NASA Conference Publication 2300

Tribology in the 80's

Volume II—Sessions 5 to 8

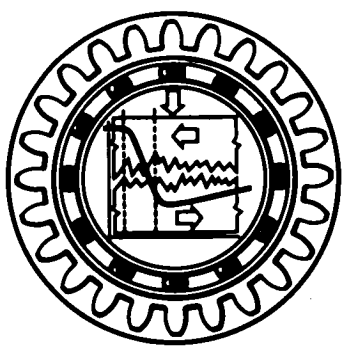

Proceedings of an International conference held at NASA Lewis Research Center Cleveland, Ohio April 18-21, 1983

NASA

NASA Conference Publication 2300

Tribology in the 80's

Volume II—Sessions 5 to 8

Proceedings of an
International conference held at
NASA Lewis Research Center
Cleveland, Ohio
April 18-21, 1983

NASA
National Aeronautics
and Space Administration

**Scientific and Technical
Information Branch**

1984

DEDICATION

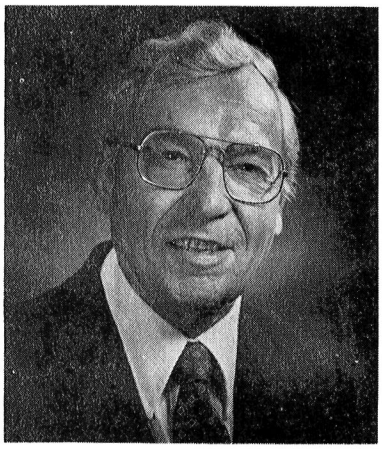

The proceedings of this conference is dedicated to Edmond E. Bisson as was the conference itself. Ed retired from NASA Lewis Research Center in 1973 and currently resides in Fairview Park, Ohio, where he writes and prepares lectures, consults, and serves as Editor-in-Chief for the American Society of Lubrication Engineers.

The tribology organization at NASA Lewis exists because of the pioneering spirit of Ed Bisson. The activity had its beginning at Langley Laboratory, Langley Field, Virginia, prior to World War II. Shortly thereafter the activity moved to the Lewis Research Center in Cleveland, Ohio. Ed recognized the need for a group dedicated to gaining a better fundamental understanding of adhesion, friction, wear, and lubrication processes. He sought the sustaining support of NACA and later NASA for the research. And he created an environment which attracted capable engineers and scientists.

Ed Bisson is a truly exceptional individual. Throughout his many years of managing the research work in tribology, bearings, gears, and seals, he demonstrated the utmost in administrative skills. More importantly, he also maintained a close contact with the technical aspects of the research work by reading and editing all technical papers emanating from the group. Many of the pioneering papers in solid film lubrication, high temperature behavior of materials, synthetic lubricants, and bearing concepts bear his name as one of the authors. His book, coauthered with William J. Anderson and entitled Advanced Bearing Technology, is widely used and referenced by tribologists throughout the world.

Researchers in this and other fields tend to gravitate to either fundamental studies or the more practical engineering applications. Ed Bisson always recognized the importance of both approaches. He knew that it was necessary to conduct fundamental research for tribology to grow as a science. He was also practical enough to recognize the need to solve existing engineering problems. He ensured that both areas were adequately addressed and helped to bring about interaction and mutual appreciation for both approaches among staff members.

A number of internationally recognized tribologists, either presently or formerly with NASA, were initiated into the field under the supervision of Ed Bisson. Literally hundreds of technical papers were published by various authors as a result of programs initiated or supported by him. A host of awards were bestowed on various members of the group through the years of his management. These recipients will readily admit that the creative environment which made these awards possible was a direct result of Ed Bisson's efforts.

Thus, in recognition of his many contributions to the field of tribology and his determined efforts in the advancement of the field, both as a scientific endeavor and an engineering discipline, we dedicated to Edmond E. Bisson the International Conference on Tribology in the 80's and its proceedings.

PREFACE

Since many of you may not be familiar with the NASA Lewis Research Center, I want to briefly introduce you to our Center and the work we do.

Lewis Research Center is one of eight major NASA field centers in the United States. In addition to these eight centers are several small satellite organizations and our Headquarters in Washington.

NASA Lewis is located on 350 acres adjacent to the Cleveland Hopkins International Airport. We have an additional 6000 acres at Sandusky, Ohio (about 60 miles west), where some larger facilities, including an experimental wind turbine, are located. Onsite we employ about 2600 civil service employees and another 700 support service contractors. Typically, our budget is about $600 million a year. About a third of that supports our inhouse research efforts, some of which you will be learning about in the next few days. The other two-thirds supports our contracts and grants with various industries and universities. You will also be hearing some results of these contractual endeavors during this conference.

Basically, there are four major program thrusts at Lewis, the largest being that of aeronautical propulsion R&T. Lewis, now over 40 years old, was formed in 1941 primarily for research on aircraft engines - originally reciprocating engines and then jet engines. That research still constitutes about half our effort here at Lewis. Aeronautical propulsion covers everything from fundamental research in materials and tribology, which you will be hearing about, through components and internal aerodynamics, and eventually to total engine systems that are tested in our various wind tunnels and engine testing facilities.

A second major thrust is space propulsion. We have people working on various types of advanced rocket engines - for example, the Centaur engine, which is a second-stage engine. The Centaur engine has been operational for 20 years. It is now being reconfigured to operate from the bay of the Shuttle as an upper-stage vehicle to deliver satellites to high Earth orbits and Earth escape trajectories. Some of our other research propulsion devices include electric thrusters and advanced chemical propulsion systems.

A third major area is space power R&T. This is an area the Center emphasized during the 1960's with such devices as solar cells, batteries, fuel cells, and various dynamic systems. Since the early 1970's and until recently only a relatively small effort had continued at Lewis in this research area. However, through our strategic planning of the last year, it was decided to make this work a major new thrust for the Center. Through such efforts, we are trying to return Lewis to its former role as NASA's lead center in space power R&D for the future.

The fourth area is communications R&T. Starting in the mid 1970's, Lewis essentially became NASA's lead center in communications technology. The Advanced Communication Technology Satellite Program is a major effort in this area. When this advanced satellite is launched in the late 1980's, it will open up the wave bands of a 20-30 GHz system.

Over the last decade we have been applying these major technologies to terrestrial-energy applications such as windmills and automotive propulsion, both gas-turbine and Stirling-cycle systems. Much of our technology is being funded and applied by the U.S. Department of Energy (DOE). Lewis Research

Center has managed and directed DOE programs through both inhouse and contracted efforts.

Another special area is launch vehicle operations for upper-stage propulsion systems. Centaur vehicle operations have been managed from Lewis for the last 20 some years. The Centaur has been a second-stage engine on both the Atlas and Titan rockets, and thus has carried many of the communications satellites to their high Earth orbits. Our Centaur program has been very successful. In fact, we have had 99 successful launches and, within the next month we will complete, hopefully, the 100th successful launch of that system.

This is just a brief overview of the work we are doing at Lewis Research Center. I hope you will find this conference rewarding, not just the formal papers that are to be presented, but also the discussions - both the more formal ones following the papers and the informal ones. And I urge you to participate actively in this conference, because participation of all attendees is the real value of any conference.

Neal T. Saunders
Director
Materials and Structures Directorate

FOREWORD

This proceedings of the International Conference in Tribology in the 80's is the result of a program by the Structures and Mechanical Technologies Division of the NASA Lewis Research Center to bring together the most outstanding and internationally known people in the field of tribology. Thirty-six invited presentations were made relative to the understanding and technical advancement of various disciplines and subdisciplines of the field. These included papers on the status of understanding on each of the eight session topics as well as an examination of the current state-of-knowledge and the directions to be taken for the remainder of the decade for each subject. Presentations by two preeminent tribologists from England, the "cradle of Tribology," set the theme for the conference. Professor David Tabor of the University of Cambridge began the conference with an overview paper on the "Status and Direction of Tribology as a Science in the 80's." Then, at the dinner meeting, Professor Duncan Dowson of the University of Leeds spoke of the future with his presentation on "Tribology for the 90's and Beyond." It is noteworthy to mention that both of these gentlemen are recipients of the prestigious Tribology Gold Medal, tribology's highest award, from the Institution of Mechanical Engineers in London. The conference was honored to have four of the ten living winners of this award in attendance, the other two being Professor Harmen Blok of The Netherlands and Robert L. Johnson of the United States.

In addition to furthering the understanding and the exchange of knowledge among some of the world's tribologists, there were several other purposes for the conference: (1) to gain attention in other scientific communities and in industry for some of the important elements being studied in tribology, (2) to help transform this information into broad, practical uses, and (3) to try to eliminate the general vagueness that exists, even among some tribologists, with the meaning of the word tribology.

Let us spend a minute with the definition and significance of the word tribology. Websters New Collegiate Dictionary has the definition "a science that deals with the design, friction, wear, and lubrication of interacting surfaces in relative motion (as in bearings or gears)." As was so succinctly stated by Professor Terence F. J. Quinn[1], "tribology is a subject which has suffered from lack of precision over the terms used to identify its various constituents." But the word itself has different connotations, according to the various authorities connected with the subject. The Jost Committee, in its report[2] to the British Government in 1966, was responsible for introducing the word tribology into current usage. The Committee defined tribology as "the study of the interactions between surfaces in relative motion and the practice related thereto." More recently, D. Scott[3], past editor of the tribology journal Wear, simply used "the science and technology of lubrication, friction and wear" as his definition. The Jost Committee's definition is perhaps deliberately vague so as to encompass the many complex interactions and practices involved and the obvious interdisciplinary nature of the science.

This conference covered a wide range of subjects extending from fundamental research with tribological materials of all kinds and their surface effects up to the final applications in mechanical components. An attempt was made to exemplify this in the design of the conference logo, which is shown on the cover. First and central to all efforts in tribology is basic research

work, which is illustrated in the middle of the logo with a drawing of the Stribeck curve[4] for delineating the various lubrication regimes. This curve is superimposed on a sketch showing two rubbing surfaces (roughness exaggerated) under load and separated by a lubricant. Around these illustrations are shown a bearing, seal, and gear to indicate the ultimate use and technology application.

The conference had a definite international flavor with 72 of the 311 registrants representing 14 countries other than the United States: 20 from Japan, 14 from England, 10 from the Federal Republic of Germany, 9 from Canada, 6 from The Netherlands, 3 each from France and Sweden, and 1 each from Australia, Finland, India, Ireland, Israel, Italy, and Switzerland.

The most important and critical elements needed for the success of this or any technical conference are the interest and support of the participants. Of the technical presentations, 11 were by NASA Lewis personnel, and the remainder were by individuals from universities, industry, and other government agencies - 12 from the United States and 13 from other countries. In addition to the 36 technical papers, there were about 70 invited discussions of these papers solicited prior to the conference plus others that were offered during and after the meeting. Those who served as chairmen of the various technical sessions were: Marshall B. Peterson, Wear Sciences; J. M. Georges, Professor, University Claude Bernard-Lyon I, France; Kenneth C. Ludema, Professor, University of Michigan; Masahisa Matsunaga, Professor, Chiba Institute of Technology, Japan; Lavern D. Wedeven, NASA Lewis Research Center; Robert L. Fusaro, NASA Lewis Research Center; Olog Vingsbo, Professor, Uppsala University, Sweden; and Robert L. Johnson, Consultant and Professor, Rensselaer Polytechnic Institute. Debra J. Drdek served as Conference Coordinator in making all the physical arrangements and Susan F. Gott was the Conference Secretary.

Many other people at the Lewis Research Center contributed to the success of this conference. Among these are some personnel of the Engineering and Technical Services Directorate and the Technical Information Services Division. I thank these people as well as the participants. In particular, a special thank you to Donald H. Buckley, Chief of the Tribology Branch, and the members of his group who helped to make this conference possible.

References

1. Quinn, T. F. J.: NASA Interdisciplinary Collaboration in Tribology - A Review of Oxidational Wear. NASA CR-3686, 1983.
2. Lubrication (Tribology), Education and Research; a report on the Present Position and industry's needs. H.M.S.O., 1966.
3. Scott, D.: Introduction to Tribology. Fundamentals of Tribology, Editors N. P. Suh and N. Saka, eds., The M.I.T. Press, 1980, pp. 1-13.
4. Stribeck, R.: Characteristics of Plain and Roller Bearings (in German), Zeit, V. D., vol. 46, 1902, pp. 1341-48, 1432-38, 1463-70.

William R. Loomis
NASA Lewis Research Center

Conference Chairman

CONTENTS

*Pages 1 to 506 are published under separate cover.

SESSION 3 - FUTURE DIRECTION OF RESEARCH IN WEAR AND WEAR RESISTANT MATERIALS
Chairman: K. C. Ludema, University of Michigan

SESSION 4 - THE FUTURE FOR LIQUID LUBRICANTS AND ADDITIVES
Chairman: M. Matsunaga, Chiba Institute of Technology

Volume II

SESSION 5 - STATUS AND NEW DIRECTIONS IN BHL
Chairman: L. D. Wedeven, NASA Lewis Research Center

ELASTOHYDRODYNAMIC LUBRICATION

Status of Understanding

Bernard J. Hamrock
National Aeronautics and Space Administration
Lewis Research Center
Cleveland, Ohio 44135

SUMMARY

The development of elastohydrodynamic lubrication can be divided into three main stages. The first stage is the development of the idealized form of elastohydrodynamic lubrication, namely where the surfaces are smooth, the fluid behavior is assumed to be Newtonian, and isothermal considerations are assumed. Results based on these assumptions are presented for the complete spectrum of contact geometries (rectangular and elliptical), contact materials (hard and soft), and lubricant availability (fully flooded and starved). The status of understanding for the idealized stage of elastohydrodynamic lubrication is fairly well covered in the existing literature. The second stage of development separately incorporates the effects of a non-Newtonian fluid model, thermal effects, and surface roughness effects into the elastohydrodynamic lubrication model developed in stage 1. Results showing recent developments in this stage are presented. The third stage collectively considers the items considered in stage 2 in investigating the lubrication of real surfaces in their operating environments.

INTRODUCTION

Dowson (1965) defines elastohydrodynamic lubrication (EHL) as "the study of situations in which elastic deformation of the surrounding solids plays a significant role in the hydrodynamic lubrication process." Elastohydrodynamic lubrication implies complete fluid-film lubrication and no asperity interaction of the surfaces. There are two distinct forms of elastohydrodynamic lubrication (EHL):

(1) Hard EHL - relating to materials of high elastic modulus, such as metals. In this form of lubrication not only is the elastic deformation important but the pressure-viscosity effects are equally as important. Engineering applications in which elastohydrodynamic lubrication is important for high-elastic-modulus materials include gears and rolling-element bearings.

(2) Soft EHL - relating to materials of low elastic modulus, such as rubber. For these materials, the elastic distortions are large, even with light loads. Another feature of the elastohydrodynamics of low-elastic-modulus materials is the negligible effect of the relatively low pressures on the viscosity of the lubricating fluid. Engineering applications in which elastohydrodynamic lubrication is important for low-elastic-modulus materials include seals, human joints, tires, and a number of lubricated elastomeric material machine elements.

Since the subject of elastohydrodynamic lubrication was introduced by Grubin (1949), there have been a number of reviews of the subject including Dowson (1965), McGrew et al. (1971), Cheng (1973), Winer (1973), and Hamrock and

Dowson (1981). It is the purpose of this paper to cover the present status of understanding of elastohydrodynamic lubrication, focusing principally on developments that have occurred in the past decade. Primary interest is in hard EHL with a section on soft EHL.

The recognition and understanding of elastohydrodynamic lubrication represents one of the major developments in the field of tribology in the twentieth century. The revelation of a previously unsuspected regime of lubrication is clearly an event of importance in tribology. Elastohydrodynamic lubrication not only explained the remarkable physical action responsible for the effective lubrication of many machine elements, but it also brought order to the understanding of the complete spectrum of lubrication regimes, ranging from boundary to hydrodynamic.

A way of coming to an understanding of elastohydrodynamic lubrication is to compare it with hydrodynamic lubrication. The major developments that have led to our present understanding of hydrodynamic lubrication (Tower, 1885; and Reynolds, 1886) predate the major developments of elastohydrodynamic lubrication (Grubin, 1949; and Petrusevich, 1951) by 65 years. Both hydrodynamic and elastohydrodynamic lubrication are considered as fluid-film lubrication in that the lubricant film is sufficiently thick to prevent the opposing solids from coming into contact. Fluid-film lubrication is often referred to as the ideal form of lubrication since it provides low friction and high resistance to wear.

CONFORMAL AND NONCONFORMAL SURFACES

Hydrodynamic lubrication is generally characterized by surfaces that are conformal. That is, the surfaces fit snugly into each other with a high degree of geometrical conformity, as shown in figure 1, so that the load is carried over a relatively large area. Furthermore, the load-carrying surface area remains essentially constant while the load is increased. Fluid-film journal bearings (as shown in fig. 1) and slider bearings exhibit conformal surfaces. In journal bearings, the radial clearance between the shaft and the bearing is typically one-thousandth of the shaft diameter; in slider bearings, the inclination of the bearing surface to the runner is typically one part in a thousand. These converging surfaces coupled with the fact that there is relative motion and a viscous fluid separating the surfaces enable a positive pressure to be developed and exhibit a capacity to support a normal applied load. The magnitudes of the pressures developed are not generally large enough to cause elastic deformation of the surfaces. The minimum film thickness in a hydrodynamically lubricated bearing is a function of applied load, speed, lubricant viscosity, and geometry. The relationship between the minimum film thickness h_{min}, the speed u, and the normal applied load F is given by

$$(h_{min})_{HL} \propto \left(\frac{u}{F}\right)^{1/2} \tag{1}$$

Many machine elements have contacting surfaces that do not conform to each other very well, as shown in figure 2 for a rolling-element bearing. The full burden of the load must then be carried by a very small contact area. In

general, the contact area between nonconformal surfaces enlarges considerably with increasing load, but it is still small when compared with the contact area between conformal surfaces. Some examples of nonconformal surfaces are mating gear teeth, cams and followers, and rolling-element bearings (as shown in fig. 2). The mode of lubrication normally found in these nonconformal contacts is elastohydrodynamic lubrication. The characteristics required for hydrodynamic lubrication (converging surfaces, relative motion, and a viscous fluid) are also required for elastohydrodynamic lubrication.

The load per unit area in conformal bearings is relatively low, typically only 1 MN/m^2 and seldom over 7 MN/m^2. By contrast, the load per unit area in nonconformal contacts will generally exceed 700 MN/m^2 even at modest applied loads. These high pressures result in elastic deformation of the bearing materials such that elliptical contact areas are formed for oil film generation and load support. The significance of the high contact pressures is that they result in a considerable increase in fluid viscosity. Inasmuch as viscosity is a measure of a fluid's resistance to flow, this increase greatly enhances the lubricant's ability to support load without being squeezed out of the contact zone. The high contact pressures on nonconforming surfaces therefore result in both an elastic deformation of the surfaces and large increases in the fluid's viscosity. The minimum film thickness is a function of the parameters found for hydrodynamic lubrication with the addition of an effective modulus-of-elasticity parameter and a pressure-viscosity coefficient.

RELEVANT EQUATIONS

The undeformed geometry of contacting solids in nonconformal contacts can be represented by two ellipsoids, as shown in figure 3. The two solids with different radii of curvature in a pair of principal planes (x and y) passing through the contact between the solids make contact at a single point under the condition of zero applied load. The radii of curvature are denoted by r's in figure 3. It is assumed that convex surfaces, as shown in figure 3, exhibit positive curvature and concave surfaces, negative curvature. Therefore, if the center of curvature lies within the solid, the radius of curvature is positive. If the center of curvature lies outside the solid, the radius of curvature is negative. It is important to note that if coordinates x and y are chosen such that

$$\frac{1}{r_{ax}} + \frac{1}{r_{bx}} > \frac{1}{r_{ay}} + \frac{1}{r_{by}} \tag{2}$$

coordinate x then determines the direction of the semiminor axis of the contact area when a load is applied and y, the direction of the semimajor axis. The direction of motion is always considered to be along the x axis.

The relevant equations used in elastohydrodynamic lubrication are given below:

Lubrication equation (Reynolds equation)

$$\frac{\partial}{\partial x}\left(\frac{\rho h^3}{\eta}\frac{\partial p}{\partial x}\right) + \frac{\partial}{\partial y}\left(\frac{\rho h^3}{\eta}\frac{\partial p}{\partial y}\right) = 12u\frac{\partial}{\partial x}(\rho h) \tag{3}$$

where

$$u = \frac{u_a + u_b}{2} \tag{4}$$

Viscosity variation

$$\eta = \eta_0 e^{\alpha p} \tag{5}$$

where η_0 is the coefficient of absolute or dynamic viscosity at atmospheric pressure and α is the pressure-viscosity coefficient of the fluid.

Density variation (for mineral oils)

$$\rho = \rho_0 \left(1 + \frac{0.6\ p}{1 + 1.17\ p}\right) \tag{6}$$

Elasticity equation

$$\delta(x,y) = \frac{2}{E'} \iint_A \frac{p(x_1,y_1)\,dx_1\,dy_1}{\left[(x - x_1)^2 + (y - y_1)^2\right]^{1/2}} \tag{7}$$

where

$$E' = \frac{2}{\frac{1 - \nu_a^2}{E_a} + \frac{1 - \nu_b^2}{E_b}} \tag{8}$$

Film shape equation

$$h = h_0 + \frac{x^2}{2R_x} + \frac{y^2}{2R_y} + \delta(x,y) \tag{9}$$

where

$$\frac{1}{R_x} = \frac{1}{r_{ax}} + \frac{1}{r_{bx}} \tag{10}$$

$$\frac{1}{R_y} = \frac{1}{r_{ay}} + \frac{1}{r_{by}} \tag{11}$$

In hydrodynamic lubrication, the solution of the Reynolds equation is such that the film shape is known and therefore the pressures can be easily determined. In elastohydrodynamic lubrication, the film shape is not known because the pressures help to determine the shape of the deforming surfaces, and therefore the solution of the Reynolds equation is considerably more complex than in hydrodynamic lubrication.

The elastohydrodynamic lubrication solution therefore requires the calculation of the pressure distribution within the conjunction, at the same time allowing for the effects that this pressure will have on the properties of the fluid and on the geometry of the elastic solids. The solution will also provide the shape of the lubricating film, particularly the minimum clearance between the solids. A detailed description of the elasticity model one could use is given by Dowson and Hamrock (1976). The complete elastohydrodynamic lubrication theory is given by Hamrock and Dowson (1976).

DIMENSIONLESS GROUPING

The variables resulting from the elastohydrodynamic lubrication theory are

E' effective elastic modulus, $2\Big/\left(\frac{1-\nu_a^2}{E_a}+\frac{1-\nu_b^2}{E_b}\right)$, N/m^2

F normal applied load, N

h film thickness, m

R_x effective radius in x (motion) direction, $1\Big/\left(\frac{1}{r_{ax}}+\frac{1}{r_{bx}}\right)$, m

R_y effective radius in y (transverse) direction, $1\Big/\left(\frac{1}{r_{ay}}+\frac{1}{r_{by}}\right)$, m

u mean surface velocity in x direction, $(u_a + u_b)/2$, m/s

α pressure-viscosity coefficient of fluid, m^2/N

η_0 atmospheric viscosity, N s/m^2

From these variables the following five dimensionless groupings can be established:

Dimensionless film thickness

$$H = \frac{h}{R_x} \tag{12}$$

Dimensionless load parameter

$$W = \frac{F}{E'R_x^2} \tag{13}$$

Dimensionless speed parameter

$$U = \frac{\eta_0 u}{E' R_x} \tag{14}$$

Dimensionless materials parameter

$$G = \alpha E' \tag{15}$$

Ellipticity parameter

$$k = \frac{a}{b} = \left(\frac{R_y}{R_x}\right)^{2/\pi} \tag{16}$$

The ellipticity parameter k is written in terms of the semimajor a and seminor b axes of the contact ellipse. The simplified expression for the ellipticity parameter given above was obtained from Hamrock and Brewe (1983) and is valid for $0 < k < 20$.

FILM THICKNESS FORMULAS

The dimensionless minimum film thickness can be written as a function of the other four dimensionless parameters, or

$$H_{min} = f(k,U,W,G)$$

The most important practical aspect of elastohydrodynamic lubrication theory is the determination of the minimum film thickness within the conjunction. That is, maintaining a fluid-film thickness of adequate magnitude is extremely important to the operation of machine elements like rolling-element bearings.

By using the numerical procedure outlined in Hamrock and Dowson (1976), the influence of the ellipticity parameter and the dimensionless speed, load, and materials parameters on minimum film thickness has been investigated by Hamrock and Dowson (1977a). The ellipticity parameter k was varied from 1 (a ball-on-plate configuration) to 8 (a configuration approaching a rectangular contact). The dimensionless speed parameter U was varied over a range of nearly two orders of magnitude, and the dimensionless load parameter W over a range of one order of magnitude. Situations equivalent to using solid materials of bronze, steel, and silicon nitride and lubricants of paraffinic and naphthenic oils were considered in the investigation of the role of the dimensionless materials parameter G. Thirty-four cases were used in generating the minimum-film-thickness formula given here.

$$\boxed{H_{min} = 3.63\, U^{0.68} G^{0.49} W^{-0.073} (1 - e^{-0.68\,k})} \tag{17}$$

In this equation the most dominant exponent occurs on the speed parameter, and the exponent on the load is very small and negative. The materials parameter also carries a significant exponent, although the range of this variable in engineering situations is limited.

From equation (17) we can write the relationship between minimum film thickness and load and speed for an elastohydrodynamic lubricated contact as

$$(h_{min})_{EHL} \propto F^{-0.073} \tag{18}$$

$$(h_{min})_{EHL} \propto u^{0.68} \tag{19}$$

Comparing the results of equations (18) and (19) with that obtained for hydrodynamic lubrication expressed in equation (1) indicates that

(1) The exponent of the normal applied load is nearly seven times as large for hydrodynamic lubrication as was found for elastohydrodynamic lubrication. This implies that in elastohydrodynamic lubrication the film thickness is only slightly affected by load while in hydrodynamic lubrication it is significantly affected by load.

(2) The exponent on mean velocity for elastohydrodynamic lubrication is slightly higher than that found for hydrodynamic lubrication.

In practical situations, there is considerable interest in the central as well as the minimum film thickness in elastohydrodynamically lubricated conjunctions. This is particularly true when traction is considered since the surfaces in relative motion are separated by a film of almost constant thickness that is well represented by the central value over much of the Hertzian contact zone. The procedure used in obtaining the central film thickness was the same as that used in obtaining the minimum film thickness. The central-film-thickness formula obtained from Hamrock and Dowson (1977a) is

$$H_c = 2.69\, U^{0.67} G^{0.53} W^{-0.067} (1 - 0.61\, e^{-0.73\, k}) \tag{20}$$

PRESSURE AND FILM THICKNESS PLOTS

A representative contour plot of dimensionless pressure is shown in figure 4 for $k = 1.25$, $U = 0.168 \times 10^{-11}$, $W = 0.111 \times 10^{-6}$, and $G = 4522$. In this figure and figure 5, the + symbol indicates the center of the Hertzian contact zone. The dimensionless representation of the x and y coordinates causes the actual Hertzian contact ellipse to be a circle regardless of the value of the ellipticity parameter. The Hertzian contact circle is shown by asterisks. Keys show the contour labels and each corresponding value of dimensionless pressure or film thickness. The inlet region is to the left and the exit region is to the right. The pressure gradient at the exit end of the conjunction is much larger than that in the inlet region. In figure 4 a pressure spike is visible at the exit of the contact.

Contour plots of the dimensionless film thickness are shown in figure 5 for the same case as in figure 4. In this figure the two minimum regions occur in well-defined side lobes that follow and are close to the edge of the Hertzian contact circle.

COMPARISON BETWEEN THEORETICAL AND EXPERIMENTAL FILM THICKNESSES

The determination of the film thickness in the lubricated conjunction is a most significant aspect of elastohydrodynamic lubrication. Film thickness dictates the extent to which the asperities on opposing surfaces can come into contact and thus has a direct bearing on the wear and fatigue failure of contacting surfaces.

For the purpose of comparing theoretical film thicknesses with those found in actual elastohydrodynamically lubricated contacts, three references will be discussed. The experimental apparatus used consisted of a steel ball rolling and sliding on a sapphire plate; this generated a circular conjunction, or an ellipticity parameter of unity. Measurements were made by using the technique of optical interferometry. Figures 6 and 7 show results from Kunz and Winer (1977) comparing the values calculated from equation (17) with their measured film thicknesses for two loads. For the smaller load, $W = 0.1238 \times 10^{-6}$ (fig. 6), the results compare remarkably well if we bear in mind the difficulties associated with the experimental determination of such small quantities under arduous conditions and the error associated with the complex numerical evaluations of elastohydrodynamically lubricated conjunctions. For the larger load, $W = 0.928 \times 10^{-6}$ (fig. 7), the agreement is not so good, with the theoretical predictions of film thickness being consistently larger than the measured values. This discrepancy is sometimes attributed to viscous heating, as discussed by Greenwood and Kauzlarich (1973), or to non-Newtonian fluid behavior, as discussed by Moore (1973).

Another comparison between experimental findings and theoretical predictions can be based on the experimental results provided by Dalmaz and Godet (1978). They measured film thickness optically in a pure-sliding, circular-contact apparatus for different fire-resistant fluids. An example of the good correlation between the theoretical predictions based on equation (20) and these experimental results is shown in figure 8. The agreement between the theoretical predictions and the experimental variation of central film thickness with speed for mineral oil and water-glycol lubricants of similar viscosity is most encouraging. The ellipticity parameter was unity and the applied load was 2.6 N for these experiments. Figure 8 also shows that for water-glycol, the film thickness generated was barely one-third of that developed for mineral oil of similar viscosity. This drastic reduction in film thickness is attributed to the pressure-viscosity coefficient of water-glycol, which is about one-fifth that of mineral oil.

One further important comparison between the theoretical film thickness equations and experimental measurements of film thickness is provided by Koye and Winer (1981). The pressure-viscosity properties of the lubricant and the effective elasticity of the crowned rollers and the sapphire disk yielded an average value for the dimensionless materials parameter G of 10 451. The dimensionless speeds U and loads W were varied by changing the rolling velocities and the applied loads such that

$$2.14 \times 10^{-11} < U < 8.90 \times 10^{-11}$$

$$0.038 \times 10^{-6} < W < 5.32 \times 10^{-6}$$

Koye and Winer (1981) found that their results suggested that both dimensionless speed U and load W had a slightly more dominant influence on minimum

film thickness than the theory indicated. A summary of the results, in which the experimental dimensionless minimum film thicknesses are plotted against the theoretical predictions, is shown in figure 9. There are two significant features of the findings of this important experimental investigation.

(1) The theoretical minimum film thickness (eq. (17)) tends to underestimate the actual minimum film thickness.

(2) The experimental findings suggest that the theoretical minimum-film-thickness formula (eq. (17)) is just as valid for ellipticity ratios less than unity as it is for ratios greater than unity.

The first conclusion appears to contradict the earlier findings of Kunz and Winer (1977), although it must be said that the overall agreement between theory and experiment in this difficult field is encouraging. If the finding that the minimum-film-thickness formula tends to underestimate the actual film thickness is confirmed, the theoretical predictions will at least possess the merit of being conservative.

SOFT EHL

The work presented in the previous sections related to materials of high elastic modulus, such as metals. In this section, the analysis is extended to materials of low elastic modulus, such as rubber. The procedure used in obtaining the soft-EHL results is given in Hamrock and Dowson (1978). The ellipticity parameter was varied from 1 (a ball-on-plate configuration) to 12 (a configuration approaching a rectangular contact). The dimensionless speed and load parameters were varied by one order of magnitude. Seventeen cases were used to generate the following minimum-film-thickness formula:

$$H_{min} = 7.43\, U^{0.65} W^{-0.21} (1 - 0.85\, e^{-0.31\, k}) \tag{21}$$

It is interesting to compare the equation for materials of low elastic modulus (soft EHL, eq. (21)) with the corresponding equation for materials of high elastic modulus (hard EHL, eq. (17)). The powers of U in equations (17) and (21) are similar, but the power of W is much more significant for low-elastic-modulus materials. The expression showing the effect of the ellipticity parameter is of exponential form in both equations, but with different constants.

A major difference between equations (17) and (21) is the absence of a materials parameter G in the expression for low-elastic-modulus materials. There are two reasons for this. One is the negligible effect of pressure on the viscosity of the lubricating fluid, and the other is the way in which the role of elasticity is simply and automatically incorporated into the prediction of conjunction behavior through an increase in the size of the Hertzian contact zone corresponding to changes in load.

From equation (21) we can write the relationship between the minimum film thickness and load and speed for a soft elastohydrodynamically lubricated contact as

$$(h_{min})_{\text{Soft EHL}} \propto F^{-0.21} \tag{22}$$

$$(h_{min})_{\text{Soft EHL}} \propto u^{0.65} \tag{23}$$

Comparing these results with the results found for hard EHL in equations (18) and (19), we find that

(1) The exponent on the normal applied load is nearly three times as large as that found for hard elastohydrodynamic lubrication. This implies that in soft EHL the film thickness is a great deal more affected by load than was found for hard EHL, but a great deal less affected by load than was found in hydrodynamic lubrication (eq. (1)).

(2) The exponent on the speed is nearly the same both for hard and soft elastohydrodynamic lubrication.

The discussion thus far has assumed that there is an ample amount of lubricant within the conjunction so that a fully flooded condition exists for both the hard- and soft-EHL results presented. The influence of lubricant starvation on film thickness and pressure has been considered for hard EHL contacts by Hamrock and Dowson (1977b) and for soft EHL contacts by Hamrock and Dowson (1979). From the results for both hard and soft EHL contacts, a simple and important dimensionless inlet boundary distance is specified. This inlet boundary defines whether a fully flooded or a starved condition exists in the contact. It is also found that the film thickness for a starved condition can be written in dimensionless terms as a function of the inlet distance parameter and the film thickness for a fully flooded condition.

STAGES OF DEVELOPMENT OF ELASTOHYDRODYNAMIC LUBRICATION

The development of elastohydrodynamic lubrication can be divided into three main stages as shown in figure 10. The first stage is the development of the idealized form of elastohydrodynamic lubrication, namely where the surfaces are smooth, the fluid behavior is assumed to be Newtonian, and isothermal considerations are assumed. Results based on these assumptions for the complete spectrum of contact geometries (rectangular and elliptical), contact materials (hard and soft), and lubricant availability (fully flooded and starved) have been considered thus far in this paper. As was shown, the status of understanding of the results from the idealized stage of elastohydrodynamic lubrication is fairly well covered in the existing literature.

That is, elastohydrodynamic lubrication theory predicts the magnitude of the film thickness quite satisfactorily over a wide range of conditions. It fails, however, to explain the behavior in traction; in particular it does not satisfactorily account for the variation of the magnitude of the traction with rolling speed or the degree of slip. These circumstances led us to the second stage of development of elastohydrodynamic lubrication, where more attention is focused on the detailed behavior within the contact zone. From figure 10 we see that the second stage of development separately incorporates the effect of the non-Newtonian fluid model, thermal effects, and surface roughness effects into the elastohydrodynamic lubrication model developed in stage 1. Results showing some of the recent developments in this stage are considered in the next three sections. The third stage shown in figure 10 involves collectively the items considered in stage 2 in investigating the lubrication of real surfaces in their operating environments.

NON-NEWTONIAN FLUID RESULTS

For the idealized stage of development of elastohydrodynamic lubrication presented in figure 10, it was assumed that the lubricant is Newtonian so that the shear stress τ is linearly related to the shear rate $\dot{\gamma}$, or

$$\dot{\gamma} = \frac{\tau}{\eta} \tag{24}$$

where η is the viscosity or constant of proportionality, which may vary with both pressure and temperature. In elastohydrodynamically lubricated conjunctions the film thickness is typically about 1 μm; the pressure, 1 GPa, and the time that the oil is subjected to the pressure, 10^{-1} s. The lubricant is subjected to very severe shear stresses and rates of shear, and it is generally accepted that in these circumstances the lubricant does not behave as a Newtonian liquid. This implies that the lubrication shear stress is still a function of the shear strain rate but the relationship is no longer linear; therefore the shear rate increases more rapidly than the shear stress. The magnitude of the critical stress determining the limit of Newtonian behavior depends on the fluid and on the pressure, but, in general, it lies within the range of stress encountered in typical elastohydrodynamic lubrication conditions. A typical nonlinear equation derived from the Ree-Eyring (1955) model of viscous flow can be written as

$$\dot{\gamma} = \frac{\tau_L}{\eta} \sinh\left(\frac{\tau}{\tau_L}\right) \tag{25}$$

where η is the viscosity at low shear stresses and τ_L is a limiting shear stress.

The relationship between the shear strain rate and shear stress is given in figure 11 (from Wilson, 1983) for a number of rheological models. For the Newtonian model (eq. (24)) and the Ree-Eyring model (eq. (25)), the shear stress increases monotonically with increasing shear strain rate. For these two models, there is no limit to the shear stresses that can be sustained by the fluid. This is in disagreement with Bair and Winer (1979), who observed that there is a limiting shear stress for a given pressure and temperature at which the lubricant will shear plastically with no further increase of shear strain rate. This type of non-Newtonian fluid behavior can be presented by

$$\dot{\gamma} = \frac{\tau}{\eta} \quad \text{when} \quad \tau < \tau_L$$

$$\dot{\gamma} = \frac{\tau_L}{\eta} \quad \text{when} \quad \tau \geq \tau_L \tag{26}$$

where

$$\tau_L = \tau_0 + \gamma p \tag{27}$$

τ_0 is the initial shear strength and γ is the limiting-shear-strength proportionality constant. Both τ_0 and γ are determined experimentally. Alternative non-Newtonian fluid models from that expressed in equation (26) are the "tanh" and "ln" models shown in figure 11.

This non-Newtonian fluid behavior can be directly related to traction behavior. The traction behavior can be divided into regimes depending on the lubricant, the solid surfaces, and the operating conditions, as pointed out by Bair and Winer (1982). They found that for slide-roll ratios greater than about 0.03 the traction behavior is plastically controlled by the limiting shear stress, which is a linear function of temperature and pressure. They therefore found that the limiting shear stress and traction increase with increasing pressure and decreasing temperature. Figure 12, obtained from Bair and Winer (1982), shows the reduced traction coefficient as a function of film parameter Λ and dimensionless speed parameter U. The reduced traction coefficient is the ratio of the measured traction coefficient to what would be expected if the traction were determined by the limiting shear stress at the same temperature. For Λ less than 2, the contact moves into the partial elastohydrodynamic lubrication regime; the load shifts away from the full EHL film to contact asperities as Λ decreases, resulting in increased traction. For Λ greater than 2, elastohydrodynamic lubrication exists. Within the elastohydrodynamic lubrication fluid-film region, there are two distinct regions. For Λ between 2 and 15, the reduced traction coefficient remains constant at 1 and this region corresponds to a situation where the fluid rheological model is non-Newtonian. For Λ greater than 15, the reduced traction coefficient decreases as a result of the decreasing pressure in the film and the lubricant behavior becomes Newtonian.

The occurrence of the Newtonian and non-Newtonian regions within elastohydrodynamic lubrication was recently investigated theoretically by Jacobson and Hamrock (1983). The approach uses a Newtonian model as long as the shear stress is less than the limiting shear stress. If the shear stress exceeds the limiting shear stress, the shear stress is set equal to the limiting shear stress. The limiting shear stress is expressed as a semiempirical linear function of pressure. The relevant equations for the shear strain rate and limiting shear stress are equations (26) and (27). The numerical solution required the coupled solution of the pressure, film shape, and fluid rheology equations while going from the inlet to the exit without making any assumptions other than neglecting side leakage effects. The influence of the dimensionless speed U, load W, and materials G parameters, the sliding velocity ($U^* = (u_a - u_b)/(u_a + u_b)$), and the limiting-shear-strength proportionality constant γ on minimum film thickness was investigated. Fourteen cases were used to generate the minimum-film-thickness equation given below for a fully flooded, hard, elastohydrodynamically lubricated rectangular contact while incorporating a non-Newtonian rheological model.

$$H_{min} = H_{min,N} \exp[-2.89\times10^{-9}(U^*)^{0.60}U^{0.23}(WG^2)^{3.80} + 1.46(\gamma - 0.07)] \qquad (28)$$

The minimum-film-thickness formula for an elastohydrodynamically lubricated rectangular contact while using a Newtonian fluid rheological model $H_{min,N}$ can be written from Hamrock and Jacobson (1983) as

$$H_{min,N} = 3.07\ U^{0.71} G^{0.51} W^{-0.11} \tag{29}$$

SURFACE ROUGHNESS EFFECTS

The relationship between the film parameter Λ and the minimum film thickness is

$$\Lambda = \frac{h_{min}}{\sigma} \tag{30}$$

where $\sigma = \left(f_a^2 + f_b^2\right)^{1/2}$ is the composite surface roughness; f_a is the rms surface finish of surface a; and f_b is the rms surface finish of surface b. The film parameter Λ is found to play a significant role in determining the fatigue life of nonconformal contacts. Specifically, if the minimum elastohydrodynamic lubrication film thickness as obtained, for example, from equation (17) is about three times the composite surface roughness ($\Lambda \approx 3$), the lubrication of the nonconformal contact is deemed to be entirely satisfactory.

Until relatively recently the roughness of bearing surfaces has been characterized by a single parameter, either R_a or rms surface finish. The value of these parameters indicates the roughness level but not the roughness texture.

A part of the description of surface texture involves the distribution function of the heights of the surface profile. That is,

$$F(z) = \int_{-\infty}^{\infty} \psi(z)\, dz \tag{31}$$

where z refers to the heights of the profile measured from the centerline and $\psi(z)$ is the probability density function of these heights. The practical derivation of such distribution curves involves taking measurements of z_1, z_2, etc., at some discrete interval ℓ and summing the number of the ordinate at any given height level. Williamson (1967-1968) has found that for surfaces finished by an abrasive process the height distribution is approximately Gaussian.

Another parameter used to define the surface texture is the autocorrelation function. It is a measure of the wavelength structure of a surface profile in a given direction. Mathematically the autocorrelation function in the x direction can be expressed as

$$R(\lambda) = \frac{1}{\ell} \int_0^{\ell} z(x) \cdot z(x + \lambda)\, dx \tag{32}$$

Whitehouse and Archard (1970) show that the autocorrelation function for most engineering surfaces is an exponentially decaying function.

A third parameter used to define the surface texture is the surface pattern parameter. Many engineering surfaces have roughnesses that are directionally oriented so that they contain long wavelengths in one direction and short wavelengths in the normal direction. The directional properties of roughness can be described by the surface pattern parameter β, first introduced by Peklenik (1968) as

$$\beta = \frac{\lambda_x}{\lambda_y} \tag{33}$$

where λ_x and λ_y are autocorrelation lengths in the x and y directions. The surface pattern parameter β may be interpreted as the length-to-width ratio of a representative asperity contact. Purely transverse, isotropic, and purely longitudinal patterns have β of 0, 1, and ∞, respectively. Surfaces with $\beta > 1$ are longitudinally oriented.

Patir and Cheng (1978) developed a method known as the average flow model to handle surface roughnesses of any arbitrary surface pattern parameter β. The average Reynolds equation is defined in terms of pressure and shear flow factors, which are obtained by numerical flow simulation. This method enables one not only to investigate the effect of more practical surface roughness textures, but also to extend the results to Λ below 3, where part of the load is shared by asperity contacts. Figure 13 shows the flow pattern for longitudinally oriented ($\beta = 6$), transversely oriented ($\beta = 1/6$), and isotropic roughness ($\beta = 1$). Figure 14, obtained from Patir and Cheng (1978), shows the ratio of actual film thickness to the smooth-surface film thickness plotted against the film parameter Λ. It is interesting to note that the roughness effect is considerably smaller for a longitudinally oriented roughness of $\beta = 6$ than for the purely longitudinal roughness of $\beta = \infty$. The case of isotropic roughness only shows a slight increase in the average film thickness over that derived from smooth-surface theory. Even for $\beta = 1/6$, the effect is not as overwhelming as that suggested by the pure transverse roughness theory.

TEMPERATURE EFFECTS

Temperature within, or adjacent to, elastohydrodynamic contacts has been recorded by embedded and trailing thermocouples and by thin films of platinum (Cheng and Orcutt, 1965-1966) and nickel (Hamilton and Moore, 1971) on insulated disks or more recently by direct measurement of infrared radiation (Ausherman et al., 1976; and Nagaraj et al., 1977). Effective lubricant temperature is particularly important in sliding elastohydrodynamic contacts because of its influence on film thickness, traction, and, in the limit, failure of the lubrication mechanism. Recently Sheu and Wilson (1982) investigated the effects of inlet shear heating on elastohydrodynamic film thickness. Some of their conclusions will be reported here. A primary reason for undertaking analyses of elastohydrodynamic lubrication using thermal Reynolds equations is to provide designers with a method of estimating lubricant film thickness under conditions where shear heating of the lubricant is considered. A relatively simple design equation is provided by Sheu and Wilson (1982). The thermal correction factor C is given by

$$C = [1 + 0.241\, L^{0.64}\, (1 + 14.8\, U^{*0.83})]^{-1} \tag{34}$$

where

$$L = \frac{\eta_0 \beta u^2}{k} \tag{35}$$

β is the lubricant thermal coefficient of viscosity, and k is the lubricant conductivity. Figure 15 shows the results of using equation (34). It is observed that under conditions of high surface speeds and high lubricant viscosities, susbstantial reductions in film thickness can occur.

A secondary reason for Sheu and Wilson's (1982) studies was to discover if there were conditions under which thermal action would prevent the formation of a lubricant film, thus leading to a catastrophic breakdown in lubrication. Their conclusions are that no conditions have been found under which a lubricant film cannot be formed nor do the forms of the relationships involved suggest that such conditions exist. Thus, the analysis seems to indicate that lubrication failure due to thermal action is not a direct result of thermal viscosity reduction due to temperature variations across the film. If thermally induced failure exists, it must be due to either surface temperature rises or changes in some property other than viscosity (such as lubricant shear strength or chemical reactivity).

CONCLUSIONS

Attention is drawn to some of the significant theoretical and experimental developments in elastohydrodynamic lubrication in the last decade. A theoretical approach has been successfully obtained by coupling the elasticity equation with the Reynolds equation for elliptical contacts such as those normally found in gears and ball bearings. Film thickness formulas considering the complete spectrum of contact geometries (ranging from circular to rectangular), materials (hard and soft), and lubricant availability (fully flooded or starved conditions) are presently available for idealized elastohydrodynamic lubricated conjunctions. Comparison between theoretical and experimental findings shows a pleasing agreement between the two. Attention was focused on film thickness calculations and measurements since this represents one of the most important practical considerations of the subject.

To be able to obtain better understanding of the failure mechanism in machine elements, the next generation of elastohydrodynamic lubrication analysis should incorporate such effects as surface roughness, non-Newtonian fluid, and temperature. The understanding of these isolated effects was presented in describing the second stage of development of elastohydrodynamic lubrication. The third stage of elastohydrodynamic lubrication, which is just at its infancy, collectively incorporates the items covered in the second stage in investigating the lubrication of real surfaces in their operating environments.

REFERENCES

Ausherman, V. K., Nagaraj, H. S., Sanborn, D. M., and Winer, W. O. (1976) "Infrared Temperature Mapping in Elastohydrodynamic Lubrication," J. Lubr. Technol., vol. 98, no. 2, 236-243.

Bair, S. and Winer, W. (1979) "Shear Strength Measurements of Lubricants at High Pressures," J. Lubr. Technol., vol. 101, no. 3, 251-257.

Bair, S. and Winer, W. (1982) "Regimes of Traction in Concentrated Contact Lubrication," J. Lubr. Technol., vol. 104, no. 3, 382-391.

Cheng, H. S. (1973) "A Review of Theoretical Elastohydrodynamic Lubrication Research," Proceedings of the Tribology Workshop Held at Georgia Institute of Technology, H. S. Cheng, F. F. Ling, and W. O. Winer, eds., NTIS, 1974, 183-206.

Cheng, H. S. and Orcutt, F. K. (1965-1966) "A Correlation Between the Theoretical and Experimental Results on the Elastohydrodynamic Lubrication of Rolling and Sliding Contacts," Elastohydrodynamic Lubrication Symposium, Institution of Mechanical Engineers, London, 1965, 111-121.

Dalmaz, G. and Godet, M. (1978) "Film Thickness and Effective Viscosity of Some Fire Resistant Fluids in Sliding Point Contacts," J. Lubr. Technol., vol. 100, no. 2, 304-308.

Dowson, D. (1965) "Elastohydrodynamic Lubrication - An Introduction and a Review of Theoretical Studies," Elastohydrodynamic Lubrication Symposium, Institution of Mechanical Engineers, London, 1965, 7-15.

Dowson, D. and Hamrock, B. J. (1976) "Numerical Evaluation of the Surface Deformation of Elastic Solids Subjected to a Hertzian Contact Stress," ASLE Trans., vol. 19, no. 4, 279-286.

Greenwood, J. A. and Kauzlarich, J. J. (1973) "Inlet Shear Heating in Elastohydrodynamic Lubrication," J. Lubr. Technol., vol. 95, no. 4, 417-426.

Grubin, A. N. and Vinogradova, I. E. (1949) "Fundamentals of the Hydrodynamic Theory of Lubrication of Heavily Loaded Cylindrical Surfaces," in Investigation of the Contact Machine Components, Kh. F. Ketova, ed. Translation of Russian Book No. 30, Central Scientific Institute for Technology and Mechanical Engineering, Moscow, Chap. 2.

Hamilton, G. M. and Moore, S. L. (1971) "Deformation and Pressure in an Elastohydrodynamic Contact," Proc. R. Soc., London, Ser. A, vol. 322, no. 1550, 313-330.

Hamrock, B. J. and Brewe, D. (1983) "Simplified Solution for Stresses and Deformations," J. Lubr. Technol., vol. 105, no. 2, 171-177.

Hamrock, B. J. and Dowson, D. (1976) "Isothermal Elastohydrodynamic Lubrication of Point Contacts, Part I - Theoretical Formulation," J. Lubr. Technol., vol. 98, no. 2, 223-229.

Hamrock, B. J. and Dowson, D. (1977a) "Isothermal Elastohydrodynamic Lubrication of Point Contacts, Part III - Fully Flooded Results," J. Lubr. Technol., vol. 99, no. 2, 264-276.

Hamrock, B. J. and Dowson, D. (1977b) "Isothermal Elastohydrodynamic Lubrication of Point Contacts, Part IV - Starvation Results," J. Lubr. Technol., vol. 99, no. 1, 15-23.

Hamrock, B. J. and Dowson, D. (1978) "Elastohydrodynamic Lubrication of Elliptical Contacts for Materials of Low Elastic Modulus, Part I - Fully Flooded Conjunction," J. Lubr. Technol., vol. 100, no. 2, 236-245.

Hamrock, B. J. and Dowson, D. (1979) "Elastohydrodynamic Lubrication of Elliptical Contacts for Materials of Low Elastic Modulus, Part II - Starved Conjunction," J. Lubr. Technol., vol. 101, no. 1, 92-98.

Hamrock, B. J. and Dowson, D. (1981) Ball Bearing Lubrication - The Elastohydrodynamics of Elliptical Contacts, Wiley, New York, N.Y.
Hamrock, B. J. and Jacobson, B. O. (1983) "Elastohydrodynamic Lubrication of Rectangular Contacts," NASA TP-2111, January 1983.
Jacobson, B. O. and Hamrock, B. J. (1983) "Non-Newtonian Fluid Model Incorporated into Elastohydrodynamic Lubrication of Rectangular Contacts," submitted to the J. Lubr. Technol. for publication.
Koye, K. A. and Winer, W. O. (1981) "An Experimental Evaluation of the Hamrock and Dowson Minimum Film Thickness Equation for Fully Flooded EHD Point Contacts," J. Lubr. Technol., vol. 103, no. 2, 284-294.
Kunz, R. K. and Winer, W. O. (1977) Discussion on Hamrock, B. J. and Dowson, D. "Isothermal Elastohydrodynamic Lubrication of Point Contacts, Part III - Fully Flooded Results," J. Lubr. Technol., vol. 99, no. 2, 275-276.
McGrew, J., Gu A., Cheng, H. S., and Murray, F. (1971) "Elastohydrodynamic Lubrication, Phase I," Technical Documentary Report AFAPL-TR-70-27.
Moore, A. J. (1973) "Non-Newtonian Behaviour in Elastohydrodynamic Lubrication," Ph.D. Thesis, University of Reading.
Nagaraj, H. S., Sanborn, D. M., and Winer, W. O. (1977) "Effects of Load, Speed, and Surface Roughness on Sliding EHD Contact Temperature," J. Lubr. Technol., vol. 99, no. 2, 254-263.
Patir, N. and Cheng, H. S. (1978) "An Average Flow Model for Determining Effects of Three Dimensional Roughness on Partial Hydrodynamic Lubrication, J. Lubr. Technol., vol. 100, no. 1, 12-17.
Peklenik, J. (1968) "New Developments in Surface Characterization and Measurement by Means of Random Process Analysis," Proc. Instr. Mech. Engrs., vol. 182, Part 3K, 1967-68, 108-114.
Petrusevich, A. I. (1951) "Fundamental Conclusion from the Contact-Hydrodyanmic Theory of Lubrication," Izv. Akad. Nauk. SSSR (OTN), vol. 2, 209.
Ree, T. and Eyring, H. (1955) "Theory on Non-Newtonian Flow" (2 parts), J. Appl. Phys., vol. 26-7, 793-809.
Reynolds, O. (1886) "On the Theory of Lubrication and Its Application to Mr. Beauchamp Tower's Experiments, Including an Experimental Determination of the Viscosity of Olive Oil," Philos. Trans. R. Soc., London, vol. A177, 157-234.
Sheu, S. and Wilson, W. R. D. (1982) "Viscoplastic Lubrication of Asperities," J. Lubr. Technol., vol. 104, no. 4, 568-74.
Tower, B. (1885) "Second Report on Friction Experiments (Experiments on the Oil Pressure in a Bearing)," Proc. Instr. Mech. Engrs., Jan. 1885, 58-70.
Whitehouse, D. J. and Achard, J. F. (1970) "The Properties of Random Surfaces of Significance in Their Contact," Proc. Roy. Soc., London, vol. 316-A, no. 1524, 97-121.
Williamson, J. B. P. (1967-1968) "Microtopography of Surfaces," Proc. Inst. of Mech. Engrs., vol. 182, part 3K, 21-30.
Wilson, W. R. D. and Sheu, S. (1983) "Effect of Inlet Shear Heating due to Sliding on Elastohydrodynamic Film Thickness," J. Lubr. Technol., vol. 105, no. 2, 187-188.
Winer, W. O. (1973) "A Review of Experimental Elastohydrodynamic Lubrication Research," Proceedings of the Tribology Workshop Held at Georgia Institute of Technology, H. S. Cheng, F. F. Ling, and W. O. Winer, eds., NTIS, 1974, pp. 207-232.

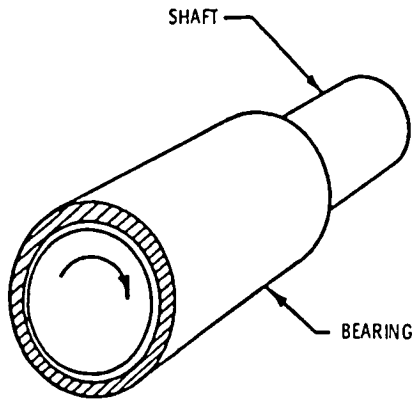

Figure 1. - Conformal surfaces.

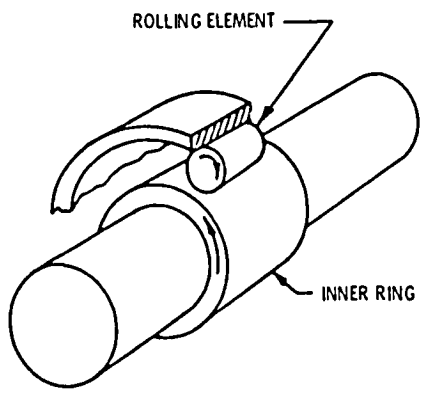

Figure 2. - Nonconformal surfaces.

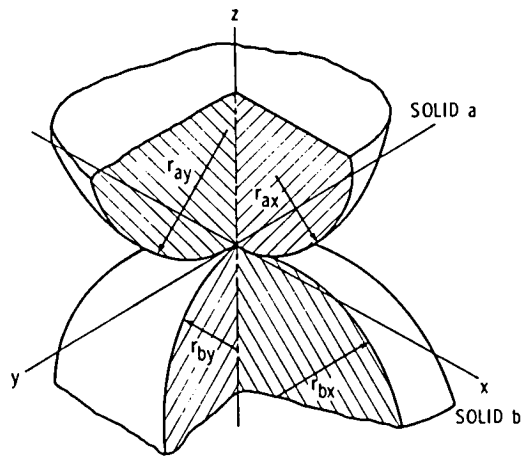

Figure 3. - Geometry of contacting solids.

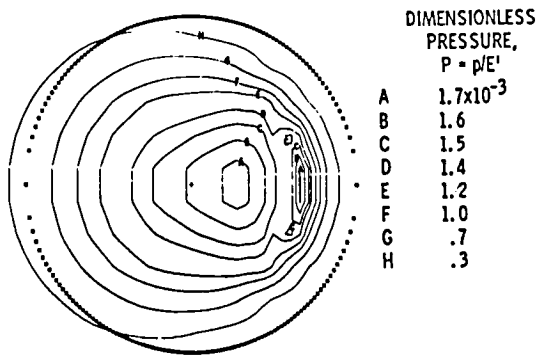

Figure 4. - Contour plot of dimensionless pressure. k = 1.25; U = 0.168x10^{-11}; W = 0.111x10^{-6}; and G = 4522.

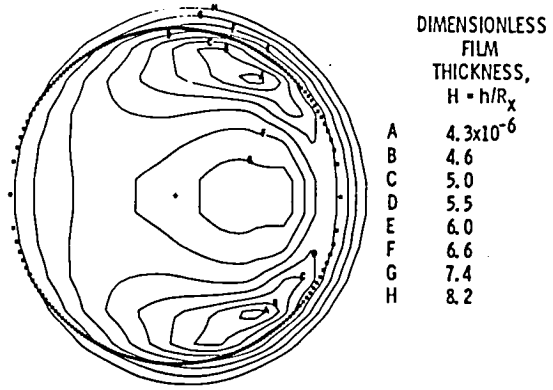

Figure 5. - Contour plot of dimensionless film thickness. k = 1.25; U = 0.168x10^{-11}; W = 0.111x10^{-6}; and G = 4522.

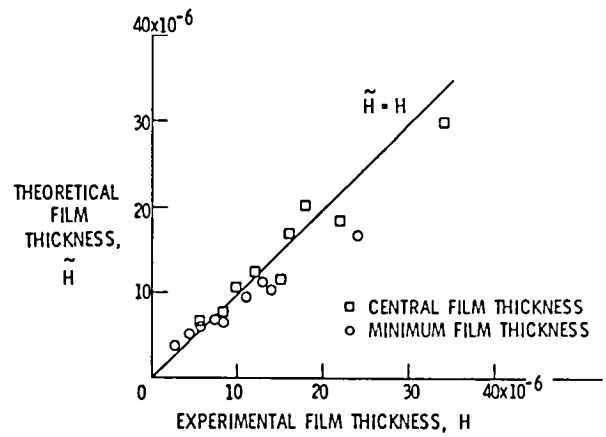

Figure 6. - Theoretical and experimental central and minimum film thickness based on optical interferometry studies. Dimensionless load parameter W = 0.1238x10^{-6}. (From Kunz and Winer, 1977.)

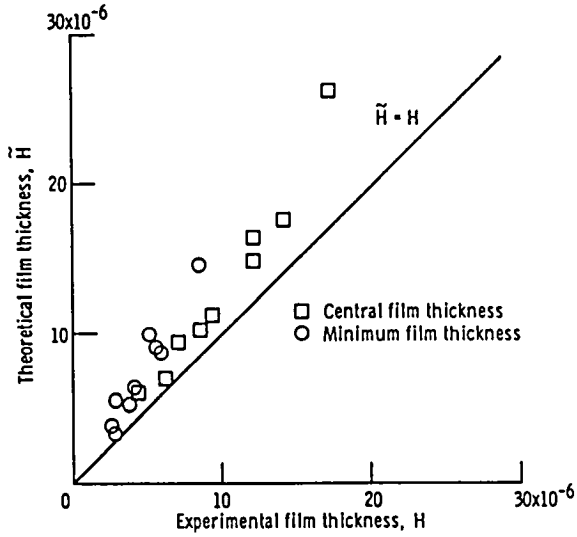

Figure 7. - Theoretical and experimental central and minimum film thicknesses for pure sliding. The dimensionless load parameter W is 0.928×10^{-6}. (From Kunz and Winer, 1977.)

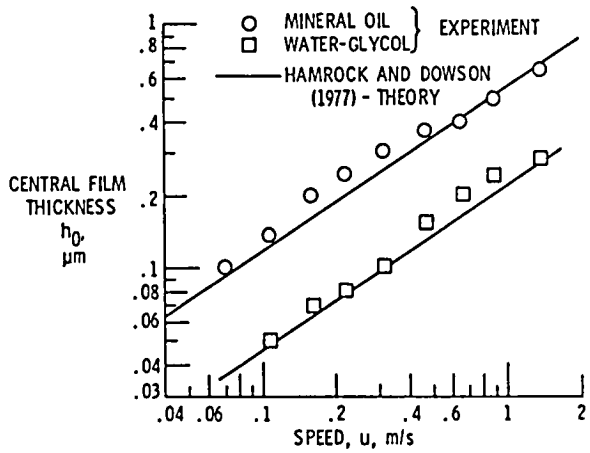

Figure 8. - Central film thickness as a function of speed at constant load (2.6 N) for mineral and water-glycol lubricants of similar viscosity. (From Dalmaz and Godet, 1978.)

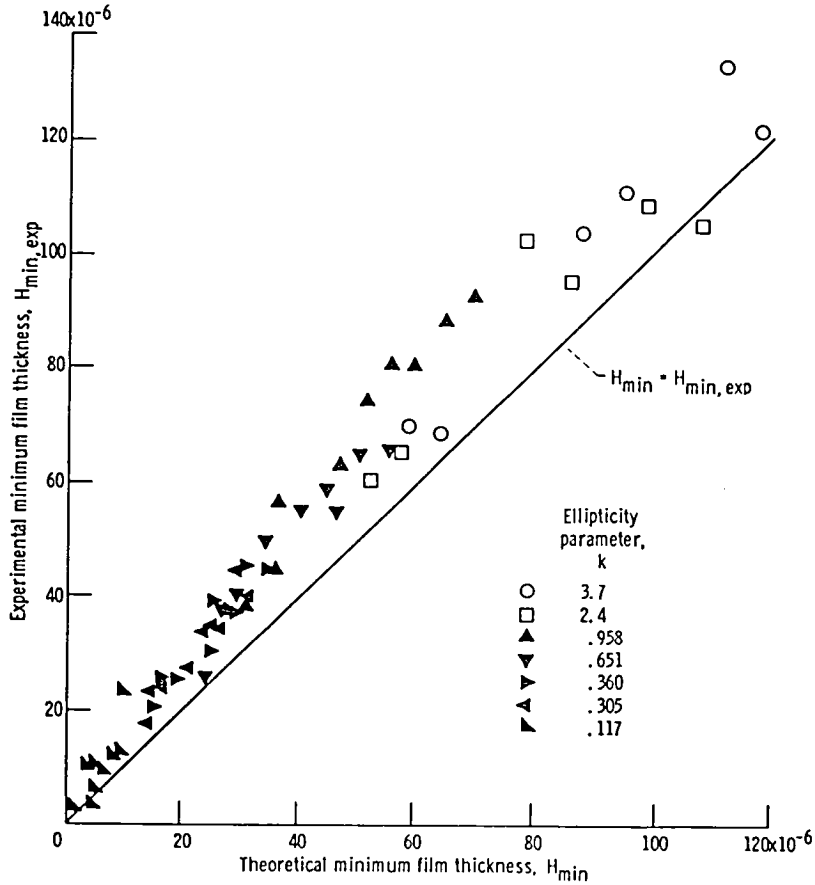

Figure 9. - Predicted dimensionless minimum film thickness (eq. (17)) as a function of measured dimensionless minimum film thickness. (From Koye and Winer, 1980.)

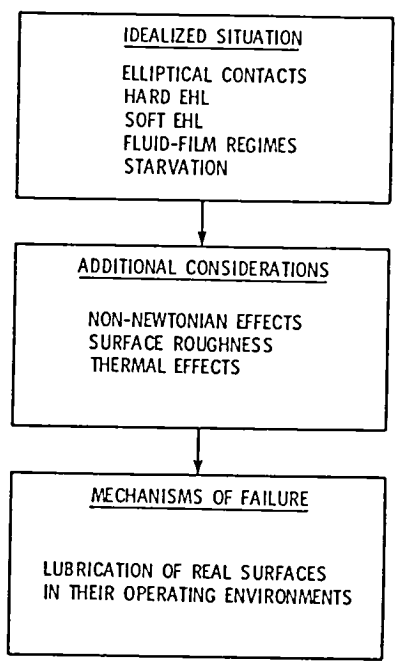

Figure 10. - Stages of development of elasto-hydrodynamic lubrication (EHL).

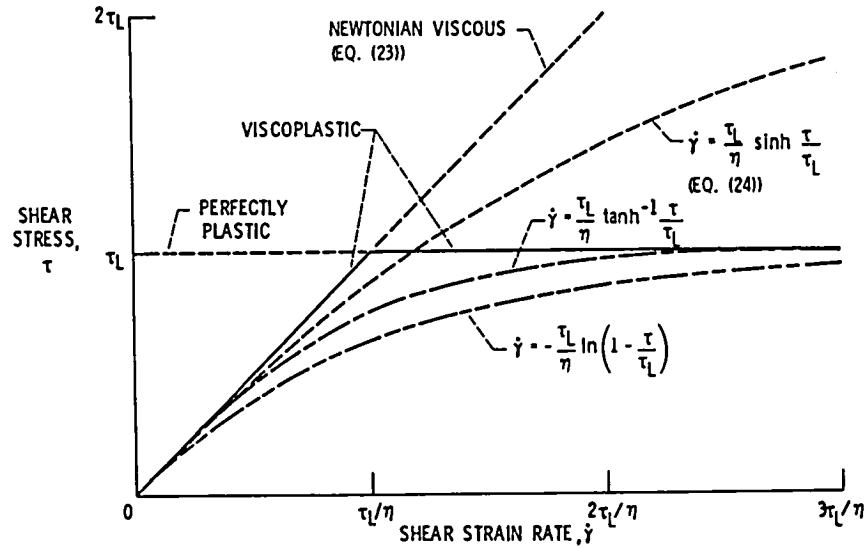

Figure 11. - Comparison of rheological models. (From Wilson, 1983.)

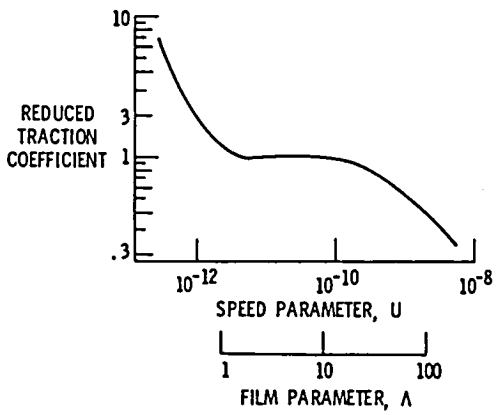

Figure 12. - Reduced traction coefficient as a function of the film and speed parameters. (From Bair and Winer, 1982.)

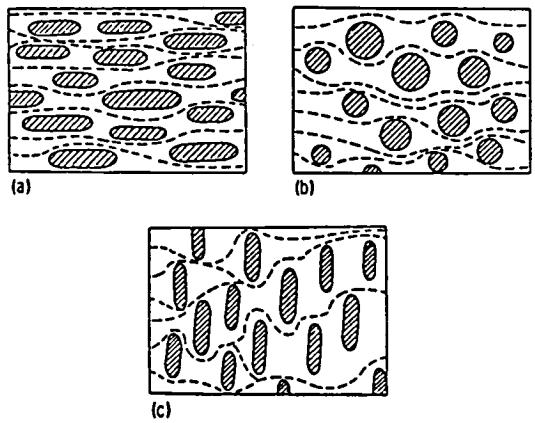

(a) $\beta = 6$. (b) $\beta = 1$.
(c) $\beta = 1/6$.

Figure 13. - Typical contact areas for longitudinally oriented, isotropic, and transversely oriented rough surfaces. (From Patir and Cheng, 1978.)

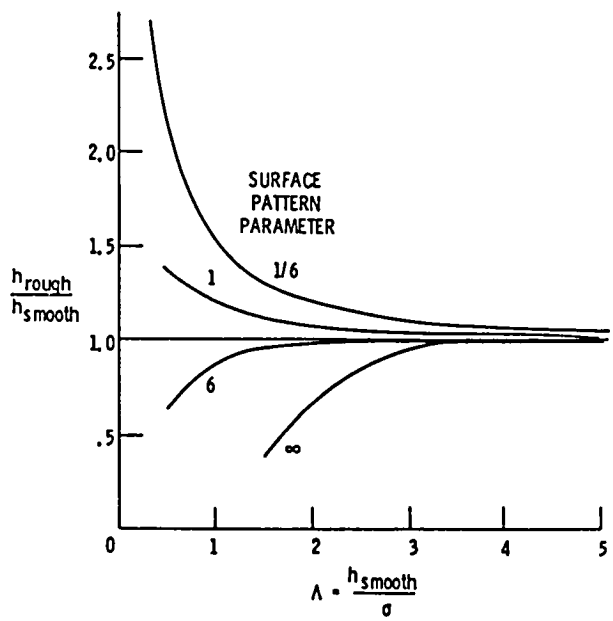

Figure 14. - Average film thickness of end contacts as a function of surface roughness. $p_0/E = 0.003$; pure rolling; $\alpha E = 3333$; $\sigma/R = 1.8 \times 10^{-5}$.

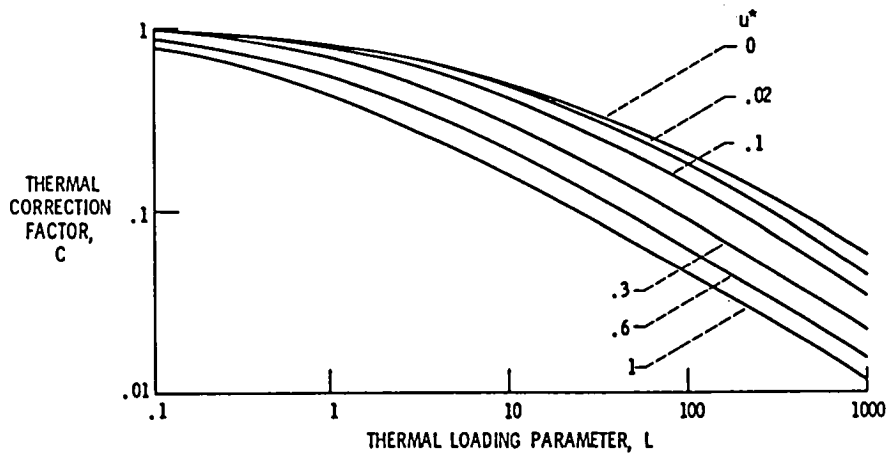

Figure 15. - Reduction in elastohydrodynamic film thickness due to thermal action. (From Sheu and Wilson, 1982.)

TEMPERATURE EFFECTS IN ELASTOHYDRODYNAMICALLY LUBRICATED CONTACTS

WARD O. WINER

Tribology and Rheology Laboratory
School of Mechanical Engineering
Georgia Institute of Technology
Atlanta, Georgia 30332

This paper gives an overview of our current understanding of thermal phenomena in elastohydrodynamic contacts and suggests some avenues for fruitful research in the next decade. Typical measured temperatures are presented for representative conditions and ranges of operating parameters. Temperatures can range from bulk ambient temperature to several hundred degrees centigrade in fully separated elastohydrodynamic films. Although attention in the past decade has been on the full film for the purposes of understanding film thickness and traction phenomena, the more interesting conditions are in the mixed elastohydrodynamic films. These mixed conditions are both common in tribological systems and they are the conditions that border on unsuccessful run-in and failure of the elastohydrodynamic contact. In mixed film conditions local hot spots can have temperatures of the order of 1000 C which cause increased reactivity of the surfaces with surrounding materials as well as changes of the surface physical properties so important to the operation of concentrated contacts.

An additional area discussed is that of the bulk system thermal transients which occur in tribological systems. These transients are frequently long in duration and have a direct bearing on the elastohydrodynamic film thickness and traction.

INTRODUCTION

The importance of thermal effects in concentrated contacts has been recognized for over four decades. In fact the recognition of the importance of high temperatures in highly loaded contacts predates the knowledge of the existence of elastohydrodynamic phenomena. The work of Bowden and Riddler (ref.1) and Blok (ref. 2,3) in the mid-thirties marks the beginning of the study of the role of thermal phenomena in concentrated contacts. Bowden and Riddler performed the first experiments in sliding contacts with and without lubricants present in which the high temperature flashes could be observed and measured with infrared detectors. Blok (ref. 2,3) published the first analytical studies

and introduced the concept of the "flash" temperature.

The Blok flash temperature concept has done much to influence thinking with regard to temperatures in concentrated contacts. The flash temperature was introduced as the increase in temperature locally in the contact above that of the bulk material. The concept was appealingly simple and caught on. It has been modified and studied in detail by many over the past forty years. The simplicity of the concept however has had the unfortunate result that the bulk temperature has been almost totally neglected. Yet the bulk temperature which is readily determined by lumped analysis, may in many engineering systems be the more important temperature to consider.

The temperature rise in the contact is the result of the frictional energy dissipation in the contact. In many engineering systems this frictional energy dissipation is the only source of thermal energy and is therefore the cause of the bulk temperature rise as well. In a fully separated elastohydrodynamic contact the energy dissipation is viscous energy dissipation in the lubricant film. In mixed film contacts there is the added energy source of the surface asperity interaction which is much more concentrated locally causing higher temperatures. Many tribologists all too readily dismiss the role of frictional energy dissipation. For those who have some difficulty appreciating the significance of this phenomena I will reiterate the analogy pointed out by Bo Jacobson in this meeting. In an average concentrated contact the energy dissipated is about 100 TW/m^3. If you have trouble relating to that figure, it might help to point out that it is like dissipating all the electrical power generated in the United States into a volume equivalent to five liters. In those terms it seems that the important questions are, what are the temperatures and can they ever be small enough to not be important? Fortunately the conditions in the concentrated contact are very beneficial to removing the energy. The film has an exceptionally high ratio of surface area to volume and the surfaces are part of massive elements with high thermal conductivity and specific heats at lower temperatures than the film. Hence the film temperature which is a measure of the energy stored in the film is the result of the difference between two very large quantities, the energy dissipated and the energy transmitted to the surroundings.

Some energy in also added to the film in the elastohydrodynamic contact by compressional heating which is the only source of energy in a pure rolling contact. Except for very high rolling speeds the resulting temperature rise is not large, e.g., about 5 C at 1 m/s rolling speed for a contact where the peak Hertz pressure is 1 GPa. The dominant source of energy dissipation is the result of the relative sliding between the surfaces. The peak temeperature is approximately proportional to the slide-to-roll ratio of the contact.

Contact temperatures are important because they influence many aspects of contact behavior. When temperatures become too high they cause contact failure. As the temperature increases the elastohydrodynamic film thickness decreases leading to lubrication on boundary films which in turn may soften or desorb resulting in contact between the two solids. The solid surface temperature can increase facilitating plastic deformation and even welding in some cases. Increasing temperatures in contacts is not always detrimental. They can cause reductions in the energy dissipation and the reaction of some boundary lubricants with the surfaces to form protective films.

The increase in lubricant temperature reduces the elastohydrodynamic film pressure generating ability and therefore the film thickness. It also decrases the friction or traction in the film. The effect on film thickness is the result of the decrease in lubricant viscosity with increasing temperature in the inlet region of the contact. This temperature is primarily determined by the bulk temperature of the elements being lubricated and not by the temperature rise in the contact zone. The effect on the traction in the contact is the result of the temperature rise in the contact itself. Because of these different effects it is possible to have in the same contact a temperature effect on the traction but not on the film thickness. In addition in some cases where both effects are present they can be of different magnitude because the viscosity which determines the film thickness is much more strongly dependent on temperature than the limiting shear stress or the limiting shear modulus which usually control the traction in the contact.

In spite of the importance of thermal effects in elastohydrodynamic contacts, the determination of temperatures in the contacts has been difficult to attain because of the size of the contact and the inaccessibility of the region of interest. Apparently the earliest attempts at measuring surface temperature in a sliding frictional contact is the work of Bowden and co-workers (ref. 1) who used an infrared cell to measure the infrared radiation through a transparent moving surface in a dry-sliding contact. They measured temperatures as high as 600C. Although they were not studying elastohydrodynamic lubrication, in some instances with their pin-on-disk experiments the surfaces were covered with a mixture of glycerin and water which probably resulted in what we would now call, a mixed mode of lubrication. They pointed out that although the extent of hot temperature flashes in such lubricated situations is greatly reduced it is clear that the presence of the liquid film does not prevent the occurrence of extremely high local temperatures as a result of local frictional heating.

Temperature measurements in elastohydrodynamic contacts have been done by relatively few people. One of the first efforts was that of Orcutt (ref. 4) who used a platinum wire as the temperature transducer, and obtained temperature profiles in moderately loaded line contacts. Moore and Hamilton (ref. 5) also used the same technique. Kannel (ref. 6) and co-workers used a similar and more sophisticated technique by using a titanium deposited transducer over a silica layer on steel disks. They developed the transducer technique in such a way that both temperature and pressure distributions could be determined. The temeperature levels measured by Kannel and co-workers were in general higher than those measured by Orcutt.

An infrared emission technique was developed in our own laboratory which can be considered a variation on the early Bowden work. Whereas the spatial and time resolution of this technique is good, it suffers from the requirement that one of the surfaces must be transparent to infrared. The most common choice of material in this work has been sapphire which does an adequate job of simulating bearing materials both thermally and mechanically. However, it does not simulate the chemistry of real bearing materials which is relevant in the mixed lubrication regime or in studying lubricant failure modes in these contacts.

There are a number of publications in the literautre on the analysis of the

temperatures in elastohydrodynamic contacts. Many of them are relatively minor variations on the original work of Blok. These include concern with the effect of somewhat different energy dissipation distributions than those considered by Blok. However, more significant studies include that of Archard (ref. 7), who presented simplified approaches to temperature calculations in concentrated contacts, those of Ling and co-workers (ref. 8), who considered the influence of asperities as well as the simultaneous solution of contact and bulk temperatures, and the recent work of Gecim (ref.9) who has studied the simultaneous effect of contact and bulk temperatures both steady and tranient as well as the effect of multiple heat sources on the same element and local temperatures resulting from asperities on rough surfaces.

ANALYTICAL STUDIES

Analytical studies of temperatures in tribological systems have almost all been concerned with the local flash temperature distribution only or the system bulk temperature only. Only recently have researchers been concerned with the solution of system and local temperature at the same time.

Both steady state and transient system bulk temperatures can be analyzed by relatively straight forward integral or lumped heat transfer analysis techniques. The system bulk temperatures play a major role in determining elastohydrodynamic film thickness. From a heat trasnfer viewpoint tribological systems are characterized by relatively low convection coefficients to transfer the heat to the surroundings, and large masses of high thermal conductivity materials resulting in low Biot numbers. A low Biot number means that the heat transfer to the surroundings by convection is poor compared to the heat transport within the solid by conduction. This results in small temperature gradients in the body except for the local flash temperature in the vicinity of the concentrated contact.

The characteristics of the typical tribological system also point to long thermal transients. This condition is generally overlooked both in tribo-element design and tribotesting in spite of the fact that it was discussed by Blok (ref. 10) in his discussion of the thermal network modelling approach to bulk temperature analysis. Blok stated that most operating transmission systems had thermal transients which lasted a few hours. The elastohydrodynamic film thickness and traction literature contain several examples of data which are almost certainly influenced by thermal phenomena. This can be recognized by the dropoff of traction with increasing slide-to-roll ratio and the dropoff of film thickness with increasing load. In fact in both types of measurements the system temperature was increasing while the measurements were made. In both of these examples there are cases in the literature where the traction does not decrease with increasing slide-to-roll ratio and the film thickness does not decrease unusually with increasing load when care was taken to eliminate the system temperature rise during the experiment.

Rarely are tribosystems constructed of single tribocontacts although virtually all analyses are of single contact systems. Gecim (ref.9) has shown that in many conditions typical of engineering systems the "flash" temperature distribution of one contact influences the others in a manner more complicated

than would be expected from simple bulk temperature considerations.

The local or flash temperature work that has been reported in the literature has been primarily concerned with relatively smooth energy distributions in the contact. This approach is acceptable for full film elastohydrodynamic lubrication conditions particularly where the traction is the result of the limiting shear stress of the material. Several works have been concerned with the importance of the various energy dissipation distributions likely in the contacts. However the difference in maximum temperatures is small, all being very similar to that first found by Blok. As a general rule the maximum temperature is proportional to the relative sliding.

The really interesting temperatures are predicted (and measured) when the ealstohydrodynamic film becomes mixed or completely disappears. When the load is shifted to the asperities the friction at first does not change significantly but the energy dissipation is concentrated over smaller areas. The friction fluctuates rapidly and can be concentrated in less than one per cent of the apparent area causing very large local temeperatures. The bulk temperature can be handled as in the full elastohydrodynamic case if an average friction coefficient can be determined as a measure of the energy dissipation. Gecim (ref. 9) has shown that in the relatively common situation of steel surfaces sliding at 2 m/s and a coefficient of friction of 0.2 the local temperature rise would be expected to be about 1100C. As will be discussed below such temperature rises have been measured.

TEMPERATURE OBSERVATIONS IN ELASTOHYDRODYNAMIC CONTACTS

Infrared Technique

The experimental results presented are based primarily on the infrared techniques developed in the author's laboratory. Some results will also be presented based on visual observation and standard photographic techniques. Two infrared detectors have been employed over the past several years. One has a fixed spot detector and the other optically scans the field of view. Both detectors are liquid nitrogen cooled Indium Antimonide detectors with high sensitivity and time resolution of about 8 microseconds. The fixed optics detector has an areal resolution of 38 micrometers and the scanning detector an an areal resolution of about one micrometer in the manner most frequently used. The elastohydrodynamic systems studied consist of a hardened steel surface loaded against a single crystal sapphire which simulates both the mechanical and thermal properties of bearing steel quite well. The apparatus and technique are described in detail in the literature (ref.11,12).

Lubricant and surface temperatures observed have ranged from as low as a few degrees to more than 1100 C above the bulk surface temperatures of the solids. This wide range of temperatures depends on the operating conditions, in particular the sliding speed, load and the film thickness to surface roughness ratio.

Lubricant Film Temperature

Lubricant film temperatures have only been measured in the sliding contacts.

The lubricant temperature obviously varies through the thickness of the film. The technique measures radiation as an integrated value through the film. Therefore the temperatures that are reported are an average value. However, because of the relationship between temperature and energy emitted, it is expected that the temperatures reported are closer to the highest value through the film than the mean.

Figure 1 shows a typical distribution of lubricant temperature rise along the centerline of a point contact moving from inlet on the left to exit on the right. The temperature rise plotted is the lubricant temperature rise above the bulk oil temperature. As the load and speed increases the lubricant temperature can become quite high even in these relatively thick film situations. The data show a significant amount of inlet oil temperature rise in the high load case where the lubricant temperature at the inlet to the Hertzian zone is as much as a 120-130 degrees above the bulk oil temperature. Given the operating conditions of the experiments, it is unlikely that this temperature rise is due to viscous heating at least according to accepted analyses. However, it may be due to the stationary surface which thermally conducts energy from the center of the Hertzian contact radially outward and into the inlet zone. This mode of inlet heating will influence film thicknesses in sliding elastohydrodynamic contacts. The inlet temeprature increase is considerably reduced at lower loads but is still as much as 80C above the bulk temperature. The unusual appearance of the temperature distribution in the low load case is believed to be a combination of the inlet conduction heating through the stationary surface and the rheological response of the lubricant in the contact.

Surface Temperatures In Sliding And Rolling Contacts

Figure 2 shows the surface temperature distributions occurring in the same contacts for which the lubricant temperatures are shown in Figure 1. In this case we are looking at the moving surface temperature which would be the lower temperature element in the contact. We see in the low load case that the inlet heating of the surface is no more than 10-15C at the entrance to the Hertzian zone, whereas in the higher load case the surface temperature at the inlet zone can be as much as 40 degrees above the ambient. Also by comparing the data in Figures 1 and 2 we see that typically the lubricant temperature in the sliding contact is from 40-50C above the moving surface temperature.

If both surfaces are moving, the surface temperatures are reduced. If the load and the rolling speed are constant, the film thickness would be expected to be essentially constant as the slide-roll ratio is varied. Figures 3a and 3b show surface temperature distributions along the centerline for fixed pressure and rolling speed with slide-roll ratio varying from -2 to +2. The -2 slide-roll ratio represents simple sliding with the temperature of the stationary surface being measured, whereas the slide-roll ratio of +2 indicates the surface temperature of the moving surface in a simple sliding contact. With both surfaces moving the inlet surface heating is reduced to less than 10C. A second observation from these data is that the temperature rise of either surface is relatively low, for example less than 20 or 30C, as long as the slide-roll ratio is less than about 0.6. A slide-roll ratio this high in an application would be considered a high sliding situation. Therefore, one would expect that the surface temperatures in rolling element bearings would be relatively low

and the major application where surface temperature effects would be important is in sliding contacts with slide-roll ratios greater than about 0.6.

Figure 4 presents the temperature distribution in a rolling contact for several different rolling speeds. Because the kinematics of the point contact sphere against rotating disk employed in this experiment, there is some twist in the contact. Also because of the relatively poor surface velocity control it is unlikely that the slide-roll ratio can be controlled within plus or minus 0.01. Nevertheless, the surface temperature rise is less than 8C up to 1.25 m/s at the relatively high Hertz pressure of 1.02 GPa. Lubricant temperatures were not obtained in the same experiment. However, they would be somewhat higher due to compressional heating.

Figure 5 presents the film thickness, lubricant temperature and both surface temperatures in a sliding contact (p_H = 1.02 GPa, bath temperature 40C). The two surface temperature distributions are remarkably similar to those presented by Blok in his early paper (ref.13). He assumed constant shear stress on the surface. In this particular case the lubricant remains about 40C above the surfaces to which it is rejecting thermal energy.

The flash temperature theory was applied to a contact consisting of the two surfaces and a lubricant film equally portioned to each surface. The energy dissipation was assumed to occur at the midplane with energy conducted through the film to each surface. The predicted surface temperatures agree well with the measured values as long as the surface of interest is moving. The comparison is shown in Figure 6. The power dependence of the surface temperature on load and speed is consistent with that in the Blok-Archard theory (ref. 14) if one accounts for the traction coefficient variation with speed in the experimental results.

Rough Surface Effects in Sliding Contacts

When the film thickess to surface roughness ratio approaches one, surface temperature fluctuations are observed on the moving rough surface (ref. 11,12). The magnitude of the temperature fluctuation can be large and decrease with time as expected from running in. The phenomena is accompanied by increased traction and wear as measured both by surface profilometry and Ferrographic analysis (ref. 15). When the temperature increases are observed, spectral analysis of the signal suggests they are the result of individual asperities passing the field of view of the detector and, curiously, they are accompanied by (followed in time) surface temperature decreases below the prevailing average surface temperature (Figure 7). Application of the Tallian (ref. 16) asperity load sharing theory indicates these fluctuations occur when the contact load is shifting from being entirely on the EHD film to partially being on the asperities and the elastohydrodynamic film load decreases.

The asperity interaction results in a time dependent system with irreversible changes occurring. When operating conditions are increased in severity for the first time, a time averaged temperature excursion occurs which then decays to a new equilibrium state as the run-in occurs. Figure 8 shows a typical example of temperature variation resulting from a step change in sliding velocity while the lambda ratio is less than one. The initial temperature excursion does not occur if the system had been previously operated until the excursion decayed to

the steady state value.

The time average surface temperature of rough surfaces, even after the run-in, is higher than for comparable operating conditions with Lambda ratioes much greater than one. A multiple regression analysis of 181 data points for cases with rough surface interaction resulted in an adjustment factor of $(1-0.7 Ra)^{-1}$ for the flash temperature equation. (Ra is the composite average surface roughness height in micrometers). This factor is similar to the $(1-0.8 Ra)^{-1}$ value recommended by the American Gear Manufacturers Association Gear Scoring Design Guide for Aerospace Spur and Helical Power Gears (AGMA Information Sheet 217.01, Oct. 1965) (ref. 12).

The spectral analysis study of surface roughness and temperature in the same experiment lead to the observation that surface roughnesses of only a particular wavelength range enter into the wear process and cause the temperature fluctuations. The significant wavelength range of surface roughness depends on the Hertz diameter of the contact and, when normalized with respect to the Hertz diameter, the range of interest is from 0.25 to 2. Surface roughness with wavelengths either longer or shorter do not interact.

Starvation Conditions in Sliding Contacts

If severe lubricant starvation occurs, surface interaction occurs no matter what the surface roughness is. A series of sliding experiments were conducted (ref. 17) with the system described above in which the initial state was steady operation with fully developed elastohydrodynamic films (lubricant naphthenic mineral oil, pressures from 1.0 to 1.25 GPa, sliding speeds from 1.0 to 4.3 m/s) where lambda ratios were greater than one. The lubricant was then drained from the system and the ball surface temperature at the contact center was monitored. Traction coefficient and surface temperature increased to an unsteady and unstable state (i.e., approximately 0.06 to 0.2 and 100 to 200C respectively). Within 15 to 30s a transient temperature spike would occur with the temperature rising to as much as 1100C in less than 8 microseconds. This appeared to be caused by an individual asperity scoring and was synchronous with ball revolution. The remainder of the ball circumference in the sliding path was apparently unaffected. Such a transient will have considerable implications with respect to surface chemical, metallurgical and mechanical phenomena.

Surface Temperatures in Dry Sliding Contacts

A few words are in order concerning the surface temperatures in dry sliding contact even though this review is about elastohydrodynamic lubrication contacts. A primary concern about the thermal phenomena in elastohydrodynamic lubrication contacts is how it relates to contact failure. In the condition of failure the elaastohydrodynamic contact must be like an unlubricated contact. Hence the behavior of dry contacts is relavent. We have recently performed dry sliding experiments of flat ended cylindrical hardened and unhardened steel pins on a sapphire disk. The pins were about 6 mm in diameter loaded with 18 N and 26 N giving a nominal pressure of 640 and 920 kPa respectively. The sliding speed was about 2 m/s. Thermocouples were implanted in the pin 3 and 8 mm back form the sliding interface. The experiments were performed in laboratory air

with an initial bulk temperature of about 23 C. These conditions are in many respects similar to the starvation elastohydrodynamic lubrication experiments described above.

Very high temperatures in localized areas on the surface were readily apparent to the naked eye and were as high as 1200 to 1500 C. No sophisticated instrumentation was necessary. The hotspots could easily be recorded on ordinary photographic film as shown in figure (9). The imbedded thermocouples in the pin permitted the extrapolation to an average surface temperature of about 70 C after 15 minutes sliding which is about what one would predict form the Archard flash temperature analysis. The photographs taken were time exposures of about one half to two seconds duration. Subsequent shorter time exposures confirm that the hot spots appearing in figure (9) were not all steady.

The limited observations that were made indicate that the hot spots were typically 35 micrometers or less in diameter with an occassional one as large as 150 micrometers in diameter. By adding up the area of hot spots during the time exposure it seems that less than one half of one per cent of the apparent area is involved in the rubbing. Because the spots intermittently participate in the rubbing probably less than one tenth of one per cent of the apparent area is ever actually loaded at one time. Analytical work by Gecim (ref.9) confirms that the temperatures observed are reasonable to expect under the conditions of the experiment.

A scanning infrared detector was used to look at the end of the pin during the sliding. The hot spots could be detected and the dynamics of them followed. However, the optics of the scanning system yielded an areal resolution of about 1 mm diamter which was too large to quantify the temperatures in the hot spots. This system did permit an estimate of the surface temperature in the vicinity of the hot spots. This estimate was between 300 and 375 C depending on whether the emmisivity of the surface was assumed to be 0.8 or 0.5 respectively. The value of 0.8 is reasonable for a rough iron oxide surface.

With these elevated temperature surfaces in air one would naturally expect surface oxidation of the steel pin. SEM and Auger electron spectroscopy of the surfaces confirmed the existence of an oxide layer of 2 to 3 micrometers thickness. The oxide layer appeared to grow and flake off in a manner predicted by the Quinn oxidational wear theory (ref. 18).

In a mixed film lubrication condition or partial elastohydrodynamic lubrication condition similar hot spots may occur. In which case reactions with the lubricant would be expected. The study of this type of phenomena may be beneficial to our understanding of the failure of elastohydrodynamic lubrication films. The concepts of thermal instability phenomena studied by Burton and co-workers (ref. 19) should be brought to bear on this area of study.

CONCLUSIONS AND RECOMMENDATIONS

Our knowledge of temperatures occuring in thick film elastohydrodynamically lubricated contacts is reasonably good. There are analytical techniques

available to predict local temperature increases and experimental techniques have verified the trends of these predictions. The infrared technique has given insight into the relationship between surface temperature and surface roughness and has lead to guidelines as to what ranges of surface roughness to be concerned with.

Bulk system temperatures can also be predicted but are believed to be afforded less attention than they deserve. A major research need in this area is better information on the values of convection heat transfer coefficients which are operative in tribosystems. Design techniques for predicting thermal transient and steady state response of tribosystems need to be developed and made accessible to the design engineer.

There are many areas of tribology where the already developed techniques for studying thermal behavior of tribosystems could be employed to further our understanding of the field. These include the study of a wider variety of materials than has been used to date including both solids and liquid lubricant formulations. The study of the relationship of local surface temperature and the effectiveness of boundary lubrication additives should be undertaken. The experimental evaluation of the existing inlet heating theories of elastohydrodynamic lubrication is another area of useful investigation.

However probably the most exciting area available to study with the experimental techniques that have been developed is that of the local high surface temperatures associated with asperity interactions. How these high temperatures relate to surface roughness, the presence of surface films, the presence of boundary lubricants, and the run-in and wear of various materials are all potential areas for advancing the field of tribology.

REFERENCES

1. Bowden, F.P.,and Tabor,D.,Friction and Lubrication of Solids - Vol.I,1954 and Vol. II 1964, Oxford University Press.

2. Blok, H., "General Discussion on Lubrication",2. Institution of Mechanical Engineers, 1937, 222.

3. Blok, H., "Surface Temperatures Under Extreme-Pressure Lubricating Conditions", Second World Petroleum Conference, Paris, 3, 4 (June 1937).

4. Orcutt, F. K., "Experimental Study of Elastohydrodynamic Lubrication", ASLE Trans. 8 (1965) 381-396.

5. Hamilton, G. M., and Moore, S. L., "Deformation and Pressure in an Elastohydrodynamic Contact", Proc. Roy. Soc. 322A (1971) 313-330.

6. Kannel, J. W., and Bell, J. C., "A Method for Estimating of Temperatures in Lubricated Rolling-sliding Gear or Bearing EHD Contacts" 1972 EHD Symposium, IME, Paper No. C24/72 (1972) 118.

7. Archard, J. F.,"The Temperature of Rubbing Surfaces", Wear, 2(6),(1959) 438-455.

8.Ling, F. F., Surface Mechanics, Wiley Interscience, New York (1976).

9.Gecim, B., Personal Communication (1983).

10.Blok, H. "The Postulate about the Constancy of Scoring Temperature", in P.M. Ku(ed.), Interdisciplinary Approach to the Lubrication of Concentrated Contacts, NASA Spec. Publ., SP-237 (1970).

11.Nagaraj, H. S., Sanborn, D. M., and Winer, W. O., "The Effect of Surface Roughness on Surface Temperature Fluctuations in EHD Contacts", Proc. Leeds-Lyon Conference (September 1977).

12.Nagaraj, H. S., Sanborn, D. M., and Winer, W. O., "Asperity Interactions in EHD Contacts", Trans. ASME, J. Lub. Tech, 100, 1 (April 1978) 246-253.

13.Blok, H., "Theoretical Study of Temperature Rise at Surfaces of Actual Contact under Oiliness Lubricating Conditions", Proc. Gen. Disc. on Lubrication and Lubricants 2, Inst. Mech. Eng. (1938) 222.

14.Nagaraj, H. S., Sanborn, D. M., and Winer, W. O., "Direct Surface Temperature Measurement by Infrared Radiation in Elastohydrodynamic Contacts and the Correlation with the Blok Flash Temperature Theory", Wear 49 (1978) 43-59.

15.Jones, W. R., Nagaraj, H. S., and Winer, W. O., "Ferrographic Analysis of Wear Particles from Sliding Elastohydrodynamic Experiments", NASA Technical Paper 1230 (April 1978).

16.Tallian, T. E., "The Theory of Partial Elastohydrodynamic Contacts", Wear 21 (1972) 49-101; Author's comments: Wear 24 (1973) 255-258.

17.Bair, S. and Winer, W. O., "Investigations of Lubricant Rheology as Applied to Elastohydrodynamic Lubrication", NASA-Lewis Research Center, NASA Grant No. NSG-3106 (July 1978).

18.Quinn, T.F.J., "A Review of Oxidational Wear", NASA Grant NCC-3-14 Interim Report (June 1982).

19.Burton, R.A.ed.,Thermal Deformation in Frictionally Heated Systems, Elsevier Sequoia S.A.,Lausanne and New York (1980).

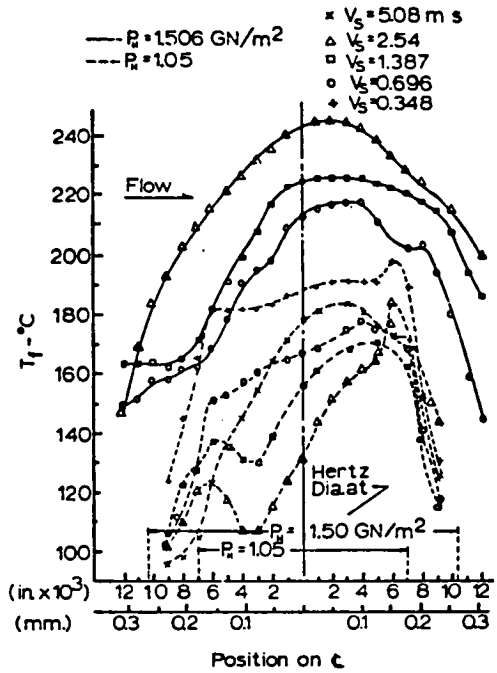

Fig. 1. Fluid film temperature on centerline versus speed and load

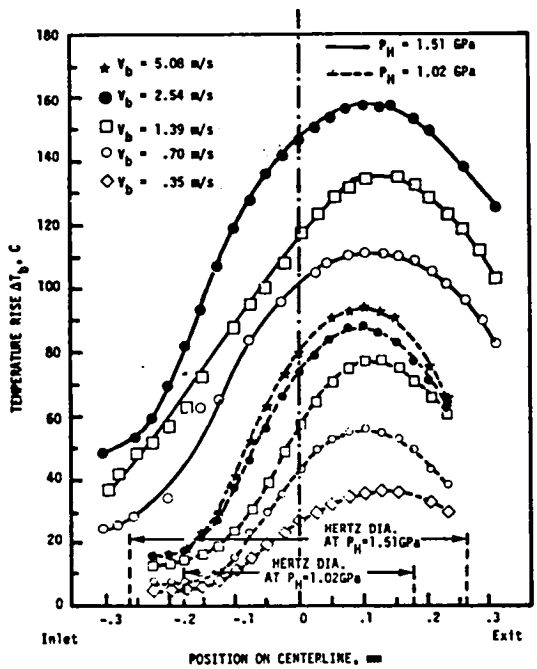

Fig. 2. Ball surface temperature rise along the centerline versus speed (smoothball: 0.011 μm Ra, fluid NI, T_{bath} = 40C, V_{sa} = 0)

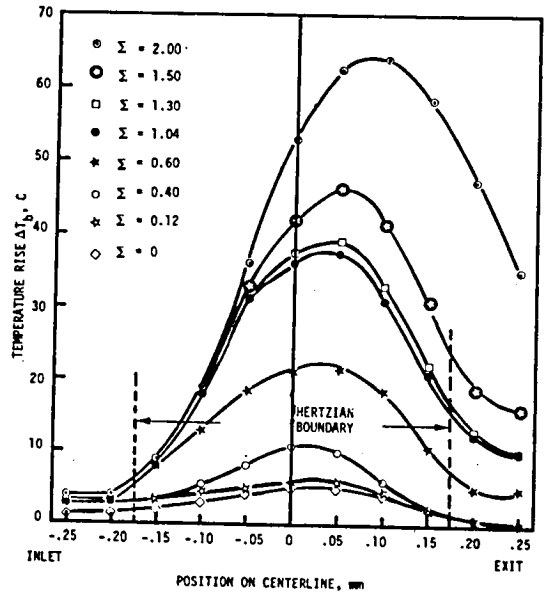

Fig. 3a. Ball surface temperature rise along the contact centerline (0.011 μm Ra roughness, P_H = 1.02 GPa, (1 m/s rolling velocity)

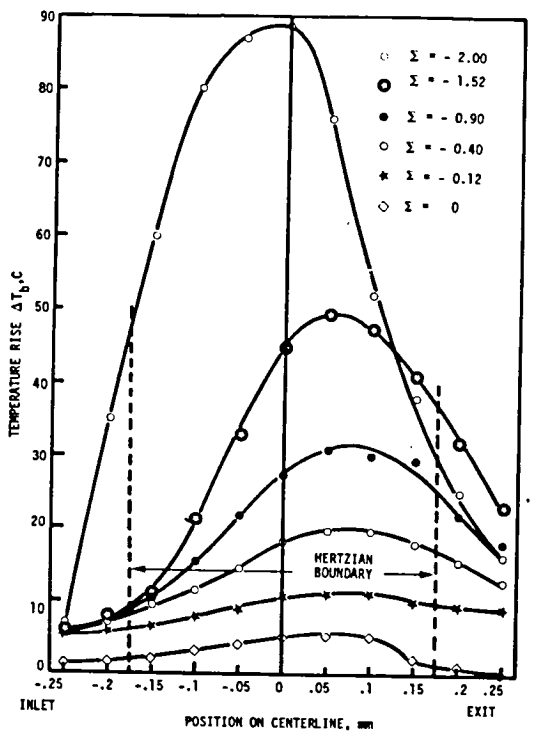

Fig. 3b. Ball surface temperature rise along the contact centerline (smooth ball → 0.011 μm Ra, P_H = 1.02 GN m^{-2}, 1 m/s rolling velocity)

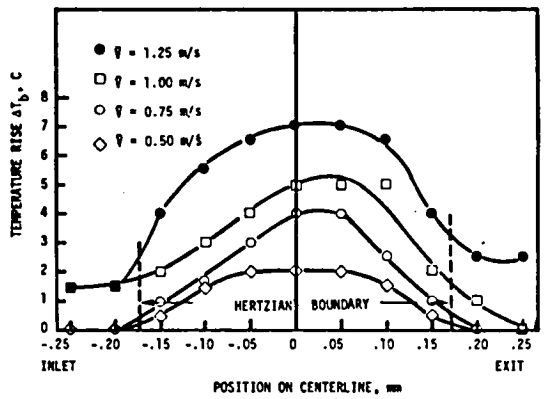

Fig. 4. Ball surface temperature rise along contact centerline (0.011 μm Ra roughness, P_H = 1.02 GPa, Σ = 0)

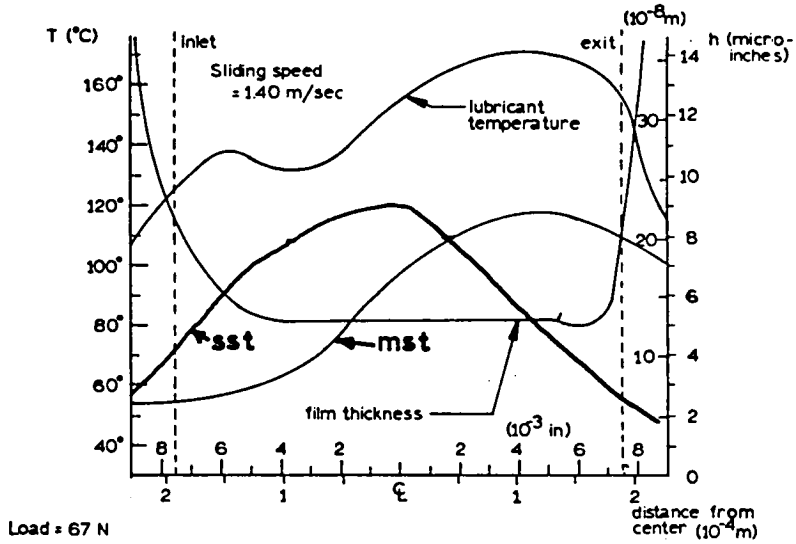

Fig. 5. Lubricant and ball surface temperatures along contact centerline (mst = moving surface temperature, sst = stationary surface temperature)

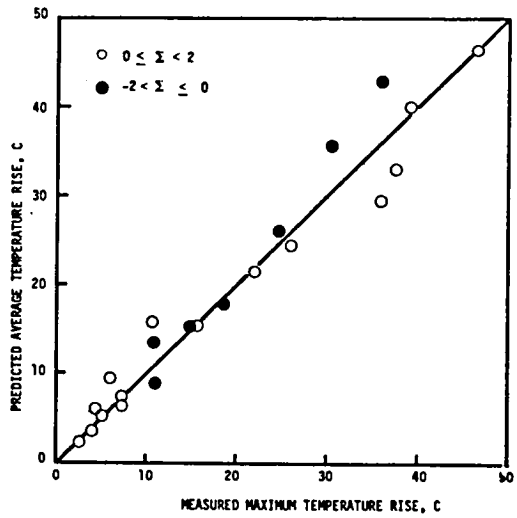

Fig. 6. Comparison of predicted average contact temperatures maximum surface and the measured maximum surface temperature rise for L > 5 (smooth ball: 0.011 μm Ra, fluid N1, V_{sa} = 0)

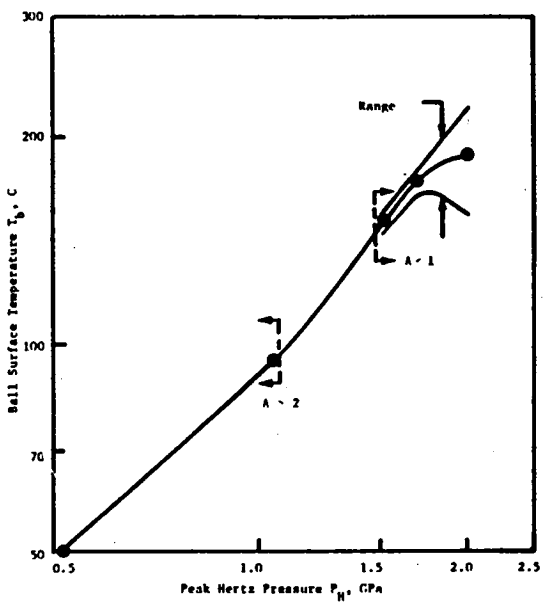

Fig. 7. Average value and range of ball surface temperature fluctuation versus peak Hertz pressure (medium rough ball: 0.76 μm Ra; fluid N1, V_s = 1.0 m/s, V_{sa} = 0)

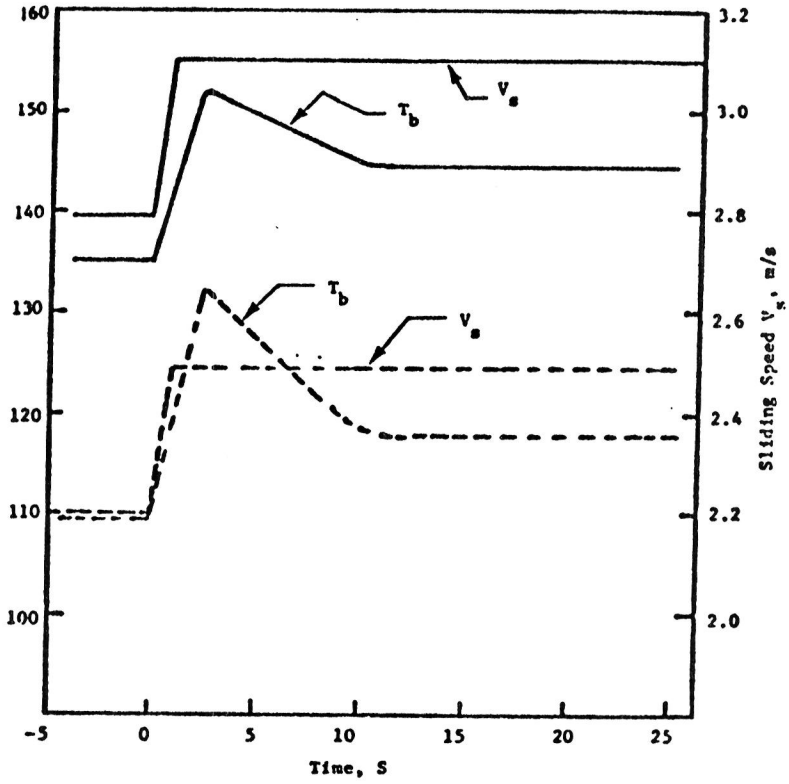

Fig. 8. Maximum ball surface temperature versus time (Time 0^+ corresponds to a velocity step) (Rough ball: 0.38 μm Ra, P_H = 1.02 GPa, fluid N1, V_{sa} = 0)

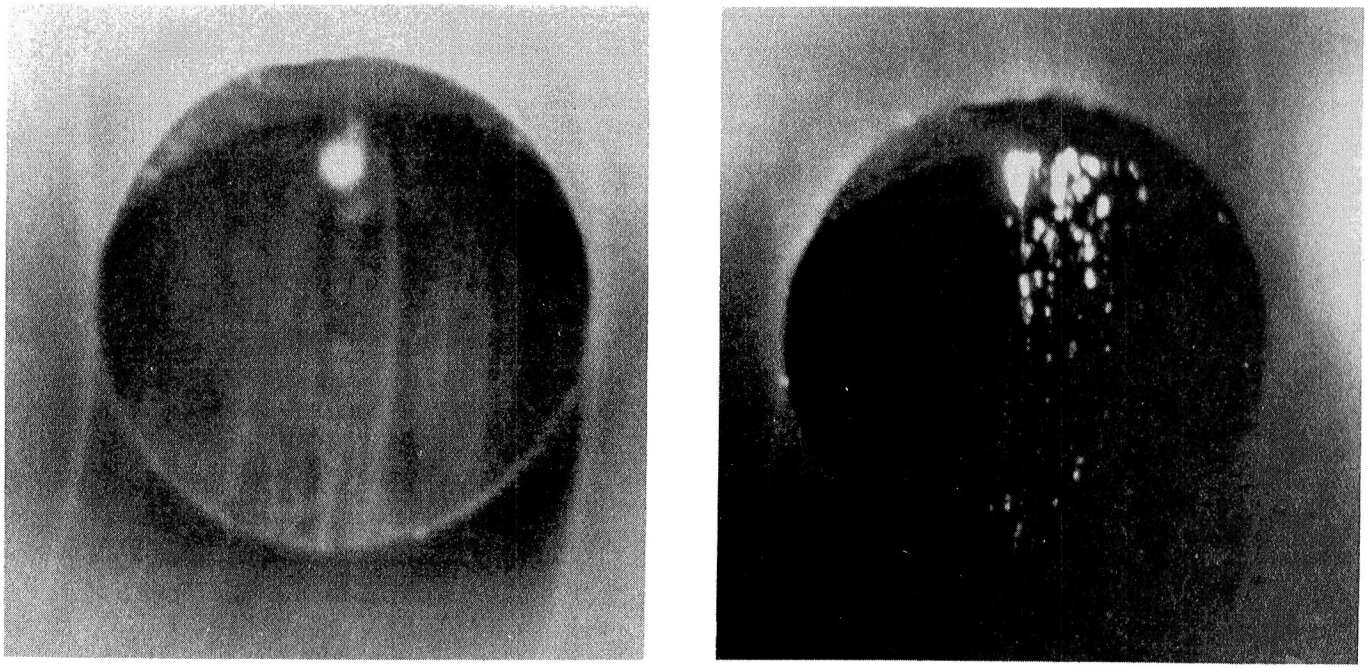

Fig. 9. Photographs of hot spots on 6 mm diameter hardened steel pin sliding on sapphire at 2 m/s and an 26N load.
a) a few seconds after the start of sliding
b) about 15 minutes after start of sliding

DISCUSSION

K. L. Johnson
Cambridge University
Cambridge, England

The author's review, backed by the excellent work of his laboratory, has shown that in the present decade we can grapple with the all-important effects of temperature in tribology in a more sophisticated way than ever before.

Flash temperatures in real situations are virtually impossible to measure. The value of the full-film infra-red experiments in the laboratory, therefore, is to investigate and to give confidence in the use of flash temperature theory to predict temperatures in practice. Early infra-red experiments were wildly at variance with theory, but the author states and shows in Fig. 6 that for moving surfaces, at least, the agreement is now good. I hope that he will expand on this aspect of his work, giving more details of the analysis and covering a wider range of conditions. Also, what about the comparison between calculated and observed film temperatures? Does this throw any light on the value of thermal conductivity of the lubricant at EHD pressures?

On the question of local temperatures in mixed lubrication conditions the author's experiments break new and important ground (though he does acknowledge the almost pre-historic work of Bowden and Riddler on this problem!). If one surface is stationary hot-spots are not unexpected: Barber and Barton have shown that thermal expansion concentrates the contact pressure and hence the heat generation into small areas. When both surfaces are moving the nature of asperity interaction is more complex. I have been struggling with this question in an attempt to estimate local flash

temperatures in railroad wheel-rail contacts when some wheel-slip takes place. The maximum flash temperature acquired by an asperity depends upon the time it is in contact with the mating surface. In the conventional wear model this is related to the length scale of the surface roughness. It seems more probable, however, that a serious high spot on one surface will maintain contact with the mating surface throughout the whole of its passage through the nominal contact area. This may be connected with the author's observations that only certain wavelengths in the roughness spectrum are related to the temperature variations. (Is the response time of the infra-red system not also important here?) Does the author think that his technique is capable of throwing light on asperity contact times as well as temperature transients?

It is clear that the remainder of the decade is going to see considerable advance in our understanding of thermal effects in tribology.

DISCUSSION

Masayoshi Muraki
Mitsubishi Oil Company
Kanagawa, Japan

Yoshitsugu Kimura
The University of Tokyo
Tokyo, Japan

Professor Winer presented a comprehensive overview of temperature effects in concentrated contacts. It enabled us to get a glimpse of his extensive investigation into this complicated problem.

He introduced the concept of flash temperature. The discussers would like to point out first that there are two different concepts of flash temperature. One is the localized instantaneous temperature rise at the points of real contact, in which case temperatures as high as 1000°C could be expected. The other, which was originally proposed by Blok as the temperature flash, is the temperature rise at the Hertzian contact area, which seldom exceeds, say, 200 or 300°C. In the case of dry or mixed lubrication conditions, the latter is considered as the mean, in a sense, of the former, but in the full EHL contacts it represents the actual temperature rise. In such a way, appropriate expression must be chosen depending upon the phenomenon on which the temperature exerts its effect.

In friction systems, practically all the heat is generated at the sliding surfaces by frictional or viscous energy dissipation. The heat thus generated is considered to flow through various passages to a body of hypothetically infinite heat capacity, whose temperature is called 'bulk temperature'. The temperature rise at the heat source, which is of the primary concern in most cases, is determined by the thermal resistance of the passages and the heat flux. Anyway, this local temperature rise must be added to the bulk temperature.

A number of analytical studies have been reported, but almost all been concerned with the estimation of local temperature rise, as Professor Winer stated. However, as is clear from the foregoing, the bulk temperature plays an equally important role in determining actual temperature of the sliding surfaces. Unfortunately, the bulk temperature depends upon non-tribological factors, which could be only insufficiently specified. If we think some bearings mounted in an automobile, the bulk temperature is primarily dependent on the place it is driven, for example. Therefore, what is important is not to pursue more rigorous solutions, but to find simple practical expressions for the temperature rise with reasonable accuracy.

In EHL contacts, an important thermal effect appears in the traction characteristics of lubricating oils. The discussers recently developed a simplified expression of the coefficient of traction[1], which will be introduced elsewhere[2]. In that, the heat is assumed to be generated uniformly in the film, and to be conducted away across the film. Then an average temperature rise of the film above the surface temperature of the rollers is given by

$$\theta_f = \bar{\tau}\Delta U h/12K_f \qquad (1)$$

where $\bar{\tau}$ is the mean shear stress, ΔU is the sliding speed, h is the film thickness and K_f is the thermal conductivity of the fluid.

The average surface temperature rise of the rollers is assumed to be given by the Crook formula[3],

$$\theta_w = 0.96b^{1/2}\bar{\tau}\Delta U/(\pi K_m \rho_m c_m U)^{1/2} \qquad (2)$$

where b is the half Hertzian width, K_m, ρ_m and c_m are the thermal conductivity, the density and the specific heat of the rollers, respectively, and U is the rolling speed.

When the local temperature rise, $\theta_m = \theta_f + \theta_w$ is thus estimated, the thermal effect on the traction can be readily determined. The theoretical result is compared in Fig.1 with the data reported by Johnson and Cameron[4], which shows satisfactory agreement. The corresponding temperature rise is shown in Fig.2. It should be remembered that the rather significant thermal effect is caused by the temperature rise of not more than 40°C in this case.

References

[1] M. Muraki and Y. Kimura : to be published in J. Japan Soc. Lub. Eng.

[2] M. Muraki and Y. Kimura : Discussion on "Lubricant Rheology in Concentrated Contacts" in the same session.

[3] K. L. Johnson and J. A. Greenwood : Wear, 61, 2 (1980) 353.

[4] K. L. Johnson and R. Cameron : Proc. Inst. Mech. Eng., 182, Pt.1, 14 (1967-68) 307.

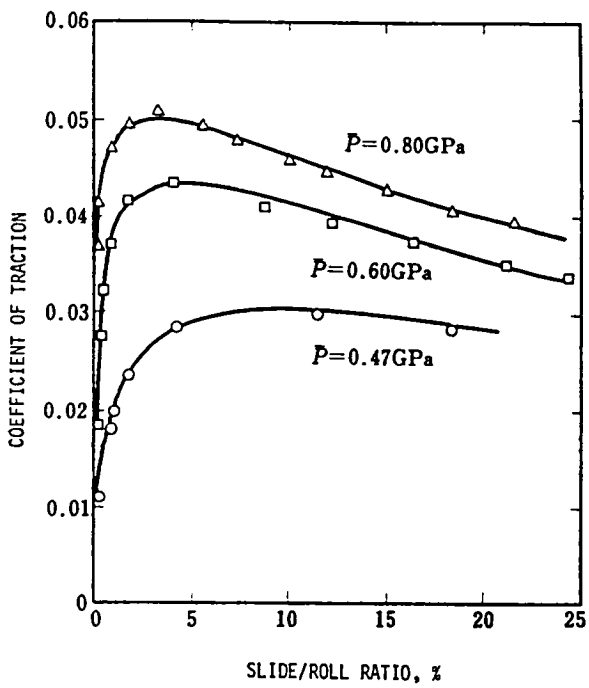

Fig.1 COMPARISON OF THEORETICAL AND EXPERIMENTAL RESULTS

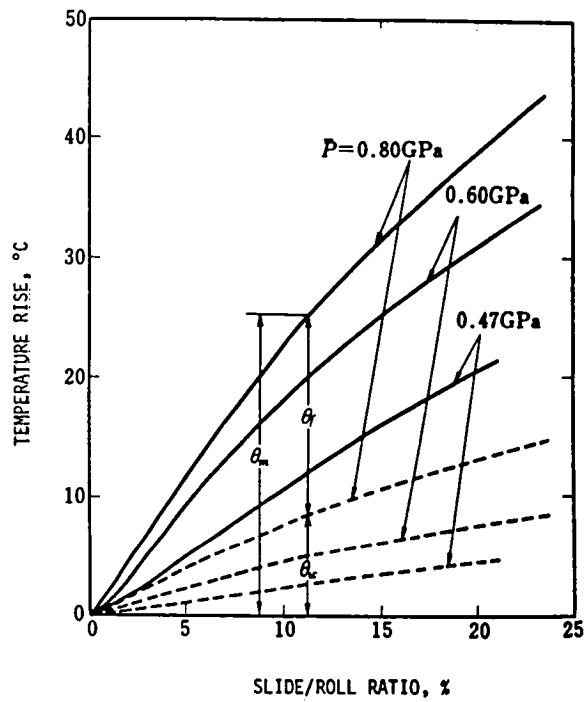

Fig.2 TEMPERATURE RISE IN THE FILM

DISCUSSION

David Tabor
Cavendish Laboratory
Cambridge, England

In my opening remarks I may have given the impression that E.H.L. had reached a plateau in knowledge and understanding. Of course this is not true. As the well coordinated session we have attended this morning shows there is a great deal of life in the subject and numerous challenging problems. But it seems to me that many of these are of a technical nature. To my mind two fundamental problems remain. First we do not understand the mechanism of film breakdown which ultimately leads to scuffing. This problem of film breakdown, of course, applies not only to E.H.L. but to the whole field of tribology. Secondly there is need for a fresh attack on the rheological properties of liquids in terms of molecular mechanisms. This should cover both the behaviour of simple lubricant liquids and liquids containing polymers or small quantities of fatty acids. I still remain very impressed with Ward Winer's results which show that at very high contact pressures the limiting shear strength of the E.H.L. film is approximately one thirtieth of the shear modulus. Such a relationship suggests that it should be possible to calculate the limiting shear strength in terms of a simple molecular model. This is a project that merits further attention.

LUBRICANT RHEOLOGY IN CONCENTRATED CONTACTS

Bo O. Jacobson
University of Luleå
Luleå, Sweden

A revue of experimental investigations of lubricant behaviour in highly stressed situations shows that a Newtonian model for lubricant rheology is insufficient for explanation of traction behaviour. The oil film build-up, on the other hand, is fairly well predicted using a Newtonian lubricant model except at high slide to roll ratios and at very high loads, where the non-Newtonian behaviour starts to be important already outside the Hertzian contact area.

Two main types of experiments are reported: static and dynamic. In static experiments the pressure is typically applied to the lubricant more than a million times longer than in an EHD contact. Depending on the pressure-temperature history of the experiment the lubricant will become a crystallized or amorphous solid at high pressures.

In dynamic experiments, where the pressure is applied as short time as in real EHD contacts, the oil is in an amorphous solid state.

Depending on the viscosity, time-scale, elasticity of the oil and the bearing surfaces, the oil film pressure, shear strain rate and the type of lubricant, different properties of the oil are important for prediction of shear stresses in the oil. This can be seen from the different proposed models for the lubricant, where it is described as being for instance a Newtonian liquid, an elastic liquid, a plastic liquid and an elastic-plastic solid.

INTRODUCTION

In lightly loaded bearings, where normal and shear stresses in the lubricant are low, the Newtonian (1) model for shear stress as a function of shear strain rate describes the behaviour of many lubricating oils very well.

If the shear stresses and velocities in the bearing are low the temperature rise is also low. When the load and speed increases, the temperature rise in the bearing increases and the viscosity of the lubricant can no longer be assumed to be constant. First the viscosity variation along the lubricating film has to be considered and at a higher power dissipation rates the temperature variation across the film thickness also gives a viscosity variation across the film. In lubricated sliding and rolling non-conformal contacts the power dissipation rate in the lubricating oil is typically of the order 100 TW/m^3, why thermal effects are important. (The total electric power installation in USA is about 0.5 TW).

In typical elastohydrodynamic contacts, where the lubricated surfaces are hard, the oil pressure is of the order 1 GPa. At these high pressures and static conditions, the viscosity of lubricating oils increases many orders of magnitude.

As long as the shear stress in the oil is low, most mineral oils behave as Newtonian liquids even at very high viscosities, but the stress level, where the oil no

longer behaves as a Newtonian liquid, is reached at a much lower shear rate.

When the shear stress in the oil is high, large molecules like multigrade additives have a tendency to break into smaller pieces. This gives a permanent viscosity loss.

At high shear stresses, elastic shear deformation of the lubricant adds to the viscous deformation, so for the same total deformation of the lubricant, the stress level will be lower. This decreases the oil film thickness and it also decreases the traction compared to the case with a Newtonian oil.

If the shear stress is further increased, the shear rate is no longer proportional to the shear stress, but the oil behaves in the same way as a metal being plastically deformed. If the pressure is high (> 1 GPa), the shear strain rate needed to reach the plasticity limit is so low that thermal effects on the pressure build-up are small compared to the effects of the plasticity.

Using a Newtonian model for the lubricant, Osborne Reynolds (2) published his famous paper, where he derived the equation for pressure build-up in a lubricating film. As long as the shear stress is proportional to the shear strain rate the equation is possible to use both for iso-viscous lubricants and for lubrication situations where the viscosity is varying along the film, but not through the oil film thickness. At high shear stresses, where the oil behaves plastically, Reynolds' equation is not applicable.

SYMBOLS

A	Constant in viscosity expression
E	Modulus of elasticity, N/m^2
E'	Effective elastic modulus $2/[(1-\nu_a^2)/E_a+(1-\nu_b^2)/E_b]$, N/m^2
F	Function, s^{-1}
G	Shear modulus, N/m^2
G	Dimensionless materials parameter, $\alpha E'$
M	Constant in viscosity expression
p	Pressure, N/m^2
R	Effective radius, m
S	Constant in viscosity expression
t	Temperature, ^oC
U	Dimensionless speed parameter, $\eta_0(U_a+U_b)/2E'R$
U*	Dimensionless sliding speed, $(U_a-U_b)/(U_a+U_b)$
U_a, U_b	Surface velocities, m/s

W	Dimensionless load parameter, $w_z/E'R$
w_z	Load per unit length, N/m
α	Pressure-viscosity coefficient of lubricant, m^2/N
γ	Limiting-shear-strength proportionality constant
$\dot{\gamma}$	Total shear rate, s^{-1}
$\dot{\gamma}_e$	Elastic shear rate, s^{-1}
$\dot{\gamma}_v$	Viscous shear rate, s^{-1}
η	Viscosity, Ns/m^2
η_0	Viscosity at contact inlet, Ns/m^2
η_a	Viscosity at atmospheric pressure and temperature 0 ^oC, Ns/m^2
μ	Coefficient of friction
ν	Poisson's ratio
τ	Shear stress, N/m^2
τ_L	Limiting shear stress, N/m^2

EXPERIMENTAL INVESTIGATIONS

The fact that lubricating oils exhibit non-Newtonian behaviour has been known for a long time. Already 1909 Bridgeman (3) showed that liquids converted to solids at high pressures, and many others (4, 5, 6, 7, 8, 9, 10, 11) also investigated solidification under pressure until Norton, Knott and Muenger in 1941 for the first time measured the yield point in oils solidified under pressure (12).

Viscosities measured in normal low shear stress viscosimeters at high pressures are so high, that the coefficient of friction μ should be of the order $\mu = 100$ if the oil was Newtonian throughout an elastohydrodynamic contact.

This led Smith in the late 1950:ies (13, 14, 15) to assume that the oil behaved as a solid with a limited shear strength in the center of the high pressure zone. This shear strength decreased with increasing temperature, so the coefficient of friction was essentially a function of the temperature.

In 1970 and -74 Jacobson (16, 17) measured the shear strength of oils solidified under hydrostatic conditions and the time for the oil to start behaving as a solid, as it was clear that the time available when the oil passed through an elastohydrodynamic contact was too short for the oil to crystallize. At pressures in the test apparatus of only 1.2 GPa (12 000 atmospheres) the oil converted to solid behaviour at room temperature in less than 9 µs. This showed that the oil must be in an amorphous solid state under these conditions.

Briscoe and Tabor (18) conclude that if an amorphous polymer such as PMMA below

its glass transition temperature is sheared, its molecules are not reoriented but the shearing possibly involves fracture-like mechanisms or true interfacial sliding.

The test procedures used so far for highly stressed oils are of two types, namely static and dynamic. In the static tests the oil is pressurized for a long time, typically more than a million times longer than in a gear or a ball bearing.

In the dynamic tests the pressure is applied approximately as long as it is in a roller bearing (milliseconds to microseconds). The last ten years a number of investigations of both types have been published.

The static experiments can be split up in two categories: Experiments where the oil crystallizes and experiments with amorphous solid oil.

Bridgeman's experiments (e.g. 3, 19) were all of the crystallization type, as he detected the solidification by the volume decrease at constant pressure when the oil crystallized. Zolotykh et. al. 1969 (20) also determined the solidification by the volume decrease.

This type of solid oil is not likely to be present in a rolling or sliding contact as the crystallization is a slow process. Winer and Sanborn (21, 22) and Bair and Winer (23, 24, 25, 26, 27) have in a series of papers measured the shear strength of oils under hydrostatic conditions. In (21) they found that isothermal compression of an oil produced a limiting shear stress lower than isobaric cooling. This is due to the fact that if the oil is compressed when the viscosity is low, the molecules are able to rearrange and this gives a higher final compression. Isobaric cooling after compression is more likely to give crystallic structures and isobaric cooling before the compression is more likely to give amorphous structures.

Figure 1 from reference (21) shows the shear elasticity and maximum shear strength for 5P4E at different temperatures and 0.275 GPa.

It is here very obvious that the oil behaves as an elastic solid and that it has a shear strength which is a function of the temperature. As these experiments were static (slow), the likelihood for elastic-plastic behaviour was even lower than in a lubrication situation, where the time for the stress pulse is short (10^{-3} s-10^{-5}s).

As mentioned earlier the shear strength of lubricating oils solidified under hydrostatic pressure was measured in 1970 by Jacobson (16).

In his apparatus (Figure 2) the shear strength of the oil or the oil-metal-interface was measured depending on which one was the weakest. In Winer et. al. (21) the shear plane was assumed to be in the middle of the oil.

Depending on the surface energies, the temperature, and stress distribution, different slip plane locations in EHD oil films are possible. In normal metal bearings and gears, where the oil is warmer than the metal surfaces, the slip plane is likely to appear somewhere in the middle of the oil. If the surface energy of the bearing is low (PTFE) or if the bearing works isothermally, the slip plane will appear at the bearing surfaces.

In static experiments it is easy to determine if the lubricant is in a liquid or a solid state. When it is solid, it can transmit shear stresses with only elastic deformations, but when it is liquid a shear rate is necessary to maintaine a shear

stress.

In dynamic experiments lubricant behaviour depends on the time-scale of the experiment. Slower straining of the oil gives a more liquid type of behaviour. This is beautifully shown in G.I. Taylor's motion picture "Laminar flow" (28), where he shows that the ice in a glacier flows like a Newtonian liquid when the stress is applied a couple of years.

As already stated it is not only important at which rate the dynamic stresses are applied but also the stress history of the lubricant. Winer and Sanborn (22) show that a rapid compression "freezes" the molecules in a non-equilibrium state, such that for instance the density of a rapidly compressed lubricant is lower than the density at the same pressure if the oil is slowly compressed. This means that experiments designed to determine physical properties of lubricants for EHD calculations should be performed at the same pressure, shear stress, temperature level and time scale as in real EHD contacts.

Equipment for dynamic experiments to determine the properties of lubricants in EHD contacts are mainly of two types: impact apparatuses and rolling contact apparatuses.

The majority of the apparatuses reported in the litterature are of the rolling contact type. Only four different impact rheometers were found in this survey. The oldest was an impact viscometer reported by Booth and Hirst (29, 30) 1969. It was of Hopkinson bar type. Paul and Cameron 1972 and 1975 (31, 32) used a dropping ball viscosimeter where the geometry was a ball impacting a flat surface. Jacobson 1974 (17) and Johnson 1978 (33) used Hopkinson bar configurations where the shear stresses in (17) were parallell to the centerline of the impacting bar and in (33) parallell to the end surface of the bar.

The impact rheometers are better suited to measure the shear stresses directly than the rolling contact rheometers where the pressure distribution in the rolling or sliding contact is given by the elastic stresses in the solid surfaces. In impact rheometers the lubricant sample can be fairly uniformly stressed, but normally the instantaneous stress value is difficult to measure and only a time mean value can be calculated.

The rolling contact apparatuses in the litterature are mainly of four different types as far as the film thickness measurement technique is concerned:

1) x-ray measurement

2) capacitance measurement

3) optical interferometry measurement

4) mechanical displacement measurement

The four different types of techniques give different values of the film thickness. The x-ray technique measures the thinnest film in the contact which means that different values will be registered for different directions of the x-rays in the plane of the contact. For a heavily loaded contact the film thickness in the side lobes can easily be five times lower than the minimum film at the trailing edge (34, 35).

x-rays have been used by Bell, Kannel et. al. (36, 37, 38) and Loewenthal (39) to determine the minimum film thickness between crowned cylindrical and conical rollers. They all found that the minimum film thickness decreased faster with increasing load than the simple EHD-theory predicted. This is due to the limited shear strength of the lubricant (13, 16, 17, 34, 35) which makes it impossible for the oil to withstand the high shear stresses induced by the steep pressure gradients at the circumference of the contact.

The capacitance method has been used by a number of authors e.g. Hamilton and Moore (40) and Hirst and Moore (41, 42, 43). In most of these experiments, except in (40), the capacitance for the total EHD contact is measured, which means that only a mean value of the film thickness can be measured. Most of the capacitance is here given by the flat central part of the contact, why the measured value is close to the central film thickness. The experimental central film thicknesses measured with this method at pure rolling agree well with Newtonian EHD-theory (42).

Using optical interferometry Cameron and Gohar (44) 1965, were able to measure the oil film thickness distribution in EHD contacts in detail. The now well known horse-shoe shape with the minimum film thickness at the sides of the contact was then shown.

Later many other investigators (e.g. 16, 22, 25, 45) have used the same method to measure film thickness. It is possible to use this method up to about 2.5 GPa Hertzian pressure with the transparent surface made from synthetic sapphire. The central film thickness from experiments in pure rolling are in good agreement with Newtonian theories (46, 47, 48).

The mechanical displacement technique developed by Münnich and Glöckner (49) is very simple. In a cylindrical roller thrust bearing, the load is applied at standstill. When the rotation is started the film thickness is measured by measuring how much the abutment height is increased by the lubricant film formation.

Traction experiments have been made by a number of authors (e.g. 13-15, 22, 25, 36-38, 41-43, 45, 49-59). The contact geometries have been cylindrical (41-43, 49, 50, 53, 58) spherical (13-15, 22, 45, 52, 54, 59) and crowned cylindrical (25, 36-38, 51, 55-57) but the main feature of the test rigs has been to measure traction in the direction of rolling or perpendicular to it. In most cases it has been difficult to distinguish between elastic and viscous forces in the contact, but Johnson and Tevaarwerk (59) could do it with their ingenious apparatus.

Jacobson (60) showed experimentally, using high speed photography, that a slight perpendicular movement (< 10% of the Hertzian width) was enough to collapse the oil film at the inlet of a rolling contact (see Figure 3).

This shows that the shear strength and traction properties of the oil are important even for the oil film build-up.

When the load is high, the tangential elastic deformations of the rollers can be larger than the elastic or viscous deformations of the oil film. It is therefore difficult to measure the properties of the oil film.

One method used by Hirst and Moore (42) has been to drive the rollers without a lubricant and then subtract the microslip and elastic deformations measured in the dry rolling situation from the lubricated case. They found that the elastic modulus

of oils increases linearily with pressure.

Experimental investigations of oil behaviour show that oils change their properties with pressure, temperature, stress level, stress rate, stress history and temperature history.

Many attempts to mathematically describe these phenomena have been made.

LUBRICANT MODELS

For prediction of oil film build-up and traction in heavily loaded contacts it is necessary to have as good a mathematical model of the lubricant as possible.

Newton (1) gave the linear relationship between shear velocity and shear stress in a liquid, but oils under high pressure get viscosities so high (61) that even small shear velocities give unreasonably high shear stresses if the Newtonian model is used. This can easily be shown by studying the shear stresses at the oil-metal-interface in the elastohydrodynamic calculations published by Grubin (62), Petrusevich (63), Dowson and Higginson (64) and others.

In the 1960:ies the capacity of computers became large enough to handle calculation of the complete elastohydrodynamic problem with Newtonian and non-Newtonian lubricants. This gave rise to a number of papers dealing with different mathematical models for lubricants.

The lubricant models can be split up in two main groups:

1. Models where the shear stresses are functions of the shear rate.

2. Models with the shear stresses independent of the shear rate.

The first group contains the Newtonian models with variable viscosity. Here the viscosity is a function of the pressure and temperature, but independent of time. For low shear stresses C.J.A. Roelands' (61, 65) model is very good:

$$\log(\eta/\eta_a) = A\left[\frac{(1+p/196.1\cdot10^6)^M}{(1+t/135)^S} - 1\right]$$

where η_a viscosity at atmospheric pressure and temperature 0 ^oC

p pressure in N/m^2

t temperature in ^oC

A, M and S are constants depending on the type of lubricant.

If the shear stress in the lubricant is higher than 1 to 5 per cent of the hydrodynamic pressure in the high pressure zone, the lubricant behaviour will be non-Newtonian and many different models have been proposed. The elasticity of the lubricant has been considered by Barlow et. al. (66, 67, 68). They found by high frequency oscillation experiments that a good lubricant model should consist of the parallel combination of the shear mechanical impedance for a Newtonian liquid and a Hookean solid.

The Maxwell model (69) for lubricants has been used by Trachman and Cheng (58), Johnson and Tevaarwerk (59, 70, 71, 72), Daniels (73) and others.

The total shear rate is here a sum of the elastic and viscous shear rates.

$$\dot{\gamma} = \dot{\gamma}_e + \dot{\gamma}_v = \frac{1}{G}\frac{d\tau}{dt} + F(\tau)$$

where $F(\tau) = \tau/\eta$ for a linear Maxwell model.

Different functions $F(\tau)$ have been used. Johnson and Tevaarwerk used

$$F(\tau) = \frac{\tau_L}{\eta}\sinh(\tau/\tau_L)$$

and Bair and Winer (24) used

$$F(\tau) = -\frac{\tau_L}{\eta}\ln(1-\frac{\tau}{\tau_L})$$

and

$$F(\tau) = \frac{\tau_L}{\eta}\tanh^{-1}(\frac{\tau}{\tau_L})$$

in different papers.

Elastic deformation of the lubricant decreases oil film thickness and traction.

The same is true for a lubricant with a delay in the viscosity increase after a pressure increase (58).

The second group contains models with a limited lubricant shear strength.

The first to propose this was Smith (13, 14, 15). He assumed that the traction was determined by the shear strength of the lubricant and the film-building ability by the viscosity.

Jacobson used the combination of a Newtonian liquid at low pressures with a plastic solid at high pressures and shear stresses (16, 34, 35, 74) as a model for the lubricant behaviour in calculations of oil film shapes and pressure distribution for point- and line-contacts.

In 1973 Allen et. al. (54) used the Dowson & Higginson formula to calculate oil film thickness. An exponential viscosity increase with pressure was used to calculate the shear stress as long as the stress was lower than 0.07 times the Hertzian pressure. If the Newtonian model gave higher shear stresses, they put the shear stress equal to 0.07 times the local pressure.

In 1982 Jacobson and Hamrock (75) used a similar model to calculate pressure distribution, oil film thickness and traction in a line-contact. As their model was isothermal, slip planes developed at the bearing surfaces if the shear stress was too high. Depending on the shear stress at the bearing surfaces three different pressure equations were used. At low loads and pure rolling, the film shapes and

pressure distributions were similar to Dowson & Higginson's. When sliding was introduced the pressure spike at the outlet decreased and the film thickness also decreased, see Figure 4.

The parameter determining the coefficient of friction (traction) at high sliding speeds was mainly the shear strength proportionality constant. This constant varies for real lubricants from 0.02 to 0.10 depending on the lubricant type. The sliding velocity needed to reach 95% of the maximum shear stress varies almost exponentially with (the load)$^{-1}$, as can be seen in Figure 5. This shows that at Hertzian pressures above 1 GPa the oil behaves as a plastic solid and the minimum film thickness decreases even for low slide to roll ratios.

CONCLUSIONS

A revue of experimental investigations of lubricant behaviour in highly stressed situations shows that a Newtonian model for lubricant behaviour is insufficient for the explanation of traction behaviour. The oil film build-up, on the other hand, is fairly well predicted using a Newtonian lubricant model except at high slide to roll ratios and at very high loads, where the non-Newtonian behaviour starts to be important already outside the Hertzian contact area.

Two main types of experiments are reported: static and dynamic. In static experiments the pressure is typically applied to the lubricant more than a million times longer than in an EHD contact. Depending on the pressure-temperature history of the experiment the lubricant will become a crystallized or amorphous solid at high pressures.

In dynamic experiments, where the pressure is applied as short time as in real EHD contacts, the oil is in an amorphous solid state.

Depending on the viscosity, time-scale, elasticity of the oil and the bearing surfaces, the oil film pressure and shear strain rate and the type of lubricant, different properties of the oil are important for the prediction of shear stresses in the oil.

This can be seen from the different proposed models for the lubricant, where it is described as being for instance a Newtonian liquid, an elastic liquid, a plastic liquid and an elastic-plastic solid.

REFERENCES

1. Newton, I.: (1687) Philosophiae Naturales Principia Mathematica. Imprimatur S. Pepys. Reg. Soc. Praeses, 5 Julii, 1686.

2. Reynolds, O.: On the theory of lubrication and its application to Mr. Beauchamp Tower's experiments, including an experimental determination of the viscosity of olive oil. Phil. Trans. Roy. Soc. 177, 1886, p. 157.

3. Bridgeman, P. W.: The Measurement of High Hydrostatic Pressure. I. A Simple Primary Gauge. Proc. Amer. Acad., vol. 44, 1909, pp. 201-217.

4. Bridgeman, P. W.: The Effect of Pressure on the Viscosity of Forty-Three Pure Liquids. Proc. Amer. Acad., vol. 61, 1926, pp. 57-99.

5. Hersey, M. D.; and Shore, H.: Viscosity of Lubricants Under Pressure. Mechanical Engineering, vol. 50, 1928, pp. 221-232.

6. Kleinschmidt, R.V.: Appendix No. 1 of Progress in Lubrication Research. Trans. ASME, vol. 50, 1928, APM-50-4.

7. Kissekalt, S.: Neuere Beitrag über den Verfestigungsdruck von Ölen. Petroleum Zeitschrift, vol. 27, Febr. 11, 1931, pp. 1-3.

8. Yoshio Suge.: Influence of Temperature and Pressure on the Viscosity of Oils (in Japanese). Bulletin Inst. of Physical and Chemical Research, vol. 12, 1933, pp. 643-662.

9. Cragoe, C. S.: Changes in the viscosity of Liquids with Temperature, Pressure and Composition. Proc. of the World Petroleum Congress, 1933, London, Eng, 1934, pp. 529-533.

10. Poulter. T.C.: The study of Extreme Pressures and Their Importance in the Investigation of Engineering Problems. Journal of Applied Physics, vol. 9, 1938, pp. 307-311.

11. Dow, R. B.: The Solidification of Fluid Lubricants by Pressure. Rheology Bulletin, vol. 13, Sept. 1942, pp. 6-7; Nov. pp. 7-8.

12. Norton, A. E.; Knott, M. J.; and Muenger, J. R.: Flow Properties of Lubricants Under High Pressure. Trans. ASME, Oct. 1941, pp. 631-643.

13. Smith, F. W.: Lubricant Behaviour in Concentrated Contact Systems - The Castor Oil-Steel System. Wear, vol. 2, 1958/59, pp. 250-263.

14. Smith, F. W.: Lubricant Behaviour in Concentrated Contact - Some Rheological Problems. Trans. ASLE, 3, 1960, pp. 18-25.

15. Smith, F. W.: The Effect of Temperature in Concentrated Contact Lubrication. Trans. ASLE, 5, 1962, pp. 142-148.

16. Jacobson, B. O.: On the Lubrication of Heavily Loaded Spherical Surfaces Considering Surface Deformations and Solidification of the Lubricant. Acta Polytechnica Scandinavica. Mech. Eng. Series No. 54, 1970.

17. Jacobson, B. O.: An Experimental Determination of the Solidification Velocity for Mineral Oils. Trans. ASLE, vol. 17, 4, pp. 290-294.

18. Briscoe, B. J.; and Tabor, D.: Rheology of Thin Organic Films. Trans. ASLE, vol. 17, 3, pp. 158-165.

19. Bridgeman, P. W.: Viscosities to 30,000 kg/cm^2. Proc. of the American Academy of Arts and Sciences, vol. 17, 1949, pp. 117-127.

20. Zolotykh, Ye. V.; et. al.: Dependence of Viscosity of Liquids on Pressure. Foreign Technology Division. Wright-Patterson Air Force Base, Ohio, May. 1973.

21. Winer, W. O.; and Sanborn, D. M.: Surface Temperatures and Glassy State Investigations in Tribology, Part I. NASA Contractor Report 3031, June. 1978.

22. Winer, W. O.; and Sanborn, D. M.: Lubricant Rheology Applied to Elastohydrodynamic Lubrication. NASA Contractor Report CR-2837, May. 1977.

23. Bair, S.S.; and Winer, W. O.: Surface Temperatures and Glassy State Investigations in Tribology - Part II. NASA Contractor Report 3162, July. 1979.

24. Bair, S. S.: and Winer, W. O.: Surface Temperatures and Glassy State Investigations in Tribology - Part III. NASA Contractor Report 3272, Apr. 1980.

25. Bair, S. S.; and Winer, W. O.: Surface Temperatures and Glassy State Investigations in Tribology - Part IV. NASA Contractor Report 3368, Jan. 1981.

26. Bair, S. S.; and Winer, W. O.: Shear Strength Measurements of Lubricants at High Pressure. Trans. ASME. Journal of Lubrication Technology, July. 1979, vol. 101, pp. 251-257.

27. Bair, S. S.; and Winer, W. O.: A Rheological Model for Elastohydrodynamic Contacts Based on Primary Laboratory Data. Trans. ASME. Journal of Lubrication Technology, July. 1979, vol. 101, pp. 258-265.

28. Taylor, Sir Geoffrey.: Film Notes for Low-Reynolds Number Flows. National Committee for Fluid Mechanics Films.

29. Booth, M. J.; and Hirst, W.: The Rheology of oils during impact. I. Mineral Oils. Proc. Roy. Soc. Lond., A 316, 1970, pp. 391-413.

30. Booth, M. J.; and Hirst, W.: The Rheology of Oils during impact. II. Silicone Fluids. Proc. Roy. Soc. Lond., A 316, 1970, pp. 415-429.

31. Paul, G. R.; and Cameron, A.: An Absolute High-Pressure Microviscometer Based on Refractive Index. Proc. Roy. Soc. Lond., A 331, 1972, pp. 171-184.

32. Paul, G. R.; Gentle, C. R.; and Cameron, A.: An Analysis of Data Taken from the Impact Viscometer at Imperial College. Office of Naval Research Contract N00014-75-C-0388, Oct. 1975.

33. Johnson, K. L.: Split Hopkinson Torsion Bar. Univ. of Cambridge.Contract No. DN875276; N00014-78-G-0013. U.S. Dept. of Defence, Navy, Office of Naval Research.

34. Jacobson, B. O.: Elasto-Solidifying Lubrication of Spherical Surfaces. ASME Paper No. 72-Lub-7.

35. Jacobson, B. O.: On the Starved Lubrication of Cylindrical Rolling Contacts, Considering Solidification of the Lubricant. Trans. of Machine Elements Division, Lund 1973.

36. Kannel, J. W.; and Bupara, S. S.: Rheology of Lubricants in Real Bearing Contacts. Trans. ASME, Journal of Lubrication Technology, Apr. 1975, pp. 228-235.

37. Bell, J. C.; Kannel, J. W.; and Allen, C. M.: The Rheological Behaviour of the Lubricant in the Contact Zone of a Rolling-Contact System. Proc. of the USAF Aerospace Fluids and Lubricants Conf., June. 1964.

38. Dow, T. A.; Kannel, J. W.; and Stockwell, R. D.: Determination of Lubricant Selection Based on Elastohydrodynamic Film Thickness and Traction Measurement. NASA CR-159428.

39. Loewenthal, S. H.; Parker, R. J.; and Zaretsky, E. V.: Elastohydrodynamic Film Thickness Model for Heavily Loaded Contacts. Trans. ASME. Journal of Lubrication Technology, July. 1974, pp. 472-481.

40. Hamilton, G. M.; and Moore, S. L.: Deformation and Pressure in an Elastohydrodynamic Contact. Proc. Roy. Soc. Lond., A 322, 1971, pp. 313-330.

41. Hirst, W.; and Moore, A. J.: Non-Newtonian Behaviour in the Elastohydrodynamic Lubrication of Rollers. Symposium on Lubricant Properties in Thin Lubricating Films presented before the Division of Petroleum Chemistry, Inc. American Chemical Society New York Meeting, Apr. 4-9, 1976.

42. Hirst, W.; and Moore, A. J.: Elastohydrodynamic Lubrication at High Pressures. Dept. of Eng. Univ. of Reading, Aug. 1977.

43. Hirst, W.; and Moore, A. J.: Elastohydrodynamic Lubrication at High Pressures. II. Non-Newtonian Behaviour. Dept. of Eng. Univ. of Reading, June. 1978.

44. Cameron, A.; and Gohar, R.: Theoretical and Experimental Studies of the Oil Film in Lubricated Point Contact. Proc. Roy. Soc. London, 1965, pp. 520-536.

45. Dalmaz, G.: Film Thickness and Traction Measurements in Small Elastohydrodynamic Elliptical Contacts. Proc. of the 5th Leeds-Lyon Symposium on Tribology, Univ. of Leeds, Sept. 1978, pp. 71-80.

46. Hamrock, B. J.; and Dowson, D.: Isothermal Elastohydrodynamic Lubrication of Point Contacts. Part II - Ellipticity Parameter Results. Trans. ASME. Journal of Lubrication Technology, vol. 98, No. 3, July. 1976, pp. 375-383.

47. Hamrock, B. J.; and Dowson, D.: Isothermal Elastohydrodynamic Lubrication of Point Contacts. Part III - Fully Flooded Results. Trans. ASME. Journal of Lubrication Technology, vol. 99, No. 2, Apr. 1977, pp. 264-276.

48. Hamrock, B. J.; and Dowson, D.: Isothermal Elastohydrodynamic Lubrication of Point Contacts. Part IV - Starvation Results. Trans. ASME. Journal of Lubrication Technology, vol. 99, No. 1, Jan. 1977, pp. 15-23.

49. Muennich, H.; and Gloeckner, H.: A new method for analysing the film building property of lubricants. Proc. of the 5th Leeds-Lyon Symposium on Tribology, Univ. of Leeds, Sept. 1978, pp. 197-203.

50. Kimura, Y.; and Muraki, M.: Evaluation of some traction fluids with a four roller machine. Tribology Int., Dec. 1979, pp. 255-259.

51. Walowit, J. A.; and Smith, R. L.: Traction Characteristics of a MIL-L7808 Oil. Trans. ASME. Journal of Lubrication Technology, Oct. 1976, pp. 607-612.

52. Lingard, S.: Development of a visco-plastic lubricant model for the synthesis of high pressure rolling contact tractions. Proc. of the Inst. of Mech. Eng., Sept. 1979, vol. 193, pp. 295-302.

53. Allen, C. W.: A Simplified Model for the Elastohydrodynamic Traction Between Rollers. Trans. ASME. Journal of Lubrication Technology, July. 1976, pp. 357-361.

54. Allen, C. W.; Townsend, D. P.; and Zaretsky, E. V.: New generalized rheological model for lubrication of a ball spinning in a non-conforming groove. NASA Technical Note. NASA TN D-7280, May. 1973.

55. Berthe, D.; Flamand, L.; and Houpert, L.: Rheological parameters of a lubricant under high speed conditions. Proc. of the 5th Leeds-Lyon Symposium on Tribology, Univ. of Leeds, Sept. 1978, pp. 188-196.

56. Gupta, P. K.; Flamand, L.; Berthe, D.; and Godet, M.: On the Traction Behaviour of Several Lubricants. Trans. ASME. Journal of Lubrication Technology, Jan. 1981, vol. 103, pp. 55-64.

57. Houpert, L.; Flamand, L.; and Berthe, D.: Rheological and Thermal Effects in Lubricated E.H.D. Contacts. Trans. ASME. Journal of Lubrication Technology, Oct. 1981, vol. 103, pp. 526-532.

58. Trachman, E. G.; and Cheng, H. S.: Rheological Effects on Friction in Elastohydrodynamic Lubrication. NASA Contractor Report NASA CR-2206, March 1973.

59. Johnson, K. L.; and Tevaarwerk, J. L.: Shear behaviour of elastohydrodynamic oil films. Proc. Roy. Soc. Lond., A 356, 1977, pp. 215-236.

60. Jacobson, B. O.: Solid Oil in rolling contacts. Sympozium Intertribo '81, Vysoké Tatry, Apr. 1981, pp. 92-98.

61. Roelands, C. J. A.; Vlugter, J. C.; and Waterman, H. I.: The Viscosity-Temperature-Pressure Relationship of Lubricating Oils and its Correlation with Chemical Constitution. Trans. ASME. Journal of Basic Engineering, Dec. 1963, pp. 601-610.

62. Grubin, A. N.; and Vinogradova, I. E.: Central Scientific Research Institute for Technology and Mechanical Engineering. Book No. 30, Moscow 1949. (D.S.I.R. translation No. 337).

63. Petrusevich, A. I.: Fundamental conclusions from the contact-hydrodynamic theory of lubrication. Izvestia Akademii Nauk, SSSR, OTN2, 1951, pp. 209-223.

64. Dowson, D.; and Higginson, G. R.: Elastohydrodynamic Lubrication, The Fundamentals of Roller and Gear Lubrication. Pergamon, Oxford, 1966.

65. Roelands, C. J. A.: Correlational aspects of the viscosity-temperature-pressure relationship of lubricating oils. Delft 1966.

66. Barlow, A. J.; and Lamb, J.: The Visco-Elastic Behaviour of Lubricating Oils under Cyclic Shearing Stress. Proc. Roy. Soc. of London, Series A, vol. 253, pp. 52-69, 1959.

67. Barlow, A. J.; Lamb, J.; and Matheson, A. J.: Viscous Behaviour of Supercooled Liquids. Proc. Roy. Soc. of London, Series A, Vol. 292, pp. 322-342, 1966.

68. Barlow, A. J.; Erginsav, A.; and Lamb, J.: Viscoelastic Relaxation of Supercooled Liquids. II. Proc. Roy. Soc. of London, Series A, vol. 298, pp. 481-494, 1967.

69. Maxwell, C.: Illustrations of the dynamical theory of gases. Phil. Mag., Series 4, 14, 19. 1860.

70. Tevaarwerk, J.; and Johnson, K. L.: A Simple Non-Linear Constitutive Equation for Elastohydrodynamic Oil Films. Wear, 35, 1975, pp. 345-356.

71. Tevaarwerk, J. L.; and Johnson, K. L.: The Influence of Fluid Rheology on the Performance of Traction Drives. Trans. ASME. Journal of Lubrication Technology, July 1979, vol. 101, pp. 266-274.

72. Tevaarwerk, J. L.: Traction Drive Performance Prediction for the Johnson and Tevaarwerk Traction Model. NASA Technical Paper 1530, Oct. 1979.

73. Daniels, B. K.: Non-Newtonian Thermo-Viscoelastic EHD Traction from Combined Slip and Spin. ASLE preprint No. 78-LC-2A-2.

74. Jacobson, B. O.: On the Lubrication of Heavily Loaded Cylindrical Surfaces Considering Surface Deformations and Solidification of the Lubricant. Trans. ASME. Journal of Lubrication Technology. Paper No. 72-Lub-44.

75. Jacobson, B. O.; and Hamrock, B. J.: Non-Newtonian Model Incorporated Into Elastohydrodynamic Lubrication of Rectangular Contacts. NASA TP, 1983.

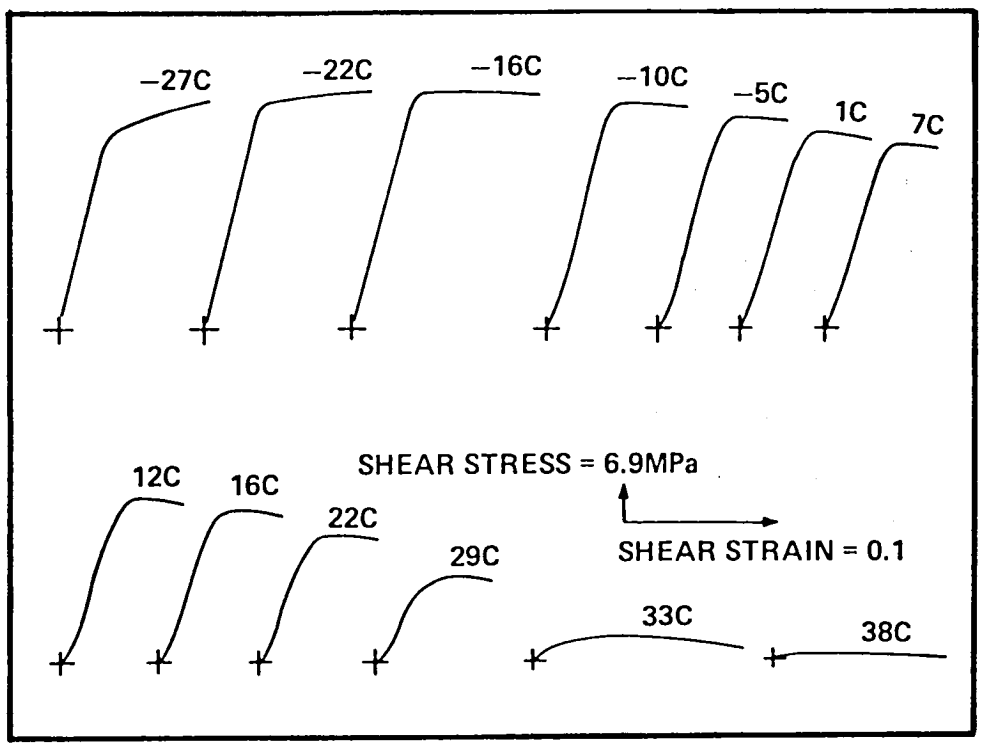

Figure 1. Shear stress versus shear strain (Winer and Sanborn (21)).

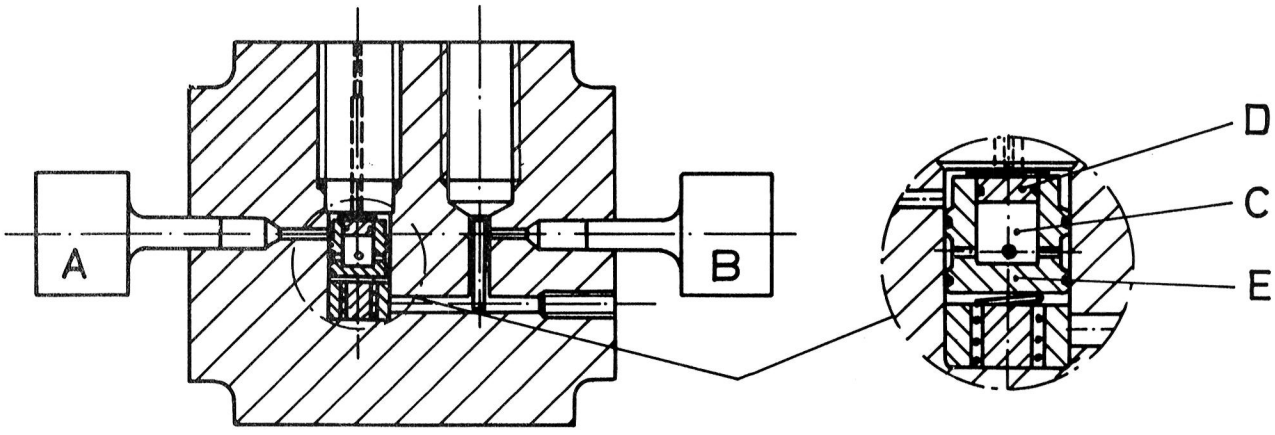

Figure 2. Shear strength apparatus.

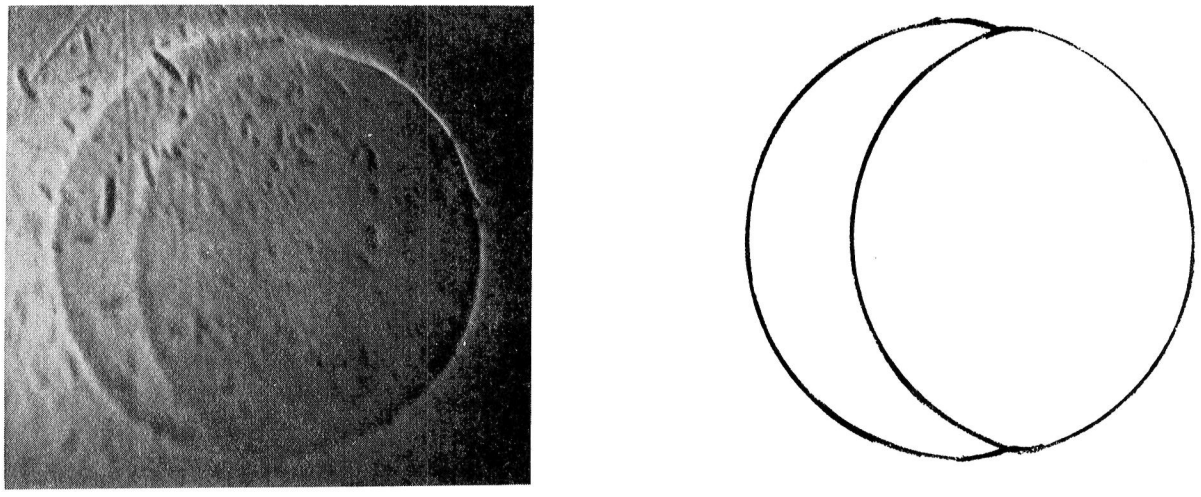

Figure 3. Oil film 2.7 ms after the start of the impact.

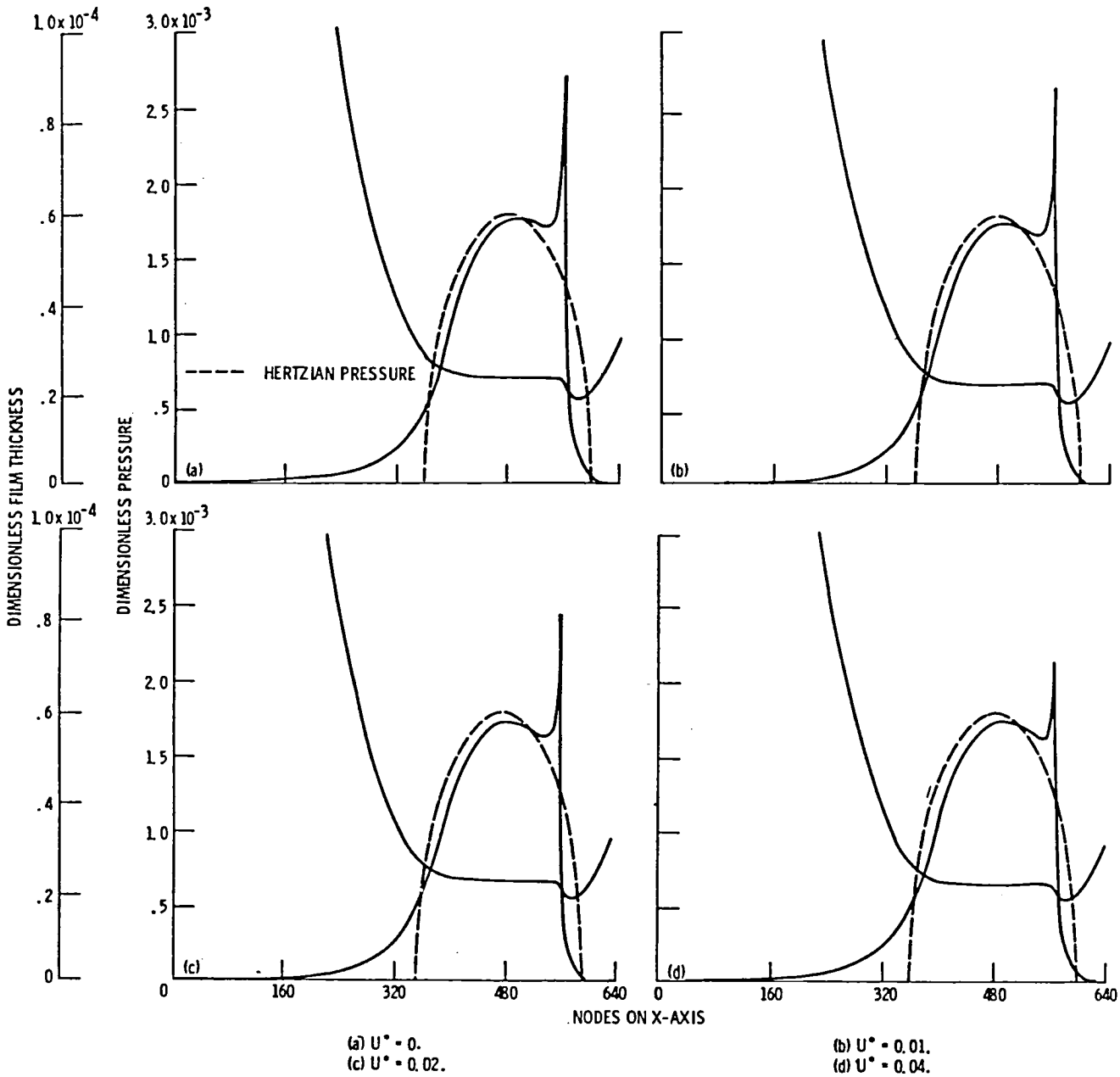

Figure 4. Pressure distributions and film shapes for different sliding velocities U*. Dimensionless load parameter W, 2.0478 x 10^{-5}; dimensionless speed parameter U, 10^{-11}; dimensionless materials parameter G, 5000; limiting-shear-strength proportionality constant γ, 0.07.

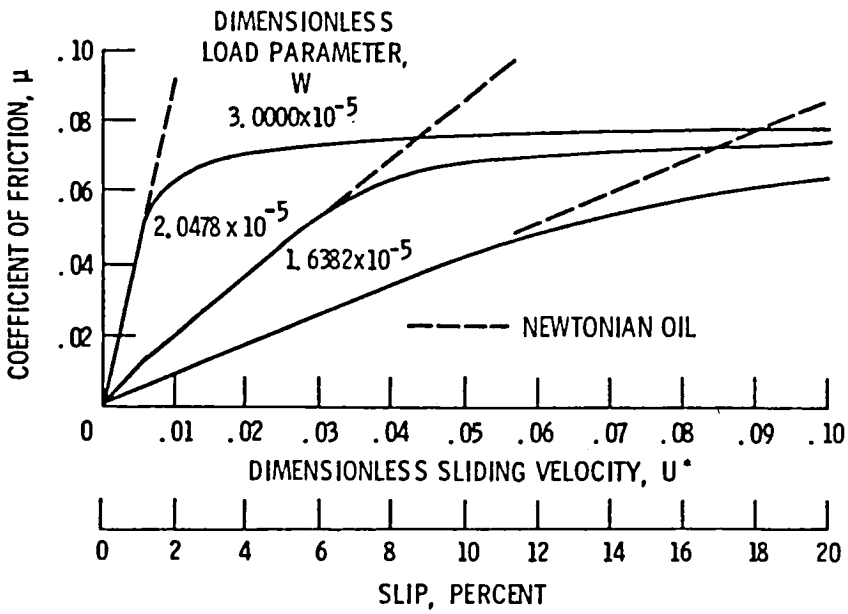

Figure 5. Coefficient of friction as a function of load and dimensionless sliding velocity. Dimensionless speed parameter U, 10^{-11}; dimensionless materials parameter G, 5000; limiting-shear-strength proportionality constant γ, 0.07.

DISCUSSION

Masayoshi Muraki
Mitsubishi Oil Company
Kanagawa, Japan

Yoshitsugu Kimura
The University of Tokyo
Tokyo, Japan

The discussers would like to congratulate the author on a very interesting paper. It is very timely and instructive to have presented a comprehensive review on the rapidly developing field of lubricant rheology in concentrated contacts. Professor Jacobson introduced a number of lubricant models, with which many attempts were made to give mathematical expressions to rheological behavior of lubricants in elastohydrodynamic films; typically, an elastic liquid, a plastic liquid, and elastic-plastic solid models. However, it should be remembered that any lubricant is neither perfectly viscous, nor elastic, nor plastic. If a certain model can describe traction behavior successfully, it means that some assumed properties of the lubricants are playing the predominating role under the specific operating condition. From such a point of view, the discussers have recently developed a thermal viscoelastic theory (1), with which it has become possible to describe traction curves with several non-dimensional parameters, with sufficient accuracy.

A nonlinear Maxwell viscoelastic model proposed by Johnson and Tevaarwerk (2) is assumed. In a dimensionless form, it can be written as

$$\Sigma = D\frac{dS}{dX} + \sinh S \qquad (1)$$

where $\Sigma=\eta\dot{\gamma}/\tau$ is the dimensionless shear rate, $D=\eta U/Gb$ is the

Deborah number, $S=\tau/\tau_L$ is the dimensionless shear stress, and $X=x/b$ is the dimensionless coordinate along the film. The nomenclature is common with the paper by Professor Jacobson; further, U is the mean rolling speed, b is the half Hertzian width.

Integration of eq.(1) is straightforward, but the solution can be approximated as,

$$S = \sinh^{-1}\Sigma \qquad \text{when } D \to 0 \qquad (2)$$

$$S = \Sigma X/D \qquad \text{when } D \to \infty \qquad (3)$$

The averaged shear stress, or traction, $\bar{S}$ is now readily obtained.

The thermal effect is considered on the Newtonian viscosity only, and an exponential dependence of the viscosity on the film temperature as well as on the mean Hertzian pressure is assumed. By a simple formulation discussed elsewhere (3), the mean film temperature rise can be expressed as the product of the viscous enegy dissipation rate and a proportionality constant. Then the thermal effect can be represented by a single dimensionless parameter Φ, which is defined as the product of the above mentioned proportionality constant, the viscosity-temperature coefficient, the representative stress τ_L squared, the film thickness and the reciprocal of the isothermal Newtonian viscosity.

When Σ and D are replaced by Σ_i and D_i defined as,

$$\Sigma = \Sigma_i \exp(-\Phi\Sigma_i\bar{S}), \qquad (4)$$

$$D = D_i \exp(-\Phi\Sigma_i\bar{S}), \qquad (5)$$

$\bar{S}$ which represents the traction is obtained in a closed form. That is,

$$\bar{S} = \left(D_i \Phi \ln 2\Sigma_i - 2(1+\Phi\Sigma_i) + 2\{(1+\Phi\Sigma_i)^2 - D_i\Phi\ln 2\Sigma_i\}^{1/2} \right) / D_i\Phi^2\Sigma_i \qquad (6)$$

The traction curve described by eq.(6) is shown in the Figure. When Σ_i is increased, $\bar{S}$ first increases along an elastic line. At a certain value of Σ_i a transition takes place and $\bar{S}$ follows an Eyring viscous curve thereafter. The viscous curve is uniquely determined by Σ_i in the isothermal region, and the thermal solution deviates downwards from it and this deviation is solely determined by Φ. Thus the entire traction curve is represented by a single formula, which shows satisfactory agreement with experimental results as exemplified elsewhere (3).

REFERENCES

1 M. Muraki and Y. Kimura : To be published in J. Japan Soc. Lub. Eng.

2 K. L. Johnson and J. L. Tevaarwerk : Proc. Roy. Soc. Lond., A356, 1685 (1977) 215.

3 Y. Kimura and M. Muraki : Discussion on " TEMPERATURE EFFECTS IN ELASTOHYDRODYNAMICALLY LUBRICATED CONTACTS " in the same session

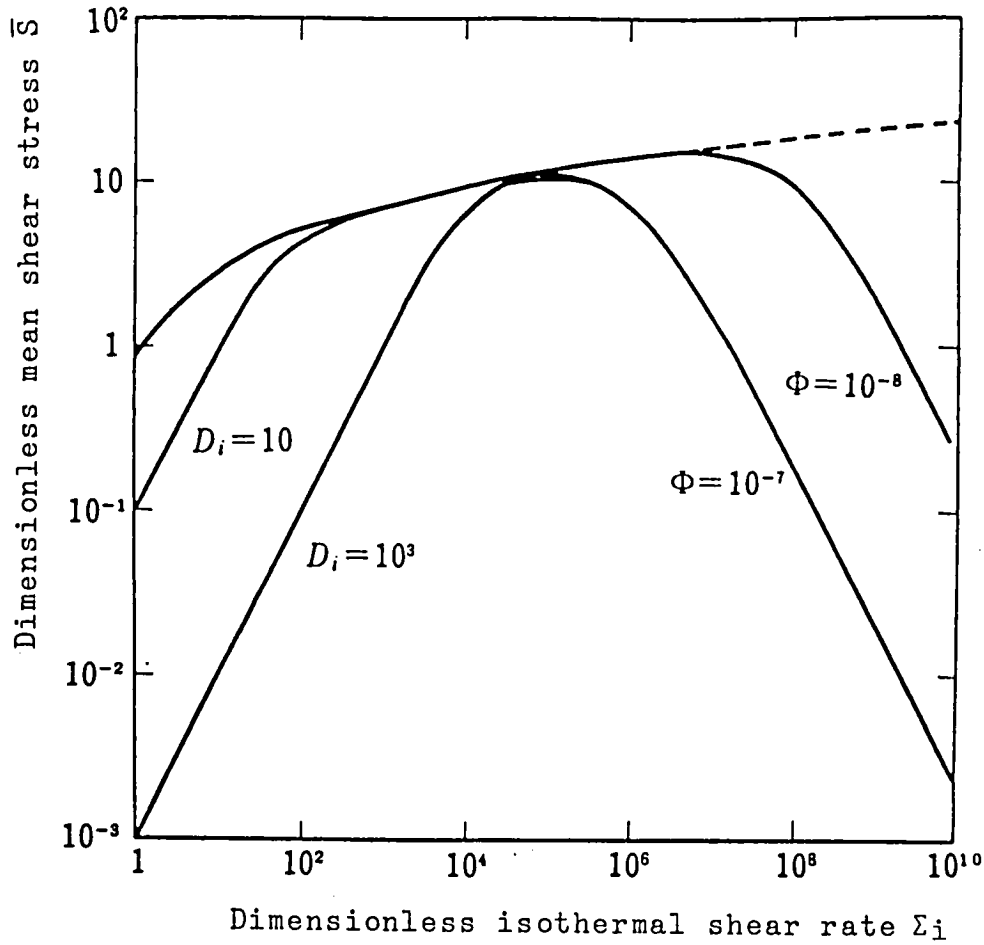

Figure Theoretical traction curves

RESPONSE

Bo O. Jacobson
Luleå University of Technology
Luleå, Sweden

As the discussors state, a lubricant is neither perfectly viscous, elastic nor plastic, so the different lubricant models are only possible to use within limited parameter ranges. This means that the lubricant models only describe some important parameters more or less accurately, but normally they do not explain what happens on the atomic level.
In Muraki's and Kimura's discussion they use this type of curve-fitting by assuming Newtonian behaviour and exponential dependence of the viscosity on temperature and mean Hertzian pressure to calculate the traction curve.

NON-STEADY STATE EFFECTS IN EHL

Duncan Dowson
Institute of Tribology
Department of Mechanical Engineering
The University of Leeds
Leeds, England

A number of lubricated machine elements are subjected to cyclic variations of load and speed, particularly in reciprocating machinery. It is well known that squeeze-film action plays an important role in preserving satisfactory lubricating films in many cases in which the entraining velocities fall to zero during each cycle, as in the reciprocating seal and synovial joints.

The essential features of combined 'entraining' and 'normal' motion are described for both hydrodynamic and elastohydrodynamic conditions. It is shown that very small squeeze-film velocities (W), or order $(h_o/\ell)U$, can lead to substantial hydrodynamic action.

A brief review of previous studies of squeeze-film lubrication between spheres or cylinders and a plane is followed by reference to a recent analysis of ankle joint lubrication. It is then shown that elastohydrodynamic lubrication might be encountered in the conjunction between a piston ring and cylinder liner and that in such cases combined entraining and squeeze-film action is important. Analysis of a 2-stroke Diesel engine shows that variations in squeeze-film velocity throughout the conjunction, associated with time rates of change of elastic deformation, must be considered in a full elastohydrodynamic lubrication analysis.

INTRODUCTION

A number of fluid-film lubricated machine elements are subjected to non-steady state, cyclic conditions. Well known examples include reciprocating seals, piston rings, cams and tappets and the bearings in reciprocating engines. In some cases the entraining velocity, which is responsible for hydrodynamic film formation in steady-state bearings, falls to zero at some stage in the cycle and the well being of the fluid-film then depends upon squeeze-film action. The survival of many non-steady state bearings is known to depend upon the powerful protection afforded by squeeze-film action. It is fortunately very difficult to reduce the film thickness rapidly by pressing two solids towards each other in the presence of a viscous fluid and hence effective lubricating films often survive the intervals of adverse entraining action in reciprocating machinery.

Even if the entraining velocity does not fall to zero it might vary throughout the cycle, as in the big-end bearing of a reciprocating engine, and this alone can lead to a cyclic variation in film thickness. Furthermore, the loading on such bearings is often severe and dynamic and elaborate methods have therefore been developed to predict the orbits of journals within them. The mobility and similar approaches to dynamically loaded bearing problems accommodate both 'entraining' and 'squeeze-film' action within the lubricating film and now provide reliable guidance

to designers on the question of cyclic variation of minimum film thickness.

Such procedures are not generally available for lubricated machine elements presenting non-conformal surfaces, like many reciprocating seals, piston rings and cams and tappets, although numerical solutions of varying degrees of sophistication based upon time-stepping procedures and an initial estimate of the film thickness at some point in the cycle can now be computed for all these applications. In each case it is found that squeeze-film action plays a vital role in the preservation of finite, but often very small, film thicknesses in relation to the composite surface roughness during periods of low entraining velocity.

It is now well established that elastic deformation of the solids bounding non-conformal conjunctions can readily lead to a transition from hydrodynamic to elasto-hydrodynamic lubrication. This action dominates the performance of low elastic modulus materials in reciprocating seals and might yet prove to be of significance in piston rings and cams and tappets. If elastohydrodynamic lubrication prevails, the analysis of non-steady state conditions is more complicated than in simple hydrodyanmic lubrication between rigid solids, since the shape and not just the minimum thickness of the lubricating film varies with time. Blok and Koens (ref. 1) provided a fine illustration of the phenomenon, described as a breathing film, based upon optical interferometric studies of lubricating films developed between a low elastic modulus rubber cylinder and a glass plate. Blok (ref. 2) had also outlined in some detail an inverse hydrodynamic procedure for analysing the pressure distributions responsible for observed film shapes under known conditions.

In elastohydrodynamic studies of machine components subjected to cyclic events like the meshing of gear teeth or the lubrication of individual balls or rollers in rolling element bearings, attention is generally focussed upon the most severe conditions and a 'static' solution suffices. Yet a sequence of quasi-static solutions for the cycle of events implies that both the film shape and minimum film thickness are functions of time. There is thus a normal motion or squeeze-film action between the surfaces which is generally neglected in elastohydrodynamic analysis, A particular example which spans hydrodynamic and elastohydrodynamic conditions and which still awaits detailed analysis is the entry of a ball or roller into the loaded segment of a rolling element bearing after passing through the lightly loaded arc. In this region, where skidding or slip is often encountered, the minimum film thickness and film shape both experience rapid changes with time and squeeze-film effects might well be significant.

In this paper the influence of combined 'entraining' and 'normal' motion upon elastohydrodynamic conjunctions will be illustrated by the somewhat unexpected case of piston ring lubrication.

NOTATION

h lubricant film thickness.

h_o film thickness on line of closest approach between a rigid parabolic solid and a plane surface.

ℓ effective length of bearing in entraining direction.

p hydrodynamic pressure.

q reduced pressure $\left(= \frac{1}{\alpha} \left[1 - e^{-\alpha p}\right]\right)$

s coordinate in elasticity calculations

t thickness of layer of elastic bearing material on rigid backing.

u entraining velocity $\left(= \frac{1}{2} \left[u_1 + u_2\right]\right)$

u_1, u_2 surface velocities.

v elastic deformation perpendicular to the surface.

x coordinate,

A, B constants,

E modulus of elasticity.

H dimensionless film thickness $\left[\frac{h}{h_o}\right]$

R radius of equivalent cylinder near a plane.

U dimensionless sliding speed of plane surface.

W velocity of approach or squeeze-film velocity of a curved solid towards a plane.

X dimensionless coordinate in entraining direction $\left[\frac{x}{\ell}\right]$

α viscosity pressure exponent $\left[\eta = \eta_o e^{\alpha p}\right]$

η lubricant viscosity.

η_o lubricant viscosity at atmospheric pressure.

σ Poisson's ratio.

HYDRODYNAMIC LUBRICATION

The Reynolds equation of fluid-film lubrication is formed from the continuity equation, representing conservation of mass flow, and the equations of motion, representing conservation of momentum. It is customary to neglect both inertia and body-force terms in the equations of motion and hence to balance the resulting 'pressure' and 'viscous' forces.

There are thus only two physical mechanisms contributing to fluid flow in a bearing, one associated with the motion of the bounding solids (entraining or Couette flow and normal motion) and the other with pressure gradients (Poiseuille flow).

For two dimensional flow of an incompressible lubricant, the Reynolds equation can be written in the form;

$$\frac{\partial}{\partial x}\left[\frac{h^3}{\eta}\frac{\partial p}{\partial x}\right] = 12u\left[\frac{\partial h}{\partial x}\right] + 12\left[\frac{\partial h}{\partial t}\right] \qquad (1)$$

Poiseuille — Entraining (Couette) — Normal Motion (Squeeze)

For the conjunction shown in Figure 1,

$$u = \frac{1}{2}\left[u_1+u_2\right] = \frac{U}{2} \qquad \frac{\partial h}{\partial t} = -W$$

- and the Reynolds equation reduces to,

$$\frac{\partial}{\partial x}\left[\frac{h^3}{\eta}\frac{\partial p}{\partial x}\right] = 6U\left[\frac{\partial h}{\partial x}\right] - 12W \qquad (2)$$

In dimensionless terms,

$$\frac{\partial}{\partial X}\left[\frac{H^3}{\eta}\frac{\partial p}{\partial X}\right] = 6\frac{\partial H}{\partial X} - 12\left[\frac{W}{U}\cdot\frac{\ell}{h_o}\right] \qquad (3)$$

Entraining — Squeeze

The ratio of 'squeeze-film' to 'entraining' terms is thus,

$$\frac{\text{Squeeze}}{\text{Entraining}} = \frac{W}{U}\cdot\frac{\ell}{h_o}\left[\frac{1}{\frac{\partial H}{\partial X}}\right] \simeq \frac{W}{U}\cdot\frac{\ell}{h_o} \qquad (4)$$

Squeeze-film action will thus assume an importance comparable to that of entraining action when,

$$W \simeq \left[\frac{h_o}{\ell}\right] U \qquad (5)$$

Since $\left(\frac{h_o}{\ell}\right)$ is generally of order 10^{-3} and not infrequently as small as 10^{-4}, it is clear that very small velocities of approach can introduce significant hydrodynamic effects.

ELASTO-HYDRODYNAMIC LUBRICATION

The modifications to simply hydrodynamic theory associated with very high pressures in many non-conformal machine elements are well known and come under the

heading of elasto-hydrodynamic lubrication. There are two beneficial effects associated with the high pressures, the elastic deformation of the bounding solids and the increase in lubricant viscosity.

Elasticity

In many cases the bearing solids can be modelled by an equivalent, rigid, curved component adjacent to a semi-infinite, elastic solid. The surface deformation due to the distributed normal, hydrodynamic pressure (p) can then be determined by summation from the expression,

$$v = A \int p \log_e (x-s)^2 \, ds + \text{constant} \tag{6}$$

It is customary to consider blocks of uniform pressure, but more complete approximations to the actual pressure distribution can be accommodated.

When the bearing structure can be represented by a thin layer of elastic material of thickness (t) on a relatively rigid backing, as in the case of many plain journal bearings and also of synovial joints, it can often be assumed that the elastic deformation (v) is related to the local surface pressure (p) by the simple relationship,

$$v = B\,p \tag{7}$$

where (B) is an equivalent elastic constant defined by,

$$B = \frac{(1+\sigma)(1-2\sigma)}{(1-\sigma)E} \tag{8}$$

It can be seen that the utility of this expression depends upon a knowledge of Poisson's ratio, and this is rather critical for elastomeric materials and articular cartilage where $\sigma \to 0.5$.

Viscosity at High Pressure

Much of elastohydrodynamic theory has been developed for isothermal conditions in which film thickness can be predicted with adequate accuracy on the basis of the simple Barus relation.

$$\eta = \eta_o e^{\alpha p} \tag{9}$$

This readily permits the Reynolds equation to be solved in terms of a reduced pressure (q) defined as,

$$q = \frac{1}{\alpha}\left[1 - e^{-\alpha p}\right] \tag{10}$$

Once solutions of the modified Reynolds equation have been obtained for (q) in terms of the constant viscosity (η_o), the real pressure (p) can be ascertained by noting that,

$$p = -\frac{1}{\alpha} \log_e [1-\alpha q] \tag{11}$$

Film Shape

Many conjunctions encountered in machine elements subjected to elastohydrodynamic conditions can be represented, in the undeformed state, by a rigid parabolic profile of local radius (R) near a plane. In this case the film thickness (h) at a distance (x) from the line of closest approach where the film thickness is (h_o) can be written as,

$$h = h_o + \frac{x^2}{2R} \tag{12}$$

If the film shape is subsequently modified by elastic deformation v = f(x), then the local film thickness becomes,

$$h = h_o + \frac{x^2}{2R} + v \tag{13}$$

Numerous solutions to the steady-state elastohydrodynamic lubrication problem have now been presented on the basis of this representation of film shape and such solutions are often adopted in quasi-static situations.

It has already been pointed out that significant hydrodynamic effects are achieved by modest normal approach velocities and if combined 'entraining' and 'squeeze-film' action is considered, the full implications of equation (13) for normal approach velocities must be examined. It can be seen that,

$$\frac{\partial h}{\partial t} = \frac{\partial h_o}{\partial t} + \frac{\partial v}{\partial t} \tag{14}$$

The total normal velocity at any location thus consists of the familiar rigid-body action represented by $\left[\frac{\partial h_o}{\partial t}\right]$ together with the time rate of change of the local elastic deformation. The $\left[\frac{\partial h}{\partial t}\right]$ total normal velocity term in the Reynolds equation will thus vary along the length of the conjunction at any instant and this is likely to be particularly significant in reciprocating machinery where the film shape is subjected to the cyclic or 'breathing' action described by Blok and Koens (ref. 1).

APPLICATIONS

The problem of pure squeeze-film action between a ball or cylinder and a plane has been discussed elsewhere in some detail. The central pressures can produce a dimple in the approaching solids as illustrated in Figure 2 and it is evident that the time rate of change of both the rigid body film thickness and the elastic deformation must be considered in a full theoretical analysis.

Squeeze-film motion between a rigid sphere and a plane in the presence of an isoviscous fluid was first analysed by G.I. Taylor and presented at the Bakerian Lecture on boundary lubrication by Sir William Bate Hardy (ref. 3). Christensen (ref. 4) considered the approach of elastic cylinders separated by a piezo-viscous fluid and account was taken of the rate of change of both the rigid body film

thickness and the local elastic deformation. He subsequently presented a similar and full analysis for spheres (ref. 5). Herrebrugh (ref. 6) also recognized the twin elements of local squeeze-film velocities between cylinders in normal approach, but neglected their variation throughout the conjunction when he sought solutions through a single integral equation. Gould (ref. 7) also noted that if the effect of pressure upon viscosity was important in squeeze film action, the influence of temperature rise would also be significant.

The relative importance of elastic deformation and rigid body geometry in the overall squeeze-film action between approaching cylinders was discussed by Lee and Cheng (ref. 8) and by Conway (ref. 9).

In all these analyses of squeeze-film action between spheres and cylinders attention has been focussed upon pure normal approach. In many reciprocating machine elements, normal approach is combined with entraining action which varies in a cyclic manner and it is the purpose of the present paper to illustrate the latter situation.

Medley (ref. 10) has analysed the problem of elastohydrodynamic lubrication in the human ankle joint. It has been shown (ref. 11) that the geometry of the ankle joint can be represented by a circular cylinder near a plane, with the surfaces being formed by articular cartilage on a bone backing. The average radius of this equivalent cylinder near a plane was found to be 0.35m and the cartilage thickness on both the tibia and talus to be about 1.2 mm.

Medley (ref. 10) found that the cyclic pattern of loading and motion in walking permitted the generation of lubricating films having a thickness of about half a micron. He found that squeeze-film action sustained a substantial proportion of the film thickness generated by entraining action during the period of active sliding between the joint surfaces, even though the entraining velocity fell to zero on two occasions in each complete cycle of reciprocating motion. He further found that a simple plane inclined surface slider bearing model, based upon the notional length of the Hertzian contact zone, yielded predictions similar to those obtained from an elastohydrodynamic analysis based upon the model of an elastic layer on a rigid parabolic solid. The latter analysis revealed a remarkably constant film thickness between the cartilage surfaces throughout the cycle in which both the load and the entraining velocities varied considerably. It did not, however, take account of the role of the time rate of change of the local elastic deformation in the analysis $(\partial v/\partial t)$ and squeeze-film action was related to the overal or rigid body motion $(\partial h_o/\partial t)$ alone. Medley (ref. 10) assessed the maximum error in film thickness prediction resulting from this assumption to be about 12 percent.

Piston Ring Lubrication

A good deal of interest has been generated in the tribological performance of the piston seal in reciprocating engines in recent years. The conjunction between the piston ring and cylinder liner is subjected to exceptionally severe dynamic conditions, since the normal load, sliding velocity, temperature and hence lubricant viscosity, all vary throughout the cycle. Furthermore, the conjunction may be starved of lubricant and the influence of each ring upon its neighbour has to be considered in a complete ring pack. In addition, the shape of the conjunction might also change throughout the cycle due to elastic and thermal distortion and wear of

the piston ring, the piston and the cylinder liner.

Analytical procedures have nevertheless been developed (ref. 12,13,14) which enable the cyclic variation of film thickness to be predicted for both 2- and 4-stroke engines. The analysis is based upon the assumption that the conjunction develops a lubricating film between smooth surfaces and account is taken of both entraining and squeeze-film action. All the solutions indicate that hydrodynamic lubrication must give way to boundary or mixed film lubrication in the vicinity of top-dead-centre, where the loads are high and the entraining velocities low.

Recent studies by Dowson et al (ref. 15), have drawn attention to the somewhat surprising result that piston rings might well operate in the elasto-hydrodynamic regime in the vicinity of top dead centre and this provides an opportunity to examine the respective roles of the rigid body and elastic displacement components of squeeze-film action.

The general geometry of the conjunction is shown in Figure 3. Details of the numerical analysis for elastohydrodynamic conditions have been presented in Ref. 15, but it should be noted that elastic deformations were calculated according to equation 6 and that the Baras relation was adopted for viscosity calculations (equation 9).

The cyclic conditions encountered in some eight 4-stroke and six 2-stroke engines were considered and all appeared to operate in the elasto-hydrodynamic regime of lubrication close to top-dead-centre. A particular 2-stroke engine of bore 550 mm, ring height 12 mm and ring face radius 0.75 m operating at 150 r.p.m. (7.85 rad/s) was analysed in detail and illustrations of the ring profile, pressure distribution and squeeze-film velocities 3^{o} before and after top-dead-centre are shown in Figure 4.

The cyclic variation of predicted film thickness is shown in Figure 5. When it was assumed that the lubricant viscosity was not affected by pressure and that the solids were rigid, normal piston ring lubrication theory predicted a cyclic minimum film thickness of 0.05 μm. When account was taken of the influence of pressure upon viscosity, this prediction was lifted to 0.11 μm. A simple elasto-hydrodynamic analysis in which squeeze-film action was associated with rigid-body motion alone brought the prediction up to 0.17 μm, thereby confirming the significance of elastohydrodynamic action in the vicinity of top-dead-centre in this engine. Finally, when the rate of change of elastic deformation with time was considered in the mixed entraining and squeeze-film action, according to equation (14), the predicted minimum film thickness was raised to 0.20 μm.

The analysis confirmed the likelihood of some elastohydrodynamic action in the conjunction between a piston ring and cylinder liner in the vicinity of top-dead-centre. It further indicated that in this somewhat severe condition, involving changes in both the magnitude and direction of the entraining velocity and the application of high loads, squeeze-film action was particularly important.

The cyclic minimum film thicknesses predicted for a piston ring are, nevertheless, small compared with the surface roughnesses of cylinder liners and piston rings. It therefore seems to be inevitable that a mixed film mode of lubrication will apply in these critical regions. It is particularly important that the fluid-film lubrication contribution to this mixed film operation should be recognized, particularly when the influence of load sharing between the lubricant and asperity interactions is considered in power loss calculations.

CONCLUSIONS

Attention has been drawn to the significance of squeeze-film action in both hydrodynamic and elasto-hydrodynamic lubrication. In the latter mode of fluid-film lubrication, the overall squeeze-film action arises from a combination of both rigid body and local elastic deformation motion.

Squeeze-film action associated with time rates of change of elastic deformation within a conjunction undoubtedly complicates numerical analysis and in some cases it is totally neglected. However, in the case of reciprocating motion, it is generally necessary to include it in any full appraisal of hydrodynamic action. This has been illustrated in relation to piston ring lubrication.

The two essential elements of elastohydrodynamic action, namely the influence of high pressure upon lubricant viscosity and the modifications to film shape associated with elastic deformation, both enhance the lubricating film thickness experienced by piston rings in the vicinity of top-dead-centre. The variation of squeeze-film velocity through the conjunction attributable to local changes in elastic deformation has been shown to play an important and far from negligible role in this film thicknesses enhancement process.

REFERENCES

1. Blok, H. and Koens, H.J.: The 'Breathing' Film Between a Flexible Seal and a Reciprocating Rod, The Institution of Mechanical Engineers, Proceedings 1965-66, Volume 180, Part 3B, 1966, pp 221-223.

2. Blok, H.: Inverse Hydrodynamics, in Proceedings, International Symposium on Lubrication and Wear, Ed. D. Muster and B. Sternlicht, McCutchan Publishing Corporation, Ca., 1965, pp 1-151.

3. Hardy, W.B. and Doubleday, I.,: Boundary Lubrication - Plane Surfaces and the Limitations of Amonton's Law, Proc. R. Soc., London, A. 108, (1925), pp.1-27.

4. Christensen, H.: The Oil Film in a Closing Gap, Proc. R. Soc. London, A. 266, (1962), pp. 312-328.

5. Christensen, H.: Elastohydrodyanmic Theory of Spherical Bodies in Normal Approach, A.S.M.E. Journ. Lub. Tech., Series F, Vol. 92, (1970), pp. 145-154.

6. Herrebrugh, H.: Elastohydrodynamic Squeeze Films Between Two Cylinders in Normal Approach, A.S.M.E., Journ. Lub. Tech., Series F, Vol. 92, No. 2, (1970), pp. 292-302.

7. Gould, P.: High-Pressure Spherical Squeeze Films, A.S.M.E., Journ. Lub. Tech., Series F, Vol. 91, No. 1 , (1971), pp 207-208.

8. Lee, K.M. and Cheng, H.S.: The Pressure and Deformation Profiles Between Two Normally Approaching Lubricated Cylinders, A.S.M.E., Journ. Lub. Tech., Series F, Vol. 95, (1973), pp. 308-317.

9. Conway, H.D.: The Rate of Change of Film Thickness in the Elastohydrodynamic Squeeze-Film Process, A.S.M.E., Journ. Lub. Tech., Series F, Vol. 95, No.2, (1973), pp. 391-393.

10. Medley, J.B.: The Lubrication of Normal Human Ankle Joints, Ph.D. Thesis, Department of Mechanical Engineering, The University of Leeds, 1981.

11. Medley, J.B., Dowson, D. and Wright, V.: Surface Geometry of the Human Ankle Joint, Engineering in Medicine, Mechanical Engineering Publications, Volume 12, Number 1, pp. 35-41.

12. Dowson, D., Economou, P.N., Ruddy, B.L., Strachan, P.J. and Baker, A.J.S.: Piston Ring Lubrication. Part II, Theoretical Analysis of a Single Ring and a Complete Ring Pack, in Energy Conservation Through Fluid Film Lubrication Technology: Frontiers in Research and Design, Ed. S.M. Rohde, D.F. Wilcock and H.S. Cheng, 1979, pp. 23-52.

13. Ruddy, B.L., Economou, P.N. and Dowson, D.: The Theoretical Analysis of Piston Ring Performance and its Use in Practical Ring Pack Design, Proceedings of the 14th International Congress on Combustion Engines, 1981, Paper D52, pp 1-24.

14. Ruddy, B.L., Dowson, D. and Economou, P.N.: A Theoretical Analysis of the Twin-Land Type of Oil-Control Piston Ring, Journal of Mechanical Engineering Science, 1981, Volume 23, Number 2, pp. 51-62.

15. Dowson, D., Ruddy, B.L. and Economou, P.N.: The Elastohydrodynamic Lubrication of Piston Rings, Proc. R. Soc. London, 1983, To be published.

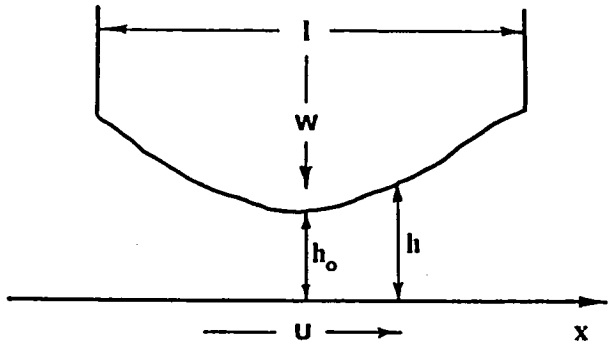

FIGURE 1 ENTRAINING AND SQUEEZE—FILM ACTION

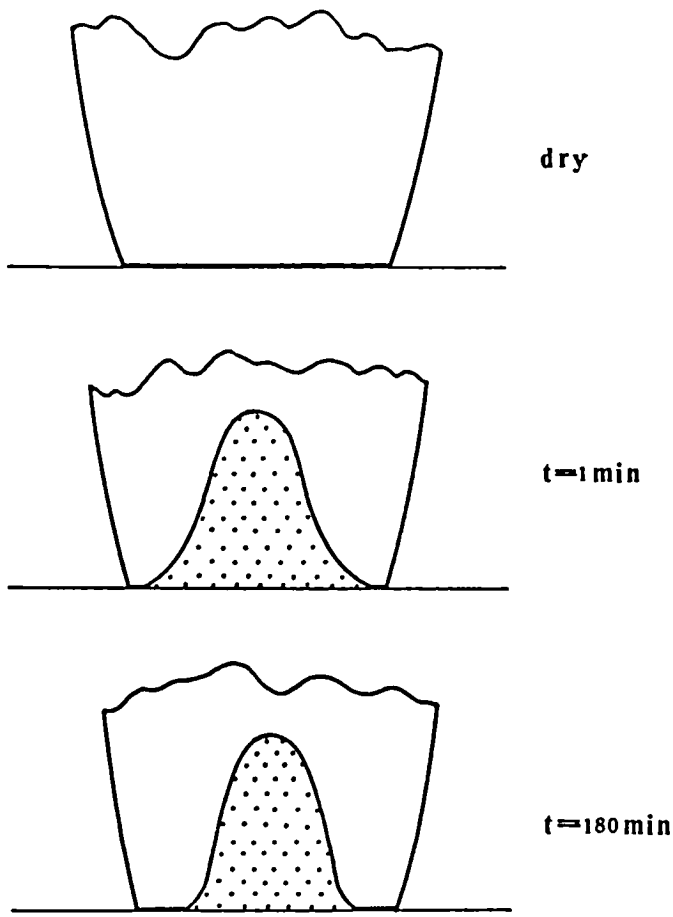

FIGURE 2 SQUEEZE FILMS AND FLUID ENTRAPMENT

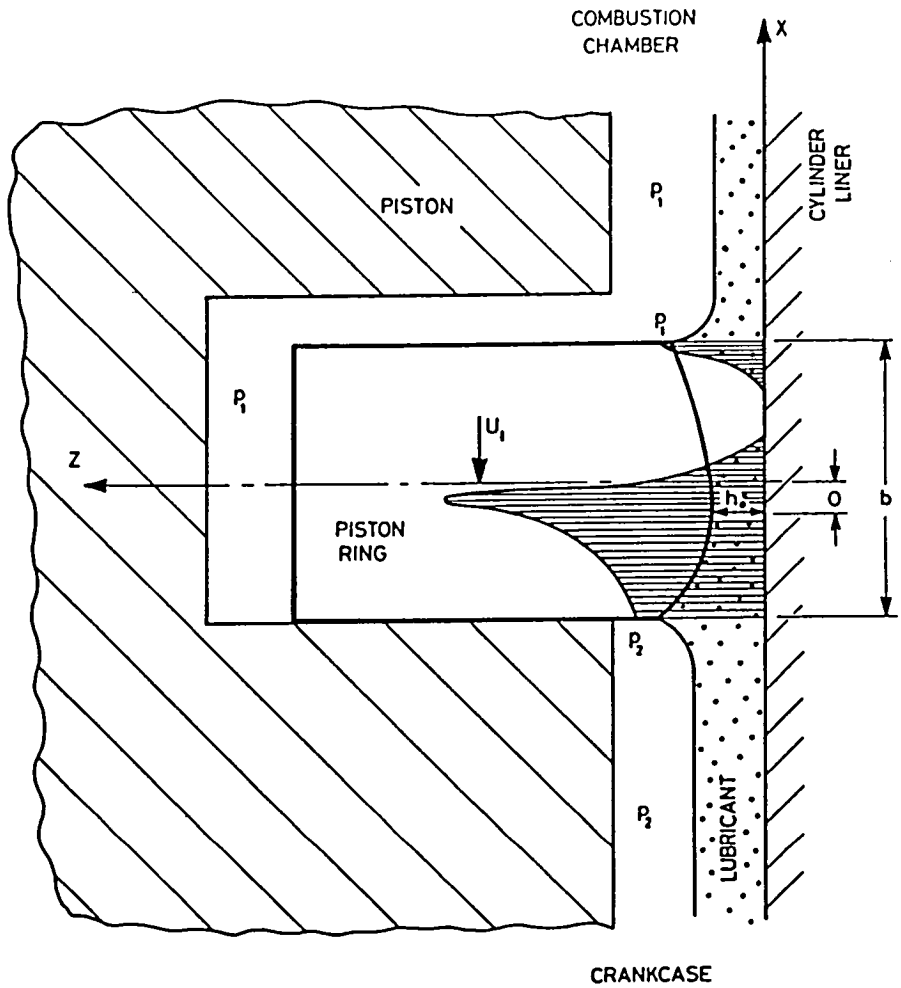

FIGURE 3 PISTON RING GEOMETRY AND SURROUNDING PRESSURES

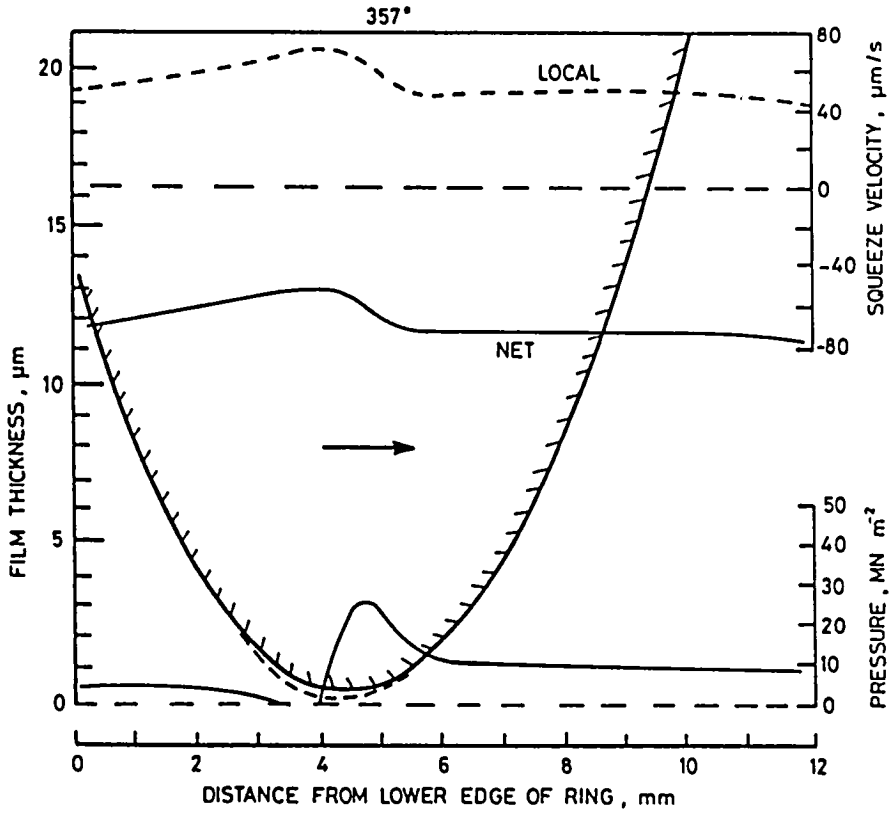

FIGURE 4 (a) PRESSURE, FILM SHAPE AND SQUEEZE VELOCITY FOR PARABOLIC PISTON RING 3° BEFORE TOP DEAD CENTRE

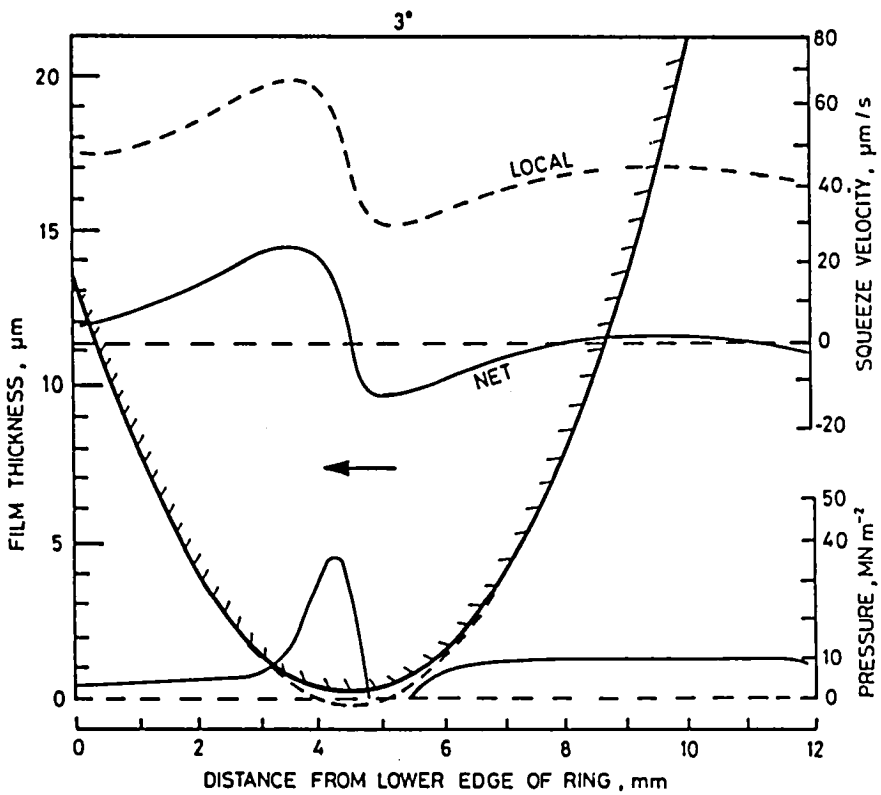

FIGURE 4 (b) PRESSURE, FILM SHAPE AND SQUEEZE VELOCITY FOR PARABOLIC PISTON RING 3° AFTER TOP DEAD CENTRE

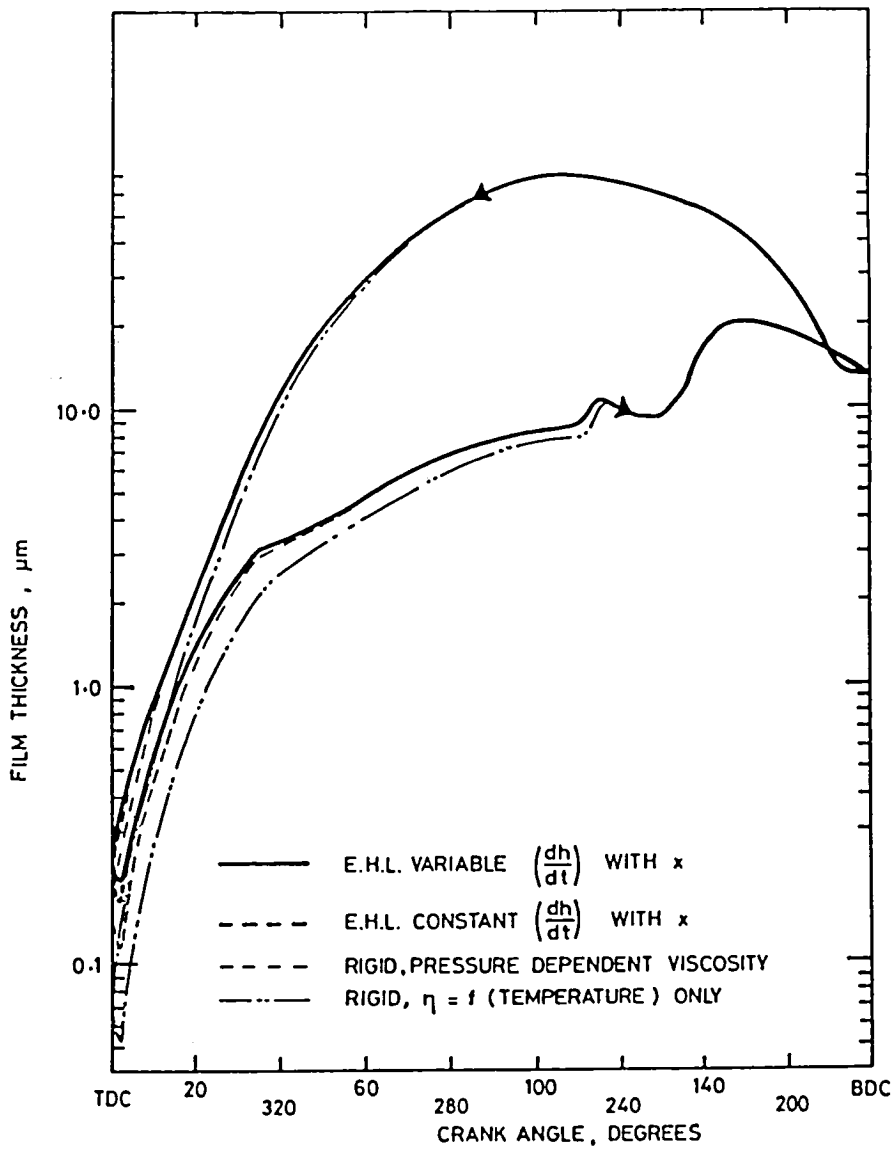

FIGURE 5 CYCLIC VARIATION OF FILM THICKNESS IN 2-STROKE DIESEL ENGINE PREDICTED BY VARIOUS ANALYTICAL PROCEDURES

DISCUSSION

Alastair Cameron
2 Bottisham Place
Cambridge, England

Professor Dowson has indeed put his finger on the next goal of theoretical analysis, the solution of the EHL problem, both hard and soft, taking squeeze films into account. It is extremely difficult, as Ettles and James (ref. 1) found in their study of it, as well as the other authors Prof. Dowson quotes.

It has occurred to me that the importance of squeeze films can be highlighted by rewriting the right hand side of Reynolds equation ($U\, dh/dx + 2\, dh/dt$). If the velocity U is written dx/dt then the first term reduces to dh/dt, showing that all hydrodynamic lubrication is effectively a squeeze film affair. The converging gap and the movement of the surfaces combine to squeeze the lubricant, thus generating a pressure.

If the squeeze film equations for EHL - which one might call SEHL - are solved, it might help explain the very mysterious drop in load carried by discs shown by Smith and Cameron (ref. 2).

Squeeze films can produce puzzling results. In a series of papers from the Imperial College Lubrication Laboratory (ref. 3) the viscosity of oils at high pressures can be evaluated, using an impact viscometer. At low pressures - up to 0.1 GPa - the viscosities so found agree with conventional values. Above this, however, they are a factor of 10 below those determined by the more conventional traction tests, even when these are carried out in the same laboratory using the same fluids (ref. 4).

REFERENCES

1. N. James and C. M. McC. Ettles: Solutions for the Normal Approach of an Axisymmetric EHL Contact. 5th Leeds-Lyons Conference, 1978.
2. A. G. D. Smith and A. Cameron: Scuffing under Cyclic Loading. ASLE Trans., Vol. 26, pp. 236-242, 1983.
3. G. R. Paul and A. Cameron: An Absolute High Pressure Impact Microviscometer. Proc. Roy. Soc., 1972, A331, 171. Ultimate Shear Stress of Fluids at High Pressures Using a Modified Impact Viscometer. ibid. 1979, A.365, 31-41.
4. R. F. Duckworth, G. R. Paul, and A. Cameron: Elastic Properties of Films in EHL Contacts. Proc. Roy Soc., 1980, A372, 155-168.

REAL SURFACE EFFECTS IN ELASTOHYDRODYNAMIC LUBRICATION

John H. Tripp*
Case Western Reserve University
Cleveland, Ohio

Following a general discussion of real effects in EHL, consideration is given in detail to the role played by stochastic roughness superimposed on the nominal solid boundaries. Particular attention is given to the full-film EHL regime where incipient asperity contact bears a negligible fraction of the load. Flow, from which an averaged Reynolds equation can be formed, is nonetheless modified by the amplitude and texture of the roughness patterns. In describing these effects by means of certain well-defined flow factors, it is found that only two extra parameters are needed - the rms surface height and the ratio of the correlation lengths in the two principal roughness directions. In a lowest order perturbation expansion of these flow factors in powers of the ratio of rms roughness to nominal film thickness, no other properties of the roughness appear. In most cases of practical interest, the factors describing Poiseuille flow are separable into the sum of two single-surface flow factors which means that a combination of a single equivalent rough surface versus an ideal smooth surface can always be found. For flow entrained by slip velocity the factors separate instead into a difference of single-surface factors and it becomes significant which of the two surfaces carries the equivalent roughness.

Results are discussed of some applications of the averaged Reynolds equation based on the flow factor method to the EHL line contact problem. Finally, the partial EHL regime is considered where comparable load fractions are carried by the hydrodynamic film and by incipient mechanical contact. An extension of the method into this regime by combining it with asperity contact models appears most encouraging.

INTRODUCTION

Ideal Elastohydrodynamic Lubrication

Over the last 30 or so years, major strides have been made in the understanding of the mechanisms of fluid lubrication in nonconformal machine elements, where the mechanical load is supported by the lubricant film over an area several orders of magnitude less than the cross-sectional area of the bearing elements themselves. The development of the concepts required for this has been reviewed thoroughly elsewhere, most recently by Hamrock and Dowson (ref. 1), and basically reduces to an appreciation of the crucial role played by both the deformation of the solid bearing materials and the viscous behavior of the lubricant. The high local pressures generated in the film cause changes in the shapes of the ideal bearing surfaces and also a sharp increase in the lubricant viscosity coefficient.

In most cases, standard elastic analysis suffices to handle the strain fields set up in the solids, leaving nothing worse than a boundary-value problem, albeit one whose boundary conditions are coupled to its solution by the necessity of simultaneously satisfying the hydrodynamic equation on the film side of the boundary. Viscous effects, on the other hand, demand an

*NRC Associate at the NASA Lewis Research Center, Cleveland, Ohio.

advance beyond the simple constant coefficient of viscosity by introducing more detailed rheological features for the fluid. In the sense that further material properties provide additional degrees of freedom, greater flexibility appears in constructing theoretical models for this hydrodynamic part of the problem, though ultimately of course such models must conform to experimental observation. The simplest step beyond isoviscosity is probably to the Newtonian fluid whose viscosity coefficient μ obeys the exponential Barus Law

$$\mu = \mu_0 e^{\alpha p} \tag{1}$$

where p is the film pressure, α the pressure viscosity coefficient, and μ_0 the value of μ at ambient pressure $p = 0$. Equation (1) not only reproduces observations satisfactorily but also leaves the hydrodynamics, which is taken to be adequately described by a Reynolds equation, in readily managed form. Perhaps for this latter advantage the exponential model has gained acceptance as the ideal lubricant behavior. Although for many purposes the parameter α may be taken as a fluid constant, further refinements allow it some pressure or temperature dependence.

These preliminary comments introduce the three main elements of ideal EHL: linear elasticity, exponential Newtonian viscosity, and a Reynolds equation for pressure generated in the film. Understanding EHL has rested largely on these basic factors, and the variety of successful applications is gratifyingly diverse. This basic formulation must, however, be broadened if it is to handle the variety of effects found in real bearing systems.

Real Elastohydrodynamic Lubrication

Two such realities of particular interest are the friction and wear behavior found universally in machine elements of the kind considered here. While the ideal model does predict friction behavior within a range of the operating conditions of load and speed, it is inadequate to deal with many of the more extreme situations encountered in today's technology. For wear, the situation is even worse since no physical mechanism is incorporated in conventional EHL allowing for surface wear.

Extensions to the rheological behavior of the lubricant are thus required. One possibility, for example, is to introduce temperature effects on viscosity and density, while another is to abandon proportionality of shear stress to strain rate for a more general non-Newtonian fluid behavior. Similarly, for the solid boundaries it is necessary to consider departures from the nominal geometry, having regard to the types of surface finish actually achieved in engineering practice. The continuum picture of the solid, moreover, should be replaced by one recognizing its microstructure since it is here, in conjunction with the surface finish, stress, and temperature distributions, that wear phenomena find their explanation. In making these extensions to the rheology and morphology of the model it is necessary to ensure their compatibility with the many physical assumptions built into a Reynolds equation. In particular, the condition for laminar flow throughout the film is easily violated if turbulence or recirculation regions form in the presence of real surface texture. Under such conditions it is necessary to modify the third ingredient of standard EHL and to consider alternatives to a Reynolds equation (ref. 2).

On the basis of this brief summary, the many new problems encountered in real EHL fall into fairly obvious categories according to which of the restricting ideal conditions are relaxed. Such a scheme might be visualized

along the lines of figure 1, which selects from numerous possibilities only those interrelationships of EHL subelements mentioned in this article. Within such a general scheme the present work focuses on the effects of surface roughness and texture on lubricant film shapes and pressure distributions, accepting the standard lubricant rheology and conditions for validity of Reynolds-type hydrodynamics.

ROUGHNESS

General Considerations

This subfield may itself be further divided according to how the roughness is modeled. In general nonrigorous terms, roughness of a surface is any departure of the actual surface height from the ideal datum level, also known as the nominal or desired level, occurring as a result of the physical and chemical methods used to prepare the final surface as well as from microstructure of the material. One of the most fundamental and fascinating questions prompted by such a definition of roughness is that of the length scale at which roughness is specified. A surface profile in fact has a fractal behavior, which means that it preserves the same appearance when either enlarged or reduced in size. This property is shared by a wide class of pseudorandom physical phenomena, including coastlines and the borders of various types of cloud (ref. 3). Both in developing mechanical models of solid boundaries and in deriving techniques of surface measurement it is desirable to know the relevant scale(s) of the surface features involved. The only natural physical limits are the atomic structure of the materials, of order 10^{-10} m, and the dimensions of a typical contact area, say 10^{-4} m, which leaves considerable freedom in choosing a bandwidth. It must be assumed here that the appropriate scale has been determined, although it is not always clear just how this is to be accomplished, particularly for the short wavelength cutoff (ref. 4).

Within any bandwidth roughness may display both an ordered and a random component, making necessary a further distinction on this basis. Model studies may emphasize one or other of these components.

Deterministic Roughness

If the profile at the chosen scale is modeled by some stated function of whatever complexity, then the EHL problem is deterministic and remains strictly in the ideal category. The complexity alone does not violate standard conditions. This includes the periodic or ordered components of roughness. Earlier studies of real surface effects often were of this deterministic type (ref. 5), superimposing on a simple plane or cylindrical surface a regular array of striations, furrows, or other features. From solutions of a Reynolds equation with appropriate boundary conditions, effects of amplitude, array spacing, etc., on film properties could be investigated.

Apart from their intrinsic interest, such studies are of value for two further reasons. First, it may be possible to obtain the expected behavior of random asperity arrays, thereby approaching chaos as a limit of order, by judiciously averaging solutions for deterministic roughness patterns representing a variety of asperity shapes. Insofar as the randomness hidden by the averaging process is brought into the problem after solving the hydrodynamic equation, such an approach is valid. Difficulties are experienced only in

incorporating all the parameters needed for the averaging, since, besides varying the size and shape of the asperities, randomness may also change the boundary conditions on pressure seen by the typical asperity from those originally imposed.

The second point of interest arising from deterministic models is known as micro-EHL (ref. 6), which is the study of just one or a few asperities of known shape superimposed on the nominal film boundary. While much can be learned from the study of global or average behavior of EHL films between rough surfaces, certain failure mechanisms such as scuffing are determined principally by the largest surface features, where reduction in film thickness is greatest. Average behavior tells little about such extreme events which accordingly are studied separately under the heading micro-EHL, essentially the performance of an asperity of known shape embedded in a lubricant film already subject to macro-EHL ambient conditions. Neither of these deterministic aspects of real surfaces will be considered further here. Emphasis instead will be on the random component of roughness.

Stochastic Roughness

Within the general framework of hydrodynamics governed by a Reynolds equation, the variables of importance in determining film pressure p are the film thickness h and its spatial derivatives. When these become stochastic variables by virtue of their spatial randomness, it is necessary to consider what information about the film stresses might usefully be sought from the theoretical model, as well as what information is available for input.

The most obvious quantities to look for are time averages of such variables as load W and friction coefficient f as well as of the distribution of p itself, each of which is determined at each instant by the particular configuration of the roughness in the conjunction. In addition to mean values, however, it may also be possible to observe fluctuations (ripple) within some specified frequency range governed by the response characteristic of the sensing device. Given such information about the statistical distribution of these quantities, some progress toward understanding those extreme events governing failure becomes possible.

In a statistical sense, a complete description of the rough surface requires knowledge of the height distribution and the correlation functions (CF) for these heights. Both of these, as it turns out, depend on the scale selected for measuring the surface features (ref. 4) and hence are not intrinsic properties of the surface. The height distribution is simply the probability that a single point in the surface selected at random lies at or below a given height, while the correlation functions describe how the probability of finding one point at given height depends on the heights of a number of other points in its vicinity. This is best illustrated by the two-point CF which is the ensemble-averaged product of heights at two points selected at random with fixed spacing between them. If heights are measured from their mean value in units of their own standard deviation σ, this CF is unity (high correlation) when the two points lie close together. It becomes zero (no correlation) when they are far apart, since statistical independence then allows the averaged product to be replaced by the product of averages. The correlation length is the distance over which the CF falls to some specified small value, say 0.1. While it provides one important characteristic length against which to calibrate surface features, it leaves unresolved the question of scale raised earlier. For a general surface, correlation depends on direction as well as magnitude of the displacement of the two points and is

determined by the typical dimensions of surface features in that direction. If the CF's and the height distribution function are the same wherever they are measured across the surface, the stochastic process is said to possess stationarity. As a function of the two-dimensional vector displacement, the two-point CF may easily be expressed as the Fourier transform of a two-dimensional power spectral density of the surface heights. For the special case of an isotropic surface, the CF depends on the magnitude of the displacement alone and the corresponding Fourier transform becomes the familiar power spectral density, a function of a single spatial frequency.

Although further statistical information is certainly contained in the higher-order CF's, defined analogously for any number of surface points, in practice it turns out that the height distribution and the two-point CF contain essentially all that is required to model both fluid flow and mechanical contact behavior. This is perhaps fortunate since the necessary information on these two functions may readily be extracted from experimental surface data, obtained for example from optical scattering or digital profilometry (ref. 7).

Roughness Regimes

One of the best known but incompletely understood results in tribology is the manner in which the friction of sliding or rolling bearings varies with the operating variables of load W and velocity U, summarized in the famous Stribeck curve (ref. 8). As shown in figure 2 the coefficient of friction f plotted against the combination $\mu U/W$ displays a minimum preceded by a steep drop and followed by a more gentle, almost linear, increase. For present purposes, another equally famous result may be borrowed from ideal EHL stating that the minimum film thickness is a monotonic increasing function of this same parameter group so that the Stribeck curve actually illustrates friction versus some nominal film thickness h^*.[1] When σ is used as the natural unit in which to measure a distance normal to the surface (such as film thickness), the curve is transformed into a plot of f against $\Lambda \equiv h^*/\sigma$. The variable Λ is the reciprocal of Dawson's D-ratio which he originally introduced to correlate observations on the pitting failure of EHL contacts (ref. 9).

With this viewpoint, the qualitative explanation of the Stribeck behavior becomes almost self-evident, and it is even possible to put approximate numbers on the abscissa. For the types of height distribution found on most surfaces, only about 0.1 percent of the surface lies above a height of 3 so that the linear region of the curve is associated with full film EHL and almost negligible solid contact between the film boundaries. On the other hand, some 15 percent of the surface exceeds a height of 1 so that for $\Lambda < 1$ the lubricant must flow between patches of incipient contact where the surfaces either make direct dry contact or are separated at most by a boundary layer or a thin micro-EHL film. The open flow paths between these regions become ever more tortuous until eventually they are blocked off. Friction in this regime arises from both dry contact and boundary layers. Wear is often high and scuffing is an important failure mode (refs. 10 and 11). The intermediate range, say $1 < \Lambda < 3$, defines the partial EHL regime (refs. 12 and 13) where the fractions of the load shared by EHL film and incipient contact, while

[1]The ensemble averaging process, which is the average taken over all possible samples of roughness having the specified statistical properties, is denoted by the superscript * or, when more convenient, by < >.

varying in opposite directions through the range, are nevertheless comparable. The dominant failure mode in this regime is by fatigue or pitting.

The principal physical concepts distinguishing the three roughness regimes have been mentioned briefly. Attention will now be concentrated on the full film regime where a statistical description of the film boundaries combined with the standard lubricant model suffices to explain real surface effects. In the final section consideration is also given to the partial EHL regime, where it becomes necessary to provide descriptions of asperity deformation and changes in statistical properties resulting from incipient contact. With recent advances in the dry contact problem at these intermediate levels of contact (ref. 14), good progress in this regime seems possible. In the boundary region, however, there are several gaps in knowledge that must be filled, including an understanding of percolation of fluid through those few channels remaining open at high degree of contact (ref. 15) and an adequate treatment of contact mechanics when, due to their interaction, asperities persist under unexpectedly high local pressures (ref. 16). This regime is perhaps more usefully regarded as an aspect of dynamical sealing than of lubrication.

STATISTICAL ASPECTS OF FLOW

Based on the general outlines sketched in the preceding section, it is now straightforward to put together the mathematical details of a statistical theory of flow. The class of film problems we shall consider in detail, while not completely general, is broad enough to illustrate the important ideas. The primitive parameters of the problem are given in figure 3, which shows the x-dimension of a lubricant film moving between two rough solid boundaries at heights z_1 and z_2. The translational velocities $\vec{u}_1$ and $\vec{u}_2$ of these boundaries lie in the (x,y) plane and are independent of position and time. Thus, there is no rigid-body rotation and no transient effect. The true surface height is the sum of a specified nominal height $z^*_{1,2}$ and its random component $\delta_{1,2}$ of zero mean and standard deviation (rms value) $\sigma_{1,2}$. The standard deviation of the composite roughness $(\delta_2 - \delta_1)$ is the quantity already referred to as σ, which is just $\left(\sigma_1^2 + \sigma_2^2\right)^{1/2}$ in the usual case when there is no cross-correlation between the two surface topographies.

While subscripts 1 and 2 denote, respectively, the lower and upper surfaces, we adopt a notation which eliminates individual reference to them by using the following set of parameters with more direct significance for flow problems:

Mean surface velocity:

$$\vec{U} \equiv \frac{1}{2}\left(\vec{u}_2 + \vec{u}_1\right)$$

Slip velocity:

$$\vec{V} \equiv \vec{u}_2 - \vec{u}_1$$

Mean film level:

$$Z \equiv \frac{1}{2}(z_2 + z_1)$$

Film thickness:

$$h \equiv z_2 - z_1$$

Roughness sum:

$$\lambda^+ \equiv (\delta_2 + \delta_1)/h^*$$

Roughness difference:

$$\lambda^- \equiv (\delta_2 - \delta_1)/h^*$$

(2)

The use of h^* in defining the nondimensional roughness sum and difference follows standard EHL practice, but to regain σ as the natural vertical measure, h^* may always be replaced by $\Lambda\sigma$. In the absence of cross-correlation, the standard deviation of $\lambda^{\pm}$ is Λ^{-1}. With these new variables, subscripts will now denote Cartesian vector components $(x_1,x_2) = (x,y)$, and summation on any index repeated in a product is implied.

The volume flow Q_i per unit width due to the pressure gradient $\partial_i p$ and the entraining velocity U_i, under the normal assumptions of a Reynolds equation, is given by

$$Q_i = -\frac{h^3}{12\mu}\partial_i p + hU_i \tag{3}$$

where the true film thickness h is given by the stochastic process $h^*(1 + \lambda^-)$. This expression connects Q_i and p to h so that one or both of them is also a random variable.

The continuity equation for incompressible flow is

$$\partial_i Q_i + \partial h/\partial t = 0 \tag{4}$$

which leads by a Euler transform to Reynolds equation

$$\partial_i\left(\frac{h^3}{12\mu}\partial_i p\right) = -V_i\partial_i Z \tag{5}$$

When the ideal rheological fluid of equation (1) is used and the reduced nondimensional pressure q defined by

$$q = (1 - e^{-\alpha p}) \tag{6}$$

is introduced, the Reynolds equation becomes

$$\partial_i\left(h^3\partial_i q\right) = -12\alpha\mu_0 V_i\partial_i Z \tag{7}$$

This shows that so far as fluid properties are concerned the hydrodynamic pressure is determined solely by the combination $\alpha\mu_0$.

In the stochastic case, solution of equation (7) may be approached in two ways. The more direct method, which has become feasible with the help of high capacity computers, is to generate a sample of the rough boundaries according to the desired statistical behavior and to find q by straightforward numerical integration. Carrying out the complete EHL procedure using this pressure distribution to evaluate the elastic displacement of the sample boundaries then leads to the actual film shape for this particular sample. Repetition of the whole procedure generates a population of such film shapes from which suitable mean values and fluctuations (for example, of the minimum film thickness) may be derived and related to the statistical parameters used to generate the roughness samples. While this method suffers from all the usual disadvantages of finite sampling in determining ensemble averages, it has the prime advantage of avoiding the need for additional assumptions concerning flow or pressure fluctuations. In principle the method can also handle the problem of contact in the partial EHL regime by introducing an asperity de-

formation model and an appropriate boundary condition on flow at the borders of contact areas. Such a complete numerical simulation, however, has so far never been done.

The alternative approach to solution of equation (7) is to average the equation itself. Since nominal surface shapes are known, there is no difficulty with the right side. However, when h and q are correlated stochastic variables, the left side needs careful handling. The ideas may be illustrated by the work of Christensen (ref. 17) which applies to a class of real boundaries where the averaging can be performed directly. This is the class of one-dimensional roughness for which surface profiles taken in one special direction, the lay direction, display the nominal shape of the surface and hence are nonrandom. Roughness features in this class include ridges, grooves, etc., and their orientation (arbitrarily assigned the x-direction) must be the same on both surfaces.

It is a reasonable assumption that sampling the pressure at points along a line parallel to the lay will result in a smooth (i.e., nonrandom) pressure variation, while along any line crossing the lay, a pressure ripple will be superimposed. Conversely, the component of flow perpendicular to the lay will be nonrandom, with fluctuations appearing in any other direction. These two assumptions enable the correct averaging of Reynolds equation to be achieved.

Since $\partial_1 q$ is nonrandom, it may be removed from the ensemble averaging of the $i = 1$ term on the left of equation (7), which then becomes $\partial_1(\langle h^3\rangle \partial_1 q^*)$. We note $\langle \partial_i q\rangle = \partial_i \langle q\rangle \equiv \partial_i q^*$ because ∂_i and $\langle\ \rangle$ are commuting operations. Next we arrange equation (3) to give $\partial_2 q$ and take its ensemble average using the determinacy of Q_2. Rearranging to recover Q_2 we set this equal to the average of the original expression to yield the average of the $i = 2$ term on the left of equation (7), namely

$$\partial_2\left(\langle h^{-3}\rangle^{-1}\partial_2 q^*\right) - 12\mu_0\alpha U_2\partial_2\left(\langle h^{-3}\rangle^{-1}\langle h^{-2}\rangle - h^*\right)$$

The averaged form of equation (7) for q^* thus becomes

$$\partial_1\left(\langle h^3\rangle\partial_1 q^*\right) + \partial_2\left(\langle h^{-3}\rangle^{-1}\partial_2 q^*\right) = 12\alpha\mu_0\left[U_2\partial_2\left(\langle h^{-3}\rangle^{-1}\langle h^{-2}\rangle - h^*\right) - V_i\partial_i Z^*\right] \qquad (8)$$

This is the generalized version of Christensen's equations derived originally only for two special cases of one-dimensional roughness on a slider bearing. All the required averages of h can be expressed in terms of the statistical parameters of the roughness distribution.

The feature of general interest to emerge from equation (8) is that it contains two distinct averaging processes for h^3 on the left associated with components of flow parallel and transverse to the lay. Clearly, passing to two-dimensional roughness brings into play a continuum of such averaging processes of which an appropriate average is needed to represent average flow. Unfortunately, despite the ingenuity of the arguments leading to equation (8), their generalization has proved elusive and a somewhat different approach has been developed (refs. 18 to 20).

The central idea is simply to express the flow equation (3) in terms of readily averaged quantities and to allow for the fluctuations by introducing a set of so-called flow factors. One of several ways to accomplish this is to write

$$Q_i = -\frac{h^{*3}}{12\alpha\mu_0}\varphi^p_{ij}\partial_j q^* + hU_i - \frac{\sigma}{2}\varphi^s_{ij}V_j \tag{9}$$

where tensors φ^p_{ij} and φ^s_{ij} are termed, respectively, the Poiseuille (or pressure) and shear flow factors. Since as a definition, equation (9) is exact, the φ factors must themselves be stochastic. Flow, however, is determined globally by the continuity requirement, so that its relative fluctuations, in common with those of the φ factors, are certainly less than the fluctuations of h or q. The Reynolds equation formed from Q^*_i is thus assumed to be adequate. When both equations (3) and (9) are averaged, the definition of the ensemble averaged flow factors is contained in

$$\langle h^3\partial_i q\rangle = \varphi^{p*}_{ij}h^{*3}\partial_j q^* + 6\alpha\mu_0\sigma\varphi^{s*}_{ij}V_j \tag{10}$$

The diagonal elements of φ^{p*} are recognized as the ratios of the appropriate average value of h^3 to h^{*3}, while the remaining elements arise from various modes of flow entrainment not present in the smooth case.

The average Reynolds equation resulting from equation (10) is easily found to be

$$\partial_i\left(\varphi^{p*}_{ij}h^{*3}\partial_j q\right) = -12\alpha\mu_0 V_j\partial_i\left(Z^*\delta_{ij} + \frac{\sigma}{2}\varphi^{s*}_{ij}\right) \tag{11}$$

Once the flow factors are known in terms of the roughness parameters, this equation serves in place of the ideal form in the complete EHL procedure. It is one form of the required generalization of equation (8).

A RIGOROUS SOLUTION

Evaluation of the flow factors rests on the assumption that, since they depend on the local value of h^*, the particular choice of nominal film geometry used to find them is immaterial. Once known, they are thus applicable to any bearing geometry.

The simplest rough Reynolds equation to solve which still contains all the flow components is one describing flow between nominally parallel rough planes, separation h^*, with constant applied nominal pressure gradient g_i and nonzero slip velocity V_i. For this configuration,

$$Z = \frac{1}{2}h^{*\lambda^+}$$

which may be substituted into the exact Reynolds equation (7). The solution q of this is then inserted in equation (10) and the ensemble average formed, whereupon the flow factor components can be individually identified. The important step here is solving for q which, since it precedes ensemble averaging, must not itself involve any such process.

The original approach of Patir and Cheng followed the simulation method described earlier from which they deduced by numerical experiment the salient features of the flow factors (refs. 18 and 19). On the other hand, the present method is analytic and generalizes the earlier simulation work. While

details of this solution by means of a Green function are supplied in reference 20, the basic statistical features of the approach are of interest here.

The pressure is expanded as a perturbation series in powers of Λ^{-1}. Since the equation determining q in any order depends on all lower order pressures, an iterative approach is required with the consequence that, in each order n, the combined roughness variables $\lambda^{\pm}$ from n different surface points are involved. The ensemble average of the series for the flow factors then requires CF's up to and including the n-point CF. In the full film EHL regime of interest, where the physical model is most applicable, the series are, in fact, truncated at second-order terms. Thus, according to equation (10) the pressure flow factors require only the 2-point autocorrelation function (ACF) of λ^{-} while the shear flow factors require the 2-point CF of λ^{-} and λ^{+}. In most cases there is no cross-correlation between the roughness on the two surfaces, so that from the definition of $\lambda^{\pm}$ the required CF's are readily expressed in terms of the individual ACF's of the two surfaces, $\rho_{1,2}$:

$$\langle \lambda^{-}(x_i)\lambda^{\pm}(x_i') \rangle = \Lambda^{-2}\left[\left(\frac{\sigma_2}{\sigma}\right)^2 \rho_2(x_i - x_i') \mp \left(\frac{\sigma_1}{\sigma}\right)^2 \rho_1(x_i - x_i')\right] \tag{12}$$

As discussed in the Stochastic Roughness section, the ACF's generally depend on both the magnitude and direction of the vector difference $(x_i - x_i')$ but not, according to stationarity, on x_i or x_i' individually. By virtue of equation (12) both shear and pressure flow factors separate into two parts, each of which depends on the roughness of one surface alone.

Upon investigating the problem of the sensitivity of flow to the actual form of the ACF, we find little that can be stated in general about this function. It manifests great variety of form according to the surface finishing processes used (ref. 21) but also displays a simple symmetry. Whenever there exists a lay direction in the surface, this direction and its normal constitute a pair of orthogonal lines of reflection symmetry for ρ. Observation of the correlation lengths in these two special directions provides a measure of the size and shape of the typical topographical feature. From the theoretical expressions for the flow factors it is found, perhaps surprisingly, that they are sensitive principally to the ratio γ of these two correlation lengths rather than to the individual values. This is, in fact, a consequence of the failure of the hydrodynamic model to furnish any absolute length scale for roughness. When this texture or anisotropy factor γ is 0 or ∞, the roughness degenerates to the one-dimensional grooves already considered, while $\gamma = 1$ denotes an isotropic surface. Implicit in this sensitivity to γ is the equally surprising lack of dependence on other details of the ACF. This recalls the analogous independence of the φ factors of the height distribution function, the effects of which enter mainly through its standard deviation.

According to this theory then, the principal effects of roughness on flow may be described by just two extra parameters, σ and γ, for each of the two real surfaces. It is fortunate, since the form of the ACF is often not well known particularly for small distances, that so little information about it is actually needed for the hydrodynamic model.

Taking the coordinates x_i along the principal roughness axes, the symmetry of the ACF diagonalizes the flow factor tensors and furthermore, since interchanging x and y merely changes γ to $1/\gamma$, it is necessary to

calculate only one component each of φ_{ij}^{p*} and φ_{ij}^{s*}, say the (1,1) term. As representative of the general ACF shape and because it yields a closed algebraic result, the Gaussian form may be adopted:

$$\rho = \exp\left(-\beta^{-2}\right)\left[(x - x')^2 + \gamma^2(y - y')^2\right] \tag{13}$$

In the x-direction this ACF falls from 1 to 0.1 in a distance 1.5β while the corresponding y correlation length is $1/\gamma$ times this. The result for the φ factors is independent of the scale factor β and finally reduces to

$$\varphi_{11}^{p*}(\Lambda,\gamma_1,\gamma_2) = \left(\frac{\sigma_1}{\sigma}\right)^2 \Phi^p(\Lambda,\gamma_1) + \left(\frac{\sigma_2}{\sigma}\right)^2 \Phi^p(\Lambda,\gamma_2) \tag{14}$$

$$\varphi_{11}^{s*}(\Lambda,\gamma_1,\gamma_2) = \left(\frac{\sigma_1}{\sigma}\right)^2 \Phi^s(\Lambda,\gamma_1) - \left(\frac{\sigma_2}{\sigma}\right)^2 \Phi^s(\Lambda,\gamma_2) \tag{15}$$

where Φ^p and Φ^s are the single surface flow factors given by

$$\Phi^p(\Lambda,\gamma) = 1 + 3\Lambda^{-2}(\gamma - 2)(\gamma + 1)^{-1} \tag{16}$$

$$\Phi^s(\Lambda,\gamma) = 3\Lambda^{-1}(\gamma + 1)^{-1} \tag{17}$$

These factors, illustrated in figure 4, embody all the obvious features expected on physical grounds from equation (10). At large Λ, Φ^p becomes unity and Φ^s becomes zero for any anisotropy. More detailed requirements can, however, be derived by comparing the generalized Christensen equation (8) with the averaged Reynolds equation (11). Since equation (8) describes flow for the case $\gamma \to \infty$, corresponding terms on the left sides show that

$$\Phi^p(\Lambda,\infty) = \langle\xi^3\rangle \tag{18}$$

$$\Phi^p(\Lambda,0) = \langle\xi^{-3}\rangle^{-1} \tag{19}$$

where ξ is the nondimensional ratio h/h^*. Similarly, the right side yields

$$\Phi^s(\Lambda,\infty) = 0 \tag{20}$$

$$\Phi^s(\Lambda,0) = \Lambda\left(1 - \langle\xi^{-3}\rangle^{-1}\langle\xi^{-2}\rangle\right) \tag{21}$$

Evaluating these expectations shows perturbation theory to be asymptotically correct.

Finally, equation (14) shows that the effect of two-sided roughness on pressure flow can be reduced to that of a single equivalent surface. The same

is true for shear flow, but because of the minus sign in equation (15), the equivalent roughness must be given to the surface with the larger flow enhancement capability, as measured by the product of ϕ^s and the variance for each surface.

APPLICATION TO EHL

The Reynolds equation (11) together with the flow factors of equations (14) to (17) constitute a firm basis from which to approach the EHL problem in the Λ regime where mechanical contact carries an insignificant fraction of the total load. In the period since the equation, somewhat simplified, was introduced by Patir and Cheng, few applications of it to an EHL problem have been made, although the results of two calculations may be of interest here. Both of these include some effects of asperity contact, but only results for $\Lambda \gtrsim 2$ will be discussed here, where partial EHL is negligible. The first is by Patir and Cheng themselves (ref. 22) who studied the rough line contact problem by looking at just the inlet half of the film region. The Reynolds equation was solved in this region subject to specifying the value of the pressure at two points, finite at the center and zero far upstream of the inlet, while the pressure gradient was taken as zero at these two points. Flow factors were computed by their simulation approach and are shown for comparison with the perturbation result in figure 4. The asymptotic agreement is seen to be good, while the systematic deviations have been discussed in reference 20.

From the present viewpoint the interest of this application of the method is not so much in the accuracy of the flow factors themselves but in their effects on the film thickness and pressure distribution. Figure 5, taken from reference 22, shows how the central film thickness varies with Λ and γ in a case of no sliding at constant central pressure (or effectively constant load). In the full EHL regime, where their model works best, the effect on the film thickness does not exceed 25 percent, falling to zero with increasing Λ. The enhanced flow produced by a longitudinal pattern ($\gamma > 1$) decreases the film thickness for given load, while transverse roughness ($\gamma < 1$) inhibits flow and consequently increases the film thickness. As noted by these authors, the results of earlier calculations based on the Christensen equation (8) for one-dimensional roughness patterns agree qualitatively with this behavior but appear to exaggerate it. Even for Λ as large as 6, the pure transverse curve still lies well above the smooth and the pure longitudinal well below it. At such large separations, it might be expected that the average roughness effects considered here would be almost negligible.

In the inlet, longitudinal roughness leads to a slightly longer and more gradual pressure buildup than for the smooth case, with opposite effects for transverse roughness. However, as discussed later, the largest effects of roughness on pressure are expected in the outlet region associated with the EHL spike and the minimum film thickness.

The second more recent application of flow factors is that of Majumdar and Hamrock (ref. 23) who also examined the line contact but who computed the full solution from inlet to outlet. Their boundary conditions set the pressure and its gradient zero at both inlet and outlet, with the inlet fixed at 2.5 Hertz radii upstream of center while the outlet floated, being determined as the first downstream point where the numerical solution fitted the boundary condition. Two striking results were obtained, illustrated for a typical case in figure 6. First, for constant nominal central film thickness (i.e., constant total flow), the rougher the surfaces, the less the load supported for

any value of γ. This is in contrast to other results where transverse roughness has been found to cause an increased load capacity, (e.g., refs. 12 and 24). The other finding is that, again at constant central thickness, greater roughness causes the minimum film thickness to increase for longitudinal roughness but to decrease for the isotropic and transverse cases. While holding central thickness or central pressure constant are clearly different physical constraints, this result and that of reference 22 just described are hard to reconcile. This is particularly so in the longitudinal case where the condition of constant central pressure happens also to be approximately maintained in the calculation of reference 23 due to the very slight dependence of load on Λ.

Further calculations have recently been initiated by the author similar to those of Majumdar and Hamrock but keeping the total load fixed so that both central and minimum film thickness become computed quantities. It is hoped that this new investigation will resolve the seeming inconsistencies. As expected, the work of reference 23 shows a sensitivity of both the amplitude and location of the pressure spike to the roughness parameters. The physical reason for this can be seen from the Reynolds equation (11) which, it will be recalled, is for incompressible flow. The role of density in this equation has been taken over by the pressure flow factors, and roughness effects are the analogue of compressibility effects, except that Λ rather than p is the controlling variable. Any small change in the local Λ value within the piezoviscous zone thus has an additional effect on the reduced pressure gradient, with possibly dramatic consequences for the real pressure. Thus, while the investigation of real surface effects was originally motivated by the need to understand scuffing failure modes, it may well turn out also to have deep implications for pitting or fatigue failure, once the effects of roughness on the pressure spike are understood.

EXTENSION AND OUTLOOK

The flow factor approach to understanding real surface EHL effects has been emphasized in this article for a number of reasons. First, it rests on a good physical foundation using the concept that relative fluctuations in flow are small compared to those of the surface roughness itself. When this holds, the average Reynolds equation for the expectation of the pressure is an excellent approximation. Insofar as the equation reduces to the more intuitive forms for the two cases of one-dimensional roughness, it represents a sound interpolation between these extremes.

Second, the method may be applied directly to EHL calculations without the added complications entailed by a simulation approach. The influence of relevant surface parameters σ and γ then emerges quite naturally.

A further consideration is that the perturbation approach to evaluating the flow factors does not constitute any fundamental limitation on the method since it is possible to calculate to any order in Λ^{-1}. Use of diagrammatic techniques already familiar in theoretical physics to sort out the relevant terms in the iterative series provides a powerful tool for this otherwise lengthy task.

Finally, the extension of the range of Λ to the partial EHL regime by means of asperity contact models is facilitated by the intense activity over the last two decades in this area of dry tribology. There is now a good understanding of the dependence of real contact area and load on surface compliance, as well as of the effect of contact on height distributions. These are the principal mechanical features which need to be brought into the flow model.

Thus, in the simple picture given in reference 12, the partial EHL condition is represented as the equilibrium of the three spring forces shown in figure 7, for which the individual load-compliance relations must be known:

(1) The bulk deformation spring is that of the classical elastic contact problem, just as in full EHL.

(2) The hydrodynamic spring is modified by two additional effects, both resulting from growth of incipient contact. First, it alters the surface height distribution and ACF, and second, if contact is not lifted by micro-EHL, it blocks the flow locally perpendicular to the boundary of the contact region. Attempts have been made to introduce local boundary conditions (ref. 18) and modified height distributions (ref. 25), although there seems to have been no consideration given to the ACF. However, since the influence of the ACF is through γ whose value is unlikely to be changed significantly by contact, this effect may well be the least important.

(3) The asperity spring is well understood, at least for $\Lambda > 1$ (ref. 14). When asperity contacts are mechanically independent, the load is closely proportional to the area of real contact, not because of plastic deformation but through the statistical manner in which new lightly loaded contact spots counterbalance old heavily loaded ones as the total load increases. This is almost independent of the actual force law of the individual asperity, with the result that the asperity spring is dominated by the height distribution.

For yet smaller Λ values, asperity interaction begins to increase the stiffness of the asperity spring quite sharply as the fraction of incipient contact area increases (ref. 16). This marks the beginning of the boundary lubrication regime and the end of the regime where an average flow approach can make a useful contribution.

REFERENCES

1. Hamrock, B. J.; and Dowson, D.: Ball Bearing Lubrication. J. Wiley and Sons, 1981.
2. Sun, D.-C.; and Chen, K. K.: First Effects of Stokes Roughness on Hydrodynamic Lubrication. J. Lubr. Technol., vol. 99, no. 1, Jan. 1977, pp. 2-9.
3. Mandelbrot, B. B.: The Fractal Geometry of Nature. W. H. Freeman, 1982.
4. Thomas, T. R.; and Sayles, R. S.: Some Problems in the Tribology of Rough Surfaces. Tribol. Int., vol. 11, no. 3, 1978, pp. 163-168.
5. Elrod, H. G.: A Review of Theories for the Fluid Dynamic Effects of Roughness on Laminar Lubricating Films. Surface Roughness Effects in Lubrication, D. Dowson, C. M. Taylor, M. Godet, and D. Berthe, eds., Mechanical Engineering Publications, London, 1978, pp. 11-26.
6. Cheng, H. S.: On Some Aspects of Microelastohydrodynamic Lubrication. Surface Roughness Effects in Lubrication, D. Dowson, C. M. Taylor, M. Godet, and D. Berthe, eds., Mechanical Engineering Publications, London, 1978, pp. 71-79.
7. Bennett, J. M.: Measurement of the RMS Roughness, Autocovariance Function and Other Statistical Properties of Optical Surfaces Using a FECO Scanning Interferometer. Appl. Opt., vol. 15, no. 11, Nov. 1976, pp. 2705-2721.
8. Czichos, H.: Tribology. Elsevier, Amsterdam, 1978, p. 130.

9. Dawson, P. H.: Effect of Metallic Contact on the Pitting of Lubricated Rolling Surfaces. J. Mech. Eng. Sci., vol. 4, no. 1, Mar. 1962, pp. 16-21.
10. Dyson, A.: Scuffing - A Review. Tribol. Int., vol. 8, no. 2, Apr. 1975, pp. 77-87.
11. Dyson, A.: Scuffing - A Review - Part II. The Mechanism of Scuffing. Tribol. Int., vol. 8, no. 3, June 1975, pp. 117-122.
12. Johnson, K. L.; Greenwood, J. A.; and Poon, S. Y.: A Simple Theory of Asperity Contact in Elastohydrodynamic Lubrication. Wear, vol. 19, 1972, pp. 91-108.
13. Tallian, T. E.: The Theory of Partial Elastohydrodynamic Contacts. Wear, vol. 21, 1972, pp. 49-101.
14. Thomas, T. R.: Recent Advances in the Measurement and Analysis of Surface Microgeometry. Wear, vol. 33, 1975, pp. 205-233.
15. Shante, V. K. S.; and Kirkpatrick, S.: An Introduction to Percolation Theory. Adv. Phys., vol. 20, 1971, pp. 325-357.
16. Pullen, J.; and Williamson, J. B. P.: On the Plastic Contact of Rough Surfaces. Proc. Roy. Soc., London, vol. A327, no. 1569, Mar. 1972, pp. 159-173.
17. Christensen, H.: Stochastic Models for Hydrodynamic Lubrication of Rough Surfaces. Proc. Inst. Mech. Eng., London, vol. 184, pt. 1, no. 55, 1969-1970, pp. 1013-1022.
18. Patir, N.; and Cheng. H. S.: An Average Flow Model for Determining Effects of Three-Dimensional Roughness on Partial Hydrodynamic Lubrication. J. Lubr. Technol., vol. 100, no. 1, Jan. 1978, pp. 12-17.
19. Patir, N.; and Cheng, H. S.: Application of Average Flow Model to Lubrication Between Rough Sliding Surfaces. J. Lubr. Technol., vol. 101, no. 2, Apr. 1979, pp. 220-230.
20. Tripp, J. H.: Surface Roughness Effects in Hydrodynamic Lubrication: The Flow Factor Method. J. Lubr. Technol., vol. 105, 1983 (to appear).
21. Peklenik, J.: New Developments in Surface Characterization and Measurements by Means of Random Process Analysis. Proc. Inst. Mech. Eng., London, vol. 182, pt. 3K, 1967-1968, pp. 108-126.
22. Patir, N.; and Cheng, H. S.: Effect of Surface Roughness Orientation on the Central Film Thickness in E.H.D. Contacts. Elastohydrodynamics and Related Topics, D. Dowson, C. M. Taylor, M. Godet, and D. Berthe, eds., Mechanical Engineering Publications, London, 1979, pp. 15-21.
23. Majumdar, B. C.; and Hamrock, B. J.: Effect of Surface Roughness on Elastohydrodynamic Line Contact. J. Lubr. Technol., vol. 104, no. 3, July 1982, pp. 401-409.
24. Bush, A. W.; Gibson, R. D.; and Skinner, P. H.: Discussion to B. C. Majumdar and B. J. Hamrock, "Effect of Surface Roughness on Elastohydrodynamic Line Contact." J. Lubr. Technol., vol. 104, no. 3, July 1982, pp. 407-408.
25. Teale, J. L.; and Lebeck, A. O.: An Evaluation of the Average Flow Model for Surface Roughness Effects in Lubrication. J. Lubr. Technol., vol. 102, no. 3, July 1980, pp. 360-366.

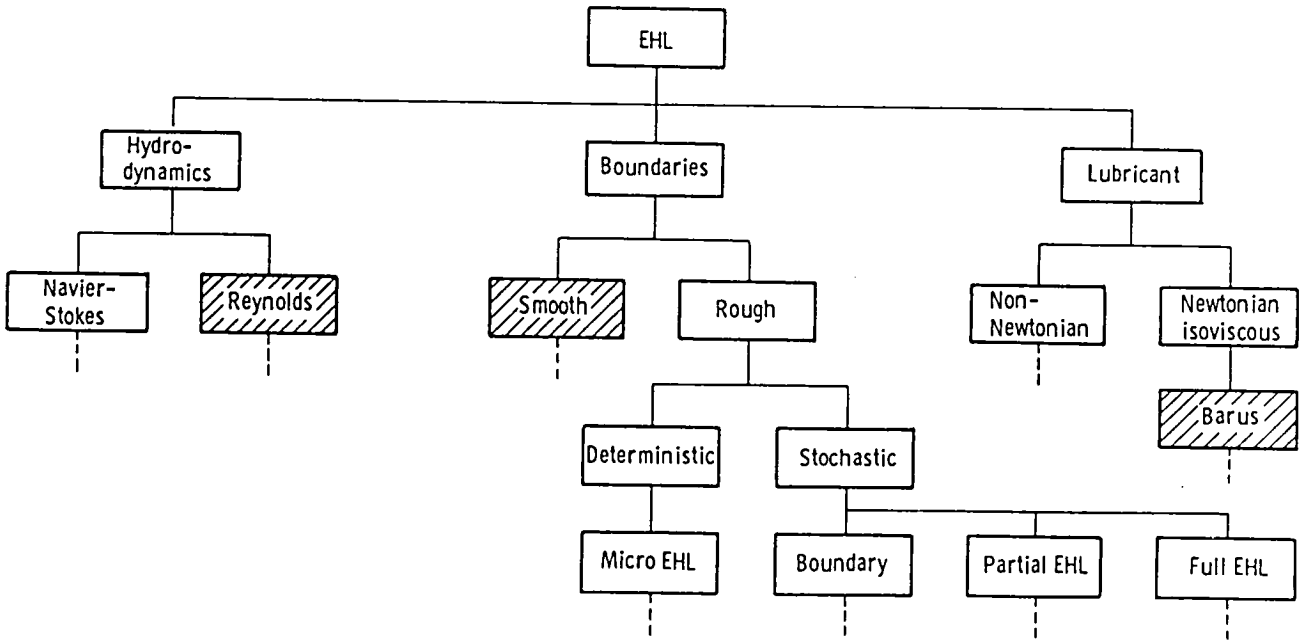

Figure 1. - Some elements contributing to EHL. Only those interrelationships considered in the text are included. Elements of ideal EHL are shaded.

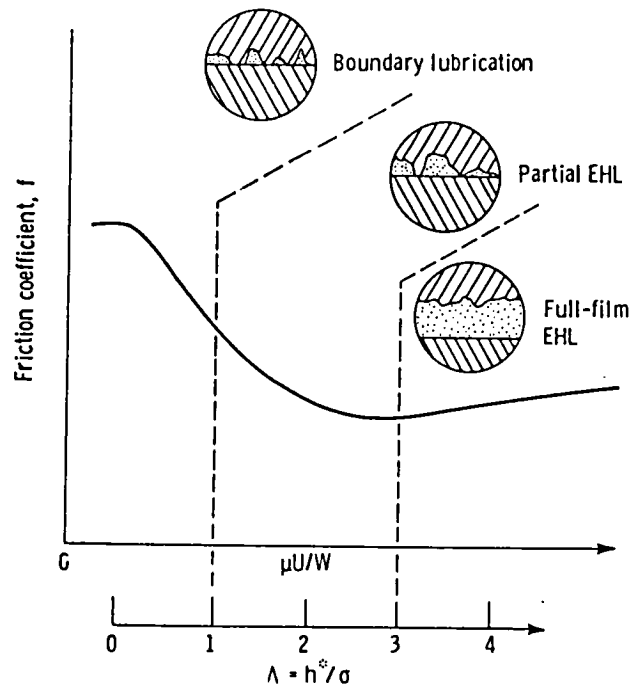

Figure 2. - Regimes of lubrication in lubricated contacts and the Stribeck curve.

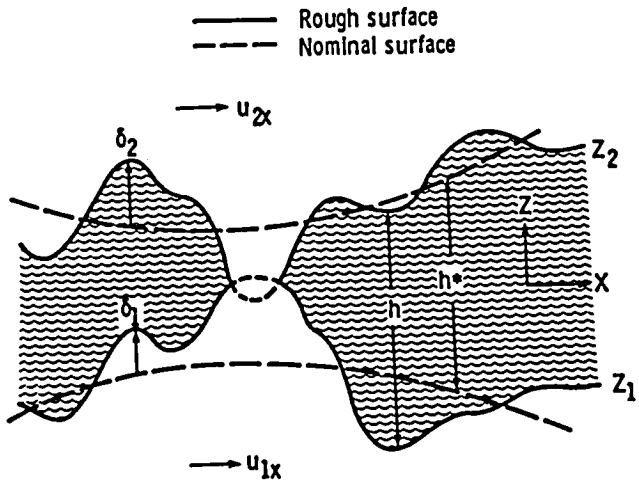

Figure 3. - Variables used to describe lubrication of moving rough surfaces.

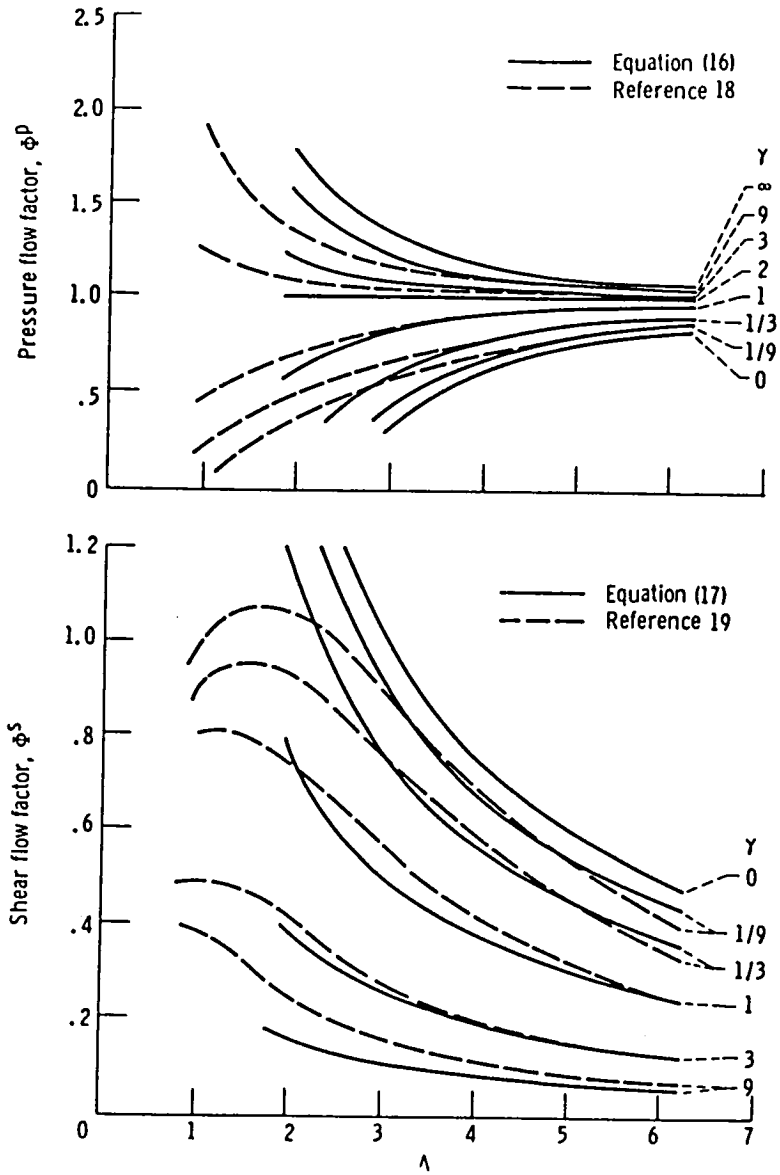

Figure 4. - Comparison of calculated flow factors with those of Patir and Cheng.

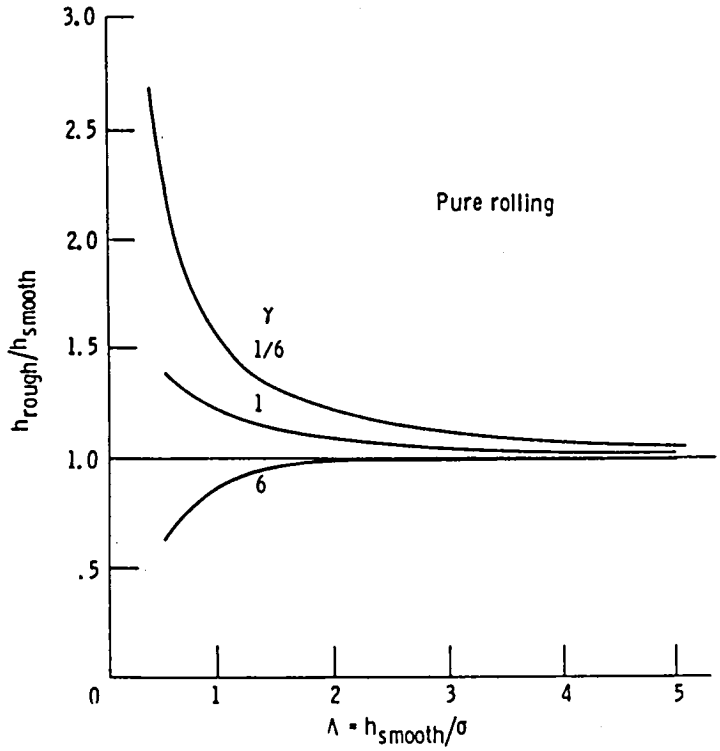

Figure 5. - Effect of Λ on ratio of EHL central film thickness based on rough surfaces to that based on smooth surfaces (ref. 22).

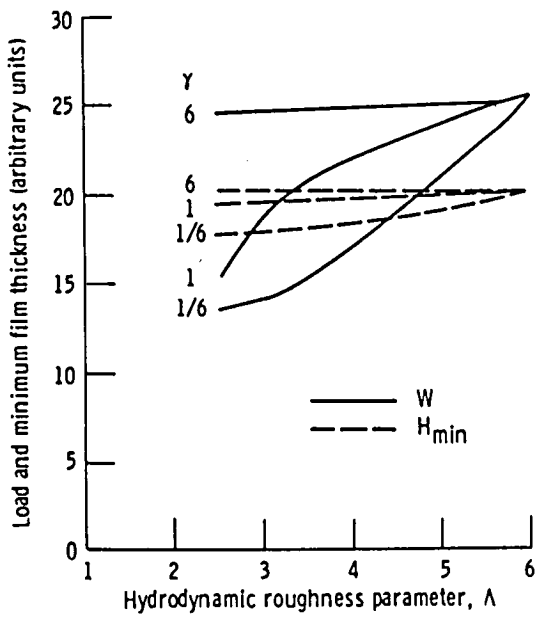

Figure 6. - Variation of EHL load and minimum film thickness for various surface pattern parameters (ref. 23).

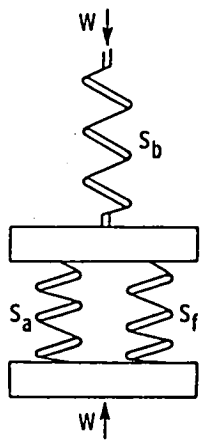

Figure 7. - Diagrammatic representation of flexible elements in partial EHL contact. Spring S_b represents bulk deformation of both bodies; spring S_a represents elastic stiffness of asperities; spring S_f represents hydrodynamic action of oil film. Total load W is shared by S_a and S_f acting in parallel.

MICRO-ELASTOHYDRODYNAMIC LUBRICATION

H. S. Cheng
Department of Mechanical and Nuclear Engineering
Northwestern University
Evanston, Illinois

Conventional elastohydrodynamics, which is based on assumption of smooth surfaces, is reviewed briefly to show its insufficiency for explaining the failure processes in these contacts. For conditions approaching failure, lubrication breakdown occurs locally at asperity contacts where the lubrication behavior is controlled by micro-elastohydrodynamic lubrication (Micro-EHL).

Description is given to the film formation mechanisms in micro-EHL conjunctions. An assessment is made to the level of film thickness due to normal approach and sliding of a single asperity and due to asperity-asperity collision between two asperities. Possible influence of the micro-EHL to incipient scuffing failure, surface crack propagation and wear are discussed.

INTRODUCTION

In lubricated Hertzian contacts, pitting, scuffing and wear are mitigated by lubrication at the interacting asperities. Understanding of the lubrication mechanisms at these small asperity tips has long been recognized as the key for establishing better criteria for prediction of pitting life, onset of scuffing, and wear rate.

It is generally accepted that an asperity has three protective films against surface damage during sliding. These include a thin oxide film immediately adjacent to the substrate, an absorbed or reactive surface film over the oxide film, and a thin oil film just enough to keep the asperity from metallic contact, figure 1(b). Figure 1(b) shows some typical orders of magnitude of the film thickness for the oxide film, adsorbed film, and reactive surface film. For any adhesive damage to occur between sliding asperities, all three films must be broken through either successively or simultaneously. Clearly the first line of defense is the thin oil film at the asperity. The mechanics of oil film formation at the asperity is similar to the conventional elastohydrodynamics but smaller in scale, and, therefore, is generally referred to as micro-elastohydrodynamics (refs. 1,2).

Asperity oil film can be formed by the squeeze film action as the asperity enters the main Hertzian conjunction. This kind of squeeze film analysis is known as the normal approach elastohydrodynamic problem (refs. 3,4). The apserity oil film is enhanced in the interior of the Hertzian conjunction by the wedge action if sliding is present at the interface. In the event that two asperities collide, the film is formed by a combined squeeze and wedge action as indicated by Fowles (refs. 5,6,7).

This paper describes the major features of micro-EHL and gives an assessment of the level of asperity oil film thickness expected between two circumferentially ground rollers due to the three above mentioned micro-EHL mechanisms. Since what occurs at the asperities is strongly dependent on the surrounding average ambient lubricant pressure and temperature, a review is also given to the aspects of macroscopic elastohydrodynamics and their influence on the micro-event. Finally the significance of micro-EHL is illustrated by its possible role on the initiation of cracks on or near the surface and on the adhesion failure at the sliding asperity junction.

SYMBOLS

a^*	semi-axis of elliptical micro-conjunction normal to the surface velocities
b^*	semi-axis of elliptical micro-conjunction parallel to the surface velocities
C	asperity height
E'	$2(1-\nu_1^2/E_1+1-\nu_2^2/E_2)-1$
E_1, E_2	Young modulus of surfaces 1 and 2
G	$\alpha E'$
h	average film thickness in the macro-conjunction
h_T	total film thickness
h_n^*	micro-EHL film thickness due to normal approach of an asperity
h_s^*	micro-EHL film thickness due to sliding of an asperity
h_c^*	micro-EHL film thickness due to asperity-asperity collision
k^*	a^*/b^*, ellipticity ratio of micro-conjunction
p	pressure distribution in the macro-conjunction
Q	$1-e^{-\alpha p}$
R_x^*	asperity radius along the rolling or sliding velocity
R_y^*	asperity radius normal to the rolling or sliding velocity
T_1, T_2	surface temperatures of surfaces 1 and 2 in the macro-conjunction
T_f	mid-plane film temperature in the macro-conjunction
T^*	asperity contact temperature

u	rolling velocity, $(u_1+u_2)/2$
u_1, u_2	velocity of surfaces 1 and 2
u_s	sliding velocity, u_1-u_2
U	$\mu_o U/E'R_x^*$
w	load per unit length of a line contact
w_T	total load of a point contact
W	$w/E'R_x^*$ for line contacts, $w_T/E'R_x^{*2}$ for point contacts
x	coordinate in the rolling or sliding direction
y	coordinate normal to the rolling and sliding direction
α	pressure viscosity coefficient
γ	surface pattern parameter, $\gamma > 1$ for longitudinal asperities and $\gamma < 1$ for transverse asperities
σ	$(\sigma_1^2+\sigma_2^2)^{1/2}$
σ_1, σ_2	r.m.s. surface roughness of surfaces 1 and 2
μ	viscosity of lubricant
μ_o	ambient lubricant viscosity
τ	shear stress distribution in the macro-conjunction

REVIEW OF MACRO-EHL

In most EHL contacts, the shape of the conjunction is an ellipse with its major axis normal to the motion as shown in figure 2. The surfaces in the conjunction zone are either totally or partially separated by the oil pressure generated hydrodynamically at the inlet. The level of separation is determined by the ratio of the average film thickness h_o to the composite surface roughness* σ. When h_o/σ is greater than three, the surfaces are totally separated, the conjunction operates in the full-film mode. In most machine components, this full-film mode is rather infrequent. Most EHL contacts operate in partial-EHL mode ($h_o/\sigma < 3$) where asperities come in close proximity with the opposing surfaces.

Macro-elastohydrodynamics deals with the variation of the average quantities in the conjunction. These include the average film thickness h,

*$\sigma = \sqrt{\sigma_1^2+\sigma_2^2}$, where σ_1 and σ_2 are the r.m.s. roughness of the two surfaces.

pressure p, shear stress τ, surfaces temperatures T_1 or T_2, and oil film temperature T_f. Even though most EHL contacts operate in the regime where the roughness plays a significant role, the characteristics of macro-EHL has been developed on the basis of smooth surface theories. The variation of h and p is best seen in the line contact solution by Dowson and Higginson (ref. 8) for highly loaded contacts. Over the major portion of the conjunction, the film thickness is essential uniform and the lubricant pressure profile is primarily Hertzian. The only deviation from the Hertzian profiles is at the exit end where there is a film constriction accompanied with a secondary pressure peak.

For point contacts having an elliptical conjunction, the film and pressure distributions were analyzed numerically by Hamrock and Dowson (refs. 9-12). Their calculated film thickness contours for a circular contact, figure 3, reveals that the minimum film thickness is at the two sides, not at the center of the contact. The film shape and the minimum film thickness formula based on the numerical results for a wide range of ellipticity ratios were substantiated by film thickness measured optically (refs. 13,14,15).

Most contacts operate in the regime $h/\sigma < 3$. In this regime, the pressure and temperatures are not smooth functions as predicted by the full-film EHL theories; they contain fluctuations due to the asperity interactions. The macro-EHL problem in the partial-film mode primarily deals with the analysis of all average quantities in the conjunction as influenced by the surface roughness. Developments in partial-EHL is still in its early stage; however, there is already evidence showing that the full-film EHL theory is not adequate in predicting (refs. 16,17) the average film thickness in the regime $h_o/\sigma < 3$. In figure 4, the results by Patir and Cheng (ref. 18) are plotted as the ratio the average film thickness including the roughness to that based ons mooth surface EHL theory. They are dependent not only on the film thickness level relative to σ but also on a surface roughness pattern parameter γ. γ can be interpreted physically as the ratio of the average wavelength of the roughness profiles in the direction of flow to that normal to the direction of flow. For $\gamma = 1$, the roughness structure is said to be isotropic. For $\gamma < 1$ the lays are normal to the flow, and the average film becomes much larger than the smooth-surface film thickness as h_o/σ decreases. For lays running in the direction of flow ($\gamma > 1$), the average film thickness is reduced by the longitudinal roughness.

Among the macro-EHL variables, the average film thickness is the most influential variable on micro-EHL because it governs the density of interacting asperities and the severity of each asperity deformation. Besides the film thickness, some evidence is given in (refs. 17,18) that the average lubricant viscosity is also important for determining micro-EHL performance. For a fully pressurized conjunction, the lubricant viscosity can be several decades higher than the ambient viscosity, and the possibility of building a healthy asperity oil film at the micro-EHL conjunction is much higher. The viscosity enhancement can be indicated by a non-dimensional quantity Q where

$$Q = 1 - \frac{\mu_o}{\mu} \tag{1}$$

with $Q = 0$ corresponds to $\mu \to \mu_o$ and $Q = 1$ corresponds to $\mu/\mu_o \to \infty$.

Comparison of partial-EHL analysis (ref. 19) rollers with longitudinal roughness and a large number of scuffing data by Bell et al. (ref. 20) shows that the transitional region from scuffing to non-scuffing corresponds very well to the region where $Q \rightarrow 1$.

MICRO-ELASTOHYDRODYNAMICS

There are three aspects to the micro-EHL problem. The first aspect is the normal approach to the problem which concerns mainly the lubricant film and pressure around single asperity as it enters the Hertzian conjunction. This aspect is more evident in pure rolling contacts. The second aspect occurs when sliding is present. Both the film thickness and the pressure is significantly altered by the wedge action when a single asperity slides over the opposing surface. The third aspect is related to the film and pressure characteristics when two asperities collide during sliding. In this process, both the squeeze-film and wedge-film mechanisms are present. In all three aspects, the lubrication is highly dependent on the asperity geometry and the orientation of the asperity tip with respect to the surface velocities. The micro-EHL film thickness generated by the normal approach, sliding, and asperity-asperity collision are denoted by h_m^*, h_s^*, and h_c^* respectively.

Asperity Geometry

The geometry of asperity tips at the summit of a rough surface depends on the topography resulting from various manufacturing methods. For ground surfaces in gears and rolling bearings, the roughness consists essentially of asperities and depressions in the form of ellipsoidal tips with very high ratios of major to minor axis. Typical profilometer traces (ref. 21) for a run-in ground surface with a CLA roughness of 0.4 μm are shown in figure 5(a) and (b). An analysis of the tip geometry at several maxima for the trace transverse to the lays reveals a distribution of tip radii shown in figure 6(a), which gives a mean tip radius of 117.5 μm. Likewise, the distribution of longitudinal radii is plotted in figure 6(b), which gives a mean tip radius of 4.312×10^4 μm. These average radii were used in assessing the level of film thickness in each of the three micro-EHL mechanisms, h_n^*, h_s^*, and h_c^*.

A Longitudinal Elliptical Asperity

Figure 7 depicts the geometry of a longitudinal elliptical asperity as it transverses through the Hertzian conjunction. The dotted line represents the average film thickness profile obtained from the macro-EHL analysis. Two typical longitudinal asperities are shown here with a normal-approach asperity shown left at the inlet of the macro-conjunction and a sliding asperity shown in the middle of the conjunction.

The normal-approach film thickness h_n^* during touchdown of a longitudinal asperity is considered first. The normal velocity of the asperity at the inlet is $-\mu\ \partial h/\partial x$ where μ is the rolling velocity, $(u_1+u_2)/2$, $\partial h/\partial x$ is the slope of the macro-EHL film profile. The development of micro-EHL film and pressure depends strongly on the ratio of c to h_o, where c is the height of

asperity and h_o is the uniform film thickness in the conjunction. When $c/h_o < 1$, no significant asperity deformation and pressure would build up at the inlet section (ref. 22). However, if c is much greater than h_o, there would be considerable pressure generated due to the squeeze-film action by the downward velocity $-u\ \partial h/\partial x$. The normal approach problem here is mainly to determine the film thickness when the pressure at the center of the asperity becomes sufficiently high to reach the condition $(1-e^{-\alpha p})$ or $Q \to 1$.

If one assumes that the lubricant pressure is high enough to cause $Q \to 1$ but still not high enough to cause any significant elastic deformation, one can use the rigid asperity squeeze-film solution to predict h_n^* when $Q \to 1$.

The pressure generated by the squeeze-film $-u\ \partial h/\partial x$ at a rigid longitudinal ellipsoidal tip is governed by

$$\frac{\partial}{\partial x}\left(\frac{h_T^3}{12\mu}\frac{\partial p}{\partial x}\right) + \frac{\partial}{\partial y}\left(\frac{h_T^3}{12\mu}\frac{\partial p}{\partial y}\right) = u\frac{\partial h}{\partial x} \tag{2}$$

where p is the pressure at the asperity, μ is the viscosity, h_T is the total film thickness including the asperity height, and h is the thickness without considering the asperity height. For very large b^*/a^*, $\partial p/\partial x$ can be neglected in comparison to $\partial p/\partial y$, equation (2) without the first term can be readily integrated to determine h_n^* when $Q \to 1$. The resulting normal approach film thickness at the inlet section is

$$h_n^*/R_y^* = \sqrt{-12\,\frac{\mu_o u \alpha}{R_y^*}\frac{\partial h}{\partial x}} \tag{3}$$

where R_y^* is the local radius of the asperity in y direction (normal to the surface velocity, μ_o the ambient viscosity, α the pressure viscosity coefficient, and $\partial h/\partial x$ the slope of film profile, excluding the asperity, at the inlet of the macro-conjunction.

Values of h_n^*/R_y^* can be calculated using c/h_o and p_o/E' as parameters ($\partial h/\partial x$ is determined by p_o/E' and the Hertzian profile at the inlet of the macro-conjunction). Figure 8 shows some results for $p_o/E' = 0.003$. It is seen that h_n^*/R_y^* is higher for larger c/h_o because a greater asperity height touches down farther from the inlet edge and introduces a larger normal approach velocity $u\frac{\partial h}{\partial x}$. Figure 8 can also be used to assess the level of h_n^* expected in circumferentially ground rollers with a mean value of $R_y^* \simeq 117$ µm (0.0047 in.). Using u = 10 m/sec. (400 in/s) and μ_o = 10 c.p. (1.45×10^6 lb.s/in^2), h_n^* is only about 35Å (0.14 µ in.) a very small film thickness.

The micro-EHL film for a sliding longitudinal asperity h_s^*, shown in figure 7, can be estimated by the point contact formula due to Hamrock and Dowson (refs. 9-12). Even though their analysis was primarily intended for elliptical contacts with the long axis normal to the motion, it was confirmed recently by Koye and Winter (ref. 15) with optical measurements that Hamrock and Dowson's formula also yields a reasonable approximation for elliptical

contacts with the long axis oriented in the direction of motion.

According to Hamrock and Dowson (ref. 12), the minimum film thickness in an elliptical micro-conjunction is

$$\frac{h_s^*}{R_x^*} = 3.63\, U^{0.68}\, G^{0.49}\, W^{-0.073}(1-e^{-0.68k^*}) \tag{4}$$

when U, G, W are defined in the list of symbols, and $k^* = a^*/b^*$, the ellipticity ratio of micro-conjunction. It is interesting to note that for a very small ellipticity ratio,

$$\begin{aligned}(1-e^{-0.68k^*}) &\cong 0.68k^* \\ &\cong 0.68 \times 1.03\,(R_y^*/R_x^*)^{0.64}\end{aligned} \tag{5}$$

Using this approximation, it is readily shown that

$$h_s^* \propto R_y^{*0.466}\left(\frac{R_y^*}{R_x^*}\right)^{0.174} \tag{6}$$

Thus, for micro-conjunctions with a constant k^*, the ratio (R_y^*/R_x^*) is constant, and the micro-EHL film due to sliding is, therefore, influenced more by the asperity radius R_y^* in the direction normal to sliding, and less by the larger asperity radius R_x^* in the direction of sliding.

Using the mean asperity radii found earlier for typical ground rollers ($R_y^* \cong 117.5$ μm and $R_x^* = 4.312 \times 10^4$ μm), G = 3000, $p_o/E' = .003$, h_s^*/R_y^* is evaluated from equation (4) and plotted as figure 8 as a function of the sliding speed parameter $\mu_o u_s/2E'R_y^*$. If an ambient viscosity of 10 c.p. and $(1.45 \times 10^{-6}$ lb-sec/in.$^2)$ and a sliding velocity of 2.5 m/s (100 in/s.) are used, h_s^* is found to be 43Å (0.172 μ in.) a very small film thickness. However, in the interior of the conjunction the viscosity is much higher than the ambient viscosity μ_o due to a higher fluid pressure. Therefore, as the asperity moves into the interior, h_s^* becomes much thicker. A qualitatively variation of h_s^* as a function of the asperity location is shown in figure 7. A natural question here is how thick should h_s^* be for micro-EHL to be considered as effective. The answer to this question seems to depend on the details of the secondary roughness on the asperity tipe. For the purpose of this assessment, it is assumed that an effective micro-EHL is achieved if h_s^* is greater than 1/4 of the height of the asperity. The mean height for the group of asperities tips in figure 5 was found to be 0.3 μm (12 μ in.). The viscosity to increase h_s^* form 43Å (.172 μ in.) at the inlet to 0.075 μm (3 μ in.) in the interior is approximately 67 times the ambient. This would require Q = 0.985 and a lubricant pressure p = 0.290 GPa (42,000 psi) with α = 14.5 1/GPa (.0001 in^2/lb), to achieve an effective micro-EHL.

A Transverse Elliptical Asperity

Figure 9 shows three possible situations for developing a micro-EHL film for an elliptical asperity oriented transversely with respect to the flow. At the inlet, a film is developed due to the touch down of the asperity. The mechanism for forming this normal-approach film is similar to that discussed earlier for the longitudinal asperity. Since the level of normal approach film for a transverse asperity is expected to be small in comparison to the film developed by sliding, it is not considered in this section.

The film thickness developed by sliding against a transverse elliptical asperity of a large R_y^*/R_x^* can be estimated by using the following line contact formula by Dowson and Higginson (ref. 8).

$$\frac{h_s^*}{R_x^*} = 2.65\, U^{0.7}\, G^{0.54}\, W^{-0.13} \tag{7}$$

For G = 3000 and $p_o/E' = 0.003$, h_s^*/R_x^* is plotted on figure 10 to compare with the film thickness generated during collision between two identical transverse elliptical asperities. Using u_s = 2.5 m/s (100 in./s), μ_o = 10 c.p. (1.45×10^{-6} lb.sec/in.^{2}), R_x^* = 117 μm (0.0047 in.), one obtains h_s^* = 240Å (0.96 μ in.). Thus, by turning a sliding longitudinal elliptical asperity 90° with its major axis normal to the flow, a five times more film thickness can be generated in the micro-conjunction. In the interior the the macro-conjunction, h_s^*, as shown in figure 9, is expected to be thicker for the reason discussed earlier. If one uses a h_s^* of 0.075 μm (3 μ in.) as the minimum film thickness for achieving an effective micro-EHL, the required Q and lubricant pressure p are found to be 0.813 and .115 GPa (16,750 psi) respectively. These results indicate that it requires only a moderate increase in viscosity to achieve an effective micro-EHL.

The film thickness generated during a collision between two identical asperities can be estimated from the asperity-asperity EHL solutions by Fowles (refs. 5,6,7). By plotting his isothermal results for collisions with a large interference at the tips, one can arrive at the following formula for predicting the non-dimensional film thickness

$$\frac{h_c^*}{R_x^*} = 0.149\sqrt{\frac{\alpha\mu_o u_s}{R_x^*}} \tag{8}$$

This relation is valid for an interference $\phi/R_x^* > 2 \times 10^{-5}$ and G > 1500. It should also be noted that in Fowles' solution h_c^* is the minimum film thickness in the micro-conjunction, not the center film thickness. Results based on equation (8) is plotted in figure 10. It is seen that the asperity-asperity collision process is more effective in generating a micro-EHL film than sliding against a single asperity. If one uses the same conditions considered earlier (G = 3000, u_s = 2.5 m/s (100 in./s), R_x^* = 117 μm (0.0047 in.)), the viscosity μ required inside the conjunction to achieve a minimum effective

micro-EHL film thickness h_c^* = 0.075 μm (3 μ in.) is found to be 59.5 c.p. which is certainly an easily achievable viscosity in a macro-EHL conjunction.

A Transverse Asperity Ridge

When the ratio of asperity radii R_y^*/R_x^* becomes infinity, an elliptical asperity degenerates into an asperity ridge. Such geometries are highly idealized limiting cases of surfaces containing long lays. The case of transverse asperity ridges is of particular interest because its pressure and film characteristics can be readily analyzed with an extension of the present line contact EHL theory. Moreover, the pressure perturbations caused by sliding against a transverse asperity ridge represent probably the most severe case among all possible micro-EHL geometries.

The extension of a line contact EHL solution to determine the pressure and subsurface stresses around an asperity ridge was carried out by Cheng and Bali (ref. 23). In their analysis, a surface shear stress proportional to the normal stress is also included. Figure 11 shows typical film thickness profiles and pressure intensifications caused by sliding against a stationary transverse asperity ridge located at x/b = -0.5, i.e., halfway between the inlet and the center of the conjunction. Two cases are shown here, the solid curves are for a taller asperity ridge with a height three times the nominal film thickness h_o. The dotted curves are for an asperity height 1.5 times h_o. It is seen that the asperity height is completely flattened out due to sliding and the flattening gives rise to a local pressure increase very similar to a Hertzian elliptical distribution. Figure 12 shows the contours of the octahedral shear stresses for the pressure profile shown in figure 11 for the taller asperity. The maximum shear stress is subsurface and occurs at about a depth 1/2 b^* where b^* is the half width of the micro-conjunction. For a tall asperity ridge, the maximum shear stress can easily exceed the shear yield stress of the material.

Viscoplasticity of the Lubricant

In recent years, traction measurements in sliding EHL contacts (refs. 24,25) have proven that lubricant under high pressure inside the conjunction is non-Newtonian. It behaves like a viscoplastic substance with a limiting shear stress when sheared under a high pressure. This non-Newtonian behavior has a strong effect in reducing the traction but its effect on the film forming mechanism at the inlet of an EHL conjunction does not appear to be too significant. In micro-EHL conjunctions, the surrounding lubricant viscosity in the valleys can become extremely high. Under this high ambient lubricant pressure, the lubricant can reach its limiting shear stress quickly at the inlet of a micro-conjunction, and, therefore, may drastically reduce the film forming capability as predicted from the Newtonian model.

The limiting shear stress model was recently used by Sheu and Wilson (ref. 26) to study the film forming capability in sliding against rigid triangular ridges. They conducted an isothermal analysis and demonstrated that for ridges with extremely small slope and height, the minimum film thickness initially increases with the product of viscosity and sliding speed until the shear stress at the sliding fluid-solid interface reaches the

limiting shear stress. At that point, the film would suddenly collapse. Since the ambient viscosity around the sliding asperities is expected to be very high, it is possible that the same phenomenon may also occur leading to a film breakdown at the inlet of these sliding micro-conjunctions.

While Sheu and Wilson's provocative analysis seems to cast some doubt on the validity of all Newtonian analyses in predicting the micro-EHL film thickness, there are also other recent positive evidences which seem to support the existence of a reasonable film thickness in micro-EHL contacts. Gecim and Winer (ref. 27) recently conducted a Grubin type inlet analysis considering a limiting shear model for the lubricant. They found that the reduction in film thickness due to the limiting shear effect is dependent on the slide to roll ratio. For small slide to roll ratios, this non-Newtonian effect is hardly noticeable. Even for the simple sliding case, only a 40% decrease in film thickness is found. They did not find a film collapsing caused by the shear stress reaching its limiting value at the sliding interface.

Cusano and Wedeven (refs. 28-30) recently measured the optical film thickness between a sapphire flat and a ball which contains three man-made asperity ridges. Figure 13 shows typical measured film thickness profiles for a pure rolling as well as a sliding case. It is seen that the asperity ridges for the sliding case is deformed locally and lifted up by micro-EHL. The level of micro-EHL film appears to be somewhat higher than that calculated from Dowson and Higginson's theory 0.04 μm (1.6 μ in.).

Asperity Temperature

Figure 14 depicts the temperature rise within a micro-conjunction. In this model, the average macroscopic surface temperature T_1 and T_2 is permitted to be unequal to account for any insulating effect from the average lubricant thickness in the valleys. However, within the micro-conjunction the temperature for both surfaces are matched. By matching the conjunction temperature, it can be readily shown (ref. 31) that the asperity temperature T^* is

$$T^* = \left(\frac{T_1}{\Delta T_{1P}} + \frac{T_2}{\Delta T_{2P}} + 1\right)\left(\frac{1}{\Delta T_{1P}} + \frac{1}{\Delta T_{2P}}\right)^{-1} \tag{9}$$

where ΔT_{1P} or ΔT_{2P} are the conjunction temperature rise of surface 1 or 2 if each were to receive the entire heat flux. It should be noted here that if $T_1 = T_2$, equation (9) reduced to the harmonic mean temperature relation proposed by Archard (ref. 32).

$$\frac{1}{\Delta T^*} = \frac{1}{\Delta T_{1P}} + \frac{1}{\Delta T_{2P}} \tag{10}$$

The macro-temperatures T_1 and T_2 in EHL contacts can be calculated numerically by using Pu and Ling's method (ref. 33) and the asperity temperature rises ΔT_{1P} and ΔT_{2P} for ellipsoidal asperities without considering matching of

conjunction temperature can be calculated by Lowen and Shaw's formula (ref. 34) for a stationary surface and by Jaeger's formula (ref. 35) for a fast moving surface. The entire numerical procedure is recently demonstrated by Lai and Cheng (ref. 31) for calculating the distribution of asperity temperatures in simple sliding EHL contacts.

Micro-EHL and Surface Damage

Among the many failure modes in EHL contacts, surface pitting and scuffing are more related to micro-EHL. Surface pitting are originated from micro-cracks initiated near the surface in the early stages during the entire life. The depth of these micro-cracks usually is of the same order of the minor width of the asperity conjunctions. In some cases, these micro-cracks merge or branch to the surface to form groups of shallow micro-pits known as surface peeling or gray staining. In other cases, one of the deeper cracks gradually propagate inwardly along an inclined plane usually 20-30° from the surface in the direction opposite to the rolling direction. As the propagating crack reaches the vicinity of maximum shear stress, the crack tip may breakaway to form a deep pit.

The above description of surface pitting indicate clearly that the initiation of surface cracks and formation of shallow pits is influenced by the variation of the local asperity pressure p^* and local shear stress τ^* as it traverses through the macro-conjunction. What is needed is a criterion to relate the density and size distribution of these surface cracks as a function of the distribution of p^* and τ^* which can be predicted from micro-EHL analysis.

Scuffing is characterized by local transfer of materials generally from a hot asperity tip onto a colder surface through plastic deformation of the hot asperity followed by gross adhesion on to the colder surface. As mentioned earlier in the introduction, scuffing is protected not only by the micro-EHL but also by a boundary type surface film and oxide film. Micro-EHL is the first line defense. There is insufficient evidence to support whether a micro-EHL breakdown would automatically lead to surface film failure. However, there is overwhelming evidence that failures of all three films are linked to asperity temperature T^* even though the exact mechanisms are still unclear. Since prediction of T^* requires p^* and τ^*, a thorough understanding of scuffing seems to need a complete knowledge of micro-EHL performance.

CONCLUDING REMARKS

Origins of surface pitting and scuffing damage in elastohydrodynamic contacts are identified at individual asperities where the failure mechanisms are influenced strongly by micro-EHL characterized by the local aspserity oil film thickness, local pressure fluctuation, shear stress, and temperature.

Asperity tip geometry varies widely in shape. For ground surfaces, the tip of an ellipsoid can be used as an idealized geometry for analysis. Analysis of a typical run-in ground surface with an r.m.s. roughness of 0.4 μm (16 μ in) gives two mean principal radii of 117 μm (.0047 in) and 4.32 ×

10^4 μm (1.73 in).

The asperity oil film developed at an ellipsoidal tip is dependent on: (1) the orientation of its major axis with respect to the surface motion; (2) the degree of viscosity enhancement around the asperities in the macro-EHL conjunction; (3) the relative sliding velocity at the asperity.

For longitudinal asperities with the major axis parallel to the surface the asperity film thickness generated based on a sliding speed of 2.5 m/s (100 in/s) without considering any viscosity enhancement is extremely small and is not expected to provide much protection against sliding damage. To provide an effective micro-EHL film a 100 times increase in viscosity in the macro-conjunction is needed.

For transverse asperities, the film forming capability is much improved. The film thickness in a sliding transverse asperity is found to be approximately five times more than that developed in longitudinal asperities under the same conditions. However, without any viscosity enhancement the level of film thickness is still insufficient as an effective micro-EHL film. An increase in viscosity approximately 10 times is found to be sufficient to provide a protective film.

Recent analysis of viscoplastic effect of lubricant using rigid triangular asperities (ref. 26) demonstrated that a thin film can collapse if the shear stress at the interfaces in the inlet region reaches the limiting shear stress. It is not certain whether the same film collapsing mechanism exists in micro-EHL conjunction sliding in a pool of pressurized lubricant. Further work is needed.

ACKNOWLEDGMENT

This paper represents a part of the research efforts on thin film lubrication supported by gifts received from ALCOA Foundation and Mobil Foundation.

REFERENCES

1. Christensen, H.: Microelastohydrodynamics. Chapter IV of Technical Report MTI 67TR23, May 1967.

2. Cheng, H. S.: On Some Aspects of Micro-Elastohydrodynamic Lubrication. Proceedings of 4th Leeds-Lyon Symposium on Lubrication, pp. 71-76, April 1977.

3. Christensen, H.: The Oil Film in A Closing Gap. Proc. Roy. Soc. A 266, 312, 1962.

4. Lee, K. M. and Cheng, H. S.: The Pressure and Deformation Between Two Normally Approaching Lubricated Cylinders. Journal of Lubrication Technology, ASME Trans., Vol. 95, pp. 308-321, July 1973.

5. Fowles, P. E.: The Application of Elastohydrodynamic Theory to Individual Asperity-Asperity Collisions. Journal of Lubrication Technology, ASME Trans., Vol. 91, pp. 464-476, 1969.

6. Fowles, P. E.: A Thermal Elastohydrodynamic Theory for Individual Asperity-Asperity Collision. Journal of Lubrication Technology, ASME Trans., Vol. 93, pp. 383-397, 1971.

7. Fowles, P. E.: The Statistical Application of a Thermal EHL Theory for Individual Asperity-Asperity Collision to the Sliding Contact of Rough Surfaces. Journal of Lubrication Technology, ASME Trans., Vol. 97, pp. 311-320, 1975.

8. Dowson, D. and Higginson, G. R.: The Effect of Material Properties on the Lubrication of Elastic Rollers. Fluid Mech. Engng Sci. 2(3), 188.

9. Hamrock, B. J. and Dowson, D.: Isothermal Elastohydrodynamic Lubrication of Point Contacts. Part I - Theoretical Formulation. Journal of Lubrication Technology, Vol. 98, No. 2, pp. 223-229, April 1976.

10. Hamrock, B. J. and Dowson, D.: Isothermal Elastohydrodynamic Lubrication of Point Contacts. Part II - Ellipticity Parameter Results. Journal of Lubrication Technology, Vol. 98, No. 3, pp. 383-385, July 1976.

11. Hamrock, B. J. and Dowson, D.: Isothermal Elastohydrodynamic Lubrication of Point Contacts. Part III - Fully Flooded Results. Journal of Lubrication Technology, Vol. 99, No. 2, pp. 264-276, April 1977.

12. Hamrock, B. J. and Dowson, D.: Isothermal EHD Lubrication of Point Contacts. Part IV - Starvation Results. Journal of Lubrication Technology, Vol. 99, No. 1, pp. 15-23, January 1977.

13. Sanborn, D. M., and Winer, W. O.: Fluid Rheological Effects in Sliding Elastohydrodynamic Point Contacts with Transient Loading: I - Film Thickness. Journal of Lubrication Technology, ASME Trans., Vol. 93, No. 2, pp. 262-271, 1971.

14. Koye, K. A. and Winer, W. O.: An Experimental Evaluation of the Hamrock and Dowson Minimum Film Thickness Equation for Fully Flooded EHD Point Contacts. Journal of Lubrication Technology, ASME Trans., Vol. 103, No. 2, pp. 284-295, April 1981.

15. Westlake, F. J. and Cameron, A.: Interferometric Study of Point Contact Lubrication. EHD Lubrication Symposium, Paper C 39/72, pp. 153, 1972.

16. Chow, L. S. H. and Cheng, H. S.: The Effect of Surface Roughness on the Average Film Thickness Between Lubricated Rollers. Journal of Lubrication Technology, ASME Trans., Series F, Vol. 98, No. 1, pp. 117-124, January 1976.

17. Patir, N. and Cheng, H. S.: Effect of Surface Roughness Orientation on the Central Film Thickness in EHD Contacts. Proceedings of the 5th Leeds-Lyon Symposium on Tribology, pp. 15-21, April 1979.

18. Dyson, A.: A Failure of EHD Lubrication of Circumferentially Ground Discs. Proceedings of IME, Vol. 190, 52/76, 1976.

19. Cheng, H. S. and Dyson, A.: Elastohydrodynamic Lubrication of Circumferentially-Ground Rough Disks. ASLE Trans., Vol. 21, 1, pp. 25-40, 1978.

20. Bell, J. C.; Dyson, A.; and Hadley, J. W.: The Effects of Rolling and Sliding Speeds on the Scuffing of Lubricated Steel Discs. ASLE Trans., Vol. 18, No. 1, pp. 62-73, 1973.

21. Bell, J. C. and Dyson, A.: Mixed Friction in an Elastohydrodynamic System. Paper No. c12/72, 2nd Symposium on Elastohydrodynamic Lubrication, Institution of Mechanical Engineers, 1972.

22. Chow, L. S. H. and Cheng, H. S.: Pressure Perturbation in EHD Contacts Due to an Ellipsoidal Asperity. Journal of Lubrication Technology, ASME Trans., Series F, Vol. 98, No. 1, pp. 8-15.

23. Cheng, H. S. and Bali, M.: Stress Distributions Around Furrows and Asperities in EHL Line Contacts. Solid Contact and Lubrication, Edited by Cheng and Keer, ASME Publication AMD-Vol. 39, pp. 205-222, 1980.

24. Johnson, K. L. and Tevaarwerk, J. L.: Shear Behavior of EHD Oil Films. Proc. Roy. Soc. London, A 356, pp. 215-236, 1977.

25. Bair, S. and Winer, W. O.: Shear Strength Measurements of Lubricants at High Pressure. Journal of Lubrication Technology, ASME Trans., Vol. 101, No. 3, pp. 251-257, July 1979.

26. Sheu, S. and Wilson, W. R. D.: Viscoplastic Lubrication of Asperities. ASME Paper 81-Lub-43, Presented at the ASME/ASLE Joint Lubrication Conference, New Orleans, 1981.

27. Gecim, B. and Winer, W. O.: Lubricant Limiting Shear Stress Effect on EHD Film Thickness. Journal of Lubrication Technology, ASME Trans., Vol. 102, April 1980.

28. Wedeven, L. D.: Influence of Debris Dent on EHD Lubrication. ASLE Trans., Vol. 21, No. 1, pp. 41-52.

29. Cusano, C. and Wedeven, L. D.: Elastohydrodynamic Film Thickness Measurements of Artifically Produced Nonsmooth Surfaces. ASLE Trans., Vol. 24, No. 1, pp. 1-14.

30. Cusano, C. and Wedeven, L. D.: The Effects of Artificially-Produced Defects on the Film Thickness Distribution in Sliding EHD Point Contacts. ASME Paper 81-Lub-46, Presented at the ASME/ASLE Lubriction Conference, New Orleans, 1981.

31. Lai, W. T. and Cheng, H. S.: Asperity Temperature in Simple Sliding Contacts. Submitted for publication, 1982.

32. Archard, J. F.: The Temperature of Rubbing Surfaces. Wear, Vol. 2, pp. 438-455, 1958/59.

33. Ling, F. F. and Pu, S. L.: Probable Interface Temperature of Solids in Sliding Contact. Wear, 7(23), 1964.

34. Lowen, E. G. and Shaw, M. C.: On the Analysis of Cutting-Tool Temperatures. ASME Trans, Vol. 76, pp. 217-231, 1954.

35. Jaeger, J. C.: Moving Sources of Heat and the Temperature at Sliding Contacts. Journal Proceedings of Roy. Soc. N.S.W. 76(203), 1942.

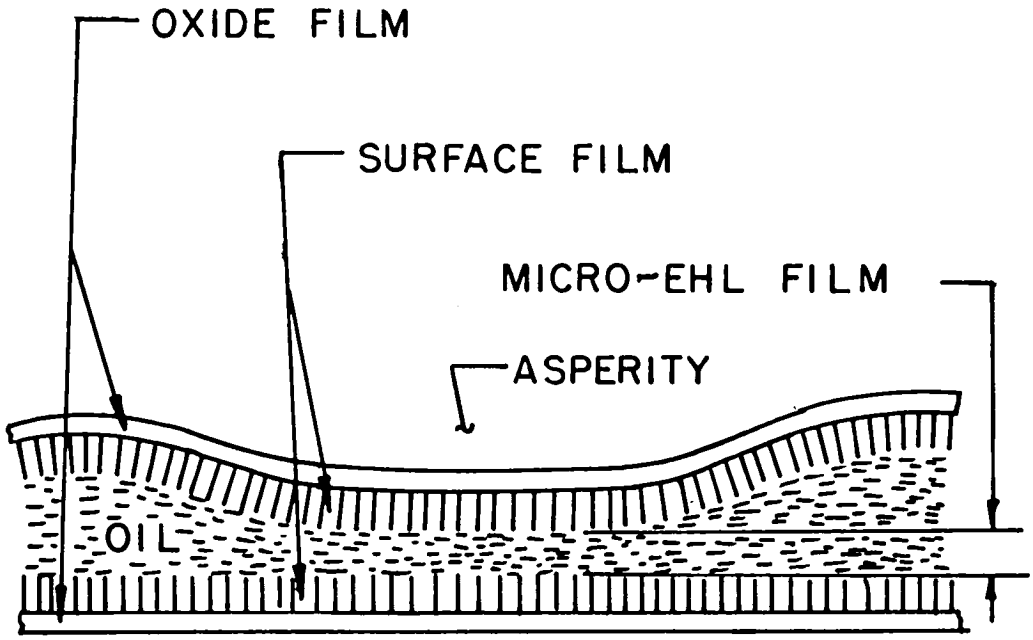

Fig. 1(a) Protective films for an asperity

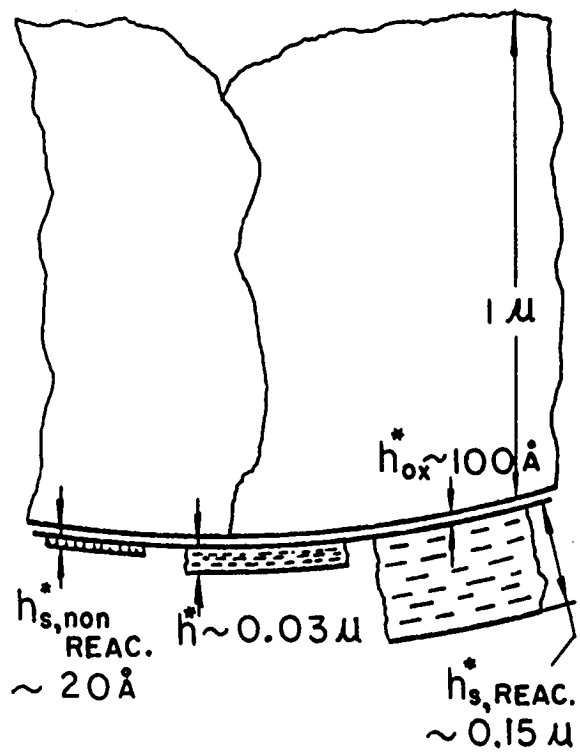

Fig. 1(b) Typical thickness of different surface films

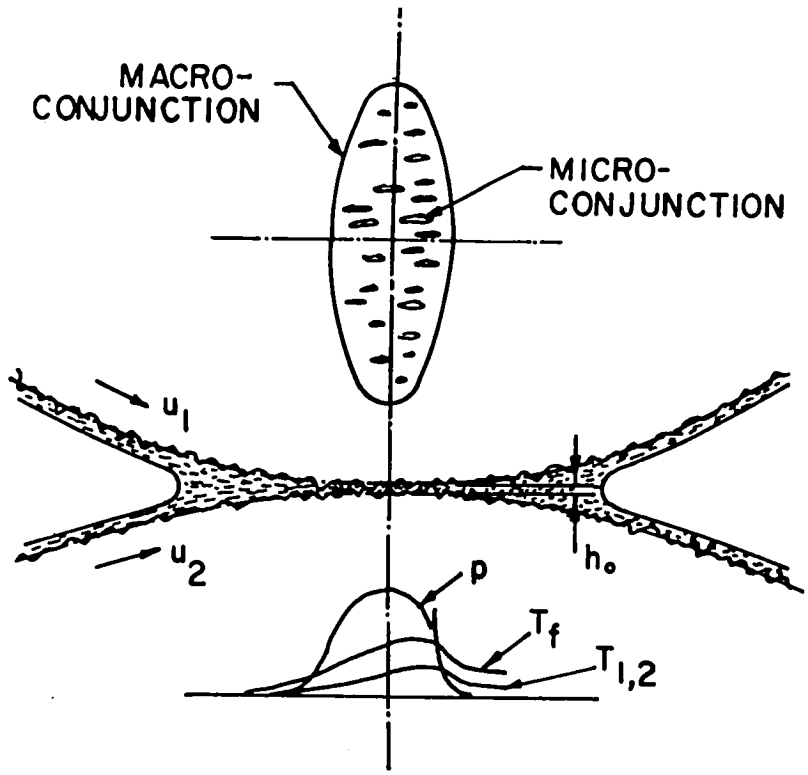

Fig. 2 Geometry of macro-EHL and micro-EHL conjunctions

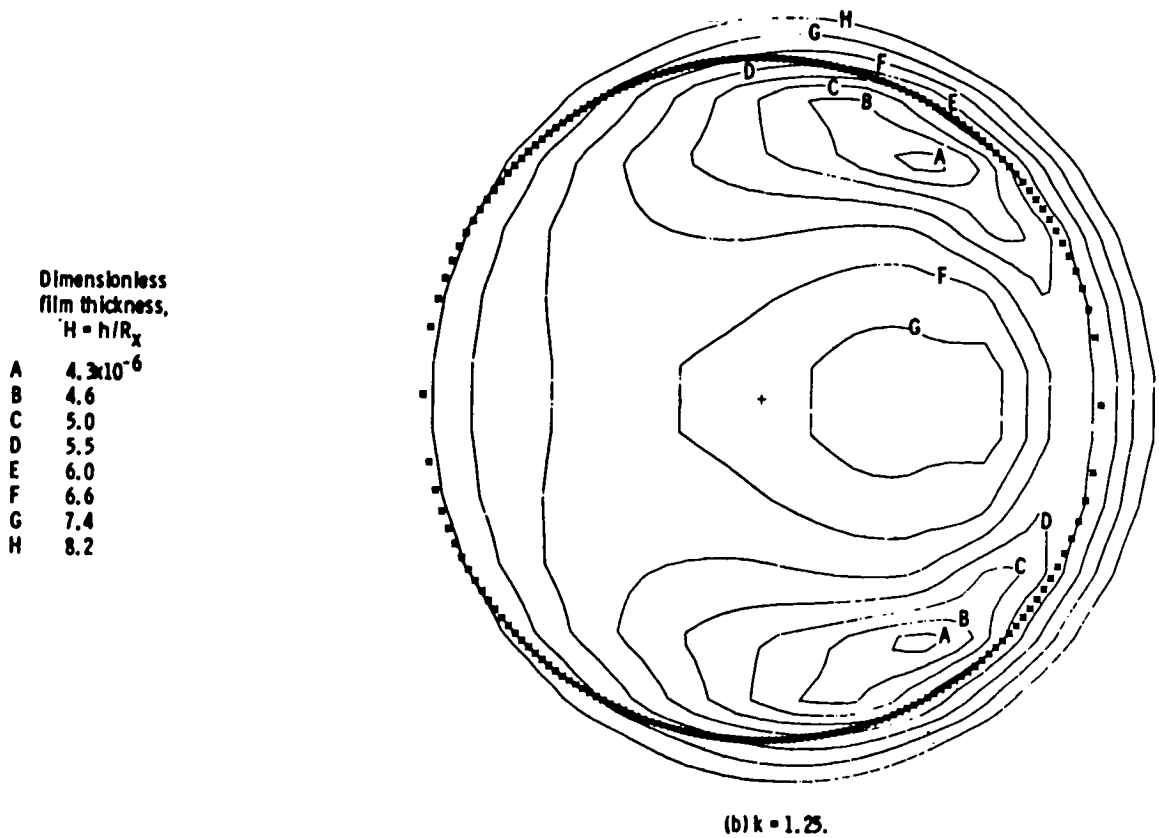

Fig. 3 Film thickness contours in EHL point contact

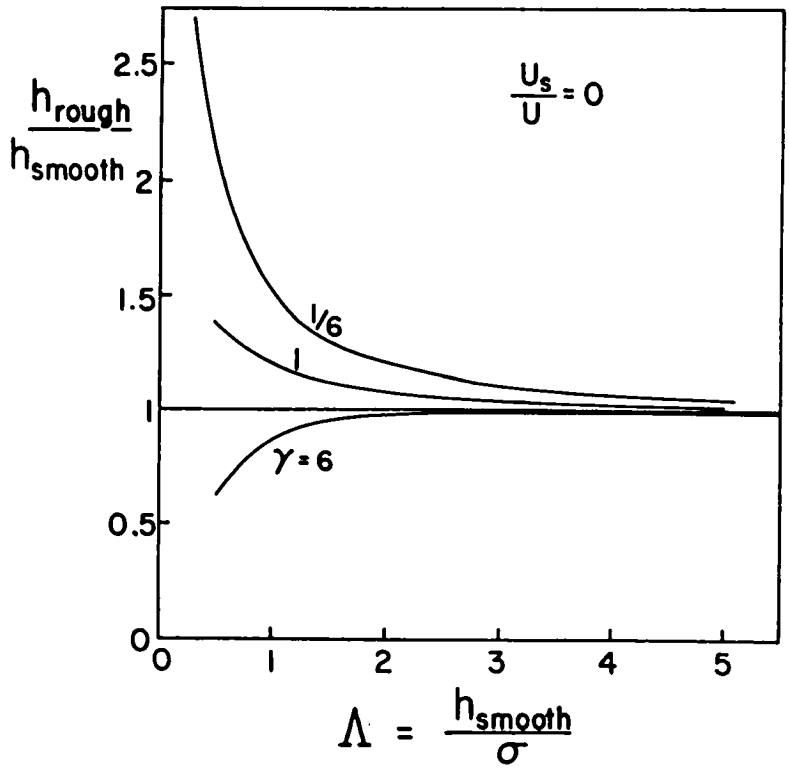

Fig. 4 Effect of roughness on average EHL film thickness

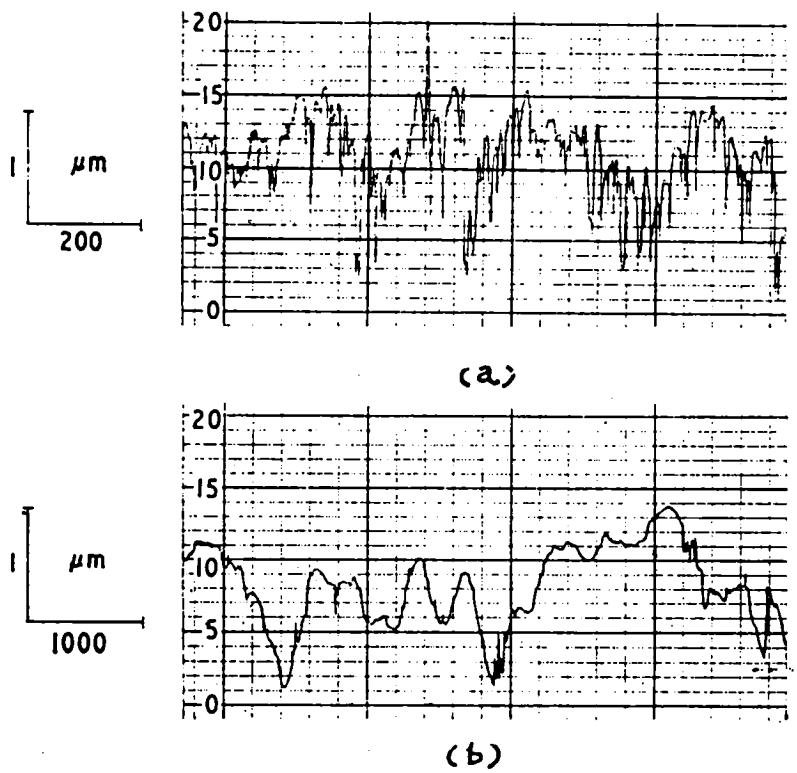

Fig. 5 Typical profiles of ground surfaces (a) axial, (b) circumferential

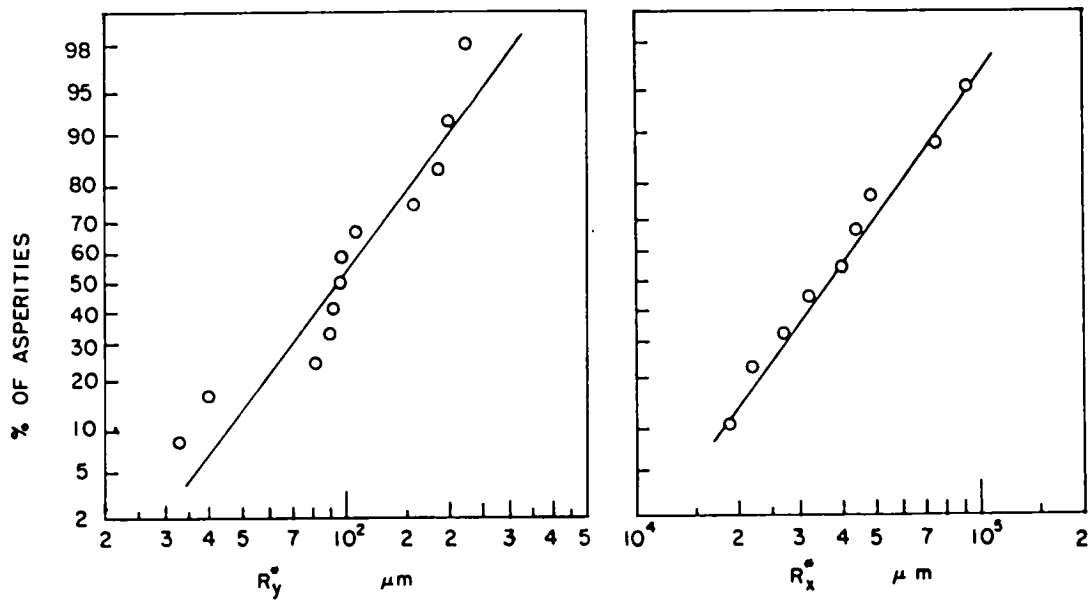

Fig. 6 Distributions of asperity tip radii (a) axial, (b) circumferential

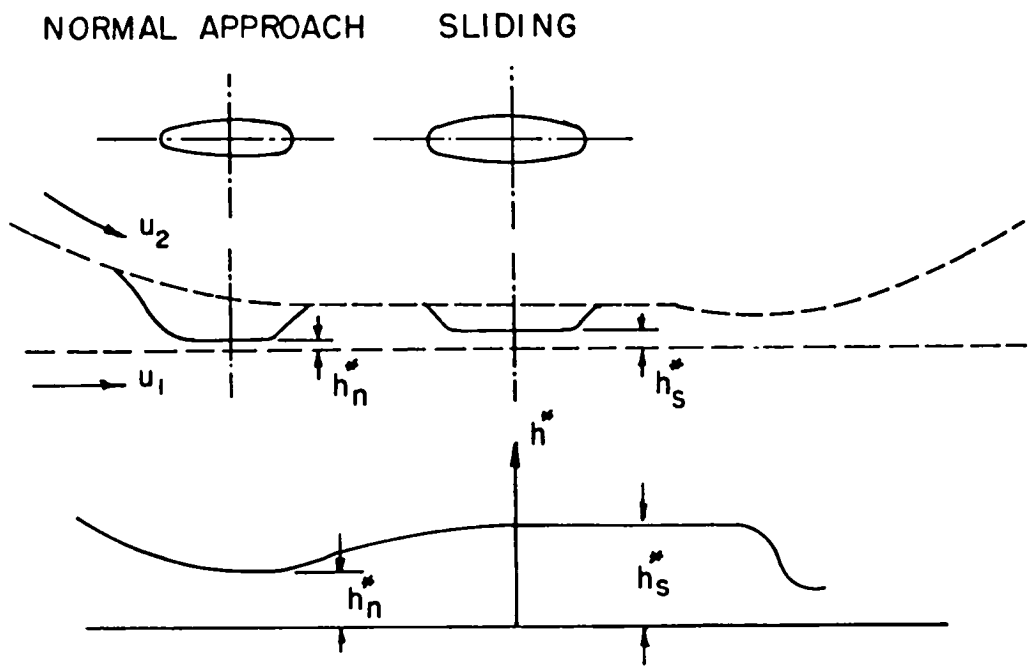

Fig. 7 Film formations by normal approach or sliding in a longitudinal asperity

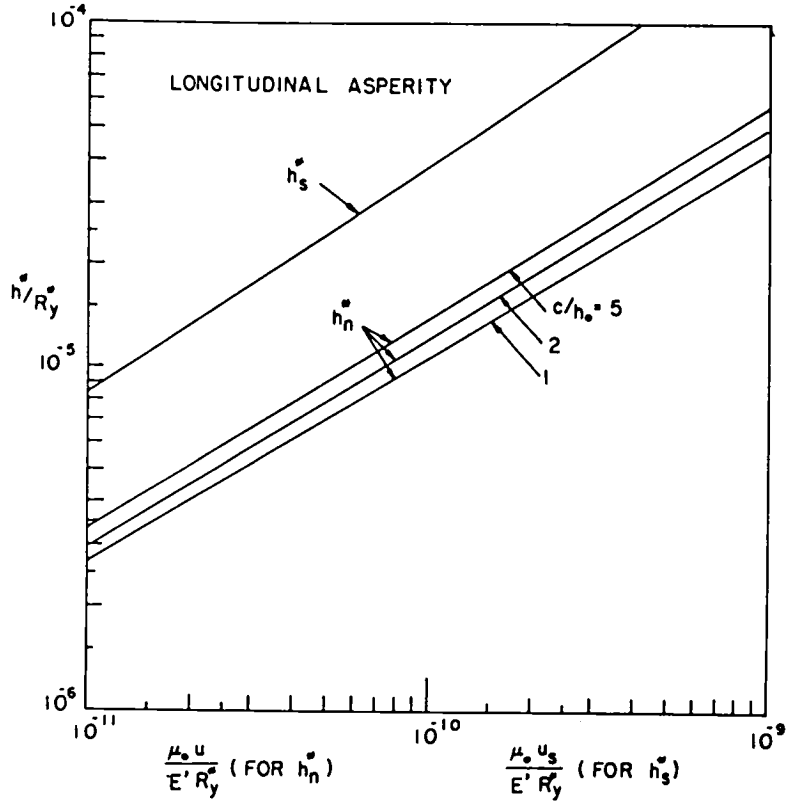

Fig. 8 Variation of h^*_n and h^*_s with the speed parameter in a longitudinal asperity

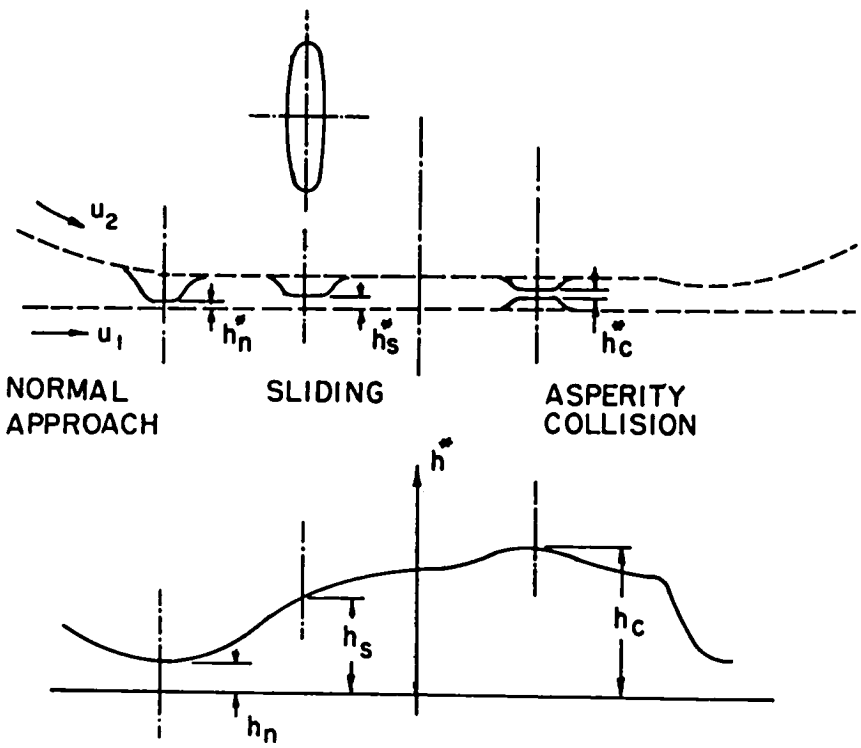

Fig. 9 Film formations by normal approach sliding and asperity collision in a transverse asperity

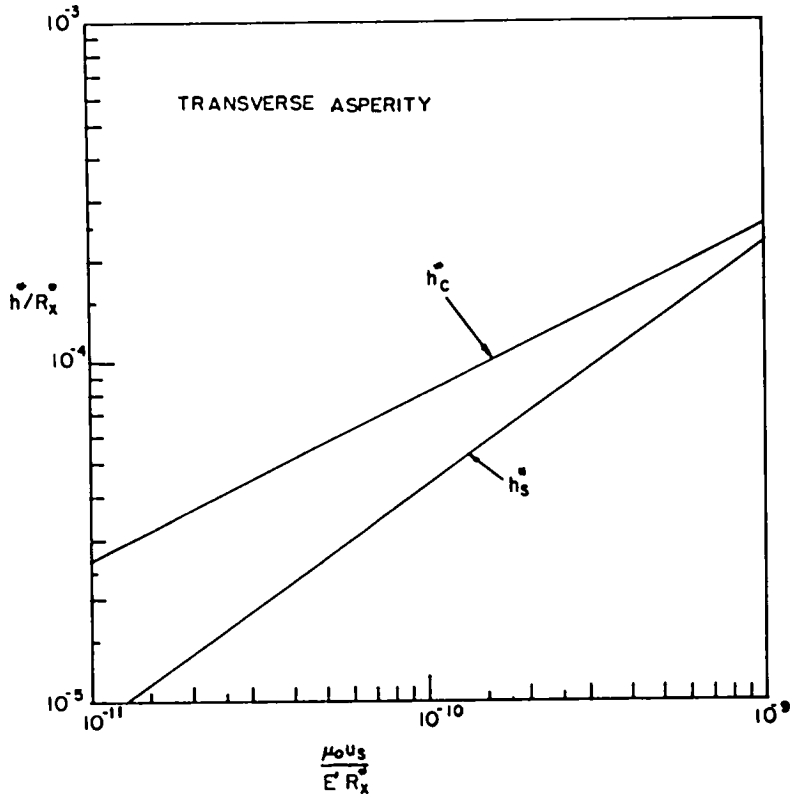

Fig. 10 Variation of h^*_c and h^*_s with the speed parameter for a transverse asperity

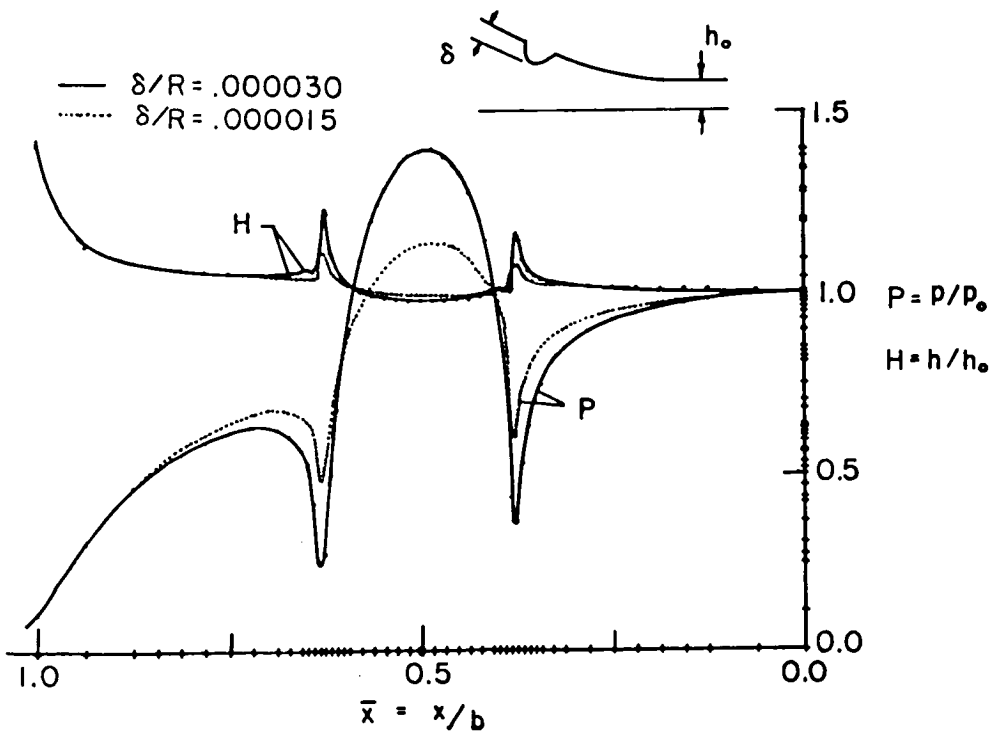

Fig. 11 Typical film thickness and pressure profiles around a sliding transverse asperity ridge

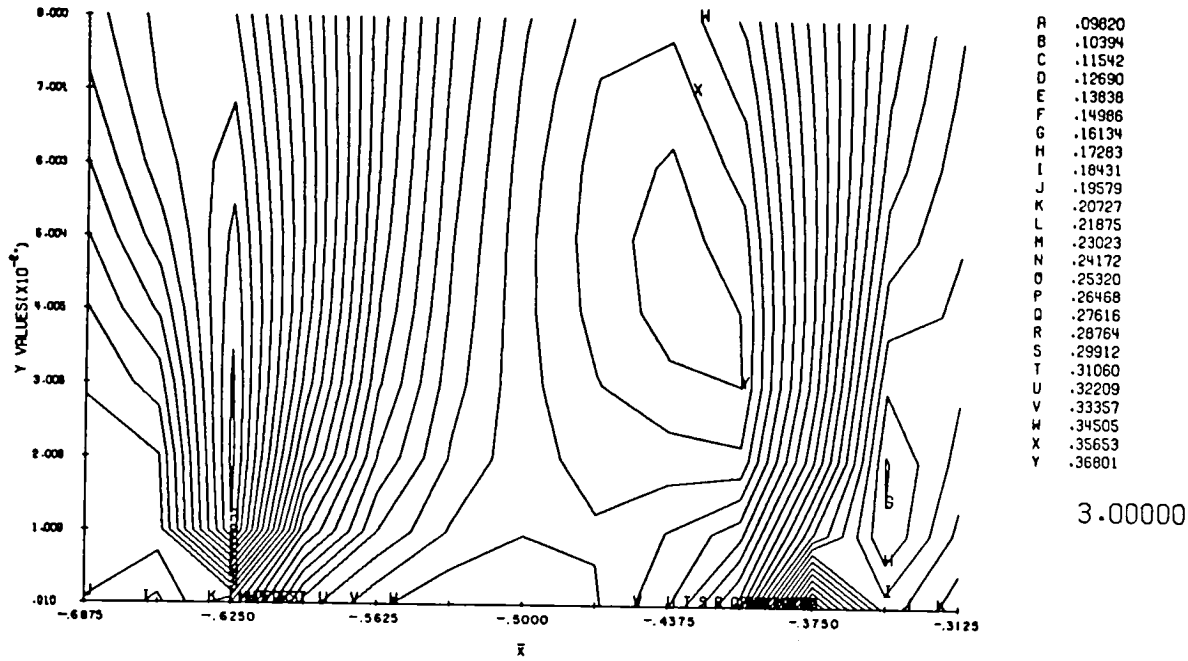

Fig. 12 Typical subsurface octahedral stress contours at a sliding transverse asperity ridge, for pressure profile for $\delta/R = 0.00003$ in Fig. 11 and local coefficient of friction of 0.25

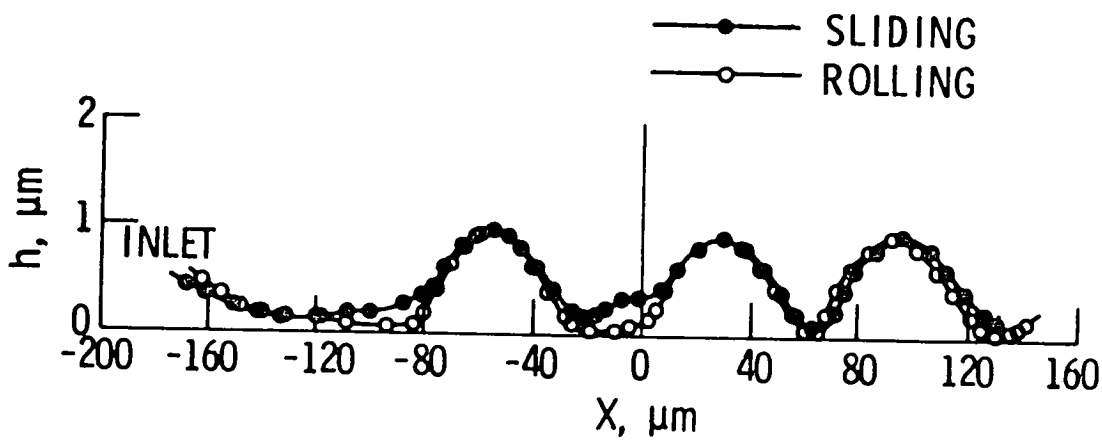

Fig. 13 Measured film thickness profiles around three asperity ridges in a circular contact

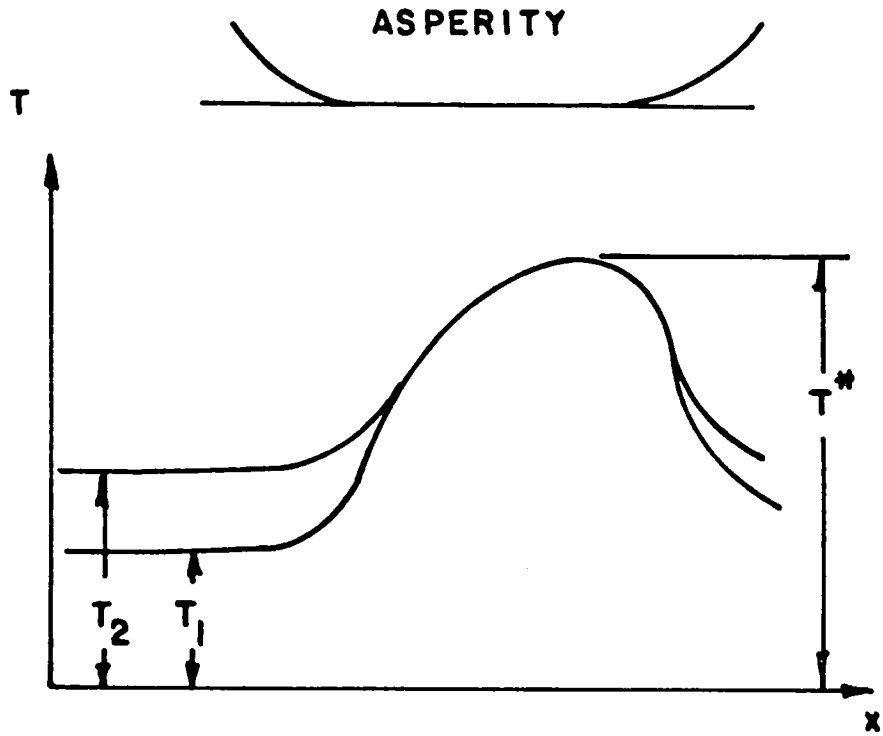

Fig. 14 Asperity temperature

DISCUSSION

Alan Dyson
Wychwood
Birkenhead, England

Microelastohydrodynamic lubrication is obviously a very important subject, and I welcome this excellent survey by Professor Cheng. I have two main comments.

The first point is that I wonder whether such detailed treatment of microelastohydrodynamics will help us in understanding or predicting failure. Conventional old theory enables us to understand how concentrated contacts may be lubricated effectively, but they do not predict failure. We can speculate that failure is unlikely if the minimum film thickness is large compared with the surface roughness (say a few tenths of 1 μm), and that failure is possible if the two quantities are of the same order. But we still cannot predict when a possible failure will become an actual one, i.e., the film thickness condition is necessary but not sufficient.

Now this paper carries the argument one step further. The surface asperities are also lubricated by an EHD mechanism, microelastohydrodynamic lubrication. The author calculates film thicknesses of a few micrometers, about two orders of magnitude lower than those for the macrosystems. The reset step is to say that the micro EHD system will fail if this film thickness is lower than a critical value which will accommodate the secondary roughness that is superimposed on the main primary roughness.

But these secondary roughnesses can be lubricated, by a secondary micro EHD system, and there is no reason why this should fail unless we go on to consider tertiary roughness and tertiary micro EHL. This is a classical infinite regress, and I have to conclude that arguments of this type do not tell us very much about failure.

Some time ago I advanced a very crude model of micro EHL (ref. D1). I suggested that if the macro EHD system could produce film pressures high compared with $1/\alpha$ (Cheng's $Q \sim 1$), then the colliding asperities would be protected by a film of lubricant of very high viscosity and the micro EHD system would be effective. But if these high pressures could not be generated by the macrosystem ($Q \sim 0$) then the microsystem would fail. This model is obviously very crude compared with Professor Cheng's, but it seems to work, to some extent, in predicting failure. Some preliminary results have already been published (ref. D2), and we hope to include more in a forthcoming paper.

My second point concerns the ratio

$$\lambda = \frac{h_{min}}{\sigma}$$

where

$$\sigma^2 = \sigma_1^2 + \sigma_2^2$$

and

h_{min} is the minimum film thickness and σ_1 and σ_2 are the standard deviations of the height distributions of the two surfaces.

The author, in common with many others, uses this ratio as a measure of the effectiveness of lubrication. But there is an implicit assumption that the roughnesses of the two surfaces are not correlated. This assumption may be true in general but some cases have recently been discovered in which there is a very strong negative correlation, the peaks of one surface fitting into the valleys of the other and vice versa (refs. D3 to D5).

The effective roughness is now that appropriate to the gap between the two surfaces, and it may be very much less than the roughness of either surface considered above. This hydrodynamic lubrication can be important even at λ ratios of 2 to 3 percent.

These are the main points that I wish to raise on Professor Cheng's paper. One point concerns the statement "there is overinvolving evidence that failures of the protective films are linked to asperity temperatures T*, even though the exact mechanism is still unclear." Could the author please provides more detail for this evidence?

My final point is that there is obviously a conflict on the effect of a shear stress limit in the lubricant. Shen and Wilson reported a sudden collapse of the film when this limit is reached, Gecun and Winer do not. This is an important point, and the conflict ought to be resolved. I do not understand why the film should collapse. On what side is Professor Cheng?

REFERENCES

D1. Dyson, A.: The Failure of Elastohydrodynamic Lubrication of Circumferentially Ground Discs. Inst. Mech. Engrs., London, 190 (52/70), 1970, 699-711.

D2. Ressides, S. D. and Suidle, R. W.: Surface Topography and the Scuffing Failure of Circumferentially Ground Discs. Surface Roughness Effects in Hydrodynamic and Mixed Lubrication. Rohde, S. M. and Cheng, H. S., eds., ASME, 1980, 93-143.

D3. Coy, R. C. and Dyson, A.: A Rig to Simulate the Kinematics of the Contact between Cam and Finger Follower. ASLE preprint no. 81-LC-2B-1, 1981.

D4. Marge, Ram, Dyson, A., and Sethuramiah, A.: Experimental Observation of the Conformity of Surface Features Produced by Wear in a Disc Machine. Wear, 73, 1981, 201-204.

D5. Bishop, I. F. and Suidle, R. W.: Some Experimental Aspects of Running-in and Scuffing Failure of Steel Discs Operated Under Elasthydrodynamic Conditions. Leeds/Lyon Symposium, Lyon, France, September 1981.

TRANSIENT EHL EFFECTS IN STARVED BALL BEARINGS

E. Kingsbury*
C. S. Draper Laboratory
Cambridge, Massachusetts 02139

The independent variables used in most calculations for EHL film thickness in ball bearings involve lubricant properties, contact elasticity, load, and bearing kinematics. The calculations are for steady state, and they give a time-constant film thickness. Experiments have shown four distinct processes in starved ball bearings which are explainable assuming a time-varying film thickness. This contribution describes these four processes as well as another transient EHL effect which does not involve the thickness of the film. A simple model, based on experimental considerations, allows direct calculation of several of the thickness transients.

INTRODUCTION

Transient EHL effects in starved ball bearings are not new. They were identified shortly after the first classical EHL solution for flooded, nonparallel films appeared in 1959 (ref. 1). An article on oil jogs (ref. 2) and a paper on a dynamic lubricating film (ref. 3) were published in 1963. These describe EHL films in instrument bearings which must have been thinner than those calculated from the fully flooded solution and which also must have been time-variable.

Interest arose in accounting for starvation film thinning within the existing fully flooded solution. The Dowson-Higginson formulation was modified for starvation first by Orcutt and Cheng (ref. 4) in 1966. A steady-state correction (an arbitrary upstream location for the beginning of pressure buildup) was added to the steady-state Reynolds and Hertz equations. As the initial lubricant boundary was brought closer to the edge of the Hertz zone, thinner EHL films were calculated. This approach has been followed in all subsequent numerical schemes for finding starved EHL film thickness, up to and including the two-dimensional solutions of Hamrock and Dowson (ref. 5).

The inlet position starvation model may be criticized on two counts:

(1) If an assumption for inlet miniscus position must be made to calculate film thickness, why not assume the thinner film straight away?

(2) No steady-state formulation can give information on film transients. An unfortunate result has been the near universal adoption of an inlet miniscus position criterion for starvation. The criterion of Horsch (ref. 3) - Starvation exists if an increase in the mass of oil available to an EHL contact gives an increased film thickness - has historical precedence, and it is a much more realistic description of the physical situation.

In this paper four bearing phenomena are explained in terms of a film thickness transient. A simple starvation model is proposed, consistent with these observations and based on much other bearing operating experience. It allows some transient EHL effects to be calculated directly. Also, for completeness, a transient in film slip velocity is reviewed.

*NRC Associate during 1983 at the NASA Lewis Reseach Center, Cleveland, Ohio.

FILM THICKNESS TRANSIENT

The four thickness transients to be described are the following: (1) the oil jag (or jog), (2) ball-race coupling variations in basic speed ratio, (3) coupling variations in orbiting drag torque, and (4) shear activated lubricant breakdown.

Oil Jag

Figure 1 (from refs. 6 and 18) shows an oil jag disturbance in gyroscope spin bearings. Observations of this sort first led to the identification of starvation. The upper trace (against time) is a record of the driving torque demand from a pair of bearings supporting a gyro wheel, spin axis horizontal. The bottom trace is a simultaneous record of the torque to balance in the gyro support servo loop. This record can be interpreted as the excursion of the wheel CG from a central position along the spin axis. The experiment shows two steps in driving torque with simultaneous motions of the wheel CG: first in one direction, then the other. Each step decays over many minutes back to its original level. The explanation (given in refs. 2 and 6) is that a small drop of oil is flung from the ball cage into the outer race Hertz track first in one bearing and then in the other. The torque steps because the balls suddenly must roll over a thicker film, and this forces the wheel assembly to move sideways along the spin axis. There is an increased film thickness when more oil enters the Hertz track (the Horsch condition), and a slow transient back to the original thickness. A realistic starvation theory ought to account for this thickness transient; in particular, it should give a quantitative prediction for the decay characteristics. Clearly, an inlet miniscus position formulation can give neither.

Basic Speed Ratio Increase with Time

Every angular contact bearing has a characteristic number, its basic speed ratio, defined as ball spin rate over total race rate (ref. 7). This number is a sensitive measure of the ball-lubricant-race coupling in a bearing, and it can easily be measured to a few parts in 10^5. For perfect coupling (no lubricant, zero drag slip), BSR has a maximum value set by bearing geometry that decreases with increasing spin drag slip (ref. 8). Figure 2 shows this number measured in a counter race rotating (zero orbit rate) retainerless bearing where there is no inflow into the Hertz track. The BSR increases with time over many minutes. Since there is no inflow, side leakage irreversibly removes oil from the Hertz track to give (according to Horsch) a continually thinning film, continually improving ball-race coupling, and a continually increasing BSR. No one-dimensional EHL theory, ignoring side flow, describes this effect.

Orbit Drag Torque Induced Slip

Internal bearing drag torques result seperately from spin and orbit motions of the ball set. If a bearing is run in the counter race rotation mode

for zero ball orbit rate, orbit induced slip is zero but can be made large by applying an external torque to the ball group (ref. 9). Figure 3 is a photograph of an apparatus to do this. A small pin inserted between the balls in a full complement group keeps the group from orbiting when the race rates are not quite correct for zero free orbit rate. The pin is connected to a dynamometer which measures the torque to force zero orbit rate (by inducing slip).

Figure 3 also shows a jag gun which throws a small mass of oil into the bearing, more or less on demand. Oil drops accumulating on the edge of the rotating disk fly off when they reach a critical size determined by a balance between surface tension and centrifugal force (ref. 2). They fly off at random, but only those aimed into the Hertz track can pass through the focusing tube. A single drop can be selected by regulating the inflow to the disk, and its mass is altered by regulating the speed of the disk.

Transients in orbit-induced slip during an oil jag can be measured by setting the inner and outer race rates for a small initial pin torque. When oil is added the pin torque steps to a new value because the thicker film changes the effective rolling geometry and free orbit rate of the bearing.

Figure 4 is a plot of pin torque versus time measured in this experiment. Also plotted are BSR and driving torque demand. The pin and driving torque curves have a similar shape, like that in figure 1, while the BSR curve is a mirror image. These results are all consistant with a sudden increase in film thickness at the jag followed by a long decay because of side leakage. Since this retainerless bearing has no oil inflow mechanism except the jag, eventually the three curves will pass through and beyond their initial levels, unless another jag is introduced. The jag oil mass used in figure 4 was 1×10^{-6} gram. Hence, to keep the film thickness constant for this particular bearing, load, and speed, about 1 microgram an hour inflow is necessary.

Lubricant Breakdown

The EHL film in a retainerless bearing running without an oiler thins by side leakage. When the film gets too thin it fails, not by asperity penetration and metallic interaction but by oxidation and polymerization: the oil changes from fluid to solid (ref. 10). Figure 5 shows BSR versus time data for the process - two experiments in the same bearing. First there is a gradual increase in BSR due to side leakage, as in figure 2, and then a sharp increase as the oil turns solid. Pictures of typical lubricant breakdown products on bearing races are shown in reference 10. These products were removed from the races between the two experiments of figure 5. It has been suggested (ref. 11) that the degradation processes, which are activated by mechanical shear, go on all the time in all bearings. The degradation rate is negligible in thick EHL films, but it becomes catastrophic if the film gets too thin.

Suppose the rate is given by

$$R = (\text{constant}) \exp [-E/S] \tag{1}$$

where E is an activation energy for the average degradation reaction and S is the shear energy dissipated in the EHL contact. For slip velocity u, film thickness h, contact transit time T, and limiting shear stress τ,

$$S = \frac{uT\tau}{h} \tag{2}$$

For a film thinning from h_1 to h_2, noticing that τ, T, and u remain constant (here u is a kinematic slip depending only on the shapes and motions of the rolling elements, e.g., pivoting or transverse precessional slip (ref. 13)),

$$\frac{R_1}{R_2} = \exp\left[-\frac{E}{uT\tau}(h_1 - h_2)\right] \tag{3}$$

For $E = 3\times10^8$ J/m^3 (energy required to add a CH_2 group to many organic forms), $\tau = 3\times10^7$ Pa (ref. 12), u = 0.04 m/sec (ref. 13), and $T = 3\times10^{-5}$ s (calculated for the bearing and running conditions of fig. 4),

$$\frac{R_1}{R_2} = \exp\left[-8\times10^6(h_1 - h_2)\right] \tag{4}$$

For a thickness difference of 4×10^{-7} m (10 microinches), we estimate a degradation rate 25 times greater in the thinner film.

The activation model for lubricant breakdown in a thin EHL film is consistant with many experiments like those in figure 5. It also explains a result reported in reference 10: A surfactant (alkyl glyceryl ether solfonate) adsorbed on bearing races greatly increases the lubricant degradation rate at a given film thickness. The surfactant, acting as an organic catalyst, simply reduces the activation energy for the degradation reactions.

FILM SLIP TRANSIENT

Occasionally a bearing ball is observed performing uniform precession. The motion is analyzed in detail in references 14 and 15. Briefly, the ball spins at rate s about its axis of figure while the axis simultaneously traces out a cone (precesses) at rate p about a fixed line. The cone half-angle θ is constant in uniform precession. If the ball angular rate as determined by bearing kinematics would be $\dot{\delta}$ without precession ($p = \theta = 0$; $s = \dot{\delta}$), it turns out that

$$p + s\cos\theta = \dot{\delta} \tag{5}$$

for uniform procession. Measurements show that s and θ are both small in the observed precessions so that $p \simeq \dot{\delta}$.

In reference 14 it is shown that precession requires a transverse ball-race slip across each Hertz area; that is, the slip is across the rolling direction, parallel to the major Hertz axis. The transverse precessional slip is found to be

$$\mathcal{S} = \frac{d}{2}(s\sin\theta\sin pt) \tag{6}$$

It is sinusoidal with time (transient) and of amplitude s_0, which is small; but frequency $p \simeq \dot{\delta}$, which can easily reach 1 kHz. Thus, EHL theory and lubricant rheology will eventually have to tolerate high frequency oscillating slip as well as long-term film thickness transients.

DISCUSSION

The central problem in EHL has been to calculate film thicknesses which are of the same order as elastic deformations in the contacts. Solutions are complicated, and until recently they have been limited to steady-state one-dimensional flow in the rolling direction. The side-leakage-dominated transient behavior observed in starved ball bearings suggests a different approach. The simple model given here is based on the way starved experiments have been made, and it has a built-in compatibility with them:

(1) Instead of calculating a film thickness, take an initial film thickness as given. This corresponds to the experimental technique of depositing a thin uniform film on bearing parts prior to any running (ref. 10).

(2) Assume one-dimensional flow inside the Hertz areas in the transverse (cross) rather than the rolling direction.

(3) Assume zero flow outside the Hertz areas everywhere in the bearing. This is a very strong form of kinematic starvation (refs. 16 and 17).

(4) As an exception, assume a well-defined inflow mechanism and rate. This corresponds to the jag gun experiment.

(5) Calculate changes in film thickness with time based on the difference between inflow and crossflow. This corresponds to a measurement of BSR.

An early application of this model (ref. 18) predicted that a step increase in load would increase EHL film thickness in a starved ball bearing previously running at constant thickness (inflow = crossflow). A load increase would not change inflow, but it would decrease crossflow since (1) the Hertz areas would get bigger, increasing the crossflow path length, and (2) oil viscosity would increase (with pressure) inside the contacts. A long increasing transient to a new thicker film was calculated. A measurement of increased thickness with load has recently been reported (ref. 19). This result seems to confirm, or at least does not contradict, the simple treatment of ball bearing starvation suggested here.

REFERENCES

1. Dowson, D.; and Higginson, G. R.: A Numerical Solution to the Elasto-hydrodynamic Problem. J. Mech. Eng. Sci., vol. 1, no. 1, June 1959, pp. 6-15.
2. Archibald, F. R.; and Blasingame, B. P.: The Jog Mechanism in Gyroscopes. Air, Space and Instruments, S. Lees, ed., McGraw-Hill, 1963, pp. 498-502.
3. Horsch, J. D.: Correlation of Gyro Spin-Axis Ball Bearing Performance with the Dynamic Lubricating Film. ASLE Trans., vol. 6, no. 2, Apr. 1963, pp. 112-124.

4. Orcutt, F. K.; and Cheng, H. S.: Lubrication of Rolling Contact Instrument Bearings. Gyro Spin Axis Hydrodynamic Bearing Symposium, Vol. 2, MIT Instrumentation Laboratory, 1966, Paper no. 5.
5. Hamrock, B. J.; and Dowson, D.: Ball Bearing Lubrication. John Wiley and Sons, 1981.
6. Kingsbury, E.: Comment on "A Theoretical Analysis of the Starved Elastohydrodynamic Lubrication Problem for Cylinders in Line Contact," by P. Castle and D. Dowson. Elastohydrodynamic Lubrication Conference Proceedings, I. Mech. E., 1972.
7. Kingsbury, E. P.: Basic Speed Ratio of an Angular Contact Bearing. J. Lubr. Technol., vol. 102, no. 3, July 1980, pp. 391-394.
8. Kingsbury, E.: Dynamic and Coupling Influences on Basic Speed Ratio of an Angular Contact Bearing. Wear, vol. 63, 1980, pp. 189-196.
9. Kingsbury, E.: Ball-Ball Load Carrying Capacity in Retainerless Angular Contact Bearings. J. Lubr. Technol., vol. 104, 1982, pp. 328-329.
10. Kingsbury, E. P.: Lubricant Breakdown in Instrument Ball Bearings. J. Lubr. Technol., vol. 100, no. 3, July 1978, pp. 386-394.
11. Kingsbury, E. P.: Lubricant Breakdown Acceleration in Instrument Ball Bearings. Presented to the 5th Inertial Guidance Contamination Control Seminiar, Hughes Aircraft Co. (El Segundo, CA), Oct. 16-18, 1979.
12. Jacobson, B. O.; and Hamrock, B. J.: Non-Newtonian Fluid Model Incorporated into Elastohydrodynamic Lubrication of Rectangular Contacts. Submitted to ASME.
13. Kingsbury E.: Pivoting and Slip in an Angular Contact Ball Bearing. Submitted to ASLE.
14. Kingsbury, E. P.: Precessional Slip in an Angular Contact Ball Bearing. Wear, vol. 77, 1982, pp. 105-114.
15. Kingsbury, E.: Ball Contact Locus in an Angular Contact Bearing. J. Lubr. Technol., vol. 105, no. 2, Apr. 1983, pp. 166-170.
16. Chiu, Y. P.: An Analysis and Prediction of Lubricant Film Starvation in Rolling Contact Systems. ASLE Trans., vol. 17, no. 1, 1974, pp. 22-35.
17. Kingsbury, E.: Discussion on Y. P. Chiu's "An Analysis and Prediction of Lubricant Film Starvation in Rolling Contact System." ASLE Trans., vol. 17, no. 1, 1974, p. 34.
18. Kingsbury, E.: Cross Flow in a Starved EHD Contact. ASLE Trans., vol. 16, no. 4, 1973, pp. 276-280.
19. Coy, J. J.; and Zaretsky, E. V.: Some Limitations in Applying Classical EHD Film Thickness Formulas to a High-Speed Bearing. J. Lubr. Technol., vol. 103, no. 2, Apr. 1981, pp. 295-304.

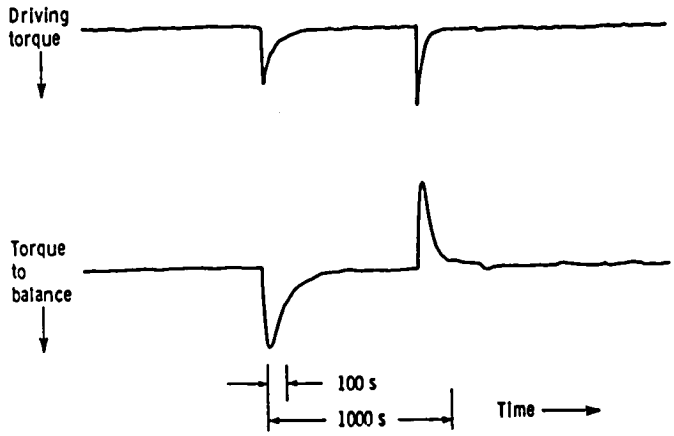

Figure 1. - Disturbances in driving torque and torque to balance during an oil jag in a gyroscope.

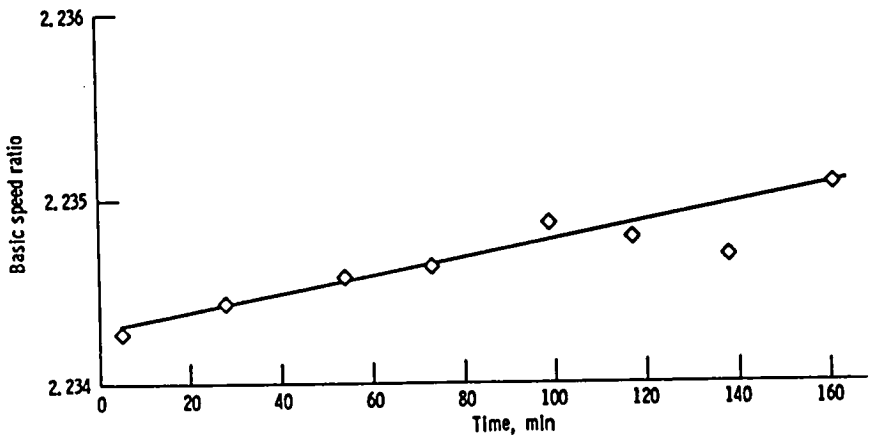

Figure 2. - BSR versus time. No inflow.

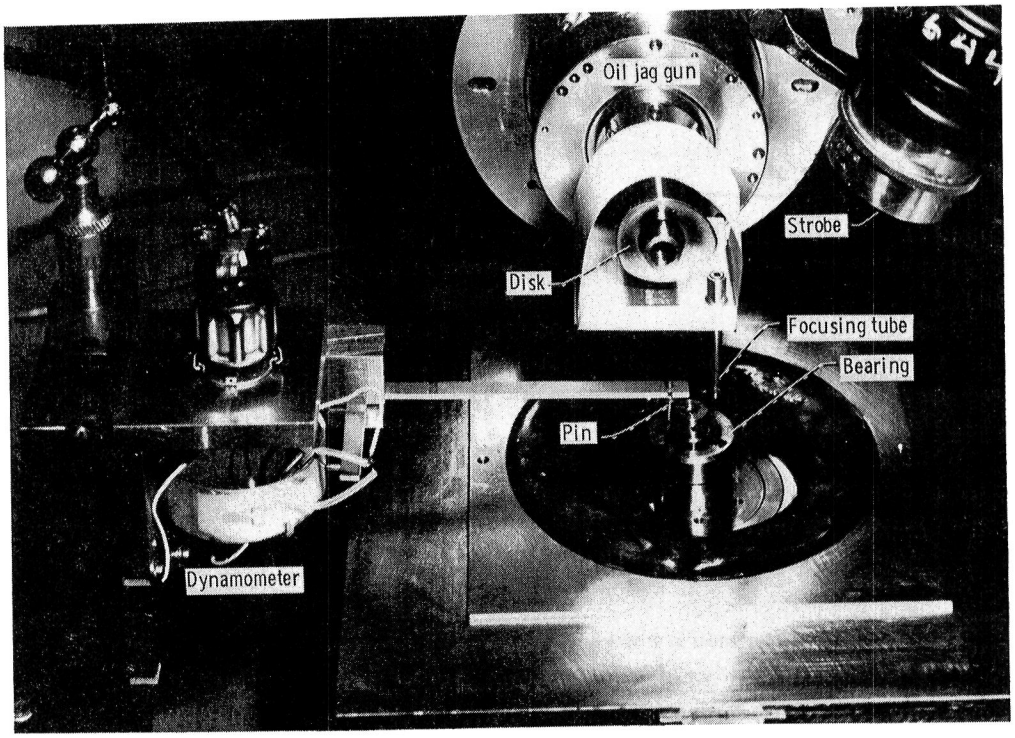

Figure 3. - Apparatus.

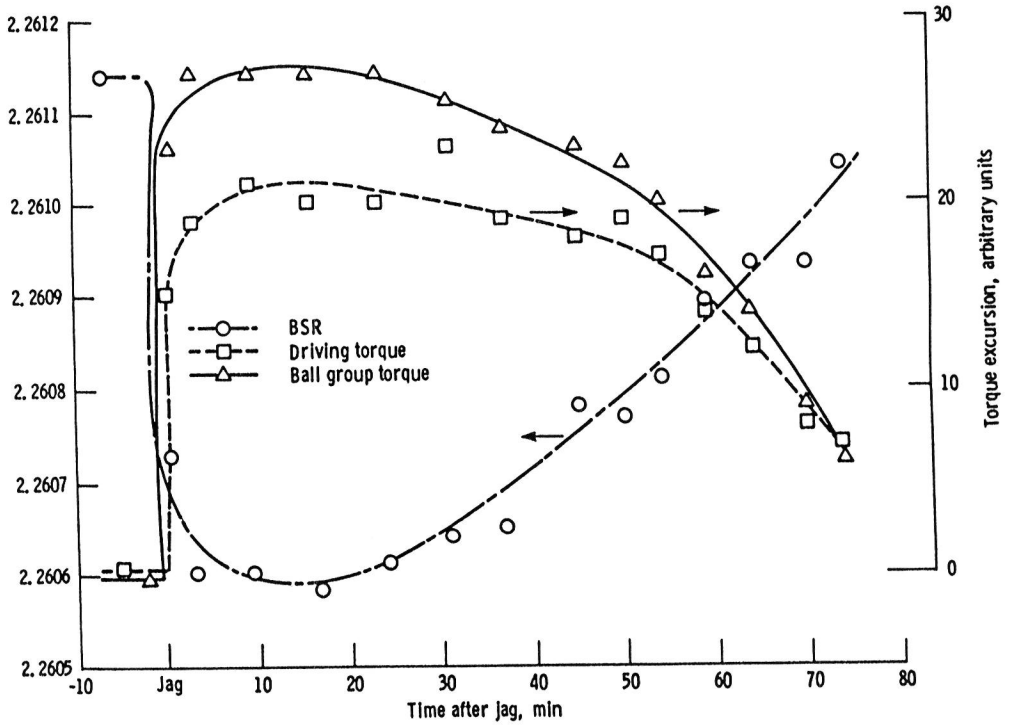

Figure 4. - BSR, orbit, and drive torque versus time during oil jag.

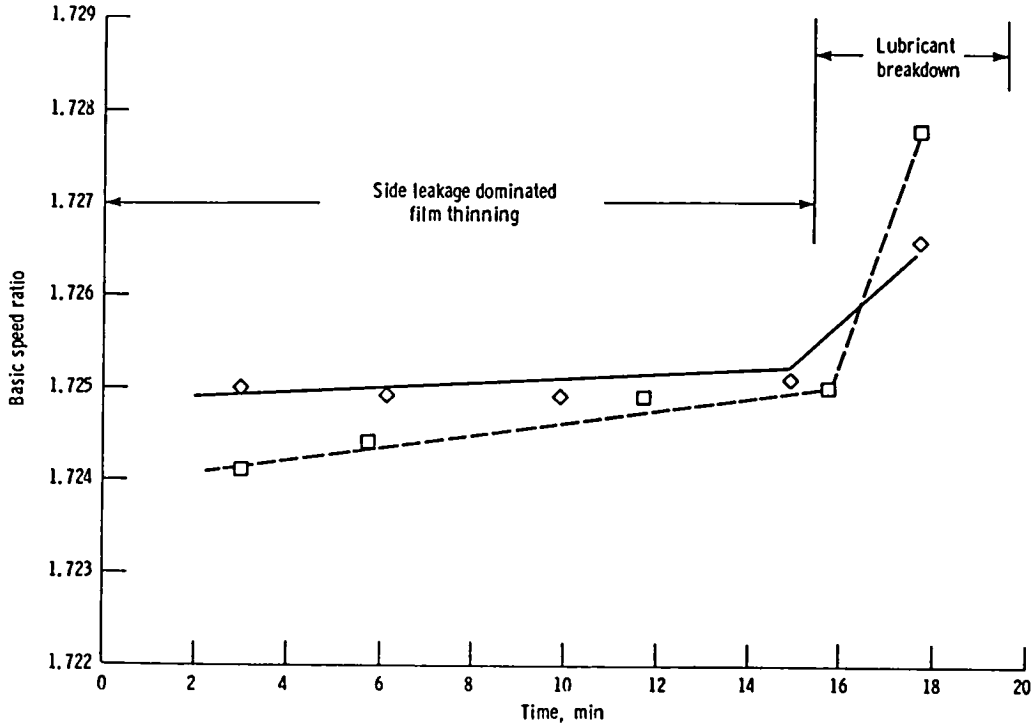

Figure 5. - Basic speed ratio as function of time for two experiments. No inflow.

DISCUSSION

L. Houpert and T. A. Harris
SKF Engineering & Research Centre B.V.
Nieuwegein, Netherlands

The paper describes experimental observations indirectly associated with lubricant film thicknesses, torque in a bearing and spin rate of a ball. Four cases are described.

a. Oil Jag

This section could be of interest for standard bearings. A sudden increase of the film thickness layer h_1 on the track, increases the torque. This torque is probably the torque due to the rolling speed and is proportional to the EHD film thickness.

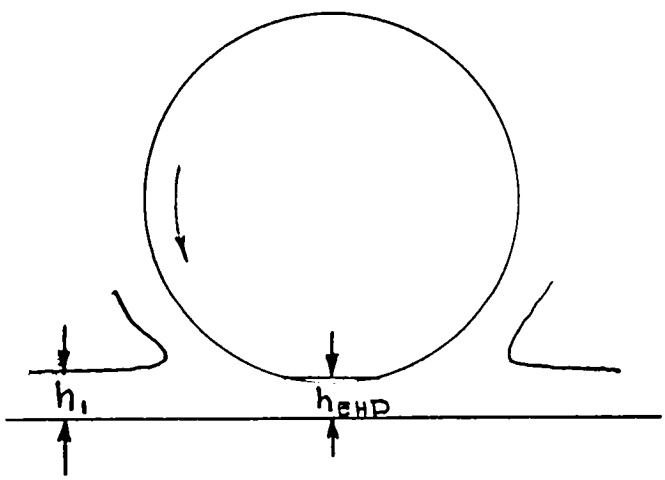

FIG. A

Referring to Fig. 1 it takes roughly 20 seconds for the torque (or film thickness h_{EHD} to reach the experimental maximum, and 100 seconds to decrease again to the original value (starved and transient value).

Let us assume that this maximum does correspond to fully flooded steady state conditions.

100 seconds is therefore the time required for the layer h_1 (see Fig. A) to flow away from the track.

Could these data be used to estimate at which speed ω_i, transient effects on film thickness occur when a ball is crossing a loaded zone in a certain time t? Considering, however, that in the author's experiment 100 seconds is required for starvation, it seems that more than ample time is available to maintain a substantially steady state condition in normal applications. Therefore the significance of "oil jag" is in question.

b) Basic Speed Ratio increases with time

FIG. B

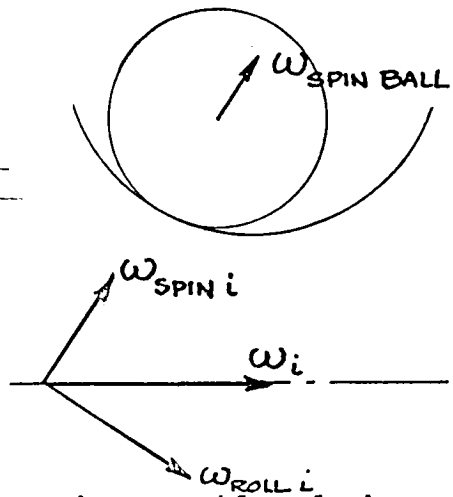

When the coupling in the contact is perfect: $\omega_{spin\ ball} = \omega_{spin\ i}$, corresponding to a maximum value of BSR, See Fig. B. The author states that the coupling becomes greater when h decreases and he attributes this decrease to transient effects in the lateral direction of the contact (hence side leakage flow)

It must be considered, however, if the decrease of film thickness might not be due to thermal effects; i.e., increase of the bulk lubricant temperature.
Furthermore, it does not appear certain that the coupling (and hence coefficient of friction μ) increases when h decreases.
A decrease of h will increase the shear rate $\dot{\gamma}$ = slip/h. The author has not stated load and speed conditions for his application; however, in most ball bearing applications, operation occurs in the decreased friction plateau region II, as shown in Fig. C

FIG. C

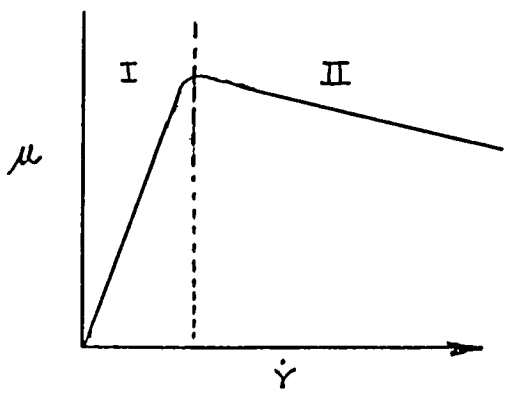

Then, in case of full separation of rolling contact surfaces, a decrease of h will increase $\dot{\gamma}$ and decrease μ , which is opposite to the effect encountered in Zone I. It appears that the author only considers conditions in the latter Zone I.

d) Lubricant Breakdown

It is observed that the author uses a limiting shear concept (Zone II of Fig. C) when calculating the dissipated energy in shear. Effectively, τ has a constant value at film thickness h_1 and h_2 in equation (3). This model appears in contradiction to the author's observations in (b) above.

e) Film slip transient

In the author's experiment, the lateral slip varies sinusoidally with time. It would be interesting to compare the slip frequency and the torque frequency. If the two signals are in phase, the behaviour of the lubricant is viscous; i.e., $\tau \sim \eta_0 \dot{\gamma}$

If the two signals are out-of-phase (90°), the rheological behaviour of the lubricant is elastic.

$$\dot{\gamma} \sim e^{i\omega t}, \quad \gamma \sim e^{i(\omega t + \frac{\pi}{2})}, \quad \tau = G\gamma$$

Thus, the lubricant rheology may be able to be assessed using a similar test method?

The frequency effect (considering pressure effect also) has been studied by many authors using sinusoidal shear waves and measuring the response of the liquid; but, the dynamic environment of the bearing was not simulated. The rolling motion probably aligns the lubricant molecules in the inlet zone; rheological characteristics of the lubricant are then changed. Using the author's method, the dynamic environment of a bearing is simulated.

General remarks

In the author's cases (b), (c) and (d), by "transient", the author considers only the lateral flow in the contact.

Hamrock and Dowson described the effect of side leakage flow by introducing the ellipse ratio "k", and it appears possible to quantify that lateral flow. Is this lateral flow considered a transient, when it occurs consistently during normally steady state operation of the bearings. It is of greater interest, rather than considering transients, to determine how much lateral flow occurs and how it is to be replenished for succeeding contacts.

DISCUSSION

J. W. Kannel
Battelle Columbus Laboratories
Columbus, Ohio

Dr. Kingsbury's work probably represents the most persistent activity in instrument bearing lubrication research over the last 15-20 years in this country. His work has given us new insights into instrument bearing performance and has continuously posed challenging questions about the real understanding of bearing performance. This paper is essentially an outline of critical bearing parameters and the effect of these parameters on performance.

Kingsbury presents four film thickness related transients in a bearing. His first transient is the famous oil jag, which was a very popular item in gyroscope bearing terminology in the 1960's. In this regard, Figure 1 from reference 6 is very reminiscent of the early research in this area for a hypothetical oil jag. However, Figure 4 taken by the author for an actual oil jag is considerably different. Would the author comment on this and also, on the lack of a torque coordinate on his graph? (Unless of course his equipment is calibrated in arbitrary units.) Figure D-1 shows an oscilloscope trace for a torque jag (taken at Comsat) for a satellite bearing. In those experiments, the film thickness was monitored simultaneously with the torque. Notice that the film thins out at the same time that the torque-jags. The thinning could be some type of contamination problem. It is possible then that oil-jags are really un-oil jags? Also, it might be noted that torque-jags can be accompanied by cage instability which is also related to lubricant film loss rather than to excessive lubricant.

Dr. Kingsbury's work with basic speed ratio (BSR) measurements have been very useful in studying lubricant film coupling. Figure 5 is intriguing especially with regards to the rise in this coupling at starvation condition. However, I am confused with Ed's explanation. In equation (2), is the arbitrary constant the same as the arbitrary torque unit mentioned earlier? Can equation (1) really predict lubricant degradation under lubricated

conditions? It would be nice to know the absolute value of R rather than just relative values. I fully suspect that lubricant degradation is the result of metal to metal contact where very high local shear occurs rather than lubricant shear stresses. The authors comments are welcomed.

Although my comments may seem picky, I believe that they are critical to the authors interpretation of his data. I think Ed's work is quite rigorous and very valuable to understanding instrument bearing lubrication. I look forward to seeing future work in this area and especially, to the new insight Ed can give us in instrument bearings.

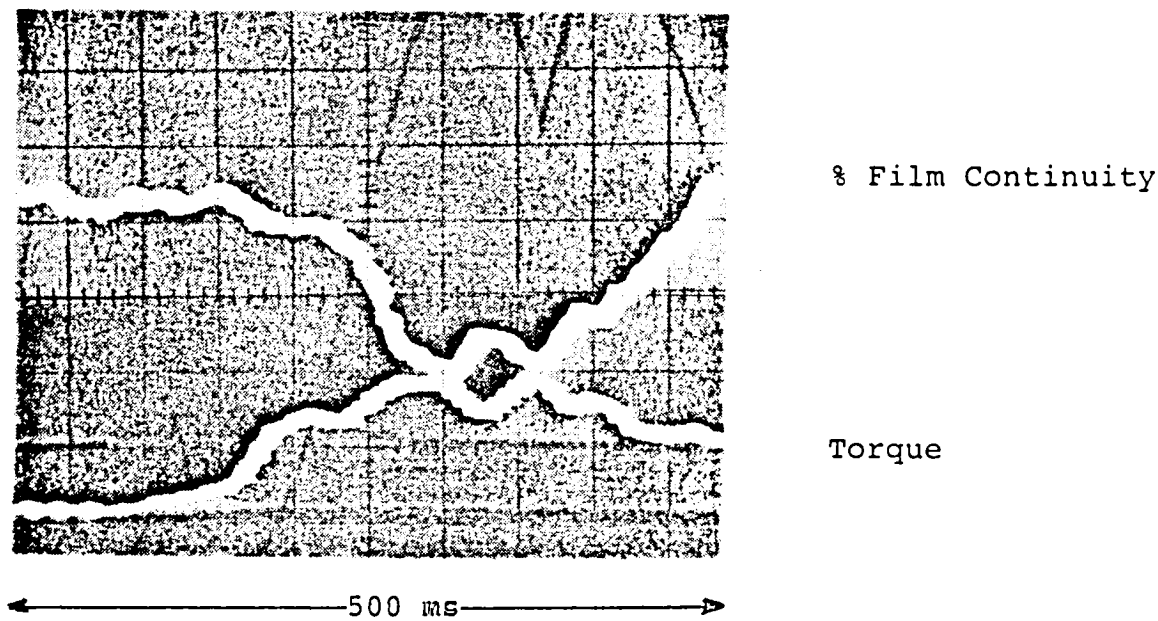

Figure D-1. Breakdown in Film Continuity during Cage Instability

DISCUSSION

T. E. Tallian*
SKF Industries, Inc.
King of Prussia, Pennsylvania

The author's concern with transient phenomena in EHD films is well founded. Both on the scale of entire contacts, and on the asperity scale, numerous transient pheonomena are known or can be conjectured. It stands to reason that a more faithful model of contact behavior will emerge if these effects are included.

We wish to illustrate another transient EHD effect, recently observed during our work supported by DOE (O. Manley, technical monitor) by N. Bhardwaj, R. Bovenkerk and L. Helwig using interferometry in a rolling contact between an optical disk and a lapped metal rolling element which was in one case a ball, in another, a toroidal roller. The interferograms were produced on a new test system with very high speed and load capabilities, and equipped to read traction force while film profile interferograms were being taken. The interferograms were recorded by high intensity electronic flash of 4-10μsec duration. The contact conditions are tabled below.

*Fellow ASME. Vice-President, Technology Services, SKF Industries, Inc.

		Roller	Ball
Profile Radii		53.340 X 7.074	6.337 mm
Disk Material		Quartz	Sapphire
Lubricant		MIL L 7808 ester	Santotrac 50 traction fluid
Exit Temperature		25.9°C	24.9°C
Rolling Speed (Pure Rolling)		10.16	7.62 m/sec
Contact Diameters:	Max.	1.24 X 0.35	0.28 mm
	Min.	1.005 X 0.28	0.23 mm
Contact Deflection:	Max.	5.7	3.1 μm
	Min.	3.5	2.1 μm
Contact Load:	Max.	174.0	84.1 N
	Min.	88.5	47.2 N
Max. Hertz Pressure:	Max.	0.76	2.03 GPascal
	Min.	0.60	1.67 GPascal
Plateau Film Thickness:	Min.	1.24	1.15 μm
	Max.	1.35	1.15 μm
Constriction Film Thickness:	Min.	0.95	0.72 μm
	Max.	1.04	0.83 μm

We show maximum and minimum values of contact diameters, contact deflection, load, pressure and film thickness for each contact. These extremes were observed among repeat interferograms taken under nominally identical conditions. It was determined that the variation occurs at frequencies (192 Hz for the roller contact and 255 Hz for the ball contact), corresponding to the fundamental rotational frequency of the rolling element. An eccentricity of the order of some micrometers was detected in the rolling elements. Calculation of the forces required to accommodate the eccentricity by deflection in the contact and in the rolling element quill, correlates with the load variation observed. While the eccentricity of the rolling element was unintentional, it

does offer the opportunity to observe relatively high frequency load transients in EHD contact. Some interesting details are as follows:

1. In neither of the experiments was there a visible meniscus near the contact, i.e. it was flooded. While it is not known that either the higher or lower of the observed loads is a true extreme value, they were selected as extremes among several interferograms. Thus a load fluctuation frequency corresponding to one complete rolling element revolution (~22 mm rolling distance) is faithfully followed by the oil supply. There is not, as one might suspect, cavitation ahead or to the two sides of the contact when its load approaches a minimum and the gap in its vicinity widens. This contrasts with the usual cavitation at the exit of any EHD contact.

2. In a detailed examination of the film shape for the roller, a slightly (0.1 μm) thinner film is observed for the higher load, in both the plateau and the constriction. There is no distortion of film shape. The film shows no unexpected reaction to the transient loads. In the ball tests, the width of the constriction increases with load, and the minimum film thickness drops. The plateau film thickness does not change observably.

3. The test system in which the described data were taken provides for direct monitoring of the traction force as a function of continuously variable slip. However, the traction force sensing system frequency response is slow. A frequency analysis of the traction force sensing circuit does not reveal significant frequencies corresponding to the load fluctuation. We can accordingly theorize on the effect of the load fluctuations on traction only from the observed behavior of time-average traction coefficient as a function of time-average load.

Using the roller contact as an example, our traction data show that the maximum traction coefficient and the initial slope of the traction vs. slip curve vary as follows with time-average load:

Load, N	μ_{max}	Initial Slope
~150	0.013	0.28
~470	0.020	0.89

For a fluctuation of ~40N around the average load of ~130N, as observed in the interferograms of the roller contact, linear interpolation projects ~30% fluctuation in initial slope and ~7% fluctuation in μ_{max}. A time-averaging traction sensor consequently overstates the initial slope by 6-8% but overstates μ_{max} by 2% at the most. Thus, it appears that time-averaged traction results are noticeably but not drastically biased by the load fluctuations observed.

4. As is the case for any fluctuating load, the fatigue life of the contact will be less than if the time-average load prevailed constantly.

These observations confirm the well-known fact that a (small) rolling bearing with rolling element diameter variations of a few m undergoes significant contact load pulsations. Such diameter variability is present in many roller bearings and the load pulsations are part of their normal operating condition. However, for bearings operating at very high speeds and with critical reliability (aircraft engine bearings) efforts to minimize load pulsations are well warranted.

RESPONSE

Edward P. Kingsbury
C.S. Draper Laboratory
Cambridge, Massachusetts

I am grateful to the discussors for their penetrating questions on this contribution. First let me make some general remarks, and then reply more specifically to Mr. Kannel and Messrs. Houpert and Harris.

There is more than one kind of slip in an angular contact ball bearing. To illustrate, and clarify the role of various slips in ball-lubricant-race coupling and lubricant degradation, consider a ball, diameter d, midway between infinite planes separated by L, the whole space between filled with lubricant.

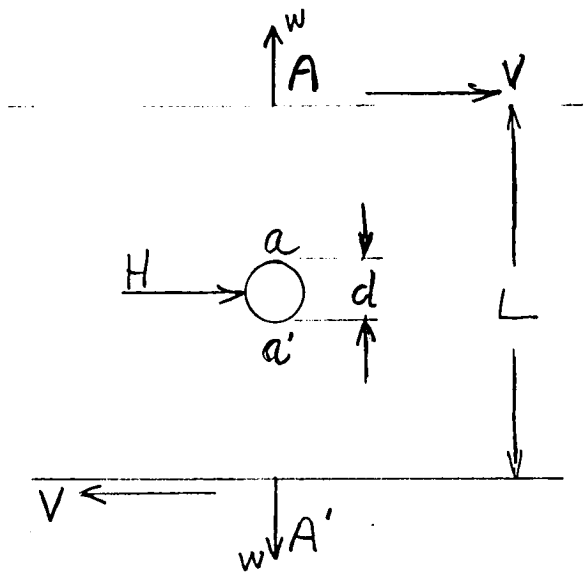

Let the planes move left and right at velocity V. When L >> d the ball does not rotate; its surface velocity is zero and the slips on the ball surface at the points a,a' momentarily coinciding with the AA' axis are V.

Now let the planes approach each other. The ball starts to rotate at $\dot{\delta} = \dot{\delta}(L)$ about an axis normal to AA' into the plane of the paper, generating surface

velocity at a and a'. Slip becomes $v = (V - \dot{\delta}d/2)$, $< V$. Eventually, when $L = d$, $v = 0$, and $\dot{\delta} = 2V/d$.

It seems reasonable to suppose that $\dot{\delta}$ is monotonic increasing as L goes from ∞ to d.

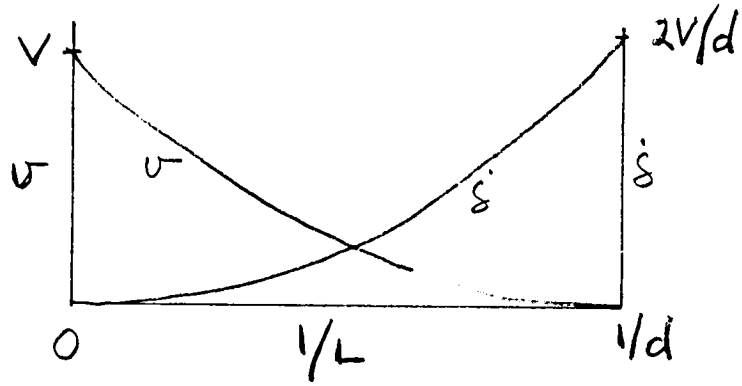

The number analogous to BSR here is $\dot{\delta}/2V$ and we expect it also always to increase as film thickness tends to zero.

Next, push on the ball with a horizontal force H to the right. It will move to the right at some velocity h for which H is balanced by viscous forces. The slips become $(v + h)$, and we have an example of induced drag slip. In a bearing there are drag torques on the ball group from orbit and separately from spin dissipations which are analogous to H. The corresponding circumferential slips become smaller as $L \dashrightarrow d$ but do not reach zero when $L = d$ (when film thickness is zero); instead they enter the regime of microslip or pseudoglissage. But such slips are in the first place small compared to rheological slip, and in the second place can't last long because the bearing will quickly fail without oil. In any case we still expect a monotonic increase in $\dot{\delta}$ (and in BSR) as the film thins.

Finally let the two planes spin about the AA' axis at $\pm w$. As the planes approach the ball any viscous spin drag will always sum to zero from symmetry, the ball does not spin, and a relative pivoting angular velocity $p = \pm w$ will appear at a and a' (this quantity is loosely referred to as spin by bearing

engineers). The associated pivoting slip is u = rw where r is measured along either plane from AA'. u remains constant as the planes approach, independent of L, and is an example of a kinematic slip. In a bearing it can be shown (13) that the sum of the liner and outer ball-race pivotings is conserved, no matter what the orientation of $\dot{s}$, so that as far as lubricant damage is concerned the kinematic pivoting slip situation in a bearing is analogous to this model. Pivoting slip, independent of film thickness, was used in the calculation for lubricant breakdown activation. It represents a minimum shear which must always be present in the oil.

Specific reply to Mr. Kannel:

The oil jags in Fig (1) were recorded more than 20 years ago with instrumentation long since abandoned. In particular, the bearings under test were the standard configuration of the time, equipped with retainers and running in outer race rotation at a large ball orbit rate. The position and trajectory of the oil drops were entirely uncontrolled. The jag of Fig (4) on the other hand was constrained to hit the outer race Hertz track between two balls in a retainerless bearing with a stationary ball group, and the overall time constant in the driving torque instrumentation was an order of magnitude smaller than previously. The results in Fig (4) are "cleaner" than Fig (1), and interestingly bring into question the term "exponential decay" which used to crop up in discussions of jags. As suggested earlier, an explanation of the shapes in Fig (4) must be given by a realistic starvation theory.
I apologize for the arbitrary torque units in the figures. A calibration was possible but not done because of time constraints. Roughly speaking, the experiment in Fig (1) associates a change in driving torque of several hundred dyne-cm and a change in film thickness of a few microns with a jag mass of

1 microgram. Specification of the multiplier in the degradation equation would require a more detailed knowledge of the chemical reactions involved. Since the reactions can now be reproduced on demand (we did not go to the trouble of setting up the video tape recording without being sure of getting a degradation failure when expected), a detailed study seems feasible. There are two reasons for discounting asperity interactions in starved lubricant breakdown failure: a) races can be cleaned after failure and reused, apparently indefinitely, b) degradation rates can be drastically altered by a surfactant.

A momentary retainer instability would indeed give a torque spike and probably have an effect on film thickness as well, as shown in Mr. Kannel's illustration. But note the time scale: some 500 ms from start to finish. Clearly this disturbance can't be used to explain long term jag transients observed in a retainerless bearing.

Specific reply to Messrs. Houpert and Harris:

Experiments measuring BSR during changes in bulk temperature of the whole apparatus do not show any temperature effect, at least over changes of 15°C. Experiments (A) have also shown that a starved bearing cannot distinguish between two lubricants of the same class having a ratio in bulk viscosity of 160 and in pressure viscosity coefficient of 1.38. Such results indicate that bulk visco-thermal changes don't affect the kinematics of starved EHL lubrication very much. I agree that an elastic response in the lubricant may be involved in high frequency transverse precessional slip. If so this is perhaps the first instance of fluid elasticity observed in a bearing as opposed to a traction device. An analysis of ball precessional dynamics will give information on the phase of the transverse stresses and displacements (B).

Dr. Hamrock and I are presently engaged in discussions as to whether and how side leakage might be incorporated into starvation theory. We are also building an apparatus similar to Fig (3), but four times larger. A starved, retainerless angular contact bearing provides an excellent vehicle to insure theoretical and experimental compatibility.

ADDITIONAL REFERENCES

A) Kingsbury, E., "Slip Measurement in an Angular Contact Ball Bearing," Trans. ASME, JOLT 105, 1983, p. 162.

B) Kingsbury, E., "Ball Motion Perturbation in an Angular Contact Ball Bearing," ASLE Trans. 25, 1982, p. 279.

STATUS AND NEW DIRECTIONS FOR SOLID LUBRICANT COATINGS AND COMPOSITE MATERIALS

Harold E. Sliney
National Aeronautics and Space Administration
Lewis Research Center
Cleveland, Ohio 44135

At one time, solid lubricants were used almost entirely in aerospace applications. Today there is a pronounced trend to use them over a much broader range of applications. For example, self-lubricating polymer-based composites have displaced traditional oil-lubricated, metallic composites for many journal bearings and thrust washers in applications as diverse as earth-moving machinery and snow blowers to aircraft applications. For moderate temperatures below 200° C, glass filament-wound epoxy bearings with PTFE lubricating liners are useful; for temperatures up to 350° C, graphite fiber reinforced polyimide bearing materials are finding applications. Molybdenum disulfide, graphite, and PTFE are the most widely known and used solid lubricants, and there is increasing interest in the relatively new solid lubricant graphite fluoride. Advanced technology engines such as the adiabatic diesel and the small, efficient gas turbine have severe lubrication and wear problems at temperatures beyond the capabilities of any of these lubricants. Here, self-lubricating ceramics and inorganic composites for use at 1000° C or higher are of interest. However, perhaps the most significant new direction for solid lubricant coatings and self-lubricating composites is their steadily increasing use in dry bearings for large volume, moderate temperature applications. This can be attributed to their simplicity of use (no supporting lubricant system needed), light weight, convenience, and general cost effectiveness.

INTRODUCTION

Forecasting can be risky in any area. However, there appear to be new directions for solid lubricant technology that are reasonably clear. In addition, we can hazard guesses on possible new directions that are less certain. The most apparent current trend is the greatly increased use of solid lubrication. The number and variety of applications for solid lubrication have been increasing steadily, and all signs indicate that we can expect that trend to continue. In the years from the 1940's through the early 1970's, solid lubrication was used predominantly in the aerospace industry with scattered, moderate volume applications throughout general industry. The new direction in recent years is the extended use of solid lubrication in the automotive, metal working, and computer/office machine industries and throughout industry in general. Only three basic solid lubricant materials are used in most of these industrial applications: molybdenum disulfied (MoS_2), graphite, and polytetrafluroethylene (PTFE). However, the variety of coating and composite formulations in which these three basic lubricating materials are used is very large and can be confusing. In fact, because of the large number of compositions available, users are inclined to depend more on performance specifications than on composition specifications.

A relatively new solid lubricant, graphite fluoride, is gaining gradual acceptance. However, its use as a lubricant is expected to increase signifi-

cantly as the material becomes more cost effective due to its increased production for use as an electrode material in lithium-graphite fluoride batteries.

There is a trend to improve corrosion protection with bonded dry film lubricants. These coatings are therefore multipurpose; they are expected to afford corrosion protection in addition to lubrication. This is accomplished largely by using a high resin to solids ratio, by eliminating graphite which at times causes galvanic corrosion problems, and by introducing oxidation inhibitors in the formulation.

The trend in advanced technology is to use solid lubrication for high-temperature applications. In engine systems currently under development (e.g., the adiabatic diesel, small gas turbine engine, and the upgraded rotory engine), high temperatures in certain areas of the engine preclude the use of oils and greases. Anticipated temperatures for the adiabatic diesel and the ceramic gas turbine are so high that the conventional big three solid lubricants and graphite fluoride are not suitable. Here, novel lubricants such as the fluorides of Group I and II metals and the rare earth fluorides are of interest. Certain soft oxides and glassy materials are also possibilties.

For temperatures of 1000° C and higher, metal structural materials and bearing materials are being replaced by ceramics. These ceramics must either be self-lubricating or coated with a solid lubricant. Fortunately, the composition of ceramics, especially oxide ceramics, are easily modified and are therefore amenable to formulation tailored for specific properties. Ceramics may be made self-lubricating by incorporating lubricating components into their basic structure or by surface diffusion of the solid lubricant material into the surficial layer of the ceramic. All of this will require a great deal of research to achieve the degree of lubrication required without being unacceptably damaging to other properties such as strength and dimensional stability.

These trends can be summarized as follows:

(1) Increased use of MoS_2, graphite, and PTFE lubricants throughout general industry
(2) Expanding use of self-lubricating composites - both polymeric and inorganic based
(3) Gradually increasing acceptance of graphite fluoride as a valuable solid lubricant, especially as it becomes more cost-effective
(4) Increased emphasis on multifunctional coatings which provide corrosion protection as well as lubrication
(5) Use of high-temperature solid lubrication in advanced technology engines, especially those with ceramic hot section structural and bearing materials

The balance of this paper will describe examples of lubricating materials relative to current trends in solid lubrication.

DISCUSSION

Polymer-Based Composites

Completely nonmetallic composite bearings are being used in an increasing number of applications. Where high compressive strength is required to achieve satisfactory bearing load capacity, fiber-reinforced polymers are used. The reinforcing fibers are usually glass, graphite, or synthetic polymers.

Aramid-fiber-reinforced epoxy. - Recently, a composite bearing was reported (refs. 1 and 2) that consists of an aramid-fiber-reinforced epoxy shell with a bonded liner of interwoven polyester and PTFE fibers. Aramid is an aromatic polyamide material that has a consideribly higher elastic modulus than glass and therefore results in a bearing structure with greater stiffness than an analagous glass-fiber-reinforced composite. Bearings of this kind have generated considerable interest in the aircraft industry for use as airframe control surface bearings. They are especially attractive for use in control surfaces made of graphite-fiber-reinforced polymer composites. The electrically conductive graphite fibers in the structural composites form galvanic couples with some metals commonly used in bearings, such as aluminum bronze, cadmium, or anodized aluminum, and galvanic corrosion becomes a serious problem especially in marine environments (ref. 1). Galvanic corrosion can of course also occur in metallic airframe structures when the structural material and the bearing material are dissimilar metals. This problem is nonexistent when completely polymeric bearings are used in either metallic or graphite-reinforced structures.

Some highlights of aramid-fiber-reinforced bearings are given in figure 1. In addition to mitigating corrosion problems, the composites are very lightweight, they can be adhesively bonded in the bearing mountings (especially in composite structures), and they are economical. As might be expected, the friction characteristics are typical of PTFE liners in metal-backed bearings with a friction coefficient of 0.06 above 20° C. Higher friction is observed at -23° C where the friction coefficient is about 0.17 at 69 MPa (10 000 psi) and decreases to about 0.10 at 276 MPa (40 000 psi).

These bearings have a lower load capacity and temperature capability than those of more conventional PTFE-lined metallic bearings. However, they have very respectable dynamic load capacities of at least 207 MPa (30 000 psi) from -23° to 121° C. This is more than adequate for most industrial applications, and it is also compatible with the load and temperature limitations of graphite fiber - epoxy structural members in which the composite bearings will be mounted in advanced airframe applications. The U.S. Airframe Bearing Committee has proposed a specification (MIL B-85560) for qualification of composite bearings for use in military aircraft.

Graphite-fiber-reinforced polyimide. - For temperatures above 125° C, the epoxy composite bearings are not suitable. Graphite-fiber-reinforced polyimide (GFRPI) composites were shown to have good tribological properties to higher temperature (ref. 3). It is now known that GFRPI composite bearing materials can be used up to 260° to 360° C depending on the specific polyimide used. The graphite fibers do not generally cause galvanic corrosion in the higher temperature application because corrosion resistant alloys are employed at these temperatures.

GFRPI composites are reinforced with either chopped graphite fibers or a woven graphite fabric. The fabric can be a two- or three-dimensional weave. Graphite-fabric-reinforced polyimide composites have been extensively studied at Hughes Aircraft in a DARPA-funded program on the subject of solid lubricated rolling element bearings (ref. 4). In that program it was demonstrated that polyimide composites with woven fabric reinforcement and suitable solid lubricant additives can be used as a self-lubricating cage material in ball bearings. Size 207 ball bearings equipped with such cages containing a complex gallium-indium, tungsten diselenide solid lubricant were successfully operated for limited duration at shaft speeds up to 24 000 rpm (ref. 5).

Most of the research on GFRPI at the NASA Lewis Research Center has been with the chopped fiber approach (e.g., refs. 6 to 9). The composite is prepared by incorporating the fiber into the still-fluid B-staged polymer, mixing

to achieve a uniform fiber distribution, then transfer molding the mix into a die where the polymerization is advanced under heat and pressure. GFRPI liners can be molded directly into plain spherical bearings by using the metal outer ring and the spherical element of the bearing itself as the mold. The outer ring is precoated with a polyimide varnish to promote adherence to its inner surface, and the spherical element is precoated with a mold release to prevent adherence to the moving bearing element.

A cutaway drawing of a GFRPI-lined plain spherical bearing is given in figure 2. The dynamic load capacities of two bearing designs are shown in figure 3. It is clear that much higher load capacities were achieved with a thin (1.5 mm) molded GFRPI liner between the ball and the outer race than with a bearing consisting of a molded GFRPI ball within a metal outer ring. For comparison, the load capacities of a conventional PTFE-lined bearing design are given. Load capacities were almost twice as high compared to the GFRPI-lined bearings but only to 175° C. At higher temperatures, the PTFE extruded from the bearing even at loads as low as 35 MPa.

Friction coefficients are not shown in figure 3 because they were not significantly influenced by bearing design differences. Friction coefficients of GFRPI bearings were typically 0.15±0.05 from room temperature to 360° C. For comparison, the friction coefficient for conventional PTFE-lined bearings is typically 0.06, but again these bearings are limited to a maximum useful temperature at high loads of about 175° C.

GRAPHITE FLUORIDE

Graphite fluoride $(CF_x)_n$, also referred to as carbon monofluoride (when $x = 1$), is a relatively new solid lubricant that can be loosely described as a layer lattice intercalation compound of graphite. It is prepared by the direct reaction of graphite with fluorine gas at controlled temperature and pressure. It is grey to pure white, depending on its stoichiometry. The subscript x in $(CF_x)_n$ can vary from about 0.3 to 1.1. For $x \geq 1$, the compound is pure white, electrically nonconductive, and nonwettable by water (hydrophobic). There is some debate about whether $(CF_x)_n$ is a true intercalation compound because the basal planes of the graphite cyrstallites are distorted to a puckered, nonplanar configuration when the compound is formed. However, there is no doubt that the orginal graphite crystal lattice is the primordial lattice from which the crystal structure of $(CF_x)_n$ is formed. The fluorine to carbon bonds are covalent with the fluorine atoms located between the distorted basal planes. The spacing between the basal planes is expanded from 3.4 Å in graphite to 7.5±1.5 Å in $(CF_x)_n$ (ref. 10). $(CF_x)_n$ is not known to oxidize in air, but it does decompose thermally above about 450° C to form carbon tetrafluoromethane, other low molecular weight fluorocarbons, and carbon (ref. 11).

Some early research on the lubricating properties of $(CF_x)_n$ is reported in reference 12. In that study, thin lubricating films of $(CF_x)_n$ and of MoS_2 were burnished on 440 C and 301 stainless steel disks and evaluated in pin on disk experiments. The $(CF_x)_n$ films were the more durable ones over the entire temperature range shown. Friction coefficients were for the most part well below 0.1 up to the failure temperatures of the coatings. Failure temperature was 400° C for MoS_2 and 480° C for $(CF_x)_n$. Similar results were obtained for the lubrication of 301 stainless steel with $(CF_x)_n$, but burnished MoS_2 films failed immediately on this alloy. General agreement with these results were obtained with burnished $(CF_x)_n$ using a flat rub block on a cylinder specimen configuration (ref. 13).

Various resin binders have been used with $(CF_x)_n$ to achieve longer wear lives and higher load capacities than can be achieved with burnished films. Good results were generally obtained in regard to low friction and wear, but there is some discrepency in reported load capacity of the coatings in Falex V-block tests. Reference 14, for example, reported a high load capacity for epoxy-phenolic resin-bonder $(CF_x)_n$, while the authors of reference 15 reported, based on their Falex evaluation, that $(CF_x)_n$ is not considered to be suitable for use in heavy load application. However, there are $(CF_x)_n$ coatings that have quite adequate load capacity for lubricating bearings with conformal contacts such as plain spherical bearings or cylindrical bushings. Polyimide-bonded $(CF_x)_n$ in particular has been extensively studied and is an excellent lubricant to about 350° C.

Polyimide-bonded graphite fluoride coatings. - Polyimide varnish films have long wear life and low friction coefficients above a friction transition temperature typically of about 100° C (ref. 16). At room temperature, short coating wear life and increased friction are observed. This transition in the tribological properties of polyimides has been attributed to second-order relaxation in the molecular bonds of the polymer above the transition temperature (ref. 17). The addition of $(CF_x)_n$ as a solid lubricant pigment to the varnish improves friction and wear life at all temperatures and completely masks the undesirable effects of the friction transition temperature of the polyimide varnish.

A promising application for polyimide-bonded $(CF_x)_n$ coatings is as a backup lubricant for compliant (foil) gas bearings at temperatures to 350° C. About 100° C higher gas temperature capability can be achieved by substituting PI-bonded $(CF_x)_n$ for the more conventional PTFE coatings. Current research by this author shows that these coatings are remarkably durable in start/stop endurance testing of foil bearings. The start/stop torque characteristics of a foil bearing lubricated with PI-bonded $(CF_x)_n$ at 300° C are shown in figure 4. The peak torque values occur before liftoff and after touchdown when the journal is in rubbing contact with the foil coating. The peak torque values are comparable to those obtained with PTFE coatings at room temperature.

Graphite fluoride availability. Factors which have so far retarded the acceptance of graphite fluoride for use as a solid lubricant in the United States are high cost, variable purity, and limited sources. These limitations should soon be alleviated. A facility for the manufacture of tonnage quantities of $(CF_x)_n$ will soon be in operation in this country (ref. 18).

The largest volume application of $(CF_x)_n$ is as an electrode material for $(CF_x)_n$ /lithium batteries. Figures 5 and 6 (from ref. 19) show typical battery construction and voltage discharge curves for this type of battery. The $(CF_x)_n$ battery has twice the output voltage and several times the watt-hour capacity of the standard carbon dry cell. The domestic production of graphite fluoride for this type of battery is expected to lower the cost of high purity $(CF_x)_n$ and make it cost effective for other applications including solid lubrication. This has been the experience in Japan where the $(CF_x)_n$ battery is already in production, and the compound is, therefore, available in quantity at prices apparently acceptable for its use as a solid lubricant. Many commercial lubricant products containing $(CF_x)_n$ are now available in Japan. Hopefully, a similar experience will occur in this country, especially since much of the pioneering research on $(CF_x)_n$ as a lubricant was performed in the U.S.A. (e.g., refs. 12, 14, and 20).

Table I lists a number of advanced technology areas and the anticipated temperatures at which components must be lubricated. It is obvious that most of these are beyond the temperature limits of oils, greases, polymers, or even known layer lattice solid lubricants. We, therefore, need to creatively search for other classes of solid materials with desirable tribological properties over a very wide temperature spectrum from atmospheric temperature to in excess of 1000° C. We also must apply creative concepts in the use of these materials. Some suggested concepts for achieving high-temperature lubrication are the following:

(1) Formulate intrinsic self-lubricating compositions
- Dispersed soft phases
- Vitrifying agents for low shear strength glaze
- Eutectic formers with components of mating surface

(2) Coatings
- Plasma sprayed
- Fusion bonded
- Surficial diffusion layer

(3) Transfer film lubrication

(4) Sputtering, ion plating
- Soft metals for lubrication
- Hard coats for wear control

Some of the materials that are appropriate to consider in applying these concepts are indicated in figure 7.

Is is now well established that chemically stable fluorides of Group I and II metals (such as LiF, CaF_2, and BaF_2) lubricate at high temperature (e.g., refs. 21 to 24). CaF_2, for example, undergoes a brittle to plastic transition at around 500° C which gives this compound the ability to function as a solid lubricant from 500° C to at least 1000° C. The lubricating properties of these compounds as powders, as fusion-bonded coatings for metals, and as components in composites have been reported. The composites are either sintered metal structures infiltrated with molten fluorides during their preparation or plasma-sprayed multicomponent coatings.

Fluoride-metal composites. - Composite bearing materials in which the solid lubricant is dispersed throughout the structure are advantageous when long lubricant life is required. In some cases, a thin, bonded solid lubricant coating is used as an overlay on the self-lubricating composite material. This assures the minimum friction coefficient obtainable by enrichment of the composite surface with lubricant while providing long life due to the underlying, self-lubricating composite material. Composites prepared by sintering and infiltration are useful materials for monolithic bearings and seals (ref. 23). Where coatings are appropriate, similar compositions can be prepared by plasma spraying (e.g., refs. 22 and 24).

Mixed powders of, for example, CaF_2 and metal can be deposited by plasma arc spraying to form a composite coating on a wrought metal substrate. Excess coating material is applied, and the coating is then surface ground to the desired thickness (usually 0.010 to 0.020 cm) and a smooth surface finish. Two coatings of this type that have been successfully applied in extreme environments such as the space shuttle airframe and the hot section of small jet engines are designated PS100 and PS101. Their compositions by weight are the following:

PS100: 67 nichrome, 16 1/2 calcium fluoride, 16 1/2 glass
PS101: 30 nichrome, 30 silver, 25 calcium fluoride, 15 glass

The glass in these compositions is a special sodium-free glass which provides oxidation protection to the nichrome. Its composition is 58 SiO_2, 21 BaO, 8 CaO, 13 K_2O.

Figure 8 (ref. 24) gives friction coefficients in air for oscillating journal bearings. The cylindrical bores of the bearings were coated with 0.025 cm of PS100 or PS101. A pre-oxidized, but otherwise uncoated, unlubricated bearing is included for comparison. The oxide film on the pre-oxidized bearing provided some protection against galling for a time but the bearing seized at 870° C. Friction coefficients for the bearing lubricated with PS100 were lower at all temperatures, and effective lubrication was achieved from about 500° to 900° C. The beneficial effect of silver in reducing low-temperature friction while only moderately reducing maximum temperature capability of the coating system is illustrated by the data for PS101. Friction coefficients of the order of 0.2 were obtained at all temperatures from -107° to 870° C.

In general, the maximum useful temperature in air for fluoride coatings with a superalloy matrix is limited by oxidation of the alloy. Even with a protective glass within the composite structure, the superalloy oxidizes more rapidly in the composite than in the wrought metal state. The oxidation temperature limit for composites with a nickel superalloy matrix is about 900° C and for cobalt matrix coatings it is about 650° C.

Fluoride-oxide composites. - Because of the limitations imposed by the oxidation of metal matrix composites and coatings, completely nonmetallic compositions are of interest. It has been reported that plasma-sprayed coatings of NiO containing about 15 percent CaF_2 have good high-temperature wear resistance (ref. 22). This coating is plasma sprayed onto seal bars for regenerators that are used in automotive gas turbine engines to improve thermal efficiency. The coatings must have wear resistance at high temperature while in sliding contact with a porous ceramic regenerator core. The core material is generally lithium-aluminum silicate (LAS), magnesium-aluminum silicate (MAS), or aluminum silicate (AS).

Current preliminary research at the NASA Lewis Research Center indicates that plasma-sprayed coatings based on zirconium oxide (ZrO_2) have attractive tribological properties. Figure 9 gives the friction coefficients of plasma-sprayed ZrO_2 and ZrO_2-CaF_2 coatings to 930° C. In these experiments, the coating was on the cylindrical surface of a rotating disk; it was placed in sliding contact with two flat nickel-base superalloy rub blocks. The beneficial effect of a 20 percent CaF_2 addition on reducing friction is clear. In an attempt to further reduce friction, silver was added to the coating composition. Friction and wear of ZrO_2-CaF_2 coatings with and without the silver addition are shown in figure 10. The silver addition was clearly detrimental, not having the beneficial effect it had on improving room temperature friction and wear of PS101. In all cases, wear of the metal rub shoes was mild, indicating that the coatings are not abrasive to the metal counterface.

Silicon carbide versus metals in air. - Silicon carbide is one of the important refractory materials being used as a structural ceramic in advanced propulsion systems. It is, therefore, of interest to determine its friction and wear properties. The friction coefficient from 25° to 930° C for silicon carbide riders sliding on the precipitation-hardened nickel-base-alloy Inconel 750 are shown in figure 11. At the sliding velocity of 9 m/s (1770 fpm) the friction coefficient decreased steadily from 0.4 at 25° to 0.2 at 930° C.

Table II gives wear coefficients for SiC riders sliding against (1) M-50 bearing steel at room temperature and at 300° C and (2) Inconel 750 at room temperature and 900° C. Wear coefficients in the 10^{-11} to 10^{-10} range are

typical of well-lubricated specimens in the boundary lubrication regime. Therefore, the wear coefficients, which are about 10^{-10} for SiC and about 10^{-9} for M-50 at room temperature and at 300° C, may be considered quite low for unlubricated sliding. Wear coefficients for the unlubricated SiC and Inconel 750 combination are higher but not extreme. Wear coefficients in the 10^{-9} range are considered moderate, and all wear coefficients were in that range except in the case of Inconel 750 at room temperature. As is usual with superalloys, both friction and wear of Inconel 750 decreased when the metal oxidized at elevated temperature.

CONCLUDING REMARKS

There appears to be a definite trend to the increasing use of solid lubrication for moderate as well as extreme environmental condition. Under mild conditions of temperature and chemical reactivity, solid lubrication is sometimes preferred for design simplicity and cost effectiveness. At high temperature beyond the capabilities of oils or greases, self-lubricated bearings or gas bearings are the only options; and even the gas bearings usually require a backup solid lubricant coating for starts, stops, and transient high-speed rubs.

Polymer-based composite bearing materials are receiving increased acceptance in a very large variety of applications. Polymer composite bearings are readily fabricated by well-known techniques of filament winding, injection molding, or transfer molding. Some polymer composites do not require a metal backing and are, therefore, completely inert to galvanic corrosion, lightweight, and inexpensive. An example is the glass or aramid-filament-wound epoxy bearings with reinforced PTFE self-lubricating liners. This bearing type is useful at high loads to a maximum temperature of about 125° C.

Graphite-fiber-reinforced polyimide composites are used as free-standing bearings (e.g., variable stator vane bushings in jet engine compressors) and as self-lubricating liners in plain cylindrical or plain spherical sliding contact bearings. They are useful to about 350° C. The graphite fibers can induce galvanic corrosion of contacting metals, but this type of bearing is usually used for moderately high-temperature applications where the surrounding metals are selected for their corrosion resistance.

For temperatures to 1000° C and higher, some inorganic composites including specially formulated metal-ceramic and all-ceramic composition have been used in some applications and will be needed in many more applications as advanced, high efficiency propulsion systems receive more attention.

REFERENCES

1. Lynn, W. F.: New Concepts in Aircraft Journal Bearings. AFFDL TR-78-97, 1978. (AD-A068619).
2. Sliney, H. E.; and Williams, F. J.: Performance of PTFE-Lined Composite Journal Bearings. NASA TM-82779, May 1982.
3. Giltrow, J. P.; and Lancaster, J. K.: Carbon-Fibre Reinforced Polymers as Self-Lubricating Materials. Tribology Convention, Pitlochry, Scotland, Institution of Mechanical Engineers, London, 1968, pp. 149-159.
4. Gardos, M. N.; and McConnell, B. D.: Development of a High-Load, High Temperature, Self-Lubricating Composite, Parts I through IV. ASLE Preprints Nos. 81-LC-3A-3 through 81-LC-3A-6, Oct. 1981.

5. McConnell, B. D.; and Mecklenburg, K. R.: Solid Lubricated Rolling Element Bearings. Presented at Symposium on Lubricants for Extreme Environments ASME/ASLE Lubrication Conference (Washington, D.C.), Oct. 1982.
6. Sliney, H. E.; and Johnson, R. L.: Graphite Fiber-Polyimide Composites for Spherical Bearings to 340 °C. NASA TN-D-7078, 1972.
7. Fusaro, R. L.; and Sliney, H. E.: Friction and Wear Behavior of Graphite Fiber Reinforced Polyimide Composites, ASLE Trans., vol. 21, no. 4, 1978, pp. 337-343.
8. Sliney, H. E.; and Jacobson, T. P.: Performance of Graphite Fiber Reinforced Polyimide Composites in Self-Aligning Plain Spherical Bearings to 315 °C. Lubr.-Eng., vol. 31, no. 12, 1975, pp. 609-613.
9. Sliney, H. E.: Some Load Limits and Self-Lubricating Properties of Plain Spherical Bearings with Molded Graphite Fiber-Reinforced Polyimide Liners to 320 °C. Lubr. Eng., vol. 35, no. 9, 1979, pp. 497-502.
10. Rudorff, W; and Rudorff, G.: Structure of Carbon Monofluoride. Z. Anorg. Chem., vol. 253, 1947, pp. 281-296.
11. Kuriakose, A. K.; and Margrave, J. S.: Mass Spectrometric Studies of the Thermal Decomposition of Poly (Carbon Monofluoride). Inorg. Chem., vol. 4, no. 11, 1965, pp. 1639-1641.
12. Fusaro, R. L.; and Sliney, H. E.: Preliminary Investigation of Graphite Fluoride as a Solid Lubricant. NASA TN D-5097, Mar. 1969.
13. Play, D.; and Godet, M.: Study of the Lubricant Properties of Carbon Monofluoride $(CF_x)_n$. NASA TM-75191, Dec. 1977. (Translation of "Etude des propietes lubrifiantes de monofluorure de graphite; $(CF_x)_n$. Proceedings Calloques Int. du CNRS, No. 233, 1975, 441-450.)
14. Gisser, J.; Petronio, M.; and Shapiro, A.: Graphite Fluoride as a Solid Lubricant. Lubr. Eng., vol. 28, no. 5, May 1972, pp. 161-164.
15. McConnell, B. D.; Snyder, C. E.; and Strang, J. R.: Analytical Evaluation of Graphite Fluoride and Its Lubrication Performance Under Heavy Load. Lubr. Eng., vol. 33, no. 4, Apr. 1977, pp. 184-190.
16. Fusaro, R. L.; and Sliney, H. E.: Lubricating Characteristics of Polyimide Bonded Graphite Fluoride and Polyimide Thin Films. ASLE Trans., vol. 16, no. 3, 1973, pp. 189-196.
17. Fusaro, R. L.: Molecular Relaxation, Molecular Orientation and the Friction Charcteristics of Polyimide Films, ASLE Trans., vol. 20, no. 1., 1977, pp. 1-14.
18. Allied Building Plant to Develop Fluorinated Carbon Products. News release, J. Commer., No. 12, 1982, p. 21. B.
19. Watanabe, N.; and Nakajima, T.: Graphite Fluoride. Preparation, Properties, and Industrial Application of Organo Fluorine Compounds, R. E. Banks, ed., John Wiley and Sons, 1982, pp. 297-322.
20. Fusaro, R. L.; and Sliney, H. E.: Graphite Fluoride $(CF_x)_n$ - A New Solid Lubricant. ASLE Trans., vol. 13, no. 1, Jan. 1970, pp. 56-65.
21. Sliney, H. E.; Strom, T. N.; and Allen, G. P.: Fluoride Solid Lubricants for Extreme Temperatures and Corrosive Environments. ASLE Trans., vol. 8, no. 4, 1965, pp. 307-322.
22. Moore, G. D.; and Ritter, J. E.: The Friction and Wear Characteristics of Plasma-Sprayed NiO-CaF_2 in Rubbing Contact with a Ceramic Matrix. Lubr. Eng., vol. 30, no. 12, 1974, pp. 596-600.
23. Sliney, H. E.: Self-Lubricating Composites of Porous Nickel and Nickel-Chromium Alloy Impregnated with Barium Fluoride-Calcium Fluoride Eutectic. ASLE Trans., vol. 9, no. 4, 1966, pp. 336-347.
24. Sliney, H. E.: Wide Temperature Spectrum Self-Lubricating Coatings Prepared by Plasma Spraying. Thin Solid Films, vol. 64, 1979, pp. 211-217.

TABLE I. - WHY HIGH-TEMPERATURE SOLID LUBRICANTS?

Application	Temperature, °C
Adiabatic diesel cylinder liner	600 to 1100
Automotive gas turbine engine:	
Regenerator wear face	260 to 1100
Foil bearing (main shaft)	650
Rotary engine for general avaition apex seals	300 to 650
Aircraft gas turbine engine:	
Variable stator vane (compressor, current)	350
Bushings (turbine, near future)	1000
Thrust reversal bearings	800
Supersonic aircraft:	
Control surface bearings	350
Control surface rub seals	650
Shuttle:	
Control surface rub seals	850

TABLE II. - WEAR COEFFICIENTS FOR SiC RIDERS SLIDING AGAINST M-50 STEEL AND INCONEL 750

Disk material	Disk temperature, °C	Wear factor, $cm^3/kg-cm$	
		SiC rider	Metal disk
M-50 steel	Room	$0.1x10^{-9}$	$1.2x10^{-9}$
	300	$.07x10^{-9}$	$1.8x10^{-9}$
Inconel 750	Room	$2.1x10^{-9}$	$18.0x10^{-9}$
	900	$1.0x10^{-9}$	$8.0x10^{-9}$

POLYMER COMPOSITE JOURNAL BEARINGS

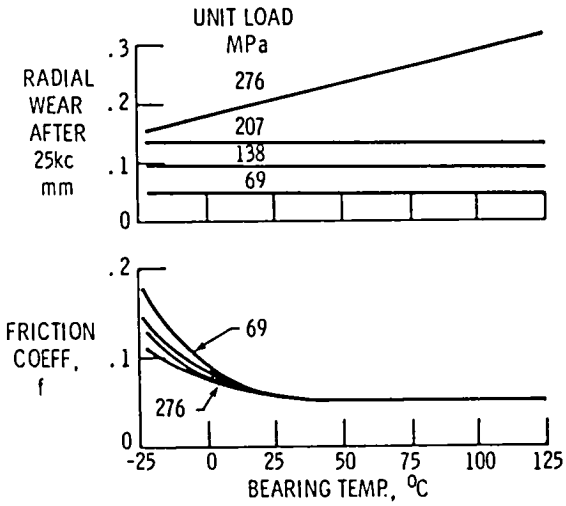

- LOW WEAR, INSENSITIVE TO TEMP. AT UNIT LOADS TO 207 MPa (30000 psi)
- LOW FRICTION (-25° TO 125° C) INVARIANT FROM 20° TO 125° C
- 200 MPa (30000 psi) DYNAMIC LOAD CAPACITY

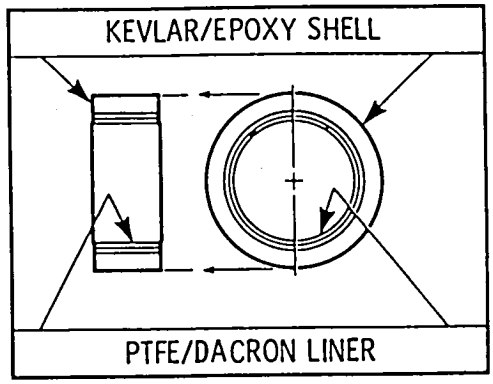

OTHER TECHNICAL GAINS

- ELIMINATES GALVANIC CORROSION (NON-METALLIC)
- LIGHT WEIGHT
- CAN BE ADHESIVELY-BONDED TO COMPOSITE STRUCTURES
- ECONOMICAL
- HIGHER MODULUS (STIFFER) THAN GLASS FIBER REINFORCED BEARINGS
- MIL-SPEC BEING WRITTEN BY A DOD AGENCY BEARING COMMITTEE BECAUSE OF FAVORABLE DATA FROM THIS PROGRAM

Figure 1.

CS-83-2148

TEST BEARING WITH MOLDED GFRPI LINER

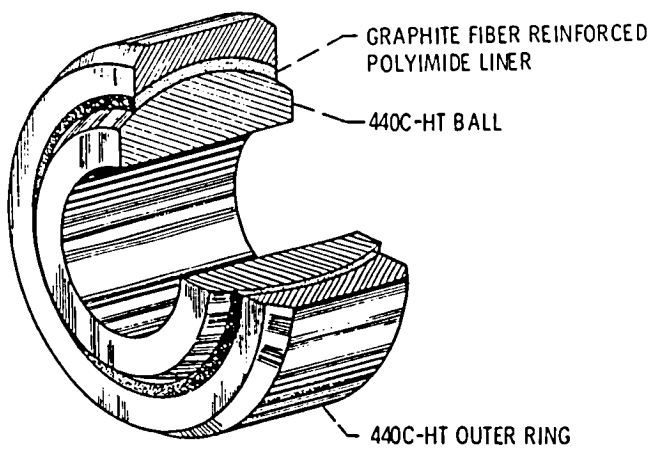

Figure 2.

CS-83-2157

DYNAMIC UNIT LOAD CAPACITIES OF THREE BEARING DESIGNS SELF LUBRICATING WITH GFRPI COMPOSITE

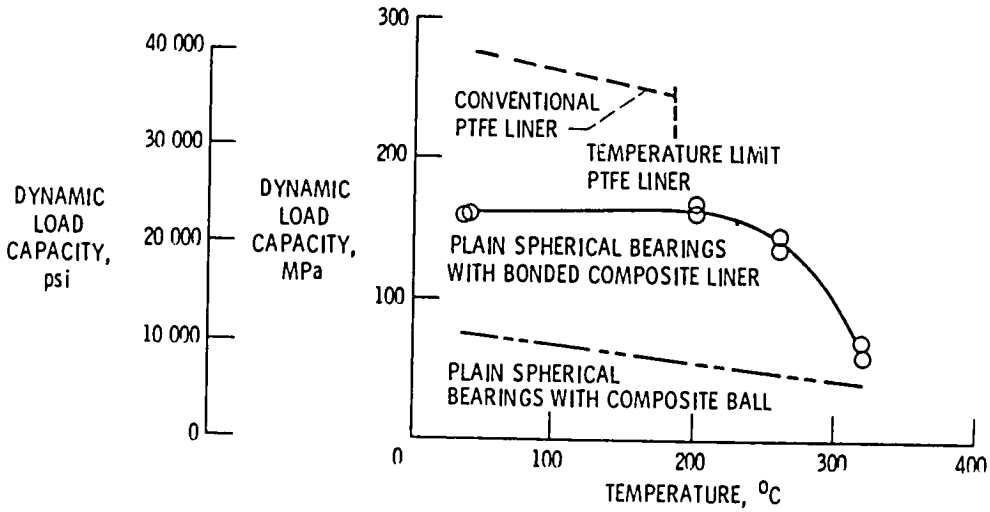

Figure 3.

CS-83-2149

START/STOP CHARACTERISTICS OF FOIL BEARING WITH PI-BONDED GRAPHITE FLUORIDE LUBRICANT

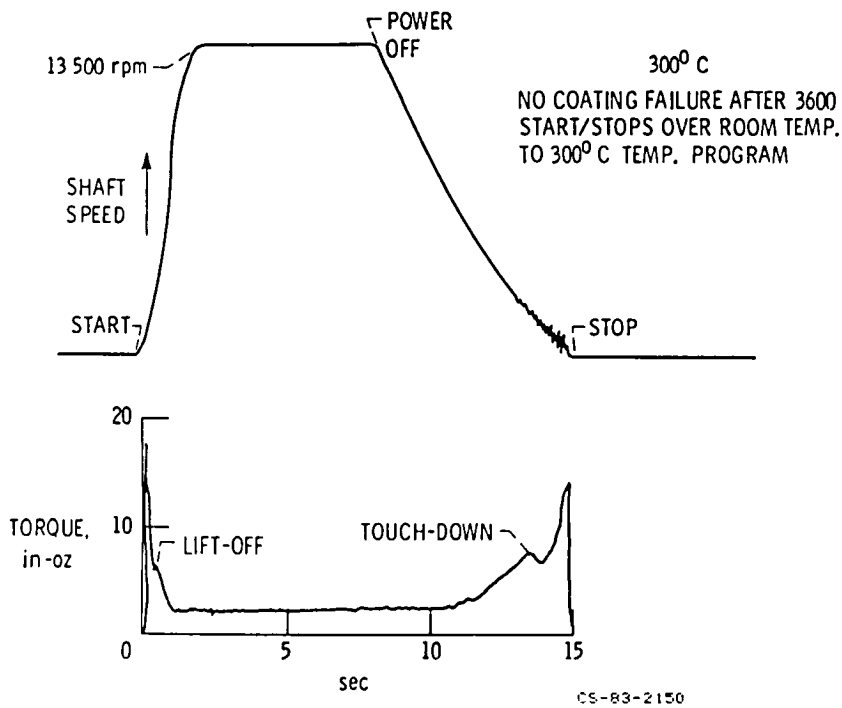

CS-83-2150

Figure 4.

INTERNAL CONSTRUCTION OF A CYLINDRICAL $[CF]_\eta$/Li BATTERY

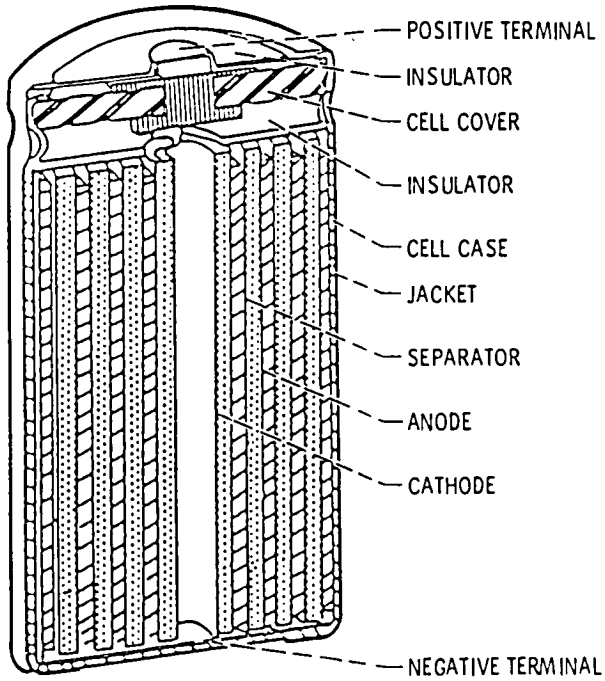

Figure 5. CS-83-2151

TYPICAL DISCHARGE CURVES FOR $[CF]_\eta$/Li AND CONVENTIONAL CARBON/ZINC BATTERIES

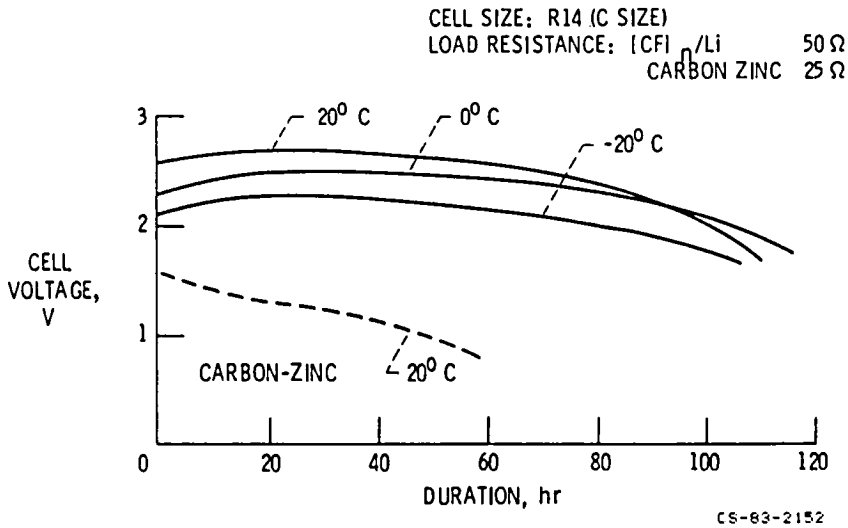

Figure 6.

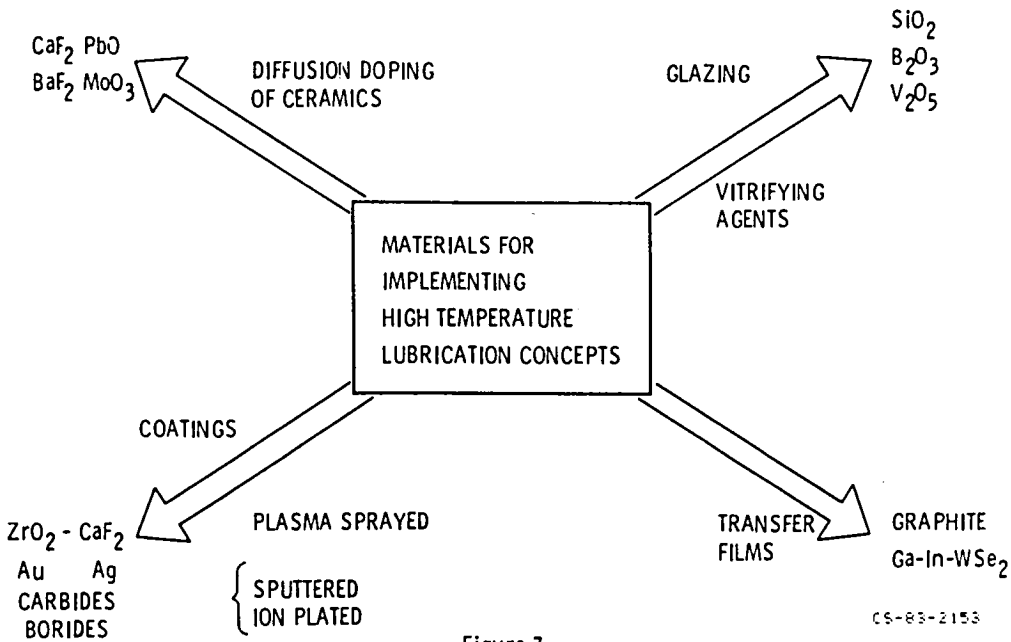

Figure 7.

PLASMA-SPRAYED COATINGS FOR SELF-ALINING OSCILLATING BEARINGS

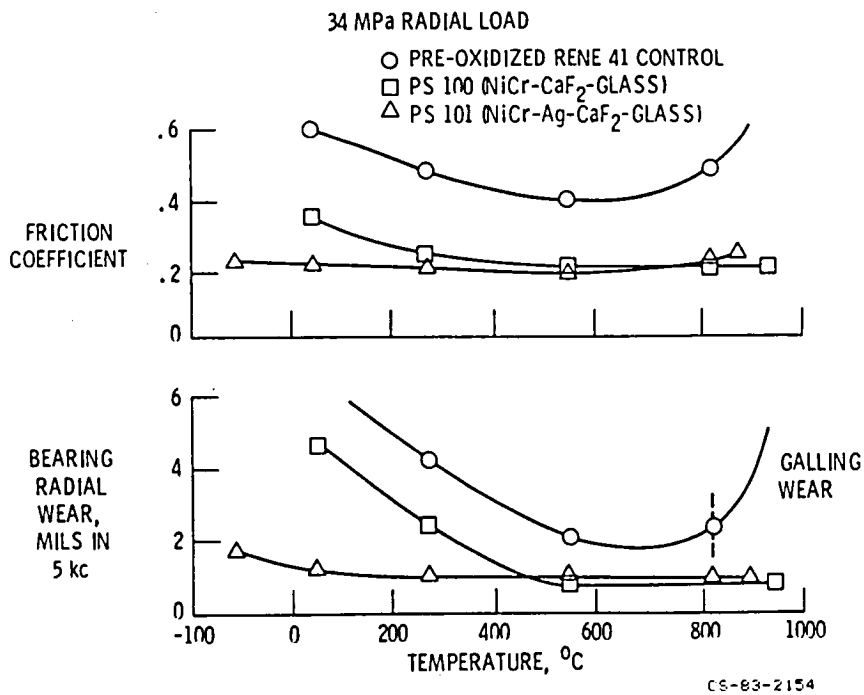

Figure 8.

FRICTION COEFFICIENTS OF PLASMA-SPRAYED COATINGS

50-PERCENT RELATIVE HUMIDITY AIR ATMOSPHERE
INCONEL 718 RUB SHOES

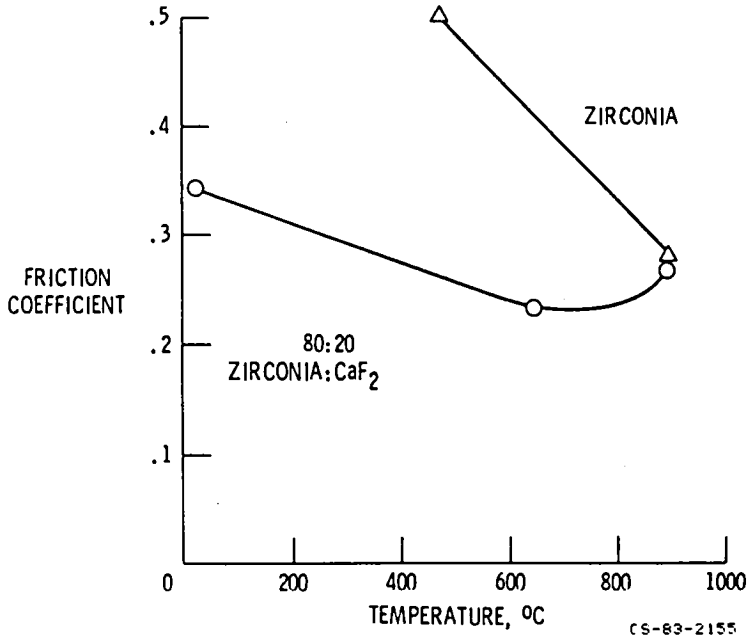

Figure 9.

WEAR AND FRICTION OF ZIRCONIA-BASED, PLASMA-SPRAYED COATINGS

50-PERCENT RELATIVE HUMIDITY AIR ATMOSPHERE
INCONEL 718 RUB SHOES

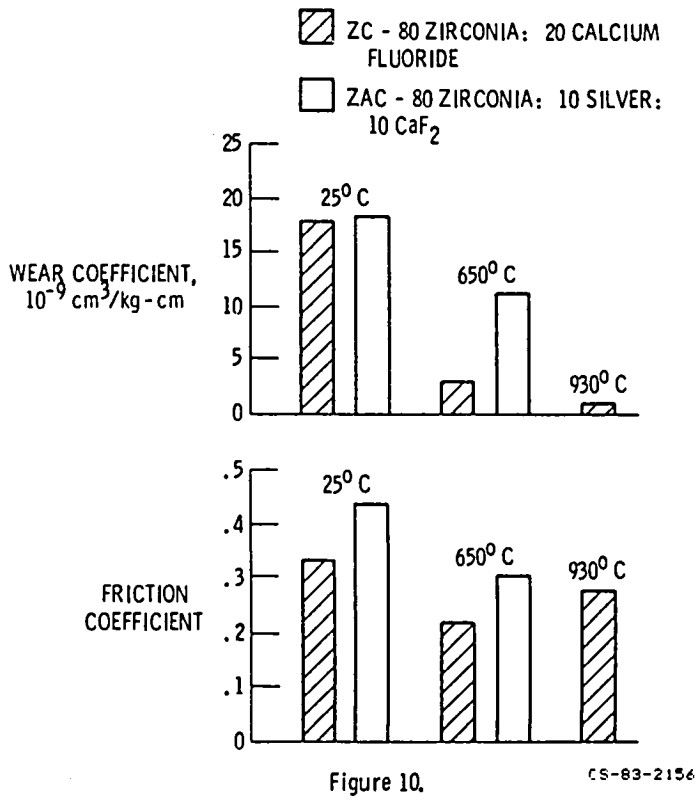

Figure 10.

FRICTION vs TEMPERATURE FOR SILICON CARBIDE vs INCONEL 750

RIDER LOAD = 500 g
DISK SPEED = 3750 rpm (9 m/s)
ATMOSPHERE: ROOM AIR(50-PERCENT RELATIVE HUMIDITY)

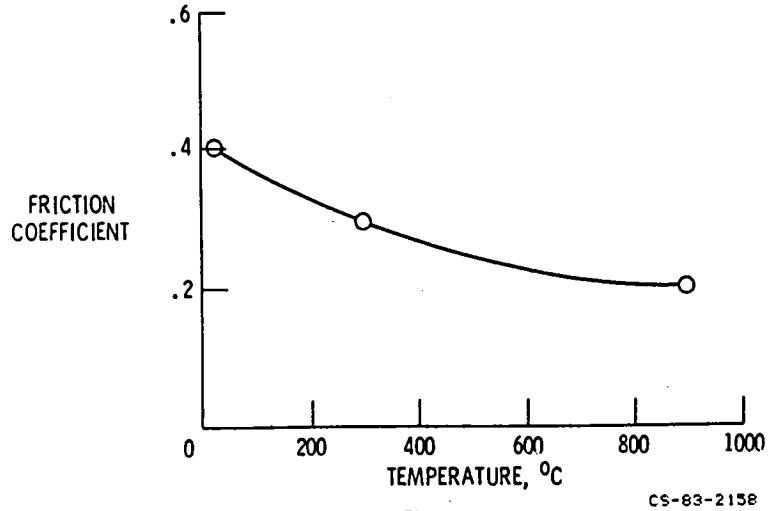

Figure 11.

PRACTICAL APPLICATIONS AND USES OF SOLID LUBRICANT FILMS

Bernard C. Stupp
Hohman Plating and Manufacturing, Inc.
Dayton, Ohio

Practical applications are illustrated with discussions covering the reasons for use of solid lubricants, required performance, lubricant selection, and results obtained for the various examples shown. The applications described cover a broad range of solid lubricants. Included are soft lamellar compounds, organic polymers, soft elemental metals, oxides and compounds for high temperature use. The illustrations selected cover a broad range of lubricant application techniques delineating the reasons for the different processing procedures which include bonded films, plasma spraying, sputtering, ion plating and electrodeposition.

INTRODUCTION

Solid lubricants or solid materials which exhibit lubricating properties have been in use for many years. In early years only materials which exhibited slipperiness to the feel were classified as lubricants. This was primarily due to the fact that most uses were under ambient operating conditions. In today's technology, solid lubricants are expected to perform over a broad spectrum of harsh environments. If a material exhibits tribological behavior under the required operating environment then it can be classified as a lubricant even if it is not slippery to the feel.

A list of common solid lubricants is shown in Table I. When used as bonded films, graphite, molybdenum disulfide and polytetrafluoroethylene (PTFE) are the most commonly used.

Graphite is a lamellar compound which lubricates because of weak van der Waals forces at the slip planes. However, as is well known, graphite depends on an intercalation of gases, liquids or other substances between its layers. It is not, therefore, useful as a lubricant in an environment where these intercalated or adsorbed materials cannot be maintained (Ref.1). Graphite has an upper operating temperature range of 823-933° Kelvin (1022-1220°F) at atmospheric pressure unless stabilized against oxidation with adjuvants.

Molybdenum disulfide is a dichalcogenide with weak van der Waals forces between the sulfur bonds and is not dependent upon adsorbed vapors for its lubricating properties. It is subject to oxidation above 573°Kelvin (572°F) and its nature is such that high humidity conditions deleteriously affects its lubricating characteristics (Ref.2). While not confirmed, it has been reported that molybdenum disulfide films sputtered at certain parameters are not as grossly affected by high humidity conditions as is the natural product (Ref.3). While

other dichalcogenides are shown in Table I, molybdenum disulfide is the most widely used.

Organic polymers such as PTFE and polymeric amides offer very low friction characteristics but generally exhibit low load carrying properties. The load carrying capabilities can be drastically improved with fillers such as carbon, oxides, molybdenum disulfide and other polymeric binders. PTFE has excellent non-wetting properties and is widely used as a release agent. As a molded article it serves for many lightly loaded applications, and in conjunction with proper fillers and binders, as a solid lubricant film.

Methods of applying the solid lubricants listed in Table I are quite varied and the technique selected will depend to a great extent upon the lubricant and the desired end result. For very thin films, less than $2x10^{-6}$m (.00008 in.), where the lubricant has a natural affinity for the substrate material, they may be burnished. This is not, however, a precise method. Thickness control is difficult and adhesion is marginal. A much more precise method is sputtering where thickness control is precise and due to the high energies involved in the deposition the adhesion is excellent. Furthermore, where noncompatibility exists between lubricant and substrate, graded coatings can be achieved with ease. Sputtering, a unique method of applying very thin films, avoids many of the common problems encountered by other application techniques. The need for binders is eliminated. The substrate surface is made atomically clean and can be textured by ion bombardment, thus providing excellent adhesion. Duplex films with enhanced properties can be produced (Ref.4). Lead, silver, gold, tin, molybdenum disulfide, PTFE and the oxides have been successfully sputtered.

Plasma spraying is used for applying coatings of calcium/barium fluoride, various oxides and hard wear resistant coatings. Plasma sprayed coatings are usually much thicker than sputtered films and generally must be finish machined after the coating is applied (Ref.5). The density of plasma sprayed coatings is lower than sputtered films and adhesion to the substrate is less.

The elemental metals listed in Table I may be electroplated, chemically deposited or ion plated. For tribological purposes ion plating is a superior method. Ion plating is accomplished by placing the component in a vacuum chamber and reducing the pressure to a low level. Following this, the chamber is back filled with a non-reactive gas such as argon to a pressure which permits a glow discharge to be sustained when the part to be coated is negatively biased. This procedure ion bombards the surface, atomically cleans it, raises the temperature and textures the surface. After the surface is sufficiently cleaned in this manner, the coating material is melted and evaporated into the glow discharge. Some of the evaporant material is ionized by collisions with electrons and is attracted to the surface of the part to be coated. The ionized evaporant arrives at the surface with high energies, in the range of $5x10^{-16}$ joule to $6x10^{-16}$ joule (3000 to 4000 electron volts) which provides excellent adhesion. Very thin films can be deposited which is very desirable for many tribological applications (Ref.6, 7 & 8).

For most applications of graphite, molybdenum disulfide and PTFE, the common method is to incorporate the lubricant pigment into various binders which can be

applied by spraying, dipping or brushing, after which they are bonded by baking or air drying.

A variety of binders used in solid lubricant compositions are listed in Table II. As would be expected, the types of binders used, their ratio to lubricant pigment and the incorporation of other adjuvants greatly influence the properties of the final coating. A high percentage of lubricant pigment to resin binders usually affords better frictional behavior but in most cases lower endurance life. Higher binder percentages can offer greater corrosion protection with a sacrifice of lubricating properties.

Other factors to be considered for proper use of bonded solid lubricant films are substrate compatibility with the particular lubricant composition to be used, substrate surface preparation and design compromises. Probably the most important consideration, assuming that the bonding agent used has good adhesion to a particular substrate material, is surface preparation (Ref.9, 10 & 11).

A number of surface preparations are listed in Table III for various substrate materials. Due to the fact that some lubricant compositions require different surface preparations for maximum performance, it is difficult to precisely describe the proper pretreatment for all situations. In many cases it must be determined empirically. However, in general, most bonded films perform best when applied over phosphated steels. Some compositions require grit blasting prior to phosphating. There are many different types of phosphating procedures used and the type of crystallography obtained is of considerable importance (Ref.11). Phosphate structures undergo phase changes at elevated temperatures and therefore the type selected should be compatible with the binder cure temperature.

Aluminum, its alloys and titanium are generally anodized prior to application of bonded films. In most instances the anodic film should be unsealed. However, in some formulations the resin binder will preferentially migrate out of the lubricant composition into the unsealed pores of the anodic film, leaving the lubricant film short of the proper ratio of binder to pigment. In these cases the anodic film should be sealed prior to lubricant application. Baking of anodic films will cause cracking of the film which reduces its corrosion resistance. Therefore, either air drying or low temperature curing binders are preferable on anodized materials.

For materials which do not phosphate or anodize, the surfaces may be chemically etched, grit blasted, vapor blasted or ion etched. Regardless of the preparation used, experience has shown that a slightly roughened or disrupted surface provides superior results for bonded films when compared to smoothly machined surfaces.

Designing for the use of bonded films is also an important consideration. These films are generally applied in thicknesses from $5x10^{-6}m$ to $2.5x10^{-5}m$ (.0002-.001 in.). As the films wear, the lubricant is gradually sluffed off. This "sluff-off" or wear debris must have someplace to go or else it expedites destruction of the film. Therefore, wherever possible the component design should incorporate recessed areas in the contact zone.

EXAMPLES OF PRACTICAL USES

The examples of practical uses of solid lubricants shown have been selected to illustrate the various materials and processing techniques discussed in the introduction.

The use of an epoxy bonded MoS_2 film is shown on a screw and slide application used for gripping perforating bars on high speed printing rolls (Fig. 1). The screw actuates a wedge slide which if not lubricated extrudes the shoulder of the screw and the wedge siezes in its guide resulting in a non-uniform pressure in the gripping action. The epoxy binder was used because of its excellent surface adhesion and load carrying capacity. The parts are fabricated of high carbon steel hardened to 553 KHN (Rc 50). They are pretreated by phosphating, sprayed with the lubricant composition to a thickness of $8x10^{-6}m$ to $2x10^{-5}m$ (.0003-.0007 inch) and baked one hour at 478°Kelvin (400°F). The load on the screw shoulder at crash gripping is $6.65x10^{4}$ Newtons/M (380 lbs/in) of bar length. The coated gripper bar is shown placed in the operating machine in Fig. 2.

A steel hand crank operated shaft using a phenolic bonded MoS_2 coating is shown in Fig. 3. The shaft is operated in a cast iron sleeve type bearing and is used to actuate a load of 222 Newtons (50 lb.) to 445 Newtons (100 lbs.) in food processing machinery where conventional grease lubrication is objectionable. The phenolic binder is used on the basis of ease of application and is sprayed over a phosphate pretreatment to a thickness of $1x10^{-5}m$ (.0005 in.) and oven baked one hour at 464° Kelvin (375°F).

This application represents a case in point, where the coating would be more effective if the shaft were machined to provide interrupted surfaces. However, the present coating system operates satisfactorily and due to increased costs the interrupted surface concept has not been implemented.

The use of a polyimide bonded MoS_2 film is shown in Fig. 4. This part has an internal acme thread and slides inside a titanium housing where high shear stress is imposed on the coating. The material is 17-4 PH hardened steel pretreated by vapor blasting. The polyimide bonding lubricant is applied to a thickness of $5x10^{-6}m$ to $1x10^{-5}m$ (.0002 to .0004 in.) and oven cured for one hour at 394° Kelvin (250°F), followed with a 90 minute cure at 589° Kelvin (600°F). This power nut is used on the Instel V satellite to position the antennas. The operational requirement is from one to two cycles per day for 16 years.

The use of an air drying alkyd bonded MoS_2 coating is illustrated in Fig. 5 & 6. In this application, aluminum tubing is coated with the air drying lubricant composition (Fig. 5) after which the tubing is swaged to a reduction of more than 30 percent (Fig. 6). After the reduction the lubricant is removed by buffing.

The above examples of bonded dry film coatings are selected to show the use of different bonding agents. Other applications include, but are not limited to, automotive ball joints, door lock mechanisms, servo motors, anti-skid brake

mechanisms, load adjustor slides on tractor trailers, starter bushings, actuator parts and universal joints.

Uses of sputtered MoS_2 films are illustrated in Fig. 7 through Fig. 10.

A sputtered MoS_2 coating on an adjusting screw is shown in Fig. 7. The screw operates in the acme thread of the power nut shown in Fig. 4. The screw is fabricated of a titanium alloy and is sputtered with $3x10^{-7}m$ (3000 Å) of MoS_2 and operates over the same cycle life as described for Fig. 4.

The assembly of the power nut and screw is shown in Fig. 8. Note that the left hand bearing diameter is also sputtered to prevent fretting corrosion against the inner race of a ball bearing fit. The ball bearing races, retainers and balls are also sputtered with MoS_2.

Sputtered ball bearing components are shown in Fig. 9. These components were used in the Viking satellite for the Mars flight. They were sputtered with $3x10^{-7}m$ to $4x10^{-7}m$ (3000 to 4000 Å) of MoS_2. The bearings operated with complete satisfaction.

The evolution of coating techniques is illustrated in Fig. 10 which shows a cam which operates in a space environment. The cam is fabricated of 17-4 PH steel and must lift a load of $4x10^{4}$Newtons (10000 lbs.) through an angle of arc of 0.61 radian (35°). The mating surface is titanium and the required operating life is 100 cycles. Although the design was improper for using standard bonded films, several were tested and on an average gave from 9 to 20 cycles to failure. When the cam was sputtered with MoS_2 to a thickness of from $2x10^{-6}m$ to $3x10^{-6}m$ (20000 to 30000 Å), this coating provided 50 to 60 cycles to failure. As described earlier, the process of sputtering is such that through some very subtle changes in processing parameters the film properties can be drastically influenced. Intentional incorporation of impurities can drastically influence performance. The final coating evolution in this case was to sputter the cam with a co-sputtered MoS_2 plus 3-5% nickel to a thickness of from $2x10^{-6}m$ to $3x10^{-6}m$ (20000 to 30000 Å). This film has consistently given a life of over 300 cycles.

An example of galvanically deposited films is illustrated in Fig. 11 which is a bearing housing fabricated of aluminum. The coating is a thin film of tin. Its use is old in the art, but it illustrates the use of solid elemental materials as lubricants. The function of the coating in this case is to allow the bearing to break in and operate properly with a marginal horsepower rating. In this instance the bearing housing is used in a compressor which is a highly competitive item and the horsepower rating is thusly reduced to a bare minimum. Without the tin coating the starting torque is high and 15 to 20% of the marginal horsepower motors are burned out in the first 15-25 hours of operation. With the tin coating, the frictional properties are such that no losses occur and the coating cost is economically necessary.

The foregoing example of tin galvanically deposited on aluminum is old in the art. A much newer technique for depositing elemental metals is ion plating. Ion plated lead on high speed ball bearing components is shown in Fig. 12. These bearing components are ion plated with thin films of lead $5x10^{-8}m$ to $1x10^{-7}m$ (500

to 1000 Å) with excellent substrate adherence. They are operated at speeds in excess of 1000 radians/seconds (10,000 RPM) at loads of $7x10^8$ newtons/m^2 (100,000 psi) in a vacuum environment.

An ion plated silver application is illustrated in Fig. 13, which shows a precision lead screw which must operate without backlash. It requires, therefore, a very thin film to prevent interfacial welding under vacuum environment. This particular part is ion plated with $1x10^{-7}$m to $1.8x10^{-7}$m (1000 to 1800 Å) of silver.

Ion plated gold bearing components are shown in Fig. 14. This photograph is of ion plated gold on 440-C stainless steel bearing components used in the Pioneer satellite. The coating process was $3x10^{-8}$m to $5x10^{-8}$m (300-500 Å) of tungsten as a barrier layer to prevent diffusion followed with $1.2x10^{-7}$m to $2x10^{-7}$m (1200 to 2000 Å) of gold. The bearings operated in an environment of space and ammonia at temperature ranges up to 478° Kelvin (400°F).

A highly loaded precision bull gear 0.51m (20 inches) in diameter which has been ion plated with $1.2x10^{-7}$m to $2x10^{-7}$m (1200 to 2000 Å) of gold is shown in Fig. 15. This particular gear is used in space environment. It transmits 136 joules (100 ft lbs.) of torque and the ion gold plate prevents cold welding of the gear pitch line (Fig. 16). The illustration serves to show that not just small parts are coated, and that coating costs are not extreme in relation to fabrication costs. It is not unusual to see metal finishing costs, even in high volume production, exceed manufacturing costs. In this illustration the gold ion plating cost is less than 5 percent of the gear cost.

Thin ion gold plated parts have operated dry at loads in excess of $1.4x10^9$ newtons/m^2 ($2.0x10^5$ psi) without cold welding.

As described earlier, PTFE is an excellent solid lubricant. Fig. 17 shows a wobble plate coated with a carbon filled PTFE composition. The part is fabricated by powder metallurgy and is pretreated with a stabilized phosphate prior to coating with PTFE and oven curing at 589° Kelvin (600°F) for one hour. The coating operates in freon and prevents seizing during intermittent operation.

Paper processing machinery such as typewriters, computer printers and copiers have the problem of paper lint collection on lubricated parts. PTFE is in many cases the perfect solution. Fig. 18 shows a chute against which paper must move with low friction. The PTFE coating performs well and does not collect paper lint.

A brass sleeve bearing coated with PTFE on the internal diameter is shown in Fig. 19. PTFE prevents metal transfer and seizing of a steel plunger which slides longitudinally in the bushing.

Many parts are in use which use PTFE as the lubricant such as throttle linkages, gate valves, solenoids, pharmaceutical equipment, industrial fasteners, carburetor shafts and centrifuges.

Plasma sprayed coatings of ceramics, oxides and other high temperature

materials are in use. Fig. 20 is a picture of a plasma sprayed calcium/barium fluoride coating on the internal diameter of a sleeve. After spraying it is ground to proper dimensions and is fitted over a shaft which is used in turbine engine diffusers. The coating operates at temperatures in excess of 1033° Kelvin (1400°F). Seal rings, bushings and bearing races are also being sprayed with calcium/barium fluoride for use in turbine engine and missile system applications, as well as shaft seals for turbo-pumps and piston rings for high performance reciprocating compressors.

Chromium oxide is a useful tribological coating and Fig. 21 shows a stainless steel shaft which has been plasma sprayed with chromium oxide and finish ground to dimension size. It operates at 755° Kelvin (900°F) in journal bearings made of tribaloy in an oscilating mode through an angle of arc of 1.6 radians (90 degrees) at 25 cycles per minute. The system has given satisfactory operation for over 40,000,000 cycles.

Dies used for high temperature hot extrusion of high melting point materials such as nickel, molybdenum, tungsten and chromium alloys use oxides as lubricant coatings. In Fig. 22 the cut away photo shows the die at the left hand side coated with a plasma sprayed coating of zirconium oxide. This coating is approximately 3.8×10^{-4}m (.015 inch) thick. The billet to be extruded is in the center section and is coated with a slurry of glass which acts as a lubricant and interacts with the zirconium oxide coating on the extrusion die. The billet is heated to 1366° Kelvin (2000°F) and extruded. The effectiveness of the coating is shown by the fact that an uncoated die requires 6.1×10^{6} newtons (690 tons) of force with an exit speed of 1.3×10^{-2} m/sec. (.50 in./sec.) at a reduction ratio of 1 to 1 whereas the zirconium oxide coated die requires only 2.1×10^{6} newtons (240 tons) at an exit speed of 3.8×10^{-2} m/sec. (1.5 in./sec.) at a reduction ratio of 19.8 to 1.

Fig. 23 shows an untrimmed extrusion with a portion of the billet remaining. Fig. 24 is the extrusion machine.

REFERENCES

1. Savage, Robert H.; "Physically & Chemically Adsorbed Films in the Lubrication of Graphite Sliding Contacts". N.Y. Acad., Sc. Vol. 53, 1951, pp 862-869.

2. Peterson, M.B., & Johnson, R.L.; "Friction and Wear Investigation of Molybdenum Disulfide and Effects of Moisture". NACA Technical Note 3055, Dec. 1953.

3. U.S. Patent 4324803, Bergmann & Melet.

4. Stupp, B.C.; "Synergistic Effects of Metals Co-Sputtered with Molybdenum Disulfide", Thin Solid Films, 84 (1981) pp 257-266.

5. Sliney, H.E.; "Plasma-Sprayed Metal-Glass & Metal Glass Fluoride Coatings for Lubrication to 900°C." ASLE Preprint 74AM-7A-3 April 28-May 2, 1974.

6. Spalvins, T.; "Energetics in Vacuum Deposition Methods for Depositing Solid Lubricants". ASLE Preprint 69AM6C-3, May 5-9, 1969.

7. Spalvins, T., Przybyszewski, J., and Buckley, D.; "Deposition of Thin Films by Ion-Plating on Surfaces Having Various Configurations". NASA-TN-D-3707 Nov. 1966.

8. Spalvins, T.; "Horizons in Ion-Plated Coatings", Metal Finishing, Vol. 12, No. 6, June 1974, pp 38-43.

9. Sonntag, A.; "The Significance of Surface Finish on Friction Lubrication & Wear", Seminar on Lubrication & Wear, Lucerone, Switz., Sept. 1959.

10. Fusaro, R.; "Effect of Surface Roughness on Lubrication & Failure Mechanisms of MoS_2 Films, NASA Tech Paper 1379.

11. Stupp, B.C.; "Effects of Surface Preparation on Wear Life of Solid Lubricant Films", Joint Air Force-Navy-Industry Conference Vol. I WADC TR-59-244, February 17, 1959.

TABLE I

Common Solid Lubricants

	Application Methods
Graphite	A
Molybdenum Disulfide	A & C
Molybdenum Diselenide	A & C
Niobium Diselenide	A & C
Tungsten Disulfide	A & C
Polytetrafluoroethylene (PTFE)	A & F
Silver	B, C & E
Lead	B, C & E
Gold	B, C & E
Tin	B, C & E
Calcium/Barium Fluoride	D
Boron Nitride	A
Oxides	C & D

A. Bonded Films
B. Ion Plated
C. Sputtered
D. Plasma Spray
E. Electrodeposition
F. Molded

TABLE II

Common Binders for Solid Lubricant Coatings

	Cure Temp. Kelvin	Max. Use Temp. Kelvin
Phenolic Resins	423	478
Cellulosic Resins	343	338
Acrylic Resins	343	338
Epoxy Resins	448-478	588
Amide Resins	573	623
Inorganic Silicates	463-523	723
Inorganic Phosphates	338-473	773
Bohemite	723	873
Alkyd Resins	343	343
Silicone Resins	533	598

TABLE III

Substrate Material	Pretreatment
Aluminum & Aluminum Alloys	Anodize
Brass & Copper Alloys	Vapor Blast, Chemical Etch
Cadmium, Tin, Zinc	Phosphate, Chromate Conversion
Magnesium	Anodize, Dow 7
Nickel & Chromium	Vapor Blast, Oxidize
Stainless Steels	Vapor Blast, Lubrite SS
Ferritic Alloys	Phosphate
Titanium	Vapor Blast, Anodize

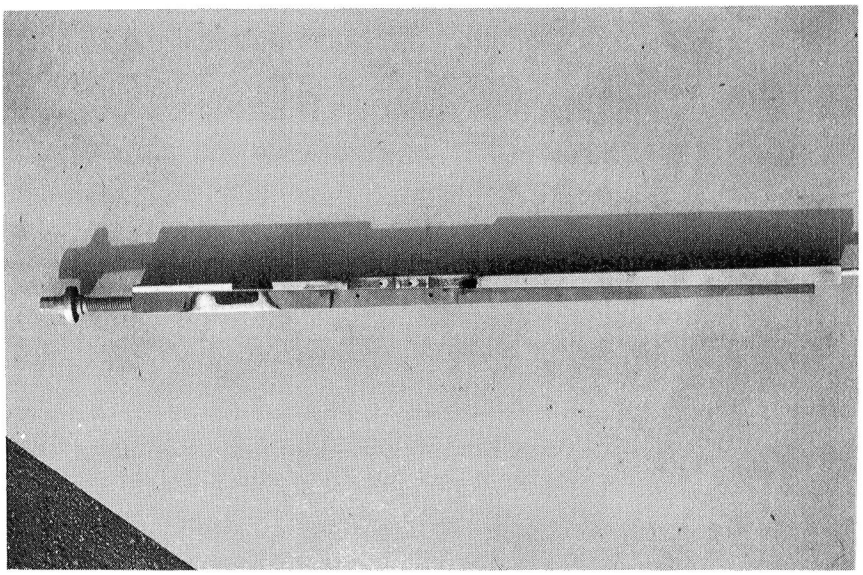

Figure 1 - Screw and slide coated with an epoxy bonded MoS_2 film.

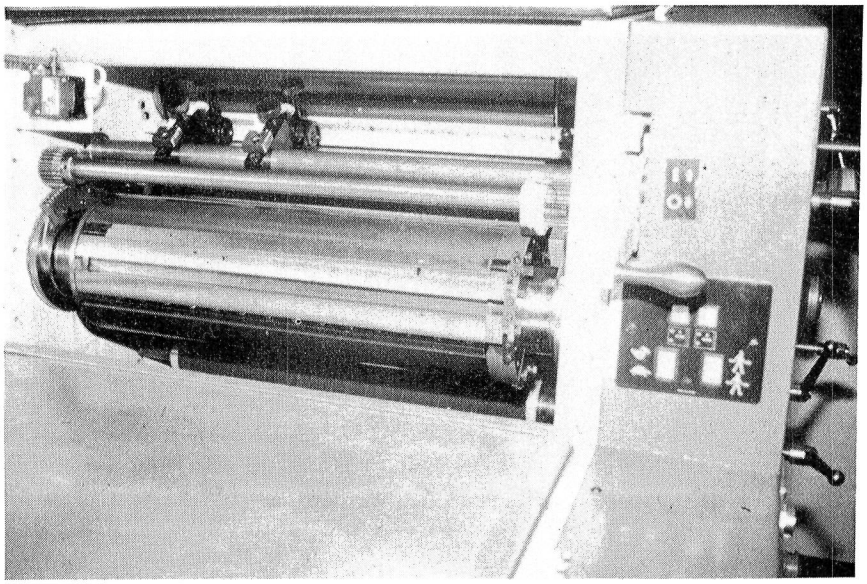

Figure 2 - Screw and slide in the operating machine.

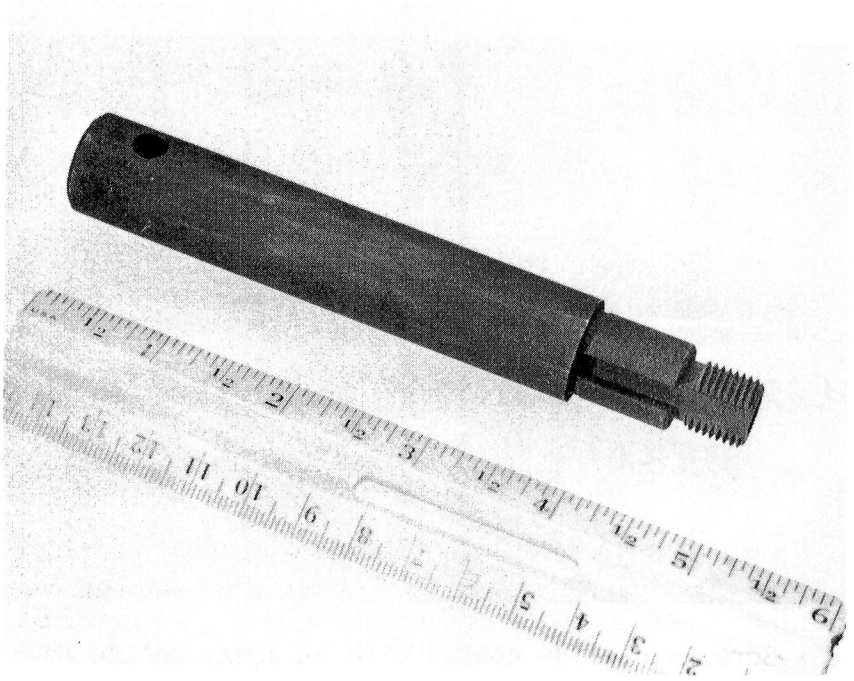

Figure 3 - Hand crank operated shaft coated with a phenolic bonded MoS_2 film.

Figure 4 - Power nut coated with a polyimide bonded MoS_2 film.

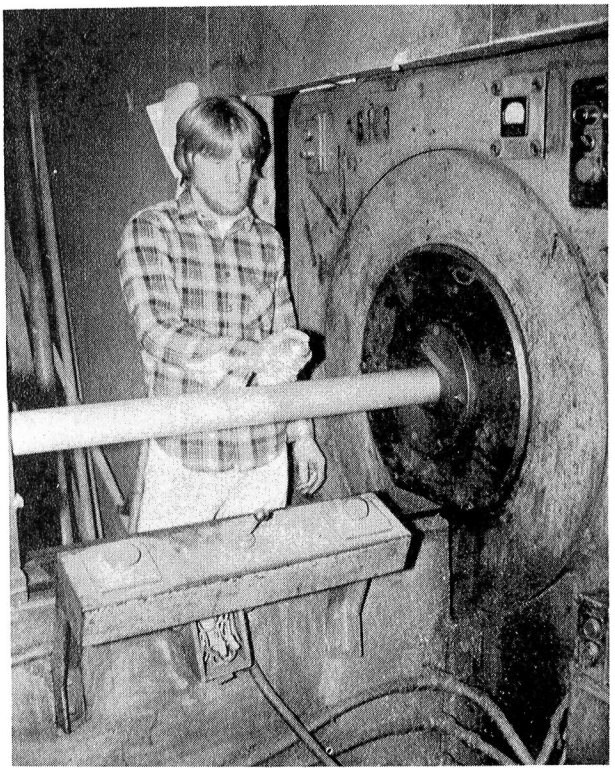

Figure 5 - Aluminum tube coated with an alkyd bonded MoS_2 film.

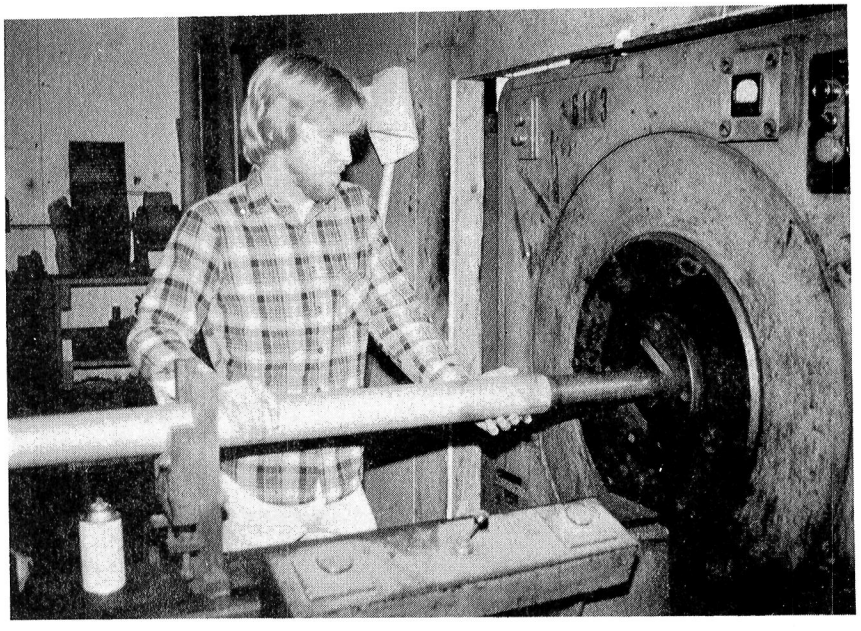

Figure 6 - Aluminum tube after swaging.

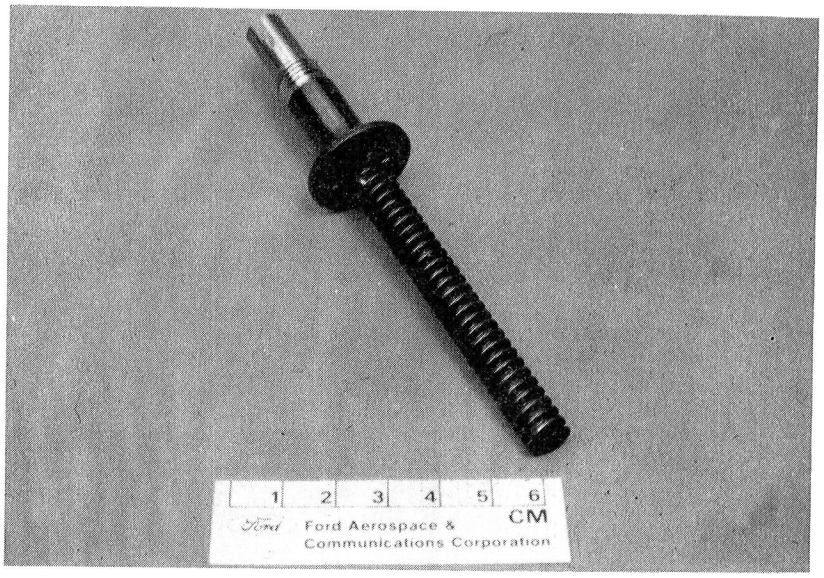

Figure 7 - Adjusting screw sputtered with MoS_2

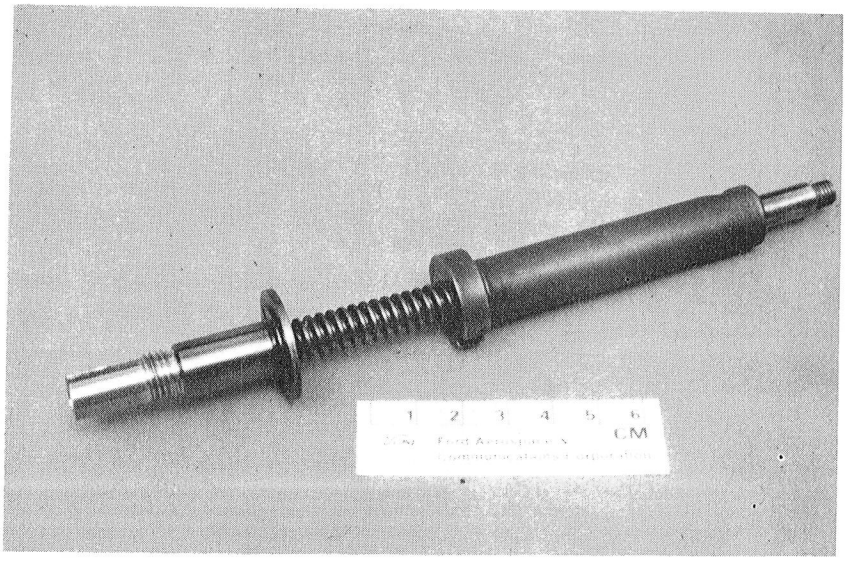

Figure 8 - Assembly of power nut and screw (Fig. 4 & 7)

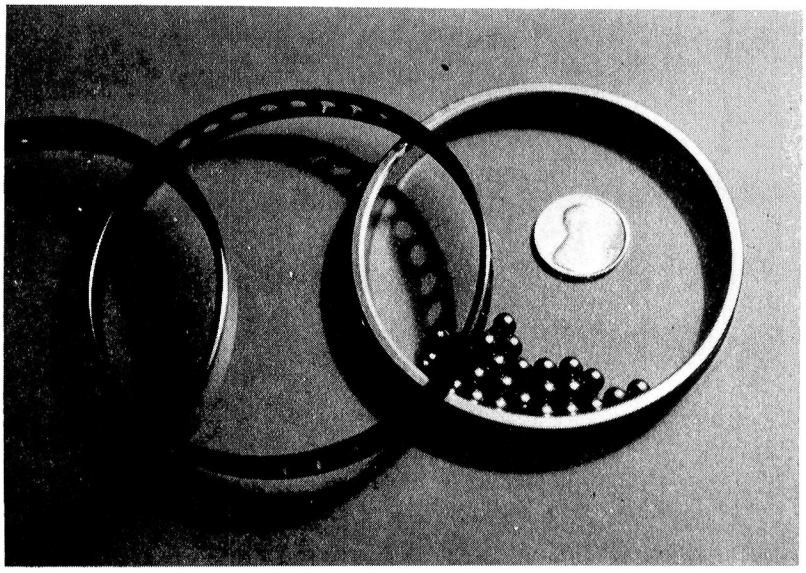

Figure 9 - Ball bearing components sputtered with MoS_2.

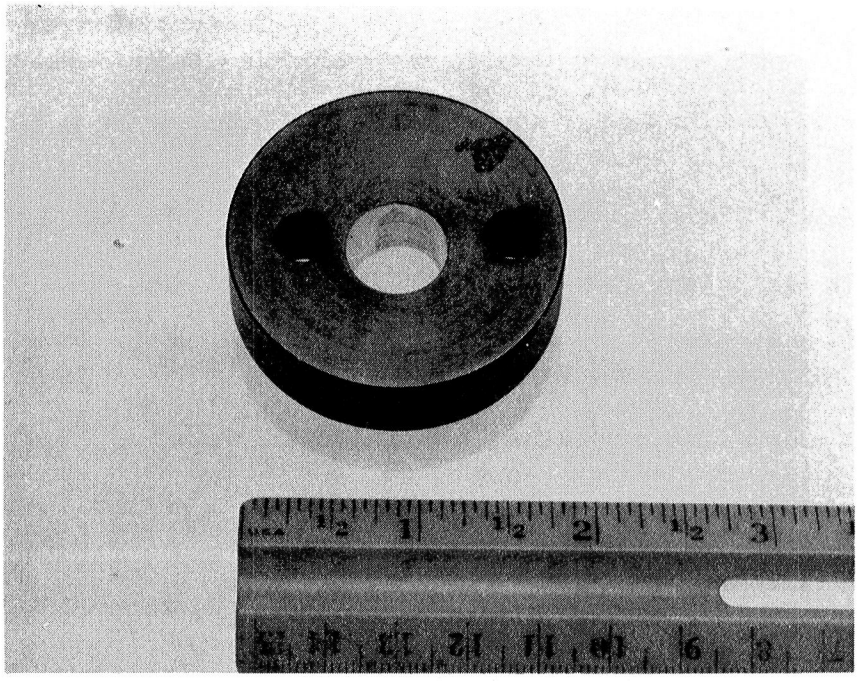

Figure 10 - Cam co-sputtered with MoS_2 and nickel.

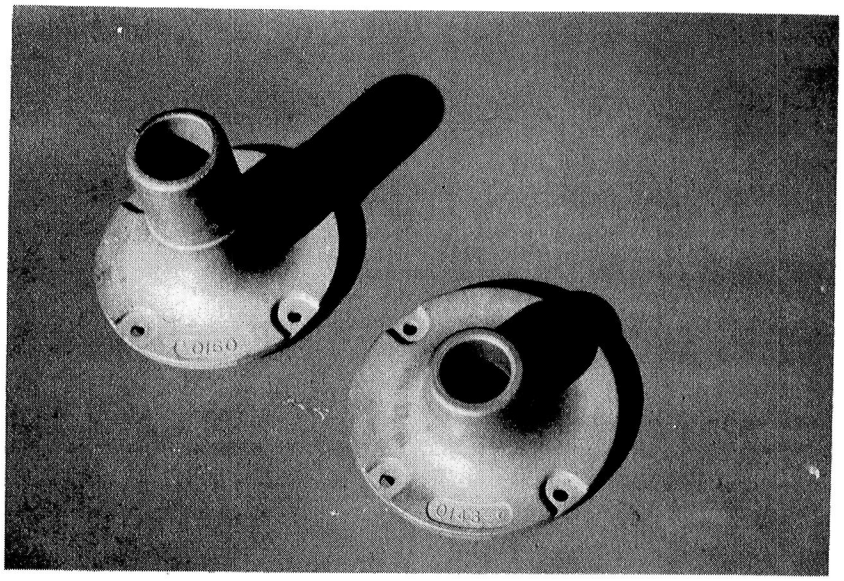

Figure 11 - Bearing housing galvanically coated with tin.

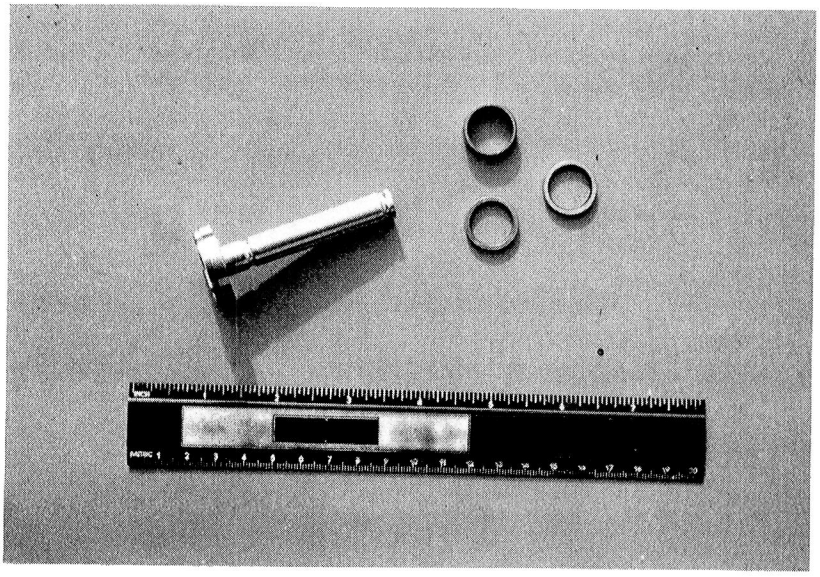

Figure 12 - Ball bearing components ion plated with lead.

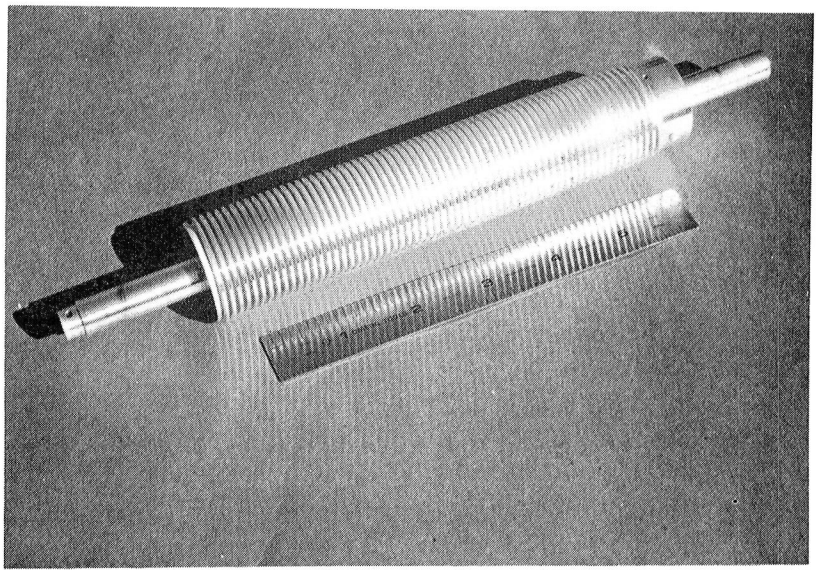

Figure 13 - Lead screw ion plated with silver.

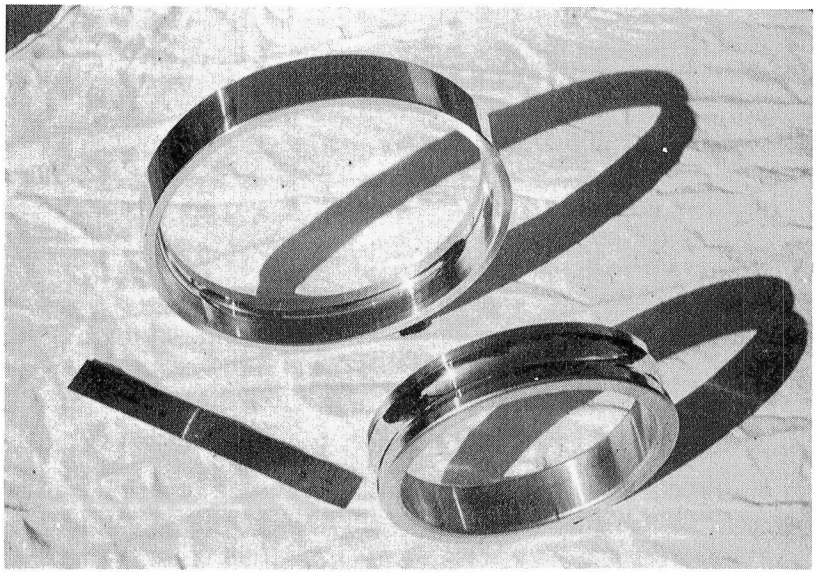

Figure 14 - Bearing components ion plated with gold.

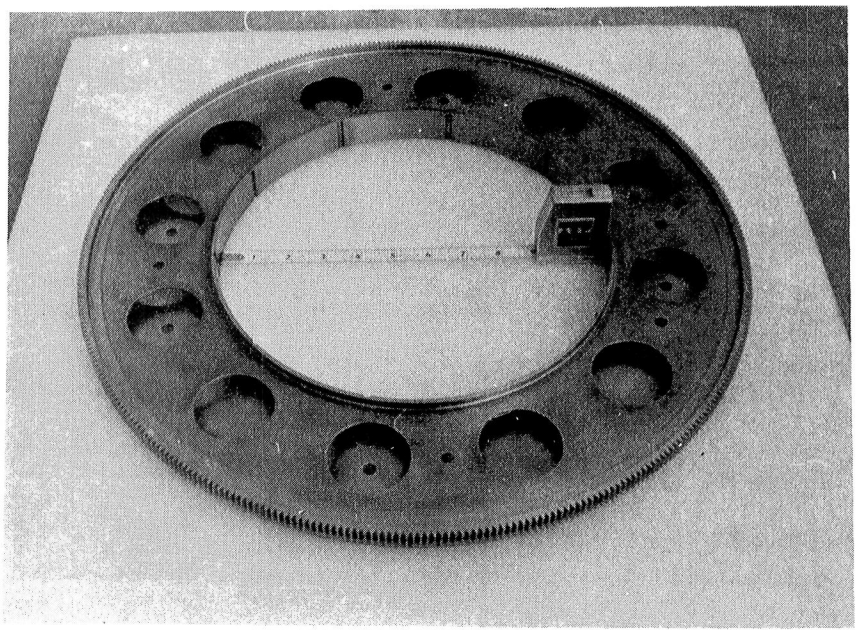

Figure 15 - Bull gear ion plated with gold.

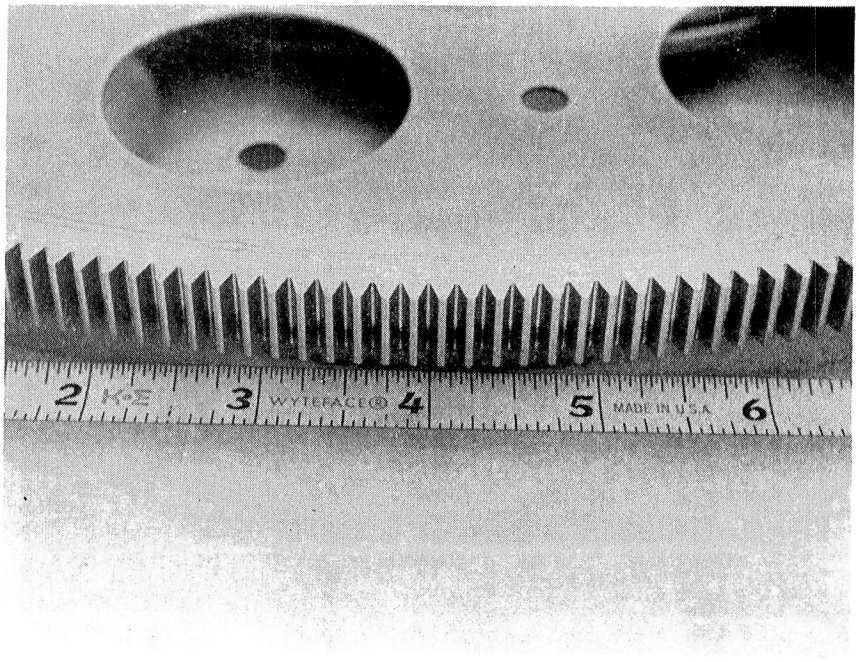

Figure 16 - Gear pitch line.

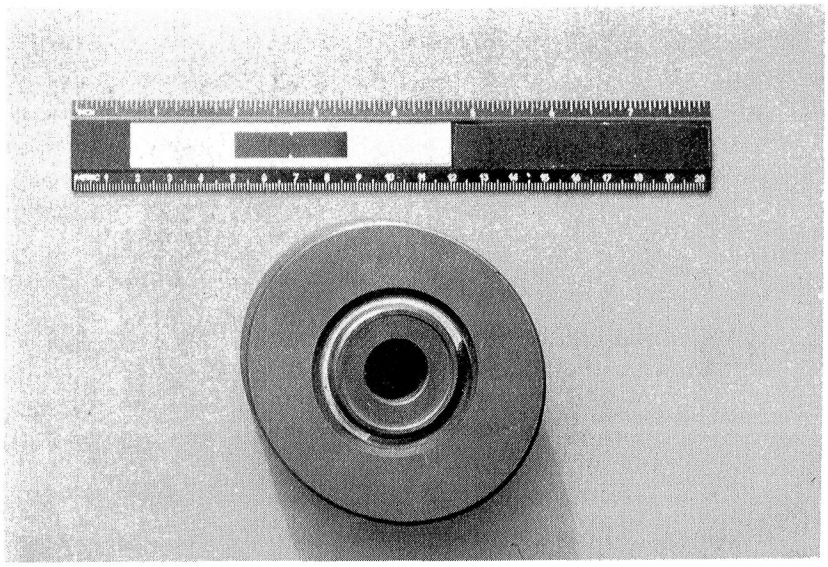

Figure 17 - Wobble plate coated with PTFE.

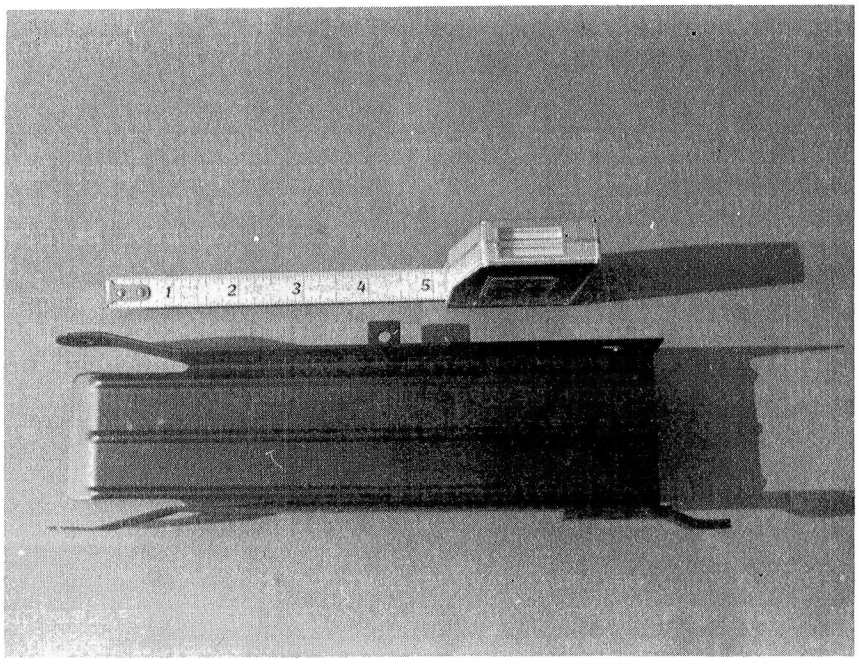

Figure 18 - Paper chute coated with PTFE.

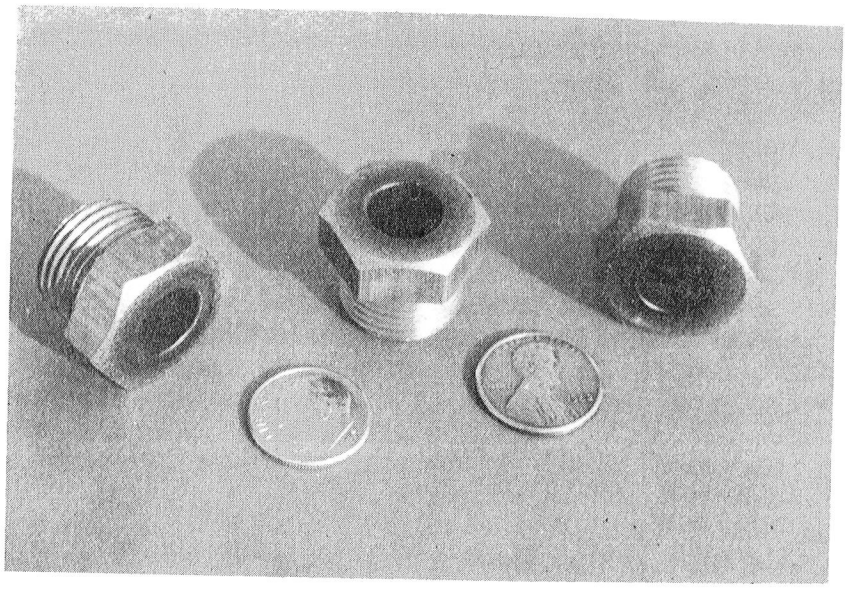

Figure 19 - Brass sleeve with internal diameter PTFE coated.

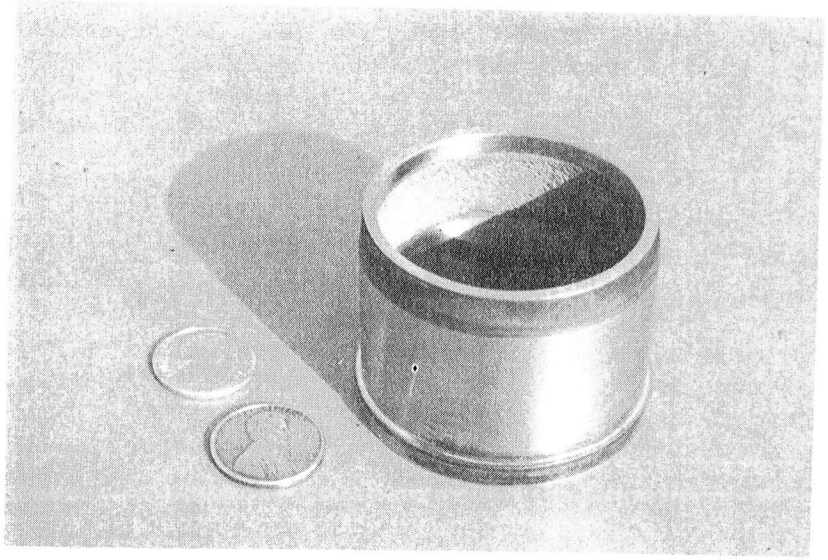

Figure 20 - Sleeve with internal diameter plasma coated with calcium/barium fluoride.

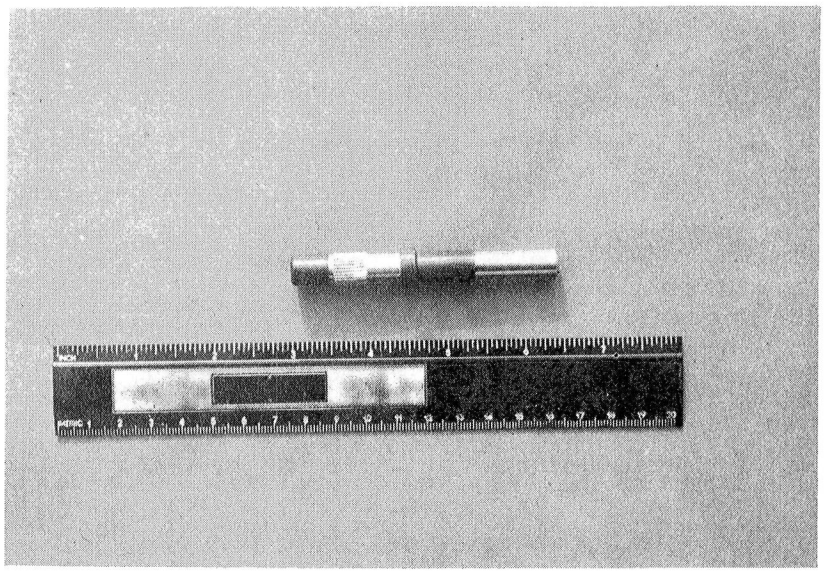

Figure 21 - Shaft plasma coated with chromium oxide.

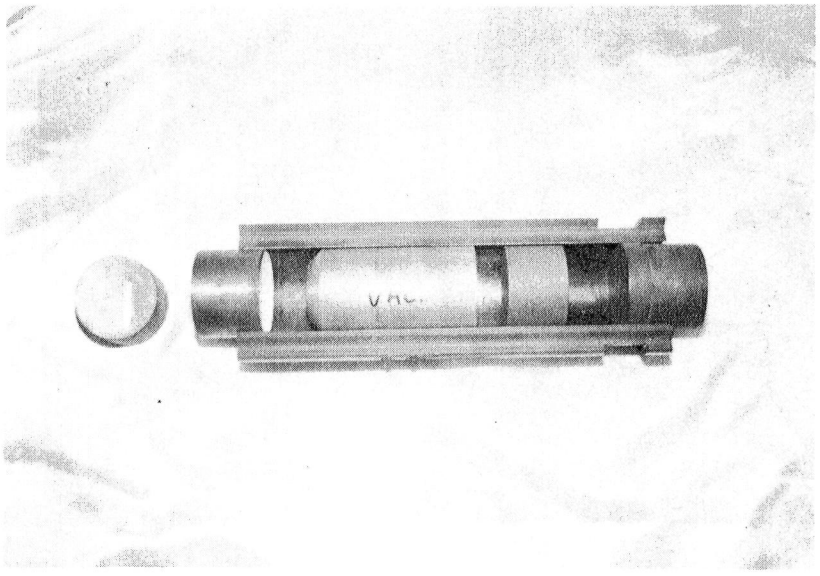

Figure 22 - Extrusion die plasma coated with zirconium oxide.

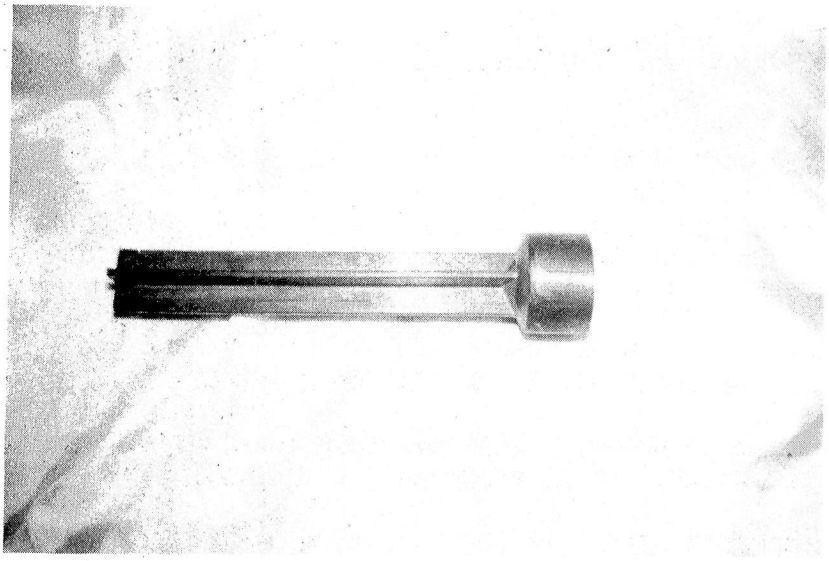

Figure 23 - Untrimmed extrusion.

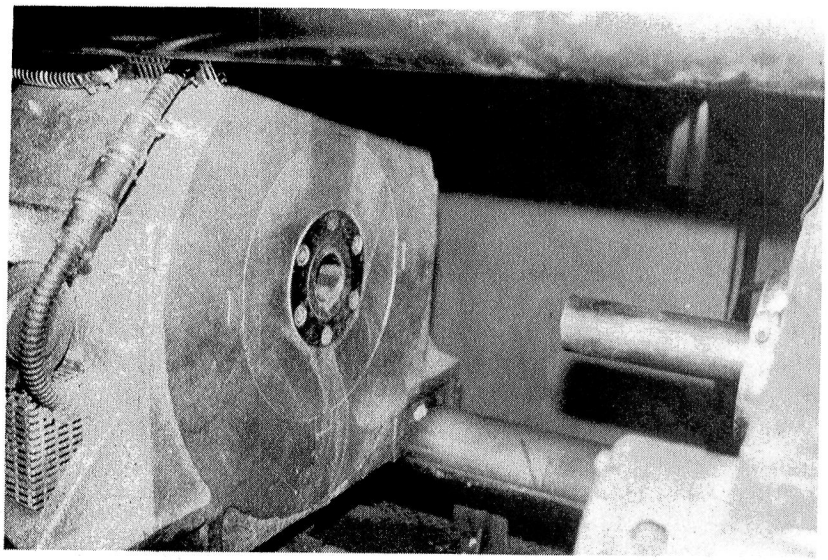

Figure 24 - Extrusion machine.

DISCUSSION

Marshall B. Peterson
Wear Sciences
Arnold, Maryland

The author has discussed some of the current practical applications of solid lubricant films. Since he has participated in most of these developments, his insight is particularly valuable for this conference as it attempts to look into the future. From his paper we can distinguish two main trends:

1. Introduction of a wider variety of lubricants and lubricating materials to meet special application requirements.

2. Developments of new film application techniques which allow for better control of film parameters and useful life.

It is useful to expand on these two points:

The search for new lubricants has been driven primarily by the need for high temperature lubricants. Through the years a variety of materials have been suggested. Some of these are summarized in Figure 1 (1). The important thing to note is that all of these materials are effective in a given temperature range. The real problem arises in trying to operate over a broad temperature range. To date almost no lubricants have been isolated which are effective at both high (>600C) and low (<200C) temperatures. Without this capability they are useless for most applications. If thirty years of research has not produced a wide temperature range lubricant, then some new approaches might be warranted; these are:

1. Conduct fundamental research to obtain a better understanding of shear process using soft solids as lubricants. Is it a flow process similar to viscous fluids or is it interface slip? If it is interface slip, where does the slip occur, within the solid lubricant or at the metal lubricant interface? What is needed is a clear model for solid lubricant behavior. With this model new advances may be possible.

2. Design components to operate with marginally effective lubricants. This is possible, for example, by choosing materials which will slide unlubricated without damage or excessive wear over that portion of the cycle where the lubricant is ineffective. It is also possible with rolling contacts which do not require low friction lubricants. Research is needed to define what film properties are required to maximize film wear life.

If the lubricants of Figure 1 are accepted, then how are they to be used to lubricate rolling contact bearings, bushings, journal bearings, gears, piston rings, valve guides etc. A variety of approaches have been tried.

For example, rolling contact bearings have been lubricated with films (2) (3) (4); reservoirs placed in the cage and lands (5); composite cages which supplied lubricants by rubbing against the balls (6) (7) (8) (9); alternative balls of metal and lubricant composite; lubricant composite balls and races (10) replacing the cage with spring loaded sticks (11) to rub against the ball; vapor lubrication with reactive gases (12) (13) either sprayed into the bearing or self contained; powders blown into the bearing (14) and finally a self contained recirculation system for powders (15). More recently a major research program was initiated to establish the feasibility of dry-lubricated, rolling contact bearings (16) (17) (18) (19) (20) using films and composite cages. Similar approaches have been used for other component types.

Of these approaches only solid lubricant films and composite materials have been adequately investigated and come into general use. Films are limited in life to several million cycles. With composite materials, the material itself must wear to supply the lubricant; accordingly, it has a limited wear life. In the other approaches the film is resupplied and the functions are separated so that a hard wear resistant bearing material may be used in combination with an effective lubricant.

Further efforts are needed to develop these resupply techniques using the available lubricants. Research should be conducted not only to better understand the parameters involved but to adapt them to specific components and specific temperature ranges. Three systems can be considered:

1. Stick lubrication
2. Vapor lubrication
3. Powder lubrication

Each of these has problems; the primary one in all three cases is lubricant film control under changing environmental conditions and wear rates. Some research along these lines would be useful.

REFERENCES

1. Peterson, M.B.; Calabrese, S.J. and Stupp, B. "Lubrication with Naturally Occurring Double Oxide Films", NTIS ADA 124248 (1983).

2. Devine, M.J.; Lamson, E.R. and Bowen, J.H., "The Lubrication of Ball Bearings with Solid Films;, 61-Lubs-11 ASME Lubrication Symposium, Miami, Floriad, May 1961.

3. Kitchen, G., "Lubrication of Small Motors in Automatic Equipment", Lubrication Eng. Vol 20 No 8 (1964) p 311.

4. Lewis, P; Murray, S.F.; Peterson, M.B.; and Esten, H., "Lubricant Evaluation for Bearing Systems Operating in Spatial Environments", ASLE Taans Vol. 6 No 1 (1963) p 67.

5. Devine, M.J.; Lamson, E.R. and Bowen, J.H., "Inorganic Solid Film Lubricants", Journal of Chemical Engineering, Vol 6 No 1, 1961.

6. Boes, D.J.; Cunningham, J.S. Jr.; and Chasman, M.R., "The Solid Lubrication of Ball Bearings Under High Speed, High Load Conditions from 225F to 1000F", Proceedings of the AFML-MRI Conference on Solid Lubricants, AFML TR-70-127 (1960).

7. VanWyk, J., "MoS_2 Solid Lubricant Composites", AFML-TR-70-127 (1970) p 291.

8. Sliney, H.E., "High Temperature Solid Lubricants - 2. Polymer and Fluoride Coatings and Composites", Mech. Eng. Vol 96 no 3, 1974 p 34.

9. Scott, D. and Blackwell, J., "Sacrificial Cage Materials for InSitu Lubrication of Rolling Contact Bearings", NASA N65-23999/6ST NTIS (1975).

10. Demorest, K.E., "Self Lubricating Gears and Other Rotating Parts", NASA Report N69-33484, 1969.

11. Mechlenburg, Karl R., "Performance of Lubricant Compact Materials in Ball Bearings", AD-787-849/9SL, 1974.

12. Gray, S., "An Accessory Manufacturers Approach to Bearing and Seal Development", Mech. Eng. vol 81 No 4 (1959) p 76.

13. Allen, G.P.; Buckley, D.H. and Johnson, R.L, "Friction and Wear with Reactive Gases at Temperatures to 1200F", NACA TN 4-316 (1958).

14. Nemeth, Z.N. and Anderson, W.J., "Effect of Air and Nitrogen Atmospheres on the Temperature Limitations of Liquid and Solid Lubricants in Ball Bearings", Lube Engineering, Vol 11 No 4, 1955, p 265.

15. Lewis, P; Murray, S.F. and Peterson, M.B., "Investigation of Complex Bearing and/or Lubrication Systems for High Speed, High Temperature Operation", FDL-TDR-64-12 (1964).

16. M.N. Gardos, "Solid Lubricated Rolling Element Bearings-Semiannual Status Report No. 6", Part 1: Executive Summary Hughes Report No. FR81-76-1047.

17. M.N. Gardos, "Solid Lubricated Rolling Element Bearings-Semiannual Status Report No. 1," DARPA Order No. 3476, AFWAL Contract No. F33615-78-C-5196, Hughes Aircraft Company Report No. FR-79-76-595, 15 February 1979.

18. Ibid, Simiannual Status Report No. 2, Hughes Aircraft Company Report No. FR-79-76-1041, 15 August 1979.

19. Ibid, Semiannual Status Report No. 3, Hughes Aircraft Company Report No. FR-80-76-714, 15 February 1980.

20. Ibid, Semiannual Status Report No. 4 & 5, Hughes Aircraft Company Report No. FR-81-76-661, 15 March 1981.

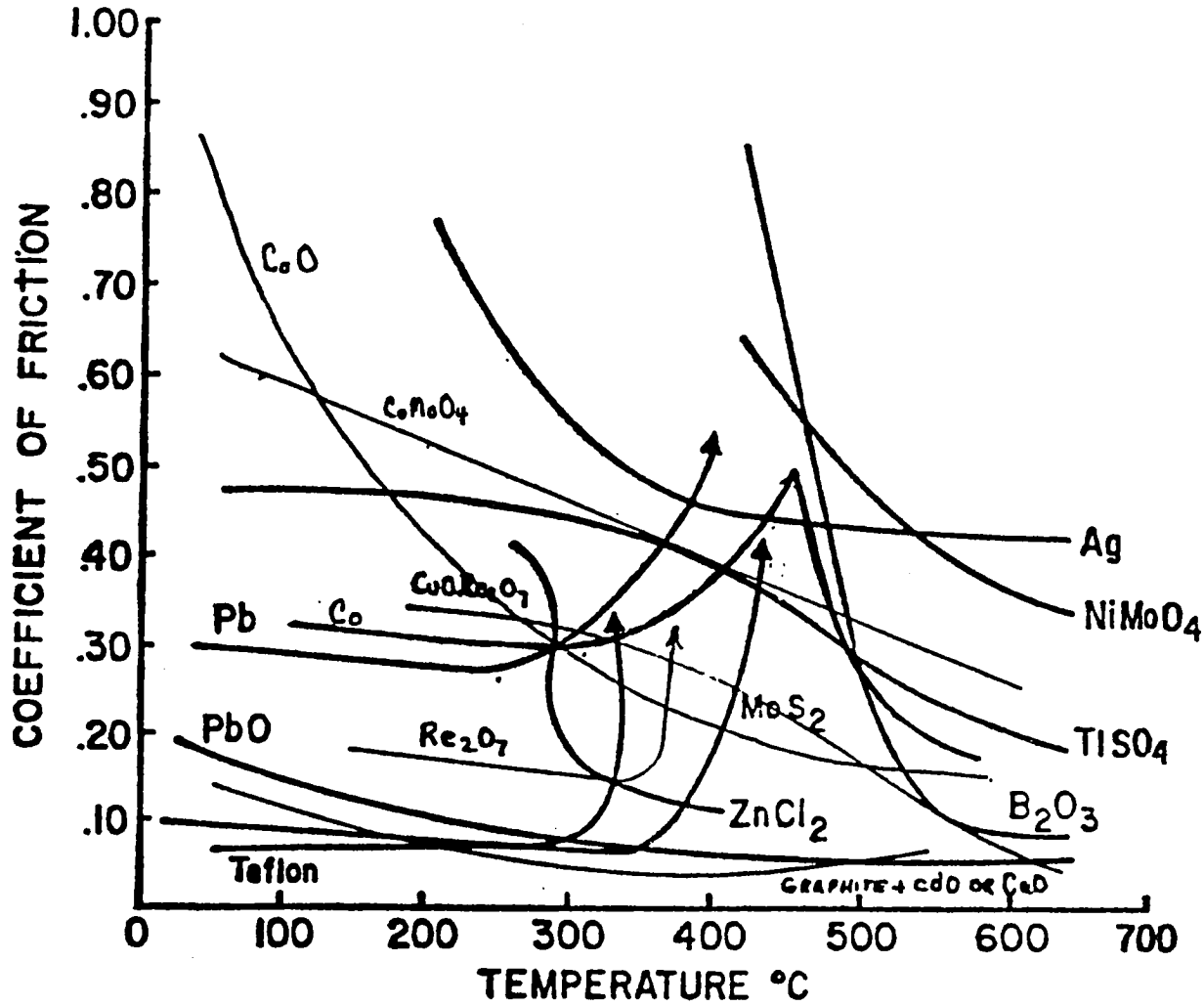

Fig. 1 Friction coefficients for a variety of solid materials vs temperature

RESPONSE

Bernard C. Stupp
Hohman Plating and Manufacturing Inc.
Dayton, Ohio

The main thrust of this paper at a highly technical conference was to interject successful uses of solid lubricant films, and as pointed out by Mr. Peterson a wide variety of materials was shown in successful applications. Film application techniques were also shown to play an important role in the effective use of solid lubricants. On expanding these two points, Mr. Peterson has shown a keen insight for the need of further fundamental research concerning the mechanism of solids as lubricants.

As relates to the broad temperature range lubricant he asks for, it may be necessary to depend upon mechanical design, such as heating or cooling components so that they work in a temperature range which can be satisfactorily lubricated, thus eliminating the ambient temperature problem.

Work is being done with interelated compounds in an effort to broaden the useful temperature range of materials and as described in reference 4 of the paper, new application techniques offer opportunities for improved materials properties.

Mr. Peterson's remarks are pertinent and offers suggestions for further investigation for which I am thankful.

SUPPORT OF OIL LUBRICATION BY BONDED COATINGS

Rüdiger Holinski
DOW CORNING W.Germany, Research and Development
Munich, West Germany

A new generation of lubricating lacquers for treatment of metal surfaces has been developed. These new coatings have proved to be oil-compatible and are used in oil-lubricated systems. The oil lubrication is supported thereby through reduction of friction and increase of load-carrying capacity during boundary conditions. For difficult tribological systems, the problem-solving lubricating concept has proved to be the beneficial combination of lubricating oil and bonded coatings. A number of practical applications are presented.

INTRODUCTION

Solid lubrication with inorganic compounds, in particular with molybdenum disulphide, has become an important branch of problem-solving lubrication. Solid lubricants have proved to be suitable for lubrication of machine components under difficult conditions such as extremely low speeds and high pressures. The greatest technical importance these solids have gained is to lubricate under dry conditions; they provide lubrication under extreme environmental conditions such as: vacuum,
extremely high temperatures,
low temperatures,
presence of radiation,
etc.
Under these conditions, oils cannot provide adequate lubrication; solid lubricants offer for these conditions suitable solutions.

The first practical application of a solid lubricant was the rubbing-in of molybdenum disulphide powder on metal surfaces. Since the platelike MoS_2 praticles adhere extremely well to metal surfaces, a homogeneous solid lubricant film is generated by polishing (fig. 1). The lubricating film is significantly smoother than the original metal surface. During the contact of two machine components, the load is distributed over a larger contact area, i.e. that the specific pressure is reduced.

The molybdenum disulphide film has a very high load-carrying capacity and protects the metal surface from wear under extremely high loads (ref. 1, 2). Furthermore, this solid film provides the metal surface with a very low friction. The coefficient of friction can go down to $\mu = 0.02$. Such dry films cannot be replaced without substantial effort, i.e. that such a film has to provide lubrication for the whole life of a machine component. Under dry conditions, the lifetime of these lubricating films is very high. When this treatment of metal surfaces and the tribological benefits became common knowledge, engineers also wanted to utilize this technology for machine components which are lubri-

cated by oils or greases. However, it was found that solid lubricant films had in oils under tribological stress only a limited lifetime. In oils, the films are stripped from the metal surface in a very short time (ref. 3, 4).

In recent years, new solid lubricant-containing coatings have been developed with oil-resistant binders. These oil-compatible bonded coatings protect metal surfaces from wear and reduce friction under boundary conditions also in the presence of oil. These coatings are well suited to provide substantially improved lubrication for machine components under difficult conditions.

COMPOSITION OF LUBRICATING LACQUERS

A typical bonded coating basically consists of three components: solid lubricant pigments, a binder, and a solvent. The binder is dissolved in the solvent and the solid lubricant particles are dispersed.

This product is applied to metal surfaces mainly by dipping or spraying. After the application, the liquid film starts to solidify by evaporation of the solvent and crystallisation of the binder. The binder can be an organic resin or an inorganic compound. It has the task to connect solid lubricant particles with each other and to bind the solid pigments to the metal surface. In most cases, the binder also has to protect the metal from corrosion by keeping water from the surface.

Figure 2 shows profiles of the metal components which have been treated with a bonded coating. On the left photo, the profile of a solid lubricant coating can be seen which has been applied to the surface by spraying. The coating appears to consist of many solid lamellae of random orientation. If such a coating is mechanically stressed by sliding or rolling contact, the solid coating is compressed. The lamellae start to orient parallelly to the frictional surface. By the applied load, the particles are pressed to the metal surface and form a very strong adhesion to the surface. During the running-in process, from the solid lubricant particles a homogeneous solid layer of a thickness of 2 /um is being formed (right part of figure 2).

When this film has been formed, there is a high degree of cohesion within the film and strong adhesion between layer and surface. Cohesion and adhesion of this homogeneous film is so strong that this surface layer can take extremely high loads and high shear forces without being destroyed or removed from the metal surface. In case of molybdenum disulphide, such a lubricating film can withstand a specific pressure of 3000 N/mm^2. The run-in film makes a very homogeneous appearance; it cannot be recognized that this film has been formed from many individual solid particles.

In an oil, a bonded coating is only stable under tribological stress when special binders are being used which have to be heat-cured after application. These oil-compatible bonded lubricants have been used successfully in many oil-lubricated tribological systems for protection of metal surfaces. Oil-compatible coatings made a significant contribution to oil lubrication.

CONTRIBUTION OF BONDED COATINGS TO OIL LUBRICATION

Solid lubricant films on metal surfaces can support oil lubrication only in the regime of boundary and mixed lubrication. Because of too high loads and/or too low speeds, the lubricating oil film becomes so thin that both moving metal components cannot be separated anymore completely from each other by the lubricant. During mixed lubrication, there is occasional metal contact and during boundary lubrication, there is primarily metal contact as is demonstrated in the Stribeck curve (fig. 3).

The shape of the Stribeck curve not only depends on speed, load, and viscosity of the oil, but also on the asperity of the metal surface (ref. 5). In case of a rough metal surface, the regime of boundary and mixed lubrication is enlarged, i.e. metal-to-metal contact occurs at relatively high speeds and low loads. If a rough metal surface has been coated with a solid lubricant-containing layer, the surface becomes significantly smoother after a short running-in of the coating. These smooth surfaces of machine components will not enter the area of mixed lubrication so soon as is the case with rough surfaces.

In figure 4, a Stribeck curve has been plotted for two different metal surfaces. In one case, the rough metal surface has been covered by a smooth lubricating film. In this case, the static friction of the break-away torque is significantly reduced in comparison to the rough metal surface because the solid lubricant film has a low coefficient of friction. Friction remains at a low level during the entire period of boundary and mixed lubricantion. Also the minimum of the Stribeck curve - that is the constellation of speed, load and viscosity where an oil film is just thick enough to separate both moving metal components - is reached at lower speeds and higher loads in case of the coated metal surface. In a certain constellation of load and speed, as demonstrated in figure 4, the moving parts with a rough metal surface are still in the regime of mixed lubrication, while the same parts with smooth coated surfaces have entered already the area of hydrodynamic lubrication.

This beneficial contribution of solid lubricant coatings to oil lubrication - as was explained by the model of the Stribeck curve - has been found in practical experiments. During friction measurement of oil-lubricated taper roller bearings, the influence of bonded coatings on friction was measured (ref. 6). In these experiments, friction of taper roller bearings has been recorded at different speeds. First, friction was measured with bearings as supplied, and in other tests, the rims of the bearings have been coated with molybdenum disulphide. The results of these experiments are given in figure 5. In case of the coated bearings, the starting friction was significantly lower in comparison to the untreated bearings; also the frictional minimum of the curve was about 25% lower. This minimum indicates the end of mixed friction and the start of hydrodynamic lubrication. Both curves demonstrate that the solid lubricant layers on metal surfaces reduce friction significantly in the regime of boundary lubrication. The area of mixed lubrication has been narrowed and hydrodynamic lubrication was enlarged. The reduction of friction means an increase of load-carrying capacity by about 25%.

In case of oil lubrication, very smooth metal surfaces are not desirable because the adhesion of oil films is not the best on these surfaces, and lubricating films may rupture. However, it has been found that oils adhere excellently to smooth metal surfaces (ref. 7, 8).

Solid lubricant coatings on metal surfaces of moving machine components contribute to oil lubrication the following benefits:

* Reduction of friction during boundary and mixed lubrication.
* Reduction of frictional temperature.
* Enlargement of hydrodynamic lubrication regime.
* Elimination of stick-slip at low speeds.
* Prevention of wear-in damages by seizure.
* Reduction of noise during boundary lubrication.
* Increase of load-carrying capacity.
* Reduction of shear stress in the area of frictional contact.

The reduction of frictional temperature means that the lubricating oil is not heated up that much, which in turn means an increase in life of the lubricant. Because of the tribological benefits of oil-compatible bonded coatings, this technology has become standard application for difficult oil-lubricated machine components.

PRACTICAL APPLICATIONS OF OIL-COMPATIBLE COATINGS

In particular in transportation systems, oil-compatible bonded coatings are being used successfully. In many cases, these lubricating lacquers are being applied to prevent surface damages during the wear-in period and to reduce break-in time. In other cases, the coatings have to support lubrication permanently. A few examples are given:

Rotary engines require a run-in period of 60 to 90 minutes on a test stand to achieve full capacity of the motor. The treatment of the sealing parts of the combustion chamber resulted in a reduction of run-in time of several minutes. The bonded coatings formed smooth surfaces in a very short time and, thereby, the needed seating of moving parts of the combustion chamber. The application of a bonded coating allowed in this case to eliminate the running-in of rotary engines on a test stand. This meant a substantial cost saving in manufacturing of rotary engines.

The first 200 to 300 rotations of a rotary engine are very critical because very high wear might be generated. This high wear during the initial run-in period is substantially reduced by a treatment of the surfaces of the trochoid with a bonded coating.

Several European car manufacturers coat gear shafts, cam shafts, and tappets of various types of passenger cars with oil-compatible lubricating lacquers (fig.6). The proven benefits of this surface treatment are reduction of run-in wear, reduction of frictional losses, and smooth trouble-free running-in of these machine components.

Automotive pistons can wear at the piston skirt under certain conditions. During cold starts, a high amount of gasoline is getting into the combustion chamber and flushes away the lubricating oil film. The piston skirt is lacking adequate lubrication. Therefore, piston skirts are coated with an oil-compatible bonded coating which protects the piston from wear during cold starts when oil lubrication is insufficient (fig. 6).

Races of constant velocity joints were coated with special bonded coatings. Extensive tests have proved that this treatment leads to an increase in load-carrying capacity, reduction of friction, and reduction of shear stress. The overall benefit was that pitting formation started much later, which increased the lifetime of constant velocity joints significantly.

At heavy service trucks, problems were encountered with the differential gears; the gear oil could not prevent wear and seizure, in particular during break-in. The various parts of the differential gear have been treated with a molybdenum disulphide-containing bonded coating (fig. 7). It was found that the surface treatment prevented seizure and wear, and the differential gears ran trouble-free.

Reduction of friction in turn means saving of energy. For this reason, the hypoid gear of the rear driving axle of a passenger car has been coated with an oil-compatible bonded coating. Extensive tests revealed a reduction of frictional losses. The efficiency of these gears has been increased from 92% to 98%.

Small driving gears of small motor cycles generated too much noise. To solve this problem, the gears have been treated with an oil-compatible coating. This bonded coating provided smooth surfaces of the gear flanks and reduced friction. Because of these effects, the running noise was reduced by several decibel.

CONCLUSION

The development of oil-compatible bonded coatings allowed a reasonable combination of solid lubrication and oil lubrication. In critical cases, these new solid lubricant-containing lacquers supported oil lubrication during boundary conditions. The proven benefits of oil-compatible coatings lead to many practical applications, especially in transportation systems. The contribution of wear reduction, friction reduction, and increase of lifetime of machine components by these bonded coatings means higher reliability and better economics of machines.

REFERENCES

1. Holinski, R.; and Gänsheimer, J: Wirkungsweise von Festschmierstoffen in Ölen und Fetten. VDI-Z 114, 1972, Nr. 2.

2. Holinski, R.: Das Geheimnis von MoS_2. Maschinen-Anlagen-Verfahren 3, 1975, pp. 28-29.

3. Holinski, R.: Dynamics of Boundary Layers. Lubrication Engineering, vol. 36, 9, pp. 530-533.

4. Holinski, R.: The influence of boundary layers on friction. Wear 56, 1979, pp. 147-154.

5. Bartel, A.: Wirkungsbereiche der hydrodynamischen Schmierung, der Teilschmierung und der Trockenschmierung. MOLYKOTE Sonderdruck 1/III, 1962.

6. Grünberg, U.: Einsatz von Festschmierstoffen bei der Schmierung von Wälzlagern. Molybdän-Dienst No. 76, Nov. 1971.

7. Braithwaite, E. R.: Penguin Science. News No. 42, 1956.

8. Braithwaite, E. R.; and Greene, A. B.: The relevance of the surface chemistry of MoS_2, particularly with its respect to wettability. Proceedings of International Solid Lubrication Symposium, Tokyo, 1975.

9. Läpple, W.: Schmierwirksame Lacke. Farben und Lack, No. 2, 1982, p. 105.

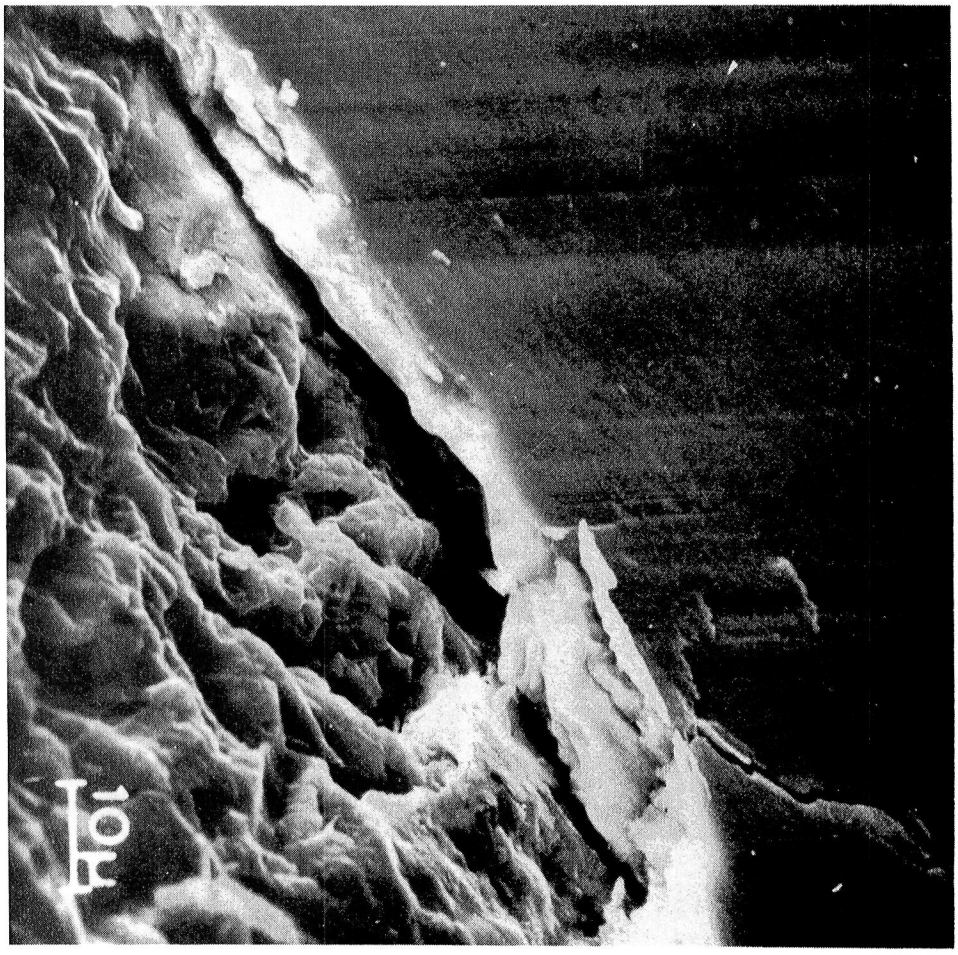

Figure 1. - SEM photograph of a runin solid lubricant film (right) on a metal surface (left). X1000.

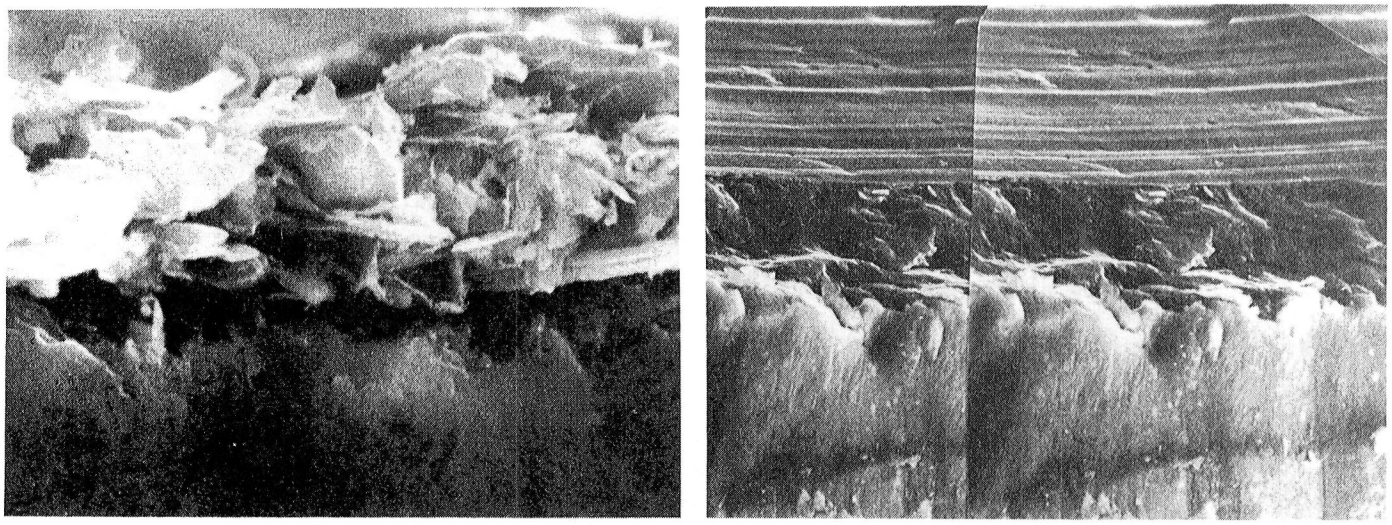

(a) After application.

(b) After running in.

Figure 2. - Profile of a solid lubricant-containing coating on metal surfaces. X2000.

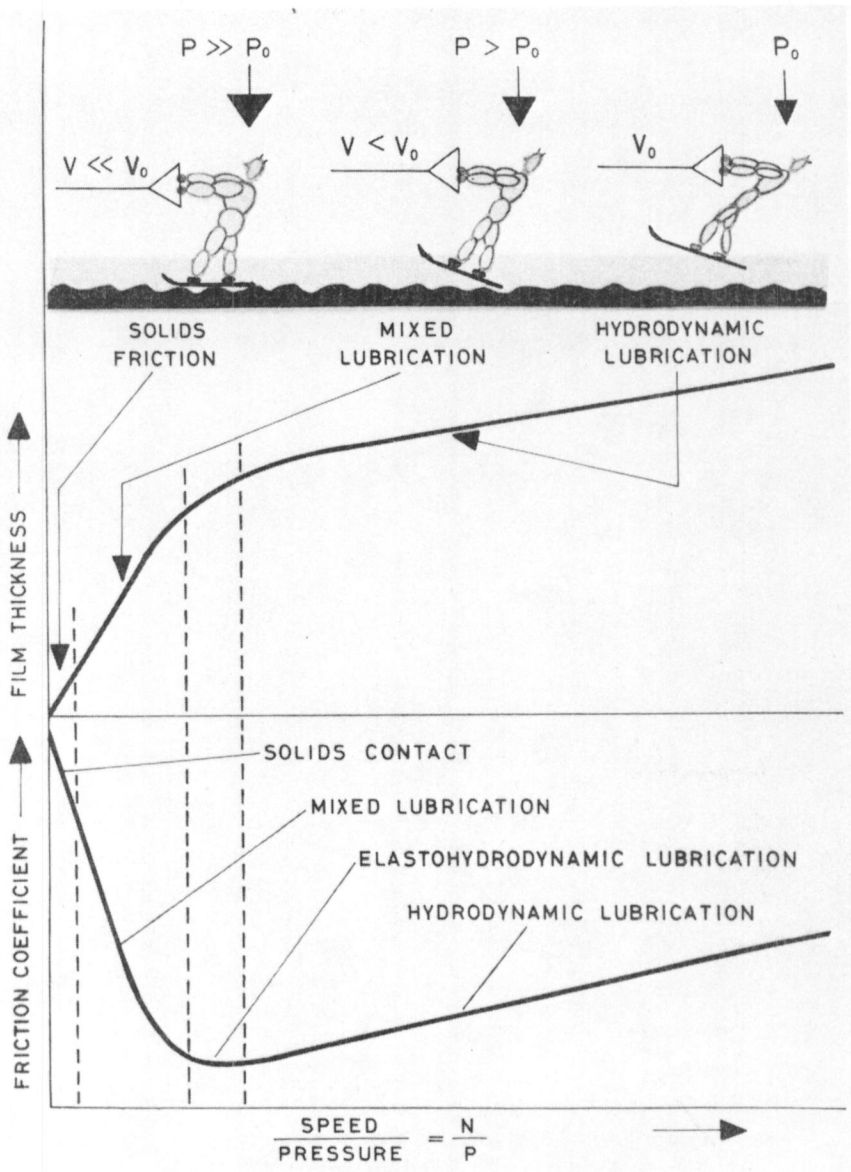

Figure 3. - Model of various lubrication regimes explained by oil film thickness and friction coefficient.

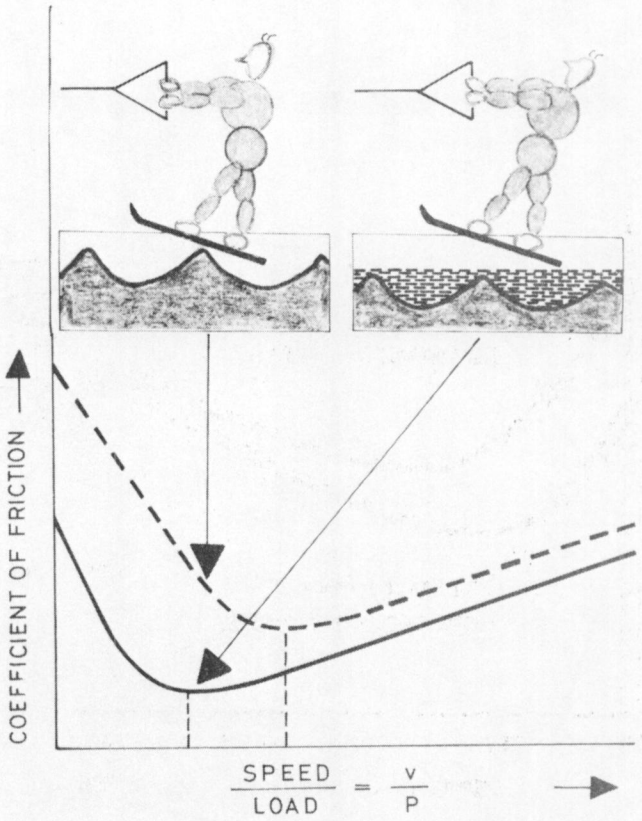

Figure 4. - Stribeck curve as function of surface roughness.

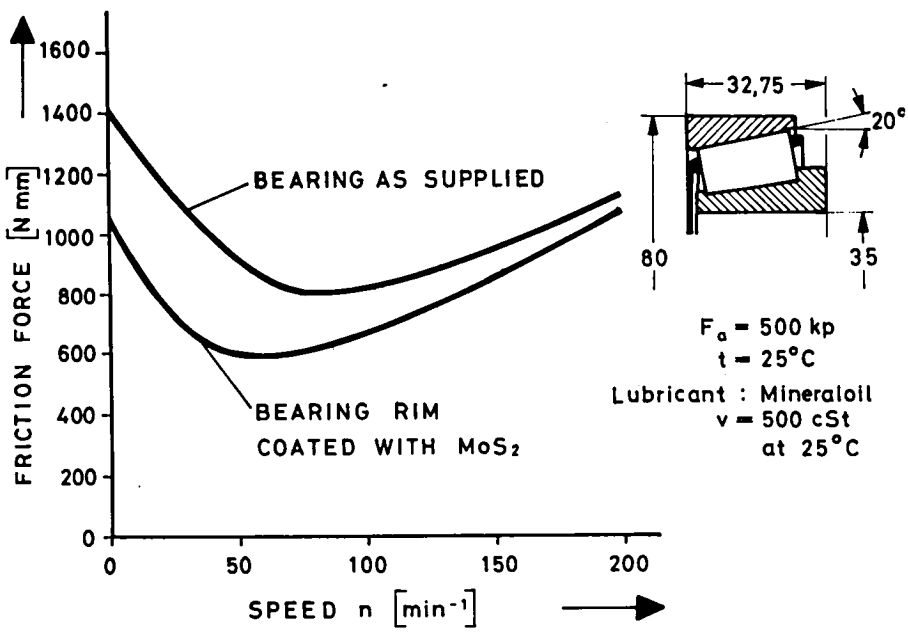

Figure 5. - Friction force as function of speed of a taper roller bearing.

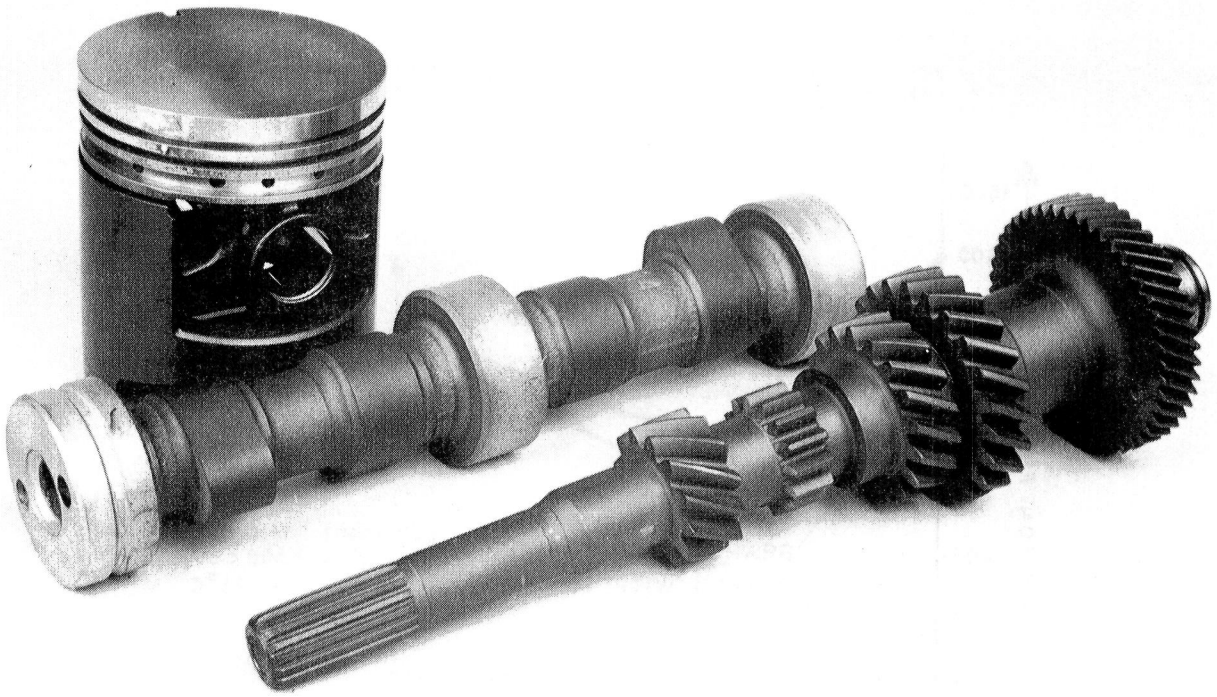

Figure 6. - Various engine parts treated with an oil-compatible bonded coating.

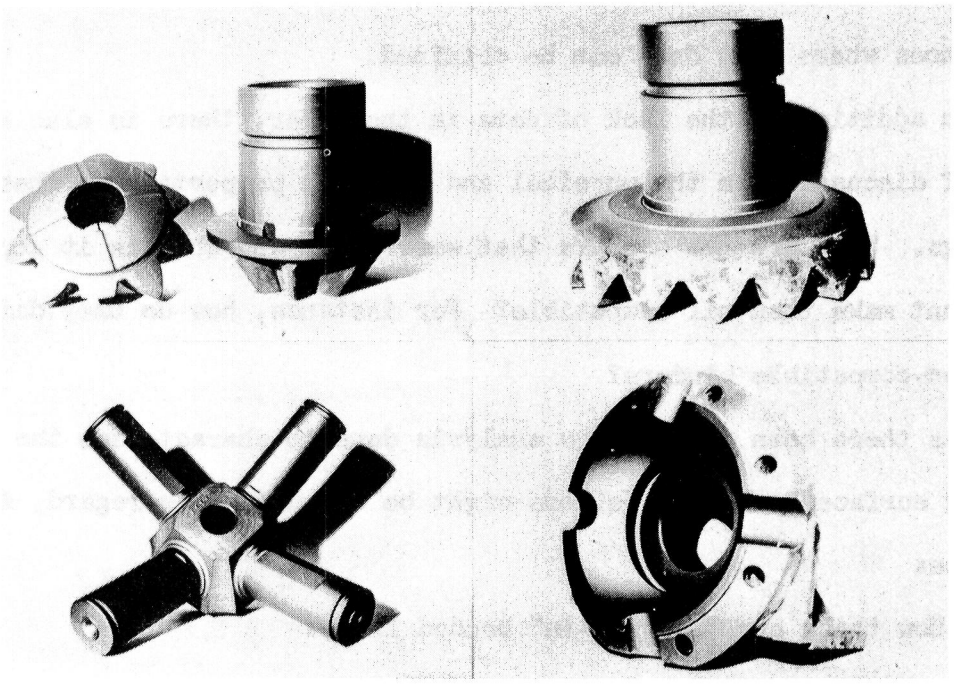

Figure 7. - Differential gear parts coated with a lubricating lacquer.

DISCUSSION

Robert L. Fusaro
National Aeronautics and Space Administration
Lewis Research Center
Cleveland, Ohio

Dr. Holinski has composed a clear, well written paper on bonded solid lubricant coatings. He has reviewed and discussed many aspects of dry solid lubrication, and he has given many benefical effects of solid lubricant coatings to oil lubrication. The one problem this discussor has with the paper is that there are no experimental data given to support these claims. No friction coefficients, wear rates or endurance lives are given. Could Dr. Holinski, at least, give some references where this data can be obtained.

In addition to the lack of data in the paper, there is also a lack of discussion on the physical and chemical properties of these coatings. What are the binders that were used, and what is it about them that make them oil compatible? For instance, how do they differ from non-compatible binders?

Has there been any surface analysis done to characterize the rubbing surfaces? Many questions might be asked in this regard, for instance:

(1) How thick are the "run-in" bonded films?

(2) Are transfer films produced and what is their character?

(3) What is the failure mechanism of the films? Do they spall or do they just gradually wear away?

(4) Is their any evidence of the oil reacting with the coatings?

(5) Is their any evidence of the additives in the oil reacting with the coatings?

(6) Does dissolved water in the oils present a problem?

(7) Are bonded film wear particles filtered out, do they remain in suspension, or do they plate out somewhere?

In conclusion, this discussor believes that the benefical effects of bonded solid lubricant coatings to oil lubrication, that Dr. Holinski depicts, could very possibly be achieved. Unfortunately, this paper does not convince this discussor that this panacea has yet been accomplished.

DISCUSSION

Masahisa Matsunaga
Chiba Institute of Technology
Narashino-shi, Japan

The work by R. Holinski is very important and interesting. Film of MoS_2 bonded by inorganic binder is stable for long times in the lubricating condition as well as in the dry condition. These results had been obtained by many workers in Japan. However, the organic binder is usually unstable in oil. For instance, the binders phenol, polyimid, and epoxy were tested at the Government Mechanical Laboratory. Their results were that these films were unstable in oil and that very severe wear occurred in oil, especially oil containing additives, even when films were fully heat-treated.

Organic films are used in Japan. For instance, Kawamura (ref. 1) reported that organic bonded films containing furan and epoxy had good "run-in" characteristics. Further, Toyo Kocyo Company has developed a method for determining the piston profile in an engine by using epoxy-bonded MoS_2 films.

In reporting their results, the Japanese give the composition and the film-making techniques are fully described. The present author, however, has not provided the reader with this necessary information. The reader would like to know more about the film. The following information should be provided:

Properties of the film.

(1) The composition of the coating agents, including additives, MoS_2, and solvents
(2) The size and shape of MoS_2 powder
(3) Surface roughness and the method of preparing the coated metal surface; for instance, pitch and depth of the surface topography as shown in figure 4

Wear characteristics of the film.

The wear of films occurs naturally even if these are strongly bonded. We would like to know the wear characteristics of the film.

(1) Initial film thickness
(2) Friction condition after the film formation
(3) Life of your film in industrial uses and at definite technical conditions
(4) Wear mechanisms of the film including chemical action
(5) Shape of the wear debris and their influence on machine parts

Friction apparatus and results.

We would like to know the apparatus for determining figure 5, and to know the measured points in the figure. The figure is too schematic.

Isn't it possible to obtain a lower friction curve if the author uses oil-containing additives instead of mineral oil?

Running-in and load-carrying capacities.

Detailed experiments that the organic binder is effectively used for the run-in process were reported by Kawamura (ref. 1). If the reduction of friction and the increase of the load-carrying capacity occur by using a smooth surface the smooth surface of the metal without MoS_2 can attain the same characteristics.

Have you compared the load-carrying capacities by increasing the applied load on the rough surface of metal, the smooth surface of metal, and the smooth surface of metal with MoS_2? We think it is not enough to estimate the load-carrying capacity from the coefficient of friction.

REFERENCE

1. Kawamura, M.; Aoki, I.; and Yoshida, Y.: ASLE Proc. of Second International Conference on Solid Lubrication. 1978.

RESPONSE

Rüdiger Holinski
Dow Corning
Munich, Federal Republic of Germany

The author would like to emphasize that the presented paper was meant to be a practical review of industrial applications and not an institute paper on test machine results: reported were those applications where oil-compatible coatings contributed substantial tribological benefits to machine components which could not be satisfactorily lubricated by an oil or grease. Most results given in this paper were received from car manufacturers which did not disclose all the detailed data the discussors are interested in. However, the important issue seems to be that oil-compatible bonded coatings are being used in production successfully to support oil lubrication in tribologically critical areas - however, there is lack of theory why these coatings work.

The author will try to respond to some of the raised questions:

1.) Composition:

The oil-compatible coating consists of a special polyimide with very good lubricating properties; the binder/pigment ratio is substantially different; this coating contains much more resin than normal bonded coatings; as pigments, molybdenumdisulphide (technical fine) in combination with organic solid lubricants are used; the film has to be heat-cured.

2.) Properties and failure mechanism of the film:

The coating is applied at a thickness of about 6/um; after running-in, the film is about 3/um thick. Transfer films have not been observed. One company checked by a special filter in a gear box for wear particles and has found only p.p.m. amounts of solid lubricant particles in the gear oil. The film is getting gradually thinner but does not spall. No evidence has been found that the oil, water in oil, or oil additives reacted with the bonded films. Test machine results revealed that the coefficient of friction of an oil (/u = 0.08) is being reduced to /u = 0.04 by the bonded coating in the oil. As a result of this, one car manufacturer reported that during a fast run the gear oil temperature was 160°C; when the hypoid gears were coated with the bonded film, the gear oil temperature dropped in the same run to 120°C. It is almost impossible to decrease coefficient of friction even more by chemical additives in the oil plus an MoS_2 bonded film. On the other hand, it is known that boundary layers generated by ZDDP in oil increase friction and frictional temperature significantly (Ref. 4 of the paper).

Surface roughness of the substrates depends on the various parts to be coated. RT = 2/um for tappet surfaces to RT = 30/um for piston skirts.

Fig. 4 is only an explanatory model: In case of a very smooth metal surface, the boundary friction is still lower for the coating because of the friction-reducing property of MoS_2. Fig. 5 is taken from Ref. 6: This SKF paper gives results from a bearing test stand using taper roller bearings with rims being bondered with MoS_2.

In essence, the author assumes that the reason for an oil-compatible coating supporting oil lubrication in many problem areas is the following: During the critical run-in period, there is sometimes lack of sufficient oil lubrication and too high specific pressure, so that often surface damage occurs such as scratches which do contribute to an early failure of machine parts like pitting. The bonded film prevents surface damages, can take high specific pressures, and contributes significantly to generating smooth surfaces of machine parts in frictional contact. Smooth surfaces can take higher loads and pitting starts much later, as has been reported by our customers.

The author does not think to have found a "panacea", but a cure for many practical applications (not all) in which oil lubrication alone does not provide adequate lubrication.

STATUS OF PLASMA PHYSICS TECHNIQUES FOR THE DEPOSITION OF TRIBOLOGICAL COATINGS

Talivaldis Spalvins

National Aeronautics and Space Administration
Lewis Research Center
Cleveland, Ohio 44135

This paper reviews the plasma physics deposition techniques of sputtering and ion-plating. Their characteristics and potentials are discussed in terms of synthesis or deposition of tribological coatings. Since the glow discharge or plasma generated in the conventional sputtering and ion-plating techniques has a low ionization efficiency (<0.1 %), rapid advances have been made in equipment design to further increase the ionization efficiency. The enhanced ionization favorably affects the nucleation and growth sequence of the coating. This leads to improved adherence and coherence, higher density, favorable morphological growth, and reduced internal stresses in the coatings. As a result, desirable coating characteristics can be precision tailored. Tribological coating characteristics of sputtered solid film lubricants such as MoS_2, ion-plated soft gold and lead metallic films, and sputtered and ion-plated wear-resistant refractory compound films such as nitrides and carbides are discussed.

INTRODUCTION

Plasma or glow discharge, often referred to as the fourth state of matter, is an ionized gas and a convenient source of energetic electrons, ions, photons, and other activated energetic particles. On the basis how these glow discharges are excited in inert gases and active gases or their mixtures, three different surface modification techniques can be distinguished: (1) the deposition of distinct overlay coatings (sputtering and ion plating); (2) the surface modification of the base materials without forming a discrete coating (ion nitriding, surface passivation, and ion implantation); and (3) the surface sputter etching or cleaning techniques.

For this review the emphasis is directed toward the plasma physics deposition techniques of sputtering and ion-plating. In these processes the coating material is passed into the vapor phase either by a momentum exchange (impact) or thermal evaporation. Condensation of the evaporant on the substrate is subjected under the direct action of either ion flows or energetic neutrals. Even without acceleration the ionized species favorably influence the critical parameters of the condensation and nucleation process for film formation. As a result, the glow discharge deposition process leads to improved film substrate adherence, favorable morphological growth, higher coherence and density, and reduced residual stresses in the film. All these film characteristics are controlled strictly by the selected sputtering and ion-plating parameters and the substrate condition, such as surface chemistry, temperature, and topography. The particular sputtering and ion-plating parameters, and the substrate conditions selected directly affect the resultant coating characteristics which are in turn strongly interrelated with tribological properties and will determine the mode of wear and the life of the coating.

The plasmas generated in the conventional direct current (dc) or radio-frequency (rf) sputtering or dc-diode ion-plating have a low degree of ionization efficiency since less than 0.1 percent of the argon gas is ionized. Intensified attempts are presently being pursued in both the design and the application to further increase the ionization efficiency of the evaporant flux, primarily for the reactive sputtering and ion-plating of the hard, wear resistant interstitial compounds such as carbides and nitrides. Glow discharge ionization can be enhanced either by incorporating additional sources for ionization (thermionic emitters) or by increasing the electron path within the discharge with the help of magnets - magnetron sputtering. The enhanced ionization very favorably affects the crystallographic structure and the morphological growth. In addition to the enhanced ionization, the activation energy is also increased. This increased energy is used to initiate chemical reactions in the reactive mode of sputtering and ion plating.

This paper reviews briefly the conventional and the enhanced glow discharge deposition techniques of sputtering and ion-plating and illustrates their resultant, unique coating characteristics. Furthermore, the tribological properties of solid film lubricants and wear resistant interstitial compound films deposited by sputtering and ion plating are reviewed.

SPUTTERING FEATURES AND ITS POTENTIALS

The sputtering technology offers a great versatility and flexibility in coating preparation, since the sputtered coatings can be tailored in any preferred chemical composition with desirable coating morphologies. The sputtering process is not regulated by classical thermodynamics and Gibb's phase rule relationships. As a result, one is not confined within the framework of the rigid phase relationships. Any combination of metal and nonmetal elements can be sputter-deposited in any composition without concern for their phase relationships.

From an industrial point of view, the following unique features of sputtering are very desirable: versatility in material deposition, momentum transfer (impact evaporation), sputter-etching, precise controls (stoichiometry, uniformity, thickness), high flexibility in selecting sputtering modes and configurations, and elimination of ecological problems. These features have been described in detail in the literature (refs. 1 to 7).

Two basic types of sputtering can be distinguished, depending on whether the glow discharge plasma is generated by direct current (dc) or radio-frequency (rf) potentials. A typical rf diode sputtering apparatus with dc bias is shown schematically and photographically in figure 1. In rf sputtering the sputtering target is energized by the application of rf (13.56 MHz) potential, thus generating the ion plasma by rf fields, which prevents charge accumulation on the target. As a result of this nonconducting materials can be sputtered. The two basic sputtering processes can have many variations of sputtering modes and configurations. All these variations arise essentially from (1) the way in which plasma is generated (dc, rf, auxiliary electrodes), (2) the target and substrate positioning and their geometrical configurations, (3) the number of sputtering targets in the system, (4) the type of gases used (inert or reactive), and (5) the use of magnetic fields to confine the plasma-magnetron sputtering.

Magnetron sputtering is a very significant, more recent development where permanent magnets are incorporated to generate more efficient plasma discharges (refs. 8 and 9). Magnetron sputtering uses a crossed electric-magnetic field

configuration to trap the secondary electrons released by the ion bombardment of the target. Trapping these electrons ensures that maximum gas ionization is achieved before they are lost to the plasma by gas collisions. A typical configuration where magnets are placed behind the target is shown in figure 2. The magnetic lines of force exit and reenter the cathode, forcing electrons into spiral motions along the field lines, and form a closed loop where the electrons are trapped. As a result, the probability of collisions between the electrons and argon gas atoms is greatly enhanced and ionization efficiency is increased. It should be recognized that the magnetic field affects and directs the electrons but not the ions. Consequently, magnetron sputtering offers higher deposition rates and low substrate temperatures in comparison with the conventional sputtering techniques.

ION-PLATING PROCESS AND ITS POTENTIALS

Ion-plating combines the high throwing power of electroplating, the high deposition rates of thermal evaporation, and the high energy impingment of ions and energetic atoms of the sputtering process. There is a basic difference between sputtering and ion-plating: in sputtering, the coating material is generated by impact evaporation and transfer occurs by a momentum transfer process; in ion-plating, generation is by thermal evaporation and transfer is by an electric field acceleration. The ion-plating process is more energetic than the sputtering process, since a high substrate bias of several thousand volts accelerates the positively ionized evaporant atoms into the substrate. The basic ion-plating system consists of a dc-diode configuration, where the specimen is made the cathode of the high-voltage dc circuit, with an evaporation source as anode (fig. 3). The ion-plating technique and the process parameters are described in the literature (refs. 10 to 15).

The interest in ion-plating originates from its three unique features:

(1) The high energy flux of ions and energetic neutrals contributes to the excellent adherence of the film to the substrate and the desirable microstructural growth of the film.

(2) When used in the reactive mode, this flux provides activation energy to synthesize stoichiometrically uniform compound films.

(3) The high throwing power provides for three-dimensional coverage to coat complex, intricate components such as bearing cages and races without rotation.

With typical ion-plating conditions (voltage is 3 to 5 kV, argon pressure is 20 mTorr, and cathode current density is 0.3 to 0.6 mA/cm^2) the ionization is relatively low, less than 1 percent. It has been estimated that under these conditions the ions carry only 10 percent of the energy dissipated while the energetic neutrals carry 90 percent (ref. 10). Thus, the plating flux consists of a small number of ions and a large number of energetic neutrals. The ions and the neutrals may have a distribution of energies from thermal 0.2 eV up to the voltage applied to the discharge. Estimates indicate that the average energies of the ions and the neutrals are of the order of 100 eV (ref. 10).

The diode or conventional ion-plating just described is primarily used for the deposition of soft, metallic lubricating films. Soft metallic films of gold, silver, and lead applied by ion-plating, in contrast to films applied by other deposition techniques, offer a lower friction coefficient and longer wear lives. They also exhibit a gradual increase in friction coefficient after the film has been worn off, which is due to the graded interface that is formed.

In recent years, the reactive mode of ion-plating is widely investigated to synthesize the hard, wear-resistant refractory coatings such as nitrides, carbides, silicides, etc. The two objectives are (1) to achieve a reaction of the metal vapor and the reactive gas, and (2) to synthesize a coating with a dense structure and strong adherence. It is important to note that, from a tribological point of view, the excellent adherence obtained from ion-plating is not the only controlling factor for optimum wear resistance. The microstructure and morphological growth of the coating is of equal importance. The conventional ion-plating process does improve the grain structure; however, the structure still tends to be columnar. The object is to increase the ionization efficiency and the kinetic energy of the evaporant flux which affect the nucleation and growth sequence of the film. Consequently, fine, equiaxed grain structures of high density can be formed.

A number of improvements in the experimental apparatus have been made to increase the ionization efficiency. Schematic diagrams for various improvements are shown in figure 4. A multicathode technique (ref. 16) is used to increase ionization with the emission of thermal electrons from hot tungsten filaments placed in the evaporation area. A high-frequency technique (rf ion-plating) (refs. 17 and 18) uses an rf coil that is connected to a 13.56-MHz (1-kW) generator through a matching box to promote ionization by a high-frequency magnetic field. Using an induction-heated evaporation source (ref. 19) where there is a high-frequency magnetic field generated by electron trapping increases the ionization. The incorporation of a positive electrode known as a positive discharge probe (ref. 20), or a low-voltage high-current electron gun with a hot hollow cathode discharge (HCD) gun, as an evaporation source (refs. 21 and 22) will also increase ionization. A combination of a thermionic emitter and a positive probe (ref. 23) will do likewise. The aforementioned techniques generally increase the ionization ratio by a factor of 10 and are mainly used for the deposition of hard wear-resistant coatings.

GLOW DISCHARGE EFFECTS ON COATING CHARACTERISTICS

During sputtering and ion-plating, the ions and energetic neutrals favorably affect the nucleation and growth sequence of the coating and the coating/substrate adherence. The understanding of the microstructure of the films deposited has progressed further than the understanding of the compositional environment of the glow discharge from which the films are formed. Gas discharges that incorporate chemical reactions comprise a reaction volume of great complexity; they consist of a melange of molecules, atoms, atomic ions in various stages of excitation, electrons, photons, etc.

Adherence

The coating/substrate interface represents a break in the normally uniform crystallinity or composition. This abrupt change or mismatch is reflected in the hardness, coefficient of thermal expansion, and thermal conductivity. This discontinuity may be reduced or eliminated by inducing a gradual transition from the interface to the outer surface of the coating. For instance, intricate, graded structures with a hardness gradient can be produced by programming the flow rates of the reactant gases either by reactive sputtering or reactive plating.

A typical TiN hardness gradient formed during reactive ion-plating is shown in figure 5. This technique is extensively used in metalworking and forming operations to improve the working surfaces of cutting and forming tools with a carbide or nitride coating.

In ion-plating, lubricating films of gold, silver, and lead can be deposited at a constant pressure due to the formation of a graded-fused interface. The graded interface, and consequently the strong adherence, is generally attributed to the sputter-etched surface and the high-energy evaporant flux. The exact mechanism for the formation of such an interface is not fully understood, but the controlling factors are a sputter-etched surface, diffusion, implantation, atomic mixing, and nucleation and growth (fig. 6). These factors can act separately or in various combinations depending on the film/substrate compatibility. The graded interface formed is not only responsible for the excellent adherence but also affects the mechanical behavior, due to a structural alteration of the crystal lattice in the surface and subsurface regions. The surface-strengthening effects created can increase the yield, tensile, and fatigue strengths (fig. 7).

Structure

It is well recognized that films prepared by sputtering and ion-plating show a wide range of microstructures as the substrate temperature increases. This has led to the development of the structure zone model (SZM) shown in figure 8 (ref. 24). The model consists of the formation of four zones which depend on the ratio of the surface temperature (T) to the melting point of the deposited material (T_m). According to this model, the microstructural growth is controlled by shadowing effects (zone 1), surface diffusion (zone T and zone 2), and bulk diffusion (zone 3) as T/T_m increases. The coatings in zone 1 have columnar grain structure with the axes of the columns along the direction of growth, normal to the substrate surface. The packing of the columns frequently is separated by voids, so that the packing density is less than unity. This structure is characteristic of most coating techniques and does not withstand high stresses and loads. Coating in the zone T (transition) region still consists of fibrous grains but more densely packed. In zone 2 the structure has columnar grains separated by distinct, intercrystalline boundaries. Finally, in zone 3 bulk diffusion has the predominant influence on the final structure of the coating and consists of equiaxed, dense, recrystallized grains.

The argon working pressure is an additional parameter which affects the structural growth as shown in figure 8. The glow discharge pressure reduction leads to a shift of more compact layers.

The equiaxed type of structure is preferred primarily in the deposition of wear resistant refractory coatings. The high T/T_m required for the formation of carbide or nitride coatings with equiaxed structures has severe limitations. For instance, the mechanical properties of tool steels are unfavorably affected at these high temperatures. Instead of increasing the bulk temperature, the zone boundaries can be shifted to lower temperatures by intensifying the glow discharge. Intensified bombardment effects generally lead to effective film-substrate temperatures (larger ratio of T/T_m) which are higher than the bulk substrate temperatures. Consequently, increasing the current density to the substrate has the same effects as raising T/T_m directly, which leads to the development of a structure characteristic of the higher zone. The enhanced ionization techniques utilize various additional

electrodes and allow for varying the discharge current independently of the bias voltage on the specimen. These techniques therefore offer a means of obtaining microstructures representative of a higher T/T_m at relatively low substrate temperatures. These techniques are primarily investigated and developed for the deposition of carbides and nitrides in the reactive sputtering and ion-plating modes.

It has been reported that high-energy (>500 eV) ion bombardment can suppress the formation of a distinct columnar structure (ref. 13). The high rate of nucleation tends to form a uniform, fine-grained, high-packing density smooth film which contributes to an increased cohesive strength. This increased cohesive strength improves the film's integrity, thereby reducing the likelihood of a breakup of the coating during the wear process. For instance, during ion-plating the evaporant ions and energetic neutrals have a strong surface interaction, thereby limiting the surface mobility and, at the same time, increasing nucleation density. This leads to the formation of a fine, uniform, and continuous grain structure. As a result, continuous dense films are obtained at a lower nominal thickness.

Internal Stresses and Film Thickness

Virtually all vacuum-deposited coatings are in a state of stress, but this effect is very pronounced in the hard wear-resistant refractory compound films. The total internal stress is composed of the thermal stress σ_t and intrinsic stress σ_i:

$$\sigma_{tot} = \sigma_t + \sigma_i$$

The thermal stress is due to the differences in the thermal expansion coefficient of the coating and the substrate material. This difference is very pronounced between the refractory compound coatings and the metallic substrate. Intrinsic stress is due to the accumulating effects of crystallographic defects or flaws formed in the coating during deposition.

Typical deposition conditions involve relatively low temperatures. At low T/T_m the intrinsic stresses dominate over thermal stresses, as shown in an idealized representation in figure 9 (ref. 25). Thus, the poor adhesion for the high-melting-point materials (carbides and nitrides) can be attributed to the intrinsic stresses. In addition to the temperature effects (T/T_m), which affect the internal stress values, the degree of ion bombardment also strongly influences the internal stresses. With increasing ion flux, the stress changes from tensile to compressive in nature. Typically evaporated films retain high tensile stresses, while sputtered films may have low tensile or compressive stresses depending on the nature of energetic ion and neutral bombardment. Ion-plating, which has the highest energy flux, generates a graded-fused interface where the compressive stresses are distributed and appreciably reduced.

The film stresses also vary with film thickness. As a critical thickness is exceeded, poor adherence is caused by cracking or buckling. Whenever the shear stress exceeds the yield stress at the interface or within the film itself, separation will occur. A typical film delamination within a sputtered Cr_3C_2 film about 3.5 μm thick is shown in figure 10.

Substrate Topography

Adherence and homogeneous growth morphology is not only affected by the coating process parameters but also by the substrate topography, which has a pronounced effect on the wear behavior. It is impossible to prepare surfaces that are atomically smooth over extended areas. Surface macrodefects can be eliminated, but microdefects such as point defects, dislocations, and embedded impurities impose limitations for obtaining a smooth surface. It is important to understand that homogeneous morphological structural growth is related to smooth, mirrorlike surfaces. Substrate irregularities or imperfections are the preferrential nucleation and growth sites of these defects. At the nucleation sites, accelerated growth occurs relative to the matrix growth, and as a consequence, the crystallographic defects extend above the matrix surface. These coating defect structures, as shown by scanning electron microscopy (SEM) in figure 11, have adverse affects on the coating. They act like stress raisers, and, therefore, weaken the mechanical properties by creating porosity and introducing cracks. These crystallographic defect structures have the greatest damaging effects on the hard wear-resistant coatings.

SOLID LUBRICANT FILM DEPOSITION IN GLOW DISCHARGE

Of the three principal classes of solid lubricants, the lamellar solids (MoS_2, WS_2, NbS_2, and other dichalcogenides) are primarily deposited by rf and dc sputtering (refs. 26 to 31), the soft metals (Au, Ag, Pb, In) by ion-plating (refs. 32 to 36), and the organic polymers (PTFE polyimides) by rf sputtering (refs. 37 to 39).

Sputtered MoS_2

Of the lamellar solids, sputtered MoS_2 films are widely used in spacecraft applications since these films in vacuum or dry air environment maintain their lubricating properties over extreme temperature ranges. Sputtered MoS_2 films about 2000 Å thick have displayed a low coefficient of friction (0.04) and long wear lives (over million cycles) and have performed better than films applied by other commonly used techniques (ref. 26) such as burnishing and spraying. It should be emphasized that the superior lubricating properties of sputtered MoS_2 films can be greatly altered by varying the sputtering parameters and substrate condition during the process. For instance, the variation of the substrate temperature from cryogenic temperatures (-195° C) to an elevated temperature of 320° C affects the nucleation and growth sequence. Amorphous films are formed at the low temperatures, and crystalline films are formed at ambient and elevated temperatures. Figure 12 illustrates how the coefficient of friction changes with the morphology and grain size. The amorphous-type structure displays a high coefficient of friction (0.4) and has no lubricating properties. On the other hand, the crystalline structure displays a low coefficient of friction (0.04) and has good lubricating properties. Simply by controlling the substrate temperature during the sputtering process the coefficient of friction can be varied accordingly as seen in the transition region.

The morphological growth zones of sputtered MoS_2 films (>1 μm thick) at ambient temperatures have been determined and the effective lubricating film thickness established. Based on scanning electron (fig. 13) and trans-

mission electron (fig. 12) microscopy, three levels of structural growth from the nano- to the microstructure were observed: (1) ridge formation during nucleation and growth, (2) equiaxed transition zone, and (3) columnar-fiberlike structure. Friction tests indicate that the film breaks within the columnar zone in the first pass as schematically illustrated in figure 14. The actual lubrication is supported by the equiaxed zone which is 0.18 to 0.22 μm thick and which is responsible for effective lubrication. This indicates that the adhesive forces between the substrate and the MoS_2 films are stronger than the cohesive forces between the columnar fibers.

Ion-Plated Gold and Lead

Of the ion-plated metallic soft lubricating films, gold and lead have found extensive uses in spaceborn bearings of satellite mechanisms such as solar array drives, despin assemblies, and gimbals. The ion-plated gold and lead films for these appliations have definite advantages in that they display a reduced coefficient of friction and extended wear life over other deposition techniques (ref. 34). These films also alter the mode of debris generation and reduce torque noise (ref. 33). The contributing factors to the superior tribological performance are the excellent adherence, and the equiaxed, dense, uniform film structure. Typical friction versus film thickness relationships for gold and lead films measured on a pin-on disk type tribotester are shown in figure 15. The effective film thickness for gold and lead films in the thickness range of 2000 to 3000 Å gives the lowest coefficients of friction - 0.085 and 0.1, respectively.

The ion-plated gold and lead films display lower friction coefficients and longer wear lives than films deposited by sputtering. The nucleation and growth characteristics during ion-plating are influenced by the increased nucleation density which leads to the formation of a fine, continuous grain structure with a high packing density.

WEAR-RESISTANT FILM DEPOSITION IN GLOW DISCHARGE

The wear-resistant coatings most widely investigated are the interstitial compounds formed between groups 4, 5, and 6 transition metals (Ti, Zr, Hf; V, Nb, Ta; and Cr, Mo, W) with the small interstitials (N, C, B). The term might be extended to encompass the oxides, which are not considered here.

Of the many potential interstitial compounds, the nitrides and the carbides are widely investigated, particularly TiN and TiC (refs. 40 to 53). These coatings possess high hardness, high corrosion resistance, low cost, and ease of Ti evaporation as compared to the W, Hf, V, Cr, Mo, and W nitrides. Characteristic bulk and coating hardness values as reported in the literature are listed in table I.

Of the possible deposition techniques available, chemical vapor deposition (CVD) has been the most widely used. However, the reactive plasma deposition techniques to synthesize and deposit interstitial compounds have expanded dramatically in the past several years. The magnetron sputtering and the enhanced (triode) ion-plating techniques in the reactive mode are being established as the preferred techniques to deposit wear-resistant carbide and nitride coatings.

It is interesting to compare the CVD and the plasma physics techniques in terms of their starting materials, byproducts, and process temperatures. CVD

processes utilize the following reaction:

$$TiCl_4 + NH_3 + 1/2\ H_2 \xrightarrow{(1000^\circ\text{-}1200^\circ\ C)} TiN + 4\ HCl$$

(volatile corrosive liquid) (toxic corrosive gas) (explosive gas) (corrosive gas)

Reactive plasma physics techniques utilize the following reaction:

$$Ti + N_2 \xrightarrow{500^\circ\ C} TiN$$

(metallic vapor) (neutral gas)

The use of nitrogen as the reactive gas in the plasma physics techniques avoids the potentially hazardous toxic gases and the high temperatures used for the CVD nitride deposition. In the reactive magnetron sputtering and reactive ion-plating the required refractory compounds are produced by sputtering and thermal evaporating the relevant metal in a reactive plasma medium. In either technique the primary objectives are to (1) achieve reaction of the metal and the reactive gas and (2) synthesize a coating with strong adherence and desirable structural morphology. With the enhanced ionization, the activation energy is also increased, and this promotes chemical reaction when the reactant gases (N_2, C_2H_2) are introduced.

The microhardness values for TiN_x that have been reported lie between 2000 and 4000 kg/mm^2. A typical hardness value is 2500 kg/mm^2. The hardness depends on the stoichiometric variation, and it can be varied by adjusting the partial pressure of nitrogen during the deposition process.

The coefficients of friction reported in the literature range from 0.08 to 0.25. The TiN coatings in addition to their wear and corrosion resistance also display an attractive goldlike color. TiN films of different colors can be obtained by varying the partial pressure of nitrogen. The color change can also be used as an indication of hardness and resistance to wear (ref. 52). The enhanced ionization, particularly in the ion-plating techniques, very favorably affects the crystallographic structure and the morphological growth of the coating. It has been demonstrated that high energy (>500 eV) ion bombardment can suppress the formation of the undesirable columnar growth and produce the dense, equiaxed film structure of the deposited coatings.

CONCLUSIONS

The plasma or ion-assisted deposition techniques such as sputtering and ion-plating have rapidly emerged to offer a great potential to precision tailor desirable morphological and tribological properties for lubricating and wear-resistant coatings. The basic processes and unique characteristics of sputtering and ion-plating should be understood in order to exploit their capabilities to synthesize films with preferred compositional and structural characteristics. The energetics of the plasma is favorably used to improve coating adherence and coherence, to develop favorable morphological growth, and to reduce residual stresses. These film characteristics are directly interrelated with friction and wear behavior. The disadvantage of these techniques and

their resultant coatings lies mainly in their newness; that is, the best coating compositions and the optimum processing parameters have yet to be established.

REFERENCES

1. Chapman, B. N.: Glow Discharge Processes, John Wiley and Sons, 1980, pp. 45-47.
2. Reinberg, A. R.: Plasma Deposition of Inorganic Thin Films. Annual Review of Material Science, Vol. 9, R. A. Huggins, R. H. Bube and D. A. Vermilyea, eds., Annual Reviews, Inc., 1979, pp. 341-372.
3. Maissel, L.: Application of Sputtering to the Deposition of Films. Handbook of Thin Film Technology, Ch. 4, L. I. Maissel and R. Glang, eds., McGraw Hill, 1970, pp. 4-1 to 4-44.
4. Holland, L.: A Review of Plasma Process Studies. Surface Technology, vol. 11, no. 3, Sept. 1980, pp. 145-169.
5. Bunshah, R. F.: Deposition Technologies for Films and Coatings, Noyes Public., 1982.
6. Vossen, J. L.; and O'Neil, J. J.: R-F Sputtering Process. RCA Rev., vol. 29, no. 2, June 1968, pp. 149-179.
7. Westwood, W. D.: Glow Discharge Sputtering. Prog. Surf. Sci., vol. 7, no. 2, 1976, pp. 71-111.
8. Thorton, J. A.: Recent Developments in Sputtering - Magnetron Sputtering. Proceedings of Society of Vacuum Coaters, vol. 21, Society of Vacuum Coaters, 1978, pp. 19-30.
9. Thornton, J. A.: Magnetron Sputtering - Basic Physics and Applications to Cylindrical Magnetrons. J. Vac. Sci. Technol., vol. 15, no. 2, Mar. 1978, pp. 171-177.
10. Teer, D. G.: Adhesion of Ion Plated Films and Energies of Deposition. J. Adhes., vol. 8, no. 4, 1977, pp. 289-300.
11. Mattox, D. M.: Fundamentals of Ion Plating. J. Vac. Sci. Technol., vol. 10, no. 1, 1973, pp. 47-52.
12. Mattox, D. M.: Sputter Deposition and Ion Plating Technology. American Vacuum Society, 1973.
13. Mattox, D. M.: Mechanisms of Ion Plating. Proceedings of IPAT 79, CEP Consultants Ltd. (Edinburgh), 1979, pp. 1-10.
14. Spalvins, T.: Survey of Ion Plating Sources. J. Vac. Sci. Technol., vol. 17, no. 1, 1980, pp. 315-321.
15. Spalvins, T.: Ion PLating for the Future. Met. Finish., vol. 80, no. 5, May 1982, pp. 47-50.
16. Kiyoshi, M.: Method for Ionization Electrostatic Plating. U.S. Patent 3,953,619, Apr. 27, 1976.
17. Murayama, Y.; and Takao, T.: Structure of a Silicon Carbide Film Synthesized by RF Reactive Ion Plating. Thin Solid Films, vol. 40, 1977, pp. 309-317.
18. Swaroop, B.; Meyer, D. E.; and White, G. W.: Ion Plated Aluminum Oxide Coatings for Protection Against Corrosion. J. Vac. Sci. Technol., vol. 13, no. 3, 1976, pp. 680-683.
19. Spalvins, T.: Ion Plating with an Induction Heating Source. NASA TM X-3330, Jan. 1976.
20. Teer, D. G.; and Delcea, B. L.: Grain Structure of Ion Plated Coatings. Thin Solid Films, vol. 54, 1978, pp. 295-301.

21. Komiya, S.; and Tsuruoka, K.: Physical Vapor Deposition of Thick Cr and Its Carbide and Nitride Films by Hollow Cathode Discharge. J. Vac. Sci. Technol., vol. 13, no. 1, 1976, pp. 520-524.
22. Wan, C. T.; Chambers, D. L.; and Carmichael, D. C.: Investigation of Hot-Filament and Hollow Cathode Electron Beam Techniques for Ion Plating. J. Vac. Sci. Technol., vol. 8, no. 6, 1971, pp. VM99-VM104.
23. Matthews, A.; and Teer, D. G.: Deposition of TiN Compounds by Thermionically Assisted Triode Reactive Ion Plating. Thin Solid Films, vol. 72, 1980, pp. 541-549.
24. Thorton, J. A.: High Rate Thick Film Growth. Annual Review of Material Science, Vol. 7, R. A. Huggins, R. H. Bube and R. W. Roberts, eds., Annual Reviews, Inc., 1977, pp. 239-260.
25. Thorton, J. A.; and Hoffman, D. W.: Stress Related Effects in Thin Films. 22nd. Annual Technical Conference Proceedings, Society of Vacuum Coaters, 1979, pp. 5-18.
26. Spalvins, T.; "Sputtering Technology in Solid Film Lubrication," Second International Conference on Solid Lubrication, ASLE Special Publication 6, ASLE, 1978, pp. 109-117.
27. Spalvins, T.: Tribological Properties of Sputtered MoS_2 Films in Relation to Film Morphology. Thin Solid Films, vol. 73, 1980, pp. 291-297.
28. Christy, R. I.: Sputtered MoS_2 Lubricant Coating Improvements. Thin Solid Films, vol. 73, 1980, pp. 299-307.
29. Christy, R. I.; and Ludwig, H. R.: R. F. Sputtered MoS_2 Parameter Effects on Wear Life. Thin Solid Films, vol. 64, 1979, pp. 223-229.
30. Stupp, B. C.: Synergistic Effects of Metals Co-Sputtered with MoS_2, Thin Solid Films, vol. 84, 1981, pp. 257-266.
31. Spalvins, T.: Morphological and Frictional Behavior of Sputtered MoS_2 Films. Thin Solid Films, vol. 96, 1982, pp. 17-24.
32. Arnell, R. D.; and Soliman, F. A.: The Effects of Speed, Film Thickness and Substrate Surface Roughness on the Friction and Wear of Soft Metal Films in Ultra High Vacuum. Thin Solid Films, vol. 53, 1978, pp. 333-341.
33. Todd, M. J.; and Bentall, R. H.: Lead Film Lubrication in Vacuum. 2nd. International Conference on Solid Lubrication, ASLE Special Publication 6, ASLE, 1978, pp. 148-157.
34. Spalvins, T.; and Buzek, B.: Frictional and Morphological Characteristics of Ion Plated Soft Metallic Films. Thin Solid Films, vol. 84, 1981, pp. 267-272.
35. Miyoshi, K.; Spalvins, T.; and Buckley, D. H.: Tribological Properties and X-Ray Photoelectron Spectroscopy Studies of Ion Plated Gold on Nickel and Iron. Thin Solid Films, vol. 96, 1982, pp. 9-16.
36. Todd, M. J.: Solid Lubrication of Ball Bearings for Spacecraft Mechanisms. Tribol. Int., vol. 15, no. 6, Dec. 1982, pp. 331-337.
37. Harrop, R.; and Harrop, P. J.: Friction of Sputtered PTFE Films. Thin Solid Films, vol. 3, 1969, pp. 109-117.
38. Morrison, D. T.; and Robertson, T.: RF Sputtering of Plastics. Thin Solid Films, vol. 15, 1973, pp. 87-101.
39. Spalvins, T.: Friction Characteristics and Lubrication with Sputtered Solid Films. Proceedings of Second German Sputtering School, Munich, Germany, Sponsored by Materials Research Corp., Orangeburg, N.Y., May 1971, pp. 150-192.
40. Spalvins, T.: Microstructural and Wear Properties of Sputtered Carbides and Silicides. Wear, vol. 46, 1978, pp. 295-304.

41. Brainard, W.; and Wheeler, D.: X-Ray Photoelectron Spectroscopy Study of Radiofrequency-Sputtered Titanium Carbide, Molybdenum Carbide, and Titanium Boride Coatings and Their Friction Properties. NASA TP-1033, Oct. 1977.
42. Chevallier, J.; and Chabert, J. P.: Microhardness of TiN Coatings Obtained by Reactive Cathodic Sputtering. Thin Solid Films, vol. 80, 1981, p. 263.
43. Sundgren, J. E.; Johansson, B. O.; and Karlsson, S. E.: Influence of Substrate Bias on Composition and Structure of Reactively RF-Sputtered TiC Films. Thin Solid Films, vol. 80, 1981, pp. 77-83.
44. Aronson, A. J.; Chen, D.; and Class, W. H.: Preparation of Titanium Nitride by a Pulsed dc Magnetron Reactive Depostion Technique Using the Moving Mode of Depostion. Thin Solid Films, vol. 72, 1980, pp. 535-540.
45. Ramalingam, S.; and Winer, W. O.: Reactively Sputtered TiN Coatings for Tribological Applications. Thin Solid Films, vol. 73, 1980, pp. 267-274.
46. Matthews, A.; and Teer, D. G.: Ion Plated TiN Coatings for Dies and Molds. Proceedings of IPAT 79, CEP Consultants, Ltd. (Edinburgh), 1979, pp. 11-18.
47. Zega, B.; Kormann, H.; and Amiguet, J.: Hard Decorative TiN Coatings by Ion Plating. Thin Solid Films, vol. 45, 1977, pp. 577-582.
48. Bunshah, R. R.: The Activated Reactive Evaporation Process: Developments and Applications. Thin Solid Films, vol. 80, 1981, pp. 255-261.
49. Nimmagadda, R. R.; Doerr, H. J.; and Bunshah, R. R.: Improvement in Tool Life of Coated High Speed Steel Drills Using the Activated Reactive Evaporation Process. Thin Solid Films, vol. 84, 1981, pp. 303-306.
50. Clarke, P. J.: Magnetron DC Reactive Sputtering of Titanium Nitride and Indium Tin Oxide. J. Vac. Sci. Technol., vol. 14, no. 1, 1977, pp. 141-142.
51. Mumtaz, A.; and Class, W. H.: Color of Titanium Nitride Prepared by Reactive DC Magnetron Sputtering. J. Vac. Sci. Technol., vol. 20, no. 3, Mar. 1982, pp. 345-348.
52. Buhl, R.; Pulker, H. K.; and Moll, E.: TiN Coatings on Steel. Thin Solid Films, vol. 80, 1981, pp. 265-270.
53. Lardon, M.; et al.: Morphology of Ion Plated Titanium and Aluminum Films Deposited at Various Substrate Temperatures. Thin Solid Films, vol. 54, 1978, pp. 317-322.

TABLE I. - MICROHARDNESS VALUES FOR NITRIDES AND CARBIDES

Material	Vickers hardness, kg/mm^2	
	Bulk	Films
TiN	2000	1500–2500
ZrN	1500	700–3600
HfN	1600	1850–2400
VN	1500	600–2000
NbN	1400	1100–3000
TaN	1000	----------
Si_3N_4	2000	----------
TiC	3500	2770–4150
VC	2500	1900–2850
WC	2050	1800–2800
TaC	2200	1280–2200

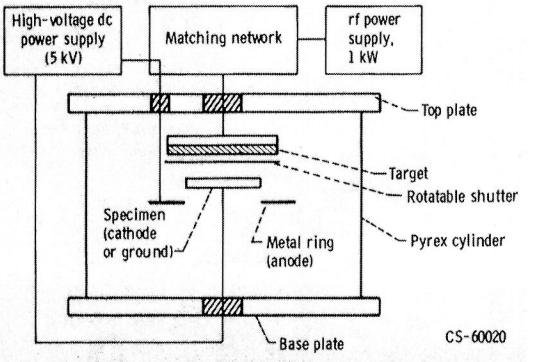

(a) Schematic diagram.

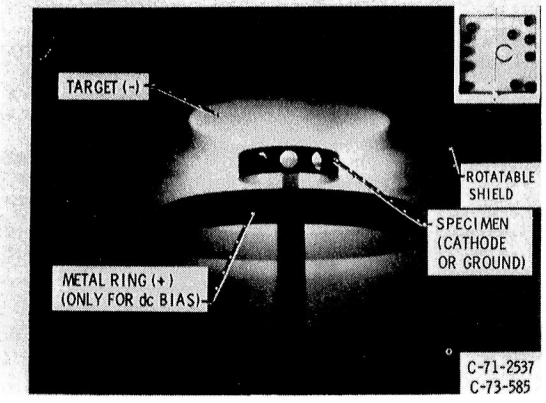

(b) View of apparatus during sputter coating.

Figure 1. - Radiofrequency diode sputtering apparatus with direct-current bias.

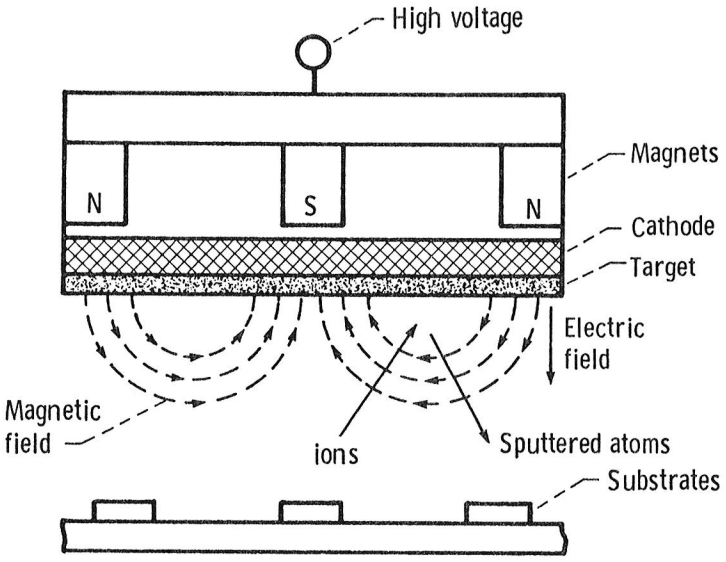

Figure 2. - Magnetron sputtering concepts.

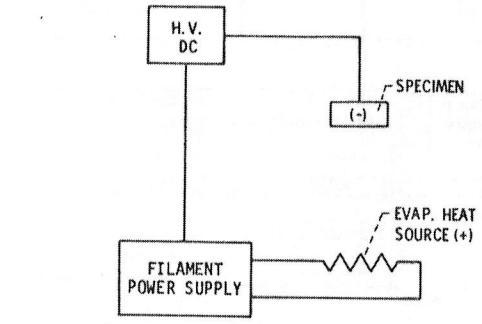

(a) SCHEMATIC.

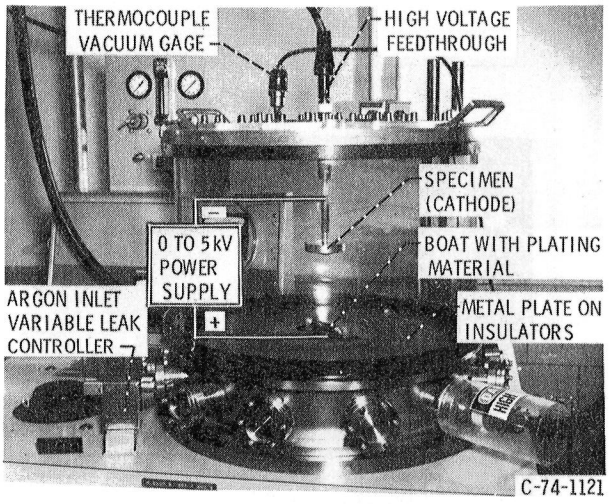

(b) ION PLATING CHAMBER.

Figure 3. - Ion plating system.

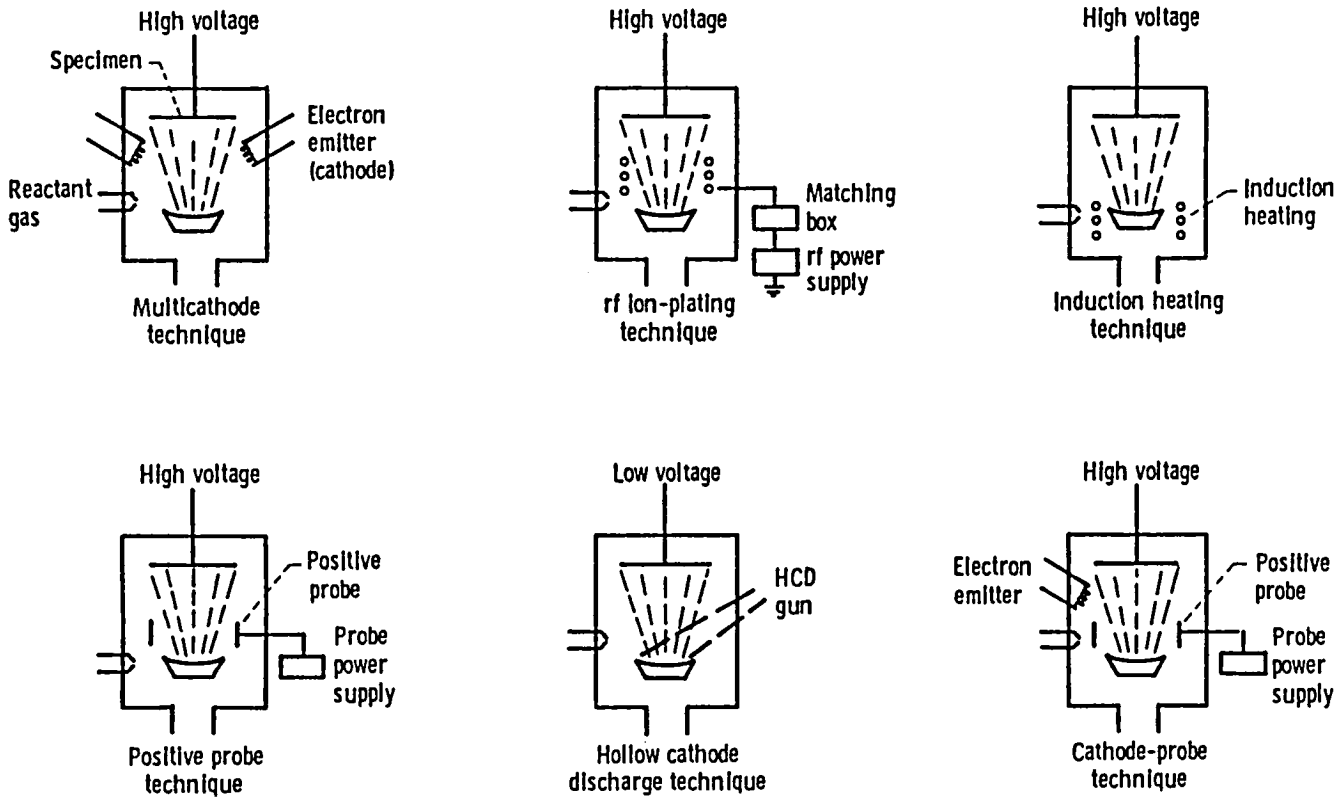

Figure 4. - Enhanced ionization techniques of ion-plating.

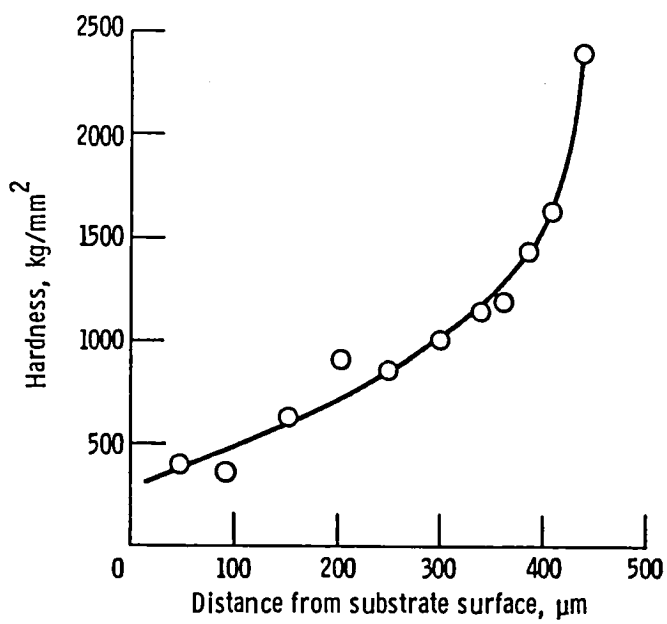

Figure 5. - Hardness gradient of TiN coating produced by reactive ion-plating.

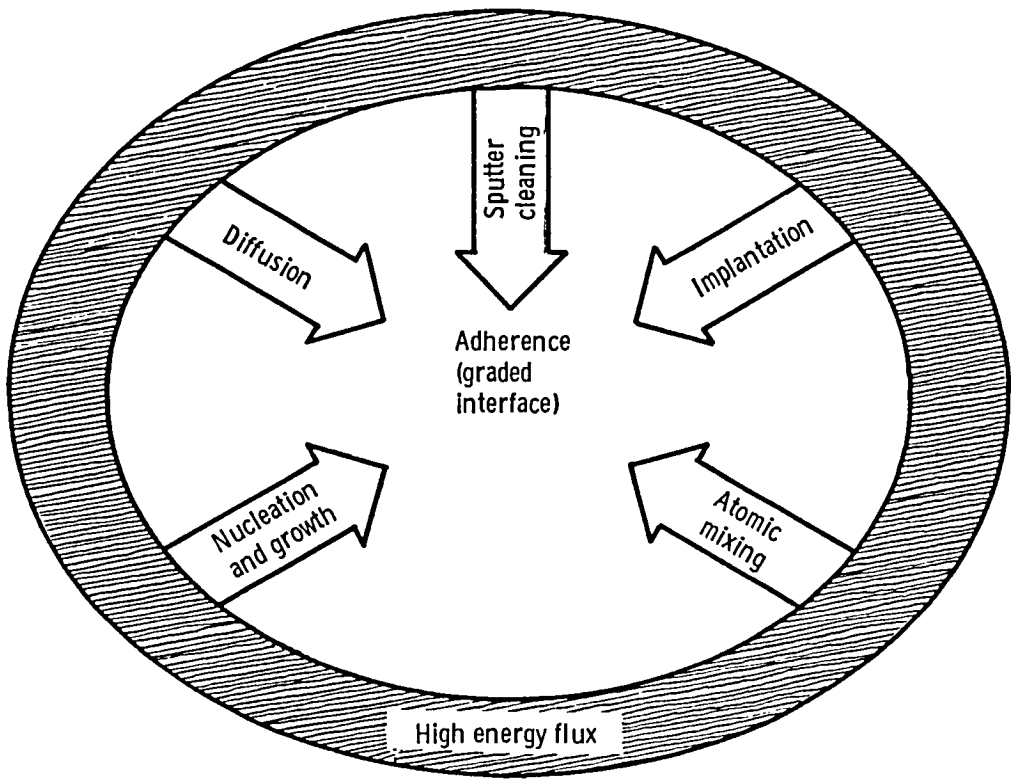

Figure 6. - Illustration of factors which influence adherence and interface formation during ion-plating.

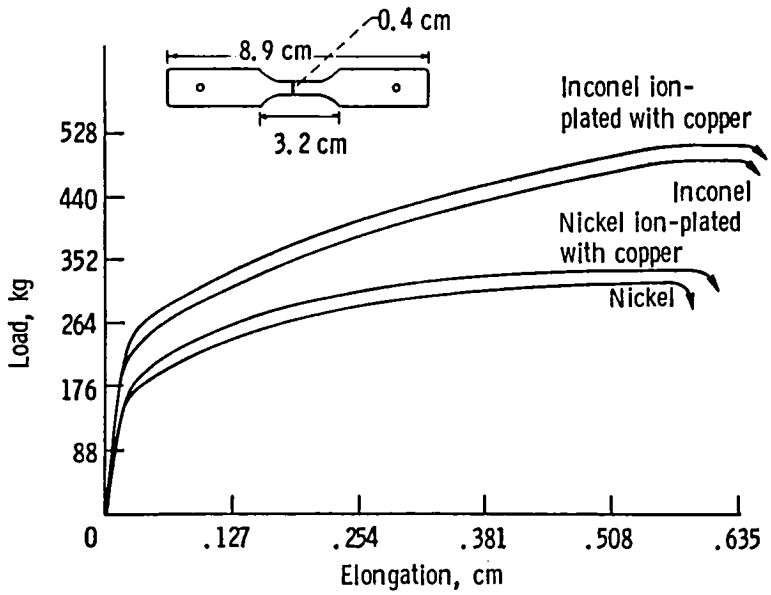

(a) Load elongation curves during tensile tests. Flat tensile specimen: nickel, 0.05 cm thick; inconel, 0.043 cm thick.

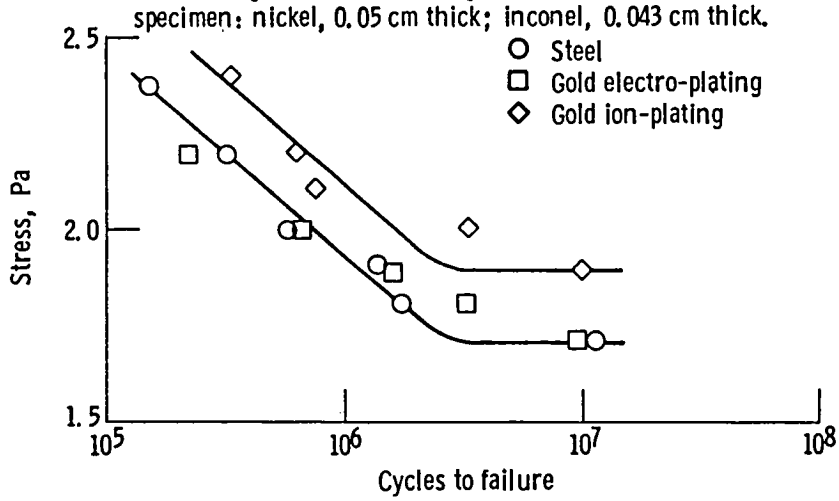

(b) Effect of ion-plating on fatigue property of low carbon steel.

Figure 7. - Surface-strengthening effects.

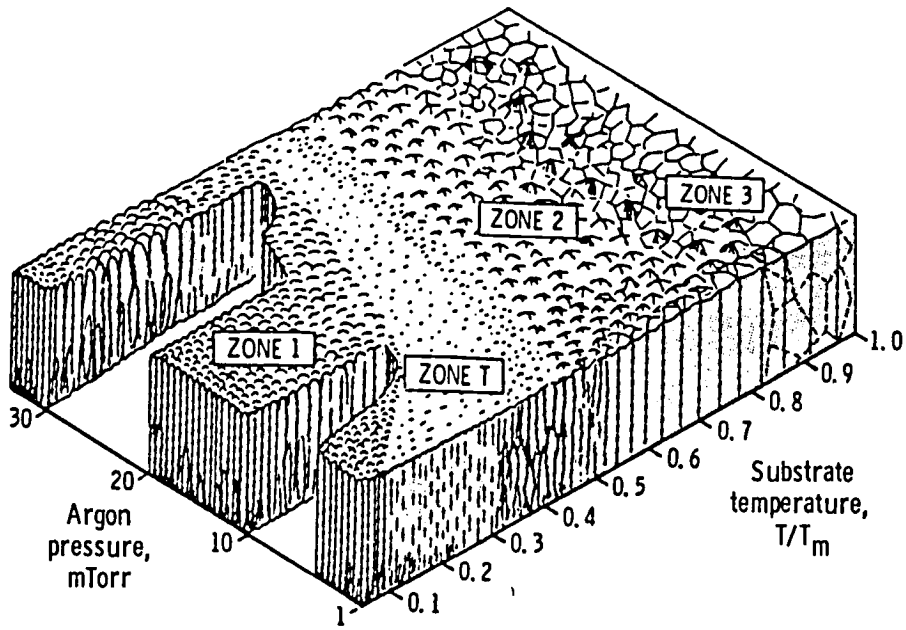

Figure 8. - Schematic representation of influence of substrate temperature and argon working pressure on structure of metal coatings deposited by sputtering using cylindrical magnetron sources. Substrate temperature, T; melting point of coating material in absolute degrees, T_m (ref. 24).

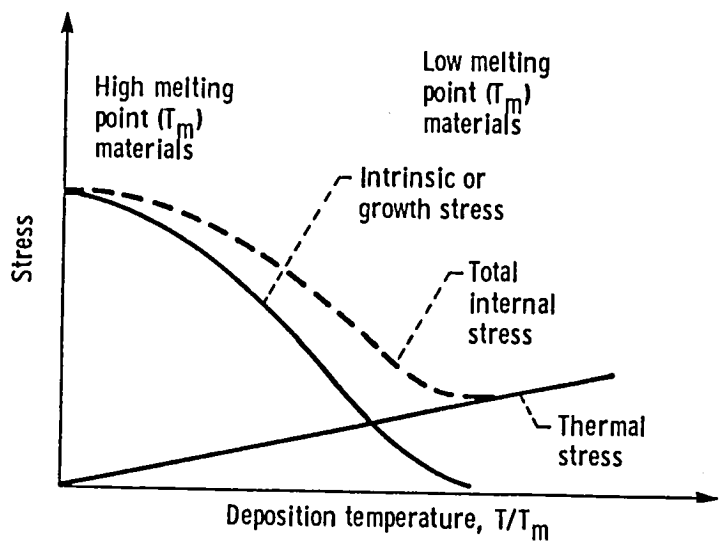

Figure 9. - Schematic representation of thermal and intrinsic stress contributions (ref. 25).

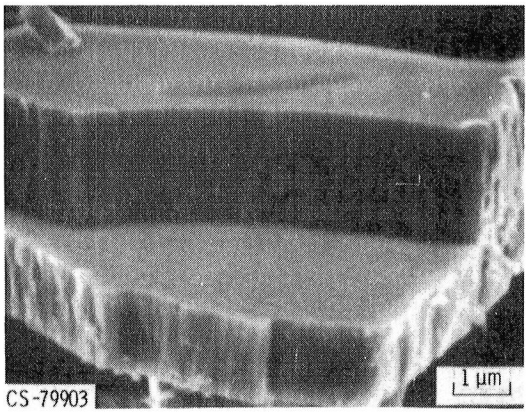

Figure 10. - Separation within a 3.5-μm film of sputtered Cr_3C_2.

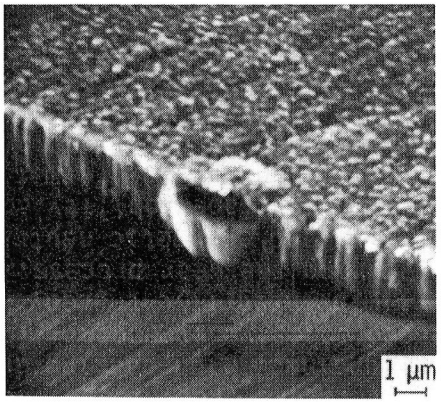

(a) Overlapping nodule.

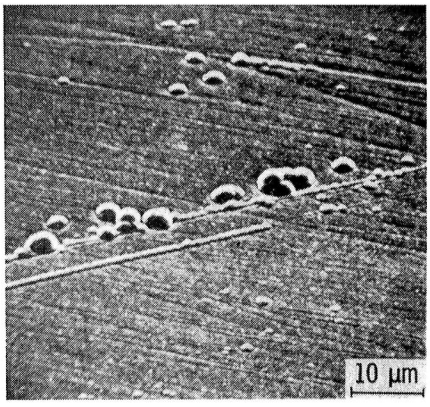

(b) Isolated and fused nodules.

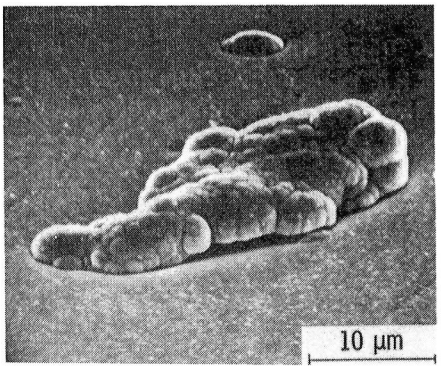

(c) Extreme localized outgrowth.

Figure 11. - Fracture cross section and surface view of defects in sputtered $MoSi_2$ and Cr_3C_2 film.

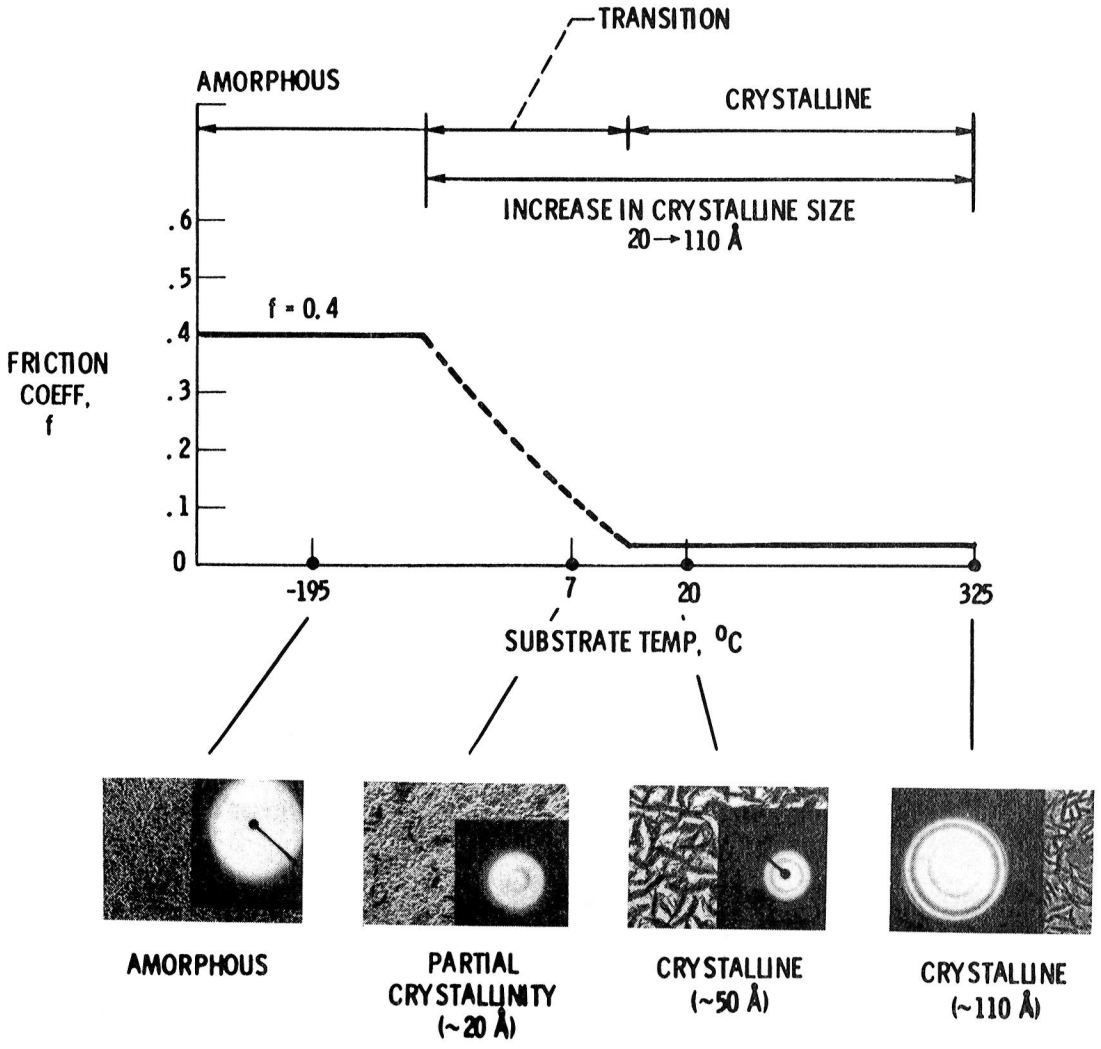

Figure 12. - Substrate temperature effects on MoS_2 film morphology and friction coefficient.

(a) Film structure after single-pass sliding.

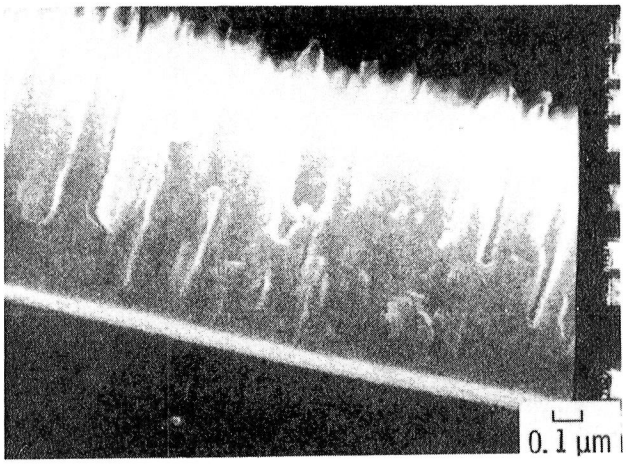

(b) Cross-sectional structure of sputtered MoS_2 film on glass.

(c) Cross-sectional structure of sputtered MoS_2 film on glass.

Figure 13. - SEM cross-sectional structures of sputtered MoS_2 films.

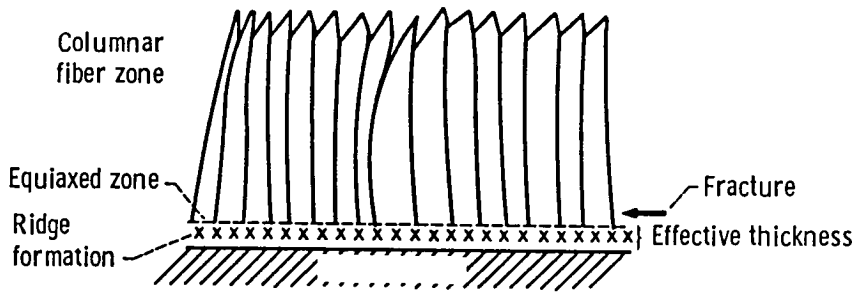

Figure 14. - Fracture during sliding of sputtered MoS_2 film in respect to morphological zones.

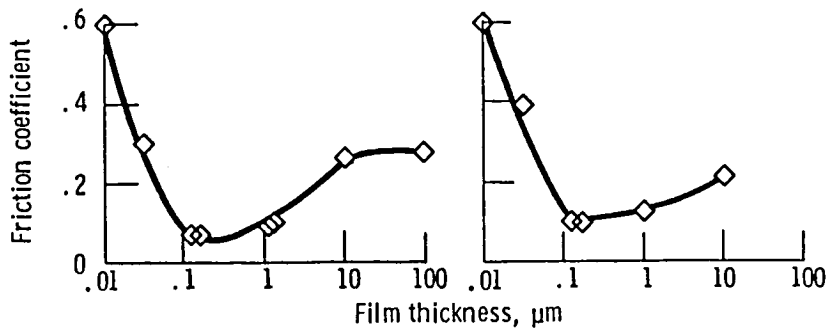

(a) Lead film. (b) Gold film.

Figure 15. - Variation of friction coefficient with film thickness.

ROLE OF CHEMICAL VAPOR DEPOSITION IN PROVIDING WEAR RESISTANT FILMS

H. E. Hintermann
Laboratoire Suisse de Recherches
Neuchatel, Switzerland

Oral presentation only.

SPUTTERING AS A TECHNIQUE FOR APPLYING TRIBOLOGICAL COATINGS

S. Ramalingam
University of Minnesota
Minneapolis, Minnesota

Friction and wear induced mechanical failures may be controlled to extend the life of tribological components through the interposition of selected solid materials between contacting surfaces. Thin solid films of soft and hard materials are appropriate to lower friction and enhance the wear resistance of precision tribo-elements. Thin film coating technologies that have been developed may be used to interpose thin solid layers between contacting surfaces to reduce friction or to extend wear life. Film deposition technologies developed include chemical vapor deposition (CVD) and physical vapor deposition (PVD).

Sputter coating is a PVD process for thin film deposition. It allows close control of coating thickness and composition and is well-suited for the deposition of tribological coatings. In this paper, the utility of magnetron sputtering for the deposition of tribological coatings is examined. Experimental results obtained when coated bodies are tested under a number of tribological operating conditions are presented. It is shown that when film adhesion problems are resolved, sputtering can be an effective means of depositing tribological coatings.

INTRODUCTION

A variety of electrically assisted, thin film deposition techniques have been developed in the last few years to deposit tribological coatings. They include ion plating, activated reactive evaporation, DC and RF sputtering, magnetron sputtering, arc coating, coating with high current plasma discharge, etc. Vapor species produced by thermal evaporation or ion bombardment are used in these processes to obtain thin coats of soft and hard materials. Coatings of virtually all of the known hard materials, soft metals, and a number of non-equilibrium materials can be produced with one or another of the electrically assisted film deposition techniques. When coatings of compounds are needed, the vapor species produced may also be reacted with process gases to concurrently synthesize and deposit needed materials.

Sputtering and magnetron sputtering are among PVD coating processes with potential for tribological applications. They are electrically-assisted, vacuum coating processes. They may be described briefly as follows. When a high DC voltage is applied to a cathode within a chamber maintained at low pressures, electrons emitted from the cathode ionize the gaseous atoms in the environment. Self-sustaining glow discharge can be obtained in such an arrangement by adjusting the chamber pressure and the applied voltage. The positive ions produced in the glow discharge, impinge on the cathode and displace the cathode atoms. The sputtered atoms diffuse through the gaseous environment and are deposited on the substrate to be coated. Over a period of time, thin films are produced. When

insulating material coatings are to be produced, radio frequency power supplies are used. Common arrangements for **DC and RF Sputtering** are shown in Figure 1.

In sputtering, the coating rates obtained depend on mass and energy of ions impinging on the cathode; target to substrate distance; sputtering gas; sputtering pressure; cathode surface condition; cathode geometry and dimensions; shielding; and target materials. Under commonly used coating conditions, the coating rates obtained are a few nanometers per minute.

Sputter coating depends on a momentum tranfer process at the cathode. Sputtered species have velocities nearly an order of magnitude larger than those produced by thermal evaporation. Good film-to-substrate adhesion can, hence, be obtained on well-cleaned substrates without much difficulty. At common operating pressures, since multiple collision occurs in the deposition ambient, coating is not a line-of-sight process. Good step coverage and coating uniformity are, hence, possible. Suitable fixturing and drive assemblies permit a wide range of complex component surfaces to be coated uniformly. Multi-cathode coating systems allow sequential coating of several layers without breaking the vacuum. This enables well-bonded, multi-layer, tribological coatings to be produced.

MAGNETRON SPUTTERING

To obtain higher coating rates than those possible with conventional DC and RF sputtering, and to coat at lower system pressures, magnetron sputtering may be used. In magnetron sputtering, crossed electric and magnetic fields are used to increase the ionization efficiency of the sputtering system. The magnetic field superposed on the electric field generates an efficient electron trap. The formation of intense glow discharge plasmas confined to the vicinity of the cathode is the result. It allows the plasma to be supported at low voltages and low pressures. "Cold sputtering" at high rates in a good vacuum is facilitated. Apart from the magnetron head, the magnetron sputtering system is identical to the conventional DC sputtering system illustrated in Figure 1.

At the operating pressures normally used, magnetron sputtering is a line-of-sight coating process. Deposition rates of several hundred nanometers per minute are obtained when the cathode power dissipation is several kilowatts.

With the use of appropriately designed anodes and floated substrates, thermal loading on the substrate is minimized during magnetron sputtering. Experimental studies (1) of temperature rise during high rate sputtering show that nearly half of the thermal loading during coating is due to condensation of the coating flux on the substrate coated. The remainder is accounted for by the kinetic energy of ionized species arriving at the substrate. In the case of aluminum sputtering, the mean energy of the coating species has been estimated and found to be several times the binding energy (1). Similar values may be expected to hold for magnetron sputtering of other materials. The high energy of the coating flux and the use of good vacuum are responsible for the well bonded films produced with magnetron sputtering.

Partial replacement of the sputtering gas with a reactive gas enables reactive sputtering to produce coatings of compounds. With commercial purity titanium targets, thin TiN films suitable for tribological applications have been successfully deposited (2-4). Both DC and RF sputtered TiN coats have been produced.

In the present work, magnetron sputtering has been used to deposit tribological coatings. The coating conditions employed and the tribological characteristics of films deposited are described in the following sections.

DESCRIPTION OF THE COATING SYSTEM AND THE COATING CONDITIONS USED

The coating system used consisted of four principal subsystems. The subsystems of the coating plant were: a vacuum plant, a high rate sputtering head, a sputtering atmosphere control system, and a power supply. It was designed to facilitate metallic coating at high rates as well as coating of hard material compounds such as TiN.

The vacuum plant used was a modified commercial CVC 14" vacuum system. A vacuum chamber defined by a 12 inch diameter by 12 inch high aluminum cylinder, a top plate, and a base plate was used. The vacuum chamber can be evacuated to pressures less than 10^{-5} torr with a diffusion pump. The system was equipped with a gate valve and roughing valves for vacuum sequencing and to control ambient pressure during sputtering. Dynamic pumping practice was employed to sweep contaminants and desorbed species. The top plate of the vacuum chamber carried the sputtering head and was electrically insulated from it with an insulator ring. It also carried a sputtering pressure monitoring gage, a shutter control, and a gas inlet.

To produce golden yellow TiN by magnetron sputtering,the system was operated at high cathode current densities, low pressures, and high voltages. In course of this work, it has been found that TiN films are best produced with this system at the following operating conditions:

System voltage:	925 to 950 V
Cathode:	1000 to 1200 ma
System pressure:	0.50 to 2.50 millitorr
Substrate-cathode distance:	4.5 to 6 cm
Argon flow rate:	2 SCCM
Nitrogen flow rate:	2.5 SCCM
Magnetron field strength on the cathode surface (central pole):	1200 Gauss
Cathode diameter:	5 cm

CHARACTERIZATION OF THE COATINGS PRODUCED

Micro-hardness measurements and x-ray diffraction techniques were used to characterize coatings deposited. Micro-hardness measurements on taper-sectioned test samples showed that coatings with hardnesses greater than H_v 2000 can be routinely produced by reactive sputtering. Titanium nitride, a defect compound, can possess a range of stoichiometries. Distinct colors are associated with specific ranges of stoichiometry, golden yellow being that of the perfect compound. This was obtained routinely.

Since, in sputtering, non-equilibrium structures are usually produced and the films deposited are under stress, x-ray analysis is not an unambiguous indicator of film stoichiometry. Additional x-ray analysis problems are introduced by preferred

texture in coatings. Despite these difficulties, x-ray analysis shows that the films produced are titanium nitride compounds. Expected x-ray peaks and those observed are in agreement. Supporting evidence is provided by microhardness measurement and film color.

TRIBOLOGICAL EVALUATION OF COATINGS PRODUCED

The tribological contact conditions encountered in engineering practice span a broad range. High contact stress, low speed sliding contacts as well as high speed, low stress contacts are common. More severe contact conditions are encountered in Hertzian contacts with non-zero slide-roll ratios. It is neither possible nor feasible to evaluate coatings produced at each combination of contact stress, relative velocity and contact type, i.e., sliding, rolling, and rolling with different slide-roll ratios, etc., encountered in practice. Three types of representative tests were hence chosen and used to evaluate the coatings produced. Two of these are sliding contact tests, LFW-1 and LFW-6 tests at high and low contact stress, respectively. The rolling contact tests carried out used a special rig which allowed the slide-roll ratio to be varied during the tests.

To assess tribological properties in high stress, low speed tests, a Faville-LaValley alpha model LFW-1 test machine was used. The test machine was calibrated following ASTM test procedures (5), and the tests themselves were conducted with a procedure similar to that used for calibration. All tests were carried out at a sliding speed of 0.13 $m \cdot s^{-1}$ with an unformulated paraffin-based mineral oil of viscosity 26 x 10^{-6} $m^2 \cdot s^{-1}$ at a bath temperature of 43°C and AISI 52100 test rings hardened to 60 R_C with an r.m.s. surface finish of 0.4 microns. The tests were 5000 revolutions of test ring in duration with a sliding distance of 550 m. The test loads used were selected to yield an initial Hertzian contact stress of 60% of the estimated yield strength of the substrate material. From calculations and observations of friction and wear, the elastohydrodynamic lubrication load-carrying component in the film was found to be insignificant. A new ring and fresh oil were used in each LFW-1 test.

For low contact stress, high speed tests, a sliding thrust washer assembly similar to that used in Faville-LaValley LFW-6 tribo-tester was employed. The test sample configuration is that of an annulus rotating on a flat. Since early tests indicated that the coatings can withstand high PV products, a contact pressure of 500 psi (3.4 MPa) and a test speed of 1800 rpm (PV product = 250,000 $psi\text{-}ft.min^{-1}$ = 9.5 MPa - $m \cdot s^{-1}$) were used. Either n-hexadecane or an unformulated mineral oil, same as that used in LFW-1 tests, was used. With either of these fluids, uncoated test samples of fully hardened T-15 high speed steel and M-50 HSS failed instantaneously under the test conditions used. Tests lasting five minutes at the specified test conditions were hence taken to indicate successful coating. Sample bulk temperatures during tests were monitored with a type K thermocouple and temperature rise of 100°C or more is common in the five minutes of tests.

A specially constructed concentrated contact simulator was used to assess traction characteristics in rolling contact tests. The test system used is described in a previous publication (3). Typically, AISI 52100 discs and rollers were used with TiN coating to assess traction characteristics as a function of the slide-roll ratio. Some test samples with duplex coatings were also used (a soft coat overlay on TiN coats). Test procedures are also described elsewhere (3).

SUMMARY OF TEST RESULTS

Since low carbon steels, cast irons, and aluminum alloys are among materials commonly used for machine construction, test samples of mild steel (SAE 1018), a gray cast iron (grade 20), and wrought aluminum alloys (2024 and 6061) were TiN coated and tested. LFW-1 tests were also carried out on two additional non-ferrous alloys, a cast magnesium alloy and Ti-6Al-4V alloy, to determine the utility of TiN coating for reduction of wear of these alloys. These non-ferrous alloys are prone to severe galling in normal sliding contacts.

The specific test conditions used and the test results obtained from LFW-1 tests are shown in Tables 1 to 4. In every instance, hardened AISI 52100 steel rings were used as counterfaces. As may be seen from the data presented, thin coats of TiN afford wear rate reductions of approximately two orders of magnitude. It is seen that films, as small as 2 micrometers in thickness, are sufficient to bestow significant wear protection.

To further illustrate the significant wear rate reduction obtained with thin films of TiN, the profiles of the wear scars produced during LFW-1 tests were recorded. Some representative data are reproduced in Figure 2. Unambiguous and striking improvement in wear resistance due to the presence of thin layers of TiN is evident. Test results from Faville-6 sliding contact tests are summarized in Table 5. While severe surface distress and large increases in friction were found to occur immediately following contact in tests with fully hardened but uncoated high speed steel samples, TiN coated samples of ferrous alloys and non-ferrous alloys survived the five minute test duration. The tests were terminated following five minutes of contact solely because of the significant temperature rise that accompanies prolonged, loaded contact at high speeds (500 ft/min; 2.5 m/s). It should be recognized that neither n-hexadecane nor the unformulated mineral oil used in the test are "lubricants" under test conditions used. Moreover, the test conditions selected are particularly severe with PV products of 250,000 psi - $ft.min^{-1}$ (9.5 MPa - $m.s^{-1}$).

In the 500 psi, 500 $ft.min^{-1}$, Faville-6 tests, both the contacting surfaces are coated. Thus, the contact is between TiN and TiN. Friction and wear processes that accompany the Faville-6 tests are those between two "ceramics" or refractory material compounds. Severe wear is not expected, and the results may be compared with alumina-on-alumina sliding contact tests where very little wear is usually found to occur. The substantial free energy of formation, -66.1 kCal/mole (6), of titanium nitride affords significant thermodynamic stability to the coated body. Corrosive wear can, therefore, be expected only at moderately high contact temperatures (of the order of 1000 - 1200°F or more). Contact surface is, hence, only expected to exhibit "burnishing" as a consequence of severe sliding contact. It was observed.

In the case of cast irons containing flake graphite, adhesion between the TiN film and the graphite phase can be a problem. The SEM micrographs from both the LFW-1 and the Faville-6 tests showed small scale debonding at graphite flakes. Despite this, test results were satisfactory. In passing, it is noted that whenever nodular cast irons with massive graphite nodules are hard-coated, there is likely to be large scale film failure. Hard coating of such materials is, hence, not preferred.

Representative test results obtained from roller-on-disc traction tests are presented in Figure 3. When TiN coated rollers are tested against TiN coated discs, although the contact stress (mean Hertzian stress) was 1 GPa and the traction coefficient in excess of 0.2 at a slide-roll ratio greater than 0.04, film failure was not observed. The test result suggests that bonding strengths, i.e., film-to-substrate adhesion strengths, will have to be in excess of 0.2 GPa for film survival. Well-bonded films are thus seen to be possible even on hardened steels. Concentrated contact tests were also carried out on TiN coated cast iron, AISI 1018, and AISI 4340. The conditions were: peak Hertz pressure 620 MPa, pure rolling at 2 m/s, and mineral oil at 43°C. Microscopic debonding was observed. With cast iron, major debonding was at the graphite flakes as expected. In the case of unhardened steels, debonding was the result of substrate collapse.

A BRIEF SUMMARY OF OTHER RESULTS

To assess if TiN coatings are feasible for use in piston ring applications where normally sprayed of chromium, molybdenum, etc., are used, preliminary coating trials have been carried out. Automotive rings of ductile iron were coated with TiN. Twist bend tests for film adhesion and fatigue tests carried out on coated rings showed that, as expected, films deposited do not bond well to the graphite nodules. Film debonding was initiated at these specific sites. Fatigue tests, on 109.22 mm diameter piston rings with 4.470 mm x 3.124 mm cross section coated with a thin layer of TiN, also showed film debonding at graphite nodule sites (50 mm fatigue displacement, unidirectional strain, 6.5 cycles/min). Observation was after 99700 cycles. It would, hence, appear that TiN coating for rings will require substrate material change. Since piston rings normally operate at contact pressures of the order of 50 psi, it should be possible to use steel rings with TiN coatings for such applications.

Solid lubricant coatings can be beneficial for friction reduction and to assist run-in process. To assess frictional and durabilitiy characteristics of solid lubricant coatings, Faville-6 thrust washer tests were carried out. Test samples were coated with a thin film of a $WeSe_2$-In-Ga alloy (commercial designation: Westinghouse Compact). Since solid lubricant films will eventually wear away in the absence of a source for replenishment, tests were carried out with a duplex coating to protect the surface following loss of soft coat, i.e., with a hard coat and a soft coat overlay. Test results obtained are presented in Figure 4. Both tests were carried out at a nominal contact pressure of 90 psi at 70 rpm.

It can be seen that duplex coated test samples in pure sliding yield frictional tractions as low as 0.06. This friction coefficient is comparable to that obtainable with (nearly) full hydrodynamic lubrication at low speeds. As may be seen from Figure 4B, satisfactory durability is attainable, at least at low contact speeds.

Results obtained in rolling contact traction tests with MoS_2 and WSe_2-In-Ga alloy are shown in Figure 5. It is recognized that tungsten diselenide is a good solid lubricant, comparable to well-established MoS_2 coatings. Scanning electron micrographic studies carried out showed that sputtered coatings are well bonded and are not easily worn away as long as the slide-roll ratio is close to or equal to zero. SEM studies also showed that at slide-roll ratios greater than 0.04, there can be substantial film loss.

The results obtained suggest that in machinery applications, soft coats are suitable provided that in sliding contacts, large life and durability are not required and contact stresses are low. These are the conditions experienced during run-in. It would thus appear that solid lubricant films may be suitable to assist run-in. In hertzian contacts, soft coat films are useful, if slide roll ratio is close to zero. This condition is experienced in many mechanical systems. Further tests and evaluation are needed to assess suitability of soft coats for such applications.

DISCUSSION

In this work, sputtered films interposed between sliding surfaces are shown to yield improved tribological characteristics. Thin hard coats improve wear resistance, while soft coats lower friction. The coating materials, coating thicknesses, and the film deposition process used in this work are somewhat arbitrary. Although technological benefits have been demonstrated, it is clear that a sound physical basis will have to be established to assist the choice of coating materials, processes, and parameters before thin film deposition techniques can be used with confidence in routine commercial practice. These issues will now be examined.

The first and foremost requirement for the use of thin film techniques in tribology is that the films deposited be well bonded to the substrate. To assure this, it should be possible to quantitatively measure the film-to-substrate bond or adhesion strength. This measurement technique will also enable the development of substrate cleaning procedures to reproducibly obtain well bonded thin film deposits.

A test method has recently been developed (7) to meet this requirement. In this test, the film is deposited over a finite region on one surface of a strip-like test sample, and the composite test sample, Figure 6, is stressed. When the film is well bonded, film and the substrate experience the same strain. However, as the film and the substrate differ in elastic properties, stressing the composite leads to the generation of a shear stress at the film-to-substrate interface. The magnitude of the shear stress generated is maximum at the longitudinal end of the film, and is a function of the material properties and test sample dimensions. By subjecting the test sample to progressively increasing applied stress, the interfacial stress can be raised till it exceeds the film-to-substrate adhesion strength and debonds the film. The adhesion of the film deposited can therefore be measured quantitatively.

With this test, Ting (7) has shown that titanium nitride films can be deposited on stainless steel strips with adhesion strengths in excess of 1 GPa when reactive magnetron sputter coating techniques are used for film deposition. It has also been shown that sputter cleaning prior to film deposition yields higher adhesion strengths than chemical cleaning procedures normally used. Hard coats of titanium nitride deposited with reactive magnetron sputtering process are, hence, able to provide improved wear resistance despite high contact stresses as in Hertzian contact with a non-zero slide-roll ratio, since the bond strength obtained is quite high.

When soft coats are used, wear of the soft film and debonding can both lead to film failure. Adhesion tests of soft coats have not been carried out. The LFW-6 sliding contact tests carried out indicate that at low contact stresses soft coats

can be retained on the contact surface. The tribological performance of the coated body then depends on the wear characteristics of the soft film deposited. As the worn film cannot be replenished in most instances, unless suitable provisions are made for film material replenishment, limits on tribological life should always be expected. The rolling contact tests carried out show that although film loss is not a serious problem in pure rolling contact, film loss occurs when the slide-roll ratio differs from zero. The performance of the sputtered films in rolling contact is better than that of burnished films, and this is probably due to a more complete coverage of the coated body possible with thin film deposition. Even with better coverage, limited life must be expected with soft coats.

Sputtering techniques have been shown to yield well bonded films. It is known that the graded interfaces produced at elevated temperatures inherent to CVD can also yield well bonded coatings suitable for tribological applications. The specific advantage offered by sputtering in comparison is the low film deposition temperature. No subsequent thermal treatment is needed as is the case with CVD when ferrous parts are coated. Moreover, precipitation hardened, lightweight non-ferrous alloys such as the aluminum alloys cannot be CVD hard coated. Absence of the need for elevated processing temperature, hence, make the PVD sputtering techniques a more flexible surface treatment process.

It is further known that when film deposition is carried out at intermediate and elevated temperatures, columnar and/or equiaxed film grain structures result. The surface finish accompanying coating under these conditions is poor due to hetrogeneous nucleation and growth. Coated bodies require refinishing to restore surface finish. Higher as-coated film thickness is then needed to allow for refinishing. Moreover, refinishing is expensive, as diamond finishing techniques are called for. Sputter deposition at low temperatures does not degrade the surface finish and yields adequate adhesion strength. Hence, sputter coating can be a powerful, finishing surface treatment for tribological components.

To improve wear life of parts, it is customary in tribological practice to raise the part hardness, H_p. As wear is a surface process, increasing the surface hardness is sufficient, and a great number of surface hardening processes are, hence, routinely used. Since both adhesive and abrasive wear theories suggest that the wear rate is inversely proportional to part hardness, raising the surface hardness to offset the wear problem is a theoretically defensible concept.

From the work of Kruschov (8), Richardson (9), etc., it is known that to significantly lower wear rates, the ratio of H_c/H_p, where H_c is the counterface hardness, will have to be less than one. At H_c/H_p ratios of 0.4 to 0.6, wear rate is negligibly small. As the counterface hardnesses, H_c, rarely exceed Vicker's hardness of 800 or so when they are made from ferrous alloys, raising the part hardness to Vicker's hardness of 1600 or more can make the part wear rate negligibly small in most instances. An enormous number of hard oxides, nitrides, carbides, silicides, borides, etc., possess inherent hardnesses in excess of Vicker's hardness 1500. The deposition of such materials can, therefore, be expected to lead to negligibly small wear rates. When wear rate is negligible, thick hard surface layers are not necessary. Well bonded thin films are sufficient, and this is precisely what sputtering techniques offer.

The thermal expansion coefficient, α, of hard metal compounds are lower than those of common engineering alloys. When ferrous parts are coated with hard materials at elevated temperatures, as in CVD, and processed to obtain martensitic structure, the accompanying specific volume change induces large tensile stresses

within the coatings. Cracking of the coating is common. Methods have been devised to render the crack pattern visible (10). Sputter coating allows pre-hardened parts to be coated. Moreover, the coating thicknesses are lower. Hence, residual stresses in the sputter coated parts with thin film coats are a lesser problem.

Residual stress considerations suggest that the $E\alpha$ product, where E is the Young's modulus, is a significant parameter in the choice of coating materials. Materials possessing $E\alpha$ products that more nearly match those of the substrate are the preferred choice. Such materials also induce lower film-substrate interfacial shear stresses during tribological operation, since the differential thermal strains induced by frictional power dissipation can be expected to be smaller. To more effectively transport the heat generated, film materials possessing larger thermal conductivities are more appropriate. Thinner films are, hence, particularly desirable to lower the propensity for film failure due to thermal stresses during sliding contact operation.

In severely loaded contacts, i.e., contacts with high PV products, power dissipation is directly proportional to the prevailing friction coefficient. Rapid transport of the dissipated energy from the contact interface requires low thermal resistance between the dissipation source and sink. Thin films or refractory metal compounds, that is ceramics, over metallic substrates is clearly more efficient in this regard than bulk ceramics with much greater thermal resistance. Even with the use of ceramic-metal composites, large interface temperatures are possible when the tribo-system is operated under severe contact conditions. At the associated high interface temperatures, tribo-chemical reactions can become severe leading to tribo-chemical or corrosive wear. This would suggest that in a choice among several coating materials for a given application, coating material with the highest thermodynamic stability is preferred for the most severe contact conditions.

In the case of hard metal compounds, it is known that, in general, oxides are thermodynamically more stable than nitrides, which in turn are more stable than carbides. Based primarily on this, nitrides are preferred over carbides, and oxides are preferred over nitrides.

The factors guiding the selection of coating material and coating thickness may now be summarized as follows. The choice of the coating material depends on the specific tribological function of the coating. Soft material and layer lattice solid coatings are appropriate to reduce friction. Life limits should be foreseen for soft coated tribo elements. Soft coats commonly used range between about 50 and 1000 nm in thickness. Despite recent theoretical analysis (11), optimum film thickness for minimum friction with a soft material coating is not yet known. Where wear resistance is the primary requirement, hard metal compound coatings are appropriate. As a very large number of materials can meet this requirement, it is appropriate to narrow the choice by considering other relevant physical properties. They are the Young's modulus, coefficient of thermal expansion, thermal conductivity, and thermal stability. Material that most nearly matches the E product of the substrate and which has the highest thermal conductivity and thermodynamic stability is the preferred choice. A sound basis for the selection of optimal coating thickness remains to be established.

Inherently hard materials may be visualized as Griffith solids. In small diameter fiber and thin film forms, Griffith solids may be expected to possess high fracture stress and fracture elongation. When continuous hard material films are deposited with techniques relying on assembly of material in the atomistic scale, the probability of geometric flaws is low in film deposition, and the film is likely

to behave as a Griffith solid. Even the roughness of engineering surface is unlikely to yield stress concentration in films.

To see this, consider an engineering surface with an RMS surface finish σ. The expected peak to valley dimension in the rough surface is 6σ. Profilometric measurements suggest that peak radii in such surfaces are typically 2 orders of magnitude higher. When a continuous film is laid over such a surface, the peaks are unlikely to represent geometric flaws as the effective $(c/\rho) = 6\sigma/100\sigma)$ is low. Hence, as long as the coating process does not produce flaws, surface finish is unlikely to act as a flaw.

When peak to valley dimensions are 6σ, to assure complete coverage and the production of a continuous film, a coating thickness of 6σ is appropriate in line-of-sight coating processes in order to avoid shadow effects. When extended coating sources are used, a thickness perhaps half this can be sufficient. On this basis, one may estimate the reasonable, minimum hard coat thickness for wear resistance as several times, 2 to 5 times the RMS surface finish. For well finished surfaces, films a few 100 nm in thickness can be sufficient. If wear of the coated hard material determines tribological life, part life increase in proportion to coating thickness may be expected as reported in the literature. It would thus appear that hard coating films, 1 to 10 micrometer in thickness, can be sufficient to significantly improve wear life.

Considerations connected with the coating process and quality control also influence the choice of coating materials in hard coating. As titanium is an efficient getter and nitrogen pumping is relatively efficient compared to hydrogen pumping, TiN coating for wear resistance yields several process advantages when vacuum techniques are used. The distinct color associated with stoichiometric TiN is another specific advantage as the production of stoichiometric coatings can be verified by optical (visual) means.

SUMMARY

Tribological characteristics of thin hard coats laid on a variety of ferrous and non-ferrous substrates have been tested. The thin hard coats used were titanium nitride films deposited by reactive magnetron sputtering of metallic titanium. High contact stress, low speed tests show wear rate reductions of one or more magnitude, even with films only a few micrometers in thickness. Low contact stress, high speed tests carried out under rather severe test conditions show that thin films of TiN afford significant friction reduction and wear protection. Thin hard coats are also suitable to improve the friction and wear performance of rolling contacts. Satisfactory film-to-substrate bind strengths can be obtained with reactive magnetron sputtering.

ACKNOWLEDGEMENTS

The author thanks S. Bair, Y. Shimazaki, and B.-Y. Ting for experimental assistance. Most of the results reported here were obtained in course of a collaborative research program witih Professor Ward O. Winer. The author is indebted to Professor Winer for his contributions.

REFERENCES

1. Hieronymi, R., et al., Thin Solid Films, 96, 1982, p. 241.

2. Bair, S., et al., Wear, 60, 1980, p. 413.

3. Ramalingam, S., et al., Thin Solid Films, 84, 1981, p. 272.

4. Ramalingam, S. and W. O. Winer, Thin Solid Films, 73, 1980, p. 267.

5. ASTM Standard D2714-68, Am. Soc. Test. Mat., Philadelphia, Pennsylvania, 1968 (reapproved 1978).

6. Weast, R. C. (editor), Handbook of Chemistry & Physics, 52nd Edition, Chem. Rubber Co., Cleveland, Ohio, 1971, p. D-71.

7. Ting, B. Y., M.S. Thesis, Georgia Institute of Technology, August, 1983.

8. Kruschov, M. M., Wear, 28, 1974, p. 69.

9. Richardson, R. C. D., Wear, 11, 1968, p. 245.

10. Gass, H. and H. E. Hintermann, Proc. 4th International Conference on CVD, The Electrochemical Society, Princeton, NJ, 1973, p. 563.

11. Heilman, P. and D. A. Rigney, Wear 72, 1981, p. 195.

TABLE 1: SUMMARY OF LFW-1 TESTS ON MILD STEEL BLOCKS

Block: AISI 1018 Mild Steel, Anneated.

Ring: AISI 52100 Hardened Steel, R_C = 62

	COATING THICKNESS (microns)			
	None	2.0	3.5	4.2
Load (kN m^{-1})	92.3	92.3	92.3	92.3
Hertz Pressure (MN m^{-2})	436.5	436.5	436.5	436.5
Coefficient of Friction[a]	.20/.16	.16/.14	.15/.15	.14/.13
Block Mass Loss (mg)	9.2	0.02	0.05	0.14
Ring Mass Loss (mg)	0.1	1.0	1.23	1.08
Block Wear Coefficient[b] K($x10^{-6}$)	32.5	0.26	0.64	1.79
Ring Wear Coefficient K($x10^{-6}$)	1.34	2.68	3.30	2.90
Sliding Distance (m)	110	550	550	550

a The coefficient of friction values quoted are the time-averaged values for the beginning and end of the tests.

b For coated specimens, a Vickers hardness of 2200 $kgmm^{-2}$ for TiN was used.

TABLE 2: SUMMARY OF LFW-1 TESTS ON CAST IRON BLOCKS

Block: Grade 20 Cast Iron, As Received
Ring: AISI 52100 Hardened Steel, R_C = 62

	COATING THICKNESS (microns)		
	None	2.0	4.2
LOAD (kN m^{-1})	122.7	122.7	122.7
HERTZ PRESSURE (MN m^{-2})	362.6	362.6	362.6
COEFFICIENT OF FRICTION[a]	.21/.25	.15/.12	.18/.15
BLOCK MASS LOSS (mg)	7.89	0.15	0.12
RING MASS[b] LOSS (mg)	-0.20	2.07	3.04
BLOCK WEAR COEFFICIENT[c] K($x10^{-6}$)	129.2	1.45	1.15
RING WEAR COEFFICIENT K($x10^{-6}$)	--	4.18	6.15
SLIDING DISTANCE (m)	16	550	550

a The coefficient of friction values quoted are the time-averaged values for the beginning and end of the tests.

b A negative loss indicates that the ring gained mass.

c For coated specimens, a Vickers hardness of 2200 $kgmm^{-2}$ for TiN was used.

TABLE 3: SUMMARY OF LFW-2 TESTS ON ALUMINUM

Block: Aluminum 6061-T651 Treatment
Ring: AISI 52100 Hardened Steel, R_c = 62

	COATING THICKNESS (microns)				
	None	2.1	2.5	3.8	4.2
LOAD (kN m^{-1})	63.0	63.0	63.0	63.0	63.0
HERTZ PRESSURE (MN m^{-2})	257.0	257.0	257.0	257.0	257.0
COEFFICIENT OF FRICTION[a]	.14/.16	.14/.13	.18/.14	.17/.13	.19/.13
BLOCK MASS LOSS (mg)	2.77	1.64	1.09	0.16	0.05
RING MASS LOSS (mg)	1.00	0.40	0.75	0.85	1.84
BLOCK WEAR COEFFICIENT[b] K($x10^{-6}$)	24.56	--[c]	19.98	3.01	0.94
RING WEAR COEFFICIENT K($x10^{-6}$)	19.65	3.15	2.95	3.34	7.24
SLIDING DISTANCE (m)	110	275	550	550	550

a The coefficient of friction values quoted are the time-averaged values for the beginning and end of the tests.

b For coated specimens, a Vickers hardness of 2200 $kgmm^{-2}$ for TiN was used.

c Mass loss is sum of TiN and Aluminum. Wear coefficient not calculated.

TABLE 4: SUMMARY OF LFW-1 TESTS ON ALUMINUM ALLOY

Block: 2024 Aluminum Alloy, T351 Condition
Ring: AISI 52100 Steel, Hardened to R_c 62

	UNCOATED	TiN COATED		
		1.0 M	3.6 M	4.5 M
LOAD (kN m^{-1})	63.0	63.0	63.0	63.0
HERTZ PRESSURE (MN m^{-2})	257.2	257.2	257.2	257.2
COEFFICIENT OF FRICTION[a]	.16/.18	.15/.16	.19/.16	.18/.16
BLOCK MASS LOSS (mg)	30	14.9	0.08	0.04
RING MASS LOSS (mg)[b]	-0.44	0.89	1.84	2.52
BLOCK WEAR COEFFICIENT K[c] ($x10^{-6}$)	102	--[d]	1.56	0.73
RING WEAR COEFFICIENT K($x10^{-6}$)	--	3.57	7.38	10.1
SLIDING DISTANCE (m)	330	550	530	550

a The coefficient of friction values quoted are the time-averaged values for the beginning and end of the tests.

b A negative loss indicates that the ring gained mass.

c For coated specimens, a Vickers hardness of 2200 $kgmm^{-2}$ for TiN was used.

d Mass loss is sum of TiN and Aluminum. Wear coefficient not calculated.

TABLE 5: SUMMARY OF TEST RESULTS LFW-6, THRUST WASHER TEST RESULTS

Contact Pressure:	500 psi	
Rotational Speed:	1,800 rpm (1.062" dia.)	
PV Product:	250,000 psi-ft/min	

Results:

Uncoated	Steel	M50	N2 Min.Oil[3]	Inst.Fail
	Steel	M50	N2 (400 psi)	Inst. Fail
	Steel	M50	Motor Oil[4]	5* Min.
TiN-Coated[2]	Aluminum	6061[1]	n-hexa dec.	9.5* Min.
	Aluminum	6061[1]	n-hexa dec.	7.5 Min.
	Mild Steel (AISI 1018)		Motor Oil	5* Min.
	Mild Steel (AISI 1018)		N-2 Oil	5* Min.
	Mild Steel (AISI 1018)		Mineral Oil[5]	5* Min.
	Cast Iron		Motor Oil	5* Min.
	Cast Iron		N-2 Oil	5* Min.
	Cast Iron		Mineral Oil	5* Min.

* Test terminated without failure.

1 Temper condition T651

2 Aluminum Sample No. 1 TiN Coating: 2.7 microns
Aluminum Sample No. 2 TiN Coating: 4.2 microns
Mild Steel and Cast Iron TiN Coating: 1.9 microns

3 N2 Min. Oil is R620-15 with 4.0% Polymer

4 SAE 10W-40 HD

5 Unformulated Paraffinic Mineral Oil

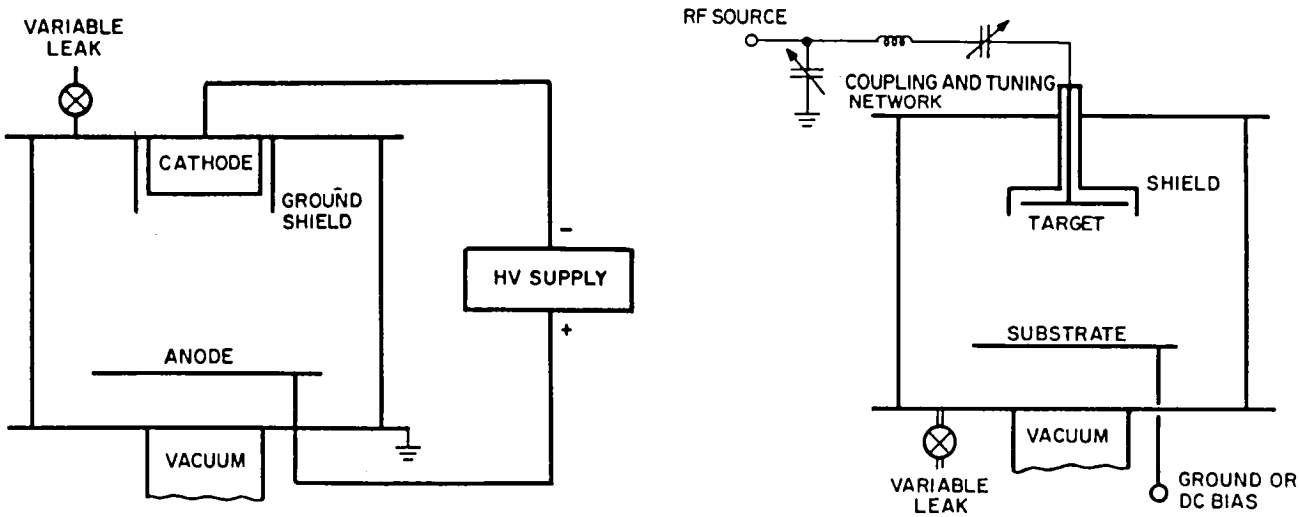

Figure 1. Schematic illustration of conventional DC and RF sputtering systems. Sample to be coated is placed on the anode.

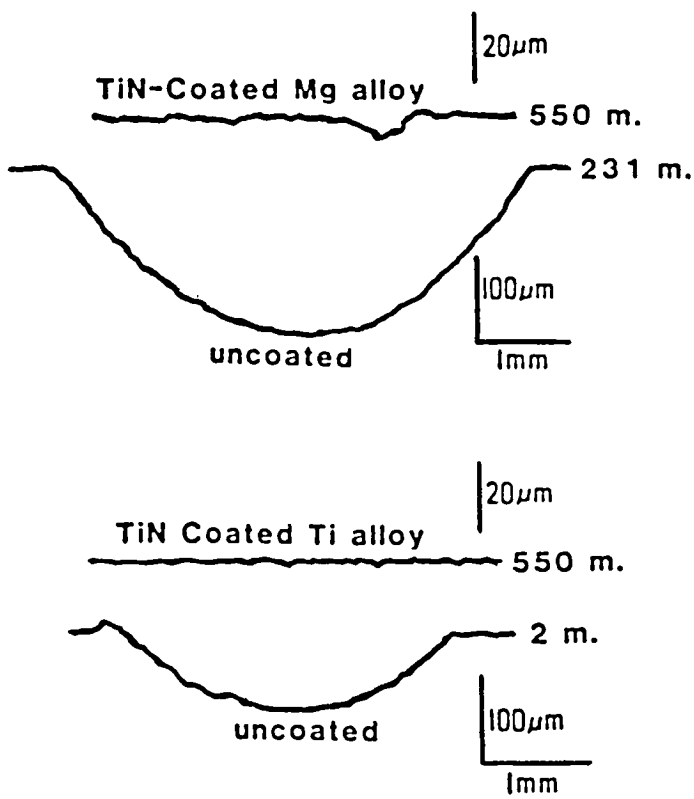

Figure 2. Wear scars produced in LFW-1 tests on test blocks without and with TiN coats. Note scales and sliding distances.

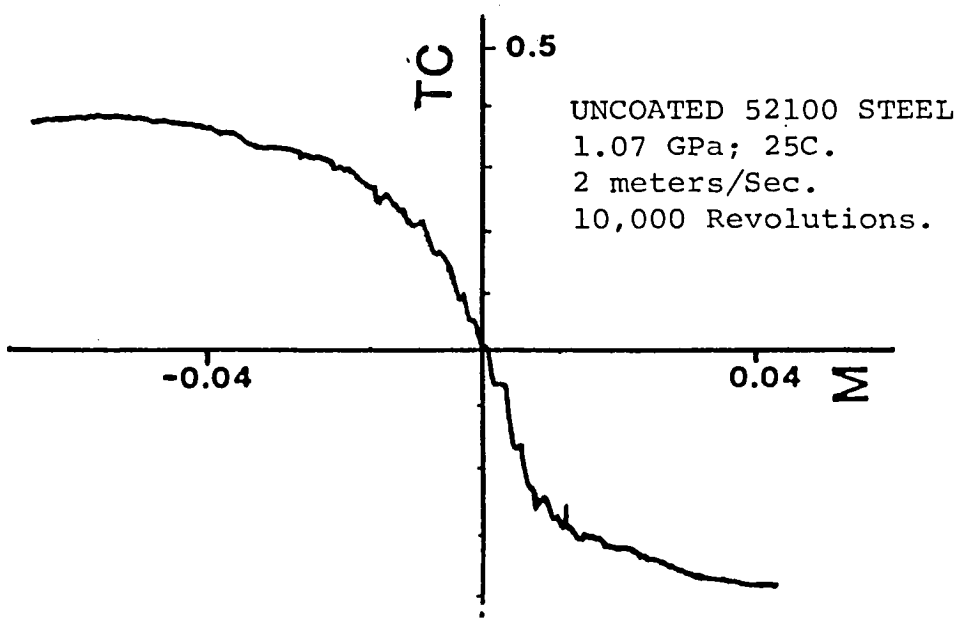

Figure 3. Representative test data from a rolling contact traction test. Traction coefficient TC is plotted against Slide-Roll ratio.

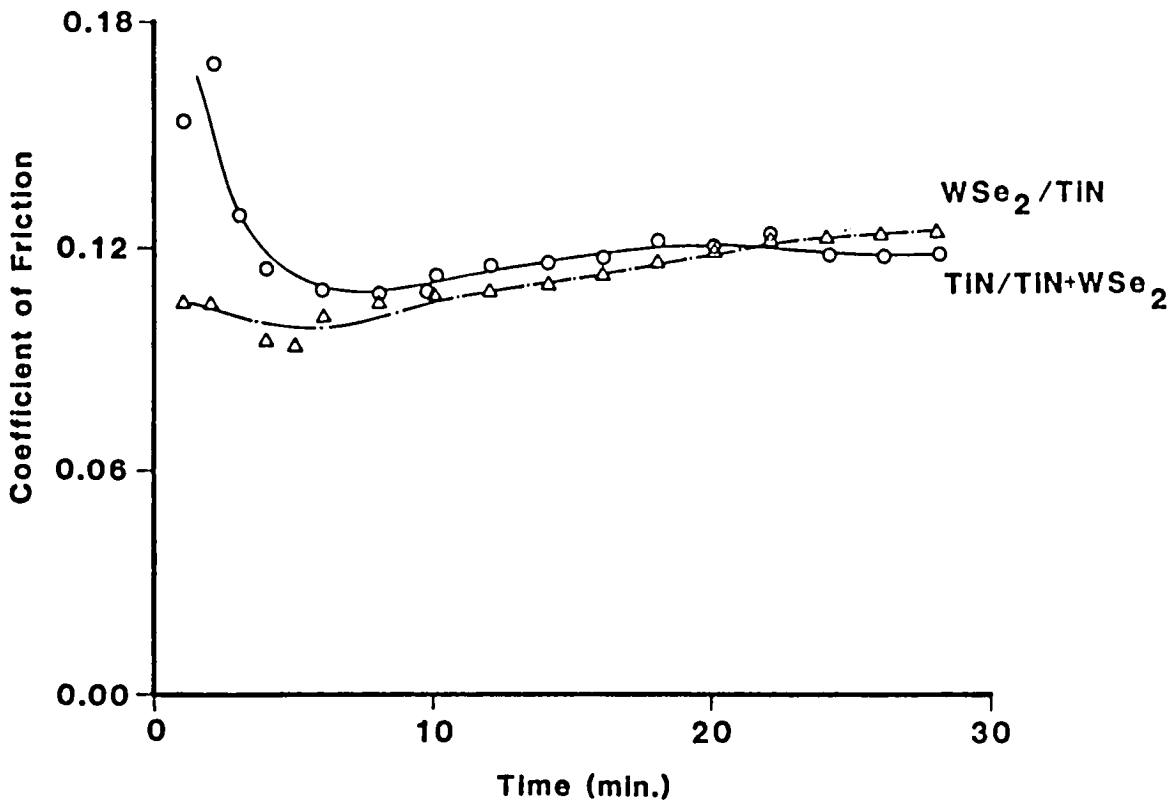

Figure 4 A. Friction Vs Time data from LFW-6 Tests at low contact stresses and sliding velocities. Hexadecane lubricant.

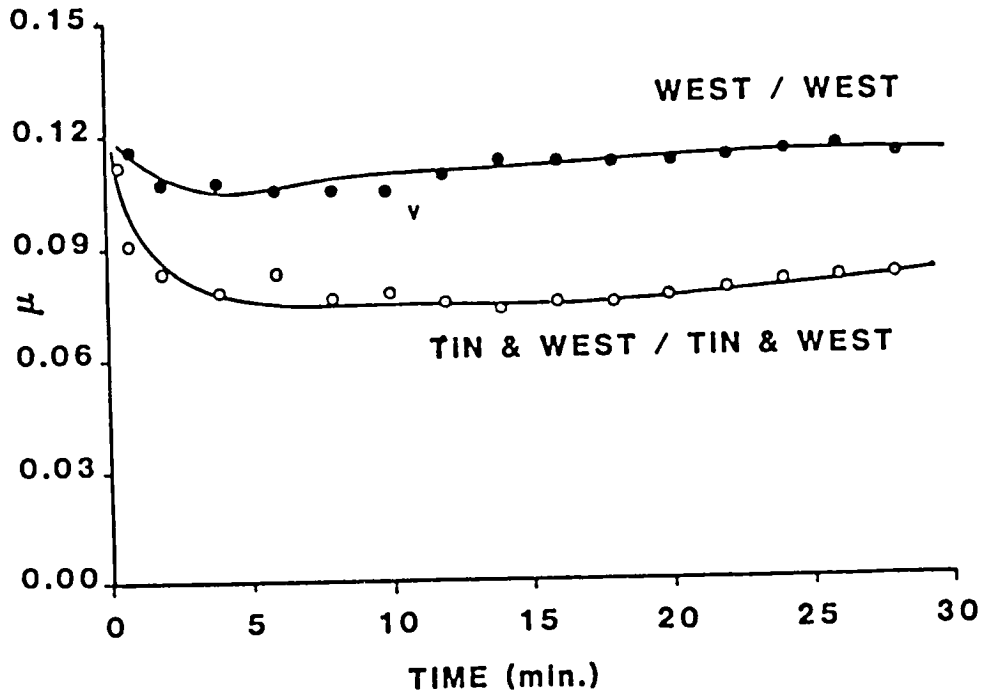

Figure 4 B. Friction Vs Time data from LFW-6 Tests. Data from soft coat and duplex coated test samples are presented.

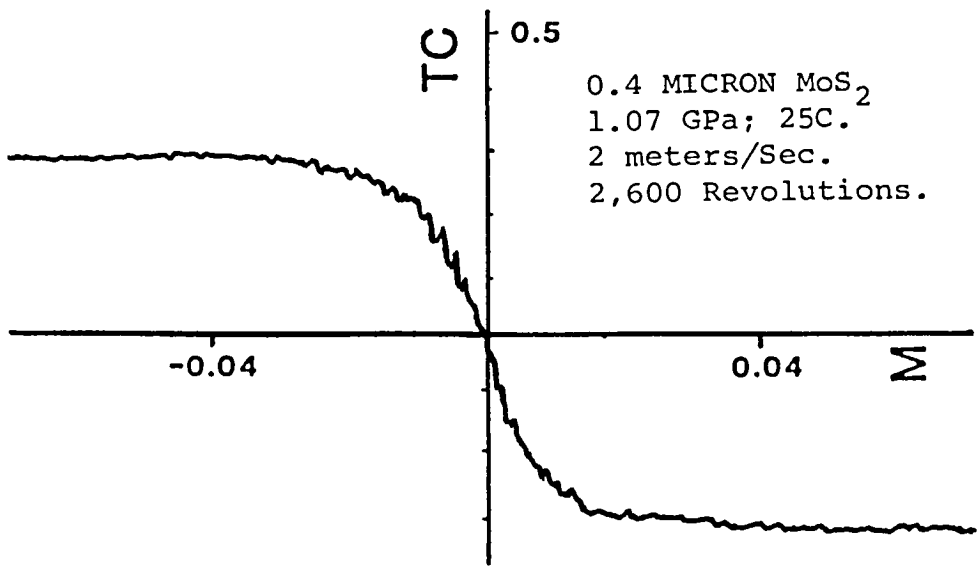

Figure 5 A. Traction Vs Slide-Roll ratio of a MoS_2 coated test sample. Contact conditions are as indicated. 'Dry' contact.

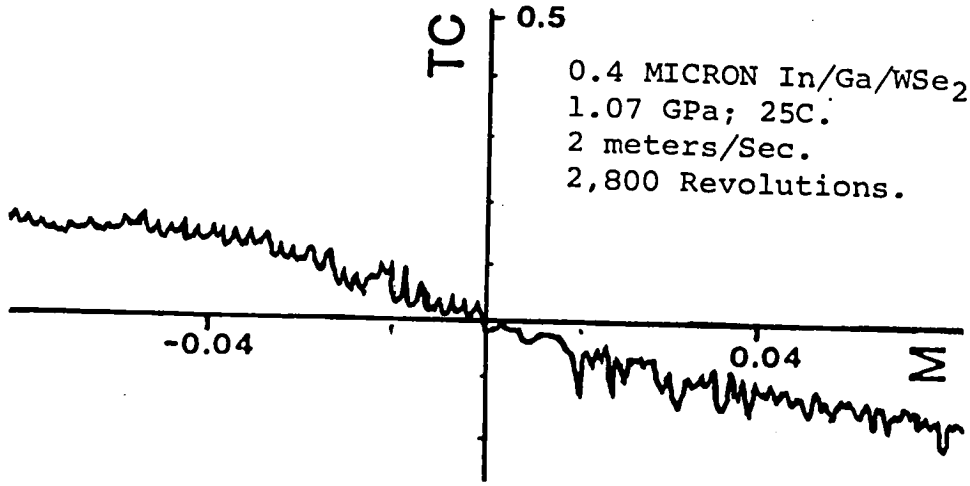

Figure 5 B. Traction Vs Slide-Roll ratio of a WSe_2 coated test sample. Test conditions are as indicated. 'Dry' rolling contact.

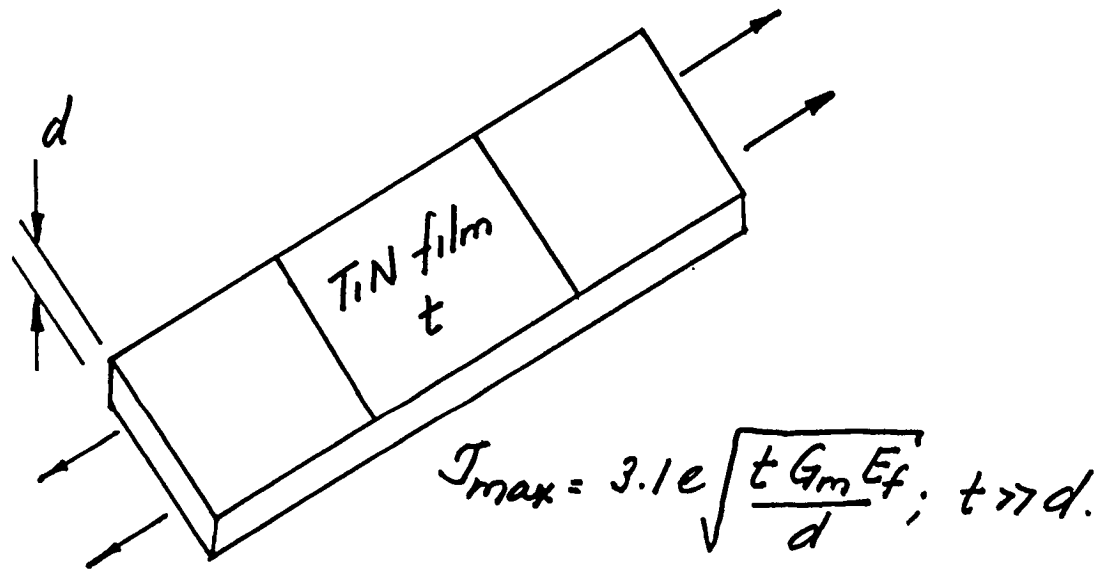

Figure 6. Schematic illustration of test sample configuration for film adhesion strength measurement. Maximum shear stress is at the longitidinal edge of the film. Applied strain is e. Subscripts m and f refer to matrix and film respectively.

STATUS OF UNDERSTANDING FOR BEARING MATERIALS

E. N. Bamberger
Aircraft Engine Business Group
General Electric Co.
Cincinnati, Ohio

The structural materials and potential failure modes for high technology aircraft gas turbine engine bearings are reviewed. It is shown that the sub-surface initiated rolling-contact fatigue failure mode is reasonably well understood and in most cases can be controlled by proper material selection and design. Current bearing materials provide long life and high reliability in existing applications. A new generation of materials are being developed which will provide improved fracture toughness, better corrosion resistance and a further extension of bearing fatigue life. Bearing problems due to surface distress, caused by a variety of surface and near surface anomalies, are less well understood. This area will require the implementation of an interdisciplinary effort to improve the level of understanding of metallic surface-lubricant reactions and interactions.

INTRODUCTION

The objective of this paper is to review the status of understanding for Bearing Materials. While at first glance this appears to be a relatively straightforward proposition, closer examination shows that the subject matter is far from simple, expecially when viewed in the context of this conference on Tribology.

To even begin to achieve a workable perspective, it is necessary to restrict the areas to be discussed, to limit the scope of those areas to be discussed and perhaps most importantly, to also look at those areas where the level of understanding is still relatively incomplete.

The subject of bearing materials obviously covers a lot of territory, encompassing a large and varied number of materials ranging from lead and babbitt to ceramics and diamonds. Because of this, a decision had to be made regarding which bearing material class or family on which to concentrate. In this paper the selection, not surprisingly, is that class of bearing materials used for mainshaft applications in aircraft gas turbine engines. These materials were selected because more than any other bearing materials, they have been the subject of substantial development efforts in the past three decades. The advent of the aircraft gas turbine engine created unprecedented needs for better materials and designs for rolling-element bearings in the engines of both subsonic and supersonic aircraft. These requirements included bearings capable of operating at increased temperatures, higher speeds and greater loads. Coupled with these requirements, and compounding the difficulty, was a continuously increasing thrust-to-weight

ratio in the engines which dictated the use of smaller and lighter bearings. Reliability of these bearings became a major consideration due not only to system and mission complexities, but also to the sizeable cost aspects involved. In response to such challenges, research and development performed by the bearing industry, engine manufacturers, and the Government have continued to provide improved bearing materials and manufacturing techniques to enhance bearing life and reliability. The selection of aircraft engine mainshaft bearings as the prime subject of discussion in this paper does not in any way infer that other high-technology bearing applications, such as those for satellite systems, space applications, nuclear reactor mechanisms, etc., are less important and/or critical. However, because the combination of severe environmental conditions, high loads, high speeds, high temperatures and the need for absolute reliability, the aircraft gas turbine engine main shaft bearing (materials and design) represents the leading edge of this technology and this paper will therefore deal with this class of bearings exclusively.

Another subject requiring some setting of limits for the purpose of this discussion is the mode of failure experienced in these bearings. All rolling element bearings have a number of competitive failure modes.(1)* Essentially, these can be grouped into the following categories:

Fatigue

Surface Distress

Corrosion

Miscellaneous

A typical fatigue spall is shown in Figure 1. Classical, sub-surface initiated fatigue is the most studied and generally the best understood failure mode in rolling element bearings. Yet when bearing failures are analyzed, a properly designed bearing, using the best available materials and processes, will rarely exhibit this failure mode. Conversely, if overload conditions are experienced or if inferior materials are used, fatigue failures will be encountered before other failure modes come into play. As an example, simulated or actual bearing life tests are usually run under very high loads to reduce the testing time; in these tests, nearly all of the failures are due to fatigue.

Consequently, that failure mode which is best understood and which is used to set the design life of the bearing is the least likely to be encountered in actual service. Over the years, it has been shown that less than 10% of all bearing failures are directly attributable to sub-surface initiated fatigue. In fairness, it should be noted that in the past, more resources have been devoted to the understanding and improvement of the sub-surface initiated mode of failure than to other bearing failure modes. Additionally, it can be postulated that until long life materials, such as VIM-VAR M-50, were available, surface distress-related problems were not as pressing because sub-surface initiated fatigue was the primary concern.

Some typical examples of the second failure mode, surface distress, are shown in Figures 2, 3 and 4. This failure mode represents the most prevalent operational failure mechanism in aircraft engine bearings, as well as in most other precision bearing applications. Surface distress is an umbrella term, covering a variety of

*Numbers in parentheses refer to references.

related failure modes. Micro-pitting, surface fatigue, scoring, debris damage, contamination, plastic deformation, smearing, and even process induced damage are all inherent in, or contribute to, surface distress. Statistically, this failure mode is seen in perhaps 70% of the operational bearing failures examined.

While bearing corrosion could be classed as a sub-category to surface distress, its impact on cost and logistics is such that it deserves a separate identity. Recent work at the Naval Air Research Facility (2) and the Air Force Wright Aeronautical Laboratories have shown that a substantial number of bearing rejections are due to the type of surface corrosion shown in Figure 5. In a recent paper (3), this subject was addressed in some detail, and it was pointed out that, while work has been done in the past on developing or utilizing more corrosion-resistant bearing alloys, the traditional approach has been to improve the bearing lubricant by the addition of corrosion-resistant additives. This approach has had a degree of success as evidenced by the data reported in Reference (4). However, to achieve a truly significant improvement in reducing bearing losses due to corrosion, it is essential to make the bearing material as impervious to corrosion as possible with current materials technology.

Both Government and industry recognize the seriousness of the corrosion problem, and there are presently a number of ongoing programs sponsored by DOD and NASA designed to develop a more corrosion-resistant material. While corrosion is a serious cost and logistics concern, the direct influence of corrosion on bearing failures per se is less well documented, although there is little doubt that if corrosion is permitted to occur on critical surfaces, such as raceways, the resultant pitting will precipitate spalling fatigue and, in the case of high DN bearings, more severe damage such as fracture can subsequently occur.

The last failure category, "Miscellaneous" covers a wide range of mostly mechanical, or handling problems which are unpredictable and statistically indeterminate. They constitute a small percentage of bearing failures although no amount of materials, design, or tribological expertise, will ever totally eradicate this failure mode. Because of the unpredictability of the "Miscellaneous" failure category and the fact that corrosion can be the subject of an entire separate conference, the emphasis in this "Status of Understanding" will therefore be restricted to the first two failure modes.

BEARING MATERIALS - FATIGUE/FRACTURE CONSIDERATIONS

Table I is a listing of typical materials used in aircraft mainshaft bearings. As can be seen, with few exceptions, iron base, low alloy steels either through-hardened or case carburized are predominant. Generally, current practice is to use through-hardened materials, although as will be discussed shortly, carburized materials are now attracting considerably more interest for mainshaft applications. The most commonly used material in the United States is AISI M-50, whereas European gas turbine engine manufacturers have traditionally used higher alloyed steels, such as 18-4-1 (T1). However, published data indicate little difference

between these two materials in terms of either rolling contact fatigue or fracture-toughness. (5,6,7)

The Cr-Mo-V high speed tool steel known as M-50 has been used since about 1957 and has logged literally millions of flight hours in U.S. commercial and military aircraft gas turbine engine bearings. M-50 is a rather remarkable material, having originally been developed as a wood-working tool steel (MV-1). However, in over two decades of evolutionary improvements, primarily in the processing of the material, it has maintained its superiority over competitive bearing alloys. This is shown in Figure 6. In a sense, the low failure rate of bearings due to sub-surface fatigue can be ascribed to the continuing improvements made in the M-50, as well as of course, improved design and analytical capabilities. For example, the widely used ASME Design Guide for Bearings (8) projects a material factor of six for M-50. In actual practice, this has proved to be a very conservative number. Operationally verified material life factors of 20-40 are the rule rather than the exception. Admittedly, since the issuance of the ASME document, further and significant improvements were made in the M-50 processing (VIM-VAR melting) as well as in bearing manufacturing techniques (controlled grain-flow, hardness and surface finish refinements). Still, the level of understanding of this material is high with extensive data available in the literature regarding types of and effects of carbide, carbide morphology, effects of residual gas contents, different melting, conversion and forging procedures, and so on. Much of this has been covered in Reference 3 and will not be repeated here. Efforts are still continuing toward improving M-50 as well as other bearing materials with new technology procedures, such as Rapid Solidification Plasma Deposition (RSPD) and Rapid Solidification Rate (RSR) produced alloys. Recent work reported in Reference (9) has shown some potential for further improvement in M-50 by alloy modification, and ongoing but as yet uncompleted work in the author's laboratory has indicated similar potential improvement trends.

However, while M-50 is clearly a superior bearing material for past and current applications, new demands made by advanced engine designs and operational conditions have indicated that it, as well as all other high hardness through-hardenable materials, has some deficiencies which need attention.

As engine speeds increase to achieve improved efficiency and better specific fuel consumption, the bearing DN* also increases. As the DN increases, the low fracture toughness (or more specifically the low stress intensity factor) of current through-hardened rolling element bearing materials becomes a critical technical barrier to the operation of advanced high performance aircraft gas turbines. At high rotational speeds (>2.4 million DN), a bearing using conventional through-hardened bearing steels, such as M-50, 52100, or 18-4-1, will be subject to race fracture either independently or as a result of a fatigue spall. This type of failure is illustrated in Figures 7 and 8. Race fracture is a totally unacceptable mode of failure because of its potentially serious secondary effect on engine integrity.

In the classical failure mode, a small crack forms below the surface, usually at a stress riser, such as a non-metallic inclusion or carbide (Figure 9). The crack propagates radially outward from the point of initiation and, upon reaching

*DN = bearing bore in mm times the shaft speed in rpm.

the surface, forms a spall. Quite often this crack will simultaneously propagate radially inward from the same point of origin, but such growth does not reach significant depth. It is assumed that the cracks that initiate race fractures are of the same nature, but the inward propagation is not arrested. Instead, a superimposed hoop tensile stress field causes them to propagate both to the surface and radially inward throughout the Hertzian stress field.

Figure 10 is a schematic representation of crack-growth rate as a function of stress-intensity range. The diagram illustrates the rapid-fracture problem. When the bearings are operated at low hoop-stress levels, the stress-intensity range is below the propagation threshold value, ΔK_{th}. In this case, the cracks formed do not propagate inward - or the propagation rate is sufficiently slow so that normal spalling fatigue will develop. While spalling is also undesirable, it is a relatively gradual fatigue process that can be detected by vibration monitors, chip detectors, or other oil system monitors. Consequently, the effected components can usually be removed before more serious secondary damage is incurred. However, as the stress level, and thus the stress-intensity range increases, the crack growth rate accelerates until a stage is reached where the stress-intensity factor is large enough to produce rapid fracture; at this point it is considered to have reached its critical value (K_{Ic}). The effect of hoop-stress on this mechanism is shown schematically in Figure 11. The time scale represents operating time measured from the initiation of a sub-surface defect. If spalls form at low hoop-stress levels and are not detected by the methods mentioned above, subsequent vibration or impact damage will eventually lead to cage failure. This is normally the final stage of a bearing failure. At increased hoop-stress levels, however, rapid fracture occurs prior to significant spalling, and consequently no warning is received. It is very likely that time-to-spall is decreased by increasing the stress level, but for the purpose of this illustration it is assumed to be independent of hoop-stress.

In typical bearing materials, such as M-50, 52100 or 18-4-1, which have an inherent low fracture toughness ($K_{Ic} \simeq 14$ - 16 MPa $\cdot$ $M^{1/2}$), this becomes a critical problem because of the small dimensions of the critical crack required to initiate fracture. This places a severe restriction on advanced engine design. Engine performance can be improved by increasing rotational speed, and additional efficiency can be realized by using multi-spool engines, where the engine shaft diameters (and consequently the bearing diameters) are increased. Both of these measures result in an increased DN value. As shown in Figure 12, current engines operate at DN values to about 2.3 million; next generation engines are expected to approach 3 million.

In addition to the fracture toughness problem, higher bearing speeds will also reduce the operating life (time) of current bearing materials. This is best illustrated in Figure 13. Because bearing materials have a finite fatigue life limit, as speed increases, the number of cycles to failure will be reached sooner. In addition, as speed increases the centrifugal load increases, further reducing life. Consequently, a material that has a safe design limit (in hours) at low speeds may become inadequate as speeds increase.

Work is currently in progress in several laboratories including the author's, on both the fracture toughness and life extension problems. Good progress has been made to date particularly in the area of fracture toughness. Figures 14 and 15 show a M-50 bearing tested under combined high hoop and Hertzian stresses.

Figure 14 is an uncontained test whereas test of the bearing in Figure 15 was terminated immediately after fracture initiation. Figure 16 shows a bearing made out of a modified carburizing grade of M-50 exposed to the same conditions as the through-hardened bearings. While the modified M-50 bearing spalled, no indication of incipient fracture or even a tendency toward fracture was noted. These tests have been repeated several times with similar results on additional modified M-50 bearings as well as bearings made out of other selected carburized materials.

The area of extended life is also being addressed, and here it appears, perhaps fortuitously, that some carburizing materials may also have an advantage. It has long been recognized that the favorable compressive residual stress patterns in carburized bearings would be beneficial in improving rolling element fatigue life. (10,11,12) However, the deterrent to using conventional carburized materials for aircraft engine, rolling-element bearings has been the relatively low operating temperature capability of conventional carburizing grades of steel. In recent years, however, carburizing steels were developed that exhibited significantly improved high temperature properties. (13) To achieve this, two different approaches in alloy design were utilized. The first was to add alloying elements (such as Si, Cr, Ni and Mo) which serve to retard martensite tempering reactions and thus help impart elevated-temperature strength to about 315°C (600°F). One of the compositions resulting from this approach is Timken CBS 600; the chemical analysis of which is listed in Table I. The second approach was designed to utilize a secondary hardening mechanism that, by the precipitation of complex alloy carbides during tempering, can raise the high temperature properties to temperatures approaching 538°C (1000°F). Secondary hardening is the basis for the excellent high temperature characteristics of high speed tool steels, such as M-50. The latter approach resulted in materials such as Timken's CBS 1000, Vasco's X-2 and General Electric's modified M-50 alloy.

Figure 17 shows recent high speed rolling contact fatigue test data on carburized modified M-50 compared to through-hardened VIM-VAR M-50. As can be seen, the carburized material has a rolling contact fatigue life twice that of the standard material at the B_{10} life. Other modifications, including Co additions mentioned in Reference (9), also indicate a similar encouraging trend toward improved fatigue life.

It is interesting to take note of several items with regard to the good progress made toward improved fatigue life. First, the research conducted brought about a much better understanding of what was needed for a good fatigue resistant material. Second, the development and continual improvement of laboratory devices (14,15,16,17) to simulate bearing operation, in parallel with the improved understanding of Elastohydrodynamics (EHD), provided an efficient means to evaluate materials that could be confidently extrapolated to practice. Third, by focusing primarily on sub-surface initiated fatigue, the complications associated with the chemical, metallurgical and mechanical interactions of the surface and near surface regions where other competitive modes of failure initiate were nicely by-passed. Thus, much could be accomplished between the materials engineer and designer. In the more recent effort on fracture toughness improvement, a similar relatively narrow focal area has helped toward what appears to be an adequate solution to the problem. In the latter area, as in the case of sub-surface fatigue, the understanding of the mechanisms and phenomenological influences had been sufficiently well established so that the approach toward achieving an improved fracture tough material was reasonably well defined. However, at the same time, a

number of interesting and potentially important observations have been made which open up a region of much less understood phenomenological behavior. It has become quite clear that the classical plane-strain fracture mechanics methodology is inadequate to provide a full understanding of crack propagation behavior in the materials being evaluated. It appears that a relatively new sub-discipline, short crack fracture mechanics,will need to be applied to better understand and explain the fracture behavior of brittle materials and crack propagation through brittle-ductile interfaces. Despite this, however, the prospect of achieving improved fracture tough bearings is good even if the precise behavior, i.e. the fundamental understanding,still lacks a rational and well defined analytical approach. In any event, the lack of full understanding of behavioral modes should not prevent this technology from entering the working environment. After all, rolling element bearings were used successfully decades before a thorough understanding was achieved as to why they worked as well as the did.

In summary, classical fatigue failure in rolling element bearings is reasonably well understood and can, in most cases, be adequately controlled. Alas, it is the least likely failure mode.

BEARING MATERIALS - SURFACE DISTRESS FAILURE MODE

The second major failure mode, surface distress, is a much more imprecise area where understanding is less clear. However, it is the area where tribological efforts can have the greatest pay off. Before summarizing the "status of understanding" in this area, some terms must again be defined.

For any load carrying surface, it can be assumed that there are three or four regions as shown in Figure 18. The surface contains the "outer layers" of oxides, absorbed films, reaction films, etc., which commands the attention of the chemists. In thickness, it is usally <1 μm. The near surface region contains the "inner layers", including the Bielby layer (if there is one) and various deformed layers. The deformed layers, perhaps of differing microstructure than the sub-surface, may arise from surface preparation, such as grinding and honing, heat treatment, or structural alterations induced during operation. Hardness and residual stresses may be significantly different than in the sub-surface region. The near surface region may be on the order of 50 μm below the surface. The sub-surface region, which may be 50-1000 μm below the surface, is generally not significantly affected by mechanical process or operationally induced physical and microstructural alterations. Its microstructure and hardness may, however, still differ from the bulk (core) material and significant bulk residual stresses may be present in the sub-surface zone. These stresses and microstructures are, however, generally the result of macro processes, such as forging, heat treating, and surface hardening. As mentioned earlier, the good progress made in understanding and improving classical fatigue related failures was the result of working basically with bulk (sub-surface) properties. In addressing surface and near surface related failures, it is no longer possible to ignore surface and lubricant chemistry, interactions, lubricant films, contamination, filtration techniques, etc.

For the surface and near surface related failures, there is as yet no specific and precise understanding relative to what is needed to reduce the problem. Perhaps even more problematical is the ability to realistically simulate these effects and correlate with real life events. Lastly, it is obvious that possible interactions between surface and near surface regions cannot be by-passed. In view of the current interest in high horsepower transmission gearing for turbo-props and the general emphasis toward higher temperature operation, the surface distress failure mode will become ever more important. However, a logical and effective means for developing materials and lubricants for this problem will likely prove much more difficult than in solving that of sub-surface initiated fatigue. The modes of failure are very much unique to the materials used, the component geometry, and the specific lubricant and operating conditions.

Because of the complicated interactions of surface and near surface failure modes, it is not easy to identify specific material needs. There is an obvious need to control and understand residual stresses and to fully understand the influence of surface finishing processes, run-in and operation on microstructural changes. But this does not seem to get at the heart of the matter. In a recent assessment of this problem (18) there was reference to the notion of tailor-making the near surface structure and even the surface region. This is a potentially attractive approach in view of the growth and understanding of surface modification techniques. The difficulty is that there is still a lack of understanding regarding what is needed for resistance to surface distress and surface initiated fatigue. The contributions of EHD, micro EHD, surface films, surface topography and near surface attributes are no doubt intimately connected in the real world. However, the lack of understanding of these connections not only inhibits the progress in surface and near surface improvements, but it also creates a bottleneck for lubricant development, and perhaps most importantly, the development of simple as well as sophisticated test devices to evaluate materials, and the ability to predict performance levels for design.

As pointed out in Reference (18), it is clear that a great deal is known about the constitutive parts of the problem. It is unfortunate that much of this knowledge has come about from isolated experiments with a variety of materials and operating conditions, generally different from practice. It is difficult to believe and even perhaps naive to think, that continued work on the constitutive parts alone will significantly move things along to a more useful end. Thus far, this approach has led to several failure concepts, all of which fall short of reality. Failure does not seem to be adequately and singly represented by the loss of an EHD film, the desorption of a surface film, the generation of critical temperature or the plastic flow of the main structure of the surface topography. The inevitable conclusion is that these generalities on the global behavior of the contact must be integrated. In addition, the sequence of behavior must be evaluated on an "asperity" scale in order to evolve a picture of what distinguished benign events from damage accumulation which could lead to a given mode of failure. Even here it is interesting to note that the scale of asperity size which may control critical events is different depending on the researcher involved. But within this general framework, it is clear that the behavior of the near surface region with regard to failure initiation is greatly influenced by the topographical structure of the surface and the relevant properties of the material in the near surface region under the stress and temperature environment it encounters. Just as has been the case with sub-surface fatigue, events are likely to be controlled by both average properties of the system as well as singular defects.

With this perspective of surface topography and near surface properties, the role of EHD, micro-EHD and boundary films seem to find their place in the whole process of friction and the initiation or accumulation of damage. They are influential in determining the magnitude of stress on both a global and a local (asperity) scale. Thinking now seems to go beyond the simple ideas of friction being derived from only adhesive junctions. A significant portion of energy can be dissipated by plastic deformation within the body of the near surface region. It is this plastic deformation that may be more detrimental than the movements and attrition of material on the surface.

In principal at least, there is no impediment to putting the competitive modes of failure which are initiated in the near surface region on a logical rather than on an empirical basis. In practice, this will prove to be a major challenge to the materials engineer, tribologist, lubricant engineer, physicist and others. It is in the truest sense of the word, an inter-disciplinary problem.

While the fundamental understanding of surface related fatigue is still in a relatively early stage, main shaft aircraft turbine engine bearings are operating under conditions which are known to contribute to surface distress. The fact that they do operate, and in general quite successfully is in part a tribute to the excellence of the design and in part to what may be relatively gross but apparently effective preventative measures. The area of filtration for instance has helped greatly in allowing bearing survival under extreme operating conditions. Work reported in References (19,20,21,22,23) has shown the effectiveness of filtration in improving bearing life. The extensive work performed by a number of researchers on surface finish effects on EHD has increased the understanding of the type of surface finish (and surface topography) needed to provide the best potential for maintaining an adequate fluid film under severe operating conditions. The work reported in Reference (24) on the effects of artificially-produced defects on the film thickness distribution in sliding EHD contacts, has provided valuable insight into the role of surface discontinuities in the critical EHD contact region.

SUMMARY

This paper has attempted to review the status of understanding for bearing materials, although as pointed out at the beginning, limits had to be set on both the materials and the failure modes discussed. Even within these relatively narrow confines, there are still areas which because of time constraints, could not be reviewed, although they do help to improve our understanding and thereby bearing life and reliability. Non-destructive inspection is one such particular area. Recent advances in scanning X-ray, ultrasonic, and eddy-current inspection techniques have helped to considerably improve not only the quality of the final product, but also helped in the understanding of why bearing materials behave either in a predictable or unpredictable manner.

Thus, considering the iron-base through-hardened bearing materials and the sub-surface initiated fatigue failure mode, it can be stated that our understanding is reasonably good. The best evidence to be offered in proof of this are the low failure rates of these materials in this mode in actual service. However, complacency is definitely not indicated, because the demands of advanced aircraft gas turbine engines continue to strain the capability of the current materials and

require the materials engineer to develop improved materials and the design community to come up with innovative design approaches.

The second primary operating failure mode comprehensively termed surface distress is less understood. Since it is accountable for the majority of operational bearing failures, it is important to increase the level of understanding of this failure mode. This is a more difficult task than the fatigue mode of failure because of the many inter-related and potentially synergistic effects. Items, such as micro-EHD, oxides, anti-wear films, asperity deformation, absorption adhesion, lubricant rheology, and surface topography, are only a few of the real and phenomenological effects to be considered. Taken as an overall picture it presents a seemingly insurmountable problem. Yet, in reviewing the literature, it is apparent that all of these areas are being worked - - - independently. To gain a better understanding (and solution) of the surface distress failure mode in rolling element bearings will require a synthesis of these divergent efforts into a cohesive technology. The key to the eventual full understanding in this area is, as was the case with the sub-surface fatigue mode, the development of realistic simulation techniques which will permit accurate extrapolation of laboratory/component tests into real world bearings.

REFERENCES

1. Tallian, T.E., "On Competing Failure Modes in Rolling Contact", ASLE Transactions; Vol. 10, October, 1967.

2. Cunningham, J.S.; and Morgan, M.A., "Review of Aircraft Bearing Rejection Criteria and Cause", ASLE Lubrication Engineering, Vol. 35, No. 8, August, 1979.

3. Bamberger, E.N., "Materials for Rolling Element Bearings", Bearing Design - Historical Aspects, Present Technology and Future Problems, W.J. Anderson, ed., ASME Publication H00160, 1980.

4. Bieberich, M.D.; Brown, C.L.; and Limpert, J.C., "Development of Corrosion Inhibited MIL-L-23699 Oils for Naval Aircraft Engines and Transmissions", D.W. Taylor Ship Research and Development Center STNSRDC/SME 80/36, September, 1980.

5. Parker, R.J.; and Zaretsky, E.V., "Rolling-Element Fatigue Life of AISI M-50 and 18-4-1 Balls", NASA Tech. Paper 1202, April, 1978.

6. Rescalvo, J.A.; and Averbach, B.L., "Fracture and Fatigue in M-50 and 18-4-1 High Speed Steels", ASM, Metallurgical Society of AIME, Metallurgical Transactions A, Vol. 10A, September, 1977.

7. Averbach, B.L., "Fracture of Bearing Steels", ASM, "Metals Progress", December, 1980.

8. Bamberger, E.N., et al, "Life Adjustment Factors for Ball and Roller Bearings", ASME Design Guide, 1971.

9. Adam, C.M.; Bourdeau, R.G.; and Broch, J.W., "Application of Rapidly Solidified Alloys", Final Report, AFWAL TR-81-4188, February, 1982.

10. Scott, R.L.; Kepple, R.K.; and Miller, M.H., "The Effect of Processing-Induced Near-Surface Residual Stress of Ball Bearing Fatigue", Rolling Contact Phenomena, J.B. Bidwell, ed., Elsevier Publ., 1962, pp. 301-316.

11. Gentile, A.J.; and Martin, A.D., "The Effects of Prior Metallurgically Induced Compressive Residual Stress on the Metallurgical and Endurance Properties of Overload Tested Ball Bearings", ASME Paper 65-WA/CF-7, 1965.

12. Almen, J.O., "Effects of Residual Stress on Rolling Bodies", Rolling Contact Phenomena, J.B. Bidwell, ed., Elsevier Publ., 1962.

13. Jatzak, C.F., "Specialty Carburizing Steels for High Temperature Applications", ASM, Metals Progress, April, 1978.

14. Zaretsky, E.V.; Parker, R.J.; and Anderson, W.J., "NASA Five-Ball Fatigue Tester - Over 20 Years of Research", Rolling Contact Fatigue Testing of Bearing Steels, ASTM STP 771, 1982.

15. Bamberger, E.N.; and Clark, J.C., "Development and Application of the Rolling Contact Fatigue Test Rig", (ibid).

16. Glover, D., "A Ball-Rod Rolling Contact Fatigue Tester", (ibid).

17. Eastaugh, P.R., "Use of Accelerated Tests to Establish the Lubricant - Interaction on Bearing Fatigue Life", (ibid).

18. Wedeven, L.D., "Interdisciplinary Approaches to Tribological Research", Extended abstract prepared for U.S.-West German Tribology Workshop - Limits on Tribo-Contact Behavior. Bundesamt für Material Prüfung, Berlin, W. Germany, 1982.

19. Loewenthal, S.H.; Moyer, D.W.; and Needelman, W.M., "Effects of Ultra-Clean and Centrifugal Filtration on Rolling-Element Life", Transactions ASME, Journal of Lubrication Technology, Vol. 104, No. 3 July, 1982.

20. Fitzsimmons, B.; and Cave, B.J., "Lubricant Contaminants and Their Effects on Bearing Performance", SAE Paper No. 750583, 1975.

21. Fitzsimmons, B.; and Clevenger, H.D., "Contaminated Lubricants and Tapered Roller Bearing Wear", ASLE Transactions, Vol. 20, No. 2, 1977.

22. Perrotto, J.A., "Effect of Abrasive Contaminants on Ball Bearing Performance", ASLE Journal of Lubrication Engineering, Vol. 35, No. 12, December, 1979.

23. Okamoto, J.; Fujita, K.; and Toshioka, T., "Effects of Solid Particles in Oil on the Life of Ball Bearings", Journal of the Mechanical Engineering Laboratory (Tokyo), Vol. 26, No. 5, 1972, (NASA Technical Translation; NASA TT-F-15,653, 1974).

24. Loewenthal, S.H.; and Moyer, D.W., "Filtration Effects on Ball Bearing Life and Condition in a Contaminated Lubricant", ASME Journal of Lubrication Technology, Vol. 101, No. 2, April, 1979.

Typical Chemical Compositions of Selected Bearing Steels

Alloying Elements (% By Weight)

Designation	C	P (max)	S (max)	Mn	Si	Cr	V	W	Mo	Co	Cb	Ni
SAE 52100	1.00	0.025	0.025	0.35	0.30	1.45	—	—	—	—	—	—
MHT*	1.03	0.025	0.025	0.35	0.35	1.50	—	—	—	—	—	—
AISI M-1	0.80	0.030	0.030	0.30	0.30	4.00	1.00	1.50	8.00	—	—	—
AISI M-2	0.83	0.030	0.030	0.30	0.30	3.85	1.90	6.15	5.00	—	—	—
AISI M-10	0.85	0.030	0.030	0.25	0.30	4.00	2.00	—	8.00	—	—	—
AISI M-50	0.80	0.030	0.030	0.30	0.25	4.00	1.00	—	4.25	—	—	—
T-1 (18-4-1)	0.70	0.030	0.030	0.30	0.25	4.00	1.00	18.0	—	—	—	—
T15	1.52	0.010	0.004	0.26	0.25	4.70	4.90	12.5	0.20	5.10	—	—
440C	1.03	0.018	0.014	0.48	0.41	17.30	0.14	—	0.50	—	—	—
AMS 5749	1.15	0.012	0.004	0.50	0.30	14.50	1.20	—	4.00	—	—	—
Vasco Matrix II	0.53	0.014	0.013	0.12	0.21	4.13	1.08	1.40	4.80	7.81	—	0.10
CRB-7	1.10	0.016	0.003	0.43	0.31	14.00	1.03	—	2.02	—	0.32	—
AISI 9310(C)	0.10	0.006	0.001	0.54	0.28	1.18	—	—	0.11	—	—	3.15
CBS 600(C)	0.19	0.007	0.014	0.61	1.05	1.50	—	—	0.94	—	—	0.18
CBS 1000M(C)	0.14	0.018	0.019	0.48	0.43	1.12	—	—	4.77	—	—	2.94
Vasco X-2(C)	0.14	0.011	0.011	0.24	0.94	4.76	0.45	1.40	1.40	0.03	—	0.10

* Also Contains 1.36% Al
C - Carburizing Grades

TABLE I

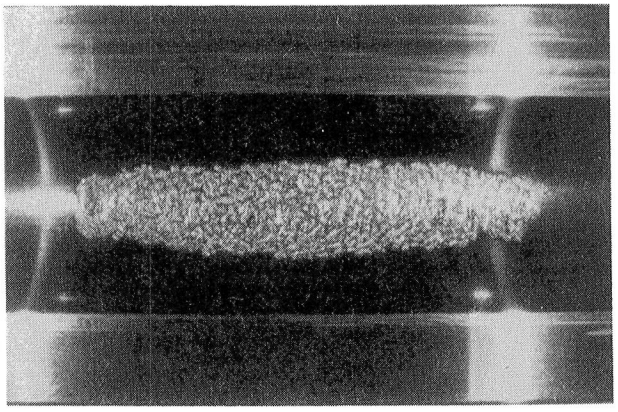

FIGURE 1: Typical Sub-Surface Initiated Fatigue Spall in Ball-Bearing Inner Race

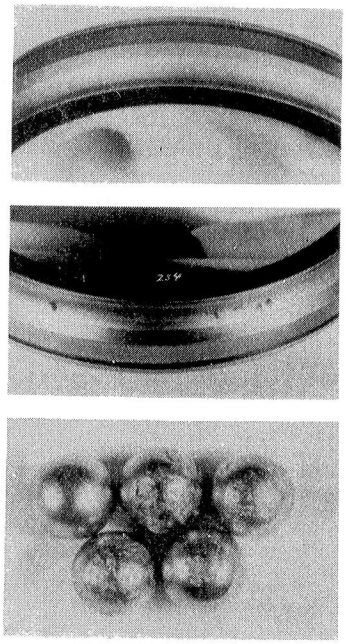

FIGURE 2: Typical Examples of Surface Distress in Ball Bearing Components

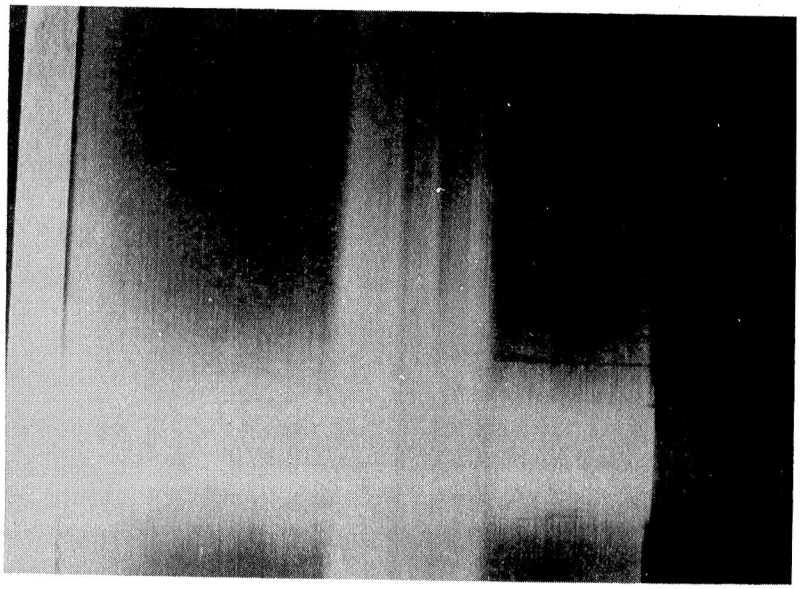

FIGURE 3: "Frosting" of Roller Bearing Raceway Due to Marginal Elastohydrodynamic Lubrication

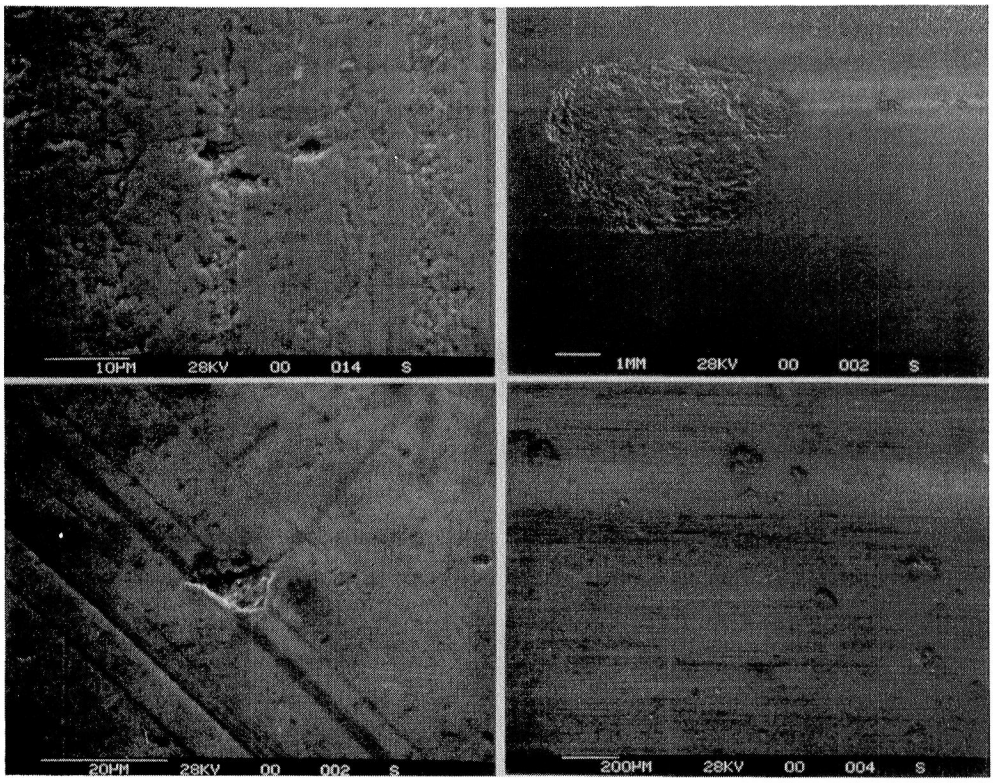

FIGURE 4: Scanning Electron Microscope Photographs Showing Micro-Pitting and Micro-Spalling in Bearing Raceway

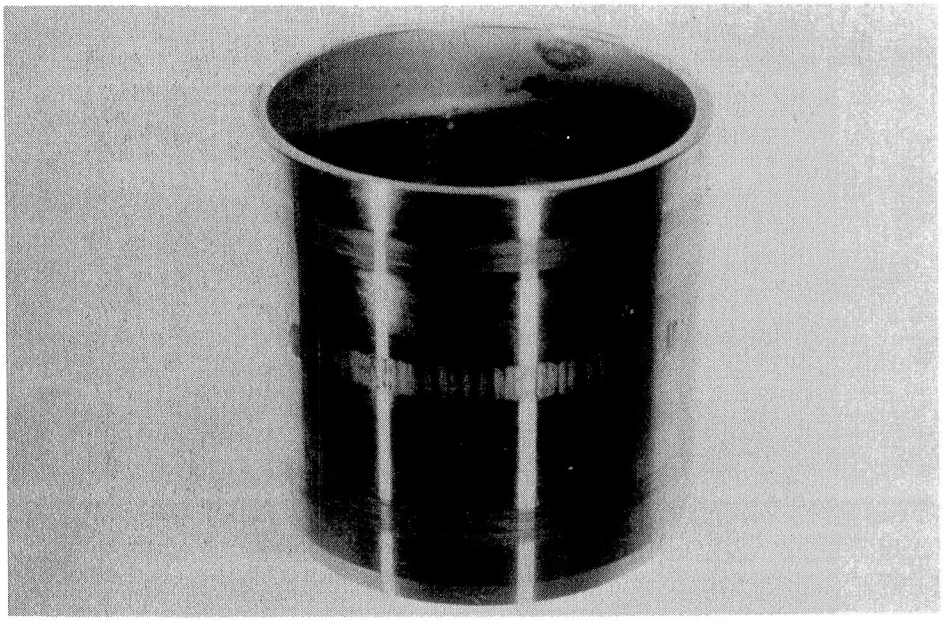

FIGURE 5: Corrosion on Roller Bearing Inner Race

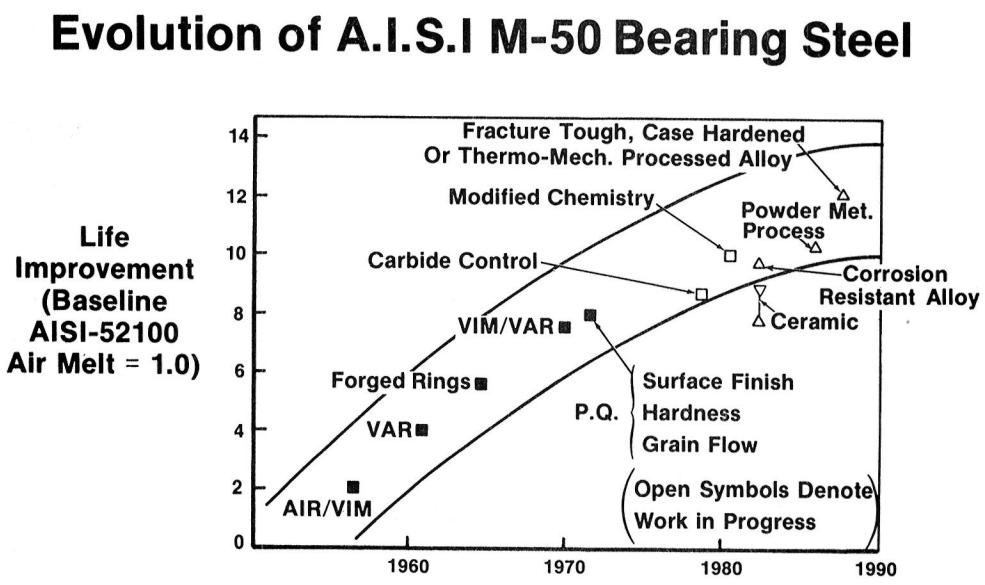

Figure 6

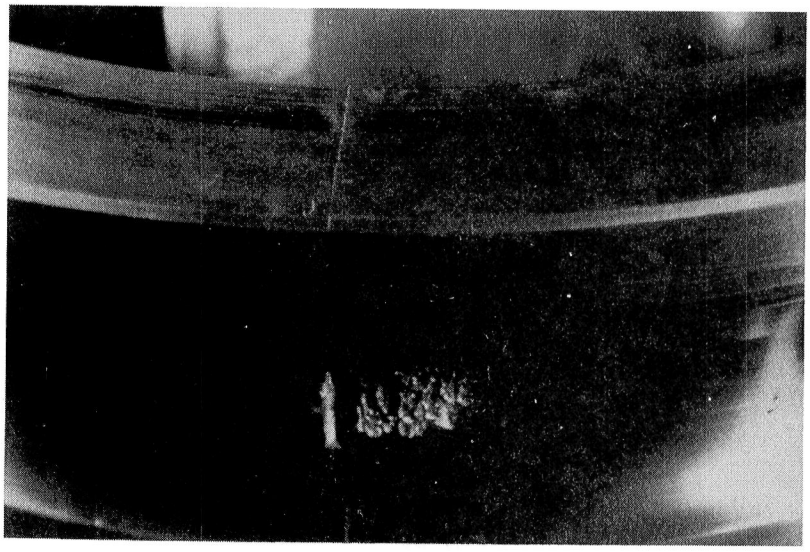

FIGURE 7: Race Fracture Caused by Combination of High Hoop and High Hertzian Stresses

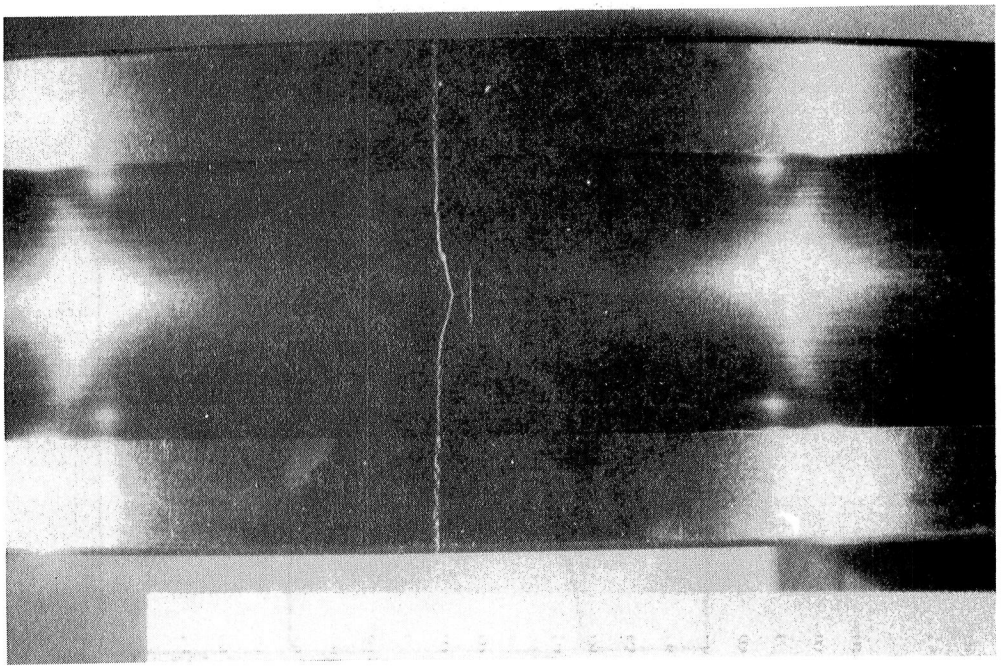

FIGURE 8: Race Fracture. Note Absence of Any Fatigue Spalling

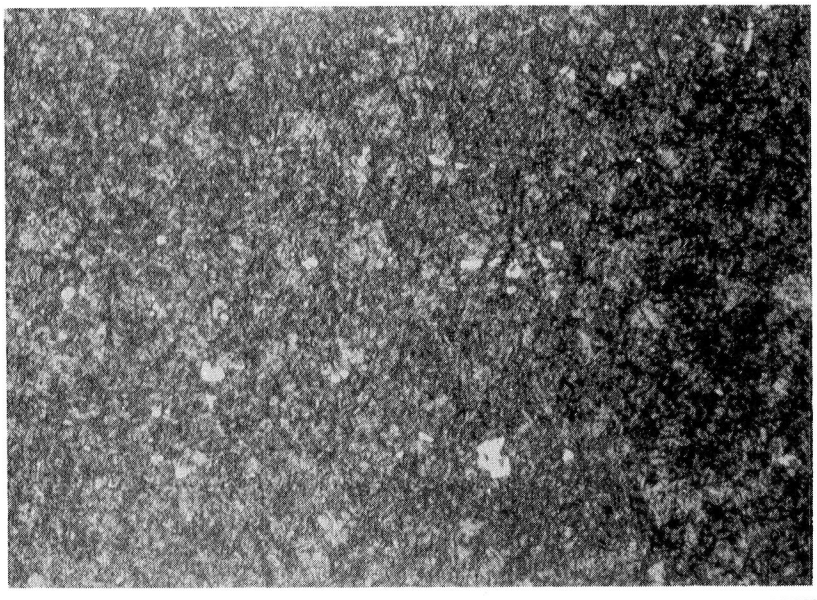

400X

FIGURE 9: Typical Microstructure of M-50 Bearing Steel. Small, White (Non-Etching), Particles are Carbides

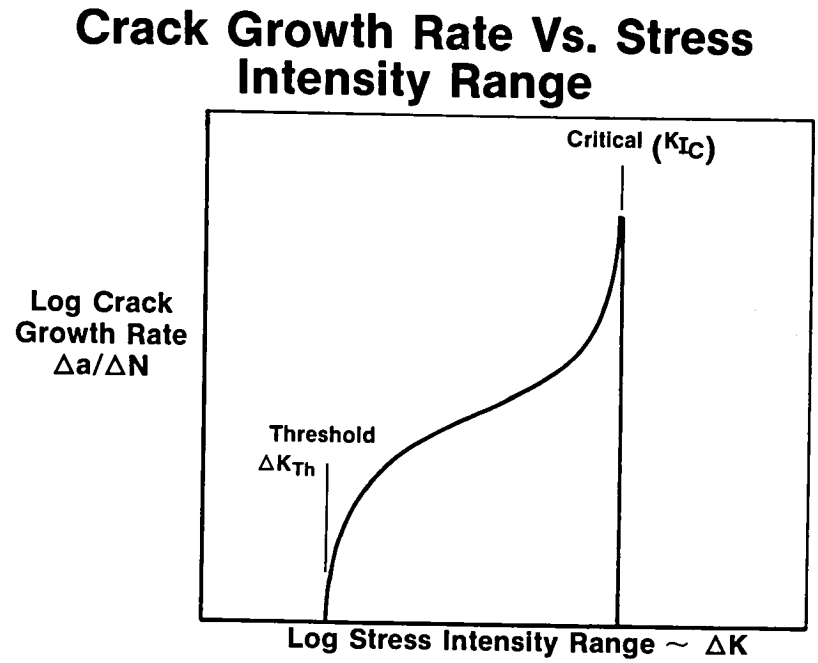

Figure 10

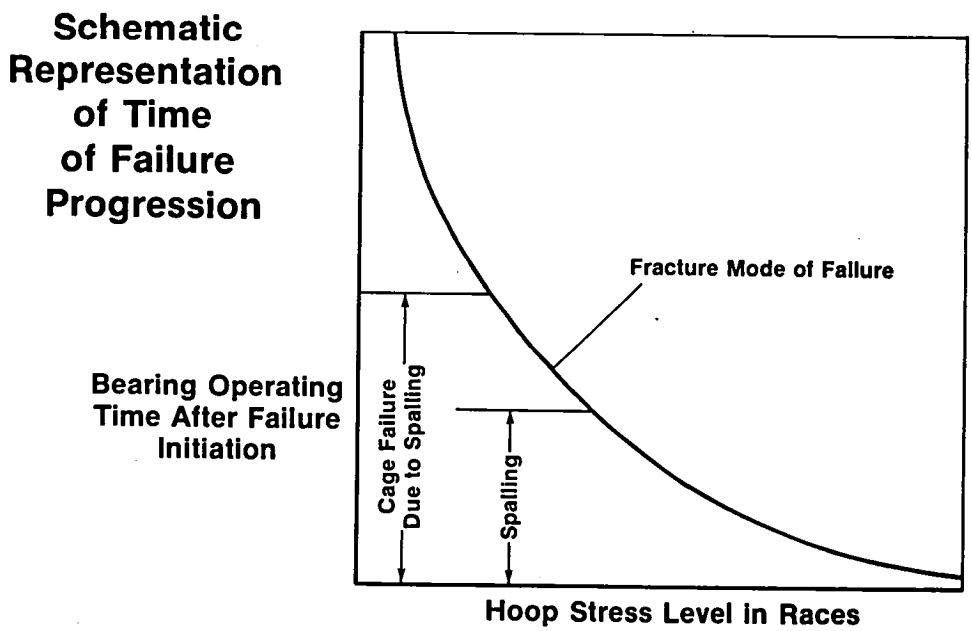

Figure 11

Trend in Aircraft Engine Main Bearing DN

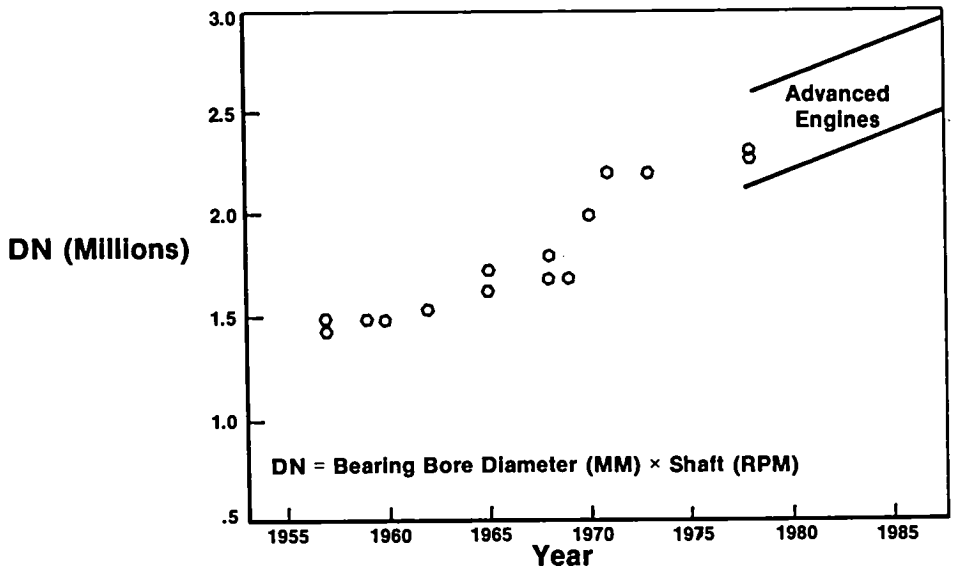

Figure 12

Mainshaft Bearing Lives & Expected Failure Mode as a Function of Speed For a Constant Bore Size

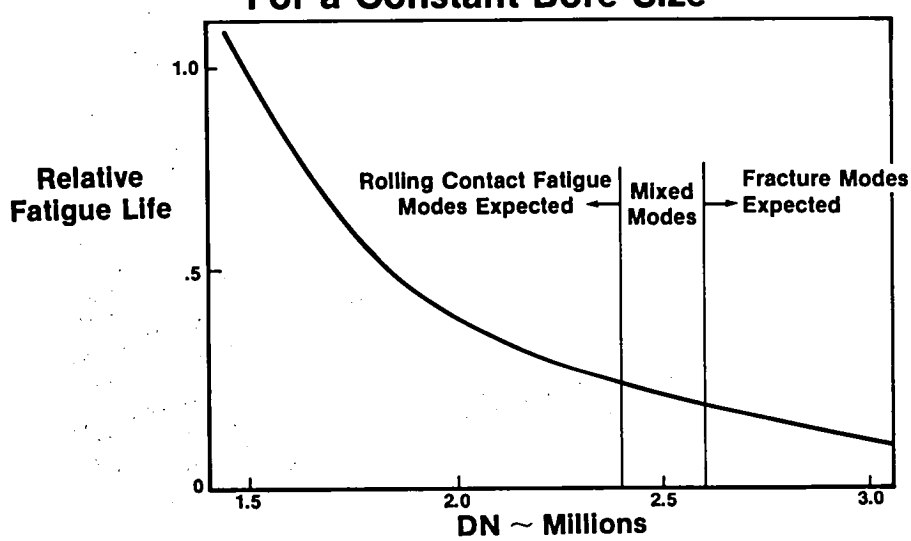

Figure 13

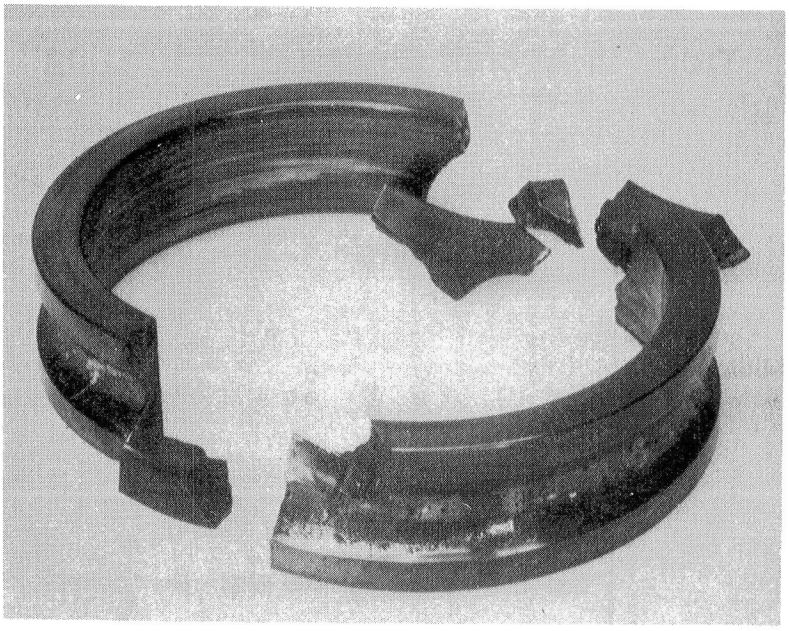

FIGURE 14: M-50 Bearing, Tested Under Combined, Very High Hoop and High Hertzian Stress

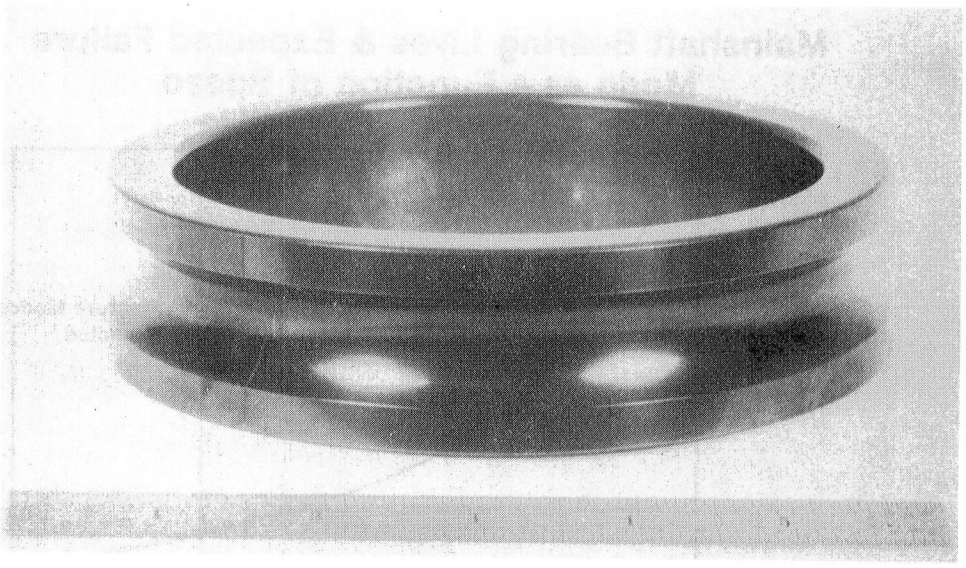

FIGURE 15: M-50 Bearing, Tested Under Combined High Hoop and High Hertzian Stress. Unlike the Bearing Shown in (Figure 14), This Test Was Terminated Immediately Upon Initial Fracture

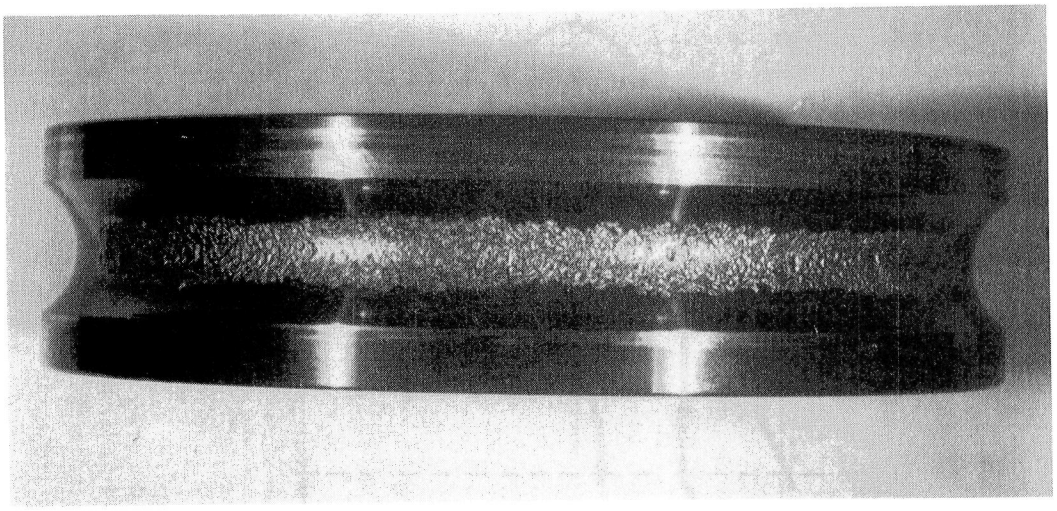

FIGURE 16: Modified M-50 Bearing Tested Under Same Load Conditions as Those in Figure 14 and Figure 15. This Bearing Spalled But Did Not Fracture

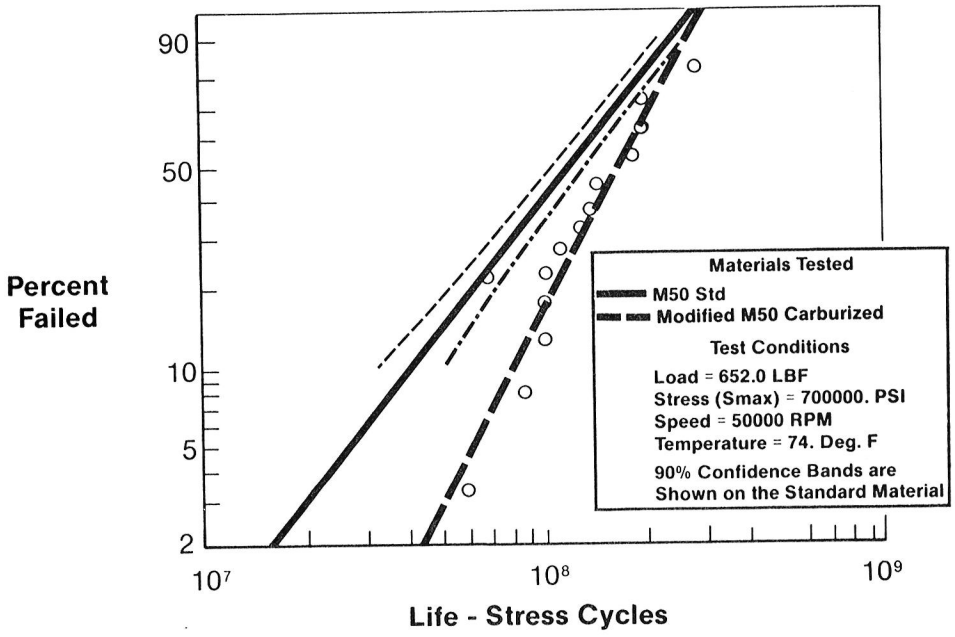

FIGURE 17: Rolling Contact Fatigue Test Results on VIM-VAR M-50 and Carburized, Modified VIM-VAR M-50

Load Regions in Contacting Bodies

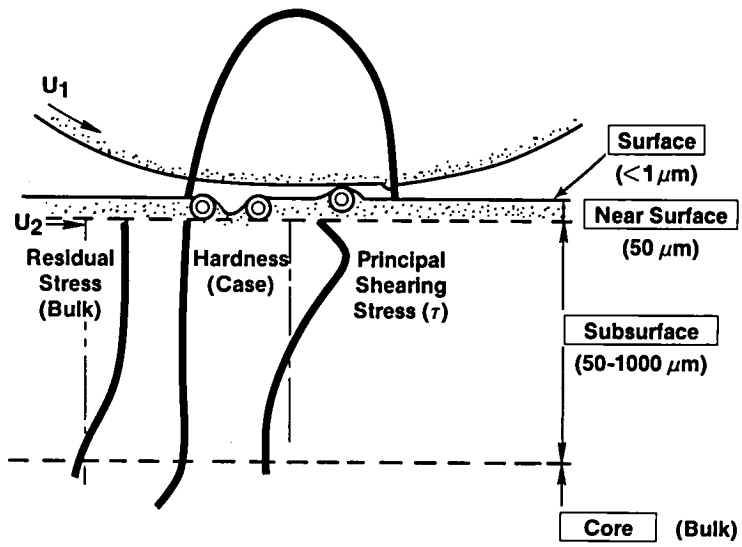

Figure 18

STATUS OF UNDERSTANDING FOR GEAR MATERIALS

Dennis P. Townsend
National Aeronautics and Space Administration
Lewis Research Center
Cleveland, Ohio 44135

SUMMARY

Today's gear designer has a large selection of possible gear materials to choose from. The choice of which material to use should be based on the requirements of the application and will include the operating conditions of load, speed, and temperature in addition to reliability, weight, noise limitation, accuracy, and cost. The plastic materials are generally low in cost with low strength capabilities and are suitable for many light-duty applications. Die-cast alloy and sintered powder-metal gears are also fairly inexpensive and will operate at higher loads and temperatures than plastic gears. The three types of cast iron offer a medium-strength gear at a cost that varies with the accuracy of machining requirements. Gears can be manufactured from several aluminum alloys for light weight and medium cost and may be anodized for improved load capacity. The copper alloys, bronze and brass, are more costly but have good sliding and wear properties that are useful for worm gear applications. The hot-forged powder-metal gears have the advantage of medium cost with good accuracy and high strength. Several low- to medium-alloy steels are available for gear design and most can be heat treated for added strength. The medium-alloy gear materials offer high strength when case hardened and will satisfy most high-load medium-temperature applications. For more severe load, speed, and temperature requirements the advanced high-temperature alloys must be used. These include EX-53, CBS 600, Vasco X-2, Super Nitralloy (5Ni-2Al), and forged AISI M-50. As the requirements become more stringent, the cost will also increase. It is necessary that the gear designer have a working knowledge of the various gear materials in order to match the most economical material with the design requirements.

INTRODUCTION

A wide variety of gear materials is available today for the gear designer. Depending on the application the designer may choose from materials such as wood (fig. 1), plastics, aluminum, magnesium, titanium, bronze, brass, gray cast iron, nodular and malleable iron, and a whole variety of low-, medium-, and high-alloy steels (fig. 2). In addition there are many different ways of modifying or processing the materials to improve their properties or to reduce the cost of manufacture. These include reinforcements for plastics, coating and processing for aluminum and titanium, and hardening and forging for many of the iron-based (or ferrous) gear materials.

In many applications the main reason for selecting a specific gear material is economic (the material strength and gear accuracy being secondary requirements). Applications such as home appliances, automobiles, recreational vehicles, instruments, and toys are but a few of the areas where high-production, low-cost, lightto medium-duty gears are used.

When selecting a gear material for an application, the gear designer will first determine the actual requirements for the gears being considered. The design requirements for a gear in a given application will depend on such things as accuracy, load, speed, material, and noise limitations. The more stringent these requirements are, the more costly the gear will become. For instance, a gear requiring high accuracy because of speed or noise limitations may require several processing operations in its manufacture. Each operation will add to the cost. Machined gears, which are the most accurate, can be made from materials with good strength characteristics. However, these gears are very expensive. The cost is further increased if hardening and grinding are required as in applications where noise limitation is a critical requirement. Machined gears should be a last choice for a high-production gear application because of cost.

Some of the considerations in the choice of a material include allowable bending and Hertz stress, wear resistance, impact strength, water and corrosion resistance, manufacturing cost, size, weight, reliability, and lubrication requirements. In aircraft applications, such as helicopter, V/STOL, and turboprops, the dominant factors are reliability and weight. Cost is of secondary importance. Off-the-road vehicles, tanks, and some actuators may be required to operate at extremely high loads with a corresponding reduction in life. These loads may produce bending stresses in excess of 150 000 psi and Hertz stresses in excess of 400 000 psi for portions of the duty cycle. This may be acceptable because of the relatively short life of the vehicle and a deemphasis on reliability. (As a contrast, aircraft gearing typically operates at maximum bending stresses of 65 000 psi and maximum Hertz stresses of 180 000 psi). Considerable research has been done on advanced aircraft gear materials at NASA Lewis Research Center in recent years (refs. 1 to 6). Some of these data are presented here.

GEAR MATERIALS

Plastics

There has always been a need for a lightweight, low-cost gear material for light-duty applications. In the past, gears were made from wood or phenolic-resin-impregnated cloth. However, in recent years with the development of many new polymers, many gears are made of various "plastic" materials. Table I lists plastic materials used for molded gears. The most common molded plastic gears are the acetate and nylon resins. These materials are limited in strength, temperature resistance, and accuracy. The nylon and acetate resins have a room-temperature yield strength of approximately 10 000 psi. This is reduced to approximately 4000 psi at their upper temperature limit of 250° F. Nylon resin is subject to considerable moisture absorption, which reduces its strength and causes considerable expansion. Larger gears are made with a steel hub that has a plastic tire for better dimensional control. Plastic gears can operate for long periods in adverse environments, such as dirt, where other materials would tend to wear excessively. They can also operate without lubrication or can be lubricated by the processed material as in the food industry. The cost of plastic gears can be as low as a few cents per gear for a simple gear on a high-volume production basis. This is probably the most economical gear available. Often a plastic gear is run in combination with a metal gear to give better dimensional control, low wear, and quiet operation.

Polyimide is a more expensive plastic material than nylon or acetate resin, but it has an operating temperature limit of approximately 600° F. This makes the polyimides suitable for many adverse applications that might otherwise require metal gears. Polyimides can be used very effectively in combination with a metal gear without lubrication because of polyimide's good sliding properties (refs. 7 to 9). However, polyimide gears are more expensive than other plastic gears because they are difficult to mold and the material is more expensive.

Nonferrous Metals

Several grades of wrought and cast aluminum alloys are used for gearing. The wrought alloys have higher strength and good machinability. The most common wrought alloy used in gearing is 2024-T4. The wrought alloy 7075-T6 is stronger than 2024-T4 but is also more expensive.

Aluminum does not have good sliding and wear properties. However, it can be anodized with a thin, hard surface layer that will give it better operating characteristics. The coating is thin and brittle and may crack under excessive load. Anodizing gives aluminum good corrosion protection in salt water applications.

Magnesium is not considered a good gear material because of its low elastic modulus and other poor mechanical properties.

Titanium has excellent mechanical properties, approaching those of some heat-treated steels with a density nearly half that of steel. However, because of its very poor sliding properties, producing high friction and wear, it is not generally used as a gear material. Several attempts have been made to find a wear-resistant coating, such as chromium plating, iron coating (refs. 10 to 13), and nitriding for titanium, with no real success. Titanium would be an excellent gear material if a satisfactory coating or alloy could be developed to provide improved sliding and wear properties.

Several alloys of zinc, aluminum, magnesium, brass, and bronze are used as die-cast materials. Many prior die-cast applications now use less expensive plastic gears. The die-cast materials have higher strength properties, are not affected by water, and will operate at higher temperatures than the plastics. As a result, they still have a place in moderate-cost, high-volume applications. Most die-cast gears are made from lower cost zinc or aluminum alloys. Copper alloys can also be used at a somewhat higher cost. The main advantage of die casting is that the requirement for machining is either completely eliminated or drastically reduced. The high fixed cost of the dies makes low production runs uneconomical. Some of the die-cast alloys used for gearing are listed in references 14 and 15.

Copper Alloys

Several copper alloys are used in gearing. Most are the bronze alloys containing varying amounts of tin, zinc, manganese, aluminum, phosphorous, silicon, lead, nickel, and iron. The brass alloys contain primarily copper and zinc with small amounts of aluminum, manganese, tin, and iron. The copper alloys are most often used in combination with an iron or steel gear to give good wear and load capacity especially in worm gear applications where there is a high sliding component. In these cases the steel worm drives a bronze gear. Bronze gears are also used where corrosion and water are a problem.

Several copper alloys are listed in table II. The bronze alloys are either aluminum bronze, manganese bronze, silicon bronze, or phosphorous bronze. These bronze alloys have yield strengths ranging from 20 000 to 60 000 psi and all have good machinability.

Ferrous Alloys

Cast iron is used extensively in gearing because of its low cost, good machinability, and moderate mechanical properties. Many gear applications can use gears made from cast iron because of its good sliding and wear properties, which are in part a result of the free graphite and porosity. There are three basic cast irons distinguished by the structure of graphite in the matrix of ferrite. These are (1) gray cast iron, where the graphite is in flake form; (2) malleable cast iron, where the graphite consists of uniformly dispersed fine, free-carbon particles or nodules; and (3) ductile iron, where the graphite is in the form of tiny balls or spherulites. The malleable iron and ductile iron have more shock and impact resistance. The cast irons can be heat treated to give improved mechanical properties. The bending strength of cast iron ranges from 5000 to 25 000 psi (ref. 16), and the surface fatigue strength ranges from 50 000 to 115 000 psi (ref. 17). In many worm gear drives a cast iron gear can be used to replace the bronze gear at a lower cost because of the sliding properties of the cast iron.

Sintered Powder Metals

Sintering of powder metals is one of the more common methods used in high-volume, low-cost production of medium-strength gears with fair dimensional tolerance (ref. 18). In this method a fine metal powder of iron or other material is placed in a high-pressure die and formed into the desired shape and density under very high pressure. The green part has no strength as it comes from the press. It is then sintered in a furnace under a controlled atmosphere to fuse the powder together for increased strength and toughness. Usually, an additive (such as copper in iron) is used in the powder for added strength. The sintering temperature is then set at the melting temperature of the copper to fuse the iron powder together for a stronger bond than would be obtained with the iron powder alone. The parts must be properly sintered to give the desired strength.

There are several materials available for sintered powder-metal gears that give a wide range of properties. Table III lists properties of some of the more commonly used gear materials although other materials are available. The cost for volume production of sintered powder metal gears is an order of magnitude lower than that for machined gears.

A process that has been more recently developed is the hot-forming powder-metals process (refs. 19 and 20). In this process a powder-metal preform is made and sintered. The sintered powder-metal preformed part is heated to forging temperature and finished forged. The hot-formed parts have strengths and mechanical properties approaching the ultimate mechanical properties of the wrought materials. A wide choice of materials is available for the hot-forming powder-metals process. Since this is a fairly new process, there will be undoubtedly be improvements in the materials made from this process and reductions in the cost. Several promising high-temperature, cobalt-base alloy materials are being developed.

Because there are additional processes involved, hot-formed powder-metal parts are more expensive than those formed by the sintered powder-metal process. However, either process is more economical than machining or conventional forging while producing the desired mechanical properties. This makes the hot-forming powder-metals process attractive for high-production parts where high strength is needed, such as in the automotive industry.

Accuracy of the powder-metal and hot-formed processes is generally in the AGMA class 8 range. Better accuracy can be obtained in special cases and where die wear is limited, which would tend to increase the cost. Figure 3 shows the relative cost of some of the materials or processes for high-volume, low-cost gearing.

Hardened Steels

A large variety of iron or steel alloys are used for gearing. The choice of which material to use is based on a combination of operating conditions such as load, speed, lubrication system, and temperature plus the cost of producing the gears. When operating conditions are moderate, such as medium loads with ambient temperatures, a low-alloy steel can be used without the added cost of heat treatment and additional processing. The low-alloy material in the non-heat-treated condition can be used for bending stresses in the 20 000-psi range and surface durability Hertz stresses of approximately 85 000 psi. As the operating conditions increase, it becomes necessary to harden the gear teeth for improved strength and to case harden the gear tooth surface by case carburizing or case nitriding for longer pitting fatigue life, better scoring resistance, and better wear resistance. An improved lubrication system may also be required to remove the heat generated by the meshing of gear teeth. There are several medium-alloy steels that can be hardened to give good load-carrying capacity with bending stresses of 50 000 to 60 000 psi and contact stresses of 160 000 to 180 000 psi. The higher alloy steels are much stronger and must be used in heavy-duty applications. AISI 9300, AISI 8600, Nitralloy N, and Super Nitralloy are good materials for these applications and can operate with bending stresses of 70 000 psi and maximum contact (Hertz) stresses of 200 000 psi. The high-alloy steels should be case carburized for AISI 8600 and 9300 or case nitrided for Nitralloy for a very hard wear-resistant surface. Gears that are case carburized will usually require grinding after the hardening operation because of distortion occurring during the heat-treating process. The nitrided materials offer the advantage of much less distortion during nitriding and therefore can be used in the as-nitrided condition without additional finishing. This is very helpful for large gears with small cross sections where distortion can be a problem. Since case depth for nitriding is limited to approximately 0.020 in., case crushing can occur if the load is too high. Some of the steel alloys used in the gearing industry are listed in table IV.

Gear surface fatigue strength and bending strength can be improved by shot peening (refs. 5 and 21). Figure 4 from reference 5 is a plot of the surface fatigue life of standard ground AISI 9310 gears and standard ground and shot-peened AISI 9310 gears. The 10-percent surface fatigue life of the shot-peened gears was 1.6 times that of the standard ground gears.

The low- and medium-alloy steels have a limited operating temperature above which they begin to lose their hardness and strength, usually around 300° F. Above this temperature the material is tempered, and early bending failures, surface pitting failures, or scoring will occur. To avoid this

condition, a material is needed that has a higher tempering temperature and that maintains its hardness at high temperatures. The generally accepted minimum hardness required at operating temperature is Rockwell C58. In recent years several materials have been developed that maintain a Rockwell C58 hardness at temper- atures from 450° to 600° F (ref. 3). Some of these materials have been or will be tested for surface fatigue life in the NASA gear test facility and the results compared with those for the standard aircraft gear material AISI 9310. Several materials have shown promise of improved life at normal operating temperature. The hot hardness data indicate that they will also provide good fatigue life at higher operating temperatures.

AISI M-50 has been used successfully for several years as a rolling-element bearing material for temperatures to 600° F (refs. 22 to 26). It has also been used for lightly loaded accessory gears for aircraft applications at high temperatures. However, the standard AISI M-50 material is generally considered too brittle for more heavily loaded gears.

AISI M-50 is considerably better as a gear material when forged with integral teeth. Figure 5(a) is a cross section through a forged AISI M-50 gear showing the excellent grain flow and good tooth shape that improves the bending strength. The grain flow from the forging process improves the bending strength and impact resistance of the AISI M-50 considerably (ref. 27).

The M-50 material can also be ausforged with gear teeth to give good bending strength and better pitting life (refs. 2 and 28). Figure 5(b) is a cross section through an ausforged gear tooth. The tooth is poorly formed because of the lower ausforging temperature (around 1400° F), and some of the good grain flow had to be cut away during finishing of the gear. Further, the ausforging temperature is so low that forging gear teeth is very difficult and expensive. As a result, ausforging for gears has considerably limited application (ref. 2).

Figure 6 is a Weibul plot comparing the forged AISI M-50 and ausforged AISI M-50 gear surface fatigue test data with the standard AISI 9310 steel data. The Weibul plot shows the percentage of specimens failed as a function of the system (two gears) life in stress cycles. These test data were taken with a superrefined naphthenic mineral oil lubricant, a speed of 10 000 rpm, a temperature of 170° F, a maximum Hertz stress of 248 000 psi with an 8-in. diametral pitch, and a 3.5-in.-pitch-diameter gear. The results show that the forged and ausforged gears can give lives approximately 5 times those of the standard AISI 9310 gears (ref. 2).

Nitralloy N is a low-alloy nitriding steel that has been used for several years as a gear material. It can be used for applications requiring temperatures of 400° to 450° F. A modified Nitralloy N called Super Nitralloy or 5Ni-2Al Nitralloy was used in the United States Supersonic Aircraft Program for gears. It can be used for gear applications requiring temperatures to 500° F. A Weibul plot of the surface fatigue data for the Super Nitralloy gears is shown in figure 7.

Two materials that were developed for case-carburized tapered roller bearings but also show promise as high-temperature gear materials are CBS 1000M and CBS 600 (refs. 29 and 30). These materials are low- to medium-alloy steels that can be carburized and hardened to give a hard case of Rockwell C60 with a core of Rockwell C38. Weibul plots of the surface fatigue test results for CBS 600 and AISI 9310 are shown in figure 7. The CBS 600 has a medium fracture toughness that could cause fracture failures after a surface fatigue spall has occurred.

Two other materials that have recently been developed as advanced gear materials are EX-53 and EX-14. Reference 31 reports that the fracture toughness of EX-53 is excellent at room temperature and improves considerably as

temperature increases. These materials are presently being evaluated for surface fatigue in the NASA gear test facility. The EX-53 surface fatigue results show a 10-percent life that is twice that of the AISI 9310.

Vasco X-2 is a high-temperature gear material (ref. 32) that is currently being used in advanced CH 47 helicopter transmissions. This material has an operating temperature limit of 600° F and has been shown to have good gear load-carrying capacity when properly heat treated. The material has a high chromium content (4.9 percent) that oxidizes on the surface and can cause soft spots when the material is carburized and hardened. A special process has been developed that eliminates these soft spots when the process is closely followed (ref. 33). Several groups of Vasco X-2 with different heat treatments were surface fatigue tested in the NASA gear test facility. All groups except the group with the special processing gave poor results (ref. 4). Figure 9 is a Weibul plot of these data showing the variation of surface fatigue life with different heat treatment processes. Vasco X-2 has a lower fracture toughness than AISI 9310 and is subject to tooth fracture after a fatigue spall.

REFERENCES

1. Townsend, D. P.; and Zaretsky, E. V.: A Life Study of AISI M-50 and Super Nitralloy Spur Gears With and Without Tip Relief. J. Lubr. Technol., vol. 96, no. 4, Oct. 1974, pp. 583-590.
2. Townsend, D. P.; Bamberger, E. N.; and Zaretsky, E. V.: A Life Study of Ausforged, Standard Forged, and Standard Machined AISI M-50 Spur Gears. J. Lubr. Technol., vol. 98, no. 3, July 1976, pp. 418-425.
3. Anderson, N. E.; and Zaretsky, E. V.: Short-Term, Hot-Hardness Characteristics of Five Case-Hardened Steels. NASA TN D-8031, 1975.
4. Townsend, D. P.; and Zaretsky, E. V.: Endurance and Failure Characteristics of Modified Vasco X-2, CBS 600 and AISI 9310 Spur Gears. J. Mech. Des., vol. 103, no. 2, Apr. 1981, pp. 506-515.
5. Townsend, D. P.; and Zaretsky, E. V.: Effect of Shot Peening on Surface Fatigue Life of Carbonized and Hardened AISI 9310 Spur Gears. NASA TP-2047, 1982.
6. Townsend, D. P.; Coy, J. J.; and Zaretsky, E. V.: Experimental and Analytical Load-Life Relation for AISI 9310 Steel Spur Gears. J. Mech. Des., vol. 100, no. 1, Jan. 1978, pp. 54-60.
7. Fusaro, R. L.: Effects of Atmosphere and Temperature on Wear, Friction and Transfer of Polyimide Films. ASLE Trans., vol. 21, no. 2, Apr. 1978, pp. 125-133.
8. Fusaro, R. L.: Tribological Properties at 25° C of Seven Polyimide Films Bonded to 440C High-Temperature Stainless Steel. NASA TP-1944, 1982.
9. Fusaro, R. L.: Polyimides. Tribological Properties and Their Use as Lubricants. Presented at the 1st Technical Conference on Polymides (Ellenville, N.Y.), Nov. 10-12 1982.
10. Johansen, K. M.: Investigation of the Feasibility of Fabricating Bimetallic Coextruded Gears. AFAPL-TR-73-112, AiResearch Mfg. Co., Dec. 1973. (AD-776795.)
11. Hirsch, R. A.: Lightweight Gearbox Development for Propeller Gearbox System Applications Potential Coatings for Titanium Alloy Gears. AFAPL-RT-72-90, General Motors Corp., Dec. 1972. (AD-753417.)
12. Delgrosso, E. J., et al.: Lightweight Gearbox Development for Propeller Gearbox Systems Applications. AFAPL-TR-71-41-PH-1, Hamilton Standard, Aug. 1971. (AD-729839.)

13. Manty, B. A.; and Liss, H. R.: Wear Resistant Coatings for Titanium Alloys. FR-8400, Pratt & Whitney Aircraft, Mar. 1977. (AD-A042443).
14. Dudley, D. W.: Gear Handbook, The Design, Manufacture and Applications of Gears. McGraw Hill Book Co., 1962.
15. Michalec, G. W.: Precision Gearing Theory and Practice. John Wiley & Sons Inc., 1966.
16. AGMA Standard for Rating the Strength of Spur Gear Teeth. AGMA 220.02, American Gear Manufacturers Association, Aug. 1966.
17. AGMA Standard for Surface Durability (Pitting) of Spur Gear Teeth. AGMA 210.02, American Gear Manufacturers Association, Jan. 1965.
18. Smith, W. E.: Ferrous-Based Powder Metallurgy Gears. Gear Manufacture and Performance, P. J. Guichelaar, B. S. Levy, and N. M. Parikh, eds., American Society for Metals, 1974, pp. 257-269.
19. Antes, H. W.: P/M Hot Formed Gears. Gear Manufacture and Performance, P. J. Guichelaar, B. S. Levy, and N. M. Parikh, eds., American Society for Metals, 1974, pp. 271-292.
20. Ferguson, B. L.; and Ostberg, D. T.: Forging of Powder Metallurgy Gears. TARADCOM-TR-12517, TRW-ER-8037-F, TRW, Inc., May 1980. (AD-A095556.)
21. Straub, J. C.: Shot Peening in Gear Design. AGMA Paper 109.13, June 1964.
22. Hingley, C. G.; Southerling, H. E.; and Sibley, L. B.: Supersonic Transport Lubrication System Investigation. (AL65T038 SAR-1, SKF Industries, Inc.; NASA Contract NAS3-6267.) NASA CR-54311, May 1965.
23. Bamberger, E. N.; Zaretsky, E. V.; and Anderson, W. J.: Fatigue Life of 120-mm-Bore Ball Bearings at 600° F with Fluorocarbon, Polyphenyl Ether and Synthetic Paraffinic Base Lubricants. NASA TN D-4850, 1968.
24. Zaretsky, E. V.; Anderson, W. J.; and Bamberger, E. N.: Rolling-Element Bearing Life from 400° to 600° F. NASA TN D-5002, 1969.
25. Bamberger, E. N.; Zaretsky, E. V.; and Anderson, W. J.: Effect of Three Advanced Lubricants on High-Temperature Bearing Life. J. Lubr. Technol., vol. 92, no. 1, Jan. 1970, pp. 23-33.
26. Bamberger, E. N.; and Zaretsky, E. V.: Fatigue Lives at 600° F of 120-Millimeter-Bore Ball Bearings of AISI M-50, AISI M-1 and WB-49 Steels. NASA TN D-6156, 1971.
27. Bamberger, E. N.: The Development and Production of Thermo-Mechanically Forged Tool Steel Spur Gears. (R73AEG284, General Electric Co.; NASA Contract NAS3-15338). NASA CR-121227, July 1973.
28. Bamberger, E. N.: The Effect of Ausforming on the Rolling Contact Fatigue Life of a Typical Bearing Steel. J. Lubr. Technol., vol. 89, no. 1, Jan. 1967, pp. 63-75.
29. Jatczak, C. F.: Specialty Carburizing Steels for Elevated Temperature Service. Met. Prog., vol. 113, no. 4, Apr. 1978, pp. 70-78.
30. Townsend, D. P.; Parker, R. J.; and Zaretsky, E. V.: Evaluation of CBS 600 Carburized Steel as a Gear Material. NASA TP-1390, 1979.
31. Culler, R. A.; Goodman, E. C.; Hendrickson, R. R.; and Leslie, W. C.: Elevated Temperature Fracture Toughness and Fatigue Testing of Steels for Geothermal Applications. TERRATEK Report No. Tr 81-97, Terra Tek, Inc., Oct. 1981.
32. Roberts, G. A.; and Hamaker, J. C.: Strong, Low Carbon Hardenable Alloy Steels. U.S. Patent No. 3,036,912, May 29, 1962.
33. Cunningham, R. J.; and Lieberman, W. N. J.: Process for Carburizing High Alloy Steels. U.S. Patent No. 3,885,995, May 27, 1975.

TABLE I. - PROPERTIES OF PLASTIC GEAR MATERIALS

Property	ASTM	Acetate	Nylon	Polyimide
Yield strength, psi	D 638	10 000	11 800	10 500
Shear strength, psi	D 732	9510	9600	11 900
Impact strength (Izod)	D 256	1.4	0.9	0.9
Elongation at yield, percent	D 638	15	5	6.5
Modulus of elasticity, psi	D 790	410 000	410 000	460 000
Coefficient of linear thermal expansion, in./in.°F	D 696	4.5×10^{-5}	4.5×10^{-5}	2.8×10^{-5}
Water absorption (24 hr), percent	D 570	0.25	1.5	0.32
Specific gravity	D 792	1.425	1.14	1.43
Temperature limit, °F	-----	250	250	600

TABLE II. - PROPERTIES OF COPPER ALLOY GEAR MATERIALS

Material	Modulus of elasticity, psi	Yield strength, psi	Ultimate strength, psi
Yellow brass	15×10^6	50 000	60 000
Naval brass	15	45 000	70 000
Phosphor bronze	15	40 000	75 000
Aluminum bronze	19	50 000	100 000
Manganese bronze	16	45 000	80 000
Silicon bronze	15	30 000	60 000
Nickel-tin bronze	15	25 000	50 000

TABLE III. - PROPERTIES OF SINTERED POWDER-METAL ALLOY GEAR MATERIALS

Composition	Ultimate tensile strength, psi	Apparent hardness, Rockwell	Comment
1 to 5Cu-0.6C-94Fe	60 000	B60	Good impact strength
7Cu-93Fe	32 000	B35	Good lubricant impregnation
15Cu-0.6C-84Fe	85 000	B80	Good fatigue strength
0.15C-98Fe	52 000	A60	Good impact strength
0.5C-96Fe	50 000	B75	Good impact strength
2.5Mo-0.3C-1.7N-95Fe	130 000	C35	High strength, good wear
4Ni-1Cu-0.25C-94Fe	120 000	C40	Carburized and hardened
5Sn-95Cu	20 000	H52	Bronze alloy
10Sn-87Cu-0.4P	30 000	H75	Phosphorus-bronze alloy
1.5Be-0.25Co-98Cu	80 000	B85	Beryllium alloy

TABLE IV. - PROPERTIES OF STEEL ALLOY GEAR MATERIALS

Material	Tensile strength, psi	Yield strength, psi	Elongation in 2 in., percent
Cast iron	45 000	------	---
Ductile iron	80 000	60 000	3
1020	80 000	70 000	20
1040	100 000	60 000	27
1066	120 000	90 000	19
4146	140 000	128 000	18
4340	135 000	120 000	16
8620	170 000	140 000	14
8645	210 000	180 000	13
9310	185 000	160 000	15
440C	110 000	65 000	14
416	160 000	140 000	19
304	110 000	75 000	35
Nitralloy 135M	135 000	100 000	16
Super Nitralloy	210 000	190 000	15
CBS 600	222 000	180 000	15
CBS 1000M	212 000	174 000	16
Vasco X-2	248 000	225 000	6.8
EX-53	171 000	141 000	16
EX-14	169 000	115 000	19

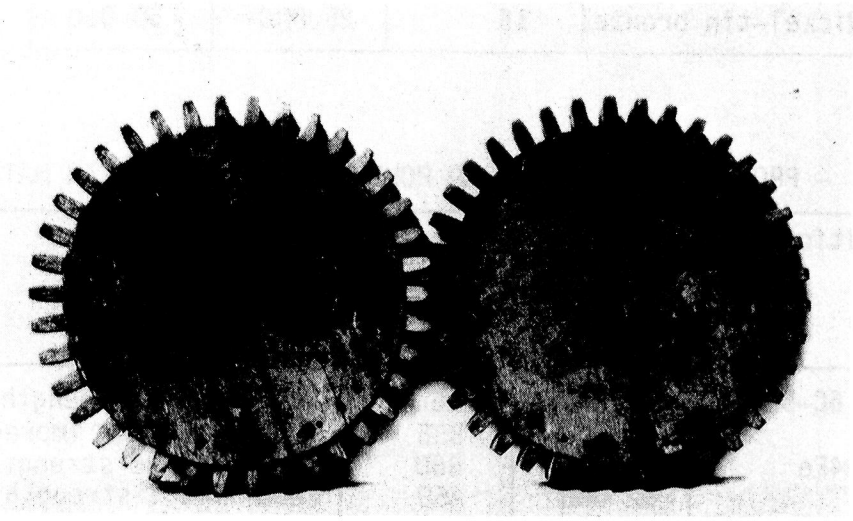

C-83-1244

Figure 1. - Early wooden gears (courtesy Smithsonian Institution).

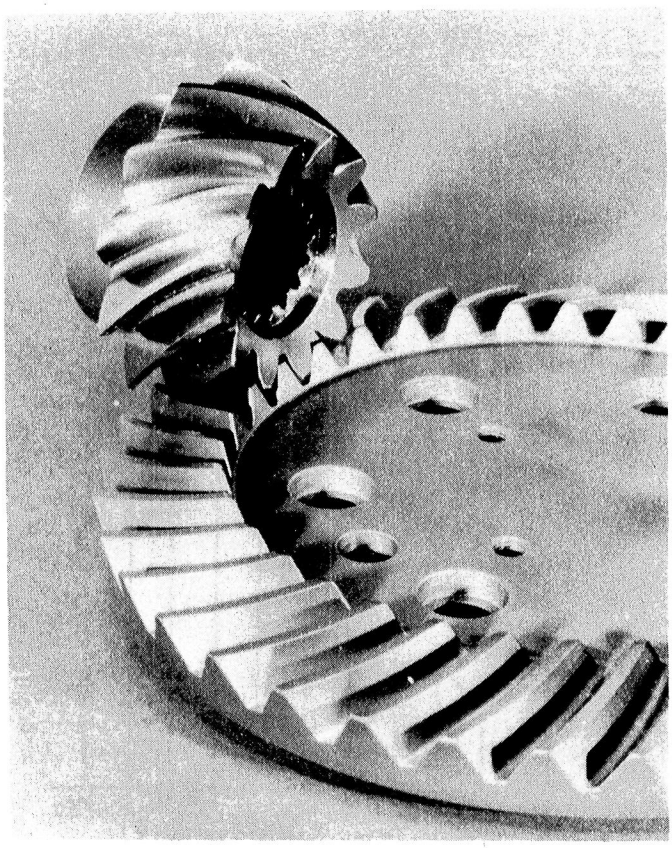

C-77-117

Figure 2. - High-alloy, precision-manufactured aircraft spiral-bevel gear set.

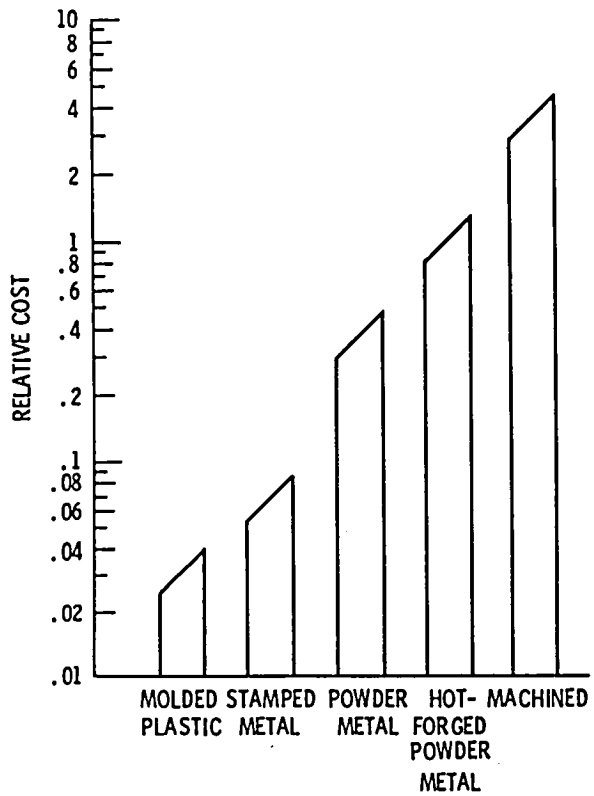

Figure 3. - Relative costs of gear materials.

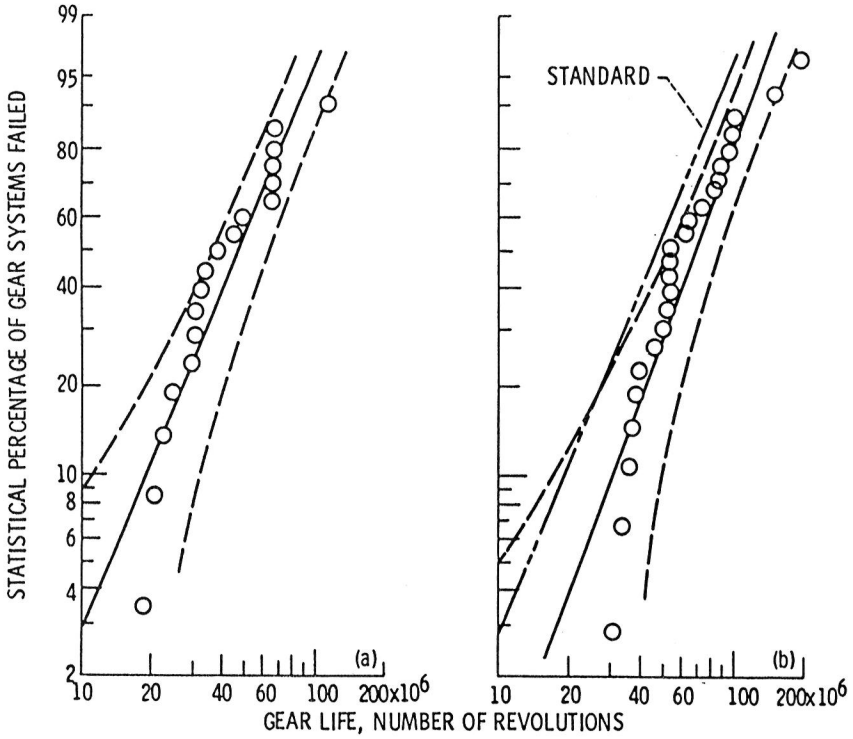

(a) Standard gears.
(b) Shot-peened gears.

Figure 4. - Surface (pitting) fatigue lives of standard ground and shot-peened carburized and hardened CVM AISI 9310 steel spur gear systems. Speed, 10 000 rpm; lubricant, synthetic paraffinic oil; gear temperature, 170° F; maximum Hertz stress, 248 000 psi.

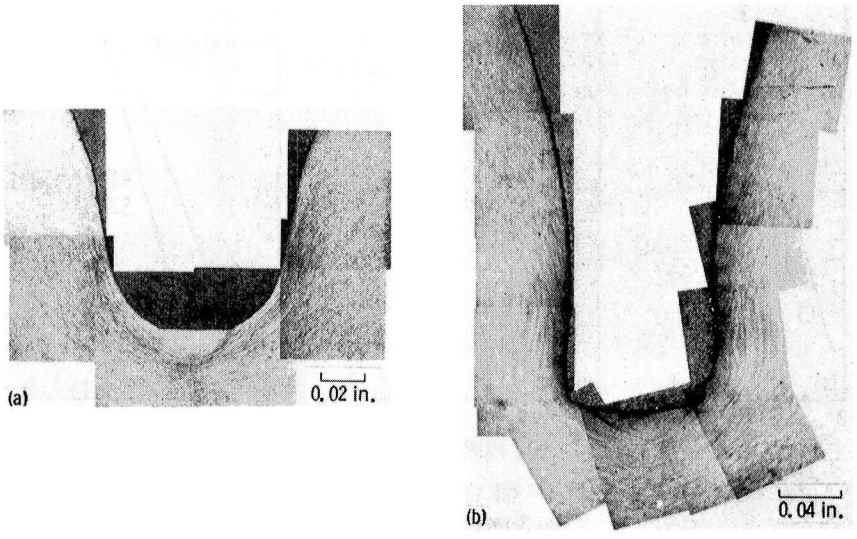

(a) Standard forged AISI M-50 gear.
(b) Ausforged AISI M-50 gear.

Figure 5. - Photomicrographs of macro grain flow patterns. Etchant, 3 percent nital.

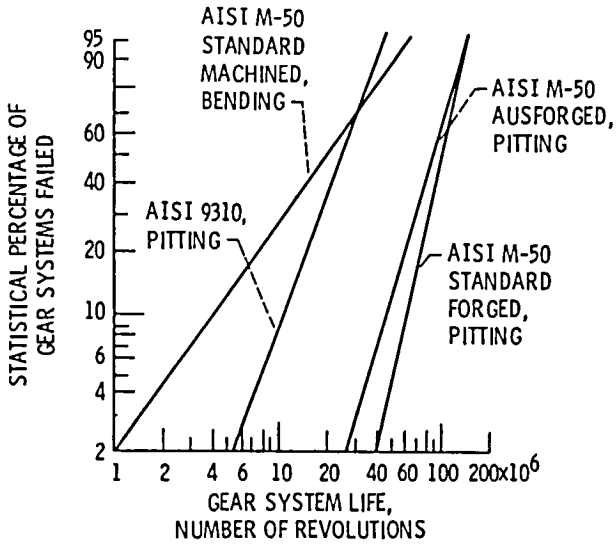

Figure 6. - Fatigue lives of spur gear systems made of VIM-VAR AISI M-50 and VAR AISI 9310. Speed, 10 000 rpm; temperature, 70° F; maximum Hertz stress, 248 000 psi; maximum bending stress at tooth root, 38 700 psi; lubricant, superrefined naphthenic mineral oil.

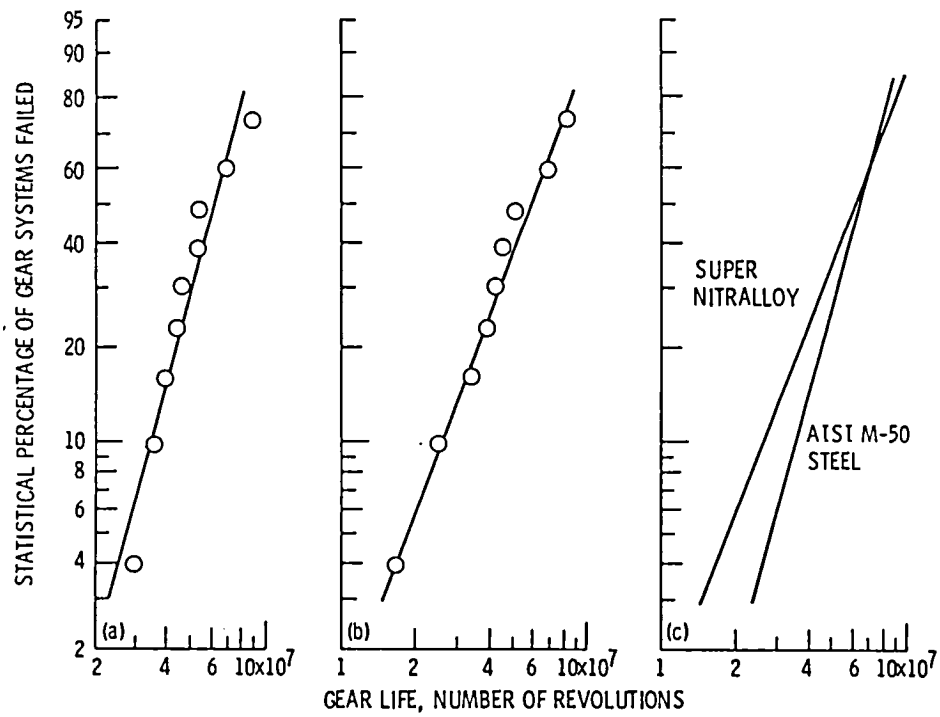

(a) AISI M-50 steel.
(b) Super Nitralloy (5Ni-2Al).
(c) Comparison of results.

Figure 7. - Surface (pitting) fatigue lives of spur gear systems made of CVM AISI M-50 steel and CVM Super Nitralloy (5Ni-2Al). Speed, 10 000 rpm; temperature, 170° F; maximum Hertz stress, 275 000 psi; lubricant, superrefined naphthenic mineral oil.

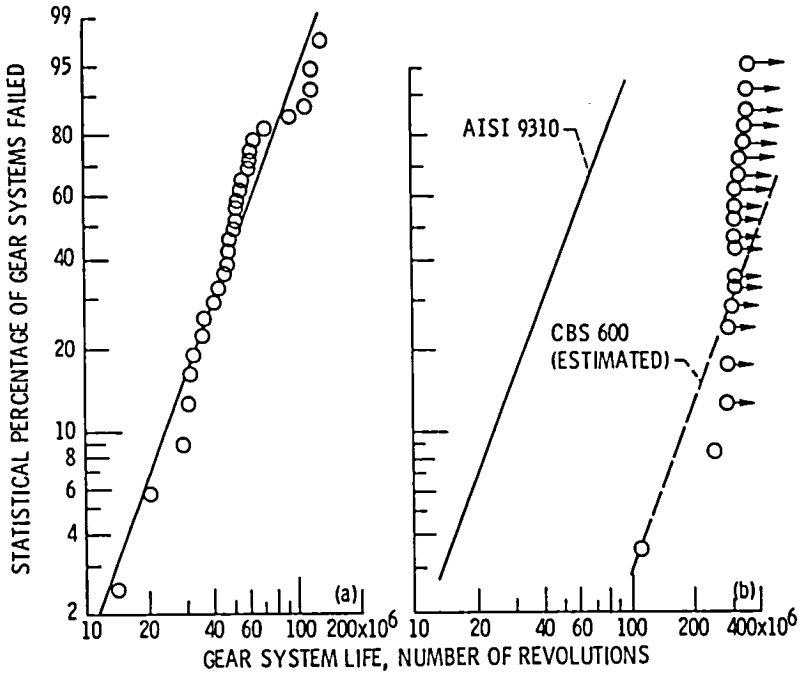

(a) CVM AISI 9310.
(b) Air-melt CBS 600.

Figure 8. - Surface (pitting) fatigue lives of spur gear systems made of CVM AISI 9310 and air-melt CBS 600. Speed, 10 000 rpm; temperature, 170° F; maximum Hertz stress, 248 000 psi; lubricant, synthetic paraffinic oil with 5 percent EP additive.

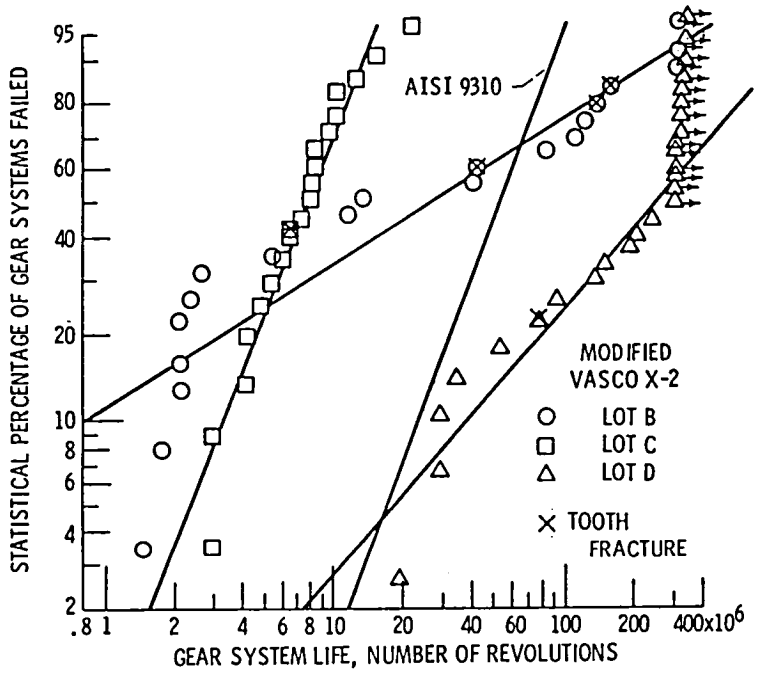

Figure 9. - Surface (pitting) fatigue lives of CVM modified Vasco X-2 spur gears heat treated to different specifications. Pitch diameter, 3.5 in.; speed, 10 000 rpm; maximum Hertz stress, 248 000 psi; lubricant, synthetic paraffinic oil.

STATUS OF UNDERSTANDING FOR SEAL MATERIALS

P.F. Brown
Pratt & Whitney Aircraft
East Hartford, Connecticut

Material selection for mainshaft face and ring seals, labyrinth seals, accessory gearbox face seals and lip seals are discussed in light of tribology requirements and a given seal application. Carbon graphite has been found to be one of the best sealing materials and it is widely used in current gas turbine mainshaft and accessory gearbox seals. Its popularity is due to its unique combination of properties which consists of dimensional stability, corrosion resistance, low friction, good self lubricating characteristics, high thermal conductivity and low thermal expansion, the latter two properties combining to provide good thermal shock resistance. A brief description of the seals and the requirements they must meet are discussed which provides an insight into the limitations and advantages of the seals in containing the lubricant. A forecast is made of the operational requirements of main shaft and gearbox seals for advanced engines and candidate materials and coatings that may satisfy these advanced engine requirements.

INTRODUCTION

Bearing compartments in gas turbine engines must be effectively isolated from the engine gases to avoid excessive heating of the bearings, contamination and degradation of the lubricant, possible combustion of the lubricant and disruption of the oil flow. In the main shaft bearing compartments, some areas are in locations that must be sealed against gases of relatively high temperatures and pressures. Other seals, used in accessory gearbox locations, must be optimized for operation at very low or zero pressure differential conditions while preventing the leakage of hot oil.

This paper focuses on material selection, including coatings, of mainshaft and accessory seals that can operate within this hostile environment. Main shaft and accessory seals depend on proper materials to provide adequate durability and to assist in minimizing leakage. Each gas turbine engine application presents a set of mainshaft sealing requirements that dictate the selection of one or more of the three basic types; ring seal, face seal and labyrinth seal. For accessory gearbox sealing, the package face seal and the elastomeric lip seal are typically used. The selection of one seal design system over another has been well described in reference 1. In commercial and military engine applications the variety of engine designs requires continued use of all the seal types mentioned. Each of these seal types will be reviewed for the impact of material selection on seal design. Operating parameters such as temperature, pressure differentials and surface speeds that influence material selection will be studied in light of current practice. With higher rotor speeds and higher cycle pressures and temperatures, the challenge of providing sealing in the rotor support system increases. These advanced engine requirements and new materials being developed to satisfy sealing requirements of future engines will be examined in this paper.

Engine Mainshaft and Accessory Seal Requirements

In a gas turbine engine that employs bearings and gears which are self-lubricating and self-cooling, only a simple rotor support system is required as described in reference 1. This system is represented in figure 1 for a simple turbojet engine. As shown, the main rotor is axially located by means of a ball thrust bearing. Primary radial support is provided by cylindrical roller bearings located on either end of the shaft. The accessory gearbox and its drive system is equally simple.

In a real engine, bearings and gears require cooling to carry away the heat generated by high speed operation. Lubricating oil is an excellent fluid for this purpose and has the advantage of providing long wear life for these mechanical components. However, this lubricant must be contained in sealed chambers as shown in figure 2. The types of seals employed to contain the lubricant and to minimize the leakage of high pressure air into the sealed compartments fall into three categories for main shaft use; namely, ring, face and labyrinth as explained in reference 2. For sealing accessory gearboxes the choices are the package face seal and the elastomeric lip seal.

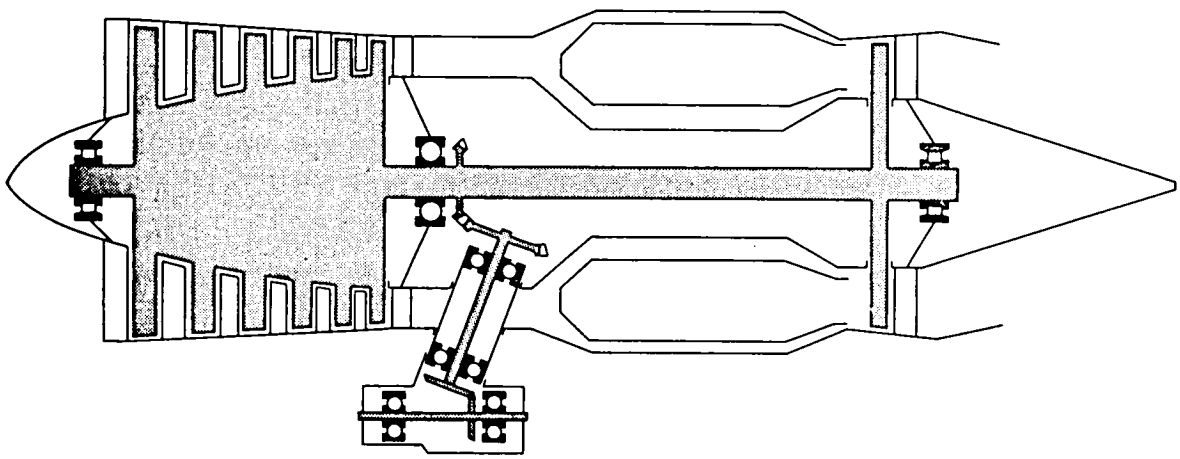

Figure 1 A Simple Gas Turbine Engine That Requires no Shaft Seal System if Self Lubricated and Cooled

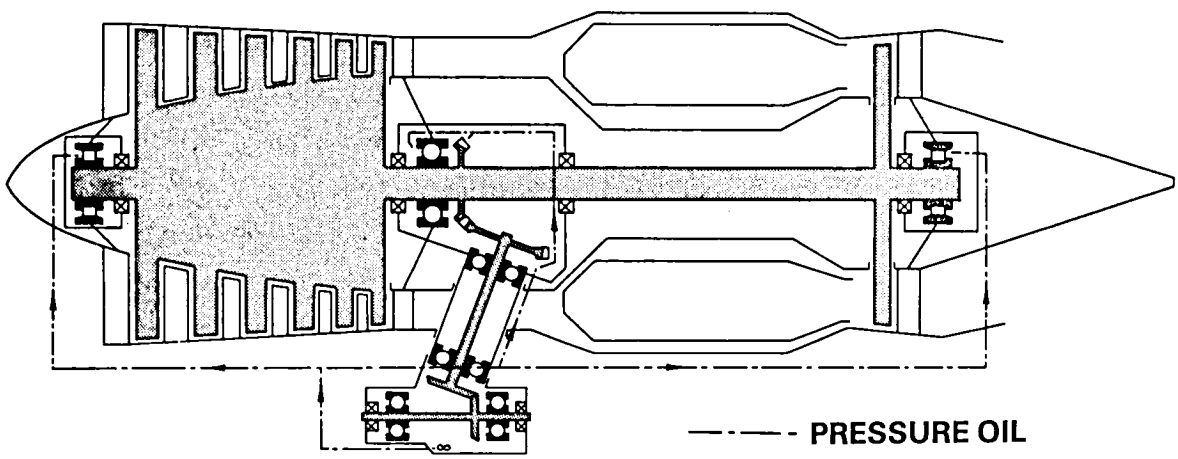

Figure 2 In Reality, Gas Turbine Engines Require Cooling Oil Adding the Complication of a Sealing System

Ring Seal

The ring seal is essentially a piston ring that may be either of the expanding or contracting design. The expanding design is the simpler of the two and is illustrated in figure 3. Other designs that can be grouped in the ring seal family include the circumferential segmented ring seal and the floating or controlled clearance ring seal as described in reference 3. The materials requirements for these seals are essentially the same as those for the expanding seal shown in figure 3. The seal rings are carbon and they seal radially against the inside diameter of the stationary cylindrical surface as well as axially against the faces of the adjacent metal seal seats. The metal seal seats are fixed to, and rotate with the shaft. The sealing closure force is provided by a combination of spring forces and gas pressures. Ring seals are employed where there is a large relative axial movement due to thermals between the shaft and the stationary structure. Ring seals are limited to operation at air pressure drops and sliding speeds that are considerably lower than those allowed for face seals. However, they can be used to gas temperature levels in the same range as for positive-contact face seals which is approximately 756K (900°F). Generally, a minimum pressure differential of 1.4 N/cm^2 (2 psi) must be maintained to prevent oil leakage from the bearing compartment.

Face Seal

The positive contact face seal was developed to provide better sealing at higher pressure differentials. A typical installation, as shown in figure 4, utilizes a carbon nosepiece to seal in the axial direction, and separate secondary seals to seal radially. The carbon nosepiece is usually assembled with a shrink fit into a metal housing called a carbon carrier. The nosepiece assembly is loaded both pneumatically and by springs to ensure contact between the carbon nosepiece and the seal seat. Torque pins are used to prevent rotation of the nosepiece assembly. The surface of the rotating seal seat which mates against the stationary carbon nosepiece is usually chrome plated or hard-face coated. The mechanical arrangements used in current applications have evolved from the early designs used in the J57 engine as outlined in reference 1. The face seal can operate at higher speeds, pressures and temperatures than ring seals since the interfacial pressures or rubbing loads can be made to approach zero by pressure balancing. This seal design can also be oil-cooled more readily.

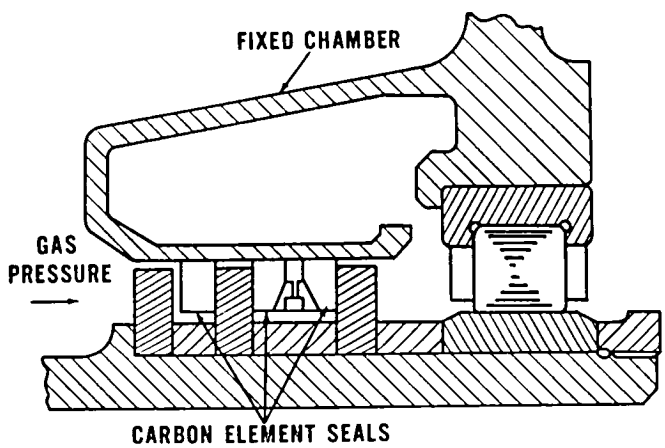

Figure 3 Expanding Type Ring Seals Are Used Where Large Thermally Induced Axial Movement Occurs

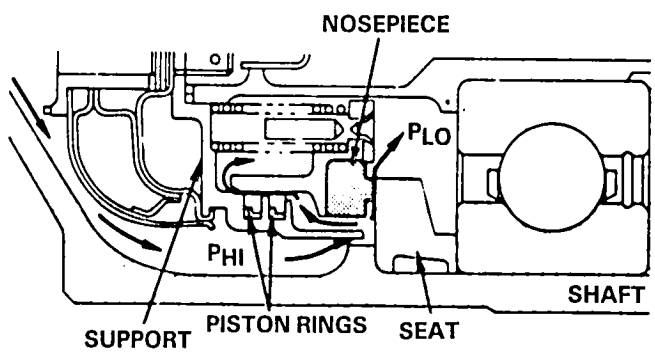

Figure 4 The Face Seal is Pressure Balanced Allowing Use at High Pressure Differentials

Current practice has been to generally limit the use of positive contact face seals to conditions not exceeding a pressure differential of 69 N/cm^2 (100 psi), a gas temperature of 756K (900°F), and a sliding speed of 107 m/sec (350 fps) although engine operation at sliding speeds to 138 m/sec (450 fps) has been achieved with this type of seal at the expense of pressure differential capability. In engines with higher pressure and temperature requirements, oil wetting of the carbon nosepiece/seal seat interface has allowed reliable operation at pressure differentials to 104 N/cm^2 (150 psi), gas temperatures to 894K (1150°F), at sliding speeds in excess of 122 m/sec (400 fps). Generally a minimum pressure differential of 2.0 N/cm^2 (3 psi) must be maintained for both types of face seals to prevent oil leakage from the bearing compartment.

Labyrinth Seal

The labyrinth seal is utilized frequently in a multiple seal configuration with pressurization and/or venting between seal stages. Early gas turbine engines employed simple nonbuffered and nonvented systems because cycle gas pressures and temperatures were low with little corresponding bearing compartment fire hazard. The more advanced engines in current use operate at high pressures and temperatures and a simple labyrinth seal system would permit excessive leakage of high temperature air which could ignite the engine lubricant. Consequently, the labyrinth seal system has evolved into a stepped, three stage system as shown in figure 5. Three stages and an extensive plumbing system are required to decrease the temperature of the air leakage into the bearing compartment to satisfactory levels. The high pressure, high temperature air must not be permitted to enter the compartment directly so it is vented overboard between the first and second stages. Relatively low temperature pressurized air must be used between the second and third stages to provide a positive pressure drop across the third stage so that the leakage flow into the bearing compartment is relatively cool air, thereby increasing fire safety. Minimization of seal clearance is of prime importance for obtaining maximum labyrinth seal effectiveness since leakage is approximately proportional to clearance. Adequate clearance to guarantee structural integrity of the seal must be established, taking into consideration dynamic growth, anticipated thermal expansion, shaft motion, tolerance buildup, and runouts.

Simple, single stage labyrinth seal systems have been used at pressure differentials up to 34 N/cm^2 (50 psi) and gas temperatures to 589K (600°F). Multistage labyrinth seal systems have been used at pressure differentials up to 280 N/cm^2 (400 psi) and gas temperatures of approximately 922K (1200°F). Rotational speed is not a limitation for this type of seal design. Generally a minimum pressure differential of 2.0 N/cm^2 (3 psi) must be maintained to prevent oil leakage from the bearing compartment.

Accessory Gearbox Face Seal

In a typical accessory gearbox face seal application (fig. 6), the primary seal ring, made of carbon graphite, is stationary and is loaded against the rotating mating ring by means of a wave spring which seats in a roll formed stainless steel cup. This cup forms a "package" around the seal and has an anti-rotation device that mates with a notch in the primary seal ring. The secondary seal is provided by an elastomeric O-ring which is held in place in its counterbore groove by a flat washer located between the back face of the primary carbon seal ring and the wave spring. This flat washer also prevents the wave spring from grooving the carbon surface. In some accessory applications the carbon primary ring is loaded to rub directly against the end of a shaft eliminating the need for the use of a separate mating ring and its

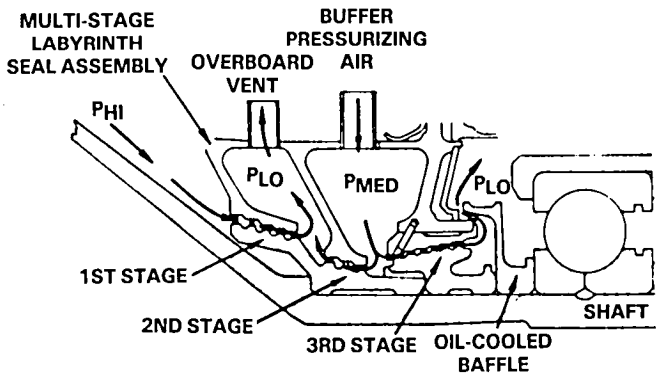

Figure 5 Labyrinth Seal Systems Feature Multiple Seal Stages to Control Leakage

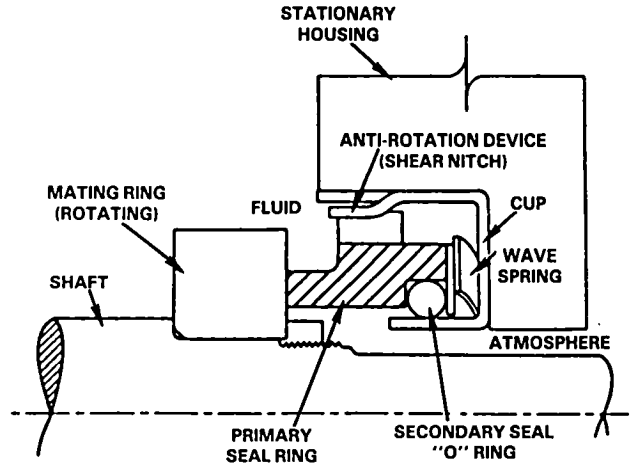

Figure 6 Accessory Gearbox Face Seals Provide Convenient Package or Cartridge Type Construction

locking nut which is required to hold it in place on the shaft. The environmental temperatures encountered in the accessory gearbox application, as described in reference 1, do not normally exceed the range of 219K to 477K (-65°F to +400°F). The accessory face seal is used to retain the lubricating oil and to exclude dirt and moisture at differential pressures in the range of 0 to 3.3 N/cm^2 (0 to 5 psi) which are quite low compared to that encountered by main shaft seals. The speed is also considerably reduced from that seen by main shaft seals, 46 m/s (150 fps) as compared to 122 m/s (400 fps).

Accessory Gearbox Lip Seal

The radial elastomeric lip seal, like the package face seal, is used in accessory gearbox installations to retain the lubricating oil and to exclude dirt and moisture. The radial lip seal is limited in its speed capability, however, but has a cost advantage compared to the face seal. The rubber lip seal functions by means of an interference fit between the flexible sealing element and a shaft, as depicted in figure 7. As described in reference 4, rubber interacts with oils and can lose tension and elasticity. As a result, a spring is provided to augment lip pressure. Fluid retention is based on a precise amount of lip contact pressure and interference. Enough interference must be designed into the seal to offset rubber tension and compression set, lip swell due to interaction with hot oils and thermal expansion. In addition, interference must be present to overcome shaft eccentricity and shaft-to-bore misalignment.

The use of radial lip seals is normally limited to applications that do not exceed 20 m/s (4000 fpm) rubbing speeds with most such seals employed at speeds below 12 m/s (2400 fpm). The higher speed applications, such as in helicopter transmissions, are correspondingly low in operating temperature, i.e., 366K (200°F) or below. Jet engine accessory applications will run hotter, sometimes above 450K (350°F), limiting lip seal surface speeds to levels below 6 m/s (1200 fpm). As cited in reference 5, these seals are not to be used at pressure differentials that exceed 4.7 N/cm^2 (7 psi) at lower speeds of 0-5 m/s (0-1000 fpm), with lower pressures of 2 N/cm^2 (3 psi) not to be exceeded when the shaft speed is above 10 m/s (2000 fpm).

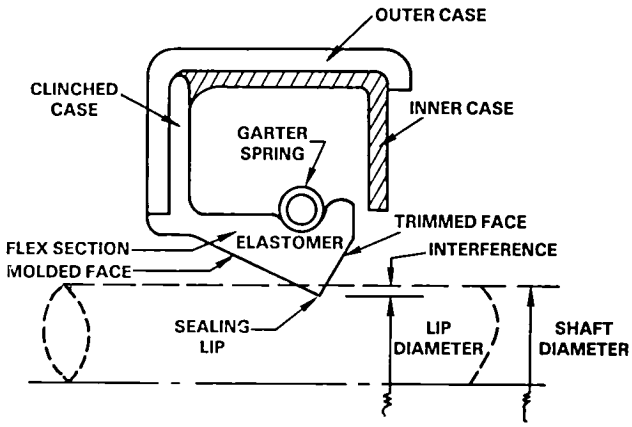

Figure 7 Radial Elastomer Lip Seal Functions by Means of Interference with the Shaft

Table 1
Ideal Properties of Seal Face Materials

Mechanical:	High modulus of elasticity High tensile strength Low coefficient of friction Excellent wear characteristics and hardness Self lubricating
Thermal:	Low coefficient of expansion High thermal conductivity Thermal shock resistance Thermal stability
Chemical:	Corrosion resistant Good wetability
Miscellaneous:	Dimensional stability Good machinability and ease of manufacture Economical and readily available

Materials for Main Shaft Face Seals and Ring Seals

The selection of the correct materials for a given seal application will ensure desired performance and durability. Components of the seal for which material selection is critical from a tribology standpoint are the stationary nosepiece or primary seal ring and the mating ring or seal seat which is the rotating element. Another important pair of tribological mating parts in the face seal assembly is the secondary seals or expanding piston rings and the mating surface upon which they must slide axially.

Considering the primary seal ring first, Table 1 lists the properties that are considered ideal for this element as described in reference 6. The material that rates high in terms of satisfying these properties is graphitic carbon which is used extensively for one of the mating faces in rubbing contact shaft seals. It is used in more than 95% of end face seal applications.

Carbon graphite as explained in reference 7 is one of the best sealing materials. It can run in face seals against itself, metals, or ceramics without galling or seizing. It is dimensionally stable over a wide temperature range and has excellent corrosion resistance. It has a high thermal conductivity which helps to dissipate heat generated at the rubbing interface of the seal. Its low thermal expansion, together with its high thermal conductivity, provide excellent thermal shock resistance. In spite of these good properties, the carbon material must be treated in order for it to satisfy the operational requirements in jet engine main rotor bearing compartment sealing applications. Typically, the seals must keep the lubricating oil system separate from air at pressures of 83 N/cm^2 (120 psig), at temperatures to 970K (1100°F) and surface speeds to 122 m/sec.(400 fps). The carbon graphite sealing rings are impregnated with other materials as discussed in reference 8 to increase strength and resistance to oxidation, adding to its ability to provide dependable service in this application.

Graphite has been referred to as self-lubricating which may be due to its sheet like structure and the weak van der Waals bonds between the sheets. This may be a factor in some applications, but generally, the lubrication results from the formation of a transfer film between the graphite and the mating surface. This film appears dependent on the presence of polar liquids, oxygen or water vapor. Graphite operating

at high temperatures, as in a gas turbine engine main shaft face seal, does not form a suitable interfacial film, in which case, special grades of graphite containing impregnants are used.

As described in reference 9, there are five general classes of seal carbons; resin impregnated, metal impregnated, film-forming impregnated, anti-oxidant impregnated and ceramic impregnated. The resin impregnated type and the anti-oxidant impregnated, are widely used in gas turbine engines. The resin impregnated type is normally limited to use in lower temperature accessory gearbox applications while the anti-oxidant impregnated type is used in the higher temperature main shaft seals.

Work on new carbon materials has resulted in making carbons with improved wear and oxidation resistance available to the seal designer. Various chemical treatments that were examined have been found to reduce oxidation rates by orders of magnitude. Seals have been tested as described in reference 10 which can be used in air at 922K (1200°F). The carbon grades that can operate at these temperatures usually contain a fine grained graphite impregnated with an inorganic salt. Improvement in oxidation resistance has been accompanied by significant advances in other material properties. Optimization of raw material powder particle size has produced grades which have isotropic fine grained microstructures. These grades can be machined to the very tight tolerances of proposed seal designs. Material permeability and porosity has been overcome by chemical impregnation of the molded product, or by a combination of filler particles, concentration of chemical binder, or by hot pressing the carbon. Various manufacturers have published the properties of commercially available grades. Table 2 taken from reference 9 summarizes typical properties of mechanical carbons.

Table 2

Carbon-Graphites for Aerospace Seals

Property/Type	Resin Impregnated	Metal Impregnated	Film Forming Impregnated	Anti-Oxidant Impregnated	Ceramic Impregnated
Strength, MPa (psi)					
Compressive	172 (25,000)	207 (30,000)	207 (30,000)	138 (20,000)	172 (25,000)
Flexural	69 (10,000)	83 (12,000)	62 (9,000)	48 (7,000)	69 (10,000)
Tensile	48 (7,000)	62 (9,000)	48 (7,000)	35 (5,000)	48 (7,000)
Modulus, GPa (psi x 10^{-6})	20.7 (3.0)	27 (3.9)	20.7 (3.0)	12.4 (1.8)	16.5 (2.4)
Density, gm/cc	1.80	2.40	1.85	1.80	2.00
Hardness, Scleroscope	75	80	85	70	80
Temperature Limit, K (°F)					
Neutral	533 (500)	1089 (1500)	1089 (1500)	1089 (1500)	950 (1250)
Oxidizing	505 (450)	533 (500)	533 (500)	866 (1100)	950 (1250)
Coefficient of Thermal Exp., m/m°K x 10^6	5.4	5.4	4.5	4.5	4.5
(in./in. °F x 10^6	(3.0)	(3.0)	(2.5)	(2.5)	(2.5)
Permeability, Darcies x 10^6	0.01	10	100	1000	0.01

In spite of these advances in carbon-graphite seal technology it is possible for materials made by different manufacturers to have identical physical properties, yet one material will perform well on an application while the other will fail miserably. Until the factors which control friction and wear are better understood, selection of carbon seal materials must remain somewhat of a trial and error process. In the 1950's and 1960's many grades of carbon were offered by the industry for use in aircraft engine seals. To evaluate the carbon material in a cost effective manner a seal material rig was developed as a screening device as described in references 1 and 11 and shown in figure 8. The rig exposes the seal ring, 12.45 cm (4.9 inch) in diameter and made of the candidate material, to increasing levels of sealing air pressure and temperature and ranks the carbon grades by wear rate. Accelerated endurance tests have been run on this rig with surface speeds to 61 m/s (200 fps) and closing forces and air temperatures high enough to cause wear rates in excess of 0.00254 cm (0.001 inch) per hour. The best of these carbon grades were subjected to engine evaluation and are providing good service even to this day. The screening rig is no longer in general use because very few advanced grades have been developed in recent years. However, the normal advanced engine development process accommodates the limited testing now required to evaluate the carbon material..

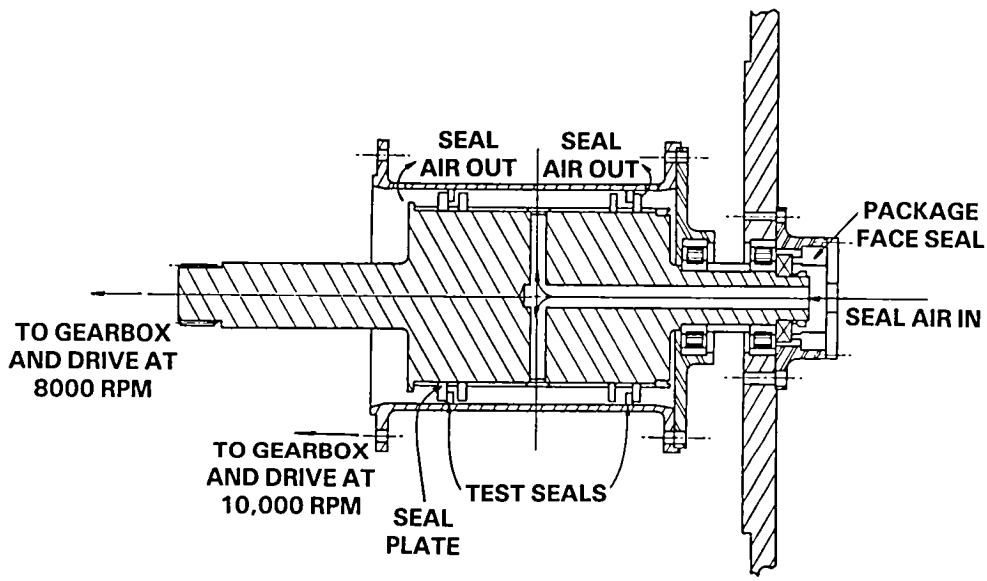

Figure 8 Seal Material Evaluation Rig

The mating ring against the engine carbon seal was developed in the 1950's. It was a fully hardened, heat and corrosion resistant wrought steel coated with a hard layer of chrome to enhance corrosion and wear resistance. Mating ring studies conducted in the 1960's on a variety of candidate metals and coatings, which were also tested in the seal materials screening rig, revealed that advanced grades of carbon were more wear compatible with a steel plate coated with flame deposited chrome carbide. This coating is still in wide use today providing good seal wear life in service engines.

The other pair of surfaces in the face seal assembly that must exhibit the proper tribological characteristics, i.e., low friction and wear, are the piston ring secondary seals and the bore surface against which it mates. In earlier designs discussed in reference 12, the cast iron, chrome flashed piston rings were seated against a carbon surface cylinder. Over long periods of time, wear of the carbon

surface in contact with the piston rings was severe enough to interfere with the axial motion of the nose piece assembly. The improved design consists of piston rings placed in contact with a hard surfaced steel cylinder. This configuration, together with improvements in piston ring material and circularity control has made the secondary seal a highly reliable, low leakage device.

Thus far in this section, attention has been limited to materials for main shaft face seals. The choice for main shaft ring seal materials is similar. In general, the ring seal is used in those sections of the engine where the pressures and shaft speeds are lower, and for the most part the temperatures are also less severe. This permits a wider latitude in selecting the carbon grade for the primary sealing ring since less resistance to oxidation is required. This, in general, allows a less expensive grade to be used. The lower oxidation resistant grades used in modern main shaft engine applications also have somewhat better mechanical properties which favors their use in ring seals as they are not mounted in a shrink fit steel carrier as in a face seal carbon ring, thus making them more exposed to mechanical damage during assembly. The ring seal, like the face seal, operate best when the carbon ring is mated against a hardened seal plate surface coated with either chrome plate or chrome carbide.

Materials for Labyrinth Seals

Bearing compartment labyrinth seals are used as primary seals to protect the compartment and as buffer seals to reduce the pressure imposed on carbon face seals. As described in reference 13 the labyrinth seal knife edges are solid metal and the lands are also solid metal or silver plate on nickel alloy substrate. Abradables used for the compressor interstage seal lands should be adequate for bearing compartment applications provided that temperature/life requirements are met, excessive debris which can contaminate the lubrication system is not generated, and heat generated during a rub does not lead to excessive oil coking or fire. A further description of abradable seal materials being developed for or currently used in modern aircraft engines is presented in references 13 and 14.

Materials for Accessory Gearbox Face Seals

Accessory gearbox face seal components for which material selection is critical from a tribology standpoint are the primary ring or nose piece and the mating or seal seat which is the rotating element (fig. 6). This is similar to the main shaft face seal which makes the graphitic carbon the best material choice for the nose piece and a hardened steel for the mating surface. As indicated in Table 3, the resin impregnated grade of carbon is the proper choice, and as described in reference 9, this type of carbon is impregnated with a low shrinkage thermosetting resin such as an epoxy, phenolic or polyester. Resin content ranges from 0.5 to 10% by weight. These types are preferred where fluid leakage through the seal must be held to a minimum. Because of their low permeability, these types have the best chance of generating a hydrodynamic film and providing very low wear rates. Generally, with these low temperature seals the mating ring does not require a corrosion resistant coating such as chrome plate used in main shaft seals. A lower cost, unplated steel surface is adequate as long as it is fully hardened with the proper surface finish and runout control. In many accessory gearbox applications the seal seat is integral with the end of a gear shaft made of a material which is carburized to a high hardness level. This provides a good mating surface for the carbon seal.

Table 3
Currently used elastomeric lip seal materials and a comparison of those characteristics of interest in jet engine applications

Properties	Nitriles (Buna N)	Acrylates	Silicones	Fluoro-elastomers	TFE Fluorocarbon
Durometer	70-80-90	70-80-90	80	80	-
Compression Set	Good	Fair	Good	Fair	Fair
Dry Running	Fair	Poor	Poor	Poor	Good
Swell	Low	Low	Medium	Low	Low to None
Abrasion Resistance	Good	Fair	Poor	Fair	Fair
Min. Operating Temp. K (°F)	219 (-65)	233 (-40)	224 (-75)	233 (-40)	189 (-120)
Max. Operating Temp. K (°F)	300 (+225)	422 (+300)	450 (+350)	477 (+400)	477 (+400)
Salt Water	Good	Poor	Good	Good	Good
MIL-L-7808 and MIL-L-23699	Fair	Poor	Good	Good	Good
Advantages	Low cost, good low temp. performance, low swell. Most commonly used in earlier engines.	Good moderate temp. performance, low swell.	Good low temp. properties	Low swell. Resistant to a wide variety of special lubricants.	Good low speed properties. Outstanding resistance to most fluids.
Disadvantages	Hardens in high temp. Not recommended for highly compounded lubricants (EP additives).	Poor low temp. properties, poor dry running.	High swell in some oils, poor dry running, more easily damaged in handling. Poor resistance to oxidized oils and some EP additives. Causes oil foaming.	High cost, special tooling.	Limited configurations available. Highest cost. More easily damaged.

The other element in the accessory seal assembly critical to its tribological performance is the secondary seal which is an elastomeric O-ring. The choice of the proper elastomer is similar for the elastomeric lip seal design but more emphasis is placed on the compression set and oil swell characteristics. A more complete discussion of elastomer types and their influence on seal performance will be presented in the following section on radial lip seals. The elastomer type most frequently chosen for the design of today's modern engines is fluorocarbon with TFE, which is described in Table 2.

The fluorocarbon elastomer has the widest temperature range capability, 189K to 477K (-120 to +400°F), outstanding resistance to most fluids and generally good to excellent swell characteristics in synthetic ester engine oils. However, fluorocarbon O-rings produced from different sources and certified to the same specification, i.e., MIL-R-83248, can behave differently when they operate in Type II engine oil per MIL-L-23699 as explained in reference 15.

Type II engine oils, available as Mobil Jet II, Exxon 2380, Aero Shell 500 and Castrol 5000 among others, contain additives which can have varied effects on fluorocarbon O-rings. Depending on the brand of fluorocarbon and the brand of oil, a permanent increase in O-ring diameter can occur that ranges from 2% minimum to over 5%. Growth levels of the O-ring in the higher end of this range can result in face seal hang up which will produce excessive leakage. The different additives and processing variations employed in making both the O-ring fluorocarbon elastomers and the different Type II lubricants obviously play a role in producing different swell rates. It is evident that a team effort by the seal manufacturer, O-ring supplier, elastomer formulator, carbon-graphite seal material manufacturer and engine designer must take place in order to develop a seal design that will function properly.

Lip Seal Materials

The basic radial lip seal came into being in the late 1930's with the advent of synthetic elastomers. They possessed a valued oil-resistant property and a higher temperature capability than natural rubber and could be molded in a variety of shapes. Buna-N, introduced in 1939, was among the first to be so employed. The introduction of quality bonding cements in the 1940's made it possible to bond the synthetic elastomer lip seal directly to its metal casing forming a unit that was ready to be installed. As a result, this oil tolerant, easily installed seal was readily adapted for use in the accessory gearbox of gas turbine aircraft engines introduced in the late 1940's. Advances in aircraft gas turbine engine design since the 50's have resulted in increases in operating temperatures and shaft speeds prompting comparable advances in elastomeric seal materials technology as well.

Further developments in synthetic elastomers produced acrylates, silicones, flouro-elastomers and the most recent fluorocarbons, the best of these being copolymerized with TFE. The base elastomer gum stocks, from which an infinite variety of formulations can be compounded, and which are all in use today are described in references 4 and 16 and summarized in Table 2.

The Buna N elastomer, which is a copolymer of acrylonitrile and butadenes, exhibits fair resistance, by today's standards, to oil and fuel at both normal and elevated temperature. At the time Buna N was developed its resistance to oils was considered outstanding but the modern fluoroelastomers and fluorocarbons are markedly better in this regard. Certain Buna N formulations exhibit improved abrasion resistance when carbon black is added.

The acrylates, which are polymers of the butyl or ethyl acrylates, were found to have somewhat higher temperature capability than Buna N, and to experience no loss in resistance to oil, or at least to the mineral oils in use in early gas turbine engines. With the advent of the higher temperature synthetic ester type aircraft engine oils; i.e., MIL-L-7808 and MIL-L-23699, this elastomer turned out to be much less compatible prompting the introduction of the silicones and the fluoroelastomers. These materials not only proved to be more compatible with the synthetic lubricants but also demonstrated a higher temperature capability. This permitted the aircraft engine designer to more completely utilize the increased temperature range of these modern lubricants.

Silicone elastomers are polymers composed basically of silicon and oxygen atoms. They are reputed to be the most stable groups of all the elastomers and are less costly than fluorocarbons. They have relatively poor mechanical properties, however, making them susceptible to handling damage. They are highly resistant to oils but have the disconcerting property of causing synthetic ester oils to foam as described in reference 17. Due to this fact, silicone elastomers are not used in the oil systems of modern gas turbine engines. These engines rely heavily on the more trouble free, yet more costly, fluoroelastomers and fluorocarbon elastomers.

Fluoroelastomers, which are fluorine containing elastomers, can be used from 233K to 477K (-40 to +400°F) and have a high resistance to a wide variety of additives and fluids. Special tooling, however, is required to mold them. The fluorocarbons can be used over a wider temperature range from 189K to 477K (-120 to +400°F) and also have better dry friction characteristics. These materials, commonly known by the trade names Viton and Flourel, contain a polymer of TFE or tetrafluoroethylene, imparting a slipperiness or a very low surface energy level that inhibits the transport of lubricating oil onto its surface. This characteristic discourages the formation of

coke that results from the thermal degradation of the synthetic engine oil and which would otherwise interfere with the sealing function. Thus, fluorocarbon elastomeric materials, though costing more tend to provide a better seal and thus pay off well in terms of reduced oil consumption and durability.

Seal Requirements for Future Engines

Future bearing and seal requirements for gas turbines are expected to be more severe than for current applications. Advanced engines for both commercial and military applications are expected to continue the trends toward lower fuel consumption and higher thrust-to-weight ratios. The trend toward lower fuel consumption, as described in reference 28, implies higher pressure ratios, higher turbine inlet temperatures and higher bypass ratios. The higher thrust-to-weight ratios are expected to place greater demands on engine structural systems. It will be difficult to develop structural systems for large transport engines which will allow the flow area needed for higher thrust without a corresponding increase in weight. "Piggyback" bearing systems* for the support of the turbine end of the rotor, while attractive for possible thrust-to-weight gains, increase certain bearing and seal requirements.

Higher levels of rotor system performance in advanced engines will result in higher rotor speeds. Increased rotor speeds, greater rotor torque capacity, and critical speed margin demands will result in higher seal surface velocity levels. The trend toward increased seal speeds is shown in figure 9. The seal surface velocity levels of 152 m/sec (500 fps) to 183 m/sec (600 fps), correspond to engines that will be in operation in the 1990's or which are under various stages of development. Advanced engine designs with counter-rotating rotors may require intershaft seals with surface velocities between 183 m/sec (600 fps) and 305 m/sec (1000 fps). The future seal requirements discussed in this paper will be limited to those required for co-rotational rotor gas turbine engine designs and the nonintershaft seals of counter-rotating rotor designs.

Increases in gas turbine pressure ratios produce corresponding increases in compressor discharge pressures and temperatures. The gas turbine pressure ratio trend is shown in figure 10. To avoid undue performance losses, particularly at the engine bearing compartment between the high compressor and turbine, low leakage seals must be developed to operate at pressures approaching high compressor discharge static pressures. Aircraft gas turbine engines in the 1990's will require seals capable of operation at pressure differentials within the 345 N/cm^2 (500 psi) to 413 N/cm^2 (600 psi) range, at gas temperatures within the 922K (1200°F) to 1032K (1400°F) range, in addition to the previously mentioned surface velocities within the 152 m/sec (500 fps) to 183 m/sec (600 fps) range.

As stated earlier, the operating conditions that are encountered by the accessory seals in current engines are sliding speeds to 46 m/s (150 fps), pressure differentials ranging from 0 to 3.3 N/cm^2 (0 to 5 psi) and environmental temperatures in the range from 219K to 477K (-65°F to 400°F). In future engines the speed and pressure differential levels are not expected to increase, however environmental temperatures are expected to rise. Maximum temperatures could rise from the present 477K (400°F) to as high as 589K (600°F). This increase is a strong

---

*"Piggyback" bearing system is a dual rotor support arrangement whereby one of the rotors is supported by the other through a bearing rather than from the engine case structure as in conventional dual rotor support arrangements.

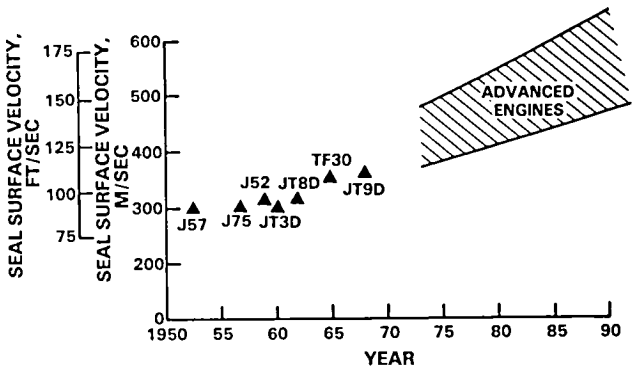

Figure 9 Trend Toward Increased Surface Speeds for Mainshaft Seals

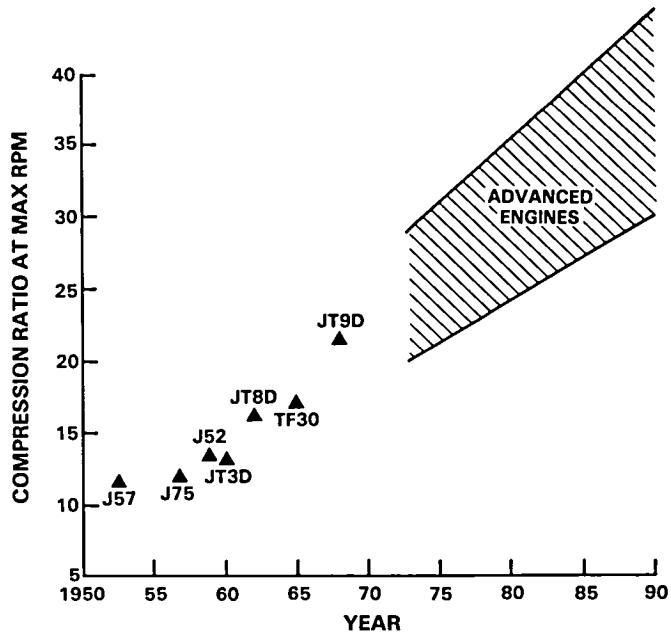

Figure 10 Trend Toward Increased Compression Ratios for Aircraft Gas Turbine Engines

possibility because operating the engine lubricating oil at higher temperature levels have certain advantages. As described in reference 26, by allowing a higher operating temperature a method for achieving 99% power gearbox efficiency can be realized, directly impacting engine fuel consumption. Also, in reference 27, for helicopter transmissions, an increase in lubricating oil temperature is identified as a means for eliminating the oil cooler or at least reducing its size, thus producing an immediate payoff in reducing both system weight and cost. With these and other such payoffs attendant to oil temperature increases it is just a matter of time before the necessary oils are developed. When this occurs then accessory seal development will be asked to keep pace.

Seal Materials for Future Engines

Matching the shaft sealing demands of each succeeding generation of engines has been possible largely because of the versatility of the rubbing contact type of face and ring seals and the carbon graphite material from which they are constructed. It is apparent that seals of the fluid film type as described in reference 12 seem to offer the best alternative for meeting the demands of the more stringent applications in future engines. A variety of research programs discussed in references 3, 10, and 18 is being conducted to demonstrate the applicability of advanced fluid film lubrication to jet engine face seals. These programs, supported on various levels by seal manufacturers, engine builders and engine users, pursued the development of oil lubrication and air lubrication methods. Materials play a key role in their design and these developments provide a glimpse into future design practices for advanced engine main shaft sealing. These concepts will not be addressed here, however experimental gas film face seals that use the properties of certain materials to advantage will be examined.

A typical advanced gas film seal designed for use in a large transport engine is shown in figure 11 which features self-acting Rayleigh step pods machined into the surface of the nosepiece portion of the assembly. This particular seal, developed in the program described in reference 19, performed successfully in rig tests to a maximum pressure differential of 345 N/cm^2 (500 psi), to a maximum sliding speed of 183 m/sec (600 fps) and to a maximum gas temperature of 922K (1200°F). Critical to the performance of this seal is maintenance of the thin gas film, as low as 0.000457 cm (0.18 mils), at the primary seal interface. This is accomplished through both geometric design and the choice of materials that have compatible thermal characteristics. The rotating seal seat was made of TZM, a molybdenum base alloy containing 0.5% Ti and 0.08% Zr, and chrome oxide coated for oxidation resistance. The high conductivity of this alloy, approximately twice that of steel, is conducive to minimizing thermal gradients in the seal seat which in turn minimizes thermally induced distortions. This aids in maintaining parallelism between the seal seat and the nosepiece which is necessary to the proper development of the dynamically generated pressures in the separating gas film. The material choice for the nosepiece was a high temperature grade of carbon-graphite which is retained in the assembly by a ring of TZM alloy. The TZM matches the thermal growth of the carbon thus again minimizing thermal gradients which otherwise would induce detrimental deformation. The piston ring secondary seal, also made of carbon graphite, is mated against a thermally compatible carrier of TZM which is, again, chrome oxide coated to provide both oxidation and wear resistance.

Figure 12 shows how this sealing concept, with its use of distortion controlling and wear resistant materials, has been adapted to an experimental seal of a smaller size for use in advanced gas turbine engines to power helicopters. This seal, as described in reference 18, operated successfully at surface speeds up to 213.4 m/s (700 ft/sec) concurrent with pressures of 182.7 N/cm^2 abs (265 psia). Maximum temperature of 677K (760°F) was reached at pressures of 148.2 N/cm^2 abs (170 psia) and speeds of 182.9 m/s (600 ft/sec). This seal design makes free use of carbon graphite in the sealing elements and TZM alloy in the seal seat. Chrome carbide is used for oxidation protection for the TZM as well as for wear control on those surfaces mating with the carbon graphite sealing elements.

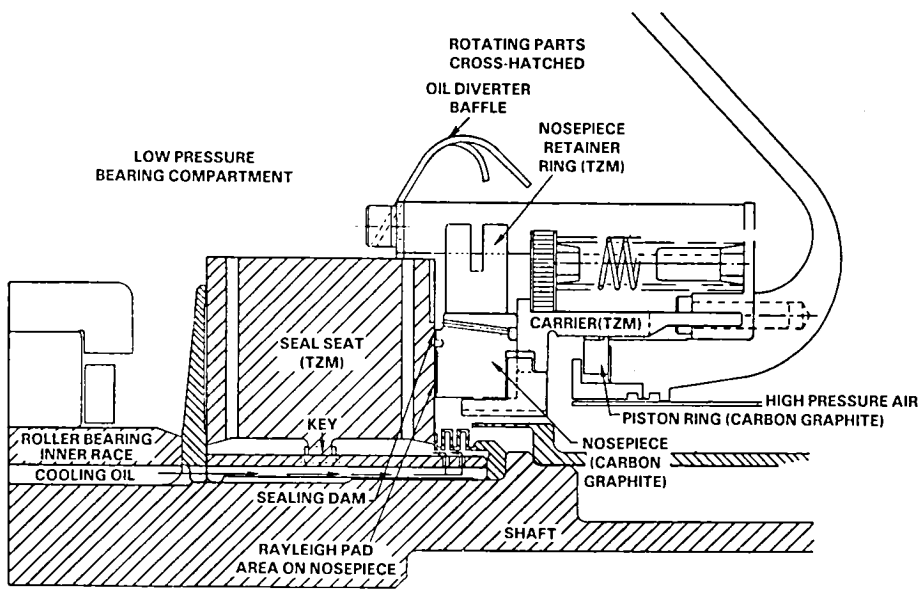

Figure 11 Advanced Gas Film Face Seal Featuring Materials for Controlling Thermally Induced Deformation

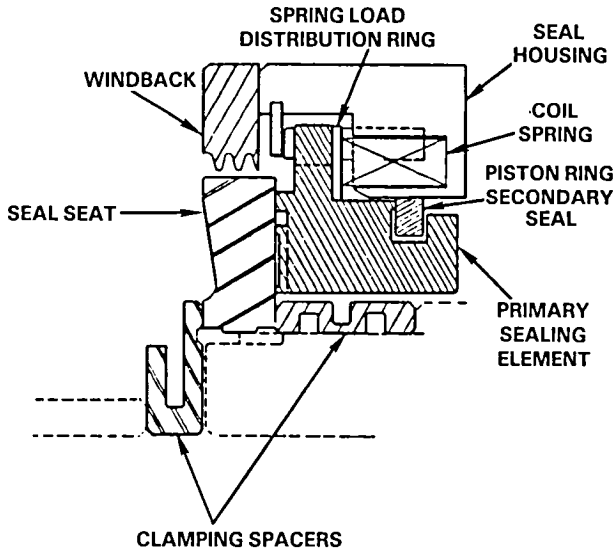

Figure 12 Advanced Gas Film Face Seal for Application to Helicopter Engines

Carbon graphite as the main sealing element in face and ring seals apparently still has potential for use at temperatures even beyond the 922K (1200°F) level employed in the gas film seal programs. This is shown in reference 20 where some carbon grades demonstrated reasonable wear rates even to the 1033K (1400°F) level. A key element to extending the useful temperature range of graphite as a face seal material is the further improvement of its oxidation resistance. References 21, 22, 23 shows there is considerable activity in this area which has contributed to a growing understanding of how both processing and impregnation can affect oxidation control. It was found that minute quantities of metal contaminants such as iron could increase oxidation rates of graphite by an order of magnitude as discussed in reference 21 and that chlorine purification of graphite can reduce its oxidation rate by an order of magnitude as shown in reference 22. Reference 22 also shows impregnation with zinc phosphate was found to give a further rate reduction. Other work provided in reference 23 demonstrated that colloidal silica plus boric oxide and P_2O_5 were also effective in reducing carbon oxidation rates. These articles represent just a sampling of the research and development activity that focuses on advancing carbon technology in the area of oxidation control. The intensity of this activity bodes well for the continued use of carbon graphite in aircraft engine seals of the future.

In addition to the TZM alloy that has exhibited promise as a mating ring for carbon graphite in gas film seals, some work has been done on some non-metallic materials that may receive more attention in the future. Power dissipation studies for a variety of non-metallics running against a carbon sealing ring in oil has been described in reference 24. Reaction bonded silicon carbide demonstrated consistently low power consumption independent of the carbon grade employed or the type of test fluid used. Other non-metallics evaluated were aluminae ceramic 85%, cobalt bound tungsten carbide and siliconized carbon. Several metals were also evaluated but they were also outperformed by the silicon-carbide. The poor performance of the alumina was not entirely unexpected. Similar high friction levels and thermal instability had been demonstrated earlier for this material and in other programs when evaluated as a gas film seal nose piece running against a TZM seat as described in reference 10.

Other work in reference 25 deals with another family of ceramics. Cast ceramics were formulated with the fluorides and silicates of calcium, lithium and barium. Good strength was reported and friction coefficients dropped from 0.4 to 0.2 as the rubbing element temperature was increased from 327K to 1088K (75 to 1500°F).

In spite of the increasing use of ceramics as one of the primary mating rings for advanced, high temperature seals, there is still a continuing interest in using metal rings due to the good thermal conductivity for metals and because special mounting practices are not required as is the case for the more rigid ceramics. Metals, however, need coatings to minimize friction and wear as influenced by oxidation which is enhanced by self induced rub temperatures. The coating used on today's wrought steel mating rings; i.e., chrome carbide, is good for operation to 1088K (1500°F) and beyond. Since today's seals operate at temperatures that generally are below 922K (1200°F), the chrome oxide coating has considerable potential for use in future engine seals. Of course, there is always interest in a coating that can be applied less expensively or in a coating that will produce even better wear performance or operate with lower friction. These factors foster considerable activity in the search for improved coatings as testified by the literature published on this subject. A number of different metallic and non-metallic materials are being explored using a variety of coating processes and surface modifications including chemical vapor deposition, plasma vapor deposition using different types of electron beam gun, electrolytic metal deposition, sprayed ceramics with fusion bonding, and surface hardening by producing amorphous alloy layers by means of laser or electron beam processing. In the effort to develop improved surface treatments for advanced engine shaft seal seats and secondary piston ring seals, the method will include one or more of the aforementioned processes.

For materials for accessory seals in future engines, it is presently anticipated that the temperature requirement is the only operating parameter that will change. An increase is anticipated by the 1990's to levels as high as 589K (600°F) compared to today's maximum temperature of 477K (400°F). The engine oil that will be developed for operation at these higher temperature levels will undoubtedly be a synthetic as those currently used. This means that the current day accessory seal materials with the exception of the elastomeric elements will most likely be usable at the higher temperatures with the new oil . The elastomer O-ring secondary seals used in the face seal assemblies may have to be replaced with some type of metal design, at least in the hottest locations. In the case of the radial elastomer lip seal, which type is used in but no more than three or four locations in a given engine accessory gearbox, higher temperatures may require their replacement with carbon face seals.

CONCLUSIONS

The workhorse material used in current day aircraft gas turbine main shaft and accessory gearbox seals is carbon graphite. This material is used in all rubbing contact seals in main shaft applications, including face and ring seals. Its popularity is due to its unique combination of properties consisting of dimensional stability, corrosion resistance, low friction, good self lubricating characteristics, high thermal conductivity and low thermal expansion, the latter two properties combining to provide good thermal shock resistance. This material which is used as the primary sealing ring mates against metal seal seats that are coated with chrome carbide. They provide reliable service in today's engines. The secondary piston ringseals are cast metal, also coated with chrome and mate against a hard surfaced steel cylinder which is integral with the main seal assembly. Other main shaft seals

used in some modern aircraft gas turbine engines are of the labyrinth type which have knife edges that are solid metal and opposing lands that are solid metal or soft abradable material applied to nickel alloy substrates.

Materials providing good performance in the accessory face seals of today's engines are also exclusively carbon graphite for the primary ring while the mating rings are commonly carburized gearshaft steel. A simple elastomeric O-ring of the fluorocarbon type is normally employed as the secondary seal and provides adequate performance for today's engines. In the lower speed accessory gearbox applications using radial lip seals modern designs employ fluorocarbon elastomers with TFE mating against hardened steel shafts.

In the 1990's, fluid film face seals may be employed to protect the main shaft bearing compartments. They will operate at higher environmental temperatures, speeds and pressure differentials. These temperature increases will most likely not exceed the capability of carbon graphite, thus permitting its continued use as the primary seal ring. Other seal seat materials such as molybdenum base alloy, TZM, protected from oxidation with a coating of chrome oxide, shows potential based on laboratory evaluation. At least one non-metallic material, silicon carbide, has demonstrated low friction as a seal seat when mating against a primary ring of carbon graphite and may benefit from further development. The currently used coatings for metal seal seats, i.e., chrome carbide, as well as the currently used piston ring secondary seals and associated coatings, are all capable of providing good service in advanced engines. In advanced engine seal designs, alternative coating processes will be evaluated as a way to reduce cost at no loss in performance.

Future accessory gearbox seal requirements will be paced by the development of higher temperature synthetic oil capability. Once higher temperature oils are available, engine performance will improve and weight will reduce, making it likely that all the accessory seals will be of the carbon face seal type to accommodate the higher temperatures. At higher temperatures, it may be necessary to replace the elastomeric secondary seals with metal designs.

REFERENCES

1. Shevchenko, R. P. and Brown, P. F., "Development of Rubbing Contact Seal Materials for Pratt & Whitney Aircraft Engines, 1961 SAE, Presented at seminar series "Rotating Seals - Design and Application" by the Southern New England Section of the SAE in Hartford, CT, March 14, 1961.

2. Povinelli, V. P., "Current Seal Designs and Future Requirements for Turbine Engine Seals and Bearings", Journal of Aircraft, Vol. 12, No. 4 April 1975, pp. 266-273.

3. Ludwig, L. P., "Gas Path Sealing in Turbine Engines" AGARD Conference Proceedings No. 237, Seal Technology in Gas Turbine Engines, London, UK, 6-7 April 1978, pp. 1-1, 1-49.

4. Horve, L. A., "Elastomeric Lip Seals", American Society of Lubrication Engineers, Fluid Sealing Education Course, May 1975.
5. Wilkinson, D. H., "Radial Lip Seals" Machine Design, Reference Issue, Seals, 4th Edition, Vol. 41, No. 14, June 19, 1969, pp. 5-9.

6. Battilana, R. E., "Mechanical Seals: Design Considerations", American Society of Lubrication Engineers, Fluid Sealing Education Course, May 1975.

7. Pure Carbon Technical Information Pamphlet, PC-5393-5M, 1979.

8. Paxton, R. R., "Carbon and Graphite Materials for Seals, Bearings and Brushes", Electrochemical Technology, Vol. 5, No. 5-6, May-June 1967, pp. 174-182.

9. Paxton, R. R. and Shobert, W. R., "Carbon-Graphite for Aerospace Seals", SAE Reprint No. 650302, Aerospace Fluid Power Systems and Equipment Conference, June 1965.

10. McKibbin, A. H. and Povinelli, V. P., "Development of Mainshaft Seals for Advanced Air Breathing Propulsion Systems", Pratt & Whitney Aircraft Reports, PWA-3933 and PWA 4263, National Aeronautics and Space Administration Reports NASA CR 72737 and NASA CR 72987, 23 June 1970 and 25 July 1971.

11. Brown, P. F., Gordon, N., and King, W. J., "A Test Method for Evaluating Gas Turbine Engine Seal Materials", Lubrication Engineering, Vol. 22, No. 1, Jan. 1966, pp. 7-16.

12. McKibbin, A. H. and Parks, A. J., "Aircraft Gas Turbine Mainshaft Face Seals - Problems and Promises" ASLE Special Publication SP-2, Fourth International Conference on Fluid Sealing, May 5-8, 1969, pp. 28-36.

13. Mahler, F. H. "Advanced Seal Technology", Pratt & Whitney Aircraft Report No. 4372, Air Force Aero Propulsion Laboratory Technical Report AFAPL-TR-72-8, February 1972.

14. Shiembob, L. T., "Development of a Sprayed Abradable Gaspath Seal", presented at 20th National SAMPE Symposium and Exhibition, April 29 - May 1, 1975.

15. Elverum, F., "Reviewing an Aircraft Gas Turbine Accessory Gearbox Seal", Rexnord, Inc., presented at NASA-Navy Liquid Lubricated Radial Face Seal Workshop, NASA Lewis Research Center, June 24-25, 1980.

16. Brady, G. S. and Clauser, H. R., Materials Handbook, Eleventh Edition, McGraw-Hill, 1977.

17. Anonymous, "Lubricant Foaming and Aeration Study, USAF, Aero Propulsion Laboratory, AFWAL-TR-82-2090, Rensselaer Polytechnic Institute, Contract F33615-80-C-2017, January 1982.

18. O'Brien, M., "Development of a Short Length Self-Acting Seal" Avco Lycoming Division Report No. LYC76-71, NASA Report No. CR 135159, November, 1976.

19. Dobek, L. J., "Development of Mainshaft Seals for Advanced Air Breathing Propulsion Systems", Pratt & Whitney Report No. PWA-4683, NASA Report No. CR 121177, March 1973.

20. Strom, N. et. al., "Wear and Friction of Impregnated Mechanical Carbons at Temperatures to 1400°F (760°C) in Air and Nitrogen", NASA TT-D 3958, May 1967.

21. Turkdogan, E. T. and Vinters, J. V., "Catalytic Oxidation of Carbon", Carbon, Vol. 10, 1972, pp. 71-111.

22. Wisander, D. W. and Allen, G. P., "Effect of Chlorine Purification on Oxidation Resistance of Some Mechanical Carbons", NASA Tech. Note D-7688, June 1974.

23. Wallough, R. W., "Treat Solution for Rendering Carbonaceous Articles Oxidation Resistant", U. S. Patent 3,351,477, Nov. 7, 1967.

24. Labus, T. J., "The Influence of Rubbing Materials and Operating Conditions on the Power Dissipated by Mechanical Seals", Lubrication Engineering, Vol. 37, No. 7, July, 1981, pp. 387-394.

25. Sliney, H. E., "An Investigation of Oxidation Resistant Solid Lubricant Materials", ASLE Transactions, Vol. 15, July 1972, pp. 177-183.

26. Godston, J. and Kish, J., "Selecting the Best Reduction Gear Concept for Prop-Fan Propulsion Systems" American Institute of Aeronautics and Astronautics Paper No. AIAA-82-1124, presented at 18th Joint Propulsion Conference, June 21-23, 1982.

27. Fitzgerald, P. C. and Gardner, G. F., "Advanced Transmission Component Development and Test Program", American Helicopter Society Propulsion System Specialists' Meeting, Preprint No. HPS-8, Washington, D.C. November, 1979.

28. Sens, W. H. and Meyer, R. M., "New Generation Engines - The Engine Manufacturer's Outlook," SAE Air Transportation Meeting, New York, April 1968, pp. 2-3.

DISTILLATION OF CONFERENCE CONCEPTS

Donald F. Hays
General Motors Research Laboratories
Warren, Michigan

I have prepared a summary of the Conference, --- a distillation of concepts if you prefer, --- that few will read, and a short discussion that fewer will remember. Such a summary is dangerous for it tends to measure the work of many. Thus, honesty of intent and accuracy of content are extremely important. Consequently, I have employed an approach typified by friendly plagiarism to minimize technical distortion and misinformation in the summary.

Now, about the distillation of concepts emerging from the Conference. Which concepts should be singled out as especially significant? What is the measure of importance? I think that the distillation of concepts has already occurred---that each of us has made his own judgment. And it will be different for you and for me, for the importance of the subject, or concept, lies in the eye of the beholder. I would not be surprised, if on reflection, we saw the Conference as somewhat of a blurred image out of which may have come one or two personally significant technical revelations and perhaps some expressions of insight, or direction, or concern expressed by others.

The point to be made is that what has been accomplished and reported here reflects today and tomorrow and not yesterday. For instance, "Tribology in the 80's" could be looked upon as where we have been and what we have accomplished; the data would be tabulated; and the reports would be closed historical documents.

In contrast to this, we have in general looked at where we are in the 80's, and talked about where we are going to be in the 90's; now we are talking about attitudes, visions, and the future. This is a dynamic, exciting experience in which the presentations are not closed, but open-ended --- the story is not yet complete.

Before discussing the many concepts that have been covered in the Conference, I would like to address some issues that were not on the program, some thoughts that were not expressed and some concerns on future directions that were not given.

First, why are we here and why are we involved in these activities, that to an outsider might appear to be much ado over something that everyone understands: friction and wear?

Are we involved because it's fun and mentally stimulating? Perhaps. I believe that we should keep in mind that we are involved in the science of tribology because our creativity is required in the development of advanced mechanical systems. These systems are characterized by mechanical linkages, power trains, bearings, seals, friction elements, cams, rotors, fasteners and other elements. They are dynamic systems; they are controlled systems; and they are composed of innumerable combinations of interacting surfaces. It is the dynamic nature of the mechanical system that introduces the issue of tribology.

A mechanical system, either simple or complex, is also a tribological system and the proper design of that system is in part a tribological issue. If the knowledge required for that design is not available, then there is a high probability that at some time there will be a tribological problem---or a tribological disaster.

Thus, we are here, making our contribution to future tribological systems. It may not be obvious as to how our contribution will be implemented. I see individual contributions, regardless of their esoteric nature, flowing along as a rivulet, being joined by other contributions until our aggregate understanding flows into the creation of new, viable and productive mechanical systems.

What we must keep in mind is that the mechanical systems of the 80's will not be sufficient as the mechanical systems of the 90's. Now I admit that there are a few problems between the concept and the implementation, and not all of these are technical. However, periodic reflection on why we are here and perhaps a visit to a failed tribological system may be helpful in terms of what we should be looking toward in the future.

And this brings us around again to the Conference. I think that Dr. Tabor has provided us with a proper guide for our endeavors: understanding of basic mechanisms, and prediction of practical performance; from the basic to the applied; we will go through the full cycle.

Now I would like to make some general observations. Experience is a great teacher, we all admit, and experience directed the design of rubbing elements long before we knew of binding energies, wear equations, EHL or transfer films. There were rules of thumb which if not providing insight, did provide a feeling of security. The developments of the 80's will hopefully provide an explanation for some of these phenomenological approaches and will provide the basis for "prediction of practical performance" in the 90's.

We will continue, however, to make tribological decisions, even if we do not have detailed knowledge of the process, just as we eat without being concerned with the technicalities of the digestive process.

In considering the future directions of tribology, it appears that there is an overabundance of areas in which fundamental work is required. The breadth of our ignorance and the rate of its growth could be discouraging except that it is this situation that keeps tribologists productive and vital.

The extent of our unknowns is perhaps best exemplified with respect to the adhesion, friction and wear of solid materials. There are many of these materials. Metals, ceramics, polymers, composites, cermets, and others are all used in tribological systems. We must gain a greater understanding of the physics and chemistry of their friction and wear characteristics.

Voices from at least two groups could be heard during the Conference. On the one hand were requests for simple, useable equations or relationships that could be employed for design purposes. This is an understandable request since life goes on with or without knowledge of all design factors. On the other hand, we find those concerned with a more extensive basic understanding of phenomena. Perhaps we must decide when we have enough of the basics, if ever, to satisfy both groups. Simple expressions are dangerous because they are incomplete; complex expressions are dangerous because their very complexity lends them perhaps undeserved credence.

Relationships, based upon correlation of data, will probably continue to be used even though the dangers were discussed on several occasions. My favorite illustration of misinformation was purposely constructed to show the misuse of data correlation. If you plot the frequency of automobile accidents by month, you see a peak in July. A remarkably similar plot is found for the consumption of ice cream cones. The way to reduce automobile accidents is then obvious; do not sell ice cream cones.

The subject of fluid lubrication seemed to fare somewhat better than solids, except for the allegation that there might not be enough fundamental work remaining to provide employment to the EHL and thick film hydrodynamicists. It has been 100 years since the discoveries of Tower and over the intervening years we have, in effect, been slipping and sliding down the Stribeck curve from the right. It appears that the hydrodynamicist will end up at the surface of the solid with three thin films.

This raises the issue of how many asperities on asperities can have smaller asperities and what effect this might have on surface phenomena. These extensions of analytical mechanics present a wonderful opportunity to the experimentalists. They must ask themselves have we overextended our analytical expressions, and, if so, what are the realities of this micro-world on the surface? Here may be a new challenge to the EHL community: the failure mode of surfaces and films.

The phrase "bridging the gap" was heard more than once during technical discussions. It seemed to be directed to the solid mechanician and the surface chemist. Don't they talk to each other? Perhaps we should not pick on these two alone. Consider who are involved in this endeavor: metallurgists, polymer chemists, analysts, rheologists, fluid analysts, physicists, ceramists, mathematicians, microscopists, solid analysts, computer analysts and designers.

There are a multitude of gaps to be bridged.

Fundamentally, it seems that we need to talk to each other. I do not really understand what you have done, but I cannot talk to you about it because I do not speak your technical language. Now I do not expect each of us to become equally familiar in all disciplines. But wouldn't it be to our mutual advantage to extend our personal boundaries so that we could more easily understand each other and share in the appreciation of the total field as it advances into the 90's?

During this Conference we have talked about many tribological phenomena. Some seem to be rather isolated; some related. If we only knew the rules, then perhaps all would ultimately be related in a sort of tribological symphony. Will we be able to bring these factors together --- and how? The only way I know is through mindful questioning -- questioning. What does this mean? How is this related? What are the contradictions? What is the mechanism?

I think that much of this will fall into place, from the micro, to the macro, to the prediction of practical performance.

The challenge is how and when.

I would like to close this discussion on concepts with a quote from Jules Henri Poincare:

"Science is built up with facts, as a house is with stones. But a collection of facts is no more a science than a heap of stones is a house."

Let us carefully, thoughtfully and purposefully build upon our discoveries --- a tribological science for the 90's. This will be the measure of us all.

*****

The following summaries are of conference papers that were available prior to the Conference.

Importance and Definitions of Materials in Tribology: Status of Understanding

by Donald H. Buckley

In a typical tribological system, we have the materials, the interspersed medium, and the environment. Of these elements, the materials provide the foundation of the system, bear the brunt of any mechanical design deficiency in the system, and are critical factors in terms of adhesion, friction and wear. The study of material surfaces is not new; however, over the years much more attention has probably been lavished on the lubricant and on the environment than on the surface and bulk properties of the materials that are so critical and fundamental to the understanding of friction, adhesion and wear. This situation was probably due to our familiarity with materials; they have been with us for ages. And, in addition, the chemistry of the lubricants seems so new and vital that it was easy to overlook the ubiquitous solid. Familiarity had bred, if not contempt, at least a misapprehension of the chemistry of the interfacial solids that were, in fact, appreciably different from the bulk material that appeared obvious as the sole interactive member.

Times have changed and today we find ourselves in the midst of an explosion of materials; we are surrounded by a host of metals, ceramics, cermets, polymers, composites, etc., that have been provided by the materials scientists and each has potential of tribological application. This situation has done much to point out our deficiency in knowledge of the material surface and bulk properties that bear upon the friction and wear properties of the solid. In the past, and to some extent today, this deficiency has spawned a multitude of empirical testing that provides data but not necessarily understanding. Today there is a new recognition of the importance of understanding the interrelations between the basic properties of the solids and their tribological performance.

But where do we start? As Buckley points out in his paper, metals and metal alloys are probably the dominant materials for components in mechanical systems. And this is where he chooses to start.

He points out that several surface events that occur on a solid surface can alter its behavior. Reconstruction occurs when the outermost layers of atoms of the solid surface undergo a change in structure, appreciably changing the coefficient of friction of the solid.

Segregation of alloy species can also occur at the surface. When this process is irreversible, the alloying elements remain on the surface. In each case, segregation has been shown to significantly affect adhesion, friction and wear.

Chemisorption impacts the adhesive properties of materials. For example, minor modifications on the hydrocarbon structure can produce marked differences in measured adhesive forces.

The last surface event is that of compound formation. When clean metal surfaces are brought into solid state contact, adhesive transfer from one surface to another always occurs. The compound formation produces strong interfacial bonds at the contacting surfaces and influences the adhesive behavior.

This last factor leads to an interesting question, What, if any, is the relationship between surface and bulk properties? If the adhesive behavior of solids is related to surface energy levels, and if there is a correlation between cohesive energy and surface energy for the elemental metals, then from reliable cohesive energy values we should be able to obtain the surface energy values which have been so difficult to obtain. Thus, it may be possible to predict adhesive transfer behavior from cohesive energy data. In addition, the basic behavior of materials in solid-state contact in the presence of oxides also show fundamental relationships to bulk properties.

Another bulk property of solids that can be related to adhesion, friction and wear behavior is the degree of d-valence bond saturation of the transition metals. In general, those metals with a high degree of valence bond unsaturation, such as titanium and zirconium, show a strong degree of adhesive bond force.

Other basic relationships have been found between the friction properties of metals and alloying elements. The abrasive wear resistance and friction coefficient for simple ferrous base binary alloys is related to the solute-to-solvent atomic radius ratio in the binary alloy. The coefficient of friction is at a minimum when the ratio is unity, and increases as the ratio varies in either direction.

More complex systems will, of course, have more than one basic property related to their tribological behavior. One of these current alloy forms is amorphous metal or metallic glass. At room temperatures, the coefficient of friction is low and wear resistance is high.

The study of tribological behavior of metals must include mechanical effects. Relative motion of surfaces under load imparts energy to the surface which may be dissipated in several ways. This can result in crystal transformations, order-disorder reactions, texturing, recrystallization, segregation and strain. These impinge on both the basic structure and properties of the substance. In addition, mechanical activity at the surface can influence the interactive chemistry between the environmental constituents and the solid surface.

Nature of Surfaces and Their Effect on Solid State Interaction
by J. M. Georges

In boundary lubrication, the chemical and mechanical properties of the surface films are of primary importance. Georges points out that while the friction of the interface layer depends on environmental conditions, the thickness of that film is small and the composition of the film is extremely difficult to determine. In many cases the components of the metallic surface are hydrated oxides and adsorbed lubricant. These are the constituents of the paste generated during surface interactions. This paste may be the material primarily responsible for wear scratches in solids.

For a sphere-plane sliding combination of 52100 steel with an adsorbed thin organic film, unidirectional sliding at low velocity produced three distinguishable zones. In zone one, which occurs during the first hertzian diameter of sliding distance, there is no observable wear and the zone corresponds to the shearing of the interposed adsorbed film. The frictional force is therefore dependent only upon the shear strength of the lubricant film.

After two or three hertzian diameters of sliding, material agglomerates in the interface but the effects are not discernible on the frictional force. This is zone two

which occurs before gross slip. These agglomerations are the beginning of third body coalescence.

In zone three, the film is disrupted, sliding occurs within a "mush" in the contact region, with piled-up material in front of the rider. For greater sliding distances, the phenomenon persists, and the coefficient of friction increases and fluctuates widely.

In tests run with a cast iron flat and a 52100 sphere with ZnDTP, Georges found that stage 1 corresponded with abrasive wear of the interface (high wear rate) and stage 2 corresponded to corrosive wear (low wear rate). At stage 3 the surface was covered with a tribological reaction film. The film products were amorphous, insulating and appeared to consist of a glassy material.

The effect of pressure on this phenomenon seemed to depend on the time required to form the film. The film is not formed at a low pressure because abrasive interface products have not been adequately sheared. With too high a pressure, seizure occurs before the protective film can form.

In essence, the effect of adsorption and chemical reactions between the environment and the solid bodies is a starting point for a very complex chemical phenomenon. Mechanical effects then create interfacial bodies, the products of which are colloidal and transformed by high pressure into a glassy material.

Importance of Properties of Solids to Friction and Wear Behavior
by Horst Czichos

We recognize that friction and wear are not "intrinsic material properties" and that a tribological system consists of three components: the interacting solids, an interfacial medium and the environment.

In designing mechanical systems a natural question to ask is, What are the material properties, or the properties of the solids, that determine the friction and wear behavior? This is an extremely difficult question to answer satisfactorily because friction and wear are influenced by a great number of processes, conditions and parameters. No simple property-behavior relations exist. The observable friction and wear are determined by interaction characteristics rather than by any intrinsic properties of single components.

In this paper, Czichos presents an extensive survey on the present state of our understanding of the importance of properties of solids to friction and wear behavior. He attempts to answer two very fundamental questions: 1) what are the fundamental friction and wear processes; and 2) how are these processes connected with the properties of solids?

First, let us turn our attention to the subject of friction. If there is no simple model to predict the friction of a given pair of materials, then what is our understanding of friction and how the properties of solids are related to this phenomenon? It is pointed out that there are three basic phenomena involved in the friction of unlubricated solids.

1. The area of real contact between the sliding surfaces.

2. The type of bond that is formed at the contact interface.

3. The way in which the material in and around the contacting regions is sheared and ruptured during sliding.

The energy loss process due to friction has been divided into different phases. First, mechanical energy is introduced into the contact zone by the formation of the real area of contact. Second, transformation of mechanical energy takes place mainly by plastic deformation, plowing and adhesion. Third, the dissipation phenomena include the effects of thermal dissipation, storage or emission.

In terms of the real area of contact, an increasing interest is being shown in surface topography and the role of the tribo contact formation in friction and wear. Real engineering surfaces are not perfectly smooth but carry the fingerprint of the manufacturing process. These asperities are the basis for the tribo contacts. The observation is made that 1) microasperities may contain no dislocations and may, therefore, be much harder than the bulk material, 2) the surface films (e.g., oxides) may change the deformation properties of the materials, and 3) the influence of temperature may lead to creep and sintering and may considerably increase the area of contact.

The adhesive component of friction is due to the formation and rupture of interfacial adhesion bonds. These bonds are the result of interfacial interatomic forces. From a consideration of metals, ceramics and polymers, it is evident that the interfacial adhesion is as natural as cohesion which determines the bulk strength of materials within a solid. It is pointed out that the simplified model of the adhesion component of friction has been extended to include a surface energy theory which introduces the surface energy of the contacting bodies as an important parameter. There is a fracture mechanic model which considers the fracture of an adhesive junction and introduces the critical crack opening factor and a work hardening factor. It is recognized that the interfacial shear strength or the surface energy are characteristics related to the given pair of materials rather than to the single components involved.

If a hard asperity penetrates into a softer surface while bodies are in relative motion, there is a plowing component of friction. In addition, plowing may be initiated by wear particles. In the plowing of brittle surface materials, the influencing parameters would seem to be material properties such as fracture toughness, elastic modulus and hardness. In the case of plowing by penetrating wear particles, consideration must also be given to the geometric properties of the asperities or penetrative wear particles.

Because of the deformation which occurs during sliding contact, mechanical energy may be dissipated through plastic deformation. In using the slip-line field model, some specific material properties should be considered and these would include:

1. Microstructure of the materials

2. Work hardening effects

3. Thermo softening

4. Influence of interfacial layers

Wear behavior of materials is a very complicated phenomenon that seems to be dictated by mechanical properties, chemical stability of the materials, temperature and operating conditions. Wear may be divided into four broad classes -- abrasion, adhesion, surface fatigue and tribochemical processes. The manner in which the various mechanisms of wear interact is very sensitive to the specific operating conditions and,

therefore, unless a single wear process dominates, the surface changes and the complex interactions make wear prediction extremely difficult. To discuss the importance of materials on the wear behavior, the chain of events which leads to the generation of wear particles must be considered. The initiation of wear particles and their removal from a tribological system is caused by two types of interactions. The first of these are stress interactions which are due to the combined action of load forces and frictional forces and these lead to wear processes described broadly as surface fatigue and abrasion. The second area is that in which the intermolecular forces between the interacting solids or between the solid bodies and the environmental atmosphere, lead to wear processes which could be described as tribochemical reactions and adhesion.

In the area of surface fatigue, it is known that under repeated tribological loading, surface fatigue may occur and lead to the generation of wear particles. These effects are due to the action of stresses in or below the surfaces without requiring a direct physical contact. This type of fatigue wear is associated with repeated stress cycling in rolling contact bearings. Several models incorporate this concept. Currently, it appears that dislocation models can now be used to explain the occurrence of sheet-like wear particles generated by this process.

In contrast to surface fatigue, abrasion occurs in those situations in which there is direct physical contact between the two surfaces. Here we find terms such as micro-plowing, micro-cutting and micro-cracking.

In the simplest model of the abrasive wear processes, the wear volume is related to the slope of the penetrating abrasive particle and to the hardness of the abraded material. More complex abrasion models have been formulated; one being related to a critical strain at which crack growth is initiated. Another model considers the detailed processes of micro-cutting, plowing and cracking. Some of the factors which are now being considered are flow pressure, hardness, capacity of work-hardening, ductility, homogeneity of strain distribution, crystal anisotropy and mechanical instability. All of these factors influence the abrasive wear mechanism.

In tribochemical wear, the environmental and the dynamic interactions between the material components and the environment determine the wear process. These interactions are cyclic processes which include the following sequence: 1) material surfaces react with the environment and reaction products are formed on the surfaces, 2) as a result of crack formation and abrasion in the contact area, an attrition of the reaction products produces "fresh" reactive surface and stage 1 repeats. As a consequence of thermal and mechanical effects, asperities undergo the following changes: 1) surface reactivity is increased due to the increased asperity temperatures which leads to the accelerated formation of surface layers, 2) the mechanical properties of the surface asperity layers are changed; in general, they have a tendency toward brittle fracture.

With the assumption that tribochemically formed surface asperity layers are detached when a certain critical thickness is reached, a tribochemical wear hypothesis has been proposed for the wear of steels. It has been concluded that tribochemical wear occurs by a process of oxidation, deformation and fracture to produce layers which are compacted into grooves in the metal surface. Oxidative surfaces become smoother with time as the troughs become filled with oxide. Then oxidative wear occurs by the fracture of plate-like debris.

Adhesive wear processes are initiated by the interfacial adhesive junctions which form when solid materials are in contact on an atomic scale. It is obvious that a number

of properties of the contacting solids influence the adhesive wear mechanism. Since adhesive wear is influenced by surface contaminants and the effect of environment, it is very difficult to relate adhesive wear processes with elementary bulk properties of materials. In vacuum, where exterior influences are eliminated, the following parameters have been seen to influence adhesive wear processes in metal/metal pairs: 1) electronic structure of the contacting surfaces, 2) crystal structure, 3) crystal orientation. Adhesive wear prediction has been described phenomenologically by the Archard equation which contains only the material property. The wear coefficient must, therefore, relate in some complex manner to the many material properties of the contacting pair.

FUTURE DIRECTIONS OF RESEARCH IN ADHESION AND FRICTION

Future Directions of Research in Adhesion and Friction: Status of Understanding
by David Tabor

In his paper, Dr. Tabor has outlined not only the basic constituents of adhesion and friction, but has also suggested a number of future research directions.

In the adhesion of clean metals, our understanding of the interfacial bonds is seemingly well in hand. However, the role of surface roughness and especially the role ductility plays in the phenomenon needs to be incorporated into an overall view of metallic adhesion. A simple method is proposed for separating ductility from bond strength, structure and geometry. This suggestion is to study diffusion of similar metals under conditions of low temperatures sufficient to freeze out the ductility.

In the case of dissimilar metals in some experiments, the surfaces do not separate at the interface but within the weaker of the two bodies. The intrinsic strength of the bond between dissimilar metals requires additional research.

Surface roughness and deformation properties of asperities are important factors in the analysis of adhesion of extended surfaces. Experiments utilizing single crystals have shown that in the absence of normal applied load, surface forces alone may be sufficient to initiate plastic flow in the contact zone. It is felt that further work is needed to establish whether these surface forces play a significant part in the adhesion of extended surfaces under extremely small loads. In addition, these studies should be extended to include sliding surfaces.

As Dr. Tabor states, "the effect of contaminant films has not gone far beyond purely descriptive language." The extent to which contaminant films reduce the pull-off force, depends upon the nature of the film, the geometry of the surface and whether surface deformation is sufficient to produce penetration of the film. Interfacial films formed by the diffusion of minor constituents or impurities to grain boundaries, also lead to a marked reduction in strength and often to embrittlement. The mechanism by which this occurs still needs a critical examination.

Although the mechanism of metallic friction is reasonably well known at a descriptive level in terms of the area of real contact, junction growth, breakdown of contaminant film, adhesion, shearing and plowing, quantitatively the picture is less satisfactory. Analytical expressions for junction growth due to combined effects of normal and tangential stresses are largely qualitative.

Although the adhesion of clean surfaces is fairly well understood, Dr. Tabor points out that the behavior of oxide coated surfaces is not. We must have a better understanding of the adhesion of the oxides, the breakup of the oxide films, the adhesion of the mixed oxide-metal interface, and the influence of surface deformation on the structure and mechanical properties of the surface layers. It is felt that the breakup of surface films is essentially speculative. The question of work hardening is still a complication in the analyses of the friction of metals. Another difficult problem now receiving attention, is the breakup of the surface and subsurface structure of the metal as a result of repeated sliding. Although there are models for the frictional heat that is generated during high speed sliding, an interesting question is posed, What is the location of the heat source? If the heat is generated in some finite volume of the material being deformed, then it would be useful to know how much our calculations of surface temperature are changed if volume deformation is taken into account.

In the case of ceramics, our understanding of adhesion is far poorer than in the case of metals. Bond formation across ceramic interfaces probably has an important bearing on the friction and wear behavior of these materials. Since these bonds may be weaker than the chemical bonds within the body of the ceramic itself, sliding will necessarily take place at the interface; the friction will not be high and in principle there will be no adhesive wear. Since ceramics are now appearing as potential engineering materials, a systematic study of the adhesion, friction and wear of clean ceramics in terms of their structure and bond type will be extremely valuable and timely.

In the case of the elastomers, the surface energy is very small and the forces between rubber surfaces are limited to van der Waals forces. The interactions across the interface will be much less than the bonding within the bulk of the rubber where strong chemical cross-links exist. Although these elastic losses will increase the work of separation, while surface roughness reduces it, it was found that the observed pull-off force may be 100-1 000 times greater than the thermodynamic energy of adhesion. The friction of soft elastomers leads to the generation of Schallamach waves which involves a continuous laying down and peeling apart of the rubber on the substrate. The frictional work is related to the surface energies and to the hysteretic loss properties of the rubber.

The adhesion of polymers is similar to that of elastomers since it includes surface energy concepts, electrical charge separation, interfacial diffusion, surface roughness and deformation losses. The friction of polymers involves adhesion and deformation as well as cracking at and below the surface. The behavior is similar to that of metals except that there is little evidence for junction growth and the deformations which occur during sliding are more dependent on temperature and shear rate. Because of poor thermal conductivity and low melting points, softening and melting take place fairly readily as a result of frictional heating. Once surface melting occurs, heat appears to be generated through viscous dissipation in the molten layer. It is suggested that there is considerable scope for examining frictional behavior in terms of a chemical structure and morphology of polymers.

Metallic Adhesion and Bonding

by John Ferrante, John R. Smith, James H. Rose

Metallic adhesion plays a central role in the area of friction and wear of rubbing tribological pairs. There are, however, few quantitative theoretical calculations regarding this phenomenon. In the study of metallic adhesion in a real world contact, we must consider the surface topography, and the mechanical properties of a solid, that is, ductile or brittle, the nature of the deformation which may be elastic or plastic, and, in addition,

the effects of surface films and adsorbates on the binding forces and on the mechanical properties of the interface. In light of these complexities, are the physics of a real metallic contact amenable to analysis? The authors feel that the single aspect of the problem that has received the least attention is the nature of the metallic bonding force. Recently, the authors have shown that the adhesive force calculations on simple metal-metal pairs may be more general than they first anticipated and may, indeed, be relevant to the case of transition metals in contact. In fact, they have shown that there are certain features in covalent bonding that are universal.

An adhesion calculation is formulated on the basis of two perfect surfaces in contact in which the binding energy is analyzed as the surfaces are pulled apart. The intent is simply to explore the nature of the bonding forces which exist in this type of metal-metal contact.

The results of the calculations show that there is a great similarity between the various binding energy curves. The question which naturally arises is: can we obtain some generalizations from these curves and can they be scaled into a universal curve? The answer is yes. Curves of dissimilar metals as well as curves of identical metal contacts can all be scaled into a universal curve. It is shown that the results of ten bi-metallic contacts all lie very close to this universal curve.

An interesting question is whether the adhesive bonding between dissimilar metal contacts is weaker, stronger or lies between forces created when the contacts are between the same metal. Although in a real contact the surfaces would probably distort and modify the interfacial energy, in general, the interfacial binding energy may be considered as comparable to the energy of the weaker partner in a contact of two dissimilar metals.

Since most engineering materials are transition metals, it is of interest to know whether this universal scaling can be applied to these metals. Using many diverse types of cohesive energy calculations, the authors show that a number of different metals fall on a single curve which indicates the generality of these scaling relations.

Since the quality of the curve fit for cohesive energies is not as close as for the adhesive energies, the authors define a new scaling length. This is a function of the second derivative of the binding energy at its minimum. With this scaling, the fit is exceptionally good.

With the previous relationships established, it seems plausible to ask whether there might be a universal curve for covalent bonding in general. A plot of molecular, chemisorptive, adhesive and cohesive bonding is shown in which the second derivative scaling technique was used. All types of covalent bonding are seen to follow the same universal curve.

With the knowledge gained, the authors then look for a relationship between surface energies and cohesive energies. Their results show that there is indeed a proportionality relationship between a metal's cohesive energy and surface energy per atom, and that this proportionality is the result of the universality of the behavior which is exhibited by binding energy relations. The question of chemisorption on transition metals is raised with respect to the scaling relationship which might exist for adsorbates on crystalline transition metals. Although there are a number of qualifiers, the results seem to show that these relationships extend to chemisorption on crystalline transition metals provided that the adsorbate does not penetrate the surface atomic layer.

The Influence of Surface Topography on Polymer Friction
by Norman S. Eiss

Increased use of polymers as components in sliding systems has resulted in the need for research directed towards the modeling of friction and wear mechanisms. If successful, such models could be used to predict tribological performance and to suggest modifications in the components to improve their tribological performance. In his paper, Eiss has attempted to determine the role of surface roughness in models of polymer friction.

It is pointed out that there are two approaches to modeling the friction of polymers; one is based on energy and the other on forces. In the energy-based models, the frictional work is equated to the energy dissipated in the materials. In the force-based models, the friction force is equated to the tangential forces generated in the interface. Energy models for polymer friction have primarily been applied to elastomers. In one model, the frictional work has been related to the energy dissipated in hysteresis losses in the material and in another model the frictional work is equated to the energy dissipated in plastic deformation. In this latter model, although energy dissipation is considered, surface roughness has not been included and the energy-based friction model does not predict friction values.

The force models of friction are based on an equality between the friction force and the sum of the forces due to adhesion and to deformation. Because the adhesion component of friction consists of a shear force developed in the contact area, the shear strength and the area being sheared are important. The real area of contact must be determined and the estimation of this parameter is still severely restricted. The relationship between the area of contact during sliding and that in static contact requires further research. It is suggested that a combination of a slip line model with the energy model may provide the basis for more advanced friction models.

In an experimental program, the wear of polymers as a function of surface roughness was studied. The results indicated that anisotropy in surface topography could be used to estimate the relative contribution of the adhesion and the deformation components of friction and provide estimates of material parameters governing shear and deformation processes. In addition, although surface topography would seem to be very important at the beginning of the test, as transfer occurs the topography is modified. It is suggested that this phenomenon may be responsible for the relative insensitivity of friction to surface roughness after steady-state friction values have been reached.

FUTURE DIRECTION OF RESEARCH IN WEAR AND WEAR RESISTANT MATERIALS

Future Direction of Research in Wear and Wear Resistant Materials: Status of Understanding
by T. Sasada

In his paper, Sasada presents a theory on new mechanisms for the formation of wear particles during adhesive wear. The author feels that the classical adhesive wear model is inadequate and that adhesion is inherently not a separation factor but rather a joining factor for interacting materials. Thus, he finds it difficult, or impossible, to show that wear particles can be formed by adhesion. In the new theory, the wear particles are not separated from the surfaces directly as a final wear particle, but rather are formed as minute adhered fragments which are later assembled and structured to form a wear

particle which is then expelled from the rubbing system. The author has observed three factors which have contributed to the structure of his model of adhesive wear. The first of these observations is that the size of observed wear particles ranges from far smaller than the real contact area to far larger than that junction. The second observation is that there is a mutual material transfer between the rubbing surfaces. The third observation is that every wear particle is composed of the two materials that have rubbed together. These phenomena are observable in metal-metal, metal-polymer, ceramics-ceramics, metal-ceramics and polymer-ceramics combinations in dry rubbing.

With this in mind, the formation process of a wear particle as perceived by the author is as follows. In the real area of contact, the geometric interference between the asperities of the two surfaces is such that there is a high probability of an oblique contact and thus it is possible for fracture to occur in the interior of either of the bulk materials even if the shear strength at the interface is weaker than in the bulk. When the system is in sliding contact, a shearing fracture occurs near the contact portion and a small fragment is produced, transferred and adhered to the opposite surface. This small transfer piece is known as a "transfer element." Because of the unsymmetric contact, shearing may occur in the harder material rather than in the softer. As the transfer elements move between the two surfaces, there will be a time when there will be a merger of two transfer elements into a "transfer particle" which will then adhere to one of the surfaces. In a repetitious process, the transfer particle gradually grows until it reaches such a size that it is removed from the surface by impingement against an asperity on the opposite surface. It is this particle that is called the "wear particle."

This model is used by the author to satisfactorily explain the three phenomena mentioned earlier; that is, the size of wear particles, the mutual material transfer, and the mixed structure of the wear particles. The model does, however, need modification if it is to account for the load-supporting mechanism.

The author has observed the growth process of a wear particle by recording the transverse movement of mechanical components of a test rig during sliding. Based upon his hypothesis of the mechanism of wear and the experimental data observed, the author has explained the size of wear particles and the effect of the lubricant on the size. Also, he has an explanation for the observed result that in practical rubbing systems the larger component wears out more rapidly than the smaller one. In addition, in a wear process in which there is repeated transfer sliding, vibration of the rubbing component is seen as a natural phenomenon. Thus, vibration is inherent to sliding wear tests and cannot be eliminated. The model is also used to explain those situations in which the harder solid has a greater degree of wear than the softer material.

Seizure of metals is also explained on the basis of this model. From the study carried out by the author, seizure is felt to be a special case of the growth of transfer particles in the sliding interface.

Microstructures Associated with Wear
by W. A. Glaeser

What is the microstructure that is associated with wear? Optical microscopy and the use of the scanning electron microscope have given us the ability to look into these intriguing microstructures. With these tools at our disposal, it seems appropriate to consider the current state of wear microstructure so that speculation can be made on the origin of wear debris.

In terms of macro deformation, dimensional changes associated with wear occur by several means. Illustrations include loss of material from the surface in the form of particulate debris, transfer of material from one surface to another, and gross plastic deformation and accumulation of plastic strain, especially during wear-in. This initial wear-in deformation may also be accompanied by changes in friction characteristics. An illustration of wear as a deformation process is given by the author where he considers the deformation of chain links under loading, and the contact wear of wire rope used in excavating machinery. Although fretting also occurs, deformation and extrusion is a major mode of plastic deformation.

Perhaps of greater interest is the study of the microprocesses that occur with the wear process. It is postulated that the near-surface structure is composed of three zones:

1. Grain deformation zone

2. Highly deformed zone (cells, subgrains, twinning)

3. Transfer layer

From stereoscopic SEM micrographs, microgrooving can be seen as well as minute extrusions, lip formations and surface tearing. From these photographs it is clear that some wear debris can originate from microextrusions and from tearing.

Asperity contact between the moving surfaces is shown to produce localized deformation in the form of scratches, furrows, grooves, etc. In the scratch zone, extreme deformation takes place as ridges are produced, ironed out and then produced again. Although some of the microgrooves and surface tearing might be associated with asperity welding, it is difficult to diagnose since many of the long scratches seem to be caused by asperity plowing.

The author points out that when a wear scar is sectioned, the directionality of the topography influences what is perceived in the section. A section in the direction of sliding will bring out the elongation and bending of grain boundaries but sections made at right angles to the direction of sliding will probably define the near surface wear microstructure more accurately.

From his studies of the microstructures associated with wear, the author indicates that strain rates during the wear process can be extremely high due to the small volume being strained. These microstructures are similar in morphology to large strain microstructures developed in metal working. In fact, the structures produced in the wear process are subject to the same controlling parameters as are found in the area of metal working. However, if we assume this, then some of the structures or effects that we might expect have not, in fact, been found in wear microstructures. This includes the area of fine twinning, strain rate effects, and the coalescence of subgrains and recrystallization. The conclusion is that more microstructural analysis is required.

The wear microstructure includes the transfer layers which are so important to the wear process. Discarding the large torn particles, the author finds a collection of very fine particles (of the order of 50 angstroms) that are layered into the surface. These particles are a mixture of materials from both sliding surfaces and appear to be sintered into continuous layers. These layers can debond and be emitted as flakes. It is assumed that the large flakes come from a detachment mechanism of the transfer layer by fracture at the boundary with the substrate.

Structures and Properties of Polymers Important to Their Wear Behavior
by K. Tanaka

Although some of the factors controlling the wear of polymers are known, many are still unknown. Since relationships between polymer structures and properties have not been completely elucidated, their effect on wear rates are discussed by the author on the basis of results obtained in experiments in which semicrystalline polymers were rubbed against a smooth steel and/or glass surface.

With respect to the effect of temperature on the wear rate of polymers, the author concludes that amorphous polymers show higher wear rates than either crystalline or semicrystalline polymers.

The friction and transfer of typical semicrystalline polymers were studied in an experimental program in which cylindrical surfaces of polymers were slid on a glass plate at a speed of 0.18 mm/s. The experiments at this very low speed indicate that the transfer characteristic of polymers are closely related to the molecular profile. The molecules of polytetrafluorethylene (PTFE) have a smooth profile, for instance, while those of polypropylene have a bulky profile. The transferred material for the polymers with a smooth molecule occurs in very thin films or streaks, while for polymers characterized by a bulky molecule, the transfer takes place in the form of thick streaks or lumps. Although temperature has an effect on the transfer of polymers, it is not uniform with all polymer structures. In the case of typical polymers having a spherulite structure, it is suggested that the size of the spherulite plays an important role in the magnitude of the wear rate. Polymers with smaller spherulites have lower wear rates. In addition, the tensile strength and melting point do not seem to be controlling factors with respect to the wear rate. From wear tests on polymers with bulky molecules and large spherulites, it is also shown that the shear strength at high temperatures near the melting point plays an important role in determining the wear rate.

Although the morphology of PTFE has not been completely understood, it is known that PTFE has a banded structure. As a result of the easy slipping of lamellae, the destruction of this banded structure occurs easily without any melting at the sliding surface. From the results of the transfer experiment carried out at very low speed, it is concluded that PTFE molecules are easily withdrawn from the lamellae at the frictional surface and a very thin film is transferred on the counter surface.

In addition, it is felt that tensile strength and melting point are not important factors with respect to the adhesive wear of polymers. The wear rate is seen to be, in general, higher when surface melting does not occur because of frictional heating than when it does occur. Although many physical, chemical, and mechanical properties are related to polymer wear, it is difficult to isolate the effect of any particular property because the wear process is complex and all effects are interrelated. The author feels, however, that it would be very useful to study the morphological and molecular characteristics of polymers that impact on the wear process. Such an understanding may well lead to the formation of a relationship explaining this phenomenon. With this understanding, one could design polymer components with the desired frictional and wear characteristics.

Ceramics in High Temperature Applications---Fundamental Considerations in Friction and Wear
by K. Miyoshi, Donald H. Buckley

Ceramics are assuming an ever-important position among the multitude of materials currently available for application in mechanical systems. Their wear properties, frictional characteristics, and their high temperature capabilities suit them particularly well for a number of applications. If these substances are to be chosen on a rational basis for tribological components, then we must be concerned with a fundamental understanding of the tribological properties of crystalline ceramics, such as adhesion, friction and wear behavior as they relate to measurable material properties. It is imperative that we gain a better understanding of the physics and chemistry of ceramics involved in tribology. In this way we may find the applications which their properties can be used to full advantage. Chemical bonding is seen to be an important aspect in the area of adhesion and friction. The removal of adsorbed films from the surfaces of ceramics and metals has been shown to result in very strong interfacial adhesion when two such solids are brought into contact. In addition, clean ceramic-to-ceramic contacts also exhibit very strong interfacial adhesion when the surfaces are brought into contact. In fact, it is found that some of these adhesive bonds are sufficiently strong that fracture of the cohesive bonds occurs.

As d-valence bonds are not completely filled in transition metals, they are responsible for such properties as cohesive energy, shear modulus, chemical stability and magnetic properties. It is hypothesized that the greater the amount of d-bond character the material possesses, the less active is its surface. It appears that this theory is the most plausible to be used in explaining the interfacial interactions of transition metals in contact with ceramics as well as with themselves. Data is presented on the coefficients of friction for some of the transition metals in contact with silicon carbide as a function of the d-bond character of the metal. These data indicate a decrease in friction with an increase in d-bond character, as predicted from theory. The more active the metal, the higher the coefficient of friction.

There also appears to be a strong correlation between the coefficient of friction and theoretical shear strength of metals. The higher the shear strength, the lower the friction.

When metals transfer to the surface of silicon carbide in a sliding pair, the morphology of metal transfer to the ceramic material reveals that the materials that have low shear strength and a low percent d-bond character exhibit much more transfer than those having higher strength and a higher percent d-bond character. From these data for metal-to-ceramic materials, it is seen that the chemical affinity and activity, tensile and shear strength all play an important role not only in the adhesion and friction, but also in the transfer and wear.

The frictional properties and the mechanical behavior of ceramic materials in sliding contact with themselves and/or metals are affected by the presence of surface films; just as in the case of metals and polymers. The surface activity related to the frictional properties for clean ceramic material contacting ceramics or metals will be strongly affected by gas or liquid interactions with the surface. The more chemically active the surface, the greater the degree of oxidation, and the higher the coefficient of friction. As might be expected, an increase in the surface temperature of a ceramic material tends to promote surface chemical reactions. These chemical reactions cause products to appear on the surface which can alter adhesion, friction and wear. As an example, the authors present experimental results showing that the surface of silicon

carbide graphitizes at high temperatures. Three questions then arise: 1) how thick is the graphite layer, 2) what is the graphitization mechanism, and 3) does the graphite affect the frictional properties of silicon carbide? It is found that the thickness of the outermost graphite layer on the silicon carbide is from 1.5 to 2.4 nm. The results suggested that the collapse of the carbon in two or three successive silicon layers after the evaporation of the silicon was the most probable mechanism for graphitization. In answering the frictional question, sliding friction experiments were conducted with silicon carbide in contact with iron. In general, there was an increase in friction with temperature which was probably due to increased adhesion and increased plastic flow in the area of contact. However, at very high temperatures the coefficients of friction for the graphitized surface of the silicon carbide were generally low.

The authors point out that very few studies of the anistrophic nature of friction and wear have been conducted from the consideration of adhesion between sliding surfaces. Test results have revealed that the highest atomic density (most closely packed) direction exhibits the lower coefficient of friction which indicates that direction is indeed important in the frictional behavior of crystalline substances. Test results have shown that the mating of crystallographic directions can play a significant role in the frictional behavior of ferrite. Sliding along the direction which is most closely packed minimizes adhesion and friction.

It is also mentioned by the authors that if friction and wear are caused by abrasion, then the primary slip system of the ceramics can explain the anisotropy of friction and deformation that has been observed. The anisotropic fracture that occurs during sliding is seen to be controlled by the surface and subsurface cracking along cleavage planes.

Composites for Increased Wear Resistance:
Current Achievements and Future Prospects
by J. K. Lancaster

Composite materials will undoubtedly find increased applications in mechanical system design. Not only do they support a load without undue distortion, deformation or fracture, but they can maintain low friction and wear over long periods without seizure. In addition, they provide the opportunity for the design of a low mass system which leads to lower dynamic loads in the system and to lower frictional losses. The topic of primary concern to the author is how the structure and composition of composites (primarily plastics-based materials) influences their friction and wear behavior.

Although composites containing PTFE have low friction and high thermal stability which is particularly attractive for sliding applications, their poor mechanical strength, excessive viscoelastic deformation under load and high rate of wear usually necessitate some form of reinforcement. The question then becomes, What is the best type of filler to choose for minimum wear? Unfortunately, there appears to be no simple answer. The reason for this should not be surprising inasmuch as there is more than one way to explain the manner in which fillers and reinforcing fibers influence wear. In the case of PTFE, for instance, the suggestion has been made that filler particles impede the drawing out process and, thus, prevent destruction of the banded structure. However, an alternative explanation is that the filler particles or fibers support load preferentially by virtue of their greater strength and stiffness. There is an added element of confusion in the literature about the effects of orientation of reinforcing fibers with respect to wear and friction. With more questions than answers, it would seem that this area would be appropriate for additional research.

The steady-state wear of a composite is seldom related directly to its bulk structure, but depends on the surface condition generated by the sliding process itself. Here we introduce the concept of "third bodies" which differ in composition and structure from the original material. And although a whole range of variables can influence third body film formation, considerable experimental effort in recent years has not enabled us to clarify more than a few specific aspects of third body film formation with PTFE composites.

An appreciable body of information has, however, been generated regarding the wear rates of composites. In general, they are very sensitive to the topography of metal counterfaces. Chain orientation within the PTFE film is also a significant factor and sliding which interferes with this orientation may be expected to produce increased wear.

PTFE transfer to a metal counterface is enhanced by the presence of copper and lead within the composite. Wear of PTFE-containing composites during oscillatory motion tends to be less than in unidirectional sliding at the same loads and speeds. Analyses of worn surfaces of composites after sliding against metals show that in general almost every element available in the system is likely to become incorporated within the third body films. This leads to the conclusion that there can be no simple mechanism for the process of film formation; debris must be transferred to and fro between the surfaces with particles being repeatedly deformed, degraded and reformed. Third body film formation from PTFE-containing composites is almost wholly inhibited in the presence of fluids and in composites containing more than one solid lubricant, interference can arise during third body film formation.

In addition to their influence on third body film formation, fillers and reinforcing fibers and polymers play another major role. Most of the materials commonly used to increase strength or stiffness are abrasive to some extent. Since polymer wear rates are influenced by counterface topography, the effect of small amounts of abrasive fillers could be beneficial in reducing wear by generating smoother surfaces. However, the choice of the optimum level of abrasiveness needed for minimum wear is by no means clearcut.

In PTFE-containing composites, the transfer film on the counterface is susceptible to abrasion by fillers. Therefore, it should be possible to control a transfer film thickness by the type and concentration of abrasive filler. Unfortunately, the relative roles of transfer and abrasion do not depend solely on the composite composition but also vary with the conditions of sliding.

Today there is a vast range of polymer/solid lubricant/fiber composites available which present the Design Room with a confusing choice since the properties of many of these composites tend to be very similar. The time may soon be approaching when rationalization and compromise formulations will be required to reduce the overall product range to a more manageable proportion.

Composites that are based on fiber-reinforced thermosetting resins have been used for many years as high load-capacity bearings in well-lubricated conditions where the fluid provides both the hydrodynamic support and cooling. Although there are several variants for these high load-capacity composites, literature appears to offer few, if any, general guidelines from which to predict the effects of changes on friction and wear performance. For unlubricated operation, the substitution of high temperature resins, such as polyimides for the usual phenolics, would be an obvious route for improving high temperature performance. However, it has not yet proven possible to establish any general trends between composite wear performance and specific resin properties, such as strength, stiffness or thermal stability.

Considering the coefficient of friction of high load composites, PTFE is usually more effective as a solid lubricant addition than MoS_2 provided the temperatures remain at less than about 250 C. This is probably due to the fact that the coefficient of friction decreases with increasing temperature for PTFE as a consequence of the reduction in shear strength; the friction also decreases with increasing load. This is probably due to the third body film being generated on the harder substrate by the sliding process. Although some of the ways are known in which a third body film influences the friction and wear of PTFE-containing composites, one of the major problems remaining is to relate the type of film used to composite structure and composition. This requires more information to characterize the films. Although numerous analytical techniques are available, considerable uncertainty exists in defining the most appropriate level of sensitivity required. For example, how relevant to the wear process is the fine scale topographical detail observed in high resolution SEM?

The author points out that the basic problem in incorporating lamellae solid lubricants such as graphite and MoS_2 is that the mechanical strength in tension is significantly reduced. Since the transfer of lamellae solids is an inefficient process, the high lubricant concentration required to achieve low friction result in mechanically weak composites giving high wear rates. It would be possible, however, to devise fabrication techniques which might result in mechanically stronger composites.

Little attention has been paid to fiber-reinforced metal composites. Carbon fibers as well as boron fibers are now available commercially and the time may be appropriate for a reassessment of their tribological prospects. Composite materials for high energy brakes have requirements which differ in several ways from those materials intended for bearings. These materials must have stability of the friction coefficient with varying load, speed and temperature, high thermal capacity, resistance to thermal shock, etc. One of the new materials is the carbon-carbon composite for aircraft brakes. The two major problems, a tendency for graphitic materials to undergo rapid wear at elevated temperatures and for non-graphitic materials to exhibit large fluctuations in friction, have been largely overcome by the introduction of additives.

THE FUTURE FOR LIQUID LUBRICANTS AND ADDITIVES

Thermal and Oxidative Stabilities of Liquid Lubricants
by William R. Jones

Liquid lubricants are being exposed to increased thermal stresses with the higher unit loadings that are being designed into mechanical systems. With the exposure to higher temperatures in oxidizing environments, the thermal and oxidative stabilities of the lubricant have become important factors.

Thermal stability is a term that defines processes occurring in the absence of oxygen. In the case of hydrocarbons and most other fluid classes, thermal decomposition or pyrolysis proceeds through a free-radical chain reaction process which yields many products. The radicals are highly reactive and start reaction chains by abstracting hydrogen atoms from the parent hydrocarbons. This chain sequence continues until the radicals are destroyed or all of the reactants are consumed. The rate of thermal decomposition usually varies with temperature according to the empirical Arrhenius rate law and one can define the rate constant for thermal decomposition by measuring the isothermal rate of vapor pressure rise at several temperatures. For standardization, an arbitrary thermal decomposition temperature is defined as the temperature at which the

isothermal rate of vapor pressure rise is 1.85 Pa/s. From data on the isothermal rate of vapor pressure increase as a function of reciprocal absolute temperature, the activation energy for decomposition can be calculated. From a knowledge of the thermal decomposition temperature and the activation energy for decomposition, the useful life of a lubricant in the absence of oxygen can be calculated. The useful life is typically defined as the time in hours for 10% decomposition.

There are a number of generalizations that can be made regarding the thermal decomposition of a variety of chemical structures.

1. The thermal decomposition temperature of a straight chain hydrocarbon is about 300 C.

2. Branched chain hydrocarbons are less stable than straight chain hydrocarbons.

3. Aromatic bonds have higher dissociation energies due to resonance and their maximum stability is approximately 450 C.

4. Esters of alcohols having β-hydrogens have a maximum thermal decomposition near 280 C.

5. Esters not containing β-hydrogens have stabilities approaching hydrocarbons.

6. Substitutions on an aromatic ring will decrease its stability.

7. Saturated ring compounds are more stable than their straight chain analogs.

8. Completely replacing hydrogen with fluorine increases the thermal stability of organic compounds (except aromatics).

There are a number of other observations that might be made with respect to the thermal decomposition temperature. Since thermal decomposition occurs at the weakest link in a compound, it should be a function of the weakest bond dissociation energy in that compound. Also, since bond length is inversely related to bond strength, it can be correlated with thermal decomposition temperature.

One of the important characteristics of a good lubricant is oxidation stability. It should be noted, however, that additives do not normally affect thermal stability of the base fluid.

The oxidation of an organic compound with molecular oxygen is referred to as autoxidation, and the process usually proceeds through a free radical chain mechanism. These reactions can become extremely complex. The liquid-phase oxidation of liquid lubricants has been extensively studied and, in general, the basic mechanism is understood. Since autoxidation proceeds through a free radical chain mechanism, it can be inhibited by the addition of scavengers which break the chain reaction by the formation of stable free radicals.

A large number of experimental methods have been used to study the reaction kinetics of the liquid phase oxidation process. In most of the oxidation studies the parameter measured is the absorption of oxygen. When this parameter is plotted as a function of time, four kinetic curves are observed. These include: 1) an autocatalytic effect, often observed with mineral oils of low aromatic content, 2) an autoretarding

effect as with highly aromatic mineral oils, 3) a linear curve which is neither autocatalytic nor autoretarding as with a polybutene, and finally 4) a curve which shows a mixed behavior as found with n-hexyldecylbenzene.

A number of micro-tests or thin film tests have been developed. In these tests, a small quantity of lubricant is injected onto the surface of a catalyst after the apparatus has been brought into equilibrium at the test temperature. A constant flow of air is maintained through the apparatus and volatile oxidation products are trapped for analysis. At the conclusion of the test, the degraded lubricant remaining on the catalyst surface is dissolved in a solvent and the solution is then analyzed by a variety of techniques to determine the rate of oxidation. The author highlights a few of the commonly used procedures.

1. High pressure liquid chromatography is used for the separation of complex mixtures of organic compounds. This method separates materials due to an equilibrium distribution of the materials between a stationary phase and a mobil phase which percolates through the stationary phase.

2. Size exclusion chromatography is the high pressure liquid chromatography mode that separates components of a mixture according to molecular size.

3. Ultraviolet-visible spectroscopy is used in identifying various components such as aromatic compounds which absorb strongly in the ultraviolet region.

4. Infrared spectroscopy is another identification technique where the spectral region of interest is from 4800 to 400 cm^{-1}.

5. Nuclear magnetic resonance is an analytical technique which may provide more structural information than is available from either the infrared or ultraviolet techniques.

6. Electron paramagnetic resonance is an analytical technique similar to nuclear magnetic resonance and can detect unpaired electrons in extremely low concentrations.

The author reviews a number of classes of lubricants in which the process of autoxidation has been investigated.

The first class is that of the hydrocarbons, and more specifically, mineral oils which constitute the bulk of conventional automotive lubricants. Esters are also discussed inasmuch as they are often used as lubricants in gas turbine engines.

The polyphenyl ether fluids have been studied because of their application to high temperature lubricants. They are thermally stable to approximately 450 C and oxidatively stable to 275 C. Most of their problems are related to poor low temperature properties and poor boundary lubricating ability.

Another class of fluids, C-ethers or thio-ethers are structurally similar to the polyphenyl ethers but they exhibit lower poor points and better boundary lubricating characteristics. Their thermal stability is somewhat lower and their oxidation stability is about 260 C. These fluids produce large quantities of a high molecular weight sludge when used as lubricants.

Perfluoroalkylethers are a class of fluids which have excellent thermal and oxidative stability. They have good viscosity characteristics, good elastohydrodynamic film forming capabilities, and good boundary lubricating characteristics.

Early data on branched perfluoroalkylethers indicated that these materials should be thermally stable and exhibit oxidation/corrosion stability.

Linear perfluoroalkylethers have a linear structure and the fluids have shown better viscosity-temperature properties than the branched class.

Behavior of Polymer Additives Under EHL and Influence of Interactions Between Additives on Friction Modification

by Toshio Sakurai

In modern formulations of lubricating oils, particularly in the case of engine oils, many types of additives are available. Polymer-type additives have become quite common in multigrade engine oils. The performance of these additives is not well understood nor are the interactions that occur between the various additives.

Although much research has been done on the effects of the addition of high molecular weight polymers to base oils, Sakurai is particularly concerned with the behavior of polymethacrylate (PMA) molecules under concentrated contact conditions. Of particular concern are the interactions which occur between lubricant additives. Although synergistic effects may exist with certain combinations of additives, there may also be antagonistic effects.

The polymer-thickened oils were formulated using selected polymer thickeners in concentrations up to 20% in a light base stock. Although polymer thickened oils exhibit distinct advantages in performance characteristics over conventional lubricants, serious problems may exist, such as unanticipated wear in cam followers, and the susceptibility of the polymer concentrates toward mechanical shear degradation.

It was noted that the film thickness of all polymer thickened oils became thinner than the film thickness with base oils. The complex behavior of polymer thickened oil may be affected by the following factors: 1) the molecular size, structure and molecular weight distribution, 2) the solubility and/or the dispersivity of polymer to the base oil, and 3) the mechanical shear degradation at or near the elastohydrodynamic (EHD) contact.

It is postulated that the larger size of PMA molecules results in their having difficulty passing through the EHD contact. Thus, the molecules may accumulate at the inlet and sweep around the contact. A number of photomicrographs are presented which show the distribution of graphite in and around an EHD contact when a graphite dispersed PMA-thickened oil has been used. However, it is observed that graphite particles in the base oil alone pass through the contact area. This is in contrast to the phenomenon when a PMA-thickened oil is used; the amount of graphite passing through the contact appears to be small. It was found that under the condition of pure sliding under boundary lubrication conditions, graphite accumulated in various degrees at the inlet and then flowed back.

These tests suggest that the high molecular weight of PMA causes an accumulation of graphite particles at the inlet region of the conjunction. One might conclude that PMA molecules are generally difficult to pass through the contact under rolling conditions. The blocking action of the polymers at the inlet region may decrease the oil supply to the contact and this may result in a condition of lubricant starvation. From these observations it is concluded that there may be a critical value of molecular weight for PMA additives which is dependent upon the structure of the polymer and on the particular contact condition.

There may be synergistic effects in some combinations of additives found in formulations of lubricating oils. Examples are additives such as organal sulfur compounds and fatty acids. There are also antagonistic effects due to the interactions involving zinc dialkyldithiophosphate (ZDP). As an example, ZDP will react with peroxy radicals and the products are not effective as anti-wear agents. Wear data indicate that the deterioration products of ZDP in a fully formulated engine oil are ineffective for anti-wear performance in normal service.

In addition, above a critical concentration, amines can cancel the anti-wear performance of ZDP as measured in a four ball machine. Also, two percent by weight of succinimide interacts with ZDP to reduce the effectiveness of its anti-wear properties. From the experimental work, it seems that the mechanism through which ZDP provides anti-wear properties is not fully understood. It is known, however, that acid phosphate formed from the decomposition of ZDP plays an important role in its anti-wear performance. The acid phosphate interacts easily with basic compounds in the lubricating oil and the resulting compounds reduce appreciably the anti-wear performance of the lubricant.

What's So Hot About Formulated Synthetics?

by Alan Beerbower

Synthetic lubricants and the additive packages that are required to make them competitive with petroleum oils have now arrived on the market. At the half-century point in their development, the author feels that a few comments are in order with respect to their applications.

The story of the use of diesters in jet engines is not due to their being "better lubricants" in some general way as compared to petroleum products. In some ways the diesters are inferior to mineral oils. They were superior however in terms of excellent volatility-viscosity relations and exhibited extremely good low temperature fluidity. The most notorious difficulty with the diesters was their poor thermal stability in the absence of oxygen. Another difficulty was that diesters can hydrolyze in storage, giving corrosive acids. In addition, diesters are not as good as mineral oils in preventing gear scuffing. Although some problems with the diesters have been solved, one that has not is their poor performance in preventing pitting fatigue.

A future trend is predicted: there will no longer be any prospect of superior base stocks. In addition, there seems little incentive for the production of better anti-oxidants since most of the oils are drained for other reasons long before serious deterioration starts. A profitable area would seem to be the search for better anti-scuff agents; perhaps additives designed to polymerize on the working surfaces. Since additive makers are secretive for competitive reasons, there may be a number of new developments occurring which we do not know.

Of all the potential markets for synthetic lubricants, that of automotive oils is by far the largest and the most attractive. It is also challenging because of the many functions provided by the lubricant in an internal combustion engine.

In view of the long success story with mineral oils, a reasonable question would be, Why use a synthetic base oil now?

By considering the physical properties of base stock, it is possible to make comparisons in terms of thickening at low temperatures. From a list of currently

available oils, it is seen that the enhancement of the mineral oil with a polymeric VI improver would still not provide as good a low temperature property as exhibited by the poorest of the synthetics.

In addition, it is seen that the volatility relations are superior for the synthetics as compared to the mineral oils.

Since heat transfer properties are important in engine lubricants, estimates were made of the specific heat and thermal conductivity of several oils. The conclusion was that the synthetics fall within the same range as mineral oils and neither offer advantages nor create problems in this context.

It is pointed out that in contrast to the aircraft turbine oil market, the synthetic automotive lubricant market is too immature to predict any trends in additives.

Currently an additional requirement is being placed upon our lubricants, energy conservation by reducing friction. The exact nature of this process is still a subject of controversy because it involves both reducing the viscosity below the level that was long regarded as the safe minimum and then using an additive to protect the rubbing surfaces from damage during asperity contacts. Some feel that classical hydrodynamics is an adequate explanation and point to the fact that colloidal graphite or molybdenum disulfide will serve as the additive. There is no doubt that such oils do reduce fuel consumption. An even more controversal matter is the addition of colloidal polytetrafluoroethene to oils. One additive that the author considers indispensable for modern engine oils is ZDP. The question is raised as to whether better varieties might be made available if consideration were given to the possibility that the way in which it works is by preventing low cycle fatigue wear rather than adhesive wear as is commonly supposed. A better understanding of the mechanism of protection could help to limit the concentration of phosphorus to avoid damage to the catalytic converters used for emission control.

In the area of industrial lubricants, it is suggested that the outlook for including the leading synthetics as industrial oil base stocks is limited since these lubricants tend to be selected by very cost-conscious personnel. In industry, however, there are many more additives used than most persons realize. The first additives to correct the lack of oiliness were nothing more than some fat to enhance the slipperiness. Stronger chemicals, such as tricresyl phosphate, now take over and bridge the gap between the oiliness agents that work by chemisorption and the extreme pressure agents that work by irreversible reactions.

The prospects for new additives in this field are not felt to be very bright because of the limited markets for individual products. Formulators tend to depend on the additive makers for research and none of the problem areas are sufficient to support other than a very modest research effort. Consequently, the result is a rather slow-moving activity, occasionally sparked by some new development.

STATUS AND NEW DIRECTIONS IN EHL

Status and New Directions in EHL: Status of Understanding
by Bernard J. Hamrock

The recognition and basic understanding of elastohydrodynamic lubrication (EHL) was one of the major developments in tribology in the 20th century. Perhaps because of

the prior analytical work in the field of full film lubrication, tools were ready for application to this new mode of lubrication and advances and understanding came fairly swiftly. Today, as Hamrock has pointed out, the status of understanding for the idealized stage of EHL is well covered in the literature. However, there is an additional stage of development in EHL which is currently being worked upon and which incorporates the effect of non-Newtonian fluid models, thermal effects and surface roughness. The final stage of development is postulated to be in lubrication of real engineering surfaces in operating environments.

The definition of EHL is taken to be, "the study of situations in which elastic deformation of the surrounding solids plays a significant role in the hydrodynamic lubrication process." The approach to the problem has been fairly straightforward -- combining the lubrication equation with the variation of lubricant viscosity and density, and incorporating elasticity into the equation of the total system.

The driving force behind the generation of understanding of this tribological mode, was the very practical consideration of the determination of the minimum film thickness within the conjunction of highly loaded bearings. This is especially important with respect to rolling element bearings which constitute elements of many mechanical systems. Design equations have been available for some time for the determination of minimum film thickness in conjunction, and experimental results have confirmed that in many cases these are reasonable values to use. It is felt that the minimum film thickness formula tends to underestimate the actual film thickness and will possess the merit of being conservative.

The initial EHD work was with materials of high elastic modulus, such as metals, and then was extended to low elastic modulus materials, such as rubber. Minimum film thickness formulas were then generated for the soft-EHL situation. It was found that in soft EHL, the film thickness is a great deal more affected by load than in hard EHL, but is less affected by load than in hydrodynamic lubrication. In addition, the exponent on speed is nearly the same for both hard and soft EHL.

At the present time, EHL theory predicts the magnitude of film thickness quite satisfactorily. However, it fails to explain behavior in traction; in particular, it does not satisfactorily account for the variation of the magnitude of the traction with rolling speed or the degree of slip. This has lead to a more detailed investigation of the behavior within the conjunction and the incorporation of non-Newtonian models, thermal effects and surface roughness effects into the EHL model.

In these high pressure conjunctions, it is accepted that the lubricant does not behave as a Newtonian fluid. A number of rheological models have been used for lubricant flow, one being the limiting shear stress model which comes from the observation that there is a limiting shear stress for a given pressure and temperature at which the lubricant will shear plastically with no further increase of shear strain rate. From these considerations, traction behavior was found to be directly related to the non-Newtonian fluid behavior.

Surface roughness effects, or surface topography, plays a very significant role in determining the fatigue life of EHL contacts. Unfortunately, the roughness of bearing surfaces is normally characterized by a single parameter which indicates the arithmetic average of the surface finish. Other parameters that will be significant include the distribution function of the heights of asperity profiles, the autocorrelation function, the surface pattern parameter, and conceivably, other characteristics that have yet to be investigated. It is an area in which a great deal of research remains to be done.

Since interacting surfaces dissipate energy, there may be an appreciable temperature rise in the conjunction. Under conditions of high surface speeds and high lubricant viscosities, substantial reductions in film thickness can occur. Thus, it is important that thermal effects be considered. An in-depth discussion of thermal effects will be included later.

Temperature Effects in EHD
by Ward O. Winer

Contact temperatures are extremely important in elastohydrodynamic lubrication (EHL). As the temperature increases, the EHL film thickness decreases which can lead to contact on boundary films which in turn may desorb and result in contact between the solids. This increase in lubricant temperature also reduces the pressure generating ability of the film and decreases the friction or traction in the film. This deleterious effect on film thickness is the result of the decrease in lubricant viscosity with increasing temperature in the inlet region of the contact. This temperature is primarily determined by the bulk temperature of the elements being lubricated and not by the temperature rise in the contact zone.

Although the thermal effects in EHL contacts is extremely important, the determination of the temperature in the contacts has been difficult to obtain because of the size of the contact and the inaccessibility of the region of interest. In fact, temperature measurements in EHL contacts have been done by relatively few people.

Both steady-state and transient system bulk temperatures can be analyzed by conventional integral or lumped heat transfer analysis techniques. It is this bulk temperature that plays a major role in determining the EHL film thickness. Heat transfer calculations in typical tribological contacts show small temperature gradients in the body except for the local flash temperature in the vicinity of the concentrated contact. In addition, typical tribological systems are characterized by long thermal transients.

Thermal analyses for full film EHL conditions have not posed any insurmountable problems. There is, however, a very practical situation which does pose considerable analytical problems. This is the area in which the EHL film becomes so thin that asperity interactions occur and energy dissipation is concentrated over extremely small areas. This is the area of mixed lubrication, a mode of lubrication that occurs frequently in heavily loaded machine elements. Analytically, the mixed lubrication regime is poorly defined and additional work will be necessary before we will be in a position to adequately predict frictional behavior of the contacts.

Surface roughness effects play an important role in EHL. When film thickness to surface roughness ratio approaches one, surface temperature fluctuations are observed on the moving rough surface; the temperature fluctuations may be large and then decrease with time as the running-in process occurs. This phenomenon is accompanied by increased traction and wear. The fluctuations in temperature occur when the contact load is shifting from being entirely on the EHL film to being partially on the asperities. This asperity interaction results in a time dependent system with irreversible changes. It was found from a spectral analysis study of surface roughness and temperature in the same experiment, that surface roughness of only a particular wavelength range entered into the wear process and caused temperature fluctuations. The significant wavelength range of surface roughness depended on the Hertz diameter of the contact. Surface roughness with wavelengths either longer or shorter did not interact.

In the case of lubricant starvation, surface interactions will occur at any level of surface roughness, and transient temperature spikes are observed. These transients, rising to as much as 1 100 C, should have considerable impact on surface chemical, metallurgical and mechanical phenomena. Whether these transient temperature spikes occur under conditions of lubricant starvation, by impending EHL film failure, or due to partial EHL in a mixed film regime, one might expect to find reactions with the lubricant. Additional attention should be addressed to these conditions, as it would enhance our understanding of the failure of EHL lubricant films. As Winer pointed out, probably the most exciting new area in EHL is the application of experimental techniques to the study of local high surface temperatures that are associated with asperity interactions. It is increasingly important that we understand how these high temperatures relate to surface roughness, the presence of surface films, the presence of boundary lubricant, and the run-in and wear of various materials.

Lubricant Rheology in Concentrated Contacts
by Bo O. Jacobson

It has been known for many years through experimental observation, that the Newtonian model for lubricant behavior in highly stressed situations is insufficient for the explanation of traction behavior. In lightly loaded bearings the behavior of many liquid lubricants is described adequately by a Newtonian model for shear stress as a function of shear strain rate. However, in a typical EHL contact, where the lubricated surfaces are hard, the oil pressure may be of the order of one GPa. At these high pressures and static conditions, the viscosity of the lubricating oil increases many orders of magnitude. Thus, lubricant rheology becomes a pivotal point in EHL analyses.

There have been a number of experimental investigations into the non-Newtonian behavior of lubricants. There are basically two types of tests: static and dynamic. In static tests, the oil is pressurized for a relatively long time, typically more than a million times longer than its transient time in a ball bearing contact. In the dynamic test, the pressure is applied approximately as long as the transient time through a roller bearing. In addition, the static experiments can be split into two categories: experiments where the oil crystallizes and experiments where the oil becomes an amphorous solid. In dynamic experiments, lubricant behavior depends on the time scale of the experiment. Not only is the rate at which the dynamic stresses are applied important, but the stress history of the lubricant must also be considered. It has been found that experiments designed to determine physical properties of lubricants for EHL calculations should be performed at the same pressure, shear stress, temperature level and time scale as in real EHL contacts.

Since experimental investigations of oil behavior show that oils change their properties with pressure, temperature, stress level, stress rate, stress history and temperature history, many attempts have been made to mathematically describe these phenemona. Thus, we have a prolification of lubricant models that have been used to predict oil film buildup and traction in heavily loaded contacts.

The lubricant models that have been considered can be split into two primary groups, 1) models where the shear stresses are functions of the shear rate, and 2) models with the shear stresses independent of the shear rate. This first grouping contains the Newtonian models with variable viscosity, the viscosity being a function of the pressure and temperature but independent of time. If the shear stress in the lubricant is higher than 1-5% of the hydrodynamic pressure in the high pressure zone, the lubricant behavior will be non-Newtonian and many different models have been proposed. The second group contains models with a limited lubricant shear strength.

Non-Steady-State Effects in EHL

by Duncan Dowson

Mechanical systems are dynamic systems, they rotate, oscillate, translate and the bearing systems are subjected to non-steady-state cyclic conditions. We find this situation in reciprocating seals, piston rings, cams and lifters and in bearings used in reciprocating engines. In these non-steady-state mechanisms, the hydrodynamic film formation ceases to exist at some time in the cycle and the functionality of the bearing is based upon squeeze film action. In the case of non-conformal lubricated components in mechanical systems, elastic deformations occur on the surfaces and the analysis is complicated since the shape, as well as the minimum thickness of the lubricating film, varies with time.

It is here that Dowson points out an interesting situation. In EHL studies of machine components, such as the meshing of gear teeth or the lubrication of balls or rollers in rolling element bearings, attention is usually focused on the most severe conditions and a static solution is obtained. Yet a sequence of quasi-static solutions for a cycle of events implies that both the film shape and minimum film thickness are functions of time. THERE IS THUS A NORMAL MOTION OR SQUEEZE-FILM ACTION BETWEEN THE SURFACES WHICH IS GENERALLY NEGLECTED IN THE EHL ANALYSIS. It is this missing term that is investigated with respect to its sensitivity on hydrodynamic effects in bearings. The starting point for an analysis is the acceptance that the total normal velocity at any location consists of the familiar rigid body action together with the time rate of change of the local elastic deformation. The total normal velocity term in the Reynolds equation varies along the length of the conjunction at any instant and this is likely to be significant in reciprocating machinery where the film shape is subjected to cyclic action.

To assess the importance of this term in Reynolds equation, Dowson analyzed the EHL behavior of a piston ring and cylinder bore. This is an appropriate application since the piston ring and cylinder bore are subject to exceptionally severe dynamic conditions. The load, sliding velocity, temperature and lubricant viscosity all vary throughout the cycle.

The results of this analysis are most interesting. When it was assumed that the lubricant viscosity was not affected by pressure and the solids were rigid, normal piston ring lubrication theory predicted a cyclic minimum film thickness of 0.05μm. When account was taken of the influence of pressure upon viscosity, this prediction increased to 0.11μm. A simple EHL analysis in which the squeeze film action was associated with rigid-body motion alone brought the prediction to 0.17μm. Finally, when the rate of change of elastic deformation with time (the missing portion) was considered in the equation, the minimum film thickness predicted was 0.20μm.

Thus, the analysis confirmed the existence of EHL action in the piston ring-cylinder bore interface in the vicinity of top dead center and, in addition, indicated that the squeeze film action was particularly important.

It is pointed out that the minimum film thicknesses predicted for the piston ring are extremely small compared to the surface roughness of the rubbing pair and therefore the mixed film mode of lubrication will undoubtedly apply in these regions. The recognition of this mode of lubrication is particularly important when one is concerned with an assessment of frictional losses.

Real Surface Effects in the Elastohydrodynamic Lubrication
by John H. Tripp

All of the papers on EHL have stressed the critical role that is played by both the deformation of the solid materials and the viscous behavior of the lubricant. The understanding of EHL has been based largely upon three factors. In the case of "ideal" EHL, these have been linear elasticity, exponential Newtonian viscosity, and a Reynolds equation for pressure generated in the film. In the present paper, Tripp considers an extension of this basic formulation as an attempt to describe bearing problems in the "real" world.

Now the realities of mechanical systems include the realities of friction and wear, and it would be extremely desirable if EHL formulations could shed some light on these factors. Although the ideal EHL model does predict frictional behavior reasonably well, it cannot add insight on wear for there is no physical mechanism incorporated in conventional EHL that would allow for surface degradation.

To predict real world phenomena, the EHL model must represent the mechanisms of surface interactions in the real world. Consequently, the model must incorporate a more general non-Newtonian viscosity formulation, consider in detail the topography of the surfaces with regard to the types of surface finish actually obtained in engineering practice, and the continuum representation of the solid must be replaced by one that recognizes its microstructure. In addition, it will be necessary to ensure that the many physical assumptions built into Reynolds equation are not violated. If such a condition should exist, then it would be necesary to determine alternative forms to Reynolds equation.

In general terms, the roughness of a solid is defined as any departure of the actual surface height from the ideal datum level, or "nominal" level. This definition raises the question of the length scale at which roughness is specified and it is seen that there is some considerable freedom in choosing this bandwidth. Then, within this bandwidth the roughness may display both an ordered and a random component. If we assume that the film thickness exhibits spatial randomness, then we must consider a stoichastic form of the Reynolds differential equation. The solution to such an equation would provide us with time-averaged values for the variables such as load, coefficient of friction, and pressure distribution.

To describe the rough surfaces in a statistical sense requires knowledge of the height distribution and the correlation functions for these heights. These depend upon the scale selected for measurement of surface features and are not intrinsic properties of the surface. The height distribution is the probability that a single point in the surface selected at random, lies at or below a given height, while the correlation functions describe how the probability of finding one point at a given height depends on the heights of some of the surrounding points.

An interesting observation is made between the lubrication regimes defined by the Stribeck curve and the result from ideal EHL which states that the minimum film thickness is a monotonic increasing function of the Stribeck parameter group. Thus, it is pointed out that the Stribeck curve illustrates friction vs some nominal film thickness. For the types of height distribution found on many surfaces, about 0.1% of the surface lies above the height of three so that the linear region of the Stribeck curve is associated with full film EHL and only negligible solid contact occurs between the film boundaries. Approximately 15% of the height distribution exceeds 1.0 so that for the parameter less than one, the lubricant flows between patches of insipient contact where the surfaces

either make direct dry contact or are separated by a boundary layer or a thin micro-EHL film. Friction in this regime arises from both dry contact and from boundary layers; wear may be high and scuffing is an important failure mode. In the intermediate range, for the parameter between one and three, we find partial EHL where fractions of the load shared by the EHL film and the insipient asperity contacts are comparable. The dominant failure mode in this regime is by fatigue or pitting.

Considerable attention is given to the full film EHL regime where insipient asperity contact carries a negligible fraction of the load.

To obtain an average solution to Reynolds equation, an approach which might be taken is to average the equation itself. This leads to a generalized averaged Reynolds equation in which it is seen that there are two distinct averaging processes required. These are associated with components of flow both parallel and transverse to the surface lay. By introducing the concept of flow factors which are known in terms of the roughness parameters, an equation is derived which may be used in place of the ideal form in the complete EHL procedure. An interesting observation is that the principle effects of the roughness on flow can be described by only two additional parameters, the RMS surface height and the ratio of the correlation lengths in the two principle roughness directions. It is also interesting to note that the factors that describe Poiseuille flow are separable into the sum of two single-surface flow factors. Thus a combination of a single equivalent rough surface vs an ideal smooth surface can always be found. Shear flow, on the other hand, factors into the difference between two single-surface factors such that it is significant as to which of the two surfaces carries the equivalent roughness.

The Reynolds equation, together with flow factors, constitute a proper basis from which to approach the EHL problem in the regime where mechanical contact carries an insignificant fraction of the total load. The reason is that the flow factor approach provides a firm foundation through the concept that relative fluctuations in flow are small compared to those of the surface roughness itself. Under these conditions, the averaged Reynolds equation for the expectation of the pressure is an adequate approximation.

Can this formulation be extended to the partial EHL regime where there is appreciable asperity contact? With an understanding of the dependence of real area of contact and load on surface compliance, as well as of the effect of contact on height distributions, then perhaps asperity contact models can be incorporated into the formulation. If the flow model can be modified for some asperity contact, then the question which remains to be answered is that of how far the averaged flow approach can be carried and still provide a meaningful contribution.

Micro-Elastohydrodynamic Lubrication
by Herbert S. Cheng

In EHL we have seen that the lubricant film thickness, pressure and surface temperatures are governed by the conditions in the conjunction. Thus, in the conjunction, the governing parameters are the deformation of the surfaces and variation of the viscosity with pressure. When one is concerned with a deterministic smooth surface, conventional EHL is insufficient to explain failure processes that may occur within the contacts. In those situations where the lubrication breakdown occurs locally at asperity contacts, conditions approaching failure occur and the lubrication phenomenon is controlled by micro-EHL. To understand failure modes, it will be necessary to turn our attention to the micro regime in which we find pitting, scuffing and wear.

In fully lubricated Herztian contacts, wear is suppressed by a series of three protective films; these include a thin oxide film, an absorbed or reactive surface film and then a thin lubricant film. If adhesive damage is to occur between sliding asperities, these three films must be broken. If asperities are to contact, the thin lubricant film at the asperity will play the critical role in mitigating failure. The mechanics of this lubricant film formation at the asperity is similar to that of the conventional EHL situation but smaller in scale, and consequently, is usually referred to as micro-EHL.

In the area of macro-EHL, we are concerned with a variation of the average quantities in the conjunction; that is, an average film thickness, pressure, and temperature. Even though most EHL contacts operate in the regime where the roughness plays a significant role, the characteristics of macro-EHL have been developed on the basis of smooth surface theories. If asperity interactions are occurring, then the pressure and temperature are not smooth functions as predicted by the full film EHL theories but contain fluctuations. The macro-EHL problem in the partial film mode primarily deals with the analysis of all average quantities in the conjunction as being influenced by the surface roughness. Developments in partial-EHL are still in the early stages. There is evidence, however, that the full film EHL theory is not adequate to predict the proper average film thickness in this regime. In the area of micro-EHL, three aspects are stressed. The first of these is the normal approach of a single asperity as it enters the Hertzian conjunction and pressure is generated. The second aspect is that of sliding in which both the film thickness and pressure are significantly altered by the wedge action as a single asperity slides over the opposing surface. The third aspect is with respect to the film and pressure characteristics occurring when two asperities collide during sliding. In this last process, both the squeeze film and wedge-film mechanisms are present.

The surface topography, which is so important in micro-EHL, is dependent upon the manufacturing process used in producing the surface. For ground surfaces, profilometry has shown that the roughness consists essentially of asperities in the form of ellipsoidal tips with very high ratios of major to minor axes. The asperity oil films that are developed at such ellipsoidal tips are dependent upon several factors which include: 1) the orientation of its major axis with respect to the surface motion, 2) the degree of viscosity enhancement around the asperities in the macro-EHL conjunction, and 3) the relative sliding velocity at the asperity.

Calculations have been made on asperity film thickness under two conditions: for a longitudinal elliptical asperity and a transverse elliptical asperity. For the longitudinal asperity, the film thickness is small and is not expected to provide much protection against sliding damage unless there can be considerable viscosity enhancement. For the case of a transverse asperity, however, the film thickness is found to be approximately five times more than that developed in the longitudinal asperity under the same conditions. In this case, the film thickness is still insufficient to provide an effective micro-EHL film.

A number of traction measurements in sliding EHL contacts prove that the lubricant under the high pressure conditions inside the conjunction is non-Newtonian. It behaves as viscous plastic substance with a limiting shear stress when sheared under high pressure. In the micro-EHL conjunctions, the lubricant viscosity in the valleys can become extremely high. Under this high ambient pressure, the lubricant can reach its limiting stress quickly at the inlet of a micro-conjunction and therefore may drastically reduce the film forming capability as predicted from a Newtonian model. Recent isothermal analyses for ridges with small slope and height have shown a limiting condition at which the film suddenly collapsed. Is it possible, then, that the same phenomenon might occur in micro-EHL and cause a film breakdown at the inlet to sliding micro-conjunctions?

Surface damage, such as surface pitting and scuffing, are related to micro-EHL. The surface pitting originates from microcracks which are initiated near the surface. With the merging of microcracks, shallow micropits are formed known as surface peeling or gray staining. The initiation of surface pitting is undoubtedly influenced by variations of the local asperity pressure and shear stress as they traverse through the macro-conjunction. To protect against such surface damage, a criterion is needed which will relate the density and size distribution of these surface cracks as a function of the distribution of pressure and shear stress. These factors can, of course, be predicted from micro-EHL analyses.

Scuffing is characterized by a local transfer of materials from one surface to the other. Surfaces are not only protected against such damage by the micro-EHL film but also by a boundary-type surface film and oxide film. There is insufficient evidence currently to support whether a micro-EHL breakdown would automatically lead to surface film failure. There is evidence, however, that failure of all three films are linked to asperity temperatures even though the exact mechanisms are still unclear. If we are to thoroughly understand the scuffing process, then we must have a much more complete knowledge of micro-EHL performance.

Transient EHL Effects in Starved Ball Bearings
by Edward P. Kingsbury

Transient EHL effects in starved ball bearings are not new. They were identified shortly after the first classical EHD solution for flooded, non-parallel films was published. Investigations of dynamic lubricating films and "oil jogs" which appeared in instrument bearings showed EHL films which must have been thinner than those calculated from the fully flooded solution. Thus, there was an increased interest in accounting for starvation film thinning in EHL.

The inlet position starvation model which has been used rather consistently is felt by the author to be open to criticism on two counts: 1) if an assumption for inlet miniscus position must be made to calculate film thickness, then why not assume the thinner film immediately? 2) a steady-state formula cannot give information on film transients. With respect to inlet miniscus position, the author feels that a much more realistic description of the physical situation would be as follows; starvation exists if an increase in the mass of oil available to an EHD contact gives an increased film thickness.

In starved ball bearings, the side leakage dominated. Transient behavior that has been observed suggests a different approach to the problem. The model presented is based on the way starved bearing experiments have been made and thus has a built-in compatibility with the experiments.

1. Instead of calculating a film thickness, assume that an initial film thickness is given. This corresponds to the experimental technique of depositing a thin, uniform film on the bearing surfaces.

2. Assume one-dimensional flow inside the Hertzian area in the transverse direction rather than along the rolling direction.

3. Assume zero flow outside the Hertzian area everywhere in the bearing.

4. Calculate changes in film thickness with time based on the difference between in-flow and cross-flow.

In this paper, four bearing phenomena are explained in terms of a film thickness transient. These four thickness transients are: 1) the oil jog, 2) ball-race coupling variations in the basic speed ratio, 3) coupling variations in orbiting drag torque, and 4) shear activated lubricant break-down.

NEW DIRECTIONS FOR SOLID LUBRICANTS

Practical Applications and Usages of Solid Lubricant Films
by Bernard C. Stupp

Solid lubricants or solid materials which exhibit lubricating properties have been in use for many years. Although there are a multitude of solid lubricants available for tribological systems, the most commonly used materials in the form of bonded films include graphite, molybdenum disulfide and polytetrafluoroethylene (PTFE).

Graphite is a lamellar compound which lubricates because of weak van der Waals forces at the slip planes. However, graphite depends on an intercalation of gases, liquids or other substances between its layers.

Molybdenum disulfide, on the other hand, has weak van der Waals forces between the sulfur bonds and is not dependent upon adsorbed vapors for its lubricating properties.

Organic polymers, such as PTFE and polymeric amides, offer very low friction characteristics but generally have low load carrying properties. The load carrying ability can, however, be improved with fillers such as carbon, oxides, or other polymeric binders. The methods of applying solid lubricants are quite varied and the techniques selected depend to a great extent upon the lubricant and the desired end result. For very thin films where the lubricant has a natural afinity for the substrate material, burnishing may be used. This is not a precise method for thickness control and consequently the technique of sputtering may provide more precise control. Plasma spraying may be used for applying coatings thicker than the sputtered films and generally must be finish machined after the coating is applied.

In many applications of graphite, molybdenum disulfide and PTFE, the common method is to incorporate the lubricant pigment into various binders which can be applied by spraying, dipping or brushing after which they are bonded by baking or air drying.

Although there are a number of surface preparations, it is difficult to describe precisely the proper pretreatment for all situations. In many cases, these pretreatments are determined empirically. It can be stated that most bonded films perform best when applied over phosphated steels. Aluminum and its alloys and titanium, are usually anodized prior to the application of the bonded film. For those materials which neither phosphate or anodize, the surfaces may be chemically etched, grit blasted, vapor blasted or ion etched. Experience has shown that a slightly roughened or disrupted surface provides better results for bonded films as compared to smooth surfaces.

Support of Oil Lubrication by Bonded Coatings
by Rudiger Holinski

As has been discussed previously, solid lubrication with inorganic compounds, such as molybdenum disulfide, has been very successful under dry conditions or under

extreme environmental conditions, such as vacuum, high and low temperatures, or in the presence of radiation. Under these conditions, lubricating oils cannot provide adequate lubrication and solid lubricants provide a viable alternative.

When these coatings are applied to a contact which is lubricated by an oil or grease, the solid lubricant film has a limited lifetime and the films are seen to be stripped from the metal surface. In recent years, new solid lubricant-containing coatings have been developed with oil-resistant binders. These oil-compatible bonded coatings protect metal surfaces from wear and reduce friction under boundary conditions in the presence of a liquid lubricant.

The typical bonded coating consists of a solid lubricant pigment, a binder, and a solvent. The binder is dissolved in the solvent and the solid lubricant particles are dispersed. The product may be applied to the metal surface by dipping or spraying. After application, the liquid film solidifies through evaporation of the solvent and crystallization of the binder. The binder connects the solid lubricant particles with each other and binds the solid pigments to the metallic surface. The film that is formed has a high degree of cohesion within the film and strong adhesion between the film layer and the surface.

A solid lubricant film on a metal surface can only be beneficial in an oil lubricated system in the regime of boundary or mixed lubrication. Since the surface topography, in conjunction with speed, load and lubricant viscosity determine the shape of the Stribeck curve, it should be possible to reduce the extent of the boundary and mixed lubrication regimes if the surface could be made smoother. It is postulated that if a rough metal surface has been coated with a solid lubricant-containing layer, the surface becomes significantly smoother after short run-in of the coating. In effect, the hydrodynamic portion of the Stribeck curve has been increased by moving the knee of the curve to the left. The author notes that solid lubricant coatings on metal surfaces of machine components contribute to the enhancement of oil lubrication and provide the following benefits:

1. Reduction of friction during boundary and mixed lubrication
2. Reduction of frictional temperature levels
3. Enlargement of the hydrodynamic lubrication regime
4. Elimination of stick-slip at low speeds
5. Prevention of wear-in damage through seizure
6. Reduction of noise during boundary lubrication
7. Increase of load carrying capacity
8. Reduction of shear stress in the area of frictional contact

Status of Use of Plasma Physics Techniques in Deposition of New Coating Materials
by Talivaldis Spalvins

The wear resistence of a rubbing pair may be enhanced through the deposition of a wear resistent tribological coating on the surfaces. Sputtering technology offers great

flexibility in the deposition of this coating since the sputtered coatings can be tailored to a preferred chemical composition and the coating morphologies can be modified as desired. Any combination of metal and non-metal elements can be sputter-deposited in any composition without concern for their phase relationships. Ion-plating techniques may also be used. The basic difference between sputtering and ion-plating is that in sputtering the coating material is generated by impact evaporation and transfer occurs by a momentum transfer process, whereas in ion-plating generation is by thermal evaporation and transfer is by electric field acceleration.

Ion-plating has three unique features: 1) a high energy flux of ions and energetic neutrals contributes to the excellent adherence of the film to the substrate and to a desired microstructural growth of the film; 2) when used in the reactive mode, this flux provides activation energy to synthesize uniform compound films; and 3) the high throwing power provides coverage of complex intricate shapes.

Conventional ion-plating is primarily used for the deposition of soft metallic lubricating films. Soft metallic gold, silver and lead films applied by ion-plating offer low friction coefficients, provide longer wear life and exhibit a gradual increase in the friction coefficient after the film has worn off.

Recently, a reactive mode of ion-plating which utilizes a reactant gas, has been investigated for depositing hard, wear-resistant refractory coatings such as nitrides, carbides, and silicides.

It has been shown that intricate graded structures with a hardness gradient can be produced by programming the flow rates of the reactant gases during reactive sputtering. The exact mechanism for the formation of this interface is not fully understood. However, the graded interface formed is not only responsible for the excellent adherence, but also effects mechanical behavior due to a structural alteration of the crystal lattice in the surface and subsurface regions. These surface-strengthening effects result in an increase in yield, tensile, and fatigue strengths of the materials.

Practically all vacuum-deposited coatings are in a state of stress. This effect is found to be more pronounced in hard wear-resistant refractory compound films. Thermal stresses exist between the refractory compound coatings and the metallic substrate, while intrinsic stresses are due to the accumulating effects of crystallographic defects or flaws formed during the coating deposition. In addition, film stresses vary with film thickness. When a critical thickness is exceeded, cracking or buckling causes poor adherence.

Of the many potential interstitial compounds used for wear-resistant coatings, the nitrides and the carbides are probably the most common. This is particularly true with titanium nitride and titanium carbide since these coatings possess the highest hardness, highest corrosion resistance, lowest cost and greatest ease of evaporation.

TRIBOLOGICAL MATERIALS FOR MECHANICAL COMPONENTS OF THE FUTURE

Status of Understanding for Bearing Materials
by Eric N. Bamberger

Since bearing materials range from lead to ceramics to diamonds, Bamberger decided to concentrate on the class of materials used for main shaft applications in aircraft gas turbine engines.

Although there are a number of failure modes for rolling element bearings, the author addresses the following categories, 1) fatigue, 2) surface distress, 3) corrosion, and 4) miscellaneous.

The classical, subsurface-initiated fatigue spall is the most studied and perhaps the best understood failure mode in rolling element bearings. Yet when bearing failures are analyzed, a properly designed bearing using the best available materials and processes rarely exhibits this failure mode. Thus, we find that the failure mode which is best understood and which is used to set the design life of bearings is the least likely to be encountered in actual service.

The second failure mode, surface distress, represents the most prevalent operational failure mechanism in aircraft engine bearings. Surface distress is a term which relates to many failure modes. Micropitting, surface fatigue, scoring, debris damage, contamination, plastic deformation, smearing, and process induced damage all contribute to surface distress.

Although corrosion could be classed as a sub-category to surface distress, Bamberger feels that its impact on cost and logistics is such that it could have a separate identity. A substantial number of bearing rejections have been shown to be due to a type of surface corrosion. To achieve a significant improvement in reducing bearing losses due to corrosion, it is essential to make the bearing material as impervious to corrosion as possible with our current materials technology.

The final failure category, miscellaneous, covers a wide range of mechanical or handling problems which are unpredictable and statistically indeterminant. They constitute a small percentage of bearing failures and no amount of materials, design or tribological expertise can ever totally eradicate this failure mode.

The most generally used aircraft mainshaft bearing materials now in the United States is AISI M-50. However, while M-50 is a superior bearing material for past and current applications, new demands made by advanced engine designs and operational conditions indicate that it, as well as other high hardness, through-hardened materials, have deficiencies which will need attention.

As engine speeds increase, the low fracture toughness of the through-hardened rolling element bearing materials becomes a critical barrier to the operation of high performance aircraft gas turbines. It is a problem because of the small dimensions of the critical crack that is required to initiate fracture. This will be an ever-increasing problem since the next generation engines are expected to have DN values approaching three million.

In addition to the problem of fracture toughness, the higher bearing speeds will reduce the operating life of current bearing materials. Consequently, a material that has a safe design limit in terms of hours of operation at low speeds, may be inadequate for future high speed applications.

Although progress is being made in solving both fracture toughness and life extension problems, there are some observations that can be made regarding future directions. For instance, it has become clear that the classical plane strain fracture mechanics methodology is inadequate to provide a full understanding of crack propagation behavior in the materials being evaluated. A relative new sub-discipline, short-crack fracture mechanics, will be needed to achieve a better understanding and explain fracture behavior of brittle materials and crack propagation through brittle-ductile interfaces.

The second major failure mode is surface distress; it is an imprecise area where our understanding is less clear. However, it is the area where tribological efforts can have the greatest payoff.

The load carrying surface is composed of several regions. The surface contains the outer layers of oxides, adsorbed films, reaction films, etc., while the near surface region contains the inner layers which include the Bielby layer and various deformed layers. The subsurface region, which may be 50-1 000 m below the surface, has a microstructure and hardness which may differ from the bulk or core material.

For surface- and near-surface-related failures, there is yet no specific and precise understanding as to what is required to reduce the severity of the problem. It is extremely difficult to realistically simulate these effects and to correlate them with real life events. As we move to future high specific energy power transmission components, the surface distress failure mode will become ever more prevalent. The modes of failure are unique to the materials used, component geometry, and specific lubricant and operating conditions.

One concept to alleviate surface failures is to tailor-make the near surface structure, and even the surface region, to control the failure mode. The difficulty is that there is a lack of understanding regarding what is needed for resistance to surface distress and surface-initiated fatigue. The contributions of EHL, micro-EHL, surface films, surface topography and the near-surface attributes are intimately connected with the real world. However, the lack of understanding of these connections not only inhibits progress and near-surface improvements, but also creates a problem in lubricant development. Perhaps most importantly, it limits the development of simple, as well as sophisticated test devices to evaluate materials and provide the knowledge required to predict performance levels for design.

Our difficulty in understanding the failure phenomena is that much of our knowledge of the separate parts of the problem have come from isolated experiments with a variety of materials and operating conditions, which generally differ from practice. Perhaps a systems-type approach would be more profitable. So far, failure does not seem to be adequately and singly represented by the loss of an EHL film, the desorption of a surface film, the generation of critical temperature or the plastic flow of the main structure of the surface topography. The conclusion is that these aspects must be integrated to achieve an understanding of the contact phenomena. In addition, it is abundantly clear that the behavior of the near surface region, with regard to failure initiation, is greatly influenced by the topographical structure of the surface and by the role of the properties of the material in the near-surface region under stress and temperature environmental conditions.

In principle, it seems that there is no problem to putting the competitive modes of failure which are initiated in the near-surface region on a logical rather than on an empirical basis. This will prove to be the major challenge to the materials engineer, tribologist, lubricant engineer, physicist and others involved in this technological area. It is certainly an interdisciplinary problem. It seems that the key to the eventual full understanding of surface induced failures is the development of realistic simulation techniques which will permit accurate extrapolations of laboratory/component tests into real world bearings.

Status of Understanding for Seal Materials

by Paul F. Brown

Bearing compartments in gas turbine engines must be isolated from the engine gases to avoid excessive heating of the bearings, contamination and degradation of the lubricant, possible combustion of the lubricant and disruption of the oil flow. To effect this isolation, a number of seal types are currently used, including ring seals, face seals, and labyrinth seals. The hostile environment in which these seals are placed makes materials selection of great importance.

In considering materials for a main shaft face seal and ring seal, it was found that graphitic carbon rates high in terms of satisfying most of the required properties. It is used in more than 95% of end face seal applications.

Carbon graphite is one of the best sealing materials and can run against itself, metals or ceramics without galling or seizing. It is dimensionally stable over a wide temperature range, has excellent corrosion resistance, high thermal conductivity, low thermal expansion and consequently provides excellent thermal shock resistance. In general, the low friction properties result from the formation of a transfer film between the graphite and the mating surface.

Although there have been advances in the carbon-graphite seal technology area, it is possible for materials made by different manufacturers to have identical physical properties, yet one material will perform well on an application while the other will fail. Thus, until the many factors which control friction and wear are better understood and perhaps controlled, the selection of carbon seal materials will remain somewhat of a trial and error process.

Accessory gear box seal components usually consist of graphitic carbon for the nosepiece and a hardened steel for the mating surface. The second element in the accessory seal assembly that is critical to its tribological performance is the secondary seal, which is an elastomeric O-ring. The choice of the elastomer is similar to that for the elastomeric lip seal but more emphasis is placed on the compression set and oil swell characteristics. Although fluorocarbon elastomers have a wide temperature range capability, an outstanding resistance to most fluids and excellent swell characteristics, O-rings produced from different sources and certified to the same specification, can behave differently when they operate in engine oils. To remedy this situation there must be a team effort by the seal manufacturers, O-ring suppliers, elastomer formulators, carbon-graphite seal material manufacturers and engine designers so that seal designs will function properly and sealing can become a tribological science rather than a tribological art.

The ubiquitous basic radial lip seal came into being in the late 1930's with the advent of synthetic elastomers. Here we have a synthetic elastomer lip seal element bonded to a metal casing with a metallic garter spring which forms a unit that can be easily installed in mechanical systems.

There are a host of synthetic lip seal materials, each having its application depending on the environment, temperature, lubricant, and speed conditions. These elastomers include buna N, acrylates, silicone elastomers, and fluoroelastomers. Of all of these elastomers, the fluoroelastomers have perhaps the highest resistance to a variety of additives in fluids and can be used over a wider temperature range. The fluorocarbon elastomeric materials, however, cost more than the other materials.

What do we see for the future? The trend toward lower fuel consumption implies higher pressure ratios, higher turbine inlet temperatures and higher bypass ratios. The higher levels of rotor system performance in the advanced engines will result in higher rotor speeds. The increased rotor speeds, greater rotor torque capacity and critical speed margin demands will result in higher seal surface velocities. Increases in gas turbine pressure ratios will produce corresponding increases in compressor discharge pressures and temperatures. The next step in seal development, therefore, seems to be directed toward higher speed seals and those which can sustain increased pressure differentials at elevated temperatures.

In terms of future engine seals, carbon graphite is still seen as the main sealing element in face and ring seals and has potential for extremely high temperature operation. There exists the need for an improvement in oxidation resistance of the graphite for face seals and currently there is an increasing understanding of how processing and impregnation can affect oxidation control. For example, chlorine purification of graphite can reduce its oxidation rate by an order of magnitude. The carbon graphite element is, however, only one-half of the seal; there is the mating ring on which it rubs with minimal friction. Reaction-bonded silicon carbide shows low power consumption. Other non-metallics evaluated included alumina ceramic 85%, cobalt bound tungsten carbide and siliconized carbon.

Although ceramics are being used, and probably will continue to be used as one of the primary mating rings for advanced, high temperature seals, there is also an interest in using metal rings due to their good thermal conductivity and because special mounting practices are not required. Metals, however, need coatings to minimize friction and wear. A number of different metallic and non-metallic materials are being explored using a variety of coating processes and surface modifications. Included are chemical vapor deposition, plasma vapor deposition using different types of electron beam guns, electrolytic metal deposition, sprayed ceramics with fusion bonding and surface hardening by means of laser or electron beam processing to produce amorphous alloy layers.

BRIEF, PREPARED DISCUSSIONS

Tribology in Material Processing

Charles Barth
TRW Bearings Division
Jamestown, New York

Tribology, or the science of surface interactions, has been aggressively applied, for example, to studies of friction and wear phenomena, surface chemistry, and elastohydrodynamic lubrication of rolling bearing elements. As this conference demonstrates, significant technical progress continues to emerge from these efforts. I would like to present an additional opportunity which has yet to receive a similar degree of attention from a tribological perspective. This area concerns the interaction of surfaces during the processing of engineering materials.

The fabrication of engineering materials involves, to a major degree, forging and machining operations to convert raw materials into useful hardware items. A great deal of friction and wear research has been focused on surfaces in sliding contact. This work, however, has been for the most part directed toward analysis of problems associated with the performance of finished structures. A significant opportunity exists to apply tribological principles to the problems inherent with interactions between the workpiece and the process tooling. I believe tribological aspects could be fruitfully applied to the physics of contact between the workpiece and the cutting tool as well as the workpiece and all the surfaces of a forging die. Cutting tool and die failure/wear mechanisms are as imperfectly understood as are the detailed interactions which occur during the processing events. Researchers in these fields have yet to develop rigorous physical models of the progress of tool failure which have application beyond very limited constraint boundaries. This is not to say that the existing models are of little value, but major voids exist in understanding the processing phenomena. Some examples might include the following:

Forging processes:

- Friction factors with and without lubrication
- Die wear mechanisms
- Heat transfer between work and die

Machining operations:

- Tool wear mechanisms
- Chemical interactions between chip and tool
- Integrity of the cut surface

In summary, I maintain that there is potential for significant synergy between researchers involved in tribology and those working in the materials processing arena. Tribologists are in a position to make significant contributions to overall materials processing technologies. The Machining

Technology Section within TRW's Materials and Manufacturing Technology Center, for one, would entertain dialogue with tribological researchers to define joint program concepts.

Boundary Lubrication

Douglas Godfrey
Chevron Research Company
Richmond, California

I would like to share with you a suggestion for the area of boundary lubrication. We should measure the physical and the mechanical properties of the antiwear and the EP films. These properties, the mechanical and the physical, actually determine the performance of the films. Even though I and many others here have analyzed the chemical composition of such films for many years, I've begun to question the value of that effort. As an example, perhaps 15 years ago we found that TCP formed iron phosphate as the antiwear agent. That information has not been of any practical use that I have seen.

Other tribologists, especially in the early days, were concerned with the mechanical and physical properties of these films. I noticed in this conference that the people who are developing the coatings are looking at optimum physical properties.

If I may be a little more specific. In the area of extreme pressure lubrication, the melting point of the material on the surface is important. I first got this idea from Zisman who said that the only effective film is a solid film. I've attempted to measure the melting points of films, with some success, and it appears to be a unifying property that may predict the performance of a film in the EP regime. One way of measuring this is through differential thermal analysis and also microscopic observation of melting of film, perhaps in a nitrogen atmosphere.

The second property I would like to mention is shear strength, which governs the friction of a surface. Shear strength has been measured. Dr. Tabor demonstrated one method between the curve microsurfaces; perhaps we can do that with other kinds of films, such as inorganic salts.

The wear resistance of films, I believe, is related to its adhesiveness to the substrate, its own cohesiveness, and also the hardness and ductility of a surface. A sliding asperity causes elastic or plastic deformation in the film on the mating surface. Because the film can't stretch or recover from this deformation, it will fail and allow intimate metal to metal contact.

Of course, the thickness of the film is important, and it has been demonstrated that there is an optimum thickness. Also, the film material should not be abrasive when it's worn from a surface: for example, generating alumina powdered particles will abrade the parent surface.

We should put more emphasis on the physical and mechanical properties of films and give a little less attention to the chemistry. That will allow further strides in understanding boundary lubrication.

Liquid Lubricants as Heat-Transfer Fluids

Ward O. Winer
Georgia Institute of Technology
Atlanta, Georgia

I've been saying that I think heat transfer is important in systems, tribological systems, and I was asked to talk about liquid lubricants as heat-transfer fluids.

I think we've been lucky in the past. Lucky in the sense that the liquid lubricants we've been using have also performed the function of a heat-transfer fluid adequately, in most cases, or we've been able to adjust things to make them work adequately. By and large, as a community, either from the design standpoint or the research standpoint, we have tended not to think much about the heat-transfer characteristics of fluids. Probably the farthest we've gone in most cases was a few references to the Prandtl number of fluids that we saw flashed on the screen this week. I submit that from the heat-transfer standpoint, in this particular field, the Prandtl number, although it's probably the only thing you can grasp, is maybe essentially irrelevant.

We need to separate our thinking. This is counter to many of the pleas we've heard about integrating our thinking, but I think we need to separate our thinking about heat-transfer functions and lubrication functions in tribology and that will help us clarify things. The Prandtl number, for those of you who are not really familiar with it, is attractive because it involves four physical properties that are measured: thermal conductivity, density, specific heat, and viscosity. At any temperature and pressure those properties can be measured and then put into a dimensionless number called the Prandtl number. The difficulty with this is that most work in heat transfer is done with materials that have a limited range of Prandtl numbers. Since the vast majority of heat-transfer literature deals with gases and water, you're dealing with Prandtl numbers from about 0.1 to 2; but, for liquid lubricants, Prandtl numbers can go as high as 1000. Beyond that, the Prandtl number makes sense only if you consider other relevant factors. It reminds me of the difference of importance in a boxing match of weight and arm length: clearly, the most important thing is the weight of a boxer, not the arm length. The Prandtl number is kind of like the arm length in this particular process. Other things need to be dealt with as far as heat transfer is concerned. If we separate the two functions of lubrication and heat transfer, then a lot of additional possibilities open up.

We have heard, and I think we have a reasonably good handle on, ways of determining temperature limitations of liquid lubricants. Elmer Klaus and others have defined ways reasonably well in terms of time and temperature behavior. That puts some clear limits on how high a temperature you can operate at and for how long. But in most advanced design systems, and we've heard about some of them here, such as adiabatic diesel concerns, people want to go to much higher temperatures for thermodynamic purposes. As many people here have said that rules out using liquid lubricants for the extreme cases.

Does that rule out a consideration of heat transfer Isn't thermal science important to an adiabatic engine If it's really adiabatic there is no upper limit and we don't have a chance of ever having any tribological success unless we consider temperature effects. Clearly, they are not talk-

ing about an adiabatic system, they are talking about a higher temperature system.

We need to direct our attention in tribology to heat-transfer mechanisms, and we need to direct our attention to clever design mechanisms for carrying the energy away. If we direct our attention to heat-transfer mechanisms in the systems, then it seems to me that we ought to consider additional possibilities such as phase changes. An example would be sodium-cooled exhaust valves for reciprocating engines. Maybe we need a look at that and at introducing heat pipe systems into tribological design mechanisms. We should not overlook the possibility of using radiation as an important means of thermal energy transport, which has been significant in space devices. It is a far more efficient procedure for removing energy from a system than any convection cooling is going to be, either with a gas or with the liquids that we use as lubricants. Maybe no one has thought about it in connection with the friction and temperature curve that I showed yesterday for the red hot glowing specimens, but you may recall that the temperature leveled off at about 650° C after only about 5 minutes. The system continued to run, which means it dissipated energy for 30 minutes. It leveled off because at 650° C and given the surface area and other relevant properties of that particular system all the energy was being very effectively and rapidly radiated away. We need to consider tribological thermal system design as a separate entity; something that receives specific additional attention compared to other areas of usual concern. Thermal control needs to be incorporated increasingly into our overall thinking of tribology. Specific attention is clearly becoming important, and we need to think in terms of separating the lubricant from the heat-transfer mechanism. If we have to go to solid lubricant systems, or hard or soft coatings, for high-temperature applications, then clearly the same material that functions as a lubricant is not going to function as a coolant.

Designing and Using Composites

Michael N. Gardos
Hughes Aircraft Company
El Segundo, California

Composites, it's not a science; I don't think it's ever been; we'd love to make it a science; but it's not going to happen in my lifetime. Take a piece of plastic which will fall apart around 600° to 700° F in air. Maybe we can reenforce it, or give it a composite body, but it would be a bowl of jello without a skeleton. Well, how would you reinforce the plastic Chopped fibers That's not enough; it wouldn't give you enough strength.

Two-dimensional graphite fabric composities depend on the shear strength. If you put a bunch of layers together and if you orient them in the wrong direction, just like a deck of cards, there will be shear failure between the layers.

We've reinforced and treated three-dimensional graphite fiber so it's not going to be an abrasive at elevated temperatures. We have compressive strength at 600° F, that's around 30 000 to 35 000 psi. And we made bearings out of it. The bearings ran at those loads at low speeds, and the wear was acceptable with a coefficient of friction of 0.2 (the magic number for solid

lubricants). Then we reduced the pressure to 4000 psi and ran it at what we call high speeds - 130 ft/min, 600 000 PV, 600° F.

How do you mold the bearing retainer from such material Since it's cylindrical you have to make a cylindrical weave. Then, you have to use a varnish and put a soluble organic salt in the composite. If you have a three-dimensional weave of graphite, you have unit cells to fill with the polymer resin. Adding an organic salt and a lubricant additive weaken the composite, so now the mechanical strengths are weakened and the tensile strength is inadequate.

All I'm saying is that it is possible to develop composite materials for tribological mechanical components, but at present it's an emperical process that may require 100 by 100 matrices. It is very difficult to understand the interaction of elements of the composites such as the graphite fiber surfaces.

Need for Design in Tribology

Harmen Blok
Rijswijk, The Netherlands

I would like to make a plea for developing tribology into tribo-technology. I will explain that. Tribology has been recognized for about two decades as a science, at that a multidisciplinary science, so at first glance tribology might look fairly complete. It is not, however, complete from the engineering viewpoint. Why It does not embody any really fundamental engineering principles and concepts, at least not explicitly. So from theories of sciences, one cannot expect results of nature not accounted for in this particular science.

There has been a gap between tribology as a science and its application to design and development. For the most part that gap exists because of the absence of fundamental design principles and concepts in tribology. Bridging this gap is all important for both rationalizing and speeding up the transfer of tribological knowledge.

To develop tribology into tribotechnology requires conceptually integrating fundamental design principles and concepts into tribology. In discussing this process I confine myself to a single concept.

This point deals with the concept of hydrodynamically self-acting lubricant films, which are rather usual and conventional. They are really pumps, and to distinguish from different types of pumps I tend to call them film pumps. By conceiving such film pumps, one may think of introducing scalloping and other new kinds of surfaces that might be used to develop pressure in lubricant films and, indeed, this has been achieved. In the bearing the lubricant film is the central element because it is hydrodynamic self-acting. In thinking of new kinds of bearings, first think of new kind of film pump for the lubricant film and then build the bearing around it.

One way of distinguishing among rubbing surfaces of systems on the basis of rigidity is developing in the field of the rigid systems. This one is that of whirl-proof bearings. Indeed, I arrived at the idea, without having any recourse to Reynold's equation, just trying to obtain a kind of pump that already exists for the purpose. The basic principle of arriving at bearings having as high a load capacity as possible was achieved by spiral grooves in different kinds of bearings. That kind of pump, call it a film pump, has much in common with many other kinds of conventional pumps.

I'm sorry there is not time to explain further, but in conclusion I want to point out that although the basic Reynolds equation is applicable to such developments none has emerged so I don't want to overemphasize the importance of this basic equation or theory in general. What I do want to point out is that to arrive at new developments, not only by invention, but by intuition, you may arrive in a very logical manner. It can be achieved by the conceptual integration of such basic design principles and design concepts into tribology. I mentioned only one such concept. That concept was obtaining hydrodynamic self-acting lubricant films using film pumps. There are many more. So that is my plea - to develop tribology into tribotechnology so as to speed up the transfer of the knowledge; that is, conceptually integrating the really fundamental principles and concepts of design and development based on tribology.

Graphite-Fiber-Reinforced Polyimide Composites

Harold E. Sliney
NASA Lewis Research Center
Cleveland, Ohio

I would like to comment on Mike Gardos' discussion relevant to graphite-fiber-reinforced polyimide composites. I agree that the three-dimensional graphite-reinforced composites developed by Mr. Gardos and his colleagues are useful self-lubricating materials. Another approach, which we have taken, also results in high, straight graphite-reinforced composites with good tribological properties. In this approach, chopped graphite fibers are used for reinforcement instead of woven fibers, and no additional solid lubricants are incorporated into the composite as they are in the three-dimensional composites described by Mr. Gardos.

I disagree with Mike's comment that the use of chopped fiber does not give a composite of adequate strength. Our experience is that chopped fibers are quite effective reinforcing agents. For example, we used chopped graphite fibers in a 1:1 weight ratio with NR150 polyimide and achieved a structure with a compressive strength of about 35 000 psi, which is quite respectable for a polymeric composite bearing material. It was also our experience that adding solid lubricants to the composite structure did not reduce the friction coefficient; in fact, it only seemed to reduce the mechanical strength of the composites. That is not to say that a solid lubricant cannot be used effectively in graphite fiber - polyimide composites, but we were unable to achieve any benefit by complicating the composition with a solid lubricant as a third component.

The preparation of chopped fiber-reinforced composites involves a relatively simple transfer molding process. In the case of plain spherical bearings, for example, a molded liner is prepared by transfer molding a mixture of chopped graphite fibers and B-staged polyimide directly into the bearing. This is done by first concentrically locating the spherical element and the outer ring in a fixture, introducing the mixture, then curing under heat and pressure. Bearings of this type have good wear resistance and have friction coefficients of the order of 0.15 to 0.20 from 250° to 350° C. They have a dynamic load capacity during low-speed oscillating motion of about 20 000 psi at 260° C and about 10 000 psi at 350° C. In most dry bearing applications, the required load capacity is less than 1000 psi and

certainly less than 20 000 or 10 000 psi. Therefore, I believe that the chopped graphite-fiber-reinforced bearing material is a very usable tribological material.

Methods for Distillation of Information

Horst Czichos
Bundesanstalt für Materialprüfung
Berlin, Federal Republic of Germany

We have had one week full of information: there have been more than 30 papers, and we've had additional discussions. Furthermore, there are about 6000 papers published annually in the field of tribology.

The question is how the existing tribological knowledge can be better used and applied in practical applications. This is an important question and a difficult one. There are two aspects. First, a proper presentation and discussion of tribolgical research results; and second, the development of away to retrieve tribological information. In Germany, we put some effort into putting things together systematically.

The first thing is how to describe the results and then to use this as a basis for retrieving tribological information. In a very simplified manner the first step is to identify all materials in the friction and wear process. We have, of course, a couple of materials with the interfacial medium and environmental medium. These components and their properties provide what we call the structure of a given situation. So this is one basic group. The other group we have is the operating variables. Most important are load and pressure, kinematic temperature, and rubbing duration. So these are the two basic groups. You can draw an analogy to a simple tensile test: you have only one piece of material, one operating variable, and the equivalent in tribology is a complex structure, and that complexity causes the difficulties. Two materials interact by means of contact friction and wear mechanisms. We have the lubricant, which has an influence on these processes as well as on the two materials, and the environment, which influences the lubricant as well as the interacting components. The multiplicity of influencing factors is the crux of all tribology.

The consequences of the action of the operating variables on the structure, via the tribological interactions, are the friction-induced energy losses and energy-induced material losses, and, further, the tribological induced changes of properties of systems components.

So there are four basic parameter groups: operating variables, external operating variables, structure components of a given system, tribological interactions, and then, also, the loss output to be described.

This is a kind of frame, and the question is how to use and apply it. To give you an example, we are operating a research program in our country which is run by the German Ministry of Research and Technology. It started in 1978 and now has about 130 projects in a 6-year program. The following are some of those 130 projects, but not in order of importance: abrasive wear, fretting and fretting fatigue, sliding bearings, EHD, mixed lubrication, measuring and testing techniques, sliding bearing materials, surface treatment, lubricants for combustion engines, manufacturing design, performance of tribological systems, diesel engines, and lifetime improvement.

In 1981 our institute was asked how this information could be described and made applicable to industry for practical applications. We tried to develop some retrieval methods, on the basis of the systematic description I showed you, and we established a descriptor system. We divided the various aspects of the tribological phenomena into seven basic groups. First, the function of the tribological system, second, the field of application (system machine apparatus component product manufacturing processes, etc.), then the operating conditions (type of contact, type of motion of operating variable), the structure (mainly the material properties and material parameters but also the geometrical parameters and design aspects), the tribological problem, the methods of investigation, and finally the background of interest. We developed a questionnaire; of course, the project leaders didn't like that but I think it was inevitable. This questionnaire contained 300 descriptive terms which were the basis for the information we obtained. When the results of these research projects are compiled, descriptors are accummulated. Now when people from industry say I have an apparatus like that, I have a type of contact like that, I have certain material processes, and I'm interested in a certain method of investigation, you can easily, by considering these parameters, distill what project is relevant. The next step may be the use of a standard data sheet. I showed one in my talk. In the future we may be able to establish a data base that can be used by industry. I know, of course, that filling in data sheets is tedious. Researchers don't like to do it, but I think that it is necessary to accomplish technological transfer from research to application.

SPECIFIC QUESTIONS AND COMMENTS

Question (L. Ting): I have two questions for Mr. Bramberger. What kind of bearing failure monitoring system did you use to conduct your simulated tests If you are using the vibration detection method, can you tell whether the bearing is beginning to fail due to bearing surface distress

Answer (E. Bramberger): We use several systems to detect bearing failure. Vibration is one. It certainly is not the best one. There are relatively sophisticated chip detection systems which detect even the very minor start of destruction of the surface, if you're talking surface distress primarily. If you're talking about more serious failures, such as fracture, we do have magnetic pickups, sensing devices, which can sense a change in the continuity of the ring if it breaks, so we can stop it immediately. I can't give you a single answer. I think it depends on the type of test that we're running. The idea, of course, in any test of this kind, where you're trying to get engineering data, is to stop the test before the bearing destructs itself to the point where you no longer have the capability of going back and analyzing exactly what happened. One of my pictures did show the bearing seriously fractured. This failure occurred in a program we're running now where we did not have adequate control in the shutdown mechanism and did get a fracture. It is obviously a very dramatic picture to show, and it illustrates a point. But from an engineering standpoint, it adds very little data, because there is not enough left for any serious analysis. One of the most important considerations, particularly when

you're trying to sense very early failure, involves a continuous evaluation of the oil contamination as the bearing begins to wear. We found this is one of the best ways of sensing very early bearing distress.

Comment (W. Winer): Several comments during the meeting were about what tribology means. It might seem redundant, but I'm concerned with whether tribology means the science of our field, the technology and applications of our field, or both. I have my idea of what it means, and I would like to at least bring it up here. If I am correct, my British colleagues can correct me on this, but it seems to me the definition that is now in the Oxford English Dictionary is that tribology is the science and technology of surfaces in relative motion and encompassing those areas known as friction, lubrication, and wear. In that definition I see no confusion and I feel badly that people are raising the issue. In my frame of reference, the term tribology means both the science and the technology, in other words, the applications, and to me that's the exciting part of it and I don't think we should try to separate the two.

By way of information, I'd like also to mention that the American Society of Mechanical Engineering, which has been a very active group in this country in the field of lubrication, or whatever you want to call it, has in the last 6 months gone through a significant change in terms of names for our field. Effective January 1, 1983, the Lubrication Division of ASME, which is where almost all the lubrication work takes place, has had its name changed from the Lubrication Division to the Tribology Division. The Research Committee on Lubrication, which prides itself on being one of the oldest research committees in ASME and one of the most active, has as of January 1, 1983, changed its name from the Research Committee on Lubrication to the Research Committee on Tribology. The Transactions of ASME Journal on Lubrication Technology, which everyone is familiar with, I hope, is going to change its name, as of the first issue in 1984, to Transactions of ASME Journal of Tribology.

Now, I'm one of the leaders or instigators of these changes, depending on how you look at it, and it has been my firm conviction in pushing for these changes and getting them approved that the name changes will, in fact, be more representative of what those groups do and what they are interested in than were the former names.

The Lubrication Division, the Research Committee on Lubrication, and the Journal of Lubrication Technology have many activities, many publications, and many interests outside lubrication in the classical sense. It has also been my firm conviction that the names do not imply that we want to go the science route but, in fact, imply that we want to tell the world that we are interested in friction, lubrication, and wear and we are interested in both the fundamental aspects and the application aspects of it. I hope nobody goes home with a confused feeling about that issue.

The people who have been involved in requesting these name changes and the ASME superstructure are firmly convinced that this is going to be more representative of the field we're really interested in and, in fact, will help people outside the field of lubrication be more comfortable participating in these activities.

As current Technical Editor of the Journal of Lubrication Technology, I want to assure everyone of that. In discussing these changes almost everyone has agreed with these changes. The only very minimal objection was on this issue of whether that name includes technology or not. I want to assure everybody that it does include the application end of things, the technology end of things, because one is rather meaningless without the other.

Comment (V. Wedeven): While we're on the subject of names, I'm sure all of you know biannually there is a Gordon Conference held in June, the next one will be in June 1984. This has been traditionally called the Gordon Conference on Friction, Wear, and Lubrication. In March 1983 this name was changed to the Gordon Conference on Tribology. As Conference Chairman for 1984, this was easy to do - it only took one telephone call.

Comment (S. Vago): I have to comment on one aspect of the word tribology. I recently was asked to write a small brochure and I used in the title the word tribology. Prior to printing it I showed it to my friends in engineering and in plant engineering and no one knew what it meant. They said not to use that word because people are going to think you're a smart so and so. Although I deleted tribology from the title, I used it in the text in an attempt to define it. If any organization, including ASME and ASLE, is going to use tribology in the broad sense, then there will have to be a maximum effort to educate the grass roots people, including general engineering, who don't belong to ASME and ASLE. We're going to have to educate these people as to the goals, meanings, and definitions of this word.

Comment (R. Johnson): This education process has been going on ever since the Jost report was first issued, and it just proves that we're all slow learners. I would hope that this move by ASME and other similar moves will help to unify the relevant technology and science in this country as it has in the United Kingdom. They have had their problems too. It's an interesting development that it will continue.

Comment (S. Hsu): I think I should raise one point about test methods. It is important, because in the next 20 years we are going to be developing materials and looking at mechanisms of what's happening in the surfaces. In spite of 6000 publications a year, we don't seem to understand what's going on. One key question is whether we're measuring the intrinsic friction and wear properties of the material or just measuring the friction and wear characteristics of the system. Is the reason we cannot advance in our technology, understanding of the science, because each of us is trying to be unique Working in ASTM at the National Bureau of Standards I have a primary responsibility for pushing and standardizing the test procedures. In ASTM we are talking about standardizing the routine tests. In our research community, in spite of all the meetings and conferences like this where we exchange information and ideas, we don't seem to have a handle on the intrinsic properties of the materials. I think this is going to be a very important issue in the next 20 years, especially when we are developing new materials and new lubricants. We always seem to select one grid in an

informational space and we measure a whole range of materials and say this is the friction of wear properties of the lubricant, or of the ceramics. I think in the future maybe we should map out the surfaces and define our space. In that way maybe the information technology exchange can push our technology further.

☆U.S. GOVERNMENT PRINTING OFFICE:1984 -739 -010/ 2 REGION NO. 4

1. Report No.	2. Government Accession No.	3. Recipient's Catalog No.
NASA CP-2300		

4. Title and Subtitle	5. Report Date
Tribology in the 80's Volume II - Sessions 5 to 8	April 1984
	6. Performing Organization Code
7. Author(s)	8. Performing Organization Report No.
	E-1559
	10. Work Unit No.
9. Performing Organization Name and Address	11. Contract or Grant No.
National Aeronautics and Space Administration Lewis Research Center Cleveland, Ohio 44135	13. Type of Report and Period Covered
	Conference Publication
12. Sponsoring Agency Name and Address	14. Sponsoring Agency Code
National Aeronautics and Space Administration Washington, D.C. 20546	

15. Supplementary Notes

16. Abstract

This 4-day international conference, held at NASA Lewis Research Center on April 18-21, 1983, was the result of an effort by the Structures and Mechanical Technologies Division at Lewis. Thirty-six invited presentations were made relative to the advancement of various disciplines and subdisciplines in the field of tribology (lubrication). These included papers on the status of understanding on each of the eight session topics, as well as the current state-of-knowledge and directions to be taken for the remainder of the decade. A wide range of subjects was covered that extended from fundamental research with tribological materials of all kinds and their surface effects up to the final technology applications in bearings, gears, and seals. The papers and the ensuing invited and spontaneous discussions on them by the participants are reported herein.

17. Key Words (Suggested by Author(s))	18. Distribution Statement
Tribology; Lubrication; Friction; Wear; Lubricants; Elastohydrodynamic lubrication; Bearing materials; Gear materials; Seal materials	Unclassified - unlimited STAR Categories 27 and 37

19. Security Classif. (of this report)	20. Security Classif. (of this page)	21. No. of pages	22. Price*
Unclassified	Unclassified	387	A17

*For sale by the National Technical Information Service, Springfield, Virginia 22161

National Aeronautics and Space Administration

Washington, D.C.
20546

Official Business
Penalty for Private Use, $300

SPECIAL FOURTH CLASS MAIL
BOOK

Postage and Fees Paid
National Aeronautics and
Space Administration
NASA-451

NASA

POSTMASTER: If Undeliverable (Section 158 Postal Manual) Do Not Return